

ABSTRACT

Small-molecule Inhibitors of Tubulin Polymerization as Vascular Disrupting Agents and Prodrugs Targeting Tumor-Associated Hypoxia

Zhe Shi, Ph.D.

Mentor: Kevin G. Pinney, Ph.D.

The tumor microenvironment provides a number of promising targets for selective treatment with anticancer agents. Aberrant tumor-associated neovascularization offers one such targeting opportunity. Compounds referred to as vascular disrupting agents (VDAs) cause morphological changes in endothelial cells lining tumor-associated vasculature leading to selective and irreversible reduction in blood flow thus starving tumors of necessary oxygen and nutrients, ultimately culminating in necrosis.

Combretastatin A-4 (CA4) and combretastatin A-1 (CA1) are natural products derived from the South African tree *Combretum caffrum* that inhibit tubulin polymerization and demonstrate dual mechanism of action functioning both as antiproliferative agents and separately as VDAs. Inspired by the molecular architecture of colchicine and the combretastatin family of natural products, several 2-aryl-3-aryol-indole analogues were designed and synthesized to further enhance structure activity relationship considerations around our previously discovered lead indole-based anticancer agent, OXi8006. These indole analogues were evaluated for their ability to inhibit tubulin assembly and for their

cytotoxicity against several human cancer cell lines. An amino analogue showed a comparable inhibition of tubulin assembly ($IC_{50} = 0.83 \mu\text{M}$) to the reference compound OXi8006. In addition to the synthesis of new analogues and prodrugs, a mechanistic study related to the formation of a key intermediate (2-arylindole) was also carried out utilizing a ^{13}C -labeled molecule.

A wide variety of solid tumor cancers are characterized by profound regions of hypoxia, which provides a unique opportunity for targeted cancer therapy. A promising strategy involves the hypoxia-selective release of potent anticancer agents facilitated through reductase-mediated cleavage of non-toxic bioreductively activatable prodrug conjugates (BAPCs). A series of BAPCs were synthesized that incorporate parent anticancer agents OXi8006 (indole), OXi6196 (dihydronaphthalene), and KGP18 (benzosuberene) that incorporate a variety of nitro-bearing heteroaromatic triggers. The cytotoxicity of these BAPCs was evaluated under both normoxic and hypoxic conditions to determine their hypoxia cytotoxicity ratio (HCR). Several of these BAPCs demonstrated promising HCR values (>7) in the A549 lung cancer cell line. The most promising BAPC (OXi6196-monomethylthiophene trigger) demonstrated anti-vascular activity in a preliminary *in vivo* study in an orthotopic syngeneic breast tumor mouse model (4T1/BALB/c), as evidenced through bioluminescence imaging (BLI) and histology.

Small-molecule Inhibitors of Tubulin Polymerization as Vascular Disrupting Agents and Prodrugs
Targeting Tumor-Associated Hypoxia

by

Zhe Shi B.S. M.A.

A Dissertation

Approved by the Department of Chemistry and Biochemistry

Patrick J. Farmer, Ph.D., Chairperson

Submitted to the Graduate Faculty of
Baylor University in Partial Fulfillment of the
Requirements for the Degree
of
Doctor of Philosophy

Approved by the Dissertation Committee

Kevin G. Pinney, Ph.D., Chairperson

Daniel Romo, Ph.D.

Robert R. Kane, Ph.D.

Mary Lynn Trawick, Ph.D.

Joseph H. Taube, Ph.D.

Accepted by the Graduate School
August 2018

J. Larry Lyon, Ph.D., Dean

Copyright © 2018 by Zhe Shi

All rights reserved

TABLE OF CONTENTS

LIST OF FIGURES	vii
LIST OF SCHEMES.....	ix
LIST OF TABLES	xi
ACKNOWLEDGMENTS	xii
DEDICATION	xiv
ATTRIBUTIONS	xv
CHAPTER ONE.....	1
Introduction.....	1
<i>Cancer</i>	1
<i>Vascular Targeting Agents</i>	2
<i>Vascular Disrupting Agents</i>	5
<i>OXi8006</i>	10
<i>Bioreductively Activatable Prodrug Conjugates</i>	11
<i>Antibody-Drug Conjugates</i>	16
<i>Mechanism of Indole Ring formation</i>	18
<i>Small-molecule Inhibitors of Cathepsin L</i>	19
CHAPTER TWO	21
Indole-Based Vascular Disrupting Agents and Antibody-Drug Conjugates	21
<i>Introduction</i>	21
<i>Synthesis of Indole Analogues</i>	22
<i>Synthesis of Bridge-Modified Combretastatin Analogue</i>	26
<i>Synthesis of OXi8006-Based Antibody-Drug Conjugate</i>	28
<i>Biological Evaluations</i>	30
<i>Materials and Methods</i>	32
CHAPTER THREE	62
Synthesis of Bioreductively Activatable Prodrug Conjugates Based on OXi8006 and 3-Bromopyruvic Acid	62
<i>Introduction</i>	62
<i>Synthesis of Bioreductive Triggers</i>	62
<i>Preparation of Normethylnitrothiophene-OXi8006 BAPC</i>	66
<i>Preparation of Bromopyruvate BAPC</i>	67
<i>Materials and Methods</i>	71

CHAPTER FOUR.....	86
Targeting Tumor Hypoxia with Bioreductively Activatable Prodrug Conjugates Derived from Dihydronephthalene, and Benzosuberene-Based Vascular Disrupting Agents	86
<i>Abstract</i>	86
<i>Introduction</i>	87
<i>Chemistry</i>	91
<i>Biological Evaluation</i>	92
<i>Conclusion</i>	97
<i>Materials and Methods</i>	97
<i>Acknowledgement</i>	106
CHAPTER FIVE	107
Mechanistic Considerations in the Synthesis of 2-Aryl-Indole Analogues under Bischler-Mohrlau Conditions.....	107
<i>Abstract</i>	107
<i>Introduction</i>	108
<i>Synthesis and Characterization</i>	112
<i>Conclusion</i>	117
<i>Experimental Procedure</i>	117
<i>Acknowledgements</i>	123
<i>Supplementary data</i>	123
CHAPTER SIX.....	124
Scale-up Synthesis of Cathepsin L Inhibitor KGP94	124
<i>Introduction</i>	124
<i>Synthesis</i>	124
<i>Materials and Methods</i>	126
CHAPTER SEVEN	132
Conclusion	132
APPENDICES	134
APPENDIX A.....	135
APPENDIX B.....	194
APPENDIX C.....	235
APPENDIX D.....	300
APPENDIX E	337
APPENDIX F	354
REFERENCES	362

LIST OF FIGURES

Figure 1.1. Top Ten Types of Cancer in Estimated New Cases and Death by Sex, United States, 2018	2
Figure 1.2. Scanning Electron Microscopy (SEM) Image of a Microvascular Cast from Normal Lung Tissue (A) and a Human Sigmoidal Adenocarcinoma (Colorectal Cancer) (B).....	3
Figure 1.3. Angiogenesis-Inhibiting Agents (AIAs) and Vascular Disrupting Agents (VDAs).....	4
Figure 1.4. Mechanism of Tumor Vasculature shutdown after administration of a VDA	6
Figure 1.5. Selected Natural Products Functioned as VDAs	7
Figure 1.6. Leading Compounds Developed in Pinney Research Group	8
Figure 1.7. Proposed VDA Mechanism of Action of OXi8007 in Activated Endothelial Cells	11
Figure 1.8. Chronic (Diffusion-Limited) and Cycling (Perfusion-Limited) Hypoxia	12
Figure 1.9. Structure of Selected Bio-reductive Prodrugs	13
Figure 1.10. Structure of Brentuximab Vedotin and Trastuzumab Emtansine	17
Figure 1.11. Structure of Cathepsin L inhibitor KGP94	20
Figure 2.1. Selected Indole-Based VDAs and their Prodrugs	21
Figure 2.2. Synthesized Indole-Based VDAs and Prodrugs	30
Figure 4.1. Structure of Selected Bio-reductive Prodrugs	87
Figure 4.2. Representative Small-molecule Inhibitors of Tubulin Polymerization.	88
Figure 4.3. Previously Reported BAPCs Based on Tubulin Binding Agents.....	89

Figure 4.4. Bioluminescence Imaging (BLI) of 4T1-luc Tumor Bearing Nude Mice at Various Times Following VDA (OXi6197) and BAPC (KGP291, Compound 13) Administration.	94
Figure 4.5. Dynamic Light Emission Time Course with Respect to Vascular Disruption.	95
Figure 5.1. Representative Examples of Inhibitors of Tubulin Polymerization Incorporating Fused Heterocyclic Ring Systems: Benzo[<i>b</i>]thiophene (A); Benzo[<i>b</i>]furan (B); and Indole (C)	107
Figure 5.2. Four Possible Indole Regioisomers from Representative Bischler-Mohlau Reaction	114
Figure 5.3. ¹³ C-NMR of Unlabeled Indole Analogue 8 , ¹³ C-NMR of ¹³ C Labeled Indole Analogue 16 (same as indole 8 but incorporating ¹³ C label), DEPT NMR of ¹³ C Labeled Indole Analogue 16	115

LIST OF SCHEMES

Scheme 1.1. Mechanism of Reductive Activation of Tirapazamine	14
Scheme 1.2. A: Proposed Strategy for Selective Release of Cytotoxic Agent from Prodrug under Hypoxic Conditions of Cancer Cells; B: Biological Reduction and Cleavage of BAPCs (CA4-gem-dimethyl Nitrothiophene as an Example).....	16
Scheme 2.1. Synthetic Route to OXi8006	22
Scheme 2.2. Synthetic Route Towards Water-soluble Disodium Phosphate Salt 5	23
Scheme 2.3. Synthetic Route Towards Indole Analogue 22	24
Scheme 2.4. Synthetic Route Towards Amino Indole Analogue 28	25
Scheme 2.5. Synthetic Route Towards the Methylene Bridge-Modified CA4 Analogue 35 from Literature	26
Scheme 2.6. Synthetic Route Towards the Methylene Bridge-Modified CA4 Analogue 35 Used in This Study.....	27
Scheme 2.7. Preparation of OXi8006-Based ADC 54	29
Scheme 3.1. Synthesis of Nitrothiophene Triggers	62
Scheme 3.2. Alternative Route towards Nitrothiophene Triggers 3 and 5	62
Scheme 3.3. Synthesis of the Nitrofurans Triggers	63
Scheme 3.4. Synthesis of the Nitroimidazole Triggers.....	63
Scheme 3.5. Attempted Methylation of Nitroimidazole Ketone	64
Scheme 3.6. Synthesis of the Nitrobenzyl Triggers.....	65
Scheme 3.7 Synthesis of BAPC 26	66
Scheme 3.8. Unsuccessful Attempts Towards BAPC 28 Utilizing Esterification Pathway.....	67
Scheme 3.9. Synthesis of Compound 32	68

Scheme 3.10. Unsuccessful Attempts Towards BAPC 28 Utilizing Bromination Pathway	69
Scheme 3.11. Successful Synthetic Route to Bromopyruvate BAPC 28	70
Scheme 4.1. Biological Reduction and Cleavage of BAPCs (Use Compound 13 as an Example).....	94
Scheme 4.2. Synthetic Routes toward BAPC 10-17	95
Scheme 5.1. Mechanistic Pathway A Associated with the Bischler-Mohrlau Reaction...	109
Scheme 5.2. Mechanistic Pathway B Associated with the Bischler-Mohrlau Reaction. ..	110
Scheme 5.3. Postulated 1,2-Aryl Shift Resulting in Rearranged Indole Analogue.	110
Scheme 5.4. Formation of Benzo[<i>b</i>]thiophene Regioisomers via Cyclization and Concomitant 1,2-Aryl Ring Migration.	111
Scheme 5.5. Potential Mechanistic Pathways Leading to ¹³ C Labeled Indole Analogues	112
Scheme 5.6. Synthesis of ¹³ C Labeled Bromoacetophenone 16	113
Scheme 6.1. Synthesis of KGP94.	124

LIST OF TABLES

Table 1.1 Inhibition of Tubulin Assembly and Cytotoxicity of Selected VDAs Table 2.1	9
Table 2.1 Inhibition of Tubulin Assembly and Cytotoxicity of Target Indole Analogs ...	29
Table 4.1. Inhibition of Tubulin Assembly and Percent Inhibition of Colchicine Binding.....	92
Table 4.2. In Vitro Potency and Hypoxia Cytotoxicity Ratio (HCR) of the BAPCs in the A549 Human Lung Carcinoma Cell Line	93

ACKNOWLEDGMENTS

First and foremost, I am deeply indebted to my advisor, Dr. Pinney. I greatly appreciated the opportunity to work in his research lab. He was incredibly supportive, understanding and encouraging as a mentor. His support and guidance were instrumental and provided foundational support for my accomplishments throughout my graduate studies.

I would like to thank my committee members Dr. Romo, Dr. Kane, Dr. Trawick and Dr. Taube for their help and suggestions with my projects and dissertation. I appreciate the valuable time they spent to ensure my success in future academia.

I also would like to express my gratitude to the Department of Chemistry and Biochemistry at Baylor University. I thank the graduate assistants for their continued hard work and support over the past six years.

Next, I would like to give my appreciation to the previous and current Pinney group members who I worked with, Dr. Jiangli Song, Dr. Matt MacDonough, Dr. Laxman Devkota, Dr. Chen-Ming Lin, Dr. Erica Parker, Dr. Christine Herdman, Dr. Deboprosad Mondal, Dr. Rajeswari Mukherjee, Casey, Haichan, Ricardo, Graham, Jake, Lauren and Wen. They provided continued support and advice that facilitate my graduate research. I also thank Cassie Robertson, Parker Korbitz and Raj Patel, who were all great undergraduates and provided helpful assistants to my research.

My thanks go to our collaborators Dr. Mary Lynn Trawick at Baylor University, Dr. Ralph P. Mason at UTSW and Dr. Ernest Hamel at NCI. Their collaborative efforts provided valuable biochemical, biological, and *in vivo* data necessary for our research.

I also would like to express my great appreciation to all the people in the Heart Failure and Muscle Metabolism DPU at GlaxoSmithKline, especially my advisor Jay Matthews. From basic lab techniques to drug design and pharmacokinetics, their expertise in medicinal chemistry and guidance will be of great benefit to my career.

I would like to thank brothers and sisters at Columbus Avenue Baptist Church and University City Chinese Christian Church. I really appreciate their continuous support and prayer.

None of this would have been possible without the loving support of my family. The financial and emotional support from my parents has allowed me to reach this stage in life. Thank you for encouraging me to always follow my dream, allowing me to study overseas and bearing the separation.

Most importantly, I want to show my greatest appreciation to my wife Lian. Her unwavering support throughout my graduate studies is undoubtedly the main reason I have completed this journey. Her love and prayers carried me through the most difficult times and helped me to move forward. I am truly blessed to have her spend the rest of her life with me. I love you so much!

DEDICATION

To my parents Zhongfa Shi, Qing Huang
and my wife Lian Liu

ATTRIBUTIONS

Some portion of Chapter Two in this dissertation is published as: Winn, B. A.; Shi, Z.; Carlson, G. J.; Wang, Y.; Nguyen, B. L.; Kelly, E. M.; Ross IV, R. D.; Hamel, E.; Chaplin, D. J.; Trawick, M. L.; Pinney, K. G. Bioreductively Activatable Prodrug Conjugates of Phenstatin Designed to Target Tumor Hypoxia. *Bioorg. Med. Chem. Let.*, **2017**, *27*, 636-641. Zhe Shi contributed to this manuscript through the preparation of all eleven bioreductive triggers which is included in Chapter Two. In addition, Zhe Shi contributed a significant amount to the preparation of the supporting information. Dr. Blake Winn (Pinney Research Group) synthesized nine of the eleven final compounds as well as characterized them by NMR, HPLC and HRMS. He also contributed to writing and editing of the manuscript. Graham Carlson (Pinney Research Group) synthesized the other two target molecules. Yifang Wang from Dr. Trawick's Research Group at Baylor University performed the enzyme cleavage assay. Dr. Benson Nguyen (Pinney Research Group) originally synthesized one of the analogues, which was resynthesized by Dr. Blake Winn. Evan Kelly (Pinney Research Group) and David Ross (Pinney Research Group) helped with the synthesis of intermediates and target molecules. Dr. Ernest Hamel (National Cancer Institute) performed the inhibition of tubulin polymerization studies.

Chapter five in this dissertation is published as: MacDonough, M. T.; Shi, Z.; Pinney, K. G. Mechanistic considerations in the synthesis of 2-aryl-indole analogues under Bischler–Mohlau conditions. *Tetrahedron Letters*, **2015**, *56*, 3624-3629. Zhe Shi contributed to this manuscript through re-synthesis of the ¹³C isotope labelled indole

analogue and full characterization of this final compound including NMR, HPLC, HRMS and crystallization. In addition, Zhe Shi contributed a significant amount to the preparation of the supporting material and editing of the manuscript.. Dr. Matthew MacDonough originally synthesized the ^{13}C isotope labelled indole analogue and characterized it with NMR. He also contributed to the writing of the manuscript.

CHAPTER ONE

Introduction

Cancer

Cancer is a group of diseases characterized by uncontrolled growth of abnormal cells and potential spread to other organs of the body.¹ It continues to be a major public health problem worldwide and is the second leading cause of death in the United States after cardiovascular disease. In 2018, it is estimated that over 1.7 million new cancer cases will occur in the United States. Moreover, 600,000 cancer deaths are projected to happen.² The top three types of cancer that occur in men are prostate, lung and bronchus, and colon and rectum cancer. On the other side, the most common types of cancer among women are breast, lung and bronchus, and colon and rectum cancer (Figure 1.1).² Statistics have also shown that approximately 40 percent of men and 38 percent of women in the U.S. will get cancer at a certain stage during their lifetime.³

Surgery, radiation therapy, chemotherapy, targeted therapy and immunotherapy are the most common cancer therapy methods.⁴ The choice of therapy depends upon the location of the tumor and the stage of the disease, as well as the performance status of the patient. In most cases, patients receive a combination of treatments, such as surgery with chemotherapy and/or radiation therapy.⁵ Immunotherapy and targeted therapy have attracted growing interest from researchers, clinicians, and pharmaceutical companies, as these therapies are expected to be more effective and less harmful in comparison to radiotherapy and chemotherapy.⁶

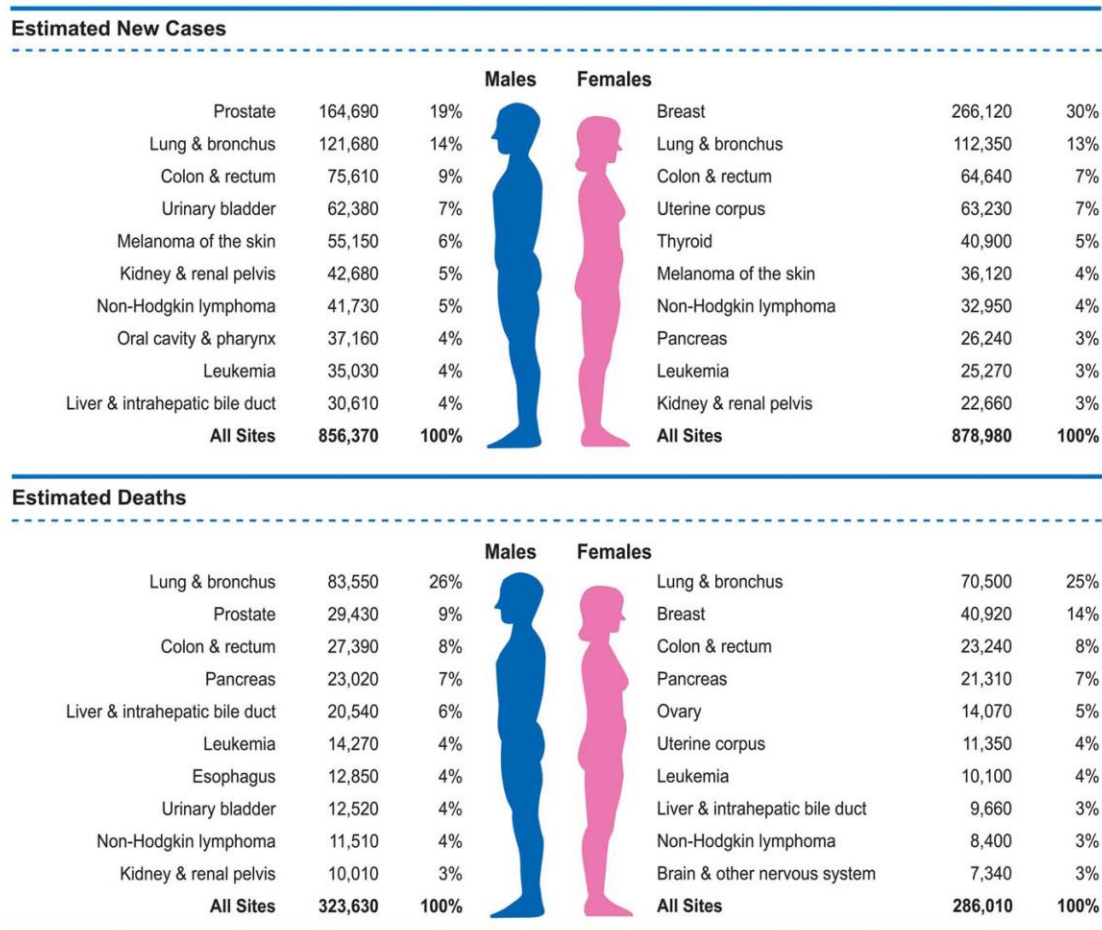


Figure 1.1. Top Ten Types of Cancer in Estimated New Cases and Death by Sex, United States, 2018²

Vascular Targeting Agents

The vascular network supporting normal tissue is hierarchically organized and evenly distributed to maintain the supply of oxygen and nutrients to all cells (Panel A in Figure 1.2).⁷ When a tumor reaches a few millimeters in size, it outgrows its blood supply,⁸ and in order to receive sufficient oxygen and nutrition, solid tumors become angiogenic and develop their own vasculature to meet the demand.^{9,10}

However, this newly-formed tumor vasculature (Panel B in Figure 1.2) is different from the vasculature in normal tissue, which might be its Achilles' heel. The

vascular network associated with tumors is typically not systemic and is unevenly distributed.¹¹ Tumor blood vessels are often immature, leaky and highly-permeable.^{12,13} This chaotic vascular network and primitive blood vessels serve as promising targets for cancer therapeutics.

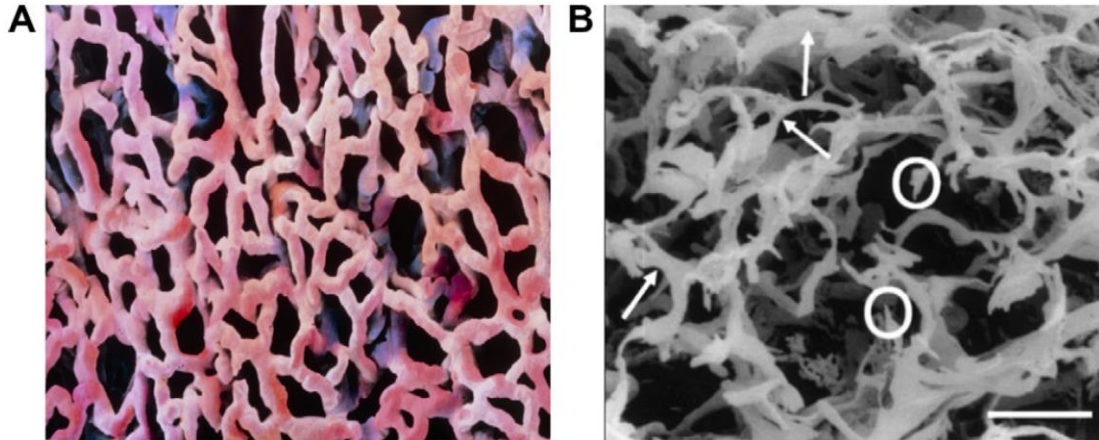


Figure 1.2. Scanning Electron Microscopy (SEM) Image of a Microvascular Cast from Normal Lung Tissue (A) and a Human Sigmoidal Adenocarcinoma (Colorectal Cancer) (B)⁷

In the early 1970s, Folkman and coworkers observed that tumors were limited in size to 1-2 mm³ if neovascularization of tumors was inhibited.^{14,15} From these observations, he proposed a well-known hypothesis that tumor growth depends on angiogenesis and suggested a potential therapeutic approach that would inhibit angiogenesis in solid tumors.⁹ He also brought up the idea of “anti-angiogenesis” and proposed that tumors would not grow beyond a few cubic millimeters in size without the development of new capillary blood vessels for the supply of oxygen and nutrients.⁹ Later in 1982, Dr. Denekamp observed that blockage of solid tumor blood vessels led to tumor necrosis.¹⁶ She then proposed that the fragile neovasculature in tumors could be a

target. This idea focused on damaging the existing new vessels, comparable to Folkman's suggestion to inhibit angiogenesis.

Vascular targeting agents generally consist of two distinct classes of compounds: angiogenesis-inhibiting agents (AIAs) and vascular disrupting agents (VDAs). AIAs are represented by a set of small-molecules that are inherently cytostatic and inhibit the development of new vasculature in the tumor region. On the other hand, VDAs cause irreversible damage to existing tumor vasculature and restrict the supply of oxygen and nutrients (Figure 1.3).

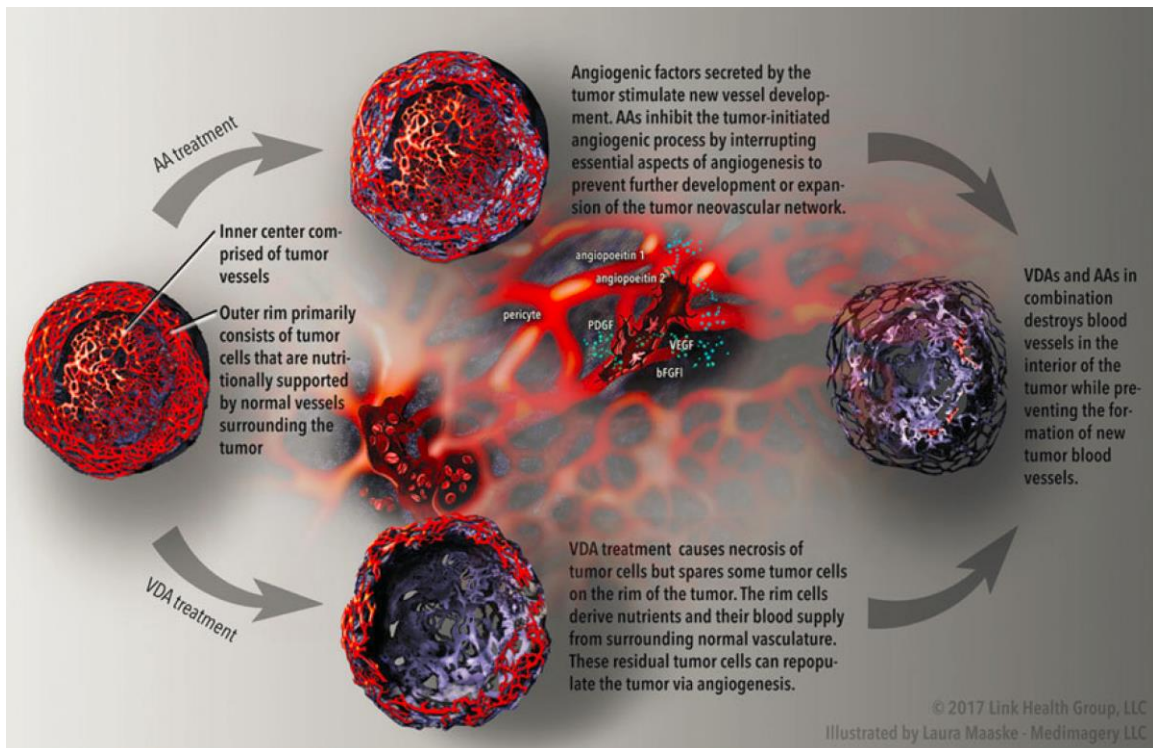


Figure 1.3. Angiogenesis-Inhibiting Agents (AIAs) and Vascular Disrupting Agents (VDAs)¹⁷

Angiogenesis is the physiological process of forming new blood vessels which involves migration, growth and differentiation of endothelial progenitor cells.¹⁸ This

process is normal and vital in growth and development, such as pregnancy, wound healing and the menstrual cycle.¹⁹ This process is regulated by several signal proteins, including vascular endothelial growth factor (VEGF) and fibroblast growth factor (FGF).^{20,21} When these endothelial growth factors bind to their receptors on the surface of endothelial cells, the development of new blood vessels are initiated.²⁰⁻²² As the tumor grows, certain growth factors are upregulated to provide sufficient tumor-associated blood supply. AIAs are unique anti-cancer agents.²² They inhibit the growth of blood vessels through interaction with these growth factors, thus restricting the supply of oxygen and nutrients, rather than blocking the growth of tumor cells.^{17,22} For example, some monoclonal antibodies specifically recognize and bind to VEGF. Once VEGF is attached to these drugs, it is unable to activate the receptor on the surface of endothelial cells.²²⁻²⁴

More than a dozen AIAs have been approved by the U.S. Food and Drug Administration (FDA) since the approval of bevacizumab (Avastin®) in 2004. Bevacizumab is a recombinant humanized monoclonal antibody that inhibits angiogenesis. It interacts with vascular endothelial growth factor A (VEGF-A), which is a growth factor overexpressed in tumors.^{23,24} It has been used as single agent or in combination therapy for the treatment colon cancer, lung cancer, glioblastoma, and renal-cell carcinoma.^{23,24}

Vascular Disrupting Agents

Distinct from AIAs, VDAs target endothelial cells and pericytes of established tumor-associated vasculature, and cause rapid occlusion of vessels, which leads to

secondary tumor-cell death.²⁵ There are two types of VDAs, small-molecule VDAs and ligand-directed VDAs.²⁶

A subset of the small-molecule VDAs are tubulin binding agents, which bind to the tubulin β -subunit at the colchicine binding site.²⁷ This binding causes depolymerization of microtubules, rearrangement of the cytoskeleton, and disorganization of actin and tubulin, which leads to rapid morphology changes of these endothelial cells in the tumor-associated blood vessels.⁷ The rounding up and blebbing of these endothelial cells increases the vascular resistance, which contributes to vascular shutdown (Figure 1.4). In addition, shape changes and apoptosis of these cells activate vasoconstriction, which also decreases the blood flow.²⁸ Moreover, the slow-down of blood flow results in promotion of red blood cell aggregation. This effect further increases viscous resistance to blood flow.²⁹ All these effects result in the occlusion of tumor-associated blood vessels.

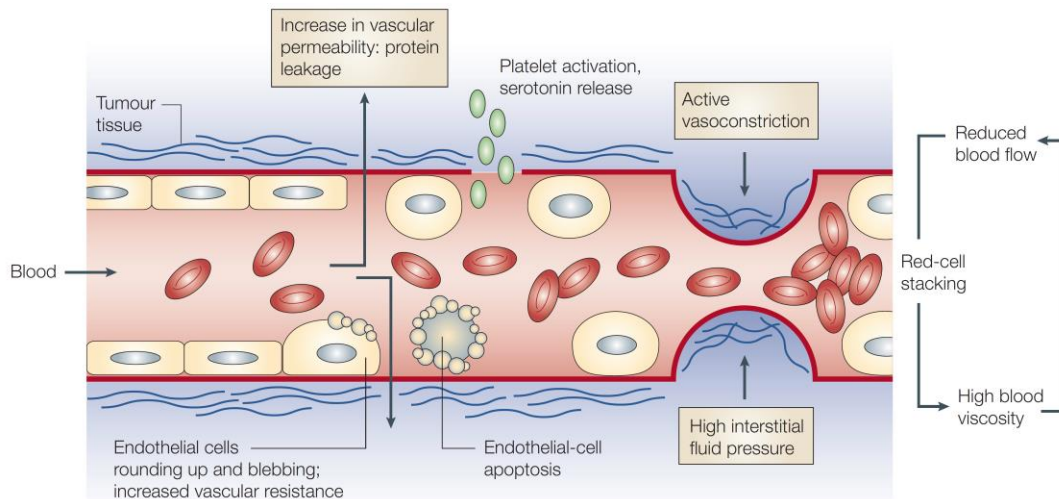


Figure 1.4. Mechanism of Tumor Vasculature Shutdown after Administration of a VDA³⁰

Colchicine, which was isolated from *Colchicum autumnale*, has been described for the treatment of gout since the first century AD (Figure 1.5).³¹ It belongs to this VDA family, which binds to the tubulin heterodimer, disrupts further polymerization to form microtubules, and inhibits mitosis.³¹⁻³⁴ It has been demonstrated to cause tumor regression and necrosis through vascular shutdown. However, due to high toxicity, its use as an anticancer agent is limited.³⁵ Combretastatins are a class of potent natural products which were first isolated by Dr. Pettit and co-workers from the South African *Combretum caffrum* tree.^{36,37} These compounds are phenolic stilbenes that bear structural similarity to colchicine. They are potent antimetabolic agents that bind to the colchicine binding site of tubulin and inhibit tubulin assembly. Combretastatin A-4 (CA4) along with Combretastatin A-1 (CA1) are the most potent members of this family.^{27,36,37} CA4, a *cis*-stilbene, is highly active against a wide-variety of human cancer cell lines and was found to exhibit an antivasular effect at one tenth of its maximum tolerated dose.³⁸ The poor solubility of CA4 led to the development of its water-soluble disodium phosphate prodrug, CA4P.³⁹

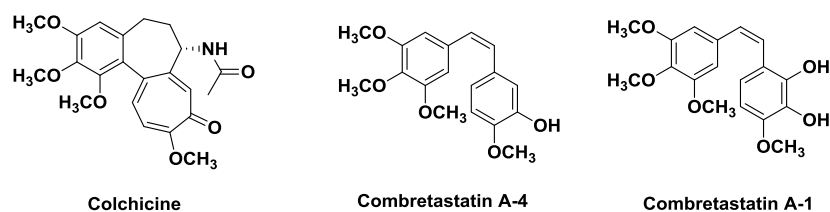


Figure 1.5. Selected Natural Products that Function as VDAs

VDAs are known to cause tumor necrosis, but tend to spare some tumor cells on the rim, which receive their blood supply from normal blood vessels (Figure 1.3).^{17,30,40} To overcome this problem, VDAs like CA4P are usually administered in combination

with other chemotherapy drugs in clinical trial.⁴¹ Four phase I clinical trials of combination therapy involving CA4P were reported.^{42–45} All these studies showed that the combination therapy was generally well tolerated and displayed promising tumor responses. However, several phase II studies involving CA4P for the treatment of anaplastic thyroid cancer (ATC) have been completed with no significant tumor response observed, including a single agent and a combination therapy with doxorubicin, cisplatin and radiotherapy.^{46,47} Combination therapy of pazopanib with CA4P for ovarian cancer and the combination of everolimus with CA4P for neuroendocrine tumors are currently undergoing clinical trials. Recently, a preclinical study has shown that the combination therapy of CA4P and an anti-CTLA-4 antibody nearly doubles the amount of tumor necrosis. This new finding showed the potential of CA4P in enhancing the efficacy of checkpoint inhibitors.⁴⁸

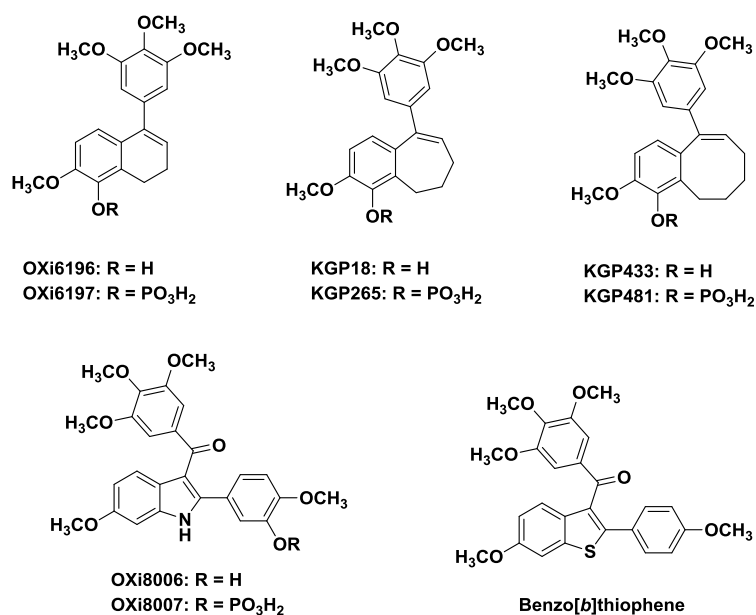


Figure 1.6. Leading Small-Molecule Inhibitors of Tubulin Polymerization Developed in Pinney Research Group: OXi6196,^{49,50} OXi6197,⁴⁹ KGP18,^{50–52} KGP265,⁵² KGP433,⁵³ KGP481,⁵³ OXi8006,^{54,55} OXi8007,⁵⁴ and Benzo[*b*]thiophene analogues.^{56,57}

Numerous structure-activity relationship (SAR) studies of CA4 have shown that the trimethoxyphenyl moiety, the *p*-methoxyphenyl moiety and a distance of 4-5 Å between the two aryl rings are essential to maintain tubulin binding activity.⁵⁸ With structural inspiration provided by colchicine, CA4 and CA1, a series of potent tubulin binding agents functioning as VDAs have been discovered by the Pinney Research Group (Baylor University), including dihydronaphthalene,⁵⁰ benzosuberene,⁵⁰⁻⁵² benzocyclooctene,⁵³ indole^{54,55}, and benzo[*b*]thiophene analogues⁵⁹ (Figure 1.6). A benzosuberene analogue KGP18 stands out among these VDAs since it combines potent inhibition of tubulin polymerization (IC₅₀= 1.1 μM) with enhanced cytotoxicity against human cancer cell lines (see Table 1.1).^{50,51} Its water-soluble phosphate prodrug KGP265 was also prepared by the Pinney Research Group.⁵²

Table 1.1 Inhibition of Tubulin Assembly and Cytotoxicity of Selected VDAs^{52-54,60,61}

Compounds	Inhibition of Tubulin Assembly IC ₅₀ (μM) ± SD	GI ₅₀ (μM) ± SD SRB assay		
		NCI-H460	DU-145	SK-OV-3
CA4	1.0 ^a	0.0022 ^a	0.00054 ^a	0.00042 ^a
CA1	1.9 ^b	0.046 ^b	0.013 ^b	n.d.
OXi6196	0.46 ± 0.01 ^c	0.0054 ^c	0.0034 ^c	0.0022 ^c
KGP18	1.4 ^d	0.000054 ^d	0.000042 ^d	0.000025 ^d
KGP433	1.2 ± 0.1 ^e	0.11 ^e	0.10 ^e	0.081 ^e
OXi8006	1.1 ± 0.04 ^f	0.038 ^f	0.036 ^f	0.0034 ^f

^a Data from ref 60.

^b Data from ref 61.

^c Unpublished data from Trawick Laboratory, Baylor University.

^d Data from ref 52.

^e Data from ref 53.

^f Data from ref 54.

n.d. = not available

OXi8006

OXi8006 (Figure 1.6) is an indole-based tubulin binding agent which was first reported by the Pinney Research Group.⁵⁴ Flynn and coworkers have subsequently obtained this compound through a separate synthetic route.⁶² OXi8006 is a potent inhibitor of tubulin assembly with an IC₅₀ value of 1.1 μM that demonstrates strong cytotoxicity against human cancer cell lines (Table 1.1). Its corresponding water-soluble disodium phosphate prodrug salt, OXi8007, demonstrated its ability to selectively decrease and shut down tumor-associated blood flow in a SCID mouse model bearing an orthotopic PC-3 (prostate) tumor.⁵⁴ A previous SAR study from the Pinney Group has identified two other indole analogues with inhibition of tubulin assembly comparable to OXi8006.⁵⁵

The mechanism of action has also been proposed (Figure 1.7).⁶³ OXi8006, generated from dephosphorylation of the corresponding phosphate prodrug salt OXi8007, enters tumor-associated endothelial cells via passive diffusion. This free phenol binds to tubulin resulting in microtubule disassembly and RhoA activation. RhoA kinase (ROCK) is activated by RhoA and phosphorylates myosin light chain (MLC) and suppresses MLC phosphatase (MP). This leads to increased levels of phosphorylated MLC and activation of non-muscle myosin II, which contributes to actin bundling and stress fiber formation. ROCK also leads to focal adhesion kinase (FAK) phosphorylation and activation contributing to increased focal adhesions.

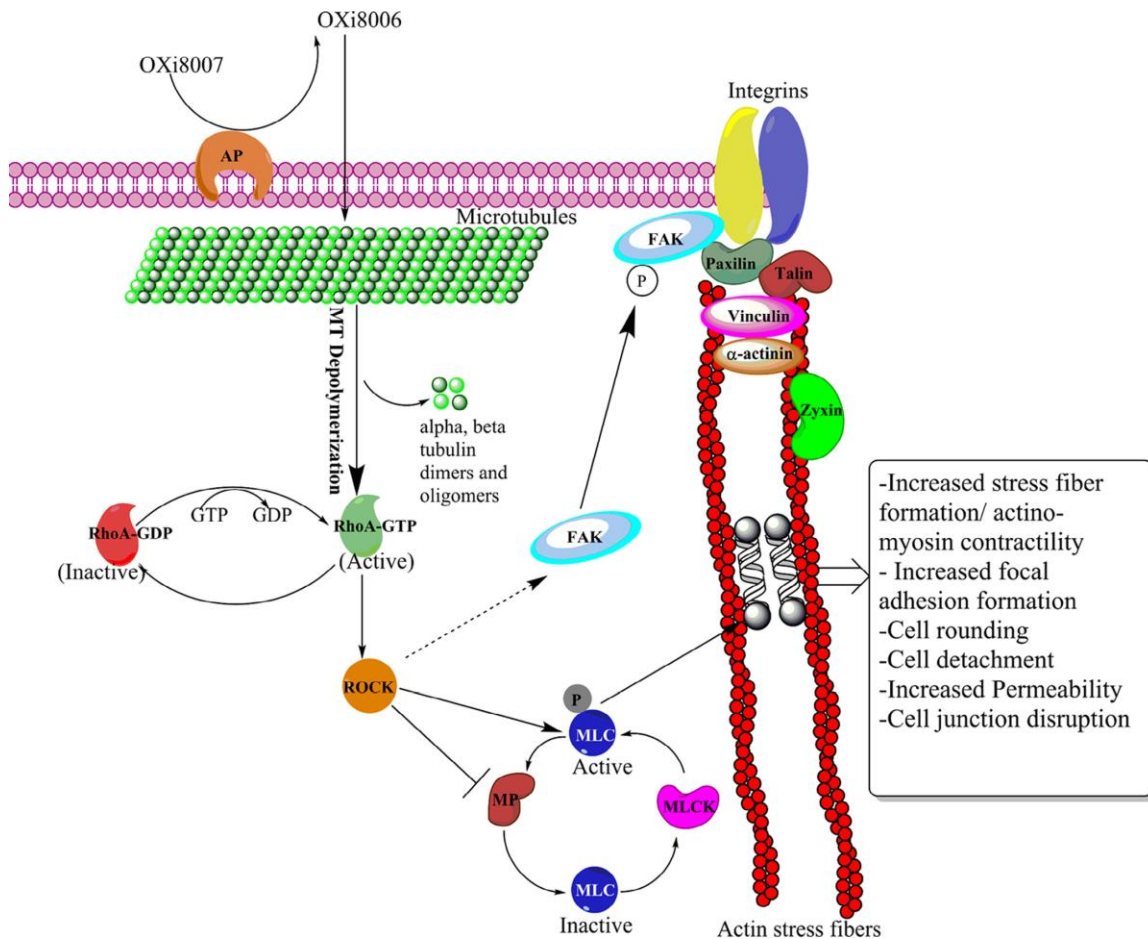


Figure 1.7. Proposed VDA Mechanism of Action of OXi8007 in Activated Endothelial Cells⁶³

Bioreductively Activatable Prodrug Conjugates

One salient feature in the solid tumor microenvironment is hypoxia.

Approximately 50–60% of solid tumors contain pronounced hypoxic regions, where the oxygen concentrations are below 1.5% - 2%.⁶⁴ Hypoxia can be divided into two major categories, perfusion-limited hypoxia and diffusion-limited hypoxia (Figure 1.8). Acute or perfusion-limited hypoxia occurs due to temporal blood vessel occlusion and unstable blood flow in tumor microvasculature.⁶⁵ The abnormal tumor vasculature structure and

enlarged distance between tumor blood microvessels may result in chronic or diffusion-limited hypoxia.⁶⁶

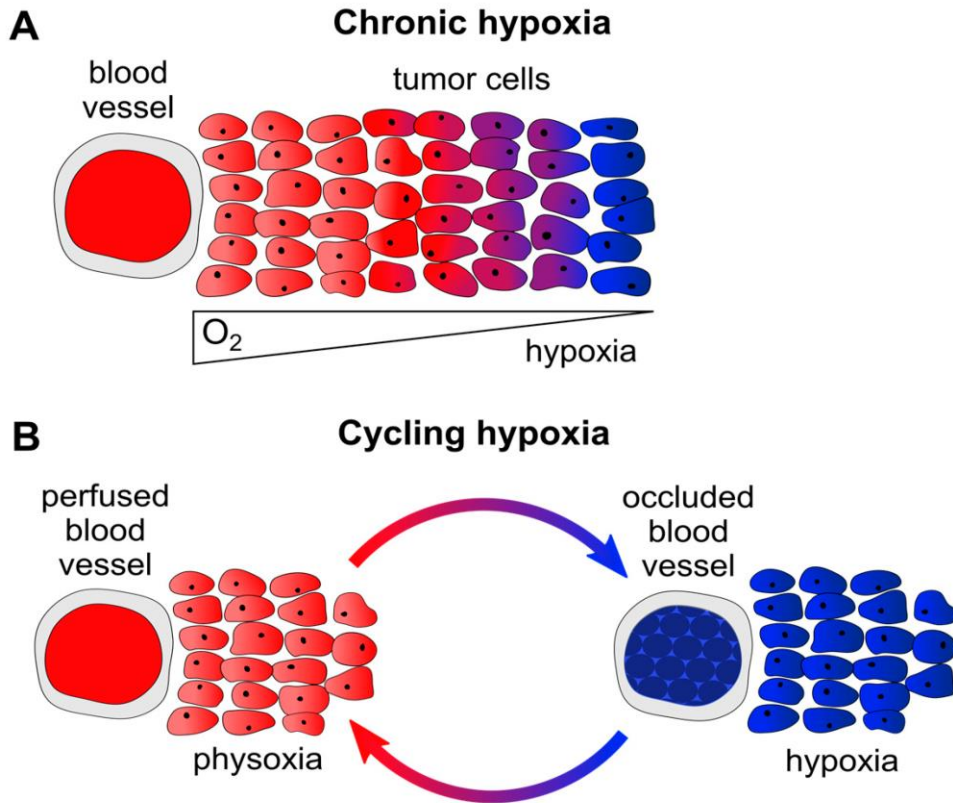


Figure 1.8. Chronic (Diffusion-Limited) and Cycling (Perfusion-Limited) Hypoxia⁶⁷

Hypoxia plays a key role in both tumor biology and prognosis. Tumor hypoxia can promote resistance to cell apoptosis,⁶⁸ downregulate DNA damage repair pathways and increase genomic instability⁶⁹, induce angiogenesis,⁷⁰ change cell metabolism to promote cell growth,⁷¹ increase invasion and metastasis,⁷² promote autophagy,⁷³ as well as suppress immunoreactivity.⁷⁴ This plethora of tumor biological effects is orchestrated largely by hypoxia-inducible factor-1 (HIF-1),⁷¹ which has been observed in most solid tumors.⁷⁵

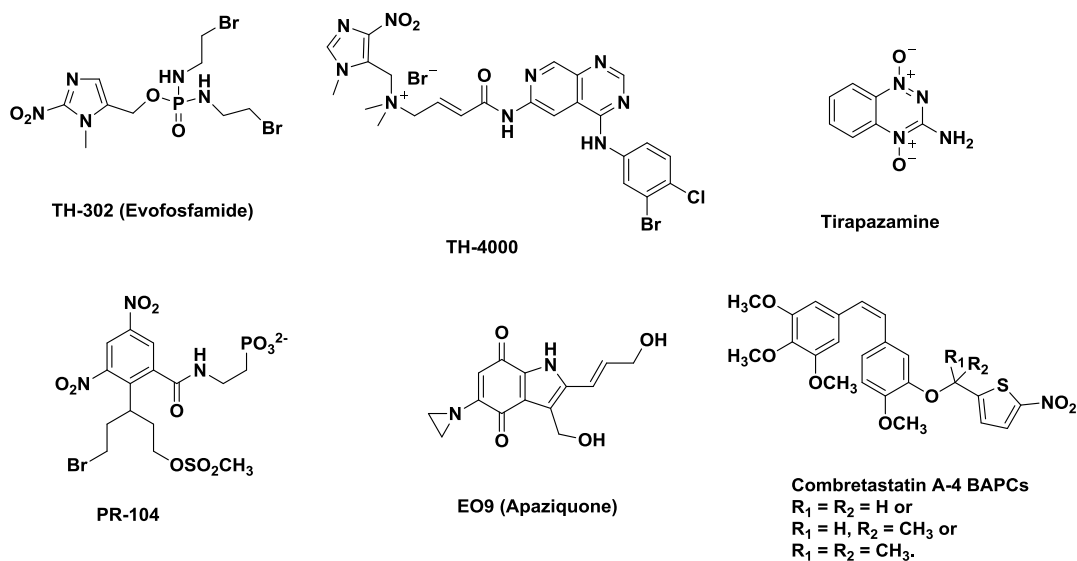
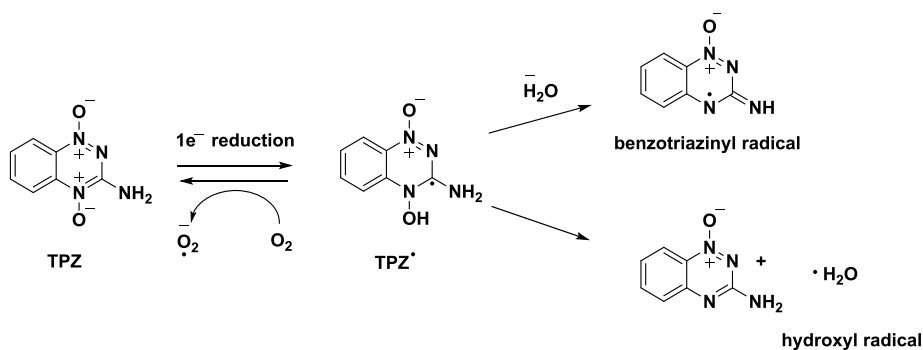


Figure 1.9. Structure of Selected Bioreductive Prodrugs: TH-302,⁷⁶ TH-4000,⁷⁷ Tirapazamine,⁷⁸ PR-104,⁷⁹ EO9,⁸⁰ and Combretastatin A-4 BAPCs.^{81,82}

Hypoxia promotes cellular resistance to many therapeutic methods including radiotherapy and chemotherapy.^{83–85} On the other hand, some cytotoxic drugs are found to be more effective in hypoxia.⁸³ Therefore, cancer hypoxia became an interesting target for new anticancer agents and treatments. Two main approaches are currently being applied: bioreductively activatable prodrug conjugates [BAPCs, also known as hypoxia-activated prodrugs (HAPs)] and small-molecule inhibitors that specifically target hypoxia, especially the HIF-pathway.⁸⁶ Herein, we are interested in developing BAPCs that incorporate small-molecule inhibitors of tubulin polymerization as the parent anti-cancer agents (effectors). These prodrugs undergo enzyme-mediated reduction in the hypoxic region through either a one- or two- electron reductase resulting in the selective release of cytotoxic agents.⁶⁶ Five different types of chemical entities have demonstrated the ability to selectively release the parent compound in hypoxia, including nitro(hetero)cyclic compounds, aromatic *N*-oxides, aliphatic *N*-oxides, quinones and

metal complexes⁸⁷ A selection of these prodrugs are shown in Figure 1.9, including tirapazamine, evofosfamide, PR-104 and TH-4000 .

Chemically, tirapazamine belongs to the aromatic *N*-oxide family. It was first prepared in a program screening for novel herbicides in 1972. Zemen and coworkers found it to be a leading compound in the development of bioreductive cytotoxic agents for cancer therapy in 1986.⁸⁸ Its triazine moiety reduces to a tirapazamine radical intermediate through a one-electron reduction. This unstable intermediate undergoes further reaction in hypoxia to produce either a benzotriazinyl radical or a hydroxyl radical, which leads to DNA damage and poisoning of topoisomerase II (Scheme 1.1).^{88–90} While tirapazamine was extensively investigated in clinic trials, and phase I and II studies showed positive results, the phase III studies utilizing a combination of tirapazamine with the conventional anticancer agent cisplatin generated limited effectiveness.^{91–93}



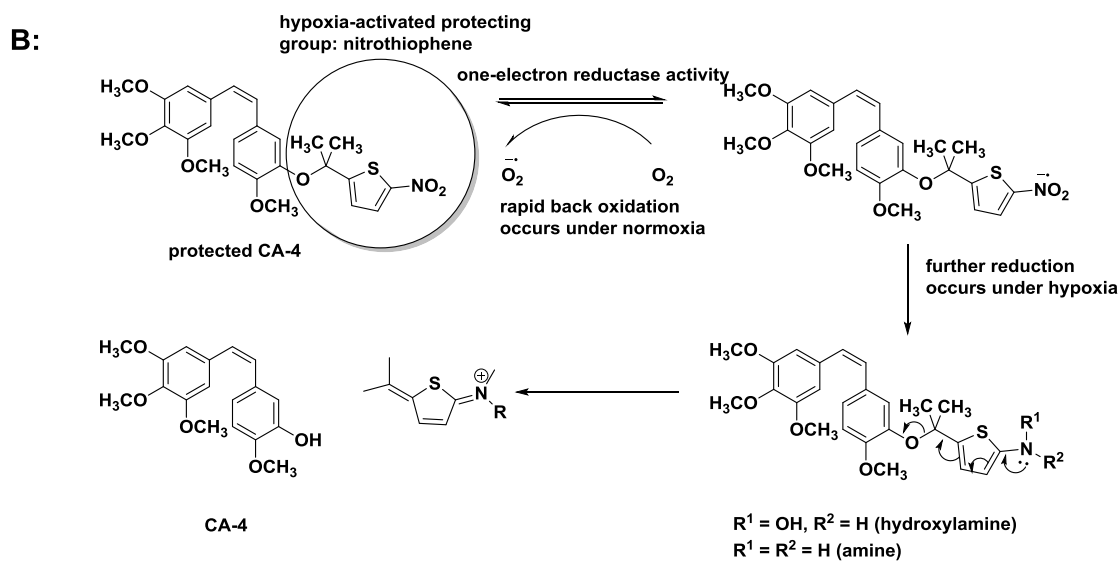
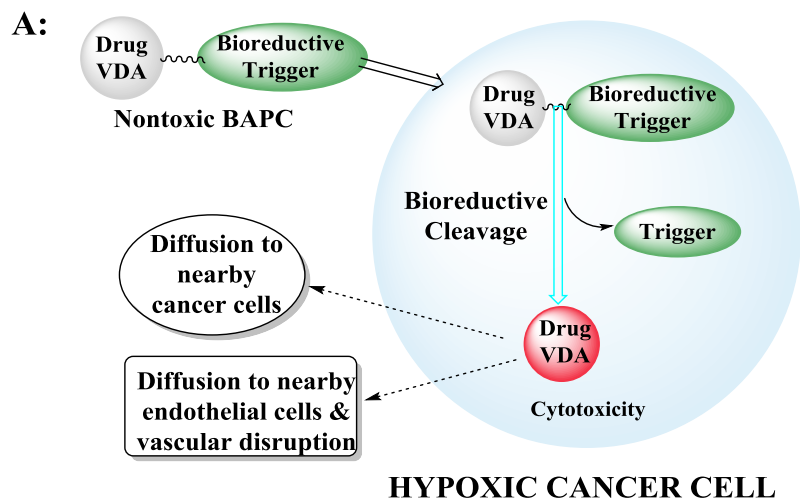
Scheme 1.1. Mechanism of Reductive Activation of Tirapazamine⁹⁰

TH-302, also known as evofosfamide, is a 2-nitroimidazole BAPC based on a bromoisophosphoramidate mustard (Figure 1.9), which releases its parent drug under hypoxic conditions.⁹⁴ This prodrug is reduced by one-electron oxidoreductases to

fragment and release the alkylating agent (bromoisophosphoramidate mustard). It also presents a high hypoxic cytotoxicity ratio (HCR: GI₅₀ ratio normoxia/hypoxia), and good pharmacokinetics and safety profiles in model animals.⁷⁶ However, Phase III clinical trials against pancreatic adenocarcinoma and soft tissue sarcoma showed no statistical significance for TH-302.^{95,96} Recently, TH-302 in clinical trials has been shown to act as a sensitizer in combination therapy with certain immune checkpoint inhibitors for the treatment of patients with advanced prostate cancer, metastatic pancreatic cancer, melanoma and glioblastoma.^{97,98}

The potent VDA CA4 was used by Davis and co-workers to prepare a series of BAPCs (Figure 1.9).^{81,82} 5-Nitrothiophene triggers were utilized as bioreductive trigger moieties and were covalently attached to CA4 through an ether linkage. These compounds were designed to release CA4 selectively in the hypoxic tumor microenvironment upon enzymatic reduction.

The BAPCs developed within the Pinney Research Group (Baylor University) followed the same strategy as TH-302 and the CA4 BAPCs shown in Scheme 1.2A.⁹⁹ Aromatic *N*-oxide moieties, including nitrothiophene, nitrofurans, nitroimidazole and nitrobenzene,^{82,100–102} were covalently linked to the small-molecule tubulin binding agents developed in the Pinney Group to target human hypoxia. These conjugates undergo bioreductive cleavage to release the cytotoxic agents. The detailed mechanism of reduction and fragmentation is shown in Scheme 1.2B.



Scheme 1.2. A: Proposed Strategy for Selective Release of Cytotoxic Agents from Prodrugs under Hypoxic Associated with Cancer Cells; B: Biological Reduction and Cleavage of BAPCs (CA4-*gem*-dimethyl Nitrothiophene as an Example)¹⁰³

Antibody-Drug Conjugates

In 1900, a German immunologist Paul Ehrlich proposed that if a compound can selectively target a disease-causing organism, then a toxin for that organism could be delivered without harming the body itself.^{104,105} This so-called “magic bullet” theory has to some extent been realized by the development of antibody-drug conjugates (ADCs). ADCs are composed of antibodies that are covalently bonded via either cleavable or non-

cleavable linkers to anticancer agents (known as payloads).^{106,107} The antibodies bind to specific antigens on the surface of tumor cells and thus deliver their payload selectively to the tumor. These ADCs are designed as targeted therapy for cancer treatment, thus killing specific tumor cells and sparing normal tissue from chemotherapeutic damage.

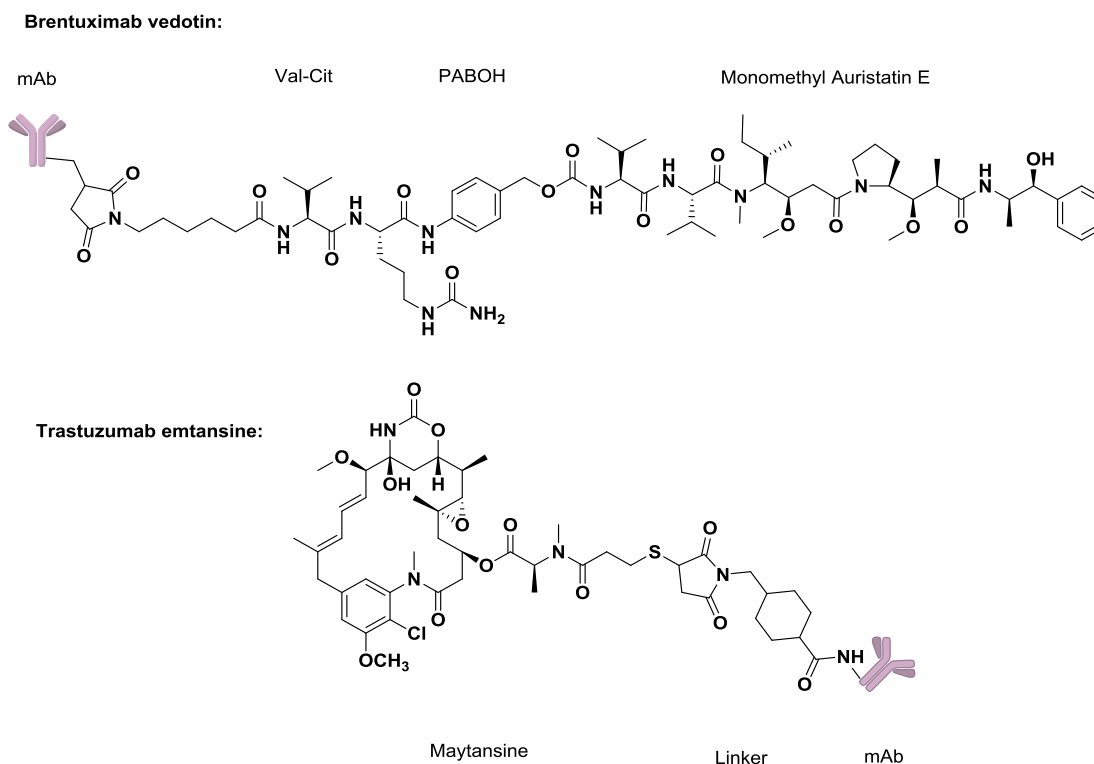


Figure 1.10. Structure of Brentuximab Vedotin¹⁰⁶ and Trastuzumab Emtansine^{108,109}

Since the discovery of monoclonal antibody (mAb) technology by Kohler and Milstein,¹¹⁰ this antibody is widely used in ADC development. The first FDA approved ADC in the oncology space was Gemtuzumab ozogamicin for the treatment of acute myeloid leukemia in 2001. After being withdrawn from the US market in 2010 due to its high fatal toxicity rate, Gemtuzumab ozogamicin was re-entered last year.¹¹¹ At the beginning of this decade, Brentuximab vedotin (Figure 1.10) for the treatment of Hodgkin Lymphoma (HL) and systemic anaplastic large cell lymphoma (ALCL),^{106,112,113}

and Trastuzumab emtansine for the treatment of HER2-positive metastatic breast cancer^{108,109} gained FDA approval. This field has generated extensive pre-clinical experimentation, and more than 60 ADCs are currently in clinical trials.¹⁰⁷

Brentuximab vedotin incorporates a cathepsin B cleavable linker containing valine-citrulline (Val-Cit).¹⁰⁶ This dipeptide is stable in the plasma, but is quickly cleaved by lysosomal enzymes such as cathepsin B.¹¹⁴ A *para*-amino benzyl alcohol (PABOH) was also used as spacer in this ADC. Inspired by this study, a series of VDAs attached to this cathepsin B cleavable linker were prepared by the Pinney Research Group.¹¹⁵ Another spacer *N,N'*-dimethylethylenediamine was installed between PABOH and the payload to generate carbamate groups instead of a carbonate moiety, since it is reported that several carbonate conjugates are less stable when compared with their carbamate derivatives.¹¹⁶

Mechanism of Indole Ring Formation

Indole is an aromatic heterocyclic compound with a benzene ring fused to a five-membered pyrrole ring. It widely exists in the natural environment. The amino acid tryptophan, neurotransmitter serotonin, and tryptamine all contain an indole core ring. Indoles are also important scaffolds in medicinal chemistry.¹¹⁷ The anticancer agents vinblastine, vincristine, and mitomycin C are well-known examples of biologically active natural products that contain an indole ring.

The preparation of indole rings has been studied for over 150 years.^{118–121} The synthetic routes available toward the indole ring are well established.^{118,120,121} Among these methods, the most versatile and well-studied approach is the Fischer indole synthesis, which involves a [3,3]-sigmatropic rearrangement followed by closure to the

fused five-membered ring.¹²² Other methods include the Leimgruber–Batcho indole synthesis, the Bischler–Mohlau indole synthesis, and the Fukuyama indole synthesis.^{120,121}

OXi8006 and its phosphate prodrug salt OXi8007 (Figure 1.6) bear an indole structure.^{54,55} OXi8006 was synthesized following the Bischler-Molhau indole methodology.^{123,124} This synthesis involved a reaction between aniline and α -halogenated acetophenone. Two recognized mechanism pathways were postulated for the formation of the 2-aryl indole product.¹²⁵ In this work, a ¹³C isotope labeling experiment was carried out to find which pathway is favored.¹²⁶

Small-molecule Inhibitors of Cathepsin L

Metastasis occurs when cancer cells invade normal tissue by spreading from a primary site to a secondary site within the host body.^{14,127–129} It is the primary reason for approximately 90% of cancer deaths.¹²⁹

Cathepsins are a group of endopeptidases which are predominately found in the lysosome.^{130,131} Some cysteine cathepsins have extracellular functions. Many mechanisms have been found to upregulate cathepsin expression in various tumor cell lines, including amplification,¹³² transcript variants^{133,134} and transcriptional regulation.¹³⁵ After being secreted from tumor cells as the proenzyme form, these proteases increase degradation of the extracellular matrix and promote metastasis.^{136–138} Cathepsin L, a member of the cathepsin family, is a ubiquitous endopeptidase which is overexpressed in cancer cells and accumulates at elevated levels in tumors and the tumor microenvironment.¹³⁹ Cathepsin L inhibitors, such as E-64 and KGP94, have shown biological activity *in vivo* and are promising for therapeutic application.^{7,140–143}

The thiosemicarbazone moiety has also been shown to exhibit anti-parasitic activity through inhibition of the cysteine proteases cruzain and falcipain.^{144–146} These discoveries inspired further investigation of the thiosemicarbazone moiety as the warhead incorporated within small-molecule inhibitors designed to target other cysteine proteases, such as cathepsin L.^{147,148}

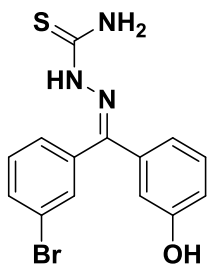


Figure 1.11. Structure of Cathepsin L inhibitor KGP94^{149–151}

KGP94 is a functionalized benzophenone thiosemicarbazone derivative developed in the Pinney Research Group, which functions as a potent inhibitor of cathepsin L.^{149–151} It significantly limits the activity of cathepsin L toward human type I collagen. It also inhibits the invasion of breast cancer cells (MDA-MB-231) through MatrigelTM by 70% at 10 μ M.¹⁴⁹ A water-soluble phosphate prodrug of KGP94 was also prepared to overcome its limited aqueous solubility.¹⁵¹ Preliminary biological evaluation has shown that this phosphate prodrug is readily hydrolyzed to KGP94 by alkaline phosphatase.

CHAPTER TWO

Indole-based Vascular Disrupting Agents and Antibody-Drug Conjugates

Introduction

Our previous work lead to the potent compound 2-(3'-hydroxy-4'-methoxyphenyl)-3-(3'', 4'', 5''-trimethoxybenzoyl)-6-methoxyindole (OXi8006)¹⁵² and its corresponding water-soluble disodium phosphate prodrug salt, OXi8007.⁵⁴ A previous structure activity relationship (SAR) study of OXi8006 from the Pinney Group identified indole analogues **3** and **4** (Figure 2.1) that demonstrate inhibition of tubulin assembly comparable to OXi8006 with IC₅₀ value of 1.1 μM and 1.0 μM.⁵⁵ Herein the synthesis and preliminary biological evaluation of the corresponding water-soluble disodium phosphate salts of indole analogues **3** and **4**, along with several other indole-based analogues is described. Synthesis of a bridge-modified combretastatin analogue is also included. In addition, a drug-linker construct of OXi8006 covalently bonded to a cathepsin L cleavable linker was synthesized. This drug-linker construct is suitable for attachment to a monoclonal antibody in future studies.

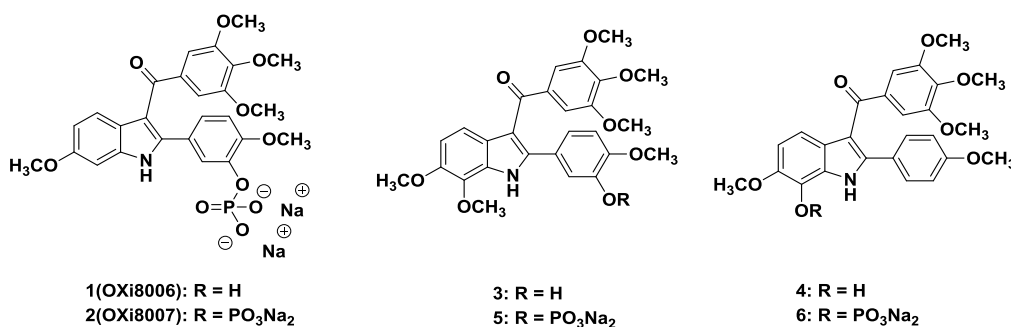
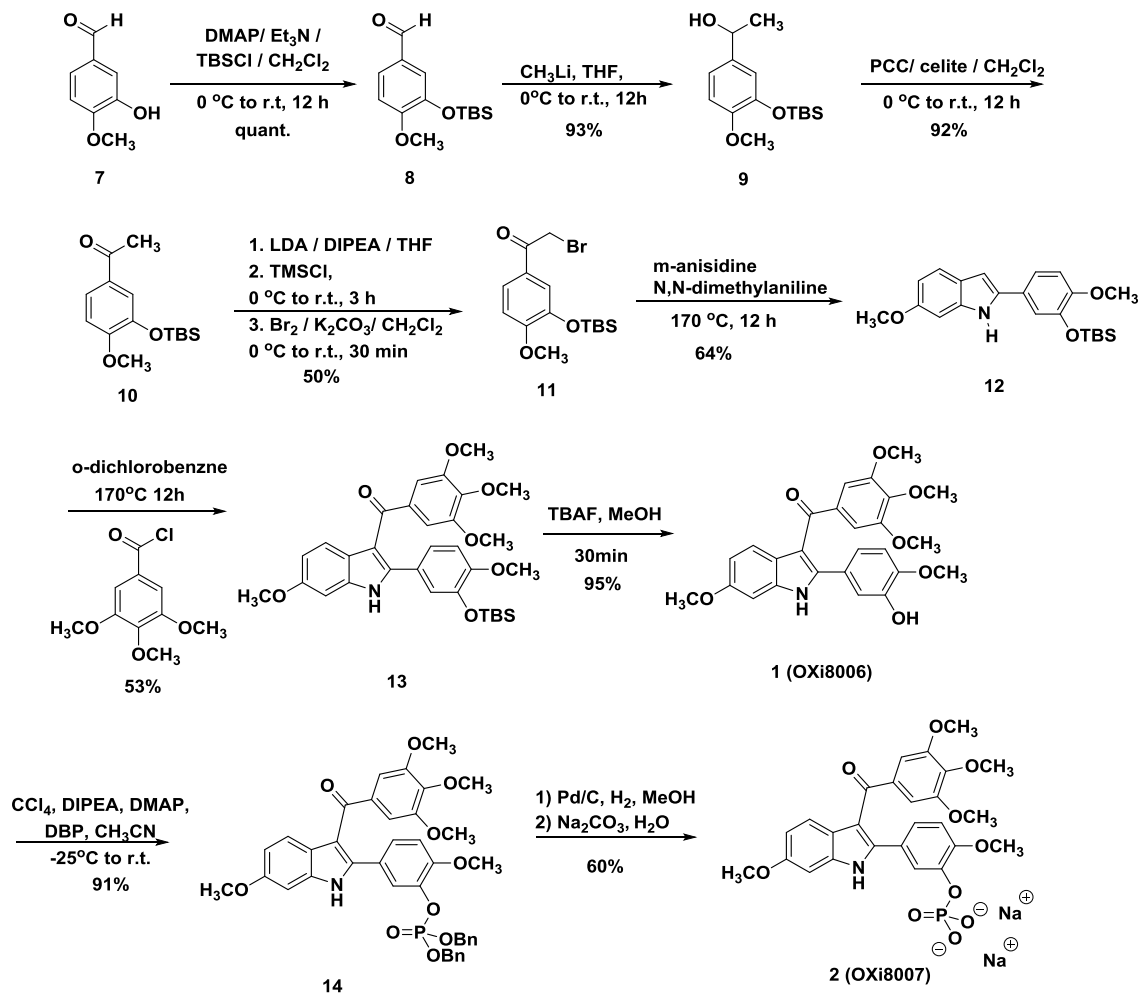


Figure 2.1 Selected Indole-based VDAs and Their Prodrugs^{153,154}

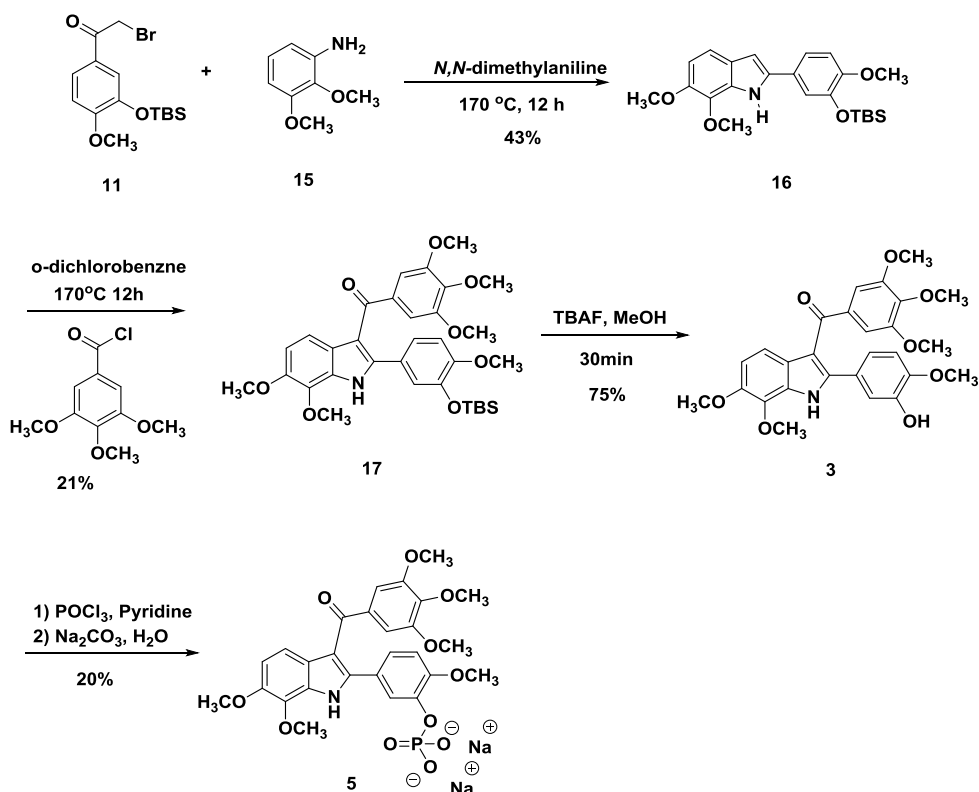
Synthesis of Indole Analogues



Scheme 2.1. Synthetic Route to OXi8006⁵⁴

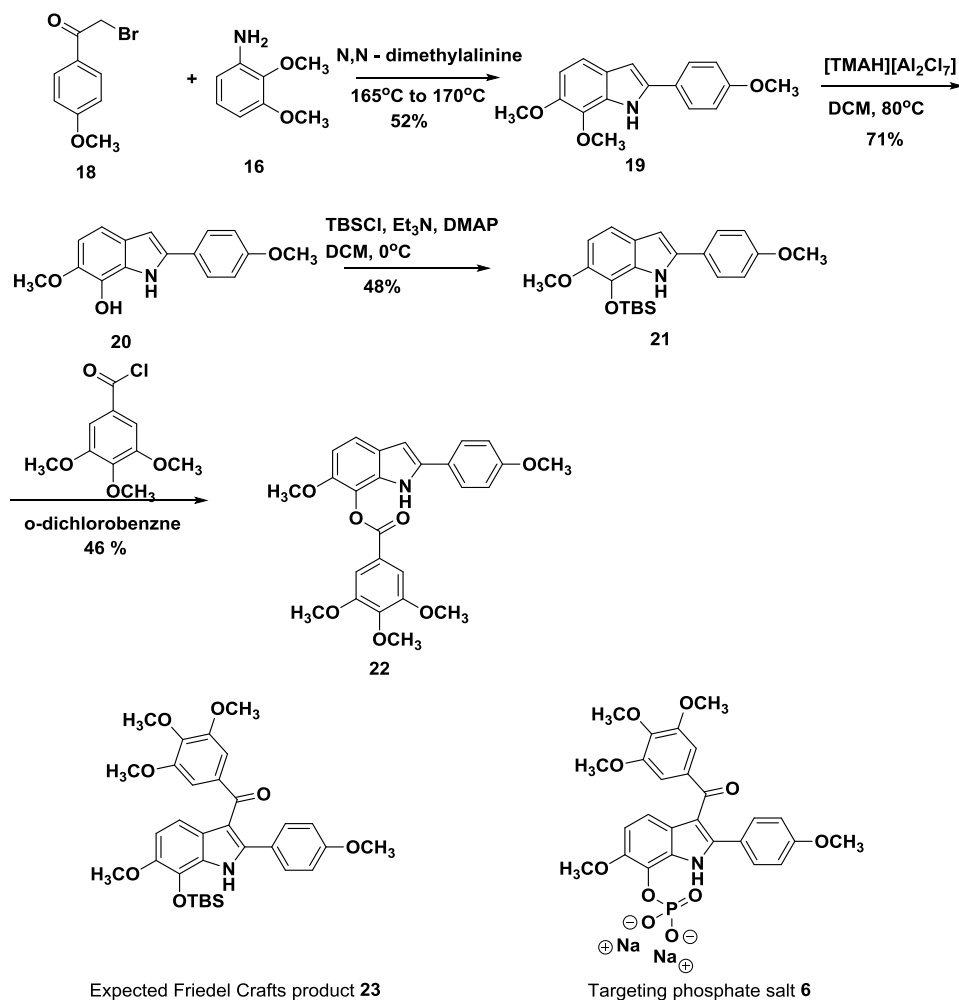
The synthetic route towards OXi8006 (**1**) and OXi8007 (**2**) are shown in Scheme 2.1, which utilizes 2-arylidole **12** as a key intermediate. The synthesis started from the commercially available isovanillin **7**. After protection of the phenol as its corresponding silyl ether **8**, addition of methyl lithium formed the secondary alcohol **9**, which was subsequently oxidized by pyridinium chlorochromate to afford the expected acetophenone **10**. The α -brominated acetophenone **11** was prepared by treatment of

compound **10** with LDA to form the corresponding silyl enol ether followed by bromination with bromine. The key step relied on a Bischler-Mohlau indole synthesis to obtain indole **12** followed by the reaction with 3, 4, 5-trimethoxybenzoyl chloride. The resulting TBS-protected indole derivative **13** was desilylated by tetrabutylammonium fluoride to afford indole-based phenol **1** (OXi8006). Reaction of free phenol **1** (OXi8006) with in situ-generated dibenzyl chlorophosphite resulted in the indole-based dibenzyl phosphate ester **14**. Deprotection by hydrogen gas and palladium on activated carbon (10%), followed by an acid–base reaction between the resulting phosphoric acid and sodium carbonate, resulted in the desired disodium phosphate indole prodrug **2** (OXi8007).



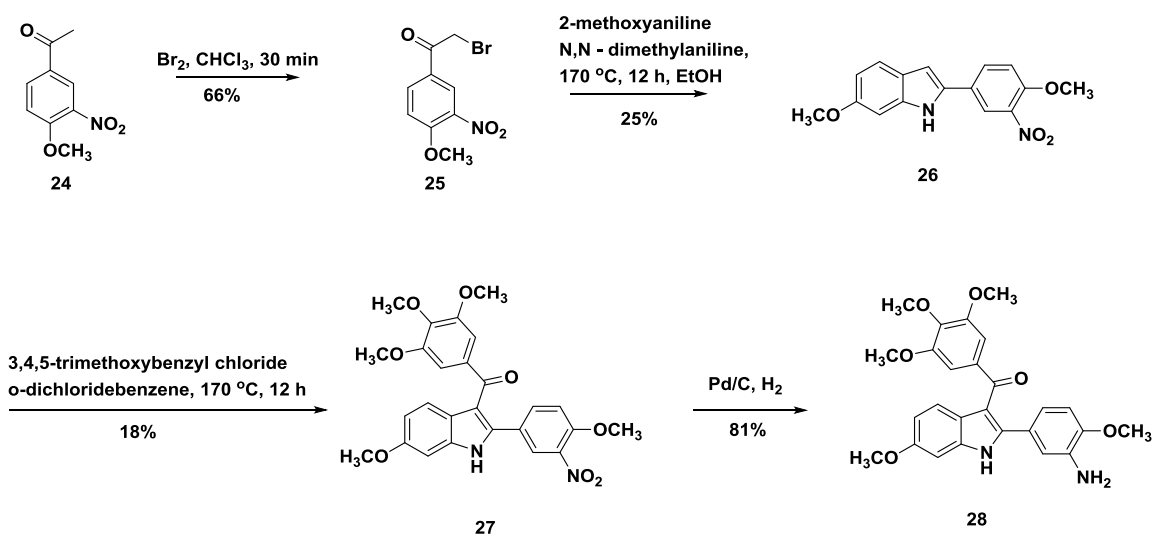
Scheme 2.2. Synthetic Route towards Water-Soluble Disodium Phosphate Salt **5**

The synthetic route towards indole-based disodium phosphate prodrug salt **5** (Scheme 2.2) started from the previously described bromoacetophenone **11**. Similar to the synthesis of **OXi8006**, 2-arylidole **16** was obtained through the Bischler-Mohlau indole synthesis and a subsequent acylation reaction with 3, 4, 5-trimethoxybenzoyl chloride resulted in the TBS-protected indole analogue **17**. After deprotection of the TBS protecting group, free phenol **3** was reacted with phosphoryl chloride to form the indole-based phosphoric acid. The corresponding phosphate salt **5** was afforded through neutralization by sodium carbonate.



Scheme 2.3. Synthetic Route towards Indole Analogue **22**

The synthesis of phosphate prodrug salt **6** was attempted through a similar route as that described for phosphate prodrug salt OXi8007 (Scheme 2.3). After the Bischler-Mohlau indole synthesis, 2-arylidole **19** was selectively demethylated in the presence of the ionic liquid [TMAH] [Al₂Cl₇] under microwave irradiation to generate the phenolic 2-arylidole **20**, which was subsequently protected as its corresponding TBS derivative **21**. In the Friedel Crafts acylation of TBS protect **21**, ester **22** was obtained instead of the expected product **23**. It is possible that due to the acidity of the reaction mixture, the TBS protecting group was cleaved and the free phenol **20** was formed, which subsequently reacted with 3,4,5-trimethoxybenzoyl chloride to afford ester **22**. Interestingly, biological evaluation of compound **20** indicated that this compound has moderate cytotoxicity against selected human cancer cell lines (GI₅₀ = 0.248 μM against DU-145 cells, for example).



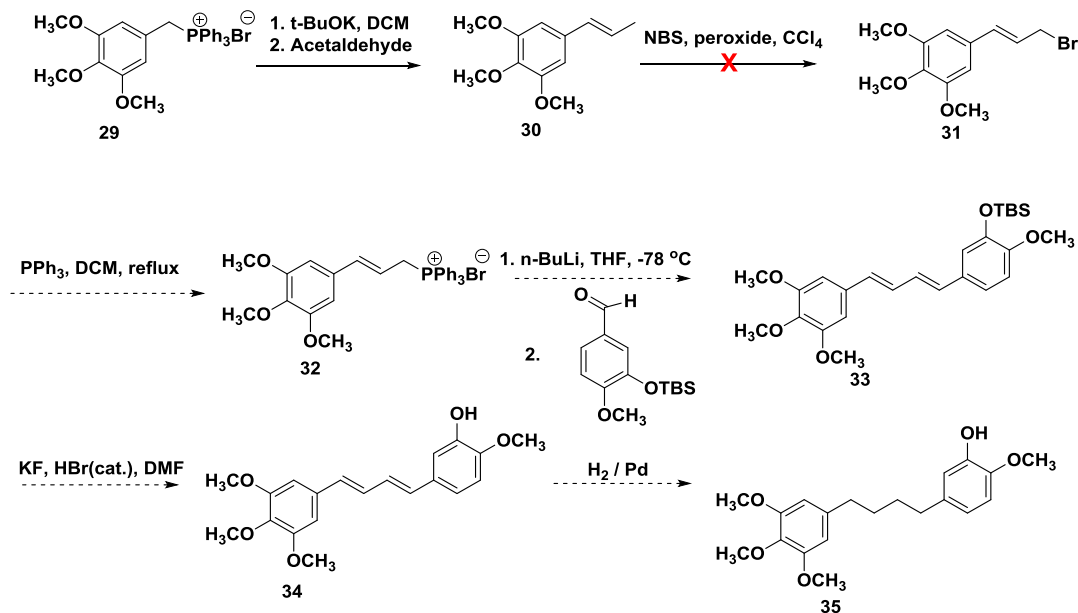
Scheme 2.4. Synthetic Route towards Amino Indole Analogue **28**

Another indole-based VDA target is the amino compound **28**. (Scheme 2.4) Bromoacetophenone **25** was obtained from the bromination of commercially available

acetophenone **24**. 2-Arylindole **26** was synthesized utilizing a similar Bischler-Mohrlau indole protocol, which was followed by acylation to afford nitro compound **27**. Reduction with hydrogen and palladium on carbon provided the final target amino compound **28**.

Synthesis of Bridge-Modified Combretastatin Analogue

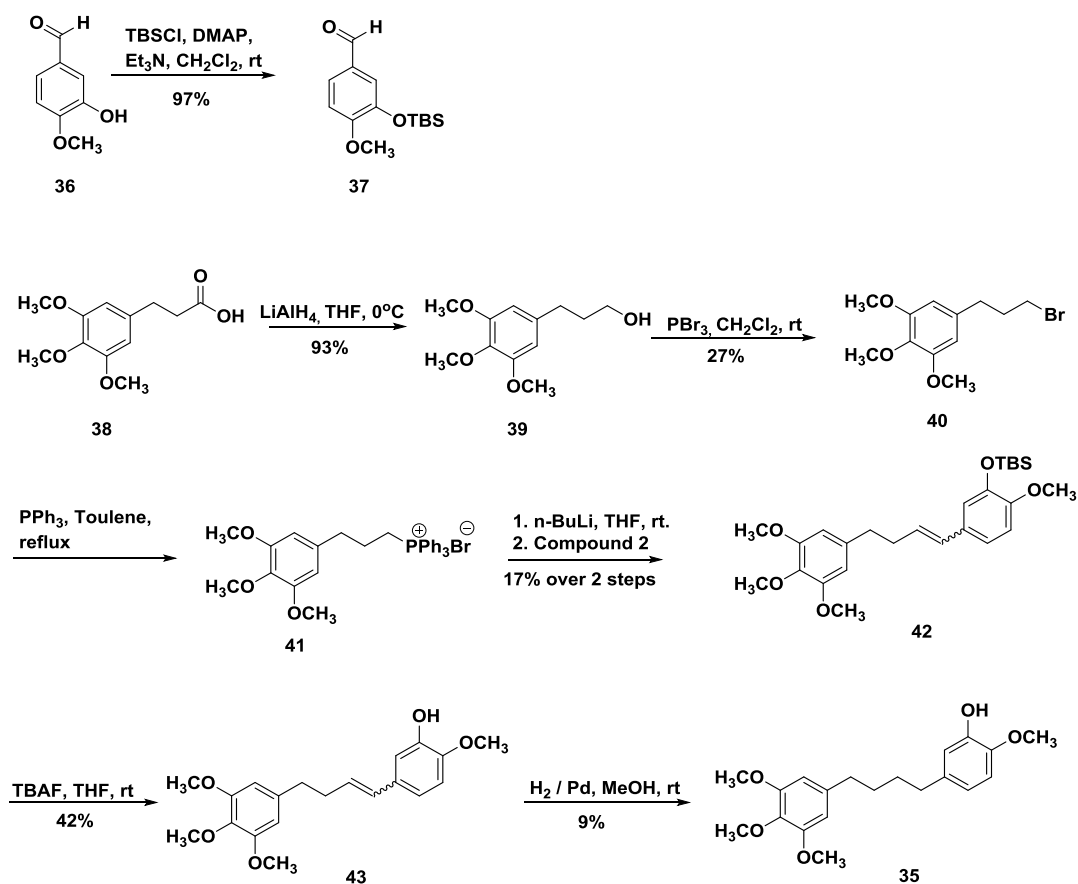
The objective for this project was to synthesize bridge-extended combretastatin analogues, in which the bridge consisted of methylene groups. As the initiation of this project, the previously reported four-carbon bridge molecule¹⁵⁵ was synthesized to lay a foundation upon which further extensions of the bridge may be fabricated in the Pinney Group Laboratory.



Scheme 2.5. Synthetic Route Towards the Methylene Bridge-Modified CA4 Analogue **35** from Literature¹⁵⁵

The synthetic pathway delineated in Scheme 2.5 represents the reported route for the synthesis of the four-carbon bridge analogue **35**.¹⁵⁵ Phosphonium bromide salt **29** was treated with potassium *tert*-butoxide to generate the corresponding ylide, which was

subsequently reacted with acetaldehyde through a Wittig reaction to yield propylene analogue **30**. Without ready access to a 500-watt lamp utilized in the literature¹⁵⁵ for radical bromination, a modification which used *N*-bromosuccinimide (NBS) as the brominating agent was pursued. Propylene analogue **30** was heated at reflux in CCl₄ with NBS and benzoyl peroxide. Unfortunately, the desired allylic bromide **31** was not obtained under these reaction conditions, and instead primarily starting material remained.



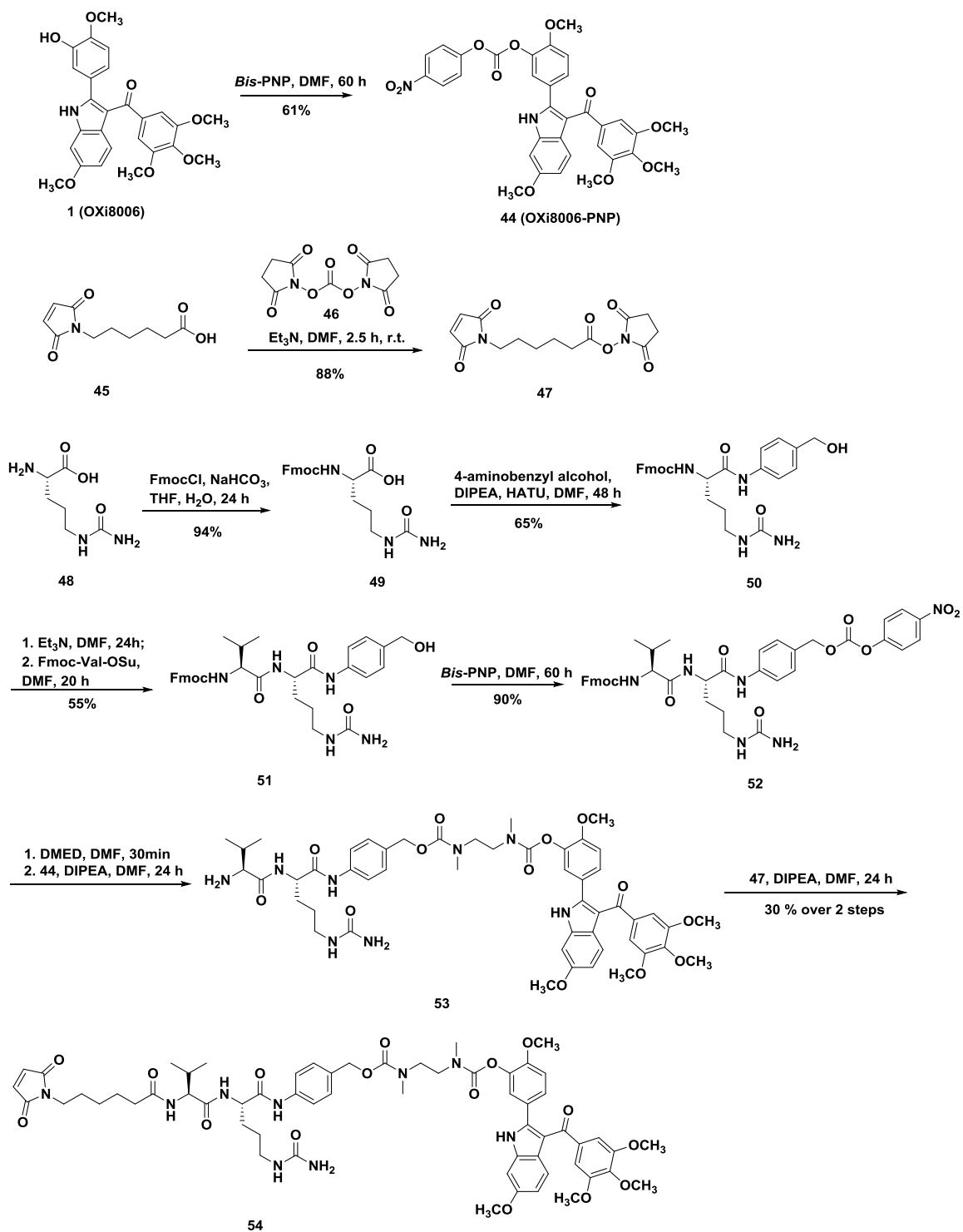
Scheme 2.6. Synthetic Route Towards the Methylene Bridge-Modified CA4 Analogue **35** Used in This Study

A new synthetic pathway, outlined in Scheme 2.6, was devised in order to avoid the fastidious radical bromination reaction. Propanoic acid derivative **38** was treated with lithium aluminum hydride to form propanol analogue **39**, which was reacted with PBr₃ to yield the propyl bromide derivative **40**. Bromide **40** was then heated at reflux in toluene with triphenylphosphine to generate phosphonium bromide salt **41**. This salt was reacted with *n*-butyllithium and successively combined with benzaldehyde **37** through a Wittig reaction, which was synthesized prior to this step though protection of isovanillin **36** by *tert*-butyldimethylsilyl chloride (TBSCl). Silyl ether **42** that resulted from the Wittig reaction was treated with tetrabutylammonium fluoride (TBAF) to yield compound **43**. Alkene **43** was then subjected to hydrogenation with palladium on carbon as the catalyst. This reaction pathway resulted in the successful synthesis of combretastatin analogue **35**.

Synthesis of OXi8006-based Antibody-Drug Conjugate

ADCs are an important class of biopharmaceutical drugs designed to selectively target identified tumor specific markers and thus function as targeted therapy. An improved methodology to synthesize a cathepsin B cleavable linker was developed in Pinney Research Group by Dr. Deboprosad Mondal and Jacob Ford (unpublished results). Following the same methodology, the leading indole-based VDA OXi8006 was covalently attached to the Val-Cit linker (Scheme 2.7).

The *para*-nitrophenyl carbonate activating group was installed onto indole-based VDA OXi8006 (**1**) through the reaction with *bis*-(4-nitrophenyl) carbonate (*bis*-PNP). The activated succinimide ester **47** was also synthesized by reacting 6-maleimidocaproic acid **45** with disuccinimide carbonate **46**.¹⁵⁶



Scheme 2.7. Preparation of OXi8006-based ADC **54**

Citrulline **48** was protected by fluorenylmethoxycarbonyl chloride (FmocCl) and then linked with 4-aminobenzyl alcohol through hexafluorophosphate azabenzotriazole tetramethyl uranium (HATU) coupling to form compound **50**. Fmoc-protected compound **50** was deprotected and coupled with Fmoc-Val-OSu to form the dipeptide **51**, which was then activated by *bis*-PNP. The carbonate **52** was treated with *N,N'*-dimethylethylenediamine (DMED) and coupled with the PNP-activated OXi8006 **44**. Finally, succinimide ester **47** was attached to the free amine **53** to provide the target conjugate **54**.

Biological Evaluation

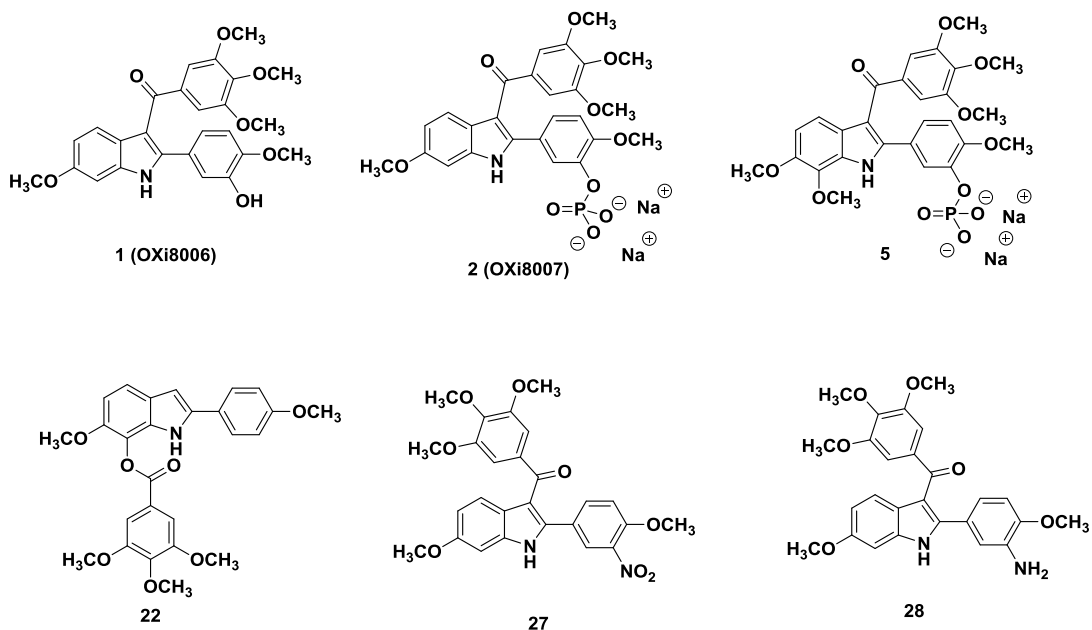


Figure 2.2. Synthesized Indole-Based VDAs and Prodrugs

All of the synthesized indole analogues were evaluated for their ability to inhibit tubulin assembly (in a cell-free, pure protein assay). The nitro indole **27** ($IC_{50} = 0.97 \mu M$) and amino indole **28** ($IC_{50} = 0.83 \mu M$) demonstrated impressive inhibition of tubulin

assembly, which is comparable to that of CA4 and OXi8006 (Table 2.1). Unlike CA4P ($IC_{50} > 40 \mu M$),¹⁵⁷ indole-based phosphate salts **2** (OXi8007) and **5** were also found to be strongly inhibitory. The inhibition of tubulin assembly assays were carried out by Dr. Hamel at National Cancer Institute.

These analogues were also tested for their cytotoxicity against selected cancer cell lines (Table 2). Amino analogue **28** demonstrated strong cytotoxicity (GI_{50} values ranging from 28 to 62 nM) against the NCI-H460 (lung), DU-145 (prostate), and SK-OV-3 (ovarian) human cancer cell lines. Comparing with compound **28**, nitro analogue **27** was somewhat less cytotoxic with GI_{50} values ranging from 99 nM to 219 nM. The ester analogue **22** demonstrated moderate cytotoxicity against these three cancer cell lines. The Sulforhodamine B (SRB) assays were carried out in Dr. Trawick's laboratory (Dr. Tracy Strecker) at Baylor University.

Table 2.1 Inhibition of Tubulin Assembly and Cytotoxicity of Target Indole Analogs^{54,60}

Compounds	Inhibition of Tubulin Assembly IC_{50} (μM) \pm SD	GI_{50} (μM) \pm SD SRB assay		
		NCI-H460	DU-145	SK-OV-3
CA4	1.0 ^b	0.00223 ^b	0.00054 ^b	0.00042 ^b
1 (OXi8006)	1.1 \pm 0.04 ^c	0.0379 ^c	0.0356 ^c	0.00345 ^c
2 (OXi8007)	4.2 \pm 0.1 ^c	0.0311 ^c	0.0297 ^c	0.0223 ^c
5	8.1 \pm 1	n. d.	n. d.	n. d.
22	n. d.	0.248 \pm 0.0853	1.00 \pm 0.158	0.429 \pm 0.0276
27	0.97 \pm 0.07	0.219 \pm 0.0419	0.151 \pm 0.00506	0.0991 \pm 0.0139
28	0.83 \pm 0.05	0.0435 \pm 0.0011	0.0622 \pm 0.0042	0.0282 \pm 0.0015

^a Average of $n \geq 3$ independent determinations

^b Data from ref. 136

^c Data from ref. 53

n.d. = not determined

Materials and Methods

General Experimental Methods

Dichloromethane, acetonitrile, dimethylformamide (DMF), methanol, ethanol, and tetrahydrofuran (THF) were used in their anhydrous forms, as obtained from the chemical suppliers. Reactions were performed under an inert atmosphere using nitrogen gas, unless specified. Thin-layer chromatography (TLC) plates (precoated glass plates with silica gel 60 F254, 0.25 mm thickness) were used to monitor reactions. Purification of intermediates and products was carried out with a Biotage isolera flash purification system using silica gel (200-400 mesh, 60 Å) or RP-18 prepacked columns or manually in glass columns. Intermediates and products synthesized were characterized on the basis of their ¹H NMR (500 or 300 MHz), ¹³C NMR (125 or 75 MHz), and ³¹P NMR (200 or 120 MHz) spectroscopic data using a Varian VNMRs 500 MHz or Bruker DPX 300 MHz instrument. Spectra were recorded in CDCl₃, D₂O, or CD₃OD. All chemical shifts are expressed in ppm (δ), coupling constants (J) are presented in Hz, and peak patterns are reported as broad (br), singlet (s), doublet (d), triplet (t), quartet (q), septet (sept), double doublet, (dd), and multiplet (m).

Purity of the final compounds was further analyzed at 25 °C using an Agilent 1200 HPLC system with a diode-array detector ($\lambda = 190\text{-}400$ nm), a Zorbax XDB-C18 HPLC column (4.6 mm - 150 mm, 5 μm), and a Zorbax reliance cartridge guard-column; method A: solvent A, acetonitrile, solvent B, 0.1% TFA in H₂O, gradient, 10% A / 90% B to 90% A / 10% B over 0 to 30 min; or method B: solvent A, acetonitrile, solvent B, H₂O, gradient, 30% A / 70% B to 90% A / 10% B over 0 to 30 min; or method C: solvent A, acetonitrile, solvent B, H₂O, gradient, 50% A / 50% B to 90% A / 10% B over 0 to 30 min;

post-time 10 min; flow rate 1.0 mL/min; injection volume 20 μ L; monitored at wavelengths of 210, 254, 230, 280, and 360 nm. Mass spectrometry was carried out under positive ESI (electrospray ionization) using a Thermo scientific LTQ Orbitrap Discovery instrument.

3-(tert-Butyldimethylsilyloxy)-4-methoxybenzaldehyde **8** ¹⁵⁸

To a solution of 3-hydroxy-4-methoxybenzaldehyde **7** (10.0 g, 65.8 mmol) dissolved in dichloromethane (150 mL) at 0 °C was added triethylamine (Et₃N) (10.1 mL, 72.3 mmol) followed by *N,N*-dimethylaminopyridine(DMAP) (0.804 g, 6.58 mmol). The reaction mixture was stirred for 10 min, and *tert*-butyldimethylsilyl chloride (TBSCl) (10.9 g, 72.3 mmol) was then added gradually. The solution was allowed to warm to room temperature over 12 h. Upon completion of the reaction, the reaction mixture was quenched with water (100 mL) and extracted with dichloromethane (3 X 50 mL). The extracted layers were combined, dried over Na₂SO₄, and concentrated under reduced pressure. The TBS benzaldehyde product **8** [17.3 g, 64.9 mmol, 99%, R_f = 0.50 (70:30 hexanes: EtOAc)] was isolated as a yellow oil and was taken to the next step without further purification.

¹H NMR (CDCl₃, 500 MHz): δ 9.80 (s, 1H, CHO), 7.45 (dd, *J* = 8.5, 2.0 Hz, 1H, ArH), 7.35 (d, *J* = 2.0 Hz, 1H, ArH), 6.93 (d, *J* = 8.5 Hz, 1H, ArH), 3.87 (s, 3H, OCH₃), 0.99 (s, 9H, C(CH₃)₃), 0.16 (s, 6H, Si(CH₃)₂).

¹³C NMR (CDCl₃, 125 MHz): δ 190.2, 156.2, 145.2, 130.0, 126.0, 119.4, 110.9, 55.1, 25.3, 18.0, -5.0.

3-tert-Butyldimethylsilyloxy-1-(1'-hydroxyethyl)-4-methoxybenzene **9** ¹⁵⁸

Crude TBS benzaldehyde **8** (4.00 g, 15.0 mmol) dissolved in tetrahydrofuran (THF, 40 mL) at 0 °C was treated with CH₃Li (12.2 mL, 1.6 M, 20 mmol) dropwise. The solution was then stirred at room temperature. After 12 h, the reaction mixture was slowly quenched with water (40 mL) and extracted with EtOAc (4 X 20 mL). The organic extract was dried over Na₂SO₄ and concentrated under reduced pressure, resulting in secondary alcohol **9** [3.84 g, 13.6 mmol, 90%, R_f = 0.40 (70:30 hexanes: EtOAc)] as a yellow oil, which was taken to the next step without further purification.

¹H NMR (CDCl₃, 500 MHz): δ 6.88 (m, 2H, ArH), 6.83 (d, *J* = 8.1 Hz, 1H, ArH), 4.81 (q, *J* = 6.3 Hz, 1H, CH), 3.79 (s, 3H, OCH₃), 1.82 (s, 1H, OH), 1.45 (d, *J* = 6.3 Hz, 3H, CH₃), 0.99 (s, 9H, (CH₃)₃), 0.15 (s, 6H, Si(CH₃)₂).

¹³C NMR (CDCl₃, 125 MHz): δ 149.7, 144.5, 138.9, 118.4, 118.0, 111.7, 69.1, 55.1, 25.5, 24.9, 18.2, -4.8.

3-tert-Butyldimethylsilylox)-4-methoxyacetophenone **10** ^{54,158}

To a solution of crude alcohol **9** (3.48 g, 12.3 mmol) and Celite® (3 g) in dichloromethane (40 mL) at 0 °C was added pyridinium chlorochromate (PCC, 2.92 g, 13.6 mmol) in small increments, allowing 10 min of stirring between each addition. The solution was then stirred at room temperature. After 12 h, the reaction mixture was filtered through a 50/50 plug of silica gel/Celite®, and the plug was rinsed well with dichloromethane. The filtrate was concentrated under reduced pressure providing the desired acetophenone derivative **10** [2.58 g, 9.20 mmol, 75%, R_f = 0.50 (70:30 hexanes: EtOAc)] as a pale yellow solid.

¹H NMR (CDCl₃, 500 MHz): δ 7.57 (dd, *J* = 8.5 Hz, 2.0 Hz, 1H, ArH), 7.46 (d, *J* = 2.0 Hz, 1H, ArH), 6.86 (d, *J* = 8.5 Hz, 1H, ArH), 3.86 (s, 3H, OCH₃), 2.52 (s, 3H, CH₃), 1.00 (s, 9H, C(CH₃)₃), 0.16 (s, 6H, Si(CH₃)₂).

¹³C NMR (CDCl₃, 125 MHz): δ 196.7, 155.3, 144.8, 130.5, 123.5, 120.4, 110.7, 55.4, 26.2, 25.6, 18.4, -4.7.

*1-(3-tert-Butyldimethylsilyloxy-4-methoxyphenyl)-1-trimethylsilylethene*⁵⁴

To a solution of diisopropylamine (7.9 mL, 56 mmol) in THF (150 mL) at 0 °C was added *n*-butyllithium (22.4 mL, 2.5 M, 56 mmol) dropwise. The LDA solution was allowed to stir for 15 min, and then a solution of TBS-acetophenone **10** (10.5 g, 37.1 mmol) in THF (50 mL) was added dropwise. The solution was stirred for 10 min, and trimethylsilyl chloride (TMSCl) (7.2 mL, 56 mmol) was added dropwise. The reaction mixture was allowed to reach room temperature overnight. After 12 h, the solution was diluted with NaHCO₃ (10%, 100 mL). The reaction mixture was extracted with Hexane (4 X 30 mL). Next the extract was dried over Na₂SO₄, and the organic phase was concentrated under reduced pressure to provide crude TMS-enol ether (14.5 g, 41.1mmol) as a dark yellow oil, which was taken to the next step without purification.

¹H NMR (CDCl₃, 500 MHz): δ 7.18 (dd, *J* = 8.5 Hz, 2.5 Hz, 1H ArH), 7.12 (d, *J* = 2.5 Hz, 1H, ArH), 6.80 (d, *J* = 8.5 Hz, 1H, ArH), 4.78 (d, *J* = 1.5 Hz, 1H, CH₂), 4.34 (d, *J* = 1.5 Hz, 1H, CH₂), 3.81 (s, 3H, OCH₃), 1.03 (s, 9H, C(CH₃)₃), 0.27 (s, 9H, Si(CH₃)₃), 0.18 (s, 6H, Si(CH₃)₂).

¹³C NMR (CDCl₃, 125 MHz): δ 155.3, 151.1, 144.4, 130.6, 118.8, 118.1, 111.2, 89.5, 55.4, 25.7, 18.4, 0.03, -4.7.

*3'-(tert-Butyldimethylsilyloxy)-4'-methoxy-2-bromoacetophenone 11*⁵⁴

To a solution of crude TMS-enol ether (14.3 g, 40.6 mmol) and anhydrous K₂CO₃ (0.240 g, 1.74 mmol) in dichloromethane (120 mL) at 0 °C was added bromine (1.24 mL, 24 mmol) dropwise. The solution was allowed to stir for 30 min, diluted with sodium thiosulfate (10%) and extracted with dichloromethane (3 X 50 mL). The extract was dried over Na₂SO₄ and concentrated under reduced pressure. Purification by flash chromatography using a prepacked 100 g silica column [solvent A: EtOAc; solvent B: hexanes; gradient: 2%A / 98%B (4 CV), 2%A / 98%B → 20%A / 80%B (10 CV), 20%A / 80%B (1.2 CV); flow rate: 25 mL/min; monitored at 254 and 280 nm] afforded bromoacetophenone analogue **11** [7.28 g, 20.2 mmol, 50%, R_f = 0.37 (90:10 hexanes: EtOAc)] as a tan red solid.

¹H NMR (CDCl₃, 500 MHz): δ 7.61 (dd, *J* = 8.5 Hz, 2.5 Hz, 1H, ArH), 7.48 (d, *J* = 2.5 Hz, 1H, ArH), 6.88 (d, *J* = 8.5 Hz, 1H, ArH), 4.37 (s, 2H, CH₂), 3.88 (s, 3H, OCH₃), 1.00 (s, 9H, C(CH₃)₃), 0.17 (s, 6H, Si(CH₃)₂).

¹³C NMR (CDCl₃, 125 MHz): δ 189.8, 156.1, 145.1, 127.1, 124.2, 121.0, 111.0, 55.5, 30.7, 25.6, 18.4, -4.6.

*2-(3'-tert-Butyldimethylsilyloxy-4'-methoxyphenyl)-6-methoxyindole 12*¹⁵⁹

To a solution of *m*-anisidine (5.16 mL, 46.2 mmol) dissolved in *N,N*-dimethylaniline (50 mL) at 170 °C was added dropwise bromoacetophenone **11** (5.03 g, 14.0 mmol) in EtOAc (10 mL). The reaction mixture was stirred at 170 °C for 12 h. Upon completion of the reaction, the reaction mixture was cooled to room temperature and extracted with EtOAc (3 x 30 mL). The combined organic extract was dried over Na₂SO₄ and concentrated under reduced pressure. Purification by flash chromatography using a

prepacked 100 g silica column [solvent A: EtOAc; solvent B: hexanes; gradient: 12%A / 88%B (4 CV), 12%A / 88%B → 100%A / 0%B (10 CV), 100%A / 0%B (2.6 CV); flow rate: 25 mL/min; monitored at 254 and 280 nm] resulted in the desired 2-phenylindole derivative **12** [3.44 g, 8.97 mmol, 64%, R_f = 0.48 (50:50 hexanes: EtOAc)] as light tan crystals.

¹H NMR (CDCl₃, 500 MHz): δ 8.11 (br s, 1H, NH), 7.47 (d, *J* = 8.5 Hz, 1H, ArH), 7.16 (dd, *J* = 8.5 Hz, 2.0 Hz 1H, ArH), 7.13 (d, *J* = 2.5 Hz, 1H, ArH), 6.90 (d, *J* = 8.5 Hz, 1H, ArH), 6.89 (d, *J* = 2.5 Hz, 1H, ArH), 6.79 (dd, *J* = 8.5, 2.5 Hz, 1H, ArH), 6.64 (dd, *J* = 2.0, 1.0 Hz 1H, ArH), 3.86 (s, 3H, OCH₃), 3.84 (s, 3H, OCH₃), 1.04 (s, 9H, C(CH₃)₃), 0.21 (s, 6H, Si(CH₃)₂).

¹³C NMR (CDCl₃, 125 MHz): δ 156.3, 150.5, 145.4, 137.4, 136.9, 125.8, 123.7, 120.9, 118.2, 117.8, 112.4, 109.9, 98.6, 94.5, 55.6, 55.4, 25.7, 18.5, -4.6.

*2-(3'-tert-Butyldimethylsiloxy-4'-methoxyphenyl)-3-(3'',4'',5''-trimethoxybenzoyl)-6-methoxyindole 13*¹⁵²

To a solution of compound **12** (3.12 g, 8.14 mmol) in *o*-dichlorobenzene (30 mL) was added 3,4,5-trimethoxybenzoylchloride (2.82 g, 12.2 mmol). The reaction mixture was heated to reflux at 170 °C for 12 h. The *o*-dichlorobenzene was removed by simple distillation, and the resulting dark colored crude oil was subjected to flash chromatography using a prepacked 100 g silica column [solvent A: EtOAc; solvent B: hexanes; gradient: 10%A / 90%B (4 CV), 10%A / 90%B → 80%A / 20%B (10 CV), 80%A / 20%B (2.8 CV); flow rate: 40 mL/min; monitored at 254 and 280 nm] resulting in TBS-indole analogue **13** [1.60 g, 2.77 mmol, 34%, R_f = 0.38 (60:40 hexanes:EtOAc)] as a yellow powder.

¹H NMR (CDCl₃, 500 MHz): δ 8.42 (br s, 1H, NH), 7.93 (d, *J* = 9.5 Hz, 1H, ArH), 6.99 (s, 2H, ArH) 6.94 (dd, *J* = 8.0, 2.0 Hz 1H, ArH), 6.91 (dd, *J* = 9.0, 2.0 Hz, 1H, ArH), 6.91 (d, *J* = 2.0 Hz, 1H, ArH), 6.77 (d, *J* = 2.0 Hz, 1H, ArH), 6.70 (d, *J* = 8.5 Hz, 1H, ArH), 3.87 (s, 3H, OCH₃), 3.79 (s, 3H, OCH₃), 3.74 (s, 3H, OCH₃), 3.69 (s, 6H, OCH₃), 0.94 (s, 9H, C(CH₃)₃), 0.04 (s, 6H, Si(CH₃)₂).

¹³C NMR (CDCl₃, 125 MHz): δ 191.9, 157.4, 152.6, 151.6, 145.2, 142.1, 141.3, 136.5, 134.6, 125.2, 123.4, 122.6, 122.3, 121.9, 112.9, 111.8, 111.7, 107.4, 94.6, 60.9, 56.1, 55.9, 55.5, 25.8, 18.5, -4.7.

2-(3'-Hydroxy-4'-methoxyphenyl)-3-(3'',4'',5''-trimethoxybenzoyl)-6-methoxyindole 1 (OXi8006)^{152,160}

To a well-stirred solution of compound **13** (0.796 g, 1.49 mmol) in THF (15 mL) at 0 °C was added tetrabutylammonium fluoride (TBAF·3H₂O, 0.707 g, 2.24 mmol). The reaction mixture was stirred for 30 min while warming to room temperature. The reaction mixture was quenched with water (10mL) and extracted with EtOAc (3 x 10 mL). The combined organic extract was dried over Na₂SO₄ and concentrated under reduced pressure. Purification by flash column chromatography using a prepacked 50 g silica column [solvent A: EtOAc; solvent B: hexanes; gradient: 12% A / 88% B (1 CV), 12% A / 88% B → 100% A / 0% B (10 CV), 100% A / 0% B (5 CV); flow rate: 40 mL/min; monitored at 254 and 280 nm] afforded the desired phenolic indole **1** (OXi8006) [0.661 g, 1.43 mmol, 95%, R_f = 0.28 (50:50 hexanes: EtOAc)] as a yellow powder.

¹H NMR (CDCl₃, 500 MHz): δ 8.30 (br s, 1H, NH), 7.93 (d, *J* = 9.5 Hz, 1H, ArH), 6.96 (s, 2H, ArH) 6.95 (d, *J* = 2.0 Hz, 1H, ArH), 6.93 (dd, *J* = 9.5, 2.5 Hz, 1H, ArH), 6.92 (d, *J* = 2.5 Hz, 1H, ArH), 6.78 (dd, *J* = 8.0, 2.0 Hz, 1H, ArH), 6.65 (d, *J* = 8.5

Hz, 1H, ArH), 5.55 (s, 1H, OH) 3.89 (s, 3H, OCH₃), 3.84 (s, 3H, OCH₃), 3.80 (s, 3H, OCH₃), 3.71 (s, 6H, OCH₃).

¹³C NMR (CDCl₃, 125 MHz): δ 192.7, 157.1, 152.5, 147.0, 145.3, 143.3, 141.0, 136.6, 135.0, 125.1, 123.0, 122.1, 121.5, 115.1, 112.6, 111.6, 110.3, 107.4, 94.8, 60.8, 56.0, 55.8, 55.6.

HPLC: Method B, 6.8 min.

HRMS (ESI⁺): *m/z* calculated for C₂₆H₂₆NO₇ [M+H]⁺ 464.1704, found 464.1706.

*2-(3'-Dibenzyl phosphate-4'-methoxyphenyl)-3-(3'',4'',5''-trimethoxybenzoyl)-6-methoxyindole 14*⁵⁴

To a solution of compound **1** (1.90 g, 4.09 mmol) in acetonitrile (70 mL) at -25 °C was added CCl₄ (3.50 mL, 36.0 mmol). The solution was stirred for 10 min, and diisopropylethylamine (1.50 mL, 8.63 mmol) and DMAP (0.050 g, 0.41 mmol) were added. After 5 min of stirring, dibenzyl phosphite (1.36 mL, 6.17 mmol) was added, and the reaction mixture was stirred for 2 h while allowing the solution to reach room temperature. After 2 h, the reaction was terminated by adding a solution of KH₂PO₄ (15 mL, 0.5 M) and extracted with EtOAc (3 × 50 mL). The combined organic extract was dried over Na₂SO₄ and concentrated under reduced pressure. Purification by flash column chromatography using a prepacked 25 g silica column [solvent A: EtOAc; solvent B: hexanes; gradient: 12% A/88% B (4 CV), 12% A/88% B → 100% A/0% B (10 CV), 100% A/0% B (5.2 CV); flow rate: 25 mL/min; monitored at 254 and 280 nm] afforded the desired phosphate ester **14** [2.71 g 3.75 mmol, 91%, R_f = 0.57 (hexanes:EtOAc, 50:50)] as a yellow powder.

¹H NMR (CDCl₃, 500 MHz) δ 9.20 (1H, br s, NH), 7.78 (1H, d, J = 8.5 Hz, ArH), 7.35 (1H, m, ArH), 7.25 (1H, m, ArH), 6.96 (1H, dd, J = 9.0, 2.5 Hz, ArH), 6.93 (2H, s, ArH), 6.91 (1H, d, J = 2.0 Hz, ArH), 6.86 (1H, dd, J = 9.0, 2.5 Hz, ArH), 6.51 (1H, d, J = 8.5 Hz, ArH) 5.17 (4H, d, J = 8.0 Hz, CH₂), 3.82 (3H, s, OCH₃), 3.79 (3H, s, OCH₃), 3.65 (6H, s, OCH₃), 3.54 (3H, s, OCH₃).

¹³C NMR (CDCl₃, 125 MHz) δ 192.1, 157.3, 152.7, 150.73, 150.69, 141.3, 141.2, 136.7, 135.6 (d, J = 7.3 Hz), 135.0, 128.84, 128.78, 128.1, 127.8, 124.6, 123.1, 122.3, 121.4, 112.8, 112.0, 111.7, 107.4, 94.9, 70.3 (d, J = 6.0 Hz), 60.9, 56.2, 55.8, 55.7.

³¹P NMR (CDCl₃, 200 MHz) δ -6.1.

2-(3'-Disodium phosphate-4'-methoxyphenyl)-3-(3'',4'',5''-trimethoxybenzoyl)-6-methoxyindole 2 (OXi8007)^{152,160}

To a solution of dibenzyl ester (0.827 g, 1.14 mmol) in methanol (25 mL) was added 10% palladium–carbon (0.365 g). The flask was evacuated under vacuum, and H₂ gas was introduced via a balloon. The reaction proceeded for 30 min, and the solution was filtered using Celite with EtOAc. The filtrate was concentrated under reduced pressure to give the crude phosphoric acid derivative as a greenish-yellow oil. The oil was dissolved in a solution of sodium carbonate (5.0 mL, 0.50 M in H₂O) was added. The reaction mixture was stirred at room temperature for 12 h, and the methanol was removed under reduced pressure. Purification by flash chromatography using a prepacked 25 g reversed-phase silica column [solvent A: water; solvent B: acetonitrile; gradient: 100% A/0% B (3 CV), 100% A/0% B → 20% A/80% B (10 CV), 0% A/100% B (7.3 CV); flow rate: 25 mL/min; monitored at 254 and 280 nm] resulted in the desired disodium phosphate salt **2** (OXi8007) [0.399 g, 0.682 mmol, 60%] as a yellow powder.

¹H NMR (D₂O, 500 MHz) δ 8.03 (1H, d, J = 9.0 Hz, ArH), 7.71 (1H, m, ArH), 7.21 (1H, d, J = 2.0 Hz, ArH) 7.03 (1H, dd, J = 9.0, 2.5 Hz, ArH), 6.93 (2H, s, ArH), 6.67 (1H, d, J = 8.5 Hz, ArH), 6.63 (1H, dd, J = 9.0, 2.0 Hz, ArH), 3.95 (3H, s, OCH₃), 3.77 (3H, s, OCH₃), 3.75 (6H, s, OCH₃), 3.72 (3H, s, OCH₃).

¹³C NMR (D₂O, 125 MHz) δ 195.1, 156.3, 151.7, 150.5, 150.4, 147.7, 142.8 (d, J = 5.6 Hz), 139.7, 136.6, 135.4, 125.8, 123.8, 122.2, 121.5, 120.4, 111.7, 111.2, 107.8, 94.5, 60.8, 56.1, 55.8, 55.7.

³¹P NMR (D₂O, 200 MHz) δ 0.57.

HPLC: Method A, 13.3 min.

HRMS (ESI⁺): *m/z* calculated for C₂₆H₂₅NNa₂O₁₀P [M+H]⁺ 588.1006, found 588.1008.

2-(3'-tert-Butyldimethylsilyloxy-4'-methoxyphenyl)-6,7-dimethoxyindole 16

To a solution of 2,3-dimethoxyaniline **15** (2.19 mL, 16.3 mmol) dissolved in *N,N*-dimethylaniline (20 mL) was added bromoacetophenone **11** (2.93 g, 8.16 mmol). The solution was heated to reflux and stirred at 150 °C for 12 h. Upon completion of the reaction, the reaction mixture was cooled to room temperature and extracted with EtOAc (3 X 50 mL). The combined organic extract was dried over Na₂SO₄ and concentrated under reduced pressure. Purification by flash chromatography using a prepacked 50 g silica column [solvent (A) EtOAc; solvent (B) hexanes; gradient: 5%A/95%B (4 CV), 5%A/95%B→40%A/60%B (10 CV), 40%A/60%B (2 CV); flow rate: 50 mL/min; monitored at 254 and 280 nm] resulted in the desired 6,7-dimethoxy-2-phenylindole **16** (1.41 g, 3.42 mmol, 42%, R_f = 0.40 (80:20 hexanes: EtOAc)) as a tan solid.

¹H NMR (CDCl₃, 500 MHz): d 8.63 (br s, 1H, NH), 7.33 (d, J = 8.5 Hz, 1H, ArH), 7.28 (d, J = 2.2 Hz, 1H, ArH), 7.26 (dd, J = 8.5 Hz, 2.2 Hz, 1H, ArH), 6.92 (dd, J = 8.4 Hz, 1.4 Hz, 2H, ArH), 6.71 (d, J = 2.2 Hz, 1H, ArH), 4.15 (s, 3H, OCH₃), 4.01 (s, 3H, OCH₃), 3.88 (s, 3H, OCH₃), 1.15 (s, 9H, C(CH₃)₃), 0.31 (s, 6H, Si(CH₃)₂).

¹³C NMR (CDCl₃, 125 MHz): d 150.7, 147.1, 145.4, 137.9, 134.2, 131.2, 126.0, 125.7, 118.4, 118.1, 115.2, 112.3, 108.7, 99.0, 60.9, 57.3, 55.4, 25.8, 18.5, -4.5.

2-(3'-tert-Butyldimethylsiloxy-4'-methoxyphenyl)-3-(3'',4'',5''-trimethoxybenzoyl)-6,7-dimethoxyindole 17

To a solution of compound **16** (1.36 g, 3.28 mmol) in o-dichlorobenzene (20 mL) was added 3,4,5-trimethoxybenzoyl chloride (1.14 g, 4.92 mmol). The reaction mixture was heated to reflux at 160 °C for 12 h. The o-dichlorobenzene was removed by simple distillation, and the resulting dark green colored solid was subjected to flash chromatography using a prepacked 50 g silica column [solvent (A) EtOAc; solvent (B) hexanes; gradient: 7%A/93%B (4 CV), 7%A/93%B → 60%A/40%B (10 CV), 60%A/40%B (5.2 CV); flow rate: 50 mL/min; monitored at 254 and 280 nm] resulting in a TBS protected indole analogue **17** as yellow powder (0.44 g, 0.72 mmol, 22%, R_f = 0.17(70:30 hexanes:EtOAc)).

¹H NMR (CDCl₃, 500 MHz): d 8.53 (br s, 1H, NH), 7.71 (d, J = 8.5 Hz, 1H, ArH), 6.98 (m, 4H, ArH), 6.77 (d, J = 2.0 Hz, 1H, ArH), 6.73 (d, J = 8.5 Hz, 1H, ArH), 4.06 (s, 3H, OCH₃), 3.96 (s, 3H, OCH₃), 3.79 (s, 3H, OCH₃), 3.76 (s, 3H, OCH₃), 3.69 (s, 6H, OCH₃), 0.94 (s, 9H, C(CH₃)₃), 0.03 (s, 6H, Si(CH₃)₂).

¹³C NMR (CDCl₃, 125 MHz): δ 191.8, 152.6, 151.8, 148.0, 145.2, 142.8, 141.3, 134.6, 134.0, 130.2, 125.2, 125.1, 122.3, 122.2, 116.8, 113.1, 111.8, 110.4, 107.4, 61.3, 60.9, 57.3, 56.1, 55.5, 25.8, 18.5, -4.7.

2-(3'-Hydroxy-4'-methoxyphenyl)-3-(3'', 4'', 5''-trimethoxybenzoyl)-6,7-dimethoxyindole 3

To a well-stirred solution of compound **17** (0.380 g, 0.625 mmol) in THF (10 mL) at 0 °C was added TBAF (0.296 g, 0.938 mmol). The reaction mixture was stirred for 30 min while warming to room temperature. The reaction mixture was quenched with water (10 mL) and extracted with EtOAc (3 X 10 mL). The combined organic extract was dried over Na₂SO₄ and concentrated under reduced pressure. Purification by flash column chromatography using a prepacked 25 g silica column [solvent (A) EtOAc; solvent (B) hexanes; gradient: 12% A/88% B (4 CV), 12% A/88% B?100% A/0% B (10 CV), 100% A/0% B (2 CV); flow rate: 25 mL/min; monitored at 254 and 280 nm] resulting in free phenol indole **3** as a dark brown powder (0.233 g, 0.472 mmol, 75%, R_f = 0.14 (50:50 hexanes: EtOAc)).

¹H NMR (CDCl₃, 500 MHz): δ 8.57 (br s, 1H, NH), 7.71 (d, J = 9.0 Hz, 1H, ArH), 6.972 (d, J = 9.0 Hz, 1H, ArH), 6.971 (d, J = 2.0 Hz, 1H, ArH), 6.94 (s, 2H, ArH), 6.79 (dd, J = 8.3, 2.0 Hz, 1H, ArH), 6.64 (d, J = 8.3 Hz, 1H, ArH), 5.63 (br s, 1H, OH), 4.06 (s, 3H, OCH₃), 3.96 (s, 3H, OCH₃), 3.83 (s, 3H, OCH₃), 3.79 (s, 3H, OCH₃), 3.71 (s, 6H, OCH₃).

¹³C NMR (CDCl₃, 125 MHz): δ 192.0, 152.6, 148.1, 147.2, 145.7, 143.2, 141.1, 135.0, 134.0, 130.2, 125.4, 125.0, 122.0, 116.8, 114.8, 113.4, 110.52, 110.45, 107.3, 61.3, 60.9, 57.4, 56.17, 56.15.

Sodium 5-(6,7-dimethoxy-3-(3,4,5-trimethoxybenzoyl)-1H-indol-2-yl)-2-methoxyphenyl phosphate **5**

To a well-stirred solution of phenol (100 mg, 0.202 mmol) in dichloromethane (10 mL), POCl₃ (0.076 mL, 0.81 mmol) and pyridine (0.059 mL, 0.72 mmol) were added into the reaction flask. After the reaction mixture was stirred at room temperature for 15 hours, the solvent was evaporated under reduced pressure. 0.25 M Na₂CO₃ solution (9.5 mL) was added into the flask until the pH of the solution was neutral, and the reaction mixture was allowed to stir for another 2 hours. The reaction mixture was concentrated to dryness with a stream of nitrogen gas and purified by flash chromatography using a prepacked C-18 12 g silica column affording phosphate salt as a yellow solid **5** (24.5 mg, 0.0397 mmol, 20%).

¹H NMR (500 MHz, Deuterium Oxide) δ 7.58 (d, J = 8.7 Hz, 1H), 7.48 (s, 1H), 6.89 (d, J = 8.8 Hz, 1H), 6.63 (s, 2H), 6.37 – 6.26 (m, 2H), 3.77 (s, 3H), 3.77 (s, 3H), 3.54 (s, 3H), 3.52 (s, 6H), 3.49 (s, 3H).

¹³C NMR (126 MHz, D₂O) δ 195.00, 151.58, 150.43 (d, J = 5.5 Hz), 148.52, 147.66, 142.67 (d, J = 5.9 Hz), 139.52, 135.32, 133.57, 130.05, 125.95, 124.34, 123.44, 120.42, 116.52, 111.68, 111.52, 110.25, 107.66, 61.33, 60.71, 56.98, 55.94, 55.65.

HPLC: Method A, 13.2 min.

HRMS [M+H]⁺: 385.2031 (calcd for [C₂₁¹³CH₃₀NO₃Si]⁺, 385.2023).

2-(4'-Methoxyphenyl)-6, 7-dimethoxyindole **19**

To a solution of 2,3-dimethoxyaniline **15** (2.19 mL, 16.3 mmol) dissolved in *N,N*-dimethylaniline (20 mL) was added 4-methoxybromoacetophenone **18** (1.87 g, 8.15 mmol). The solution was heated to reflux and stirred at 150 °C for 12 h. Upon completion

of the reaction, the reaction mixture was cooled to room temperature and extracted with EtOAc (3 X 50 mL). The combined organic extract was dried over Na₂SO₄ and concentrated under reduced pressure. Purification by flash chromatography using a prepacked 100 g silica column [solvent (A) EtOAc; solvent (B) hexanes; gradient: 5% A/95% B (4 CV), 5% A/95% B - 40% A/60% B (10 CV), 40% A/60% B (4 CV); flow rate: 40 mL/min; monitored at 254 and 280 nm] resulted in the desired 6,7-dimethoxy-2-phenylindole **19** (1.20 g, 4.24 mmol, 52%, R_f = 0.35 (80:20 hexanes: EtOAc)) as a tan solid.

¹H NMR (CDCl₃, 500 MHz): d 8.61 (br s, 1H, NH), 7.61 (d, J = 8.7 Hz, 2H, ArH), 7.28 (d, J = 8.5 Hz, 1H, ArH), 6.97 (d, J = 8.7 Hz, 2H, ArH), 6.87 (d, J = 8.6 Hz, 1H, ArH), 6.66 (d, J = 2.1 Hz, 1H, ArH), 4.09 (s, 3H, OCH₃), 3.97 (s, 3H, OCH₃), 3.85 (s, 3H, OCH₃).

¹³C NMR (CDCl₃, 125 MHz): d 159.2, 147.1, 138.0, 134.2, 131.3, 126.4, 126.0, 125.3, 115.3, 114.5, 108.5, 98.8, 61.1, 57.4, 55.4.

2-(4'-Methoxyphenyl)-6-methoxy-7-hydroxyindole 20

Trimethoxyindole **19** (0.613 g, 2.16 mmol) was dissolved in a solution of [Al₂Cl₇][TMAH] (6.3 mL, 3.1 mmol, 0.496 M in dichloromethane). The reaction mixture was sealed and subjected to microwave irradiation at 80 °C for 1 h. Upon completion of the reaction, the reaction mixture was diluted with NaHCO₃ and extracted with CH₂Cl₂ (3 X 20 mL). The combined organic extract was dried over Na₂SO₄ and concentrated under reduced pressure. Purification by flash chromatography using a prepacked 100 g silica column [solvent (A) EtOAc; solvent (B) hexanes; gradient: 7% A/93% B (4 CV), 7% A/93% B - 60% A/40% B (10 CV), 60% A/ 40% B (2 CV); flow rate: 40 mL/min;

monitored at 254 and 280 nm] resulted in the desired 6-methoxy-7-hydroxy-2-phenylindole **20** (0.420 g, 1.55 mmol, 71%, R_f = 0.36 (70:30 hexanes: EtOAc)) as a tan solid.

¹H NMR ((CD₃)₂CO, 500 MHz): δ 10.11 (br s, 1H, NH), 7.85 (d, J = 8.7 Hz, 2H, ArH), 7.66 (s, 1H, OH), 6.98 (m, 3H, ArH), 6.81 (d, J = 8.5 Hz, 1H, ArH), 6.66 (d, J = 2.2 Hz, 1H, ArH), 3.83 (s, 3H, OCH₃), 3.81 (s, 3H, OCH₃).

¹³C NMR ((CD₃)₂CO, 125 MHz): δ 159.9, 142.5, 138.8, 133.1, 128.4, 127.2, 127.1, 126.5, 115.0, 111.3, 108.9, 99.0, 58.3, 55.7.

2-(4'-Methoxyphenyl)-6-methoxy-7-tertbutyldimethylsilyloxyindole 21

To a solution of free phenol indole **20** (0.328 g, 1.22 mmol) in dichloromethane (20 mL) at 0 °C was added Et₃N (0.19 mL, 1.3 mmol) and DMAP (0.015 g, 0.12 mmol). The reaction mixture was stirred for 10 min, and TBSCl (0.202 g, 1.30 mmol) was added gradually. The solution was allowed to warm to room temperature over 12 h. Upon completion of the reaction, water (10 mL) was added, and the reaction mixture was extracted with dichloromethane (3 X 20 mL). The combined organic extract was dried over Na₂SO₄ and concentrated under reduced pressure. Purification by flash chromatography using a prepacked 50 g silica column [solvent (A) EtOAc; solvent (B) hexanes; gradient: 2% A/98% B (4 CV), 2% A/ 98% B to 20% A/80% B (10 CV), 20% A/80% B (5.2 CV); flow rate: 35 mL/min; monitored at 254 and 280 nm] resulted in the TBS indole product **21** (0.366 g, 0.90 mmol, 74%, R_f = 0.64 (70:30 hexanes: EtOAc)) as a light tan solid.

¹H NMR (CDCl₃, 500 MHz): δ 8.03 (br s, 1H, NH), 7.53 (d, J = 8.7 Hz, 2H, ArH), 7.13 (d, J = 8.5 Hz, 1H, ArH), 6.98 (d, J = 8.7 Hz, 2H, ArH), 6.80 (d, J = 8.5 Hz,

1H, ArH), 6.61 (d, $J = 2.2$ Hz, 1H, ArH), 3.86 (s, 6H, OCH₃), 1.11 (s, 9H, C(CH₃)₃), 0.24 (s, 6H, Si(CH₃)₂).

¹³C NMR (CDCl₃, 125 MHz): δ 159.3, 145.2, 137.5, 131.2, 130.2, 126.2, 125.9, 125.6, 114.6, 112.9, 108.5, 99.0, 57.0, 55.5, 26.3, 18.8, 4.2.

2-(4'-Methoxyphenyl)-3-(3'',4'',5''-trimethoxybenzoyl)-6-methoxy-7-tert-butyltrimethylsilyloxyindole 22

To a solution of compound **21** (0.417 g, 1.09 mmol) in *o*-dichlorobenzene (30 mL) was added 3,4,5-trimethoxybenzoyl chloride (0.376 g, 1.63 mmol). The reaction mixture was heated to reflux at 160 °C for 12 h. The *o*-dichlorobenzene was removed by simple distillation, and the resulting dark green colored solid was subjected to flash chromatography using a prepacked 25 g silica column [solvent (A) EtOAc; solvent (B) hexanes; gradient: 10% A/ 90% B (4 CV), 10% A/90% B - 80% A/20% B (10 CV), 80% A/20% B (2 CV); flow rate: 25 mL/min; monitored at 254 and 280 nm] resulting in **22** as a tan solid (0.26 g, 0.56 mmol, 46%, $R_f = 0.36$ (60:40 hexanes:EtOAc)).

¹H NMR (600 MHz, CDCl₃) δ 8.70 (s, 1H), 7.60 (d, $J = 8.8$ Hz, 2H), 7.44 (s, 2H), 7.41 (d, $J = 8.6$ Hz, 1H), 6.91 (d, $J = 8.8$ Hz, 2H), 6.87 (d, $J = 8.6$ Hz, 1H), 6.67 (d, $J = 2.1$ Hz, 1H), 3.93 (s, 3H), 3.88 (s, 6H), 3.86 (s, 3H), 3.81 (s, 3H).

¹³C NMR (151 MHz, CDCl₃) δ 164.1, 159.2, 152.7, 146.5, 142.5, 138.4, 130.8, 126.4, 126.3, 125.1, 124.9, 123.9, 117.8, 114.3, 107.5, 107.4, 98.9, 61.0, 57.2, 56.1, 55.4.

HPLC: Method B, 10.9 min.

HRMS (ESI⁺): m/z calculated for C₂₆H₂₅NO₇Na [M+Na]⁺ 486.1521, found 486.1523.

4'-Methoxy-3'-nitro-2-bromoacetophenone **25**

To a well-stirred solution of 4-methoxy-3-nitroacetophenone **24** (2.00 g, 10.3 mmol) in chloroform (10 mL) at room temperature, was added dropwise a solution of bromine (0.53 mL, 10 mmol) in chloroform (2 mL). The reaction mixture was stirred for 30 mins. Water (10 mL) was added upon the completion of the reaction, the organic layer was separated and the aqueous layer was extracted with dichloromethane (3 X 15 mL). The combined organic layer was dried over Na₂SO₄ and concentrated under reduced pressure. The crude product was then recrystallized from hot ethanol to afford the desired bromoacetophenone derivative as yellow needle-shaped crystals **25** (1.38 g, 4.98 mmol, 50%), R_f = 0.40 (EtOAc/Hexanes: 40/60).

¹H NMR (600 MHz, CDCl₃) δ 8.49 (d, *J* = 2.3 Hz, 1H), 8.22 (dd, *J* = 8.9, 2.3 Hz, 1H), 7.20 (d, *J* = 8.8 Hz, 1H), 4.40 (s, 2H), 4.07 (s, 3H).

¹³C NMR (151 MHz, CDCl₃) δ 188.5, 156.8, 139.4, 134.9, 126.9, 126.2, 113.6, 57.1, 29.9.

6-methoxy-2-(4-methoxy-3-nitrophenyl)indole **26**

To a solution of *m*-anisidine (4.7 mL, 42 mmol) in *N,N*-dimethylaniline at 150 °C, a warm solution (60 °C) of bromide **25** (3.50 g, 12.8 mmol) in ethanol (15 mL) was added dropwise. The reaction mixture was stirred at 160 – 170 °C for 12 hours. Water (20 mL) was added into the solution and organic layer was separated in a separation funnel. Aqueous layer was then extracted with EtOAc (3 X 30 mL). The combined organic phase was dried over Na₂SO₄ and concentrated under reduced pressure to afford a dark colored solid. This crude product was further purified by recrystallization from EtOAc to form the desired product as dark red powder **26** (1.13 g, 3.80 mmol, 30%).

¹H NMR (600 MHz, Acetone-*d*₆) δ 10.65 (s, 1H), 8.23 (d, *J* = 2.1 Hz, 1H), 8.08 (dd, *J* = 8.8, 2.2 Hz, 1H), 7.45 (t, *J* = 8.5 Hz, 2H), 6.95 (d, *J* = 2.0 Hz, 1H), 6.89 (d, *J* = 2.0 Hz, 1H), 6.73 (dd, *J* = 8.7, 2.1 Hz, 1H), 4.04 (s, 3H), 3.82 (s, 3H).

¹³C NMR (151 MHz, CDCl₃) δ 157.8, 152.1, 141.4, 139.4, 135.3, 130.8, 126.8, 124.3, 121.8, 121.4, 115.6, 111.0, 100.5, 95.2, 57.2, 55.7.

(6-methoxy-2-(4-methoxy-3-nitrophenyl)indol-3-yl)(3,4,5-trimethoxyphenyl)methanone
27

To a solution of 6-methoxy-2-(4-methoxy-3-nitrophenyl)indole **26** (1.59 g, 5.32 mmol) in *o*-dichlorobenzene (45 mL) at 150 °C, was added 3,4,5-trimethoxybenzoyl chloride (2.1 g, 9.1 mmol) in portions. The reaction mixture was stirred at 160-170 °C for 12 hours. It was allowed to cool down to room temperature, filter and rinsed with a small amount of EtOAc. The residue was further purified by recrystallization from dichloromethane-hexanes to afford a greenish-yellow solid **27** (0.48 g, 0.97 mmol, 18%).

¹H NMR (600 MHz, Acetone-*d*₆) δ 11.08 (s, 1H), 7.90 (d, *J* = 8.8 Hz, 1H), 7.86 (s, 1H), 7.70 (dd, *J* = 8.7, 2.3 Hz, 1H), 7.25 (d, *J* = 8.7 Hz, 1H), 7.04 (d, *J* = 2.2 Hz, 2H), 6.92 – 6.88 (m, 4H), 3.95 (s, 3H), 3.86 (s, 3H), 3.70 (s, 6H), 3.67 (s, 3H).

¹³C NMR (151 MHz, Acetone-*d*₆) δ 190.9, 157.5, 152.9, 152.2, 141.1, 140.2, 139.2, 137.1, 136.9, 135.4, 134.7, 125.8, 125.0, 122.8, 122.2, 113.6, 111.7, 107.0, 94.4, 59.6, 56.4, 55.4, 54.9.

HPLC: Method C, 5.5 min.

HRMS (ESI⁺): *m/z* calculated for C₂₆H₂₅N₂O₈ [M+H]⁺ 493.1605, found 493.1604.

(2-(3-amino-4-methoxyphenyl)-6-methoxy-1H-indol-3-yl)(3,4,5-trimethoxyphenyl)methanone 28

To a round-bottom flask containing nitro compound **27** (246 mg, 0.497 mmol), 10% palladium on carbon (52.9 mg, 0.050mmol) was added under nitrogen followed by MeOH (50 mL). Hydrogen was introduced through a balloon. The reaction mixture was then stirred at room temperature for 2 h examining periodically by TLC. It was filtered and the filtrate was concentrated under reduced pressure to achieve a yellow solid. The crude product was subjected to flash column chromatography using a pre-packed 50 g silica gel column [solvent A, 50% EtOAc, 50% dichloromethane, solvent B, hexanes; gradient 20%A / 80%B (1CV), 20%A / 80%B → 90%A / 10%B (15 CV), 90%A / 10%B (6 CV); flow rate, 36 mL/min; monitored at 254 and 280 nm]. The final product amine **28** (0.186 g, 0.402 mmol, 81%) was isolated as a yellow solid, $R_f = 0.35$, (EtOAc/Dichloromethane/hexane: 40/40/20).

¹H NMR (600 MHz, CDCl₃) δ 8.46 (s, 1H), 7.90 (d, $J = 9.3$ Hz, 1H), 6.97 (s, 2H), 6.90 (dd, $J = 4.7, 2.4$ Hz, 2H), 6.69 (dd, $J = 8.2, 2.1$ Hz, 1H), 6.63 (d, $J = 2.1$ Hz, 1H), 6.59 (d, $J = 8.2$ Hz, 1H), 3.87 (s, 3H), 3.80 (s, 3H), 3.78 (s, 3H), 3.70 (s, 6H).

¹³C NMR (151 MHz, CDCl₃) δ 192.0, 157.2, 152.4, 147.7, 143.1, 140.9, 136.2, 136.2, 134.9, 124.8, 123.1, 122.4, 119.2, 115.2, 112.6, 111.4, 109.9, 107.1, 94.5, 60.8, 56.0, 55.7, 55.5, 53.4.

HPLC: Method C, 3.8 min.

HRMS (ESI⁺): m/z calculated for C₂₆H₂₇N₂O₆ [M+H]⁺ 463.1864, found 463.1868.

3-(tert-Butyldimethylsilyloxy)-4-methoxybenzaldehyde 37

3-Hydroxy-4-methoxybenzaldehyde **36** (2.00 g, 13.2 mmol) was dissolved in CH₂Cl₂ (40 mL) and cooled to 0 °C. Triethylamine (Et₃N) (2.0 mL, 15 mmol) and *N,N*-dimethylaminopyridine (DMAP) (0.161 g, 1.31 mmol) were added, and the solution was stirred for 10 minutes. *tert*-Butyldimethylsilyl chloride (TBSCl) (2.18 g, 14.5 mmol) was added gradually. The reaction mixture was allowed to warm to room temperature over 12 hours. It was then quenched with water, extracted with CH₂Cl₂ three times. The combined organic layers were dried over sodium sulfate, and concentrated under reduced pressure to afford aldehyde **37** as a dark tan oil (3.42 g, 12.8 mmol, 97%).

¹H NMR (CDCl₃, 500 MHz): δ 9.80 (s, 1H, CHO), 7.45 (dd, *J* = 8.5, 2.0 Hz, 1H, ArH), 7.35 (d, *J* = 2.0 Hz, 1H, ArH), 6.93 (d, *J* = 8.5 Hz, 1H, ArH), 3.87 (s, 3H, OCH₃), 0.99 (s, 9H, C(CH₃)₃), 0.16 (s, 6H, Si(CH₃)₂).

¹³C NMR (CDCl₃, 125 MHz): δ 190.2, 156.2, 145.2, 130.0, 126.0, 119.4, 110.9, 55.1, 25.3, 18.0, -5.0.

3-(3,4,5-Trimethoxyphenyl)propanol 39

To a stirred suspension of lithium aluminum hydride (16.7 mL, 33.4 mmol) in dry THF (25 mL) at 0 °C, compound **38** (5.02 g, 20.8 mmol) in THF (25 mL) was added dropwise. The reaction mixture was stirred from 0 °C to room temperature overnight. It was then cooled to 0 °C, quenched by dropwise addition of 20% H₂O in THF (50 mL), filtered and washed with Et₂O. A yellow oil **39** (4.37 g, 19.3 mmol, 93%) was isolated under reduced pressure.

¹H-NMR (CDCl₃, 500 MHz): δ 6.41 (s, 2H, ArH), 3.83 (s, 6H, OCH₃), 3.81 (s, 3H, OCH₃), 3.68 (t, 2H, CH₂), 2.64 (t, 2H, CH₂), 1.87 (pent, 2H, CH₂), 1.74 (s, 1H, OH).

¹³C-NMR (CDCl₃, 125 MHz): δ 153.1, 137.6, 136.1, 105.3, 62.2, 60.8, 56.0, 34.3, 32.5.

HRMS (ESI⁺): m/z calculated for C₁₂H₁₈O₄ [M + Na]⁺ 249.1097, found 249.1094.

5-(3-Bromopropyl)-1,2,3-trimethoxybenzene 40

To a solution of compound **39** (4.05 g, 17.9 mmol) in CH₂Cl₂ (25 mL), PBr₃ (9.0 mL, 9.0 mmol) in CH₂Cl₂ (25 mL) was added dropwise. The solution was stirred at room temperature for 1 hour. It was then washed several times with water until pH of the rinse was neutral. The organic phase was dried and concentrated under reduced pressure.

Purification by flash chromatography using a prepacked 100 g silica column [solvent A: n-Hexane; solvent B: ethyl acetate (EtOAc); gradient: 7% A / 93% B (1.0 CV), 7% A / 93% B → 60% A / 40% B (10.0 CV), 60% A / 40% B (2.0 CV); flow rate: 50 mL/min; monitored at 254 nm and 280 nm] afforded bromide derivative **40** (1.52 g, 4.86 mmol, 28%) as a pale-yellow oil.

¹H-NMR (CDCl₃, 500 MHz): δ 6.41 (s, 2H, ArH), 3.85 (s, 6H, OCH₃), 3.82 (s, 3H, OCH₃), 3.41 (t, 2H, CH₂), 2.72 (t, 2H, CH₂), 2.15 (pent, 2H, CH₂).

¹³C-NMR (CDCl₃, 125 MHz): δ 153.2, 136.3, 136.2, 105.4, 60.8, 56.1, 34.3, 34.1, 33.1.

HRMS (ESI⁺): m/z calculated for C₁₂H₁₇O₃Br [M + Na]⁺ 311.0253 and 313.0233, found 311.0258 and 313.0234.

Triphenyl(3-(3,4,5-trimethoxyphenyl)propyl)phosphate Bromide 41

To a round-bottom flask with a condenser, triphenylphosphine (1.27 g, 4.84 mmol), compound **40** (1.52 g, 4.84 mmol), and toluene (15 mL) were added. The reaction was refluxed for 5 hours. The solution was then poured out and the precipitate washed with diethyl ether. Bromide salt **41** (1.77 g, 5.57 mmol, 57%) was advanced to the next step without further purification.

tert-Butyl(2-methoxy-5-(4-(3,4,5-trimethoxyphenyl)but-1-en-1-yl)phenoxy)dimethylsilane 42

Bromide salt **41** (2.67 g, 4.84 mmol) was suspended in THF (15 mL) and purged with N₂. While being stirred at room temperature, 2.5 M n-BuLi (2.0 mL, 4.84 mmol) was added dropwise. The reaction was stirred for 15 minutes and the solution changed color from orange to red. Aldehyde **37** (1.29 g, 4.84 mmol) in THF (15 mL) was then added dropwise and the reaction mixture was stirred for 24 hours. The color of the solution changed to light orange. The reaction was poured onto ice and diluted with ethyl acetate. It was extracted three times with ethyl acetate, dried over sodium sulfate, and concentrated. Purification by flash chromatography using a prepacked 100 g silica column [solvent A: n-Hexane; solvent B: ethyl acetate (EtOAc); gradient: 2% A / 98% B (1.0 CV), 2% A / 98% B → 20% A / 80% B (10.0 CV), 20% A / 80% B (2.0 CV); flow rate: 50 mL/min; monitored at 254 nm and 280 nm] afforded alkene **42** (0.380 g, 0.832 mmol, 17%) as a white solid. Note that this is a mixture of *E* and *Z* isomers.

¹H-NMR (CDCl₃, 500 MHz): δ 6.87 (m, 3H, ArH), 6.44 (s, 2H, ArH), 6.31 (d, 1H, CH), 6.08 (m, 1H, CH), 3.83 (s, 3H, OCH₃), 3.82 (s, 6H, OCH₃), 3.79 (s, 3H, OCH₃), 2.68 (m, 4H, CH₂), 0.15 (m, 15H, CH₃).

$^{13}\text{C-NMR}$ (CDCl_3 , 125 MHz): δ 153.0, 149.8, 144.5, 137.4, 130.6, 130.1, 129.0, 122.3, 121.5, 119.7, 118.2, 112.0, 111.7, 105.4, 60.8, 56.0, 55.5, 36.4, 34.9, 30.2, 25.7, 18.4, -4.6.

HRMS (ESI^+): m/z calculated for $\text{C}_{26}\text{H}_{38}\text{O}_5\text{Si}$ [$\text{M} + \text{Na}$] $^+$ 481.2381, found 481.2383.

2-Methoxy-5-(4-(3,4,5-trimethoxyphenyl)but-1-en-1-yl)phenol 43

Compound **42** (0.38 g, 0.83 mmol) was dissolved in THF (10 mL). TBAF (1.3 mL, 1.0 M, 1.3 mmol) was added and the solution was stirred for 30 minutes. The reaction was quenched with water, extracted with ethyl acetate three times, and dried over sodium sulfate. Compound **43** (0.12 g, 0.35 mmol, 42%) was advanced to the next step without further purification.

HRMS (ESI^+): m/z calculated for $\text{C}_{20}\text{H}_{24}\text{O}_5$ [$\text{M} + \text{Na}$] $^+$ 367.1516, found 367.1518.

2-methoxy-5-(4-(3,4,5-trimethoxyphenyl)butyl)phenol 35

10% Pd/C (0.090 g, 0.085 mmol) was added to compound **43** (0.120 g, 0.351 mmol) under N_2 , and methanol (10 mL) was added. The reaction was stirred under H_2 (in balloons) for 12 hours. The product was filtered, washed with ethyl acetate, and evaporated under reduced pressure. Purification by flash chromatography using a prepacked 10 g silica column [solvent A: n-Hexane; solvent B: ethyl acetate (EtOAc); gradient: 8% A / 92% B (1.0 CV), 8% A / 92% B \rightarrow 60% A / 40% B (10.0 CV), 60% A / 40% B (2.0 CV); flow rate: 12 mL/min; monitored at 254 nm and 280 nm] afforded derivative **35** (11.4 mg, 0.033 mmol, 9.5%) as a white solid.

¹H-NMR (CDCl₃, 500 MHz): δ 6.76 (d, 2H, ArH), 6.64 (dd, 1H, ArH), 6.38 (s, 2H, ArH), 5.56 (s, 1H, OH), 3.86 (s, 3H, OCH₃), 3.84 (s, 6H, OCH₃), 3.82 (s, 3H, OCH₃), 2.56 (dd, 4H, CH₂), 1.64 (m, 4H, CH₂).

¹³C-NMR (CDCl₃, 125 MHz): δ 153.0, 145.4, 144.6, 138.4, 136.0, 135.9, 119.6, 114.6, 110.5, 105.2, 60.8, 56.0, 56.0, 36.2, 35.1, 31.1, 31.0.

HPLC: Method C, 7.4 min.

HRMS (ESI⁺): m/z calculated for C₂₀H₂₆O₅ [M + Na]⁺ 369.1672, found 369.1674.

OXi8006-PNP 44

To a solution of OXi8006 (200 mg, 0.431 mmol) and *bis*-PNP (394 mg, 1.30 mmol), was added triethylamine (0.18 mL, 1.3 mmol) dropwise. The reaction mixture was stirred at room temperature for 24 h and then concentrated under reduced pressure. The residue was purified by flash column chromatography using 15-100% hexanes-EtOAc as solvent. Compound **44** (165 mg, 0.261 mmol, 61%) was obtained as a yellow solid.

¹H NMR (600 MHz, Methanol-*d*₄) δ 8.37 (d, *J* = 9.1 Hz, 2H), 7.89 (d, *J* = 8.8 Hz, 1H), 7.55 (d, *J* = 9.1 Hz, 2H), 7.34 (dd, *J* = 8.5, 2.2 Hz, 1H), 7.26 (d, *J* = 2.2 Hz, 1H), 7.06 (d, *J* = 8.5 Hz, 1H), 7.02 (d, *J* = 2.3 Hz, 1H), 6.91 (s, 2H), 6.89 (dd, *J* = 8.8, 2.3 Hz, 1H), 4.87 (s, 6H), 3.88 (s, 6H), 3.71 (s, 3H), 3.70 (s, 6H).

2,5-dioxopyrrolidin-1-yl 6-(2,5-dioxo-2,5-dihydro-1H-pyrrol-1-yl)hexanoate 47

To a solution of 6-maleimidocaproic acid **45** (1.00 g, 4.70 mmol) and disuccinimide carbonate **46** (1.27 g, 5.02 mmol) in DMF (10 mL), was added

triethylamine (0.66 mL, 4.70 mmol) dropwise. The reaction mixture was stirred at room temperature for 2.5 h and concentrated to remove DMF. The residue was re-dissolved in EtOAc (20 mL) and washed with saturated NaHCO₃ solution (20 mL). The aqueous layer was separated and extracted with EtOAc (20 mL X 2). The combined organic layers were dried over sodium sulfate and concentrated to provide compound **47** (1.28 g, 4.20 mmol, 88%) as an oil.

¹H NMR (600 MHz, Chloroform-*d*) δ 6.70 (s, 2H), 3.54 (t, *J* = 7.2 Hz, 2H), 2.91 – 2.77 (m, 4H), 2.61 (t, *J* = 7.3 Hz, 2H), 1.79 (p, *J* = 7.5 Hz, 2H), 1.65 (p, *J* = 7.3 Hz, 2H), 1.43 (p, *J* = 7.3 Hz, 2H).

Fmoc-L-Citrulline 49

A solution of *l*-citrulline **48** (1.25 g, 7.11 mmol) in water (0.2 M) was treated with sodium bicarbonate (1.20 g, 14.2 mmol). After stirring for 1 h at room temperature, THF (0.2 M) was added followed by Fmoc-Cl (1.68 g, 6.52 mmol). The solution was stirred at room temperature for 24.0 h, at which point THF was removed under vacuum. The aqueous solution was extracted with EtOAc (20 mL X 3) and the organic layer was discarded. The aqueous layer was subsequently acidified with HCl (2 M) at which point a white precipitate was observed, which was partly soluble in water. *i*PrOH [10% by volume]-EtOAc was added followed by stirring to achieve a clear phase separation. The organic layer was collected, and the aqueous layer was extracted two more times with the same solvent system. The combined organic layer was dried over sodium sulfate. The solvent was removed under reduced pressure to afford the product as a clear viscous liquid, which was subjected to sonication in diethyl ether. After trituration the diethyl ether was decanted off. This step was repeated twice to obtain a white solid, which was

dried under reduced pressure to obtain an analytically pure sample of compound **49** (2.55 g, 6.43 mmol, 94%).

¹H NMR (600 MHz, DMSO-d₆) δ 7.90-7.89 (d, J = 7.5 Hz, 2H), 7.74-7.72 (d, J = 7.4 Hz, 2H), 7.68-7.67 (d, J = 8.0 Hz, 1H), 7.43-7.41 (d, J = 7.4 Hz, 1H), 7.42-7.41 (d, J = 7.5 Hz, 1H), 7.34-7.33 (d, J = 7.4 Hz, 1H), 7.33-7.32 (d, J = 7.4 Hz, 1H), 6.01 (s, 1H), 5.44 (s, 3H), 4.28-4.21 (m, 3H), 3.95-3.91 (m, 1H), 2.97-2.95 (t, J = 6.6 Hz, 2H), 1.74-1.68 (m, 1H), 1.60-1.52 (m, 1H), 1.48-1.37 (m, 2H);

HRMS (ESI⁺) calc. for C₂₁H₂₃N₃NaO₅ [M+Na]⁺: 420.1535. Found: 420.1529.

Fmoc-L-Citrulline-PABOH 50

A solution of compound **49** (2.55 g, 6.43 mmol) and 4-aminobenzyl alcohol (2.37 g, 19.0 mmol) in DMF (0.1 M) was treated with DIPEA (1.15 mL, 6.52 mmol) followed by stirring for 15 min at room temperature. HATU (2.68 g, 6.98 mmol) was added to the reaction mixture and stirred at room temperature for 48 hours in the dark. DMF was removed under reduced pressure and the resulting residue was purified by flash column chromatography using 2-10% MeOH-CH₂Cl₂ as solvent. Compound **50** was isolated as a white solid (2.09 g, 4.20 mmol, 65%).

¹H NMR (600 MHz, DMSO-d₆) δ 9.98 (s, 1H), 7.90-7.88 (d, J = 7.5 Hz, 2H), 7.76-7.73 (t, J = 7.1 Hz, 2H), 7.67-7.66 (d, J = 8.0 Hz, 1H), 7.57-7.55 (d, J = 8.4 Hz, 2H), 7.43-7.40 (m, 2H), 7.35-7.31 (m, 2H), 7.25-7.23 (d, J = 8.4 Hz, 2H), 6.01-5.99 (t, J = 5.4 Hz, 1H), 5.43 (s, 2H), 5.10-5.09 (t, J = 5.6 Hz, 1H), 4.44-4.43 (d, J = 5.3 Hz, 2H), 4.30-4.15 (m, 4H), 3.07-3.01 (m, 1H), 2.98-2.93 (m, 1H), 1.71-1.58 (m, 2H), 1.51-1.35 (m, 2H);

HRMS (ESI⁺) calc. for C₂₈H₃₀N₄NaO₅ [M+Na]⁺: 525.2114. Found: 525.2111.

Fmoc-Val-Cit-PABOH 51

A solution of compound **50** (2.09 g, 4.22 mmol) in DMF (0.2 M) was treated with triethylamine (11.6 mL, 83.0 mmol) followed by stirring at room temperature for 24 h. DMF and excess triethylamine were removed under reduced pressure. The resulting residue was dissolved in DMF (0.1 M) and to the solution Fmoc-Val-OSu (1.99 g, 4.98 mmol) was added. The reaction mixture was stirred at room temperature for 20 h. DMF was removed under reduced pressure and the resulting residue was purified by flash column chromatography using 3-12% MeOH-CH₂Cl₂ as solvent. Compound **51** (1.39 g, 2.31 mmol, 55%) was obtained as a white solid.

¹H NMR (600 MHz, DMSO-d₆) δ 9.96 (s, 1H), 8.10-8.09 (d, *J* = 7.59 Hz, 1H), 7.90-7.88 (d, *J* = 7.54 Hz, 2H), 7.76-7.75 (d, *J* = 7.51 Hz, 1H), 7.74-7.72 (d, *J* = 7.50 Hz, 1H), 7.55-7.53 (d, *J* = 8.40 Hz, 2H), 7.44-7.40 (m 3H), 7.34-7.32 (d, *J* = 6.80 Hz, 1H), 7.32-7.31 (d, *J* = 7.40 Hz, 1H), 7.24-7.22 (d, *J* = 8.42 Hz, 2H), 5.97-5.95 (t, *J* = 5.49 Hz, 1H), 5.40 (s, 2H), 5.10-5.08 (t, *J* = 5.75 Hz, 1H), 4.43-4.42 (d, *J* = 5.62 Hz, 2H), 4.42-4.40 (m, 1H), 4.33-4.29 (m, 1H), 4.25-4.21 (m, 2H), 3.94-3.92 (dd, *J* = 8.91, 7.05 Hz, 1H), 3.05-2.99 (m, 1H), 2.96-2.91 (m, 1H), 2.02-1.96 (m, 1H), 1.72-1.66 (m, 1H), 1.62-1.58 (m, 1H), 1.48-1.41 (m, 1H), 1.40-1.33 (m, 1H), 0.89-0.88 (d, *J* = 6.76 Hz, 3H), 0.86-0.85 (d, *J* = 6.76 Hz, 3H);

HRMS (ESI⁺) calc. for C₃₃H₃₉N₅NaO₆ [M+Na]⁺: 624.2798. Found: 624.2791.

Fmoc-Val-Cit-PABOH-PNP 52

To a solution of compound **51** (200 mg, 0.332 mmol) in DMF (6 mL), was added *bis*-PNP (303 mg, 1.00 mmol). The reaction mixture was stirred at room temperature for 72 h, followed by removal of DMF under reduced pressure. The residue was purified by

flash column chromatography using 2-15% MeOH-CH₂Cl₂ as solvent. Compound **52** (230 mg, 0.302 mmol, 90%) was obtained as a white solid.

¹H NMR (600 MHz, DMSO-*d*₆) δ 10.14 (s, 1H), 8.32 (d, *J* = 9.1 Hz, 2H), 8.14 (d, *J* = 7.4 Hz, 1H), 7.90 (d, *J* = 7.5 Hz, 2H), 7.75 (dd, *J* = 12.0, 7.5 Hz, 2H), 7.65 (d, *J* = 8.4 Hz, 2H), 7.60 – 7.56 (d, *J* = 9.1 Hz, 2H), 7.45 – 7.39 (m, 5H), 7.33 (td, *J* = 7.4, 1.1 Hz, 2H), 5.98 (s, 1H), 5.41 (s, 2H), 5.25 (s, 2H), 4.47 – 4.39 (m, 1H), 4.37 – 4.28 (m, 1H), 4.27 – 4.20 (m, 2H), 3.94 (dd, *J* = 9.0, 7.0 Hz, 1H), 3.09 – 2.99 (m, 1H), 2.99 – 3.92 (m, 1H), 2.04 – 1.96 (m, 1H), 1.75 – 1.65 (m, 1H), 1.65 – 1.57 (m, 1H), 1.50 – 1.43 (m, 1H), 1.41 – 1.34 (m, 1H), 1.32 – 1.21 (m, 1H), 0.88 (dd, *J* = 17.2, 6.8 Hz, 6H).

HRMS (ESI⁺) calc. for C₄₀H₄₂N₆NaO₁₀ [M+Na]⁺: 789.2855. Found: 789.2847.

Val-Cit-PABOH-DMED-OXi8006 53

To a solution of Fmoc-Val-Cit-PABOH-PNP **52** (152 mg, 0.200 mmol) in DMF (3 mL), DMED (0.11 mL, 1.0 mmol) was added dropwise. The reaction mixture was stirred at room temperature for 1h at which point analysis of the reaction progress (by mass spectrometry) indicated completion, and the solvent was removed under reduced pressure. The residue was then dissolved in DMF and concentrated under reduced pressure to remove DMED, followed by dissolution in DMF (5 mL). DIPEA (0.18 mL, 1.0 mmol) was added to the mixture, followed by the addition of OXi8006-PNP (190 mg, 0.304 mmol). The reaction was stirred for 2 h, checked by mass spec and then concentrated under reduced pressure. The residue was purified by flash chromatography using a prepacked 25 g silica column [solvent (A) MeOH; solvent (B) CH₂Cl₂; gradient: 2% A/98% B (1 CV), 2% A/ 98% B to 20% A/80% B (10 CV), 20% A/80% B (2 CV); flow rate: 25 mL/min; monitored at 254 and 280 nm]. Fractions contained the target product

53 was combined and concentrated to afford a mixture (122 mg) which was advanced to the next step without further purification.

HRMS (ESI⁺) calc. for C₅₀H₆₃N₈O₁₃ [M+H]⁺: 983.4509. Found: 983.4506.

Maleimide-Val-Cit-PABOH-DMED-OXi8006 54

To the solution of the previous mixture containing drug-linker conjugate **53** and activated succinimide ester **47** (93.1 mg, 0.301 mmol) in DMF (5 mL), was added diisopropylethylamine (0.11 mL, 0.61 mmol). The reaction was stirred for 4 h, checked by mass spec and then concentrated under reduced pressure. The residue was purified by flash chromatography using a prepacked 25 g silica column [solvent (A) MeOH; solvent (B) CH₂Cl₂; gradient: 2% A/98% B (1 CV), 2% A/ 98% B to 15% A/85% B (10 CV), 15% A/85% B (2 CV); flow rate: 25 mL/min; monitored at 254 and 280 nm]. Pure fractions were combined and concentrated to afford compound **54** (104 mg, 0.0880 mmol, 30% over 2 steps) as a yellow solid.

¹H NMR (600 MHz, DMSO-*d*₆) δ 12.02 – 11.94 (m, 1H), 9.96 (s, 1H), 8.06 (d, *J* = 7.3 Hz, 1H), 7.78 (d, *J* = 8.6 Hz, 1H), 7.78 – 7.69 (m, 1H), 7.60 – 7.50 (m, 2H), 7.30 – 7.20 (m, 3H), 6.99 (s, 2H), 6.96 (d, *J* = 8.5 Hz, 1H), 6.94 (s, 1H), 6.82 (d, *J* = 6.8 Hz, 2H), 6.79 (s, 1H), 5.96 (t, *J* = 5.2 Hz, 1H), 5.40 (s, 2H), 5.00 – 4.92 (m, 2H), 4.37 (q, *J* = 7.0 Hz, 1H), 4.19 (t, *J* = 7.7 Hz, 1H), 3.81 (s, 3H), 3.75 – 3.65 (m, 3H), 3.60 (s, 9H), 3.54 – 3.45 (m, 2H), 4.43 – 3.33 (m, 4H), 3.05 – 2.97 (m, 2H), 2.97 – 2.83 (m, 5H), 2.82 – 2.76 (m, 1H), 2.21 – 2.14 (m, 1H), 2.14 – 2.07 (m, 1H), 2.00 – 1.91 (m, 1H), 1.73 – 1.65 (m, 1H), 1.63 – 1.54 (m, 1H), 1.54 – 1.39 (m, 5H), 1.39 – 1.22 (m, 3H), 1.22 – 1.14 (m, 3H), 1.21 – 1.14 (m, 2H), 0.89 – 0.77 (m, 7H).

HPLC: Method B, 10.1 min.

HRMS (ESI⁺) calc. for C₆₀H₇₃N₉NaO₁₆ [M+Na]⁺: 1198.5067. Found: 1198.6086.

CHAPTER THREE

Synthesis of Bioreductively Activatable Prodrug Conjugates based on OXi8006 and 3-Bromopyruvic Acid

Some portion of this chapter is published as: Winn, B. A.; Shi, Z.; Carlson, G. J.; Wang, Y.; Nguyen, B. L.; Kelly, E. M.; Ross IV, R. D.; Hamel, E.; Chaplin, D. J.; Trawick, M. L.; Pinney, K. G. Bioreductively Activatable Prodrug Conjugates of Phenstatin Designed to Target Tumor Hypoxia. *Bioorg. Med. Chem. Let.*, **2017**, 27, 636-641.

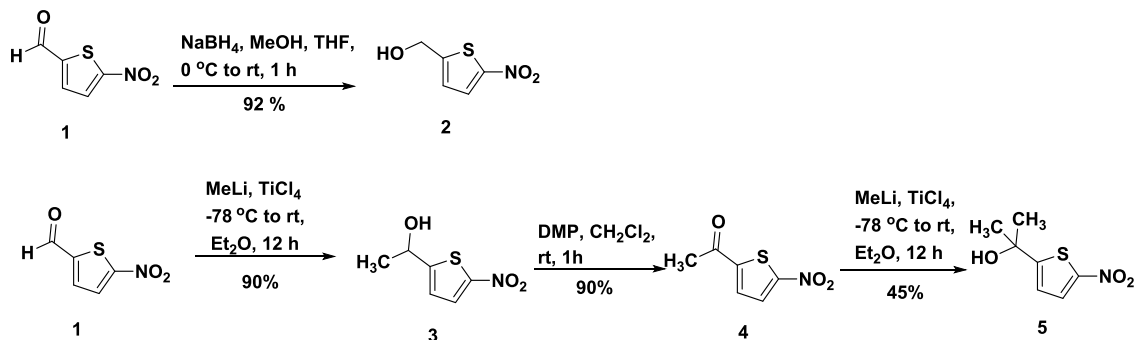
Introduction

In this chapter, synthetic efforts towards several nitro-aromatic triggers are discussed including nitrothiophene, nitroimidazole, nitrofuran and nitrobenzyl triggers. The synthesis of these triggers in the Pinney Research Group (Baylor University) supported the preparation towards bioreductively activatable product conjugates (BAPCs) of phenstatin, a potent small-molecule inhibitor of tubulin polymerization. In addition, the synthesis towards a *nor*-methylnitrothiophene-OXi8006 BAPC and a *gem*-dimethylnitrobenzyl 3-bromopyruvate BAPC are also described.

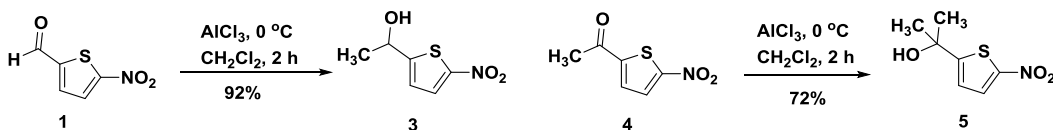
Synthesis of Bioreductive Triggers

The *nor*-methyl nitrothiophene trigger **2** was prepared in good yield through sodium borohydride reduction of aldehyde **1**.⁸¹ However, synthetic routes towards the *gem*-dimethyl nitrothiophene trigger **5** by Davis and his coworkers generated the trigger in very low yield (< 8%).^{81,82} To overcome this problem, direct methylation of ketone **4** was investigated. Methylation conditions described by Reetz et al. and adopted by us in the synthesis of nitrobenzyl triggers (described later in this chapter) provided a new

synthetic route towards both *mono*- and *gem*-dimethyl nitrothiophene triggers in good yields.¹⁶¹ Aldehyde **1** was reacted with methyllithium and titanium tetrachloride to generate the secondary alcohol **3** in 90% yield, which was oxidized by Dess-Martin periodinane to provide ketone **4**. Further methylation of compound **4** afforded the targeted *gem*-dimethyl nitrothiophene trigger **5** in 45% yield (Scheme 3.1). Discussion with Dr. Peter Davis and further investigation led to the discovery that trimethylaluminium might be a more efficient methylating agent in this type of reaction, and indeed the use of trimethylaluminium improved the yields of aldehyde **1** and ketone **3** to 92% and 73%, respectively (Scheme 3.2).



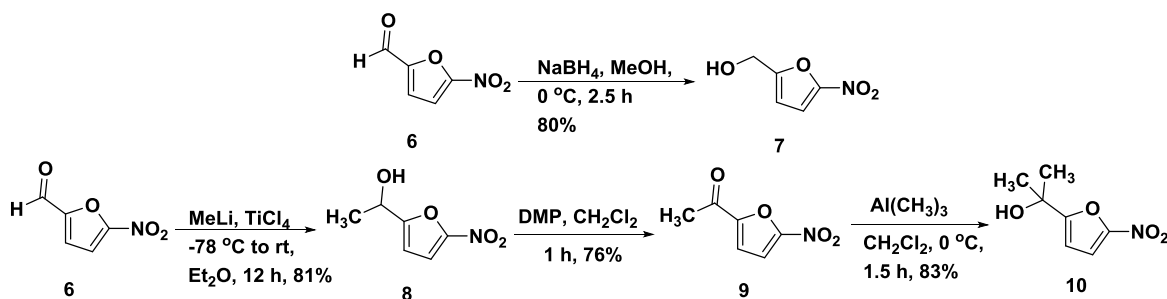
Scheme 3.1. Synthesis of Nitrothiophene Triggers^{81,161}



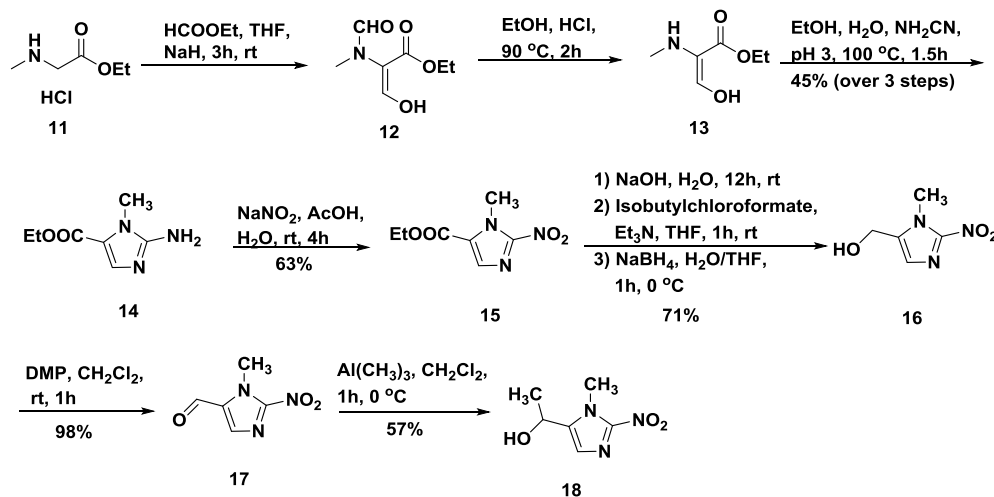
Scheme 3.2. Alternative Route towards Nitrothiophene Triggers **3** and **5**⁸²

The synthetic route towards the nitrothiophene bioreductive triggers was based on the modified route to the nitrothiophene triggers (Scheme 3.3).^{99,161} The *nor*-methyl nitrothiophene trigger **7** was prepared from the sodium borohydride reduction of aldehyde **6**.

The *mono*-methyl nitrofuran trigger **8** was prepared from methylation of **6** by titanium tetrachloride and methyllithium. Ketone **9** was synthesized from Dess-Martin oxidation of secondary alcohol **8** and followed by methylation to generate the dimethyl nitrofuran trigger **10**.



Scheme 3.3. Synthesis of the Nitrofuran Triggers^{82,99,102}



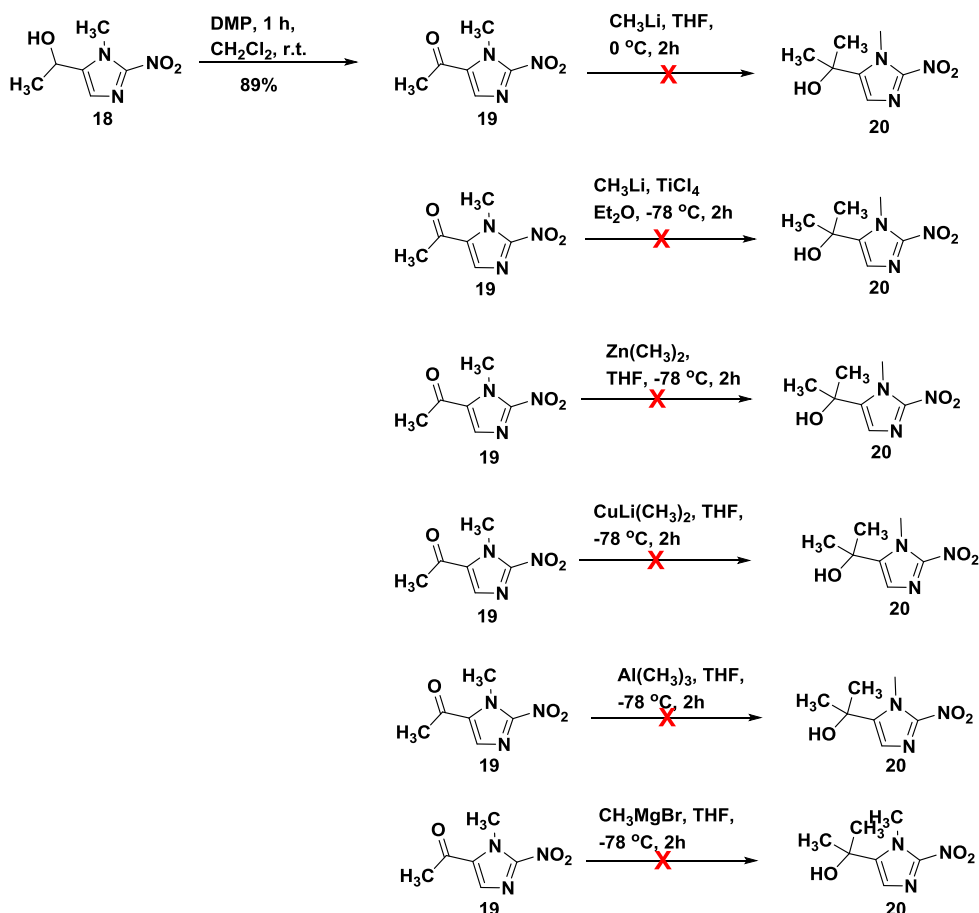
Scheme 3.4. Synthesis of the Nitroimidazole Triggers^{99,100,162}

To prepare the imidazole triggers, the first few attempts were carried out following a published route (patent) by Threshold Pharmaceuticals Inc.¹⁰⁰ However, these attempts resulted in poor yields. A similar route towards these imidazole triggers was published later by the Conway Group (Scheme 3.4)^{102,162} and was adopted in this study.

Sarcosine ethyl ester hydrochloride salt **11** was first formylated, then deformylated, and cyclized in order to generate ester **14** with a yield of 45% over the three steps.^{100,162}

Amine **14** was treated with sodium nitrite to generate nitro ester **15** through a diazonium intermediate, which was hydrolyzed and then reacted with isobutylchloroformate to form a carbonate, which was subsequently reduced to the *nor*-methyl nitroimidazole trigger

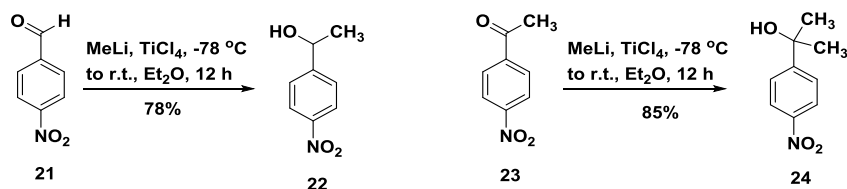
16.^{100,162} Alcohol **16** was subsequently oxidized by Dess-Martin periodinane to provide aldehyde **17**,^{100,162} which was methylated by trimethylaluminum to yield the *mono*-methyl nitroimidazole trigger **18**.⁸²



Scheme 3.5. Attempted Methylation of Nitroimidazole Ketone⁸²

Mono-methyl trigger **18** was oxidized to yield the ketone **19**. Several methylation strategies were investigated to generate the *gem*-dimethyl nitroimidazole trigger **20**, shown in Scheme 3.5. However, none of the strategies were successful and only starting material was recovered. To be best of our knowledge, only one synthetic route towards trigger **20** has been reported.¹⁶³ However, this procedure was not attempted in our laboratory due to the extremely low overall yield (< 1%) reported in the literature and the required large scale use of potassium cyanide and picric acid.¹⁶³

Preparation of *mono*-methyl nitrobenzyl trigger **21** and *gem*-dimethyl trigger **23** is shown in Scheme 3.6. Methyl lithium and titanium tetrachloride were utilized and gave good yields, while using methyl lithium directly significantly lowered the yields.



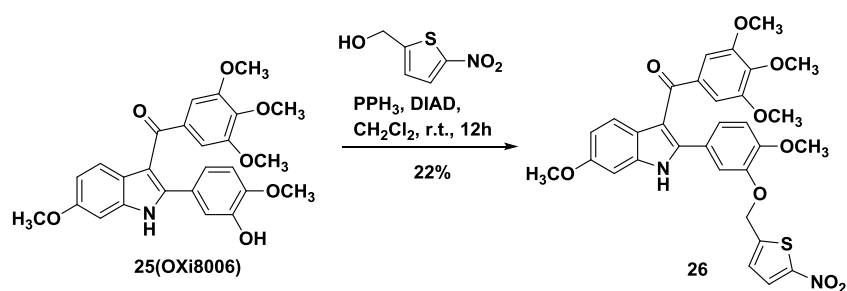
Scheme 3.6. Synthesis of the Nitrobenzyl Triggers¹⁶¹

Preparation of Nor-methylnitrothiophene-OXi8006 Bioreductively Activatable Prodrug Conjugates

OXi8006 is a leading indole-based, small-molecule inhibitor of tubulin polymerization ($IC_{50} = 1.1\ \mu\text{M}$) developed in the Pinney Research Laboratory (Baylor University) that demonstrates dual-mechanism of action functioning both as a cytotoxic agent and a VDA.^{55,160} A series of nitrothiophene-OXi8006 BAPCs were prepared by Dr. Matthew T. MacDonough a former graduate student in the Pinney Research Group. However, a compound in this series, *nor*-methylnitrothiophene-OXi8006 BAPC **26**,

required re-synthesis to provide a sample of sufficient quantity and purity to support to biological evaluation.

The parent compound OXi8006 was prepared through the procedure described in Chapter 2. OXi8006 was then subjected to a Mitsunobu reaction facilitated by diisopropyl azodicarboxylate (DIAD) and triphenylphosphine at room temperature. The reaction gave the desired BAPC **26** in 22% yield (Scheme 3.7).



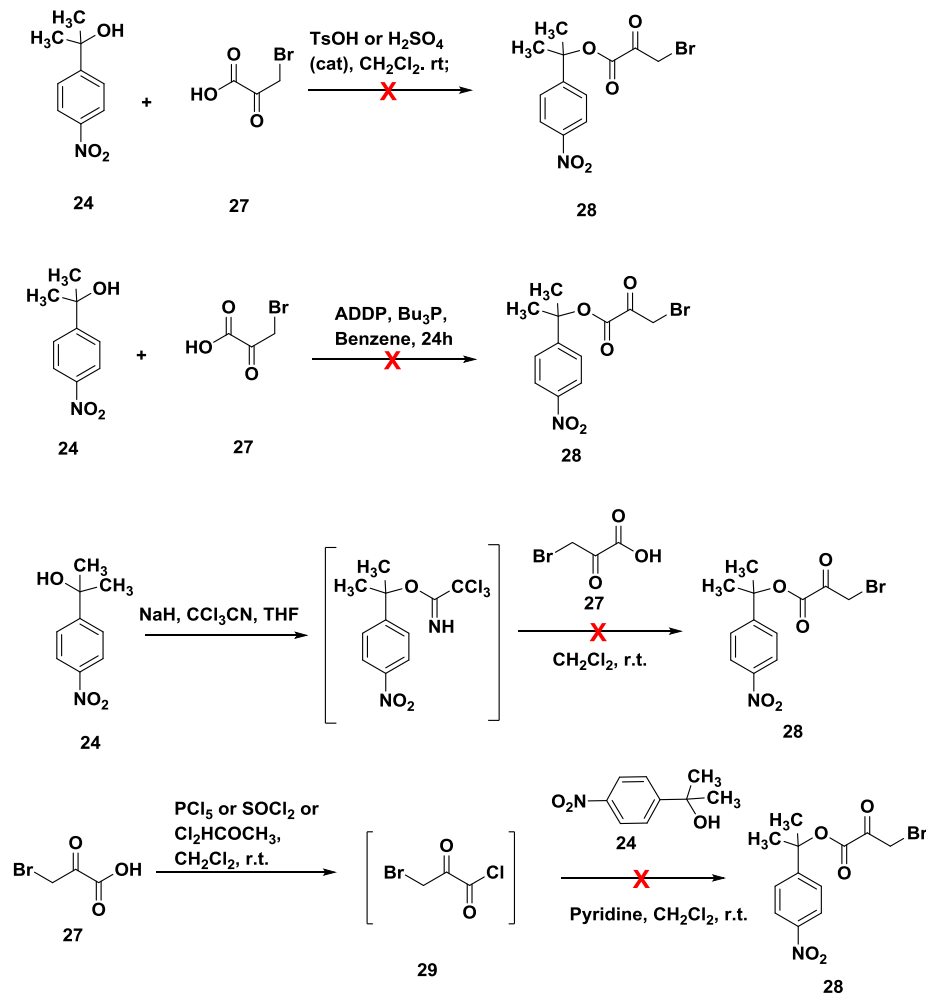
Scheme 3.7 Synthesis of BAPC **26**

Preparation of Bromopyruvate BAPC

The Warburg effect, which is defined as enhanced metabolism of glucose to lactic acid even under anaerobic conditions, has been a common observation in tumor regions for over 80 years.¹⁶⁴ 3-Bromopyruvic acid was demonstrated to be a glycolytic inhibitor which targets glyceraldehyde-3-phosphate dehydrogenase. Dr. Peter Davis proposed a series of BAPCs based on this antiglycolytic agent. Initial investigation regarding various synthetic approaches towards these bromopyruvate BAPCs was carried out by other members of the Pinney Research Group (Baylor University). Herein, attempts toward *gem*-dimethylnitrobenzyl-3-bromopyruvate **28** are described.

Retrosynthetic analysis of BAPC **28** revealed two distinct pathways to synthesize the target molecule. One pathway utilized an esterification reaction between 3-

bromopyruvic acid and *gem*-dimethylnitrobenzyl alcohol **24** as the last step. The other pathway concluded with bromination of the α -carbon of the carbonyl group to generate bromopyruvate **28**.

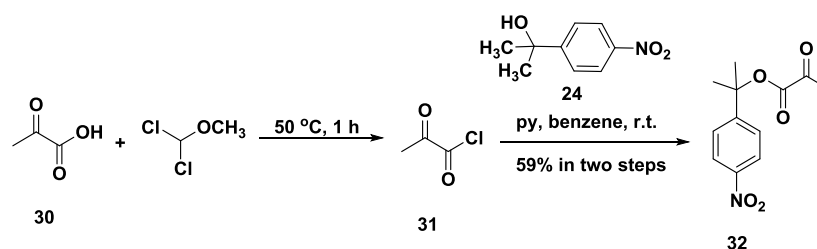


Scheme 3.8. Unsuccessful Attempts towards BAPC **28** Utilizing an Esterification Pathway

The first attempt of the coupling between tertiary alcohol **24** and bromopyruvic acid **27** utilized acid-catalyzed esterification with either *p*-toluenesulfonic acid (TsOH) or sulfuric acid. However, neither of these approaches generated the desired product. The coupling reaction was also carried out under Mitsunobu reaction conditions with 1,1'-

(azodicarbonyl)dipiperidine and diphenylphosphine as the catalyst. Unfortunately, this reaction was not successful and only the starting material alcohol was obtained. Another attempt involved the activation of tertiary alcohol **24** by trichloroacetonitrile, which did not generate the desired product.

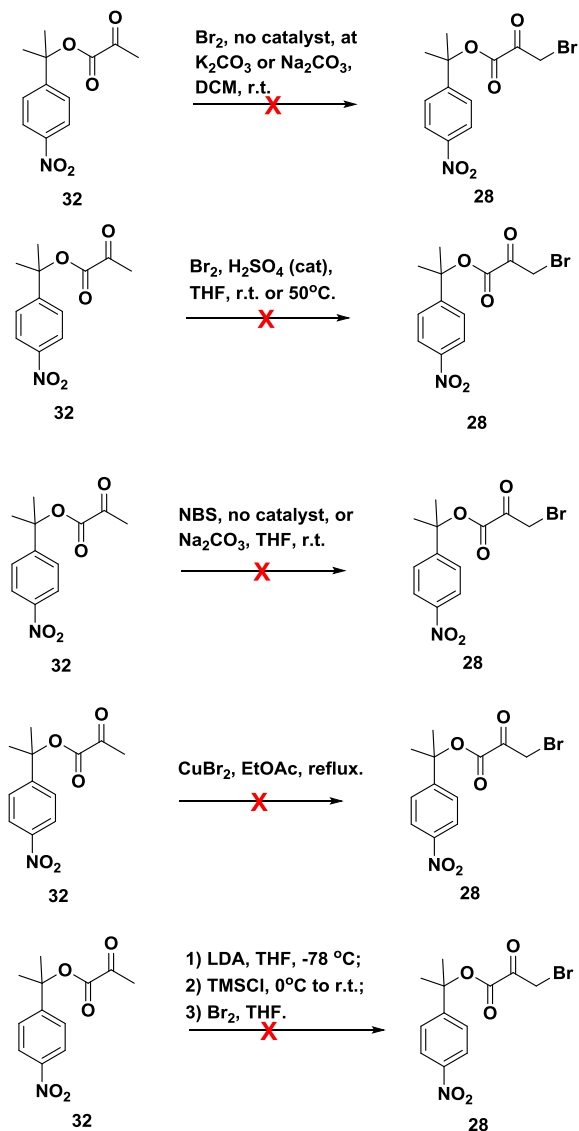
Conversion of bromopyruvic acid **27** to bromopyruvic chloride **29** was also attempted (Scheme 3.8). Chlorination was achieved by phosphorus pentachloride, thionyl chloride or 1,1-dichlorodimethyl ether. However, the reaction between chloride **29** and tertiary alcohol **24** did not generate the targeted BAPC. Pyruvic chloride **31**, synthesized by the treatment of pyruvic acid **30** with 1,1-dichlorodimethyl ether, was reacted with tertiary alcohol **24** to afford ester **32** (Scheme 3.9). With compound **32** in hand, a simple bromination to form compound **28** was proposed.



Scheme 3.9. Synthesis of Compound **32**

Pyruvate **32** was treated with bromine at room temperature, but unfortunately the desired product was not formed (Scheme 3.10). Inorganic bases, namely sodium carbonate or potassium carbonate, were employed as catalyst as well as sulfuric acid in separate attempts. However, none of these attempts were successful. *N*-Bromosuccinimide (NBS) and copper bromide were also evaluated as another bromination source with no success. Furthermore, lithium diisopropylamide (LDA) and

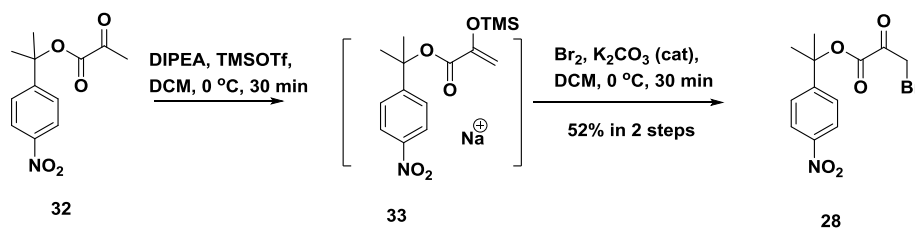
trimethylsilyl chloride (TMSCl) were applied to generate silyl enol ether **33**, followed by treatment with bromine. This route was also unsuccessful.



Scheme 3.10. Unsuccessful Attempts Towards BAPC **28** Utilizing a Bromination Pathway

Pyruvate **32** was also treated with *N,N*-diisopropylethylamine and trimethylsilyl trifluoromethanesulfonate at 0 °C for 30 minutes to form silyl enol ether **33**.¹⁶⁵ Bromine was then added to the resulting intermediate **33** with potassium carbonate as the catalyst

at 0 °C. This route (Scheme 3.11) successfully produced bromopyruvate BAPC **28** with a yield of 52% in two steps. However, final compound **28** was not stable. It partially decomposed while carefully stored under a nitrogen or argon atmosphere at -20 °C overnight.



Scheme 3.11. Successful Synthetic Route to Bromopyruvate BAPC **28**

Materials and Methods

General Experimental Methods

Dichloromethane, benzene, diethyl ether, methanol, ethyl acetate and tetrahydrofuran (THF) were used in their anhydrous forms, as obtained from the chemical suppliers. Reactions were performed under an inert atmosphere using nitrogen gas, unless specified. Thin-layer chromatography (TLC) plates (precoated glass plates with silica gel 60 F254, 0.25 mm thickness) were used to monitor reactions. Purification of intermediates and products was carried out with a Biotage isolera flash purification system using silica gel (200-400 mesh, 60 Å). Intermediates and products synthesized were characterized on the basis of their ^1H NMR (500 or 300 MHz) and ^{13}C NMR (125 or 75 MHz) spectroscopic data using a Bruker DPX 300 MHz instrument. Spectra were recorded in CDCl_3 or CD_3CN . All chemical shifts are expressed in ppm (δ), coupling

constants (J) are presented in Hz, and peak patterns are reported as broad (br), singlet (s), doublet (d), triplet (t), quartet (q), septet (sept), double doublet, (dd), and multiplet (m).

Purity of the final compounds was further analyzed at 25 °C using an Agilent 1200 HPLC system with a diode-array detector ($\lambda = 190\text{-}400$ nm), a Zorbax XDB-C18 HPLC column (4.6 mm - 150 mm, 5 μm), and a Zorbax reliance cartridge guard-column; method A: solvent A, acetonitrile, solvent B, H₂O; gradient, 50%A / 50%B to 100%A / 0%B over 0 to 40 min; post-time 10 min; flow rate 1.0 mL/min; injection volume 20 μL ; monitored at wavelengths of 210, 254, 230, 280, and 360 nm. Mass spectrometry was carried out under positive ESI (electrospray ionization) using a Thermo scientific LTQ Orbitrap Discovery instrument.

*(5-Nitrothiophen-2-yl)methanol 2*⁸¹

5-Nitrothiophene-2-carboxaldehyde **1** (1.00 g, 6.38 mmol) was dissolved in dry methanol (20 mL) in an ice bath (0 °C). NaBH₄ (0.270 g, 7.14 mmol) was added, and the reaction mixture was stirred for 2 hours. Ice was added and the solution was acidified to pH 7 with 3 M HCl. The reaction mixture was extracted with EtOAc, dried with Na₂SO₄, and evaporated under reduced pressure. Flash chromatography of the crude product using a pre-packed 50 g silica column [eluent: solvent A, EtOAc; solvent B, hexanes; gradient, 10% A/90% B (1 CV), 10% A/90% B \rightarrow 65% A/35% B (10 CV), 65% A/35% B (2 CV); flow rate 50.0 mL/min; monitored at 254 and 280 nm] afforded (5-Nitrothiophen-2-yl)methanol **2** (0.914 g, 5.74 mmol, 90% yield) as a brown oil.

¹H NMR (CDCl₃, 500 MHz): δ 7.84 (1H, d, $J = 4.1$ Hz), 6.95 (1H, dt, $J = 4.1, 1.0$ Hz), 4.90 (2H, d, $J = 5.2$ Hz), 2.15 (1H, t, $J = 5.8$ Hz).

¹³C NMR (CDCl₃, 126 MHz): δ 154.0, 150.6, 129.0, 123.5, 60.2.

*1-(5-Nitrothiophen-2-yl)ethan-1-ol 3*⁹⁹

5-Nitro-2-thiophenecarboxaldehyde **1** (1.00 g, 6.36 mmol) was dissolved in CH₂Cl₂ (50 mL) at 0 °C. Trimethylaluminum (2 M, 5.30 mL, 10.6 mmol) was added dropwise, and the reaction mixture was stirred for 2 hours. The reaction was quenched with HCl (1 M, 40 mL) and the layers were partitioned. The residue was extracted with CH₂Cl₂ (3 x 30 mL), and the combined organic phase was washed with brine (40 mL), dried over Na₂SO₄, and evaporated under reduced pressure. The crude product was purified by flash column chromatography using a pre-packed 100 g silica column [solvent A: EtOAc; solvent B: hexanes; gradient: 10%A / 90%B (1 CV), 10%A / 90%B → 70%A / 30%B (13 CV), 70%A / 30%B (2 CV); flow rate: 100 mL/min; monitored at 254 and 280 nm] to afford 1-(5-Nitrothiophen-2-yl)ethan-1-ol **3** (1.01 g, 5.85 mmol, 92%) as yellow-orange crystals.

¹H NMR (CDCl₃, 600 MHz): δ 7.82 (1H, d, *J* = 4.2 Hz), 6.91 (1H, dd, *J* = 4.2, 1.0 Hz), 5.14 (1H, qd, *J* = 6.4, 1.0 Hz), 2.14 (1H, s), 1.64 (3H, d, *J* = 6.5 Hz).

¹³C NMR (CDCl₃, 126 MHz): δ 160.0, 149.9, 129.1, 122.2, 66.3, 25.1.

*1-(5-Nitrothiophen-2-yl)ethan-1-one 4*⁹⁹

2-(1-Hydroxyethyl)-5-nitrothiophene **3** (1.04 g, 6.00 mmol) was dissolved in 70 mL CH₂Cl₂ at room temperature. Dess-Martin periodinane (3.82 g, 9.00 mmol) was added in portions to the solution, and the reaction mixture was stirred for 1 hour. Saturated solutions of sodium thiosulfate (50 mL) and NaHCO₃ (50 mL) were used to quench the reaction mixture. The layers were partitioned, and the residue was extracted with EtOAc (4 x 30 mL). The combined extracts were washed with brine, dried over Na₂SO₄, filtered, and concentrated under reduced pressure. The crude product was purified by flash

chromatography using a pre-packed 100 g silica column [solvent A: EtOAc; solvent B: hexanes; gradient: 10% A / 90% B (1 CV), 10% A / 90% B → 80% A / 20% B (13 CV), 80% A / 20% B (2 CV)]; flow rate: 100 mL/min; monitored at 254 and 280 nm] to afford 1-(5-Nitrothiophen-2-yl)ethan-1-one **4** (0.873 g, 5.10 mmol, 90% yield) as yellow-orange crystals.

¹H NMR (CDCl₃, 600 MHz): δ 7.89 (1H, d, *J* = 4.3 Hz), 7.58 (1H, d, *J* = 4.3 Hz), 2.60 (3H, s).

¹³C NMR (CDCl₃, 151 MHz): δ 190.4, 156.5, 148.7, 130.1, 128.3, 26.6.

*2-(5-Nitrothiophen-2-yl)propan-2-ol 5*⁹⁹

2-Acetyl-5-nitrothiophene **4** (0.500 g, 2.92 mmol) was dissolved in CH₂Cl₂ (20 mL) at 0 °C. Trimethylaluminum (2 M, 2.42 mL, 4.85 mmol) was added dropwise, and the reaction mixture was stirred for 2 hours. The reaction was quenched with HCl (1 M, 30 mL), and the layers were partitioned. The residue was extracted with CH₂Cl₂ (3 x 20 mL), and the combined organic extracts were washed with brine (20 mL), dried over Na₂SO₄, filtered and the solvent was evaporated under reduced pressure. The crude product was purified by flash column chromatography using a pre-packed 50 g silica column [solvent A: EtOAc; solvent B: hexanes; gradient: 10% A / 90% B (1 CV), 10% A / 90% B → 70% A / 30% B (13 CV), 70% A / 30% B (2 CV)]; flow rate: 50 mL/min; monitored at 254 and 280 nm] to afford 2-(5-Nitrothiophen-2-yl)propan-2-ol **5** (0.365 g, 2.13 mmol, 73%) as bright orange crystals.

¹H NMR (CDCl₃, 600 MHz): δ 7.80 (1H, d, *J* = 4.2 Hz), 6.89 (1H, d, *J* = 4.2 Hz), 1.69 (6H, s).

¹³C NMR (CDCl₃, 151 MHz): δ 163.5, 150.0, 128.8, 121.3, 71.9, 32.1.

*(5-Nitrofur-2-yl)methanol 7*⁸¹

5-Nitrofur-2-carbaldehyde **6** (4.00 g, 28.0 mmol) was dissolved in anhydrous methanol (80 mL) and cooled to 0 °C. NaBH₄ (1.17 g, 31 mmol) was added to the reaction mixture, which was stirred for 2.5 h. The reaction was quenched with an HCl solution (1 M, 40 mL) and extracted with EtOAc (3 x 50 mL). The combined organic layer was dried over Na₂SO₄ and concentrated under reduced pressure to afford a crude yellow oil. Purification by flash chromatography using a prepacked 100 g silica column [solvent A: EtOAc; solvent B: hexanes; gradient: 7%A / 93%B (1 CV), 7%A / 93%B → 60%A / 40%B (10 CV), 60%A / 40%B (2 CV); flow rate: 100 mL/min; monitored at 254 and 280 nm] afforded (5-nitrofur-2-yl)methanol **7** (3.23 g, 22.6 mmol, 80%) as a pale yellow oil.

¹H NMR (600 MHz, CDCl₃) δ 7.31 (1H, d, *J* = 3.6 Hz), 6.58 (1H, d, *J* = 3.6 Hz), 4.74 (2H, s), 2.09 (1H, s).

¹³C NMR (151 MHz, CDCl₃) δ 157.37, 151.92, 112.40, 110.61, 57.45.

*1-(5-Nitrofur-2-yl)ethan-1-ol 8*¹⁶¹

TiCl₄ (0.78 mL, 7.1 mmol) in Et₂O (35 mL) was treated with methyl lithium (4.4 mL, 1.6 M, 7.1 mmol) at -78 °C. The resulting solution was stirred for 1 h. A THF (10 mL) solution of 5-nitrofur-2-carbaldehyde **6** (0.500 g, 3.5 mmol) was added dropwise, and the reaction mixture was stirred for 24 h. Water (30 mL) was added and the resulting solution was extracted with EtOAc (3 x 30 mL), which was dried over Na₂SO₄ and concentrated to afford a crude brown oil. Purification by flash chromatography using a prepacked 25 g silica column [solvent A: EtOAc; solvent B: hexanes; gradient: 7%A / 93%B (1 CV), 7%A / 93%B → 60%A / 40%B (10 CV), 60%A / 40%B (2 CV); flow

rate: 75 mL/min; monitored at 254 and 280 nm] afforded 1-(5-nitrofur-2-yl)ethan-1-ol **8** (449 mg, 2.86 mmol, 81%) as a brown oil.

$^1\text{H NMR}$ (600 MHz, CDCl_3) δ 7.29 (1H, d, $J = 4.1$ Hz), 6.52 (1H, d, $J = 4.6$ Hz), 4.96 (1H, q, $J = 7.1$ Hz), 2.57 (1H, s), 1.61 (3H, d, $J = 6.8$ Hz).

$^{13}\text{C NMR}$ (151 MHz, CDCl_3) δ 161.27, 151.59, 112.51, 108.57, 63.66, 21.38.

1-(5-Nitrofur-2-yl)ethan-1-one 9

Dess-Martin periodinane (8.62 g, 20.4 mmol) was added to 1-(5-nitrofur-2-yl)ethan-1-ol **8** (3.20 g, 20.4 mmol) dissolved in CH_2Cl_2 (250 mL), and the reaction mixture was stirred for 1 h. The reaction was quenched with saturated solutions of sodium thiosulfate and NaHCO_3 , then extracted with CH_2Cl_2 (3 x 50 mL), which was washed with water and brine, dried with Na_2SO_4 , and evaporated under reduced pressure. Flash chromatography of the crude product using a prepacked 100 g silica column [eluent: solvent A, EtOAc; solvent B, hexanes; gradient, 7% A/93% B over 1.19 min (1 CV), 7% A/93% B \rightarrow 50% A/50% B over 13.12 min (10 CV), 50% A/50% B over 2.38 min (2 CV); flow rate 100.0 mL/min; monitored at 254 and 280 nm] yielded 1-(5-nitrofur-2-yl)ethan-1-one **9** (2.98 g, 19.2 mmol, 94%) as yellow solid.

$^1\text{H NMR}$ (600 MHz, CDCl_3) δ 7.38 (1H, d, $J = 3.8$ Hz), 7.28 (1H, d, $J = 3.7$ Hz), 2.61 (3H, s).

$^{13}\text{C NMR}$ (151 MHz, CDCl_3) δ 186.73, 151.91, 151.48, 116.79, 111.94, 26.27.

2-(5-Nitrofur-2-yl)propan-2-ol 10

1-(5-Nitrofur-2-yl)ethan-1-one **9** (3.00 g, 19.3 mmol) in CH_2Cl_2 (120 mL) was treated dropwise at 0 °C with trimethylaluminum (16.0 mL, 2.0 M, 32 mmol), and the

resulting yellow solution was stirred for 90 min at 0 °C. Sat. aq. NH₄Cl was added to the reaction mixture, which was extracted with CH₂Cl₂ (3 x 50 mL). The combined organic layers were dried over Na₂SO₄ and filtered, and the solvent was removed under reduced pressure to provide a yellow oil. Purification by flash chromatography using a prepacked 100 g silica column [solvent A: EtOAc; solvent B: hexanes; gradient: 7% A / 93%B (1 CV), 7%A / 93%B → 60%A / 40%B (10 CV), 60%A / 40%B (2 CV); flow rate: 1000mL/min; monitored at 254 and 280 nm] afforded 2-(5-nitrofuran-2-yl)propan-2-ol **10** (2.75 g, 16.1 mmol, 83%) as a yellow oil.

¹H NMR (600 MHz, CDCl₃) δ 7.27 (1H, d, *J* = 3.7 Hz), 6.49 (1H, d, *J* = 3.7 Hz), 2.36 (1H, s), 1.65 (7H, s).

¹³C NMR (151 MHz, CDCl₃) δ 164.05, 151.36, 112.55, 107.37, 69.30, 28.67.

Ethyl 2-amino-1-methyl-1H-imidazole-5-carboxylate **14**¹⁰¹

To a suspension of sarcosine ethyl ester **11** (4.00 g, 0.026 mol) in THF (90 mL) and ethyl formate (90 mL) was added NaH (60 % dispersion in mineral oil, 10.0 g, 0.25 mol) in several portions at room temperature. The reaction mixture was stirred for 3 hours, during this time a yellow suspension formed. The reaction mixture was concentrated and triturated with hexane (2 x 150 mL). The hexane was decanted and the resulting light tan solid **12** was dried in vacuo. Ethanol (80 mL) and concentrated aqueous HCl (16 mL) were added to the solid, and the suspension was heated to reflux for 2 hours. The reaction mixture was filtered while hot and the filter was rinsed with boiling ethanol (2 x 50 mL). The combined filtrate was concentrated to yield a brown oil **13**. The oil was diluted with ethanol (140 mL) and water (60 mL), and the pH of the solution was adjusted to 3 by using NaOH solution (2 M). Cyanamide (2.18 g, 0.052 mol)

was added, and the resulting solution was heated to reflux for 1.5 hours. After being cooled to room temperature, the reaction mixture was concentrated to approximately 1/8 of its original volume. Solid K_2CO_3 was added to adjust the pH of the concentrated reaction mixture to 8-9, resulting in the formation of a yellow precipitate. The solid was removed by filtration, washed with a K_2CO_3 solution (1 M, 1 x 20 mL) and water (2 x 20 mL) and dried to afford a pale yellow solid **14** (1.97 g, 12.0 mmol, 45% yield).

1H NMR ($CDCl_3$, 600 MHz): δ 7.45 (1H, s), 4.27 (2H, q, $J = 7.1$ Hz), 4.25 (2H, s), 3.68 (3H, s), 1.34 (3H, t, $J = 7.1$ Hz).

^{13}C NMR ($CDCl_3$, 151 MHz): δ 160.7, 151.9, 135.5, 119.1, 59.8, 30.6, 14.4.

Ethyl 1-methyl-2-nitro-1H-imidazole-5-carboxylate **15**^{100,101}

Aminoimidazole **14** (0.700 g, 4.14 mmol) in acetic acid (7.3 mL) was added dropwise to an aqueous solution of sodium nitrite (3.6 mL, 11 M). The solution was stirred at room temperature for 4 hours until no further N_2 was formed. The reaction mixture was extracted with CH_2Cl_2 (1 x 20 mL), washed with brine (1 x 20 mL) and a saturated aqueous solution of Na_2SO_3 (1 x 20 mL). The organic layer was then dried over Na_2SO_4 , filtered and concentrated to afford a crude yellow solid. Purification by flash chromatography using a pre-packed 25 g silica column [solvent A: EtOAc; solvent B: hexanes; gradient: 7%A / 93%B (4 CV), 7%A / 93%B \rightarrow 60%A / 40%B (10 CV), 60%A / 40%B (2 CV); flow rate: 70 mL/min; monitored at 254 and 280 nm] afforded Ethyl 1-methyl-2-nitro-1H-imidazole-5-carboxylate **15** (0.510 g, 2.60 mmol, 63% yield) as a yellow solid.

1H NMR ($CDCl_3$, 600 MHz): δ 7.74 (1H, s), 4.40 (2H, q, $J = 7.1$ Hz), 4.35 (3H, s), 1.41 (3H, t, $J = 7.1$ Hz).

^{13}C NMR (CDCl_3 , 151 MHz): δ 159.1, 147.5, 134.7, 126.3, 61.8, 35.4, 14.2.

(1-Methyl-2-nitro-1H-imidazol-5-yl)methanol **16**¹⁰⁰

A suspension of the nitroimidazole ethyl ester **15** (0.796 g, 4.00 mmol) in 0.75 M NaOH solution (16 mL) was stirred at room temperature overnight to give a clear light yellow solution. The pH of the reaction mixture was adjusted to 1 by adding concentrated HCl. The resulting solution was extracted with EtOAc (5 x 20 mL). The combined organic layer was dried over Na_2SO_4 , filtered and concentrated to afford a light yellow solid. The solid was dissolved in THF (8 mL) with triethylamine (0.880 mL, 6.30 mmol). Isobutylchloroformate (0.820 mL, 6.30 mmol) was added dropwise at $-40\text{ }^\circ\text{C}$, and the reaction mixture was stirred at room temperature for 1 hour. NaBH_4 (0.794 g, 21.0 mmol) was added to the solution, followed by dropwise addition of water (7 mL) over 1 hour while maintaining the temperature around $0\text{ }^\circ\text{C}$. The reaction mixture was extracted with Et_2O (3 x 20 mL), which was dried over Na_2SO_4 , filtered and the solvent was removed under reduced pressure. Purification by flash chromatography using a pre-packed 25 g silica column [solvent A: methanol; solvent B: CH_2Cl_2 ; gradient: 1%A / 99%B (4 CV), 1%A / 99%B \rightarrow 15%A / 85%B (10 CV), 15%A / 85%B (2 CV); flow rate: 75 mL/min; monitored at 254 and 280 nm] afforded *(1-Methyl-2-nitro-1H-imidazol-5-yl)methanol* **16** (0.449 g, 2.86 mmol, 71% yield) as a pale yellow solid.

^1H NMR (Methanol- D_4 , 600 MHz): δ 7.11 (1H, s), 4.68 (2H, s), 4.06 (3H, s).

^{13}C NMR (Methanol- D_4 , 151 MHz): δ 145.8, 137.9, 126.0, 53.2, 33.4.

*1-Methyl-2-nitro-1H-imidazole-5-carbaldehyde 17*⁹⁹

(1-Methyl-2-nitro-1H-imidazol-5-yl)methanol **16** (359 mg, 2.28 mmol) was dissolved in CH₂Cl₂ (10 mL). Dess–Martin periodinane (1.16 g, 2.74 mmol) was added and the reaction mixture was stirred for 1 hour at room temperature. Saturated solutions of NaHCO₃ (20 mL) and sodium thiosulfate (20 mL) were added to the reaction mixture, which was extracted with EtOAc (3 x 25 mL). The combined organic layers were dried over Na₂SO₄, filtered and the solvent was removed under reduced pressure. Purification by flash chromatography using a pre-packed 25 g silica column [solvent A: EtOAc; solvent B: hexanes; gradient: 12%A / 88%B (1 CV), 12%A / 88%B → 100%A / 0%B (10 CV), 100%A / 0%B (2 CV); flow rate: 75 mL/min; monitored at 254 and 280 nm] afforded 1-Methyl-2-nitro-1H-imidazole-5-carbaldehyde **17** (346 mg, 2.23 mmol, 98% yield) as a yellow solid.

¹H NMR (CDCl₃, 600 MHz): δ 9.94 (1H, s), 7.82 (1H, s), 4.36 (3H, s).

¹³C NMR (CDCl₃, 151 MHz): δ 180.4, 148.4, 139.4, 132.4, 35.6.

*1-(1-Methyl-2-nitro-1H-imidazol-5-yl)ethan-1-ol 18*⁹⁹

1-Methyl-2-nitro-1H-imidazole-5-carbaldehyde **17** (200 mg, 1.29 mmol) was dissolved in CH₂Cl₂ (10 mL) at 0 °C. Trimethylaluminum (2 M, 1.3 mL, 2.6 mmol) was added dropwise, and the reaction mixture was stirred for 2 hours. The reaction was quenched with HCl (1 M, 10 mL) and the layers were partitioned. The residue was extracted with CH₂Cl₂ (3 x 10 mL), and the combined organic phase was washed with brine (20 mL), dried over Na₂SO₄, and evaporated under reduced pressure. The crude product was purified by flash column chromatography using a pre-packed 25 g silica column [solvent A: EtOAc; solvent B: hexanes; gradient: 10%A / 90%B (1 CV), 10%A /

90%B → 70%A / 30%B (13 CV), 70%A / 30%B (2 CV); flow rate: 100 mL/min; monitored at 254 and 280 nm] to afford 1-(5-Nitrothiophen-2-yl)ethan-1-ol **18** (125 mg, 0.742 mmol, 57%) as a yellow solid.

¹H NMR (Acetone-D₆, 600 MHz): δ 7.07 (1H, s), 5.01 (1H, p, *J* = 6.2 Hz), 4.64 (1H, d, *J* = 6.0 Hz), 4.09 (3H, s), 1.63 (3H, d, *J* = 6.6 Hz).

¹³C NMR (Acetone-D₆, 151 MHz): δ 146.4, 141.6, 124.7, 60.4, 33.9, 21.1.

1-(4-Nitrophenyl)ethan-1-ol **20** ¹⁶¹

TiCl₄ (2.72 mL, 24.8 mmol) was slowly added (dropwise) to dry Et₂O (100 mL) in an acetone / dry ice bath (-78 °C). Methyllithium (15.5 mL, 25 mmol, 1.6 M) was then added dropwise slowly to the reaction mixture which was stirred for 1.5 h. 4-Nitrobenzaldehyde **19** (2.88g, 19.1 mmol) dissolved in Et₂O (140 mL) was added dropwise to the reaction mixture, which was stirred for 18 h. The reaction was quenched with water and extracted with CH₂Cl₂ (3 x 50 mL), which was washed with water and brine and dried over Na₂SO₄, and evaporated under reduced pressure. Flash chromatography of the crude product using a prepacked 100 g silica column [eluents: solvent A, EtOAc; solvent B, hexanes; gradient, 10% A/90% B (1 CV), 10% A/90% B → 80% A/20% B over (10 CV), 80% A/20% B (2 CV); flow rate 100.0 mL/min; monitored at 254 and 280 nm] yielded 1-(4-nitrophenyl)ethan-1-ol **20** (2.49 g, 14.9 mmol, 78%) as a yellow-orange oil.

¹H NMR (600 MHz, CDCl₃) δ 8.17 (2H, d, *J* = 8.7 Hz), 7.53 (2H, d, *J* = 8.6 Hz), 5.01 (1H, q, *J* = 6.5 Hz), 1.51 (3H, d, *J* = 6.6 Hz).

¹³C NMR (151 MHz, CDCl₃) δ 153.22, 147.09, 126.13, 123.71, 69.43, 25.44.

2-(4-Nitrophenyl)propan-2-ol **22** ¹⁶¹

TiCl₄ (3.02 mL, 27.6 mmol) was slowly added (dropwise) to dry Et₂O (100 mL) in an acetone / dry ice bath (-78 °C). Methylolithium (17.2 mL, 28 mmol, 1.6 M) was then added dropwise slowly to the reaction mixture, which was stirred for 1.5 h. 4-Nitroacetophenone **21** (3.50 g, 21.2 mmol) dissolved in Et₂O (150 mL) was added dropwise to the reaction mixture, which was stirred for 18 h. The reaction was quenched with water, and the mixture was extracted with CH₂Cl₂ (3 x 50 mL), which was washed with water and brine, dried over Na₂SO₄, and evaporated under reduced pressure. Flash chromatography of the crude product using a prepacked 100 g silica column [eluents: solvent A, EtOAc; solvent B, hexanes; gradient, 10% A/90% B (1 CV), 10% A/90% B → 60% A/40% B (10 CV), 60% A/40% B (2 CV); flow rate 100.0 mL/min; monitored at 254 and 280 nm] yielded 2-(4-nitrophenyl)propan-2-ol **22** (1.42 g, 7.84 mmol, 37%) as an orange oil.

¹H NMR (600 MHz, CDCl₃) δ 8.16 (2H, d, *J* = 8.9 Hz), 7.65 (2H, d, *J* = 8.9 Hz), 1.61 (7H, s).

¹³C NMR (151 MHz, CDCl₃) δ 156.52, 146.64, 125.51, 123.45, 72.49, 31.69.

(6-methoxy-2-(4-methoxy-3-((5-nitrothiophen-2-yl)methoxy)phenyl)-1H-indol-3-yl)(3,4,5-trimethoxyphenyl)methanone **26**

To a clean, dry round-bottom flask, nitrothiophenyl alcohol **2** (0.14 g, 0.90 mmol) was dissolved in CH₂Cl₂ (10 mL). Compound **25** (0.47 g, 1.0 mmol) and PPh₃ (0.46 g, 1.8 mmol) were added and the solution was stirred for 5 min. Diisopropylazodicarboxylate (DIAD) (0.24 mL, 1.2 mmol) was added dropwise and the reaction mixture was stirred for 12 h. The dichloromethane was removed under reduced

pressure and the crude mixture was subjected to flash column chromatography using a pre-packed 50 g silica gel column [solvent A, EtOAc, solvent B, hexanes; gradient 15%A / 85%B (4 CV), 15%A / 85%B → 100%A / 0%B (8 CV), 100%A / 0%B (7.2 CV)]; flow rate, 40 mL/min; monitored at 254 and 280 nm]. BAPC **26** (0.080 g, 0.11 mmol, 13%) was isolated as a yellow solid.

¹H NMR (CDCl₃, 500 MHz): δ 8.62 (br s, 1H, NH), 7.81 (d, *J* = 9.5 Hz, 1H, ArH), 7.78 (d, *J* = 4.0 Hz, 1H, ArH), 7.10 (dd, *J* = 8.0 Hz, *J* = 2.0 Hz, 1H, ArH), 6.99 (s, 2H, ArH), 6.95 (d, *J* = 4.0 Hz, 1H, ArH), 6.89 (m, 2H, ArH), 6.85 (d, *J* = 2.0 Hz, 1H, ArH), 6.81 (d, *J* = 8.0 Hz, 1H, ArH), 4.91 (s, 2H, CH₂), 3.85 (s, 3H, OCH₃), 3.83 (s, 3H, OCH₃), 3.82 (s, 3H, OCH₃), 3.67 (s, 6H, OCH₃).

¹³C NMR (CDCl₃, 125 MHz): δ 192.0, 157.5, 152.8, 151.8, 150.6, 148.1, 147.0, 141.8, 141.6, 136.5, 134.9, 128.5, 125.1, 124.9, 123.1, 122.9, 122.5, 117.3, 113.0, 111.94, 111.87, 107.5, 94.7, 66.9, 61.1, 56.2, 56.1, 55.8.

HPLC: 15.21 min.

HRMS (ESI⁺): *m/z* calculated for C₃₁H₂₉N₂O₉S [M+H]⁺ 605.1588, found 605.1587.

2-(4-nitrophenyl)propan-2-yl 2-oxopropanoate 32

To a round bottom flask (50-mL) with pyruvic acid **30** (1.2 mL, 17 mmol) was added (dropwise) 1,1-dichloromethyl ether (1.5 mL, 17 mmol). The reaction mixture was warmed up to 50 °C for 1.5 h and then was added (dropwise) to a benzene solution (50 mL) of 2-(4-nitrophenyl)propan-2-ol **22** (1.24 g, 6.82 mmol) and pyridine (2.5 mL, 34 mmol) at 0 °C. The mixture was stirred from 0 °C to room temperature overnight. The reaction was quenched with water, and the mixture was extracted with ethyl acetate (3 x

50 mL), which was washed with water and brine, dried over Na₂SO₄, and evaporated under reduced pressure. Flash chromatography of the crude product using a prepacked 50 g silica column [eluents: solvent A, EtOAc; solvent B, hexanes; gradient, 5% A/95% B (1 CV), 5% A/95% B to 40% A/60% B (10 CV), 40% A/60% B (2 CV); flow rate 100.0 mL/min; monitored at 254 and 280 nm] yielded 2-(4-nitrophenyl)propan-2-yl 2-oxopropanoate **32** (1.01 g, 4.01 mmol, 59%) as a tan solid.

¹H NMR (600 MHz, Chloroform-*d*) δ 8.24 (d, *J* = 8.8 Hz, 2H), 7.58 (d, *J* = 8.8 Hz, 2H), 2.45 (s, 3H), 1.91 (s, 6H).

¹³C NMR (151 MHz, Chloroform-*d*) δ 192.0, 159.7, 151.5, 147.2, 125.4, 123.9, 83.6, 28.0, 26.4.

*2-(4-nitrophenyl)propan-2-yl 3-bromo-2-oxopropanoate 28*¹⁶⁵

To a dry round bottom flask with 2-(4-nitrophenyl)propan-2-yl 2-oxopropanoate **32** (250 mg, 1.02 mmol) in dichloromethane (5 mL) at 0 °C under argon, diisopropylethylamine (0.21 mL, 1.2 mmol) and trimethylsilyl trifluoromethanesulfonate (0.22 mL, 1.2 mmol) were added. The reaction mixture was stirred at 0 °C for 30 minutes. Potassium carbonate (7.1 mg, 0.051 mmol) was added, followed by the addition of bromine (30 μL, 0.6 mmol) in dichloromethane (1 mL) solution. The resulting solution was stirred at 0 °C for an additional 30 min. The reaction was then quenched with saturated sodium thiosulfate solution, and the mixture was extracted with dichloromethane (3 x 50 mL), which was washed with water and brine, dried over Na₂SO₄, and evaporated under reduced pressure. Flash chromatography of the crude product using a prepacked 50 g silica column [eluents: solvent A, EtOAc; solvent B, hexanes; gradient, 7% A/93% B (1 CV), 7% A/93% B to 60% A/40% B (10 CV), 60%

A/40% B (2 CV); flow rate 100.0 mL/min; monitored at 254 and 280 nm] yielded 2-(4-nitrophenyl)propan-2-yl 3-bromo-2-oxopropanoate **28** (170 mg, 0.520 mmol, 52%) as a tan solid.

¹H NMR (600 MHz, Chloroform-*d*) δ 8.25 (d, $J = 8.8$ Hz, 2H), 7.60 (d, $J = 8.8$ Hz, 2H), 4.26 (s, 2H), 1.94 (s, 3H).

¹³C NMR (151 MHz, Chloroform-*d*) δ 184.6, 158.4, 150.9, 147.3, 125.5, 123.9, 84.8, 77.3, 77.0, 76.8, 30.2, 28.1.

HRMS (ESI⁺): m/z calculated for C₁₂H₁₂BrNNaO₅ [M+Na]⁺ 351.9791, found 351.9792.

CHAPTER FOUR

Targeting Tumor-Associated Hypoxia with Bioreductively Activatable Prodrug Conjugates Derived from Dihydronaphthalene and Benzosuberene-Based Inhibitors of Tubulin Polymerization

This chapter will be submitted to a peer reviewed journal with the following title and author list: “Targeting Tumor Hypoxia with Bioreductively Activatable Prodrug Conjugates Derived from Dihydronaphthalene, and Benzosuberene-Based Vascular Disrupting Agents” Zhe Shi, Rajsekhar Guddneppanavar, Blake A. Winn, Clinton S. George, Tracy E. Strecker, Jeni Gerberich, Alex Winters, Elisa Lin, Casey J. Maguire, Jacob Ford, Ernest Hamel, David J. Chaplin, Ralph P. Mason, Mary Lynn Trawick, Kevin G. Pinney.

The author Zhe Shi contributed to this manuscript through synthesizing four of the eight BAPCs reported in this manuscript and full characterization of all eight final compounds including NMR, HPLC and HRMS. In addition, Zhe Shi made significant contributions to the preparation of the manuscript and the supporting material.

Abstract

A significant percentage of solid tumors are characterized with profound regions of hypoxia, which is a hallmark of cancer. While tumor-associated hypoxia is associated with challenges in effective external beam radiation therapy, it provides a unique opportunity for targeted cancer therapy. A promising strategy involves the selective release of potent anticancer agents facilitated through reductase-mediated cleavage of non-toxic bioreductively activatable prodrug conjugates (BAPCs) in regions of pronounced tumor-associated hypoxia. Previous studies in our laboratories resulted in a series of highly potent, small-molecule anticancer agents, including dihydronaphthalene

analogue **1** and benzosuberene analogue **2**, which were inspired by the molecular architecture of the natural products combretastatin A-4 (CA4), combretastatin A-1 (CA1), and colchicine that inhibit tubulin assembly into microtubules. Compounds **1** and **2** demonstrate dual-mechanism of action functioning as both potent anti-proliferative (cytotoxic) agents and promising vascular disrupting agents (VDAs) that selectively and irreversibly disrupt tumor-associated vasculature. A series of BAPCs was synthesized that incorporate anticancer agents **1** and **2** with nitro-bearing heteroaromatic triggers. In a preliminary evaluation of this series, several BAPCs produced positive hypoxia cytotoxicity ratios (GI₅₀ ratio normoxia/hypoxia) in the A549 human lung carcinoma cell line. One of these promising BAPCs, **13**, demonstrated vascular disrupting activity in a preliminary *in vivo* study in an orthotopic syngeneic breast tumor (4T1) mouse model as evidenced with bioluminescence imaging (BLI) and histology.

Introduction

Tumor-associated vasculature is aberrant in nature and is typically characterized by a chaotic vascular network and primitive blood vessel network,⁷ which fails to sufficiently rectify oxygen deficiency and results in regions of hypoxia. In addition, temporal opening and closing of blood vessel occlusion also leads to acute perfusion-limited hypoxia.^{86,166} Tumor-associated hypoxia plays an important role in tumor progression,^{83,87} and promotes cellular resistance to many types of radiotherapy and chemotherapy.⁸³⁻⁸⁵ However, in certain cases cytotoxic drugs are more effective under hypoxic conditions.⁸³ Tumor-associated hypoxia represents a promising target for the selective delivery of potent anticancer agents through a variety of prodrug strategies.

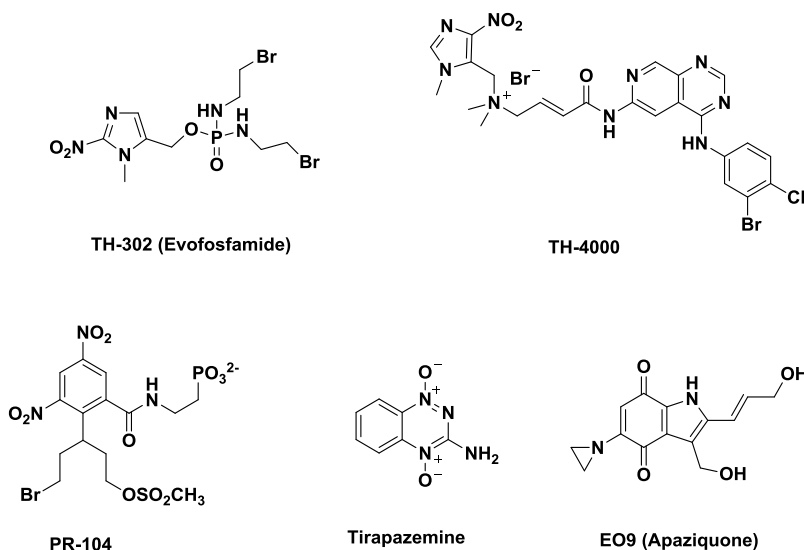


Figure 4.1. Structure of Selected Bioreductive Prodrugs

Bioreductively activated prodrug conjugates (BAPCs) also referred to as hypoxia-activated prodrugs (HAPs) facilitate the selective release of highly potent anticancer agents to tumors characterized with hypoxic fractions, and represent a promising investigative approach towards cancer therapy.^{66,83,89,167,168} The mechanism of these prodrugs involves enzymatic reduction through either one- or two- electron reductases resulting in selective release of cytotoxic anticancer agents.⁶⁶ A variety of chemical entities (triggers) are capable of undergoing enzymatic reduction to release their cytotoxic anticancer agents (effector molecules), including nitro(hetero)cyclic compounds, aromatic *N*-oxides, aliphatic *N*-oxides, quinones, and metal complexes.^{83,86,87} Clinically relevant prodrugs that undergo selective activation under hypoxia are shown in Figure 1. TH-302 is currently undergoing clinical trials in combination therapy with checkpoint inhibitor antibodies.¹⁶⁷ Despite significant progress and advances over the past 40+ years, prodrugs that target tumor-associated hypoxia have yet to reach FDA approval.

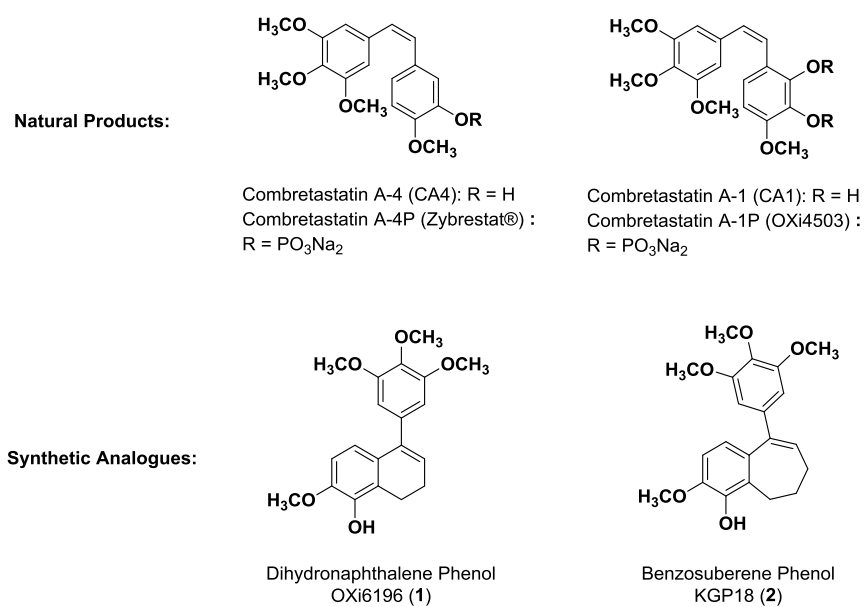


Figure 4.2. Representative Small-Molecule Inhibitors of Tubulin Polymerization.^{36,37,50–52}

In addition to hypoxia, the immature vasculature itself also represent a promising target for cancer therapy. The natural product combretastatin A-4 (CA4), originally isolated from African bush willow tree *Combretum caffrum*, is a potent inhibitor of tubulin assembly, which binds at the colchicine site.³⁷ CA4, along with another analogue in the combretastatin family combretastatin A-1 (CA1), demonstrates significant cytotoxicity (*in vitro*) against human cancer cell lines.³⁶ The necessity and challenge of improving water-solubility led to the development of their corresponding phosphate prodrug salts [combretastatin A-4P (Zybrestat®) and combretastatin A-1P (OXi4503)], which have been evaluated in clinical trials as vascular disrupting agents (VDAs).^{44,169} These VDAs induce significant morphological changes to the endothelial cells lining tumor-associated vasculature leading to microvessel occlusion and shutdown of blood flow, which restricts the supply of oxygen and nutrients, and leads to necrosis.

The potent antimitotic capability of CA4 inspired Davis and co-workers to prepare a series of BAPCs (Fig. 3) that utilize CA4 as the parent (effector) anticancer agent.^{81,82} A 5-nitrothienyl bio-reductive trigger was covalently bonded to CA4 through an ether linkage. These CA4-BAPCs were designed to release CA4 selectively in the hypoxic tumor microenvironment upon enzymatic reduction. We employed the same strategy to develop a series of BAPCs based on phenstatin,^{99,170} which is a functionalized benzophenone analogue prepared by Pettit and co-workers that mimics salient structural features of CA4. A subset of nitrothiophene, nitrobenzyl, nitrofuran, and nitroimidazole triggers was employed as the bio-reductive triggers in this study.^{99,102}

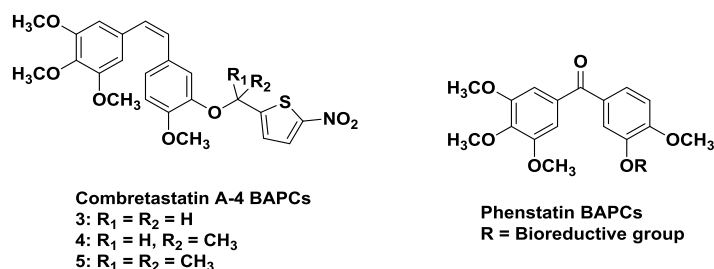
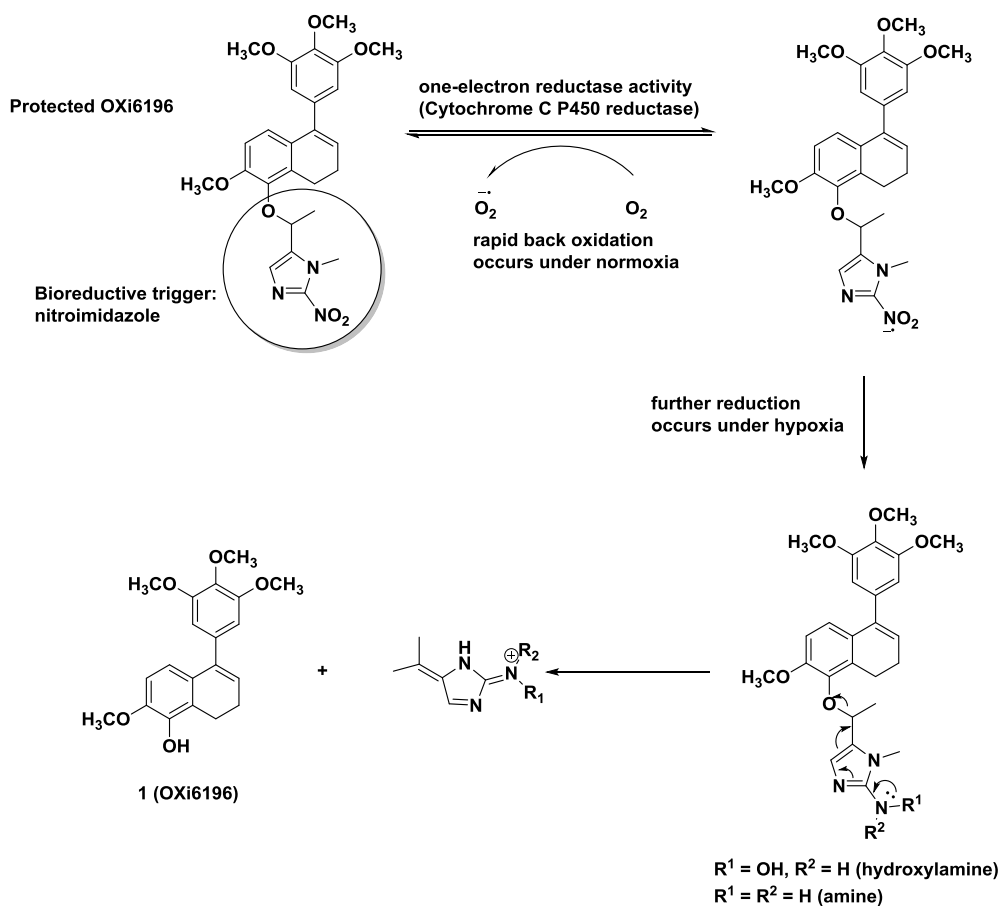


Figure 4.3. Previously Reported BAPCs based on Tubulin Binding Agents

A long-standing program in the design, synthesis, and biological evaluation of small-molecule inhibitors of tubulin polymerization resulted in our discovery and development of a wide-variety of molecules including dihydronaphthalene, benzosuberene analogues inspired, in part, by colchicine and CA4.⁵⁰⁻⁵² Utilizing a promising phenolic-based benzosuberene analogue (referred to as KGP18) and a corresponding dihydronaphthalene analogue (referred to as KGP03) as effector anticancer agents, we prepared a series of BAPCs bearing nitrothienyl and nitroimidazole

moieties as triggers, which are capable of undergoing reductase cleavage (Scheme 1) in hypoxic tumor fractions.

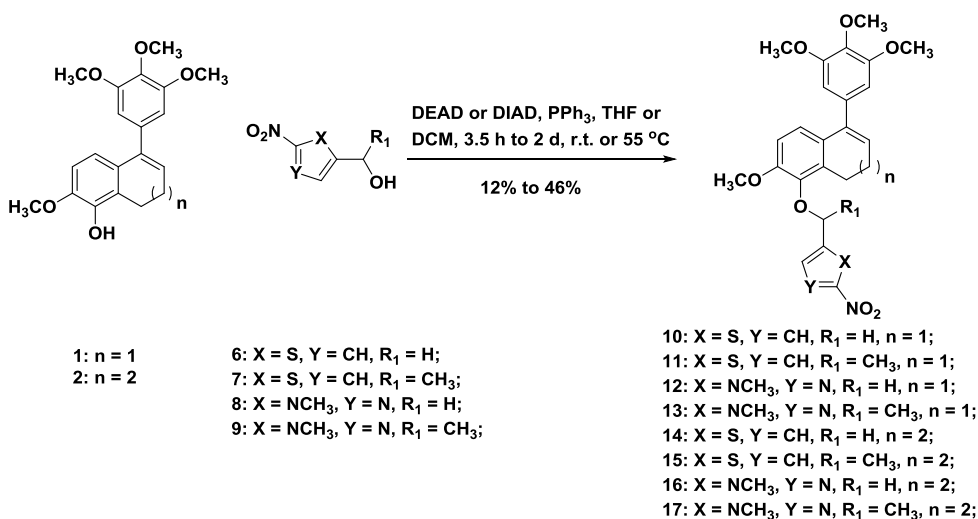


Scheme 4.1. Biological Reduction and Cleavage of BAPCs (Compound **13** as a Representative Example)

Chemistry

The synthetic strategy towards BAPCs **10** to **17** is shown in Scheme 2. Tubulin binding agents **1** (OXi6196) and **2** (KGP18) were prepared through newly developed methods published by our group.^{49–52} Bioreductive triggers **6–9** were synthesized following previously reported procedures.^{99,100,162} A Mitsunobu reaction was employed to facilitate incorporation of the bioreductive triggers with the parent agents to generate the requisite BAPCs in low to moderate yields (12% to 46%).^{81,171} Depending on the

reactivity of the nitro triggers involved in each reaction, a combination of triphenylphosphine with either diethyl azodicarboxylate (DEAD) or diisopropyl azodicarboxylate (DIAD) were used to generate the ether linkage. The order of reagent addition and the amount of solvent utilized also played important roles in the successful synthesis of these compounds.



Scheme 4.2. Synthetic Routes toward BAPC **10-17**.

Biological Evaluation

These BAPCs, as well as their parent anticancer agents, were evaluated for their ability to inhibit tubulin assembly and compete for the colchicine binding site (Table 1) through a collaboration with Dr. Ernest Hamel (National Cancer Institute). All the BAPCs were inactive ($IC_{50} > 20 \mu M$) as inhibitors of tubulin assembly. This is a desired attribute for these dihydronaphthalene and benzosuberene BAPCs. Ideally, these BAPCs will remain inactive until they undergo enzyme-mediated prodrug cleavage to generate their corresponding parent anticancer agents.

Table 4.1. Inhibition of Tubulin Assembly and Colchicine Binding.

Compound	Inhibition of tubulin assembly IC ₅₀ (μM) ± SD	Inhibition of colchicine binding % Inhibition ± SD 5 μM inhibitor
1	0.5	
2	1.4	
10	>20	9.2 ± 5
11	>20	9.4 ± 2
12	>20	9.6 ± 1
13	>20	4.8 ± 2
14	n.d.	n.d.
15	>20	4.7 ± 2
16	>20	6.1 ± 3
17	>20	25 ± 3

n.d. = not determined

The cytotoxicity (Table 4.2) of these BAPCs was also evaluated in A549 human lung carcinoma cell line through collaborative studies with the Trawick Group (Dr. Tracy Strecker) at Baylor University. These compounds were evaluated under both normoxic and hypoxic conditions utilizing the standard sulforhodamine B (SRB) assay to determine and quantify cell-based cytotoxicity. The ideal BAPC should demonstrate differential growth inhibition between normoxic and hypoxic conditions, showing enhanced cytotoxicity under hypoxic condition. Several BAPCs in this study demonstrated a positive hypoxic cytotoxicity ratio (HCR > 6), including compound **11**, **13** and **16**.

Table 4.2. *In Vitro* Potency and Hypoxia Cytotoxicity Ratio (HCR) of the BAPCs in the A549 Human Lung Carcinoma Cell Line

Compound	IC ₅₀ [oxic] (μM)±SD	IC ₅₀ [anoxic] (μM)±SD	HCR
TPZ	63.5	7.1	9.0
1	0.0066 ^b	n.d. ^c	n.d. ^c
2	0.000027 ^b	n.d. ^c	n.d. ^c
10	0.46	0.48	0.97
11	0.94	0.12	7.8
12	0.13	0.083	1.6
13	0.39	0.049	8.0
14	0.046	0.062	0.74
15	1.7	1.2	1.4
16	0.36	0.046	7.8
17	2.1	0.060	3.5

^a Average of $n \geq 3$ independent determinations

^b Values for standard SRB assay for cytotoxicity in A549 cells

^c n.d. = not determined

A preliminary *in vivo* study was carried out in collaboration with Dr. Ralph P. Mason (University of Texas Southwestern Medical Center) that utilized BALB/c mice bearing the syngeneic 4T1-luc breast cancer model with BAPC **13** to gauge initial tolerability and efficacy of this agent. 4T1 is a murine mammary tumor that arose spontaneously in an ageing BALB/C mouse and is considered to replicate many of the characteristics of human breast cancer.¹⁷² It is widely used in studies of chemotherapy, and several reports have used luciferase transfected clones to facilitate imaging of therapeutic response and metastasis.^{173–176}

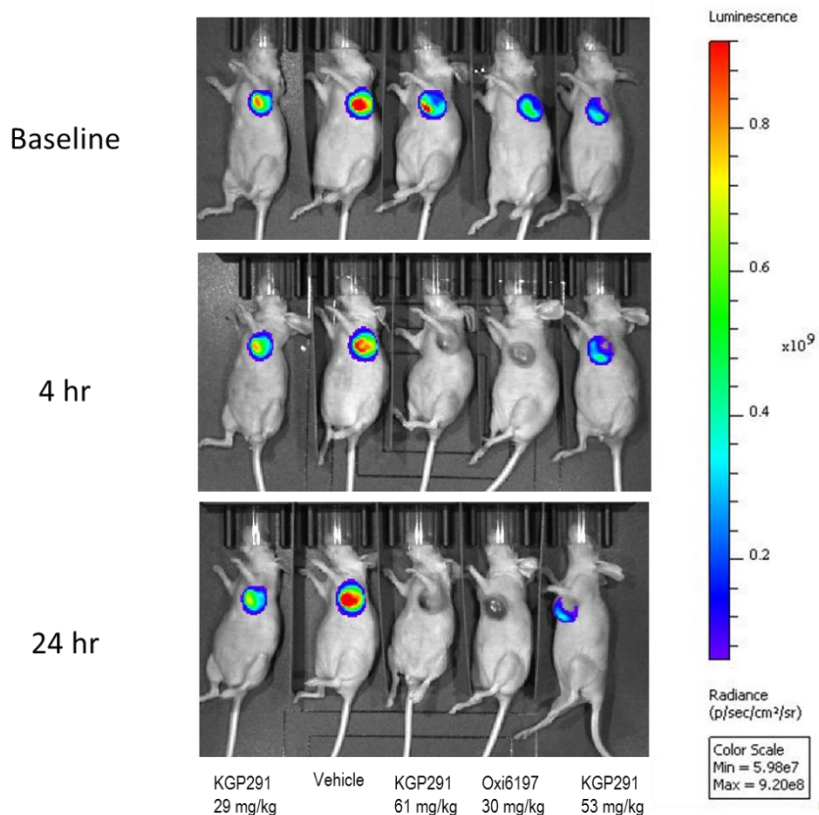


Figure 4.4. Bioluminescence imaging (BLI) of 4T1-luc Tumor Bearing Nude Mice at Various Times Following VDA (OXi6197) and BAPC (KGP291, compound **13**) Administration. Baseline shows mice at 20 min time point following administration of 120 mg/kg of luciferin subcutaneously to five athymic nude mice bearing orthotopic syngeneic 4T1-luc tumors growing in frontal mammary fat pad. Immediately following baseline BLI, mice were treated by IP injection as follows: (l to r) KGP291 (**13**) @ 29 mg/kg; vehicle (10%DMSO/90% sesame oil); KGP291 (**13**) @ 61 mg/kg; Oxi6197 @ 30 mg/kg in saline vehicle; KGP291 (**13**) @ 53 mg/kg. BLI was repeated 4 hrs and 24 hrs after treatment.

BLI was performed on a group of five mice. Three mice were treated with BAPC **13** at different doses, 29 mg/kg, 53 mg/kg and 61 mg/kg. Two mice served as controls, with one mouse treated with vehicle alone and another mouse treated with OXi6197 (30 mg/kg), the phosphate salt prodrug of compound **1**. Bioluminescent images are shown for the group of five mice at various time points (baseline to 24 hrs in Figure 5.4). Four hours following administration of BAPC **13**, one of three mice, which treated with the highest

dose showed a dramatic decrease in light emission following administration of fresh luciferin (Figures 5.4 and 5.5). At 24 h this tumor remained depressed. By comparison, CA4P caused a >99 % drop in signal within 4 h, which remained reduce up to 24 h. By contrast, the control mouse receiving vehicle alone showed relative stability up to 24 h.

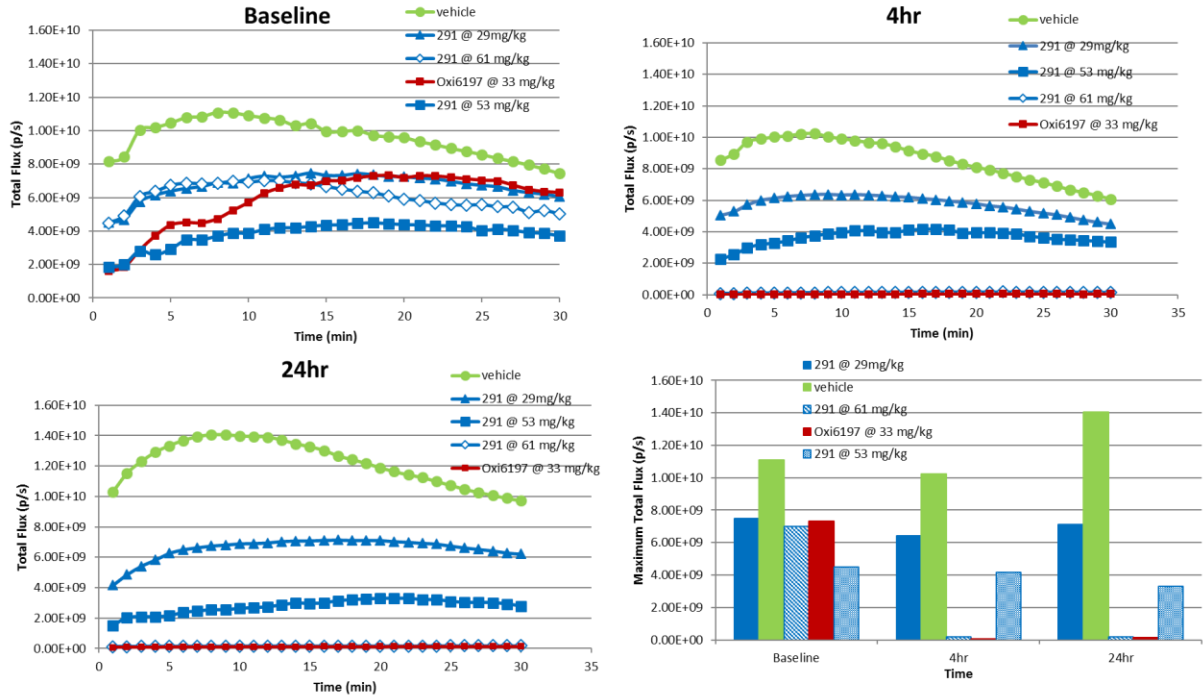


Figure 4.5. Dynamic Light Emission Time Courses with Respect to Vascular Disruption. Variation of signal intensity is shown at baseline, 4 hrs. and 24 hrs. Lines with red squares received OXi6197; green circles received vehicle; solid blue triangles was treated with KGP291 (13) @ 29 mg/kg; solid blue squares received KGP291 (13) @ 53 mg/kg and open blue diamonds received KGP291 @ 61 mg/kg. At baseline all tumors showed similar light emission kinetics (upper left). Four hrs. and 24 hrs. later (upper right and lower left, respectively), the tumors receiving Oxi6197 and the highest dose of KGP291 (13) showed substantially reduced signal, while the tumors receiving vehicle alone and two lower doses of KGP291 (13) showed little change. The histogram (lower right) shows the point of maximum light emission along the dynamic curve for each individual tumor at baseline, 4 hrs. and 24 hrs.

Conclusion

In this study, eight BAPCs based on tubulin binding agents dihydronaphthalene analogue **1** and benzosuberene analogue **2** were prepared to target tumor-associated hypoxia for selective delivery of anticancer agents. Among them BAPCs **11**, **13** and **16** produced positive HCRs (~8) in the initial assays. In a preliminary *in vivo* study, the monomethyl-nitroimidazole BAPC **11** demonstrated antivasular activity in an orthotopic syngeneic breast tumor mouse model (4T1/BALB/c) as evidenced through BLI.

Materials and Methods

General Experimental Methods

Dichloromethane, acetonitrile, dimethylformamide (DMF), methanol, ethanol, and tetrahydrofuran (THF) were used in their anhydrous forms, as obtained from the chemical suppliers. Reactions were performed under an inert atmosphere using nitrogen gas, unless specified. Thin-layer chromatography (TLC) plates (precoated glass plates with silica gel 60 F254, 0.25 mm thickness) were used to monitor reactions. Purification of intermediates and products was carried out with a Biotage isolera flash purification system using silica gel (200-400 mesh, 60 Å). Intermediates and products synthesized were characterized on the basis of their ¹H NMR (600 or 500 MHz) and ¹³C NMR (150 or 125 MHz) spectroscopic data using a Varian VNMRS 500 MHz or Bruker DPX 600 MHz instrument. Spectra were recorded in CDCl₃ or Aceton-d₆. All chemical shifts are expressed in ppm (δ), coupling constants (*J*) are presented in Hz, and peak patterns are reported as broad (br), singlet (s), doublet (d), triplet (t), quartet (q), septet (sept), double doublet, (dd), and multiplet (m).

Purity of the final compounds was further analyzed at 25 °C using an Agilent 1200 HPLC system with a diode-array detector ($\lambda = 190\text{-}400\text{ nm}$), a Zorbax XDB-C18 HPLC column (4.6 mm - 150 mm, 5 μm), and a Zorbax reliance cartridge guard-column; solvent A, acetonitrile, solvent B, H₂O; gradient, 50%A / 50%B to 100%A / 0%B over 0 to 30 min; post-time 10 min; flow rate 1.0 mL/min; injection volume 20 μL ; monitored at wavelengths of 210, 254, 230, 280, and 360 nm. Mass spectrometry was carried out under positive ESI (electrospray ionization) using a Thermo scientific LTQ Orbitrap Discovery instrument.

2-(((2-methoxy-5-(3,4,5-trimethoxyphenyl)-7,8-dihydronaphthalen-1-yl)oxy)methyl)-5-nitrothiophene **10**^{81,171,177}

Dihydronaphthalene **1** (0.340 g, 1.00 mmol), (5-nitrothiophen-2-yl)methanol **6** (0.080 g, 0.500 mmol), and triphenylphosphine (0.267 g, 1.00 mmol) were dissolved in THF (2.0 mL) at room temperature. DEAD (0.158 mL, 1.00 mmol) was added dropwise and the reaction mixture was stirred at 55 °C for 3.5 hours. The reaction was then cooled and the solvent was evaporated under reduced pressure. The crude product was purified by flash chromatography using a pre-packed 25 g silica column [solvent A: EtOAc; solvent B: hexanes; gradient 0%A / 100%B (1 CV), 0%A / 100%B \rightarrow 30%A / 70%B (13 CV), 30%A / 70%B (2 CV); flow rate: 75 mL/min; monitored at 254 and 280 nm] to afford 2-(((2-methoxy-5-(3,4,5-trimethoxyphenyl)-7,8-dihydronaphthalen-1-yl)oxy)methyl)-5-nitrothiophene **10** (0.040 g, 0.083 mmol, 17% yield) as a yellow oil.

¹H NMR (600 MHz, Acetone-*d*₆) δ 7.98 (d, $J = 4.1\text{ Hz}$, 1H), 7.24 (d, $J = 4.1\text{ Hz}$, 1H), 6.87 (d, $J = 8.6\text{ Hz}$, 1H), 6.84 (d, $J = 8.5\text{ Hz}$, 1H), 5.99 (t, $J = 4.7\text{ Hz}$, 1H), 5.31 (s,

1H), 3.91 (s, 2H), 3.81 (s, 3H), 3.76 (s, 1H), 2.87 – 2.82 (m, 2H), 2.29 (td, $J = 7.9, 4.7$ Hz, 2H).

^{13}C NMR (151 MHz, Acetone- d_6) δ 153.3, 151.8, 151.4, 149.8, 143.6, 139.5, 137.7, 136.3, 130.5, 128.8, 128.6, 125.9, 124.9, 122.1, 109.3, 106.1, 68.6, 59.7, 55.5, 55.2, 22.6, 21.1.

HRMS, m/z : observed 506.1244 [$\text{M} + \text{Na}$] $^+$, (calcd for $\text{C}_{25}\text{H}_{25}\text{NNaO}_7\text{S}^+$, 506.1244).

HPLC: 16.4 min, 100% pure at 254 nm.

2-(1-((2-methoxy-5-(3,4,5-trimethoxyphenyl)-7,8-dihydronaphthalen-1-yl)oxy)ethyl)-5-nitrothiophene **11**^{81,171,177}

Dihydronaphthalene **1** (0.342 g, 1.00 mmol), 1-(5-nitrothiophen-2-yl)ethan-1-ol **7** (0.087 g, 0.500 mmol), and triphenylphosphine (0.267 g, 1.00 mmol) were dissolved in THF (2.5 mL) at room temperature. DEAD (0.160 mL, 1.00 mmol) was added drop-wise and the reaction mixture was stirred at 55 °C for 3.5 hours. The reaction was then cooled and the solvent was evaporated under reduced pressure. The crude product was purified by flash chromatography using a pre-packed 25 g silica column [solvent A: EtOAc; solvent B: hexanes; gradient 0%A / 100%B (1 CV), 0%A / 100%B \rightarrow 30%A / 70%B (13 CV), 30%A / 70%B (2 CV); flow rate: 75 mL/min; monitored at 254 and 280 nm] to afford 2-(1-((2-methoxy-5-(3,4,5-trimethoxyphenyl)-7,8-dihydronaphthalen-1-yl)oxy)ethyl)-5-nitrothiophene **11** (0.115 g, 0.231 mmol, 46% yield) as a yellow solid.

^1H NMR (Acetone- D_6 , 500 MHz): δ 7.95 (1H, d, $J = 4.2$ Hz), 7.16 (1H, dd, $J = 4.2, 0.9$ Hz), 6.85 (1H, d, $J = 8.6$ Hz), 6.81 (1H, d, $J = 8.6$ Hz), 6.58 (2H, s), 5.98 (1H, t, J

= 4.7 Hz), 5.68 (1H, qd, $J = 6.4, 0.9$ Hz), 3.87 (3H, s), 3.81 (6H, s), 3.75 (3H, s), 2.78 (2H, ddd, $J = 10.8, 8.9, 6.7$ Hz), 2.34 – 2.14 (2H, m), 1.71 (3H, d, $J = 6.5$ Hz).

$^{13}\text{C NMR}$ (Acetone- D_6 , 126 MHz): δ 155.6, 153.3, 151.9, 150.7, 142.2, 139.6, 136.4, 130.9, 128.7, 128.6, 125.0, 124.2, 121.9, 109.3, 106.1, 106.1, 74.8, 59.7, 55.5, 55.1, 27.7, 21.7, 21.3.

HRMS, m/z : observed 520.1400 [$\text{M} + \text{Na}$] $^+$, (calcd for $\text{C}_{29}\text{H}_{27}\text{NNaO}_7\text{S}^+$, 520.1400).

HPLC: 18.7 min, 98.6% pure at 254 nm.

5-(((2-methoxy-5-(3,4,5-trimethoxyphenyl)-7,8-dihydronaphthalen-1-yl)oxy)methyl)-1-methyl-2-nitro-1H-imidazole **12**^{81,171,177}

Dihydronaphthalene **1** (0.363 g, 1.06 mmol), (1-methyl-2-nitro-1H-imidazol-5-yl)methanol **8** (0.200 g, 1.27 mmol), and DIAD (0.280 mL, 1.43 mmol) were dissolved in THF (70 mL) at room temperature. Triphenylphosphine (0.557 g, 2.12 mmol) was added and the reaction mixture was stirred for 2 days. The reaction solvent was evaporated under reduced pressure. The crude product was purified by flash chromatography using a pre-packed 50 g silica column [solvent A: EtOAc; solvent B: hexanes; gradient 10% A / 90%B (1 CV), 10%A / 90%B \rightarrow 80%A / 20%B (13 CV), 80%A / 20%B (2 CV); flow rate: 50 mL/min; monitored at 254 and 280 nm] to afford 5-(((2-methoxy-5-(3,4,5-trimethoxyphenyl)-7,8-dihydronaphthalen-1-yl)oxy)methyl)-1-methyl-2-nitro-1H-imidazole **12** (0.179 g, 0.371 mmol, 35% yield) as a yellow solid.

$^1\text{H NMR}$ (CDCl_3 , 600 MHz): δ 7.14 (1H, s), 6.85 (1H, d, $J = 8.5$ Hz), 6.69 (1H, d, $J = 8.5$ Hz), 6.54 (2H, s), 5.97 (1H, t, $J = 4.6$ Hz), 5.01 (2H, s), 4.24 (3H, s), 3.89 (3H, s), 3.85 (3H, s), 3.85 (6H, s), 2.76 (2H, t, $J = 7.9$ Hz), 2.31 (2H, td, $J = 7.8, 4.6$ Hz).

¹³C NMR (151 MHz, CDCl₃) δ 153.0, 151.6, 143.0, 139.4, 137.2, 136.4, 133.9, 130.7, 129.1, 129.0, 125.4, 122.6, 109.0, 107.2, 105.8, 63.0, 61.0, 56.2, 55.6, 34.6, 22.8, 21.1.

HRMS, *m/z*: observed 504.1740 [M + H]⁺, (calcd for C₂₅H₂₇N₃NaO₇⁺, 504.1741).

HPLC: 7.3 min, 96.2% pure at 254 nm.

5-(1-((2-methoxy-5-(3,4,5-trimethoxyphenyl)-7,8-dihydronaphthalen-1-yl)oxy)ethyl)-1-methyl-2-nitro-1H-imidazole **13**^{81,171,177}

Dihydronaphthalene **1** (0.200 g, 0.585 mmol), 1-(1-methyl-2-nitro-1H-imidazol-5-yl)ethan-1-ol **9** (0.120 g, 0.702 mmol), and DIAD (0.150 mL, 0.761 mmol) were dissolved in THF (60 mL) at room temperature. Triphenylphosphine (0.307 g, 1.17 mmol) was added to the reaction mixture and it was stirred for 2 days. The reaction solvent was evaporated under reduced pressure. The crude product was purified by flash chromatography using a pre-packed 50 g silica column [solvent A: EtOAc; solvent B: hexanes; gradient 10%A / 90%B (1 CV), 10%A / 90%B → 79%A / 21%B (13 CV), 79%A / 21%B (2 CV); flow rate: 50 mL/min; monitored at 254 and 280 nm] to afford compound **13** (0.0694 g, 0.140 mmol, 24%) as a yellow solid.

¹H NMR (CDCl₃, 600 MHz): δ 7.14 (1H, s), 6.77 (1H, d, *J* = 8.5 Hz), 6.62 (1H, d, *J* = 8.6 Hz), 6.47 (2H, s), 5.91 (1H, t, *J* = 4.6 Hz), 5.53 (1H, q, *J* = 6.6 Hz), 4.11 (3H, s), 3.82 (3H, s), 3.79 (3H, s), 3.78 (6H, s), 2.69 (2H, td, *J* = 9.3, 6.8 Hz), 2.27 – 2.14 (2H, m), 1.61 (3H, d, *J* = 6.6 Hz).

¹³C NMR (Acetone-D₆, 126 MHz): δ 153.3, 152.0, 141.6, 139.6, 138.8, 137.6, 136.3, 131.6, 128.7, 126.3, 125.0, 122.0, 109.2, 106.0, 68.9, 59.7, 55.5, 55.1, 34.1, 22.6, 21.7, 17.6.

HRMS, m/z : observed 496.2077 [M + H]⁺, (calcd for C₂₆H₂₉N₃NaO₇⁺, 496.2078).

HPLC: 10.0 min, 95.0% pure at 254 nm.

2-(((3-methoxy-9-(3,4,5-trimethoxyphenyl)-6,7-dihydro-5H-benzo[7]annulen-4-yl)oxy)methyl)-5-nitrothiophene **14**

(5-nitrothiophen-2-yl)methanol (0.129 g, 0.810 mmol) was dissolved in CH₂Cl₂ (7 mL). 3-methoxy-9-(3,4,5-trimethoxyphenyl)-6,7-dihydro-5H-benzo[7]annulen-4-ol (0.301 g, 0.844 mmol) and triphenylphosphine (0.435 g, 1.66 mmol) were added to the solution and allowed to stir until all reagents had dissolved. Azodicarbonyldipiperidine (0.333 g, 1.32 mmol) was then added to the solution. The solution was allowed to stir for 12 hours at room temperature. The solvent was removed under reduced pressure. The crude product purified on silica gel using isocratic 7.5% EtOAc: 92.5% hexanes as eluent. The solvent was removed under reduced pressure and the resultant product was crystallized using Et₂O to afford 2-(((3-methoxy-9-(3,4,5-trimethoxyphenyl)-6,7-dihydro-5H-benzo[7]annulen-4-yl)oxy)methyl)-5-nitrothiophene **14** (0.050 g, 0.010 mmol, 12% yield) as a yellow solid.

¹H NMR (CDCl₃, 500 MHz): δ 7.85 (1H, d, $J = 4.2$ Hz), 7.03 (1H, d, $J = 4.2$ Hz), 6.83 (1H, d, $J = 8.6$ Hz), 6.80 (1H, d, $J = 8.6$ Hz), 6.48 (2H, s), 6.34 (1H, t, $J = 7.3$ Hz), 5.22 (2H, d, $J = 0.5$ Hz), 3.92 (3H, s), 3.86 (3H, s), 3.81 (6H, s), 2.73 (2H, t, $J = 6.8$ Hz), 2.07 (2H, p, $J = 7.0$ Hz), 1.93 (2H, q, $J = 7.0$ Hz).

¹³C NMR (CDCl₃, 126 MHz): δ 152.9, 151.8, 151.1, 149.2, 143.8, 142.6, 138.2, 137.5, 135.9, 134.0, 128.2, 127.3, 126.1, 125.0, 109.4, 105.3, 69.4, 60.9, 56.2, 55.7, 34.4, 25.5, 24.4.

HPLC: Method C, 16.5 min

HRMS, m/z : observed 520.1394 [M + Na]⁺, (calcd for 520.1400).

2-(1-((3-methoxy-9-(3,4,5-trimethoxyphenyl)-6,7-dihydro-5H-benzo[7]annulen-4-yl)oxy)ethyl)-5-nitrothiophene **15**^{81,171,177}

1-(5-nitrothiophen-2-yl)ethan-1-ol **7** (0.650 g, 3.75 mmol) was dissolved in CH₂Cl₂ (40 mL). 3-methoxy-9-(3,4,5-trimethoxyphenyl)-6,7-dihydro-5H-benzo[7]annulen-4-ol **2** (1.50 g, 4.20 mmol) and triphenylphosphine (1.37 g, 7.29 mmol) were added to the solution and allowed to stir until all reagents had dissolved. Diisopropylazodicarboxylate (1.15 mL, 5.08 mmol) was then added to the solution. The solution was allowed to stir for 12 hours at room temperature. The solvent was removed under reduced pressure. The crude product was purified on silica gel using isocratic 5% EtOAc: 95% hexanes as eluent. The solvent was removed under reduced pressure and the resultant product was crystallized using Et₂O to afford 2-(1-((3-methoxy-9-(3,4,5-trimethoxyphenyl)-6,7-dihydro-5H-benzo[7]annulen-4-yl)oxy)ethyl)-5-nitrothiophene **15** (0.869 g, 1.70 mmol, 45% yield) as a yellow solid.

¹H NMR (CDCl₃, 500 MHz): δ 7.81 (1H, d, $J = 4.4$ Hz), 6.94 (1H, dd, $J = 4.2, 0.7$ Hz), 6.80 (1H, d, $J = 8.6$ Hz), 6.77 (1H, d, $J = 8.6$ Hz), 6.45 (2H, s), 6.32 (1H, t, $J = 7.1$ Hz), 5.62 (1H, qd, $J = 6.4, 0.7$ Hz), 3.87 (3H, s), 3.86 (3H, s), 3.80 (6H, s), 2.74 (1H, m), 2.64 (1H, m), 2.06 (1H, m), 1.91 (3H, m), 1.73 (3H, d, $J = 6.6$ Hz).

¹³C NMR (CDCl₃, 126 MHz): δ 155.3, 152.9, 151.1, 142.6, 142.4, 138.3, 137.4, 136.6, 134.0, 128.1, 127.3, 125.8, 123.3, 109.4, 105.2, 74.6, 60.9, 56.1, 55.6, 34.1, 25.6, 24.4, 21.8.

HRMS, m/z : observed 520.1394 [M + H]⁺, (calcd for 512.1737).

HPLC: 20.1 min, 99.0% pure at 254 nm.

5-(((3-methoxy-9-(3,4,5-trimethoxyphenyl)-6,7-dihydro-5H-benzo[7]annulen-4-yl)oxy)methyl)-1-methyl-2-nitro-1H-imidazole **16**^{81,171,177}

Benzosuberene analogue **2** (0.250 g, 0.702 mmol), (1-methyl-2-nitro-1H-imidazol-5-yl)methanol **8** (0.123 g, 0.842 mmol), and DEAD (0.144 mL, 0.913 mmol) were dissolved in CH₂Cl₂ (60 mL) at room temperature. Triphenylphosphine (0.368 g, 1.40 mmol) was added to the mixture and the reaction was stirred for 2 days. The reaction was evaporated under reduced pressure. The crude product was purified by flash chromatography using a pre-packed 50 g silica column [solvent A: EtOAc; solvent B: hexanes; gradient 10%A / 90%B (1 CV), 10%A / 90%B → 80%A / 20%B (13 CV), 80%A / 20%B (2 CV); flow rate: 50 mL/min; monitored at 254 and 280 nm] to afford 5-(((3-methoxy-9-(3,4,5-trimethoxyphenyl)-6,7-dihydro-5H-benzo[7]annulen-4-yl)oxy)methyl)-1-methyl-2-nitro-1H-imidazole **16** (0.143 g, 0.288 mmol, 41% yield) as an orange crystal.

¹H NMR (600 MHz, Chloroform-*d*) δ 7.15 (s, 1H), 6.84 (d, *J* = 8.5 Hz, 1H), 6.79 (d, *J* = 8.5 Hz, 1H), 6.46 (s, 2H), 6.34 (t, *J* = 7.3 Hz, 1H), 5.05 (s, 2H), 4.25 (s, 3H), 3.89 (s, 3H), 3.86 (s, 3H), 3.80 (s, 6H), 2.68 (t, *J* = 6.9 Hz, 2H), 2.07 – 1.99 (m, 2H), 1.93 (q, *J* = 7.1 Hz, 2H).

¹³C NMR (151 MHz, CDCl₃) δ 152.9, 151.1, 146.3, 142.5, 141.7, 138.6, 138.2, 137.5, 136.8, 134.3, 127.4, 126.7, 126.1, 109.2, 105.3, 68.7, 60.9, 56.2, 55.5, 34.7, 34.1, 25.6, 24.3, 18.4.

HRMS, *m/z*: observed 518.1898 [M + Na]⁺, (calcd for C₂₆H₂₉N₃NaO₇⁺, 518.1898).

HPLC: 10.7 min, 98.1% pure at 254 nm.

5-(1-((3-methoxy-9-(3,4,5-trimethoxyphenyl)-6,7-dihydro-5H-benzo[7]annulen-4-yl)oxy)ethyl)-1-methyl-2-nitro-1H-imidazole **17**^{81,171,177}

Benzosuberene analogue **2** (0.250 g, 0.702 mmol), 1-(1-methyl-2-nitro-1H-imidazol-5-yl)ethan-1-ol **9** (0.144 g, 0.842 mmol), and DIAD (0.179 g, 0.913 mmol) were dissolved in CH₂Cl₂ (60 mL) at room temperature. Triphenylphosphine (0.368 g, 1.40 mmol) was added to the mixture and the reaction was stirred for 2 days. The reaction was evaporated under reduced pressure. The crude product was purified by flash chromatography using a pre-packed 50 g silica column [solvent A: EtOAc; solvent B: hexanes; gradient 10%A / 90%B (1 CV), 10%A / 90%B → 80%A / 20%B (13 CV), 80%A / 20%B (2 CV); flow rate: 50 mL/min; monitored at 254 and 280 nm] to afford 5-(1-((3-methoxy-9-(3,4,5-trimethoxyphenyl)-6,7-dihydro-5H-benzo[7]annulen-4-yl)oxy)ethyl)-1-methyl-2-nitro-1H-imidazole **17** (0.122 g, 0.239 mmol, 34% yield) as an orange solid.

¹H NMR (600 MHz, Chloroform-*d*) δ 7.14 (s, 1H), 6.75 (d, *J* = 8.5 Hz, 1H), 6.71 (d, *J* = 8.5 Hz, 1H), 6.38 (s, 2H), 6.26 (t, *J* = 7.0 Hz, 1H), 5.57 (q, *J* = 6.6 Hz, 1H), 4.09 (s, 3H), 3.81 (s, 3H), 3.79 (s, 3H), 3.73 (s, 6H), 2.63 (dt, *J* = 12.6, 6.3 Hz, 1H), 2.54 (dt, *J* = 13.7, 6.8 Hz, 1H), 2.05 – 1.97 (m, 1H), 1.85 (m, 3H), 1.64 (d, *J* = 6.6 Hz, 3H).

¹³C NMR (151 MHz, CDCl₃) δ 152.9, 151.1, 146.3, 142.5, 141.7, 138.6, 138.2, 137.5, 136.8, 134.3, 127.4, 126.7, 126.1, 109.2, 105.3, 68.7, 60.9, 56.2, 55.5, 34.7, 34.1, 25.6, 24.3, 18.4.

HRMS, *m/z*: observed 532.2054 [M + Na]⁺, (calcd for C₂₇H₃₁N₃NaO₇⁺, 532.2503).

HPLC: 11.5 min, 97.5% pure at 254 nm.

Acknowledgements

The authors are grateful to the Cancer Prevention and Research Institute of Texas (CPRIT, Grant No. RP140399 to K.G.P., M.L.T., and R.P.M.), the National Cancer Institute of the National Institutes of Health (Grant No. 5R01CA140674 to K.G.P., M.L.T., and R.P.M.), and Mateon Therapeutics, Inc. (grant to K.G.P. and M.L.T.) for their financial support of this project. The content is solely the responsibility of the authors and does not necessarily reflect the official views of the National Institutes of Health. BLI was facilitated by the Southwestern Small Animal Imaging Resource supported in part by the NIH Comprehensive Cancer Center Grant P30 CA142543 and a Shared Instrumentation Grant 1S10 RR024757. The authors also thank Dr. Michelle Nemecek (Director) for the use of the shared Molecular Biosciences Center at Baylor University and Dr. Alejandro Ramirez (Mass Spectrometry Core Facility, Baylor University).

CHAPTER FIVE

Mechanistic Considerations in the Synthesis of 2-Aryl-Indole Analogues under Bischler-Mohlau Conditions

This chapter was published as: MacDonough, M. T.; Shi, Z.; Pinney, K. G. Mechanistic considerations in the synthesis of 2-aryl-indole analogues under Bischler–Mohlau conditions. *Tetrahedron Letters*, **2015**, *56*, 3624-3629.

The author Zhe Shi contributed to this manuscript through re-synthesis of the ^{13}C isotope labelled indole analogue and full characterization of this final compound including NMR, HPLC, HRMS and crystallization. In addition, Zhe Shi contributed a significant amount to the preparation of the supporting material and editing of the manuscript.

Abstract

Mechanistic insight into the pathway of the Bischler-Mohlau indole formation reaction is provided by isotopic labeling utilizing judicious incorporation of a ^{13}C atom within the α -bromoacetophenone analogue reactant. The resulting rearranged 2-aryl indole, isolated as the major product, located the ^{13}C isotope label at the methine carbon of the fused five-membered heterocyclic ring, which suggested that the mechanistic pathway of cyclization, in this specific example, required two equivalents of the aniline analogue reactant partner and proceeded through an imine intermediate rather than by direct formation of the corresponding 3-aryl indole accompanied by a concomitant 1,2-aryl shift rearrangement.

Introduction

In the context of a long-standing program focused on the design, synthesis, and biological evaluation of diversely functionalized small-molecule anticancer agents, a series of benzo[*b*]thiophene,^{56,57,178} benzo[*b*]furan, and indole-based^{153,154,179} analogues emerged as promising potential pre-clinical candidates (Fig. 5.1). These compounds were designed to function as inhibitors of tubulin polymerization (assembly) that bind to the colchicine site on the tubulin heterodimer and certain of these compounds demonstrated a dualistic mechanism of action functioning both as potent antiproliferative agents and as pronounced vascular disrupting agents (VDAs).¹⁸⁰ In each case, the heterocyclic fused ring was introduced synthetically through an efficient ring-closing step, and it proved intriguing to consider whether this reaction in the indole series of analogues mirrored that of the benzo[*b*]thiophene series or was mechanistically distinct.

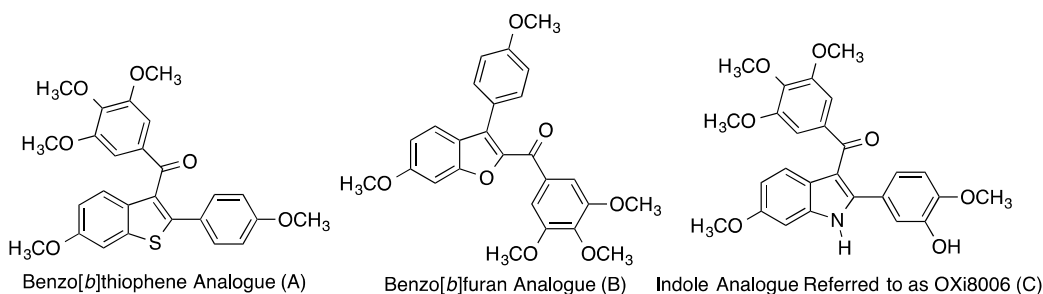
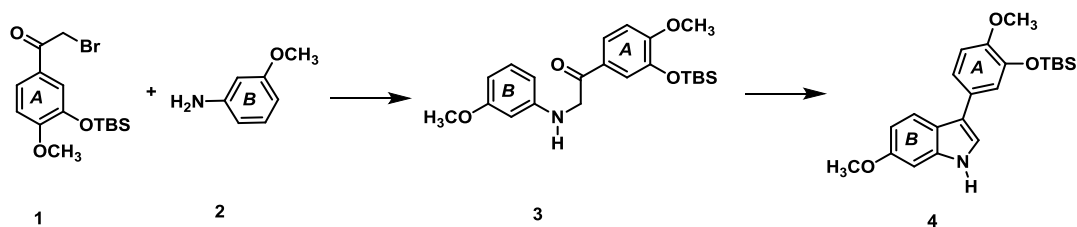


Figure 5.1. Representative Examples of Inhibitors of Tubulin Polymerization Incorporating Fused Heterocyclic Ring Systems: Benzo[*b*]thiophene (A); Benzo[*b*]furan (B); and Indole (C)

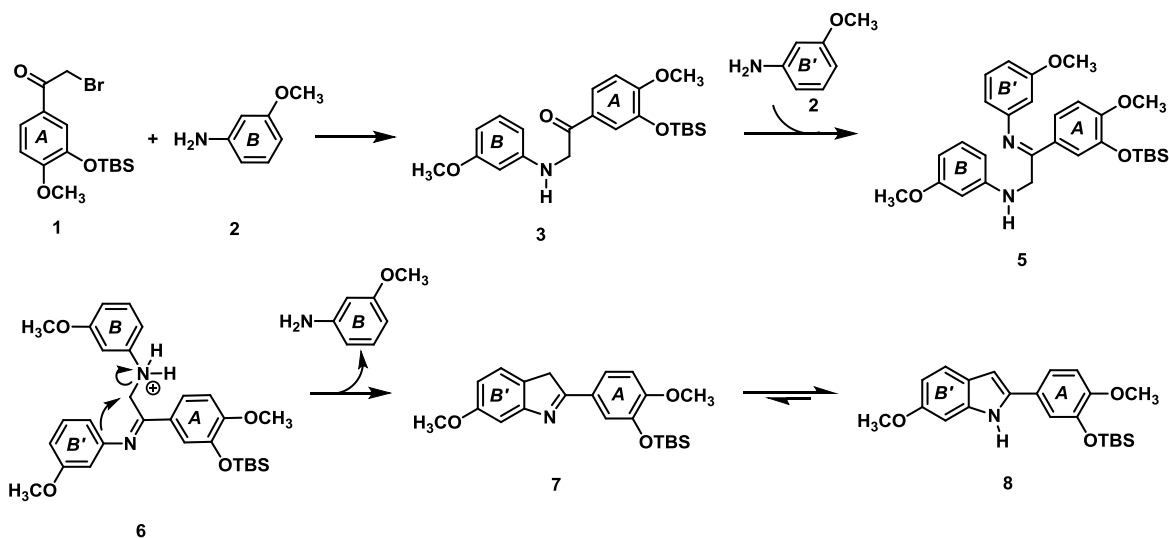
The indole core ring system continues to be utilized as an abundant molecular scaffold in medical chemistry¹⁸¹ and represent an important class of heterocycles. The mechanistic pathways and synthetic routes available towards the indole platform are well established and vary greatly.¹²¹ One established approach, referred to as the Fischer

indole synthesis, involves a [3,3]-sigmatropic rearrangement followed by closure to the fused five-membered ring. This method was first pioneered by Fischer in 1883¹⁸² and continues to be explored today.¹¹⁸ Another frequently utilized approach is the Bischler-Mohlau indole synthesis^{119,183} that involves the reaction between aniline analogues and α -halogenated ketone analogues and results in both 2-aryl and 3-aryl indole regioisomers. While the Bischler-Mohlau reaction^{120,184–188} accommodates a wide-range of functionalized α -bromoketones and aniline analogues as starting materials, low isolated yields and unpredictable regiochemistry¹⁸⁹ remain potentially problematic. The reaction is heavily substrate dependent (in terms of yield and regiochemical outcome) and modifications in reaction conditions, including microwave heating, can dramatically influence the overall process.¹⁸⁹ The perceived simplicity of the Bischler-Mohlau reaction somewhat disguises the complex mechanistic pathways which can lead to both 2-aryl and 3-aryl indole analogues. The indole product (2-aryl or 3-aryl) is dependent on one of several potential mechanistic pathways. These pathways were further investigated by Vara and co-workers by assessing the activation energies associated with intermediates and transition states.²⁶ Pathway A (Scheme 5.1) involves initial displacement of a bromine atom from 2-bromoacetophenone or an appropriately functionalized 2-bromoacetophenone analogue by aniline or an analogous aniline analogue. The pathway proceeds through intramolecular cyclization and subsequent re-aromatization to afford non-rearranged 3-aryl indole **4**.



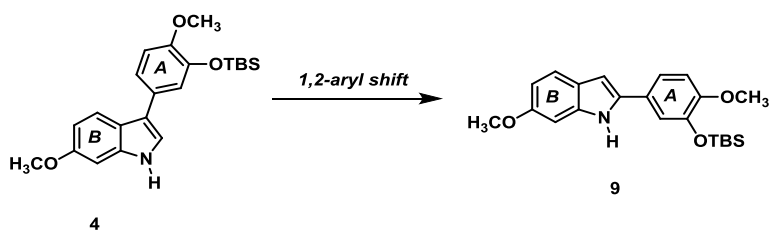
Scheme 5.1. Mechanistic Pathway A Associated with the Bischler-Mohrlau Reaction

A well-recognized competing Pathway B (Scheme 5.2), which most often is invoked as being predictive of the major product of the Bischler-Mohrlau indole synthesis, initiates in a similar fashion with the aniline analogue (3-methoxyaniline in this example) displacing the bromine atom on the α -bromoacetophenone analogue (compound **1** in this example). Condensation with a second molecule of 3-methoxyaniline results in the formation of imine intermediate **5**, which upon intramolecular cyclization involving displacement of the initial aniline molecule and subsequent tautomerization of 2-aryl indole **7**, generates the stable 2-aryl indole tautomer **8**. Previous computational and experimental studies have suggested that pathway B is preferred when an excess of aniline is used.¹⁸⁹ It should be noted that Vara and co-workers have evaluated another mechanistic possibility leading to formation of rearranged indole products (such as **8**), through an interesting carbonyl-shift rearrangement of a ketone (such as **3**) to an aldehyde prior to cyclization.^{189,190}



Scheme 5.2. Mechanistic Pathway B Associated with the Bischler-Mohrlau Reaction.

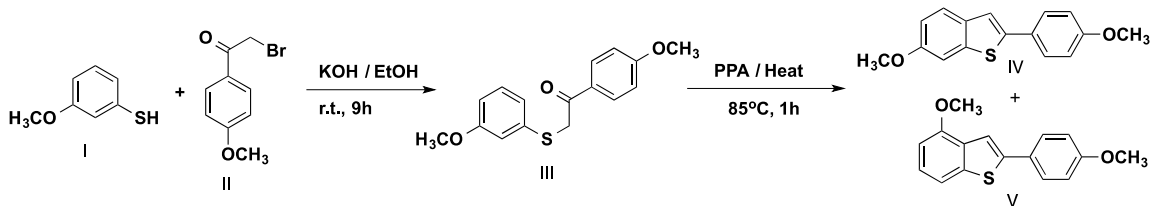
We were intrigued by the possibility that a 3-aryl-indole analogue formed through pathway A could perhaps undergo a subsequent 1,2 aryl shift (pH dependent) resulting in a rearranged 2-aryl-indole analogue as the thermodynamic sink under these reaction conditions (Scheme 5.3).¹⁹¹



Scheme 5.3. Postulated 1,2-Aryl Shift Resulting in Rearranged Indole Analogue.

This postulated methodology (1,2-aryl shift in the indole system under Bischler-Mohrlau conditions) is somewhat reminiscent of previous studies with related benzo[*b*]thiophene ring systems in which alpha-thio-ketone III (Scheme 5.4), for example, was converted to benzo[*b*]thiophene regioisomers IV and V upon treatment with PPA.^{57,192} The mechanism is widely thought to involve concomitant cyclization and

1,2 aryl ring migration. The regioisomers in this example result from initial cyclization occurring either *ortho* or *para* to the methoxy group on the aryl ring of the sulfide.^{57,192}

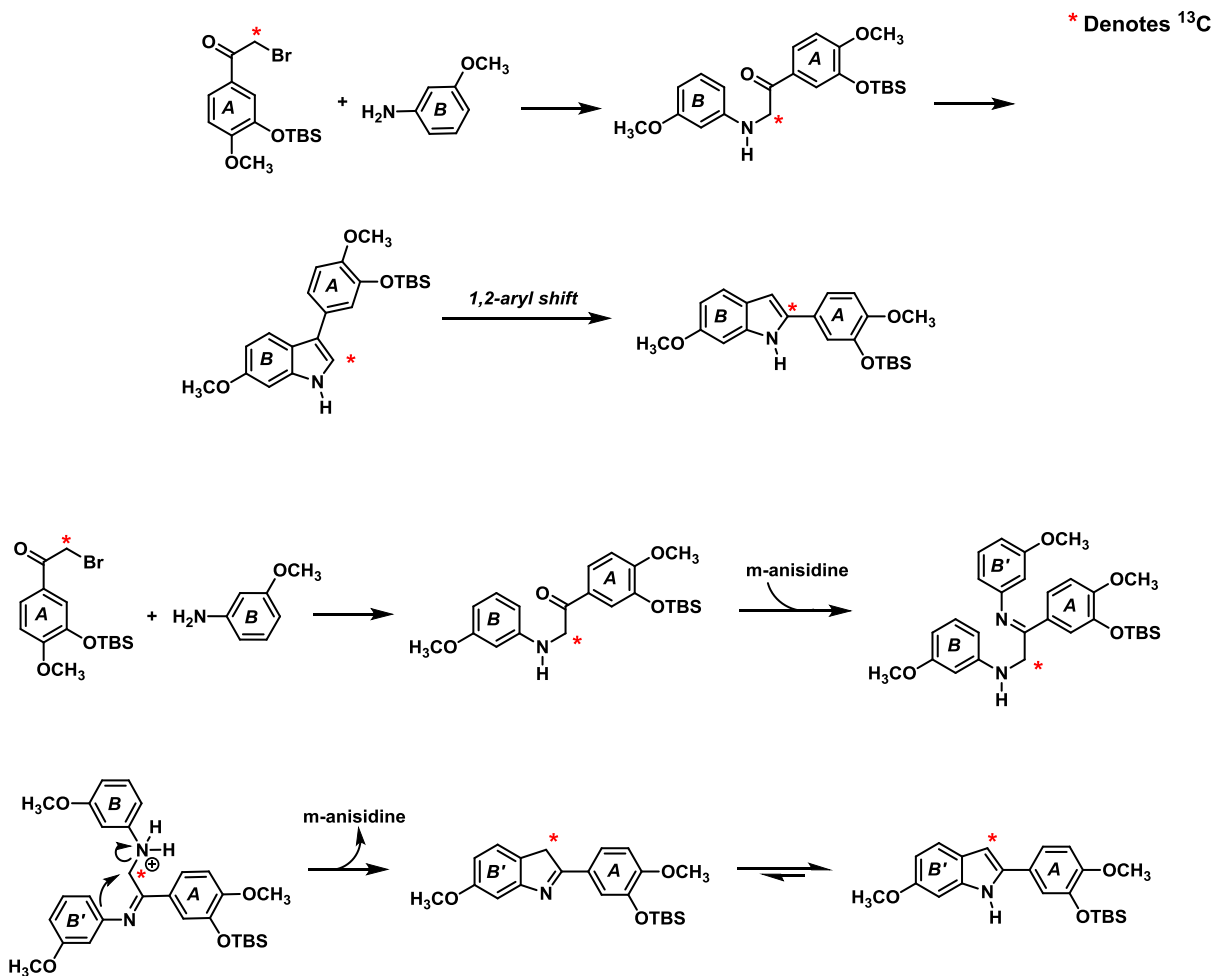


Scheme 5.4. Formation of Benzo[*b*]thiophene Regioisomers via Cyclization and Concomitant 1,2-Aryl Ring Migration.

In an effort to further explore the Bischler-Mohrlau reaction pathways a ¹³C isotopic labelling strategy was developed in which the α -carbon (to the carbonyl) was selectively labeled with ¹³C. This labeled carbon atom can be readily traced through the identification of key distinct ¹³C NMR signatures, specifically ¹³C DEPT NMR, thus providing evidence for which mechanistic pathway predominates in this specific indole-forming reaction sequence (Scheme 5.5).

Synthesis and Characterization

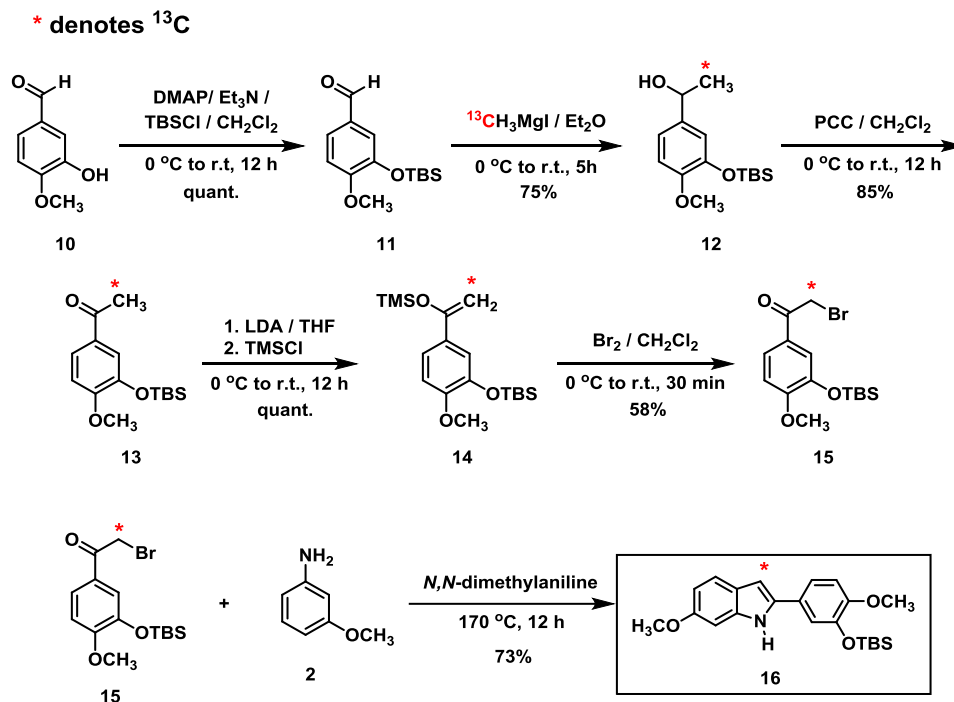
The synthetic route to ¹³C-labeled bromoacetophenone intermediate **16** followed a similar sequence as the non-labeled bromoacetophenone intermediate from our previous studies with the indole based vascular disrupting agent (VDA) OXi8006^{153,154} along with related work by von Angerer and co-workers,¹⁹³ and simply replaces the transitional methylation step reagents to install the ¹³C carbon atom at the alpha position (Scheme 5.6).



Scheme 5.5. Potential Mechanistic Pathways Leading to ^{13}C Labeled Indole Analogues

Protection of 3-hydroxy-4-methoxybenzaldehyde (*isovanillin*) with TBSCl in the presence of Et_3N and catalytic DMAP afforded TBS-aldehyde **11** which was subsequently treated with *in situ* generated $^{13}\text{C}\text{H}_3\text{MgI}$ (from commercially available $^{13}\text{C}\text{H}_3\text{I}$) to yield ^{13}C -labeled secondary alcohol **12**. PCC mediated oxidation generated ^{13}C -labeled acetophenone **13**, which after enolization was trapped as its corresponding silyl enol ether **14** upon reaction with TMSCl . Bromination of ^{13}C -labeled enol ether **14** afforded requisite ^{13}C -labeled bromoacetophenone intermediate **15**, which was treated with three molar equivalents of 3-methoxyaniline (*m*-anisidine) **2** in *N,N*-dimethylaniline

at 170 °C (Bischler-Mohrlau conditions) for 12 h to afford rearranged ¹³C-labeled 2-aryl indole **16** (Scheme 5.6).



Scheme 5.6. Synthesis of ¹³C Labeled Bromoacetophenone **16**

It is important to note that there are four possible indole regioisomers that can result from this transformation (Fig. 5.2) depending on whether the initial cyclization takes place *para* or *ortho* to the methoxy group, with or without rearrangement. In our hands, with this specific set of reactants and these reaction conditions, only one regioisomer was isolated and it was identified as the regioisomer in which the ¹³C atom label was located at the methine carbon (C-3 position of the indole core), suggesting that the system proceeded mechanistically through pathway B (imine intermediate formation) to generate the rearranged 2-aryl indole analogue **16**. The Bischler-Mohrlau reaction to form indole analogue **16** was repeated twice for verification. In the first case, the

isolated/purified yield of indole **16** was somewhat low (23%), however in the repeated experiment this yield rose to 73% (91% pure by HPLC), and a subsequent recrystallization afforded a highly pure sample (see Supplementary data for pertinent spectra). Initial comparison of the ^{13}C -NMR of indole regioisomer **16** (Fig. 5.3) with the predicted spectra (ChemBioDraw Ultra, Version 13.0.2.3020) for each of the four regioisomers, also taking into account the differences in the ^1H -NMR coupling patterns in the A-ring between the *para* and *ortho* ring closed possible products, strongly suggested regioisomer **16** as the major (and only identified and characterized) product of this reaction (both the initial reaction and the repeated reaction). DEPT ^{13}C NMR analysis (Fig.5.3) confirmed that the ^{13}C atom label was located on a methine carbon, thus providing further evidence in support of regioisomer **16**. X-ray crystallographic analysis of indole regioisomer **16** provided unequivocal confirmation of its structural assignment (see Supplementary data).

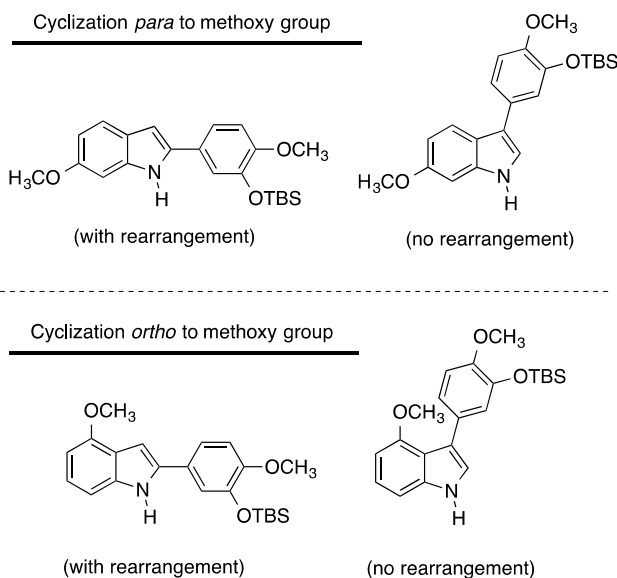


Figure 5.2. Four Possible Indole Regioisomers from Representative Bischler-Mohrlau Reaction

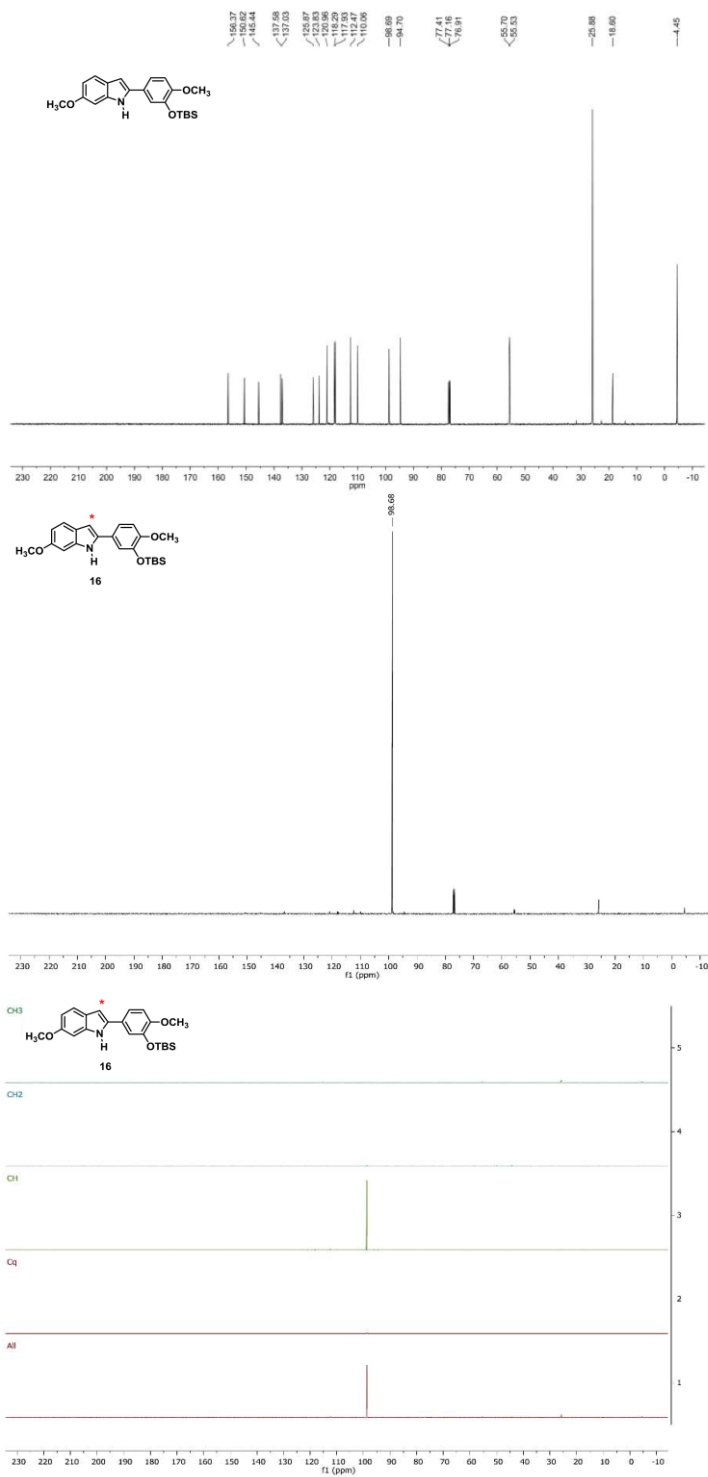


Figure 5.3. ^{13}C -NMR of Unlabeled Indole Analogue **8**, ^{13}C -NMR of ^{13}C Labeled Indole Analogue **16** (same as indole **8** but incorporating ^{13}C label), DEPT NMR of ^{13}C Labeled Indole Analogue **16**.

Conclusion

Judicious incorporation of a ^{13}C label provided compelling evidence that the indole ring closure occurred (at least in this example) through a Bischler-Mohlau pathway rather than a Friedel-Crafts type ring closure, re-aromatization, accompanied by a concomitant aryl ring migration sequence that was envisioned as a potential competing pathway based on early studies suggesting that certain benzo[*b*]thiophene systems undergo ring-closure through this pathway under polyphosphoric acid (PPA) conditions. These results suggest that further inquiry into these and related systems may prove fruitful in delineating and predicting mechanistic pathways based (perhaps) on functional group incorporation and choice of reaction conditions, thus expanding the canopy of indole, benzo[*b*]thiophene, benzo[*b*]furan, and related small-molecule anticancer agents accessible under these synthetic protocols.

Experimental Procedures

CH_2Cl_2 , THF, EtOH, and Et_2O were used in their anhydrous forms as obtained from the chemical suppliers. Reactions were performed under an inert atmosphere using nitrogen gas, unless specified otherwise. Thin-layer chromatography (TLC) plates (precoated glass plates with silica gel 60 F254, 0.25 mm thickness) were used to monitor reactions. Purification of intermediates and products was carried out with a flash purification system (Biotage Isolera 1 or 4) using silica gel (200-400 mesh, 60 Å) prepacked columns. Intermediates and products synthesized were characterized on the basis of their ^1H NMR (500 MHz), ^{13}C NMR (125 MHz), and DEPT ^{13}C NMR (125 MHz) spectroscopic data using a Varian VNMRS 500 MHz instrument. Spectra were recorded in CDCl_3 . All of the chemical shifts are expressed in ppm (δ), coupling

constants (J) are presented in Hz, and peak patterns are reported as broad (br), singlet (s), doublet (d), double doublet (dd), quartet of doublets (qd) quartet (q), and multiplet (m). ^{13}C -labeled atoms have their ^{13}C -NMR chemical shift values denoted with bold text in each appropriate experimental write-up.

3-(tert-Butyldimethylsilyloxy)-4-methoxybenzaldehyde 11

To a clean dry round bottom flask 3-hydroxy-4-methoxybenzaldehyde **10** (5.02 g, 32.9 mmol) was dissolved in CH_2Cl_2 (100 mL). The solution was cooled to 0 °C and Et_3N (5.04 mL, 36.2 mmol) was added followed by the addition of *N,N*-dimethylaminopyridine (DMAP) (0.402 g, 3.29 mmol). The reaction mixture was stirred for 10 min and *tert*-butyldimethylsilyl chloride (TBSCl) (5.29 g, 36.2 mmol) was added gradually. The solution was allowed to warm to room temperature and was stirred for 12 hours. The reaction was diluted with water (50 mL), transferred to a separatory funnel, and was extracted with CH_2Cl_2 . The organic extracts were combined, dried over Na_2SO_4 , filtered, and concentrated under reduced pressure. The TBS benzaldehyde product **11** (9.24 g, 34.7 mmol) was isolated quantitatively as a yellow oil and was taken to the next step without further purification.

$^1\text{H NMR}$ (CDCl_3 , 500 MHz): δ 9.80 (s, 1H, CHO), 7.45 (dd, $J = 8.5, 2.0$ Hz, 1H, ArH), 7.35 (d, $J = 2.0$ Hz, 1H, ArH), 6.93 (d, $J = 8.5$ Hz, 1H, ArH), 3.87 (s, 3H, OCH_3), 0.99 (s, 9H, $\text{C}(\text{CH}_3)_3$), 0.16 (s, 6H, $\text{Si}(\text{CH}_3)_2$).

$^{13}\text{C NMR}$ (CDCl_3 , 125 MHz): δ 190.2, 156.2, 145.2, 130.0, 126.0, 119.4, 110.9, 55.1, 25.3, 18.0, -5.0.

3-tert-Butyldimethylsilyloxy-1-(1'-hydroxyethyl)-4-methoxybenzene 12

To a solution of magnesium turnings (0.40 g, 17 mmol) in diethyl ether (Et₂O) was added ¹³C-labeled methyl iodide (1.00 mL, 16.0 mmol). The solution was refluxed for 30 minutes until the turnings were dissolved. The solution was cooled to room temperature and TBS benzaldehyde **11** (1.92 g, 7.20 mmol) in Et₂O was added dropwise. The reaction mixture was stirred for 5 hours. Upon completion the reaction mixture was slowly quenched with 0.1 M HCl and extracted with Et₂O. The organic extracts were washed sequentially with saturated NaHCO₃ solution and water. The organic layer was further dried over Na₂SO₄, filtered, and concentrated under reduced pressure. The crude mixture was subjected to flash chromatography using a prepacked 50 g silica column [solvent A, EtOAc, solvent B, hexanes; gradient, 7% A / 93% B (1 CV), 7% A / 93% B → 60% A / 40% B (10 CV), 60% A / 40% B (2 CV); flow rate, 40 mL/min; monitored at 254 and 280 nm] to yield ¹³C-labeled alcohol **12** (1.54 g, 5.45 mmol, 75%, R_f = 0.47 (70:30 hexanes: EtOAc)) as a yellow oil.

¹H NMR (CDCl₃, 500 MHz): δ 6.90 (dd, *J* = 8.2, 2.2 Hz, 1H, ArH), 6.88 (d, *J* = 2.2 Hz, 1H, ArH), 6.81 (d, *J* = 8.2 Hz, 1H, ArH), 4.79 (qd, *J* = 6.4, 2.0 Hz, 1H, CH), 3.79 (s, 3H, OCH₃), 1.79 (s, 1H, OH), 1.45 (dd, *J* = 6.4 Hz, *J*_{C-H} = 126.6 Hz, 3H, CH₃), 1.00 (s, 9H, C(CH₃)₃), 0.16 (s, 6H, Si(CH₃)₂).

¹³C NMR (CDCl₃, 500 MHz): δ 150.30, 145.02, 138.64, 118.50 (d, *J* = 1.9 Hz), 118.27 (d, *J* = 1.6 Hz), 111.96, 69.96 (d, *J* = 38.6 Hz), 55.56, 25.73, **24.96**, 18.45, -4.59 (d, *J* = 1.4 Hz).

HRMS [M+Na]⁺: 306.1578 (calcd for [C₁₄¹³CH₂₆NaO₃Si]⁺, 306.1577).

3-tert-Butyldimethylsilyloxy-4-methoxyacetophenone 13

The crude alcohol **12** (1.76 g, 6.23 mmol) was dissolved in CH₂Cl₂ (50 mL). Celite (1.5 g) was added and the solution was cooled to 0 °C. Pyridinium chlorochromate (PCC) (1.48 g, 6.86 mmol) was added in small increments allowing 10 minutes of stirring between each addition. The reaction was allowed to warm to room temperature and stirred for 12 hours. The reaction mixture was filtered through a 50/50 mixture of silica gel/celite rinsing well with CH₂Cl₂. The filtrate was concentrated under reduced pressure providing the desired ¹³C-labeled acetophenone **13** (1.48 g, 5.28 mmol, 85%) as a pale yellow solid.

¹H NMR (CDCl₃, 500 MHz): δ 7.58 (dd, *J* = 8.5, 2.1 Hz, 1H, ArH), 7.47 (d, *J* = 1.9 Hz, 1H, ArH), 6.87 (d, *J* = 8.3 Hz, 1H, ArH), 3.87 (s, 3H, OCH₃), 2.53 (d, *J* = 127.3 Hz, 3H, CH₃), 1.01 (s, 9H, C(CH₃)₃), 0.17 (s, 6H, Si(CH₃)₂).

¹³C NMR (CDCl₃, 500 MHz): δ 196.71 (d, *J* = 42.7 Hz), 155.31, 144.83, 130.59 (d, *J* = 13.9 Hz), 123.50, 120.47, 110.78, 55.48, **26.30**, 25.68, 18.44, -4.63.

HRMS [M+H]⁺: 282.1603 (calcd for [C₁₄¹³CH₂₅O₃Si]⁺, 282.1601).

1-(3-tert-Butyldimethylsilyloxy-4-methoxyphenyl)-1-trimethylsilylethene 14

To a solution of diisopropylamine (1.1 mL, 7.0 mmol) in THF (30 mL) at 0 °C was added *n*-butyllithium (3.2 mL, 7.9 mmol) dropwise. The LDA solution was allowed to stir for 15 minutes and a solution of TBS acetophenone **13** (1.48 g, 5.26 mmol) in THF (5 mL) was added dropwise. The solution was stirred for 10 min and TMSCl (1.0 mL, 7.9 mmol) was added dropwise and the reaction was allowed to warm to room temperature. The solution was stirred for 12 hours and was quenched using 10% NaHCO₃ (100 mL). The reaction mixture was extracted with Et₂O, dried over Na₂SO₄,

and concentrated under reduced pressure resulting in ^{13}C -labeled TMS enol ether **14** (1.95 g, 5.51 mmol) quantitatively as a dark yellow oil which was taken to the next step without purification.

$^1\text{H NMR}$ (CDCl_3 , 500 MHz): δ 7.23 (dd, $J = 8.5, 2.0$ Hz, 1H ArH), 7.18 (d, $J = 2.0$ Hz, 1H, ArH), 6.82 (d, $J = 8.5$ Hz, 1H, ArH), 4.83 (dd, $J = 1.5$ Hz, $J_{\text{C-H}} = 159.5$ Hz, 1H, CH₂), 4.38 (dd, $J = 1.5$ Hz, $J_{\text{C-H}} = 159.0$ Hz, 1H, CH₂), 3.83 (s, 3H, OCH₃), 1.08 (s, 9H, C(CH₃)₃), 0.32 (s, 9H, Si(CH₃)₃), 0.23 (s, 6H, Si(CH₃)₂).

$^{13}\text{C NMR}$ (CDCl_3 , 125 MHz): δ 155.4 (d, $J = 82.0$ Hz), 151.3, 144.6, 130.8 (d, $J = 6.9$ Hz), 118.9 (d, $J = 2.4$ Hz), 118.2 (d, $J = 2.3$ Hz), 111.3 (d, $J = 42.6$ Hz), **89.6**, 55.5, 25.9, 18.6, 0.2, -4.5.

3'-(tert-Butyldimethylsilyloxy)-4'-methoxy-2-bromoacetophenone 15

A solution of crude **14** (1.95 g, 5.51 mmol) in CH_2Cl_2 (30 mL) and K_2CO_3 (0.033 g, 0.239 mmol) was cooled to 0 °C. Bromine (0.17 mL, 3.3 mmol) was added dropwise and the solution was allowed to stir for 30 minutes. The reaction was quenched with 10 % sodium thiosulfate solution, transferred to a separatory funnel, and extracted with CH_2Cl_2 . The organic extracts were dried over Na_2SO_4 and concentrated under reduced pressure. The crude mixture was subjected to flash chromatography using a prepacked 100 g silica column [solvent A, EtOAc, solvent B, hexanes; gradient, 2% A / 98% B (4 CV), 2% A / 98% B \rightarrow 20% A / 80% B (10 CV), 20% A / 80% B (2 CV); flow rate, 50 mL/min; monitored at 254 and 280 nm] to yield ^{13}C -labeled bromoacetophenone **15** as a tan solid (1.16 g, 3.22 mmol, 58%, $R_f = 0.29$ (80:20 hexanes: EtOAc)).

¹H NMR (CDCl₃, 500 MHz): δ 7.62 (dd, *J* = 8.5, 2.2 Hz, 1H, ArH), 7.49 (d, *J* = 2.2 Hz, 1H, ArH), 6.89 (d, *J* = 8.5 Hz, 1H, ArH), 4.38 (d, *J*_{C-H} = 150.9 Hz, 2H, CH₂), 3.89 (s, 3H, OCH₃), 1.01 (s, 9H, C(CH₃)₃), 0.18 (s, 6H, Si(CH₃)₂).

¹³C NMR (CDCl₃, 500 MHz): δ 189.89 (d, *J* = 43.8 Hz), 156.10, 145.13, 127.12 (d, *J* = 17.2 Hz), 124.21, 121.10, 111.00, 55.55, **30.69**, 25.65, 18.43, -4.61.

HRMS [M+Na]⁺: 382.0533 (calcd for [C₁₄¹³CH₂₃BrNaO₃Si]⁺, 382.0526).

2-(3'-*tert*-Butyldimethylsilyloxy-4'-methoxyphenyl)-6-methoxyindole **16**

A solution of *m*-anisidine (0.41 mL, 3.7 mmol) was dissolved in *N,N*-dimethylaniline (10 mL) and was heated to reflux at 170 °C. A solution of **15** (0.40 g, 1.1 mmol) in EtOAc (1 mL) was added dropwise. The reaction mixture was stirred at 170 °C for 12 hours. The reaction mixture was allowed to cool to room temperature and was extracted with EtOAc (3 x 50 mL). The combined organic extracts were dried over Na₂SO₄ and concentrated under reduced pressure. Purification by flash chromatography using a prepacked 50 g silica column [solvent A, EtOAc, solvent B, hexanes; gradient, 2% A / 98% B (1 CV), 2% A / 98% B → 25% A / 75% B (10 CV), 25% A / 75% B (2 CV); flow rate, 40 mL/min; monitored at 254 and 280 nm] resulted in the desired ¹³C-labeled phenylindole **16** (0.312 g, 0.81 mmol, 73%, R_f = 0.48 (50:50 hexanes: EtOAc)) as a light tan solid. A portion of compound **16** was recrystallized from hexane and dichloromethane to obtain the analytical data.

¹H NMR (CDCl₃, 500 MHz): δ 8.14 (br s, 1H, NH), 7.48 (dd, *J* = 8.6 Hz, 2.9 Hz, 1H, ArH), 7.16 (m, 2H, ArH), 6.90 (m, 2H, ArH), 6.83 – 6.40 (m, 2H, ArH), 3.87 (s, 3H, OCH₃), 3.85 (s, 3H, OCH₃), 1.06 (s, 9H, C(CH₃)₃), 0.22 (s, 6H, Si(CH₃)₂).

¹³C NMR (CDCl₃, 125 MHz): δ 156.36, 150.57, 145.39, 137.37 (d, *J* = 3.3 Hz), 136.85, 125.77 (d, *J* = 3.6 Hz), 123.68 (d, *J* = 56.5 Hz), 120.89 (d, *J* = 2.4 Hz), 118.18 (d, *J* = 2.9 Hz), 117.81 (d, *J* = 2.5 Hz), 112.36, 109.89 (d, *J* = 4.6 Hz), **98.68**, 94.46 (d, *J* = 2.4 Hz), 55.68, 55.53, 25.75, 18.49, -4.57.

HPLC: Method C, 23.8 min.

HRMS [M+H]⁺: 385.2031 (calcd for [C₂₁¹³CH₃₀NO₃Si]⁺, 385.2023).

Acknowledgments

The authors are grateful to the National Cancer Institute of the National Institutes of Health (grant no. 5R01CA140674 to K.G.P.) and Oxigene Inc. (grant to K.G.P.) for their financial support of this project, and to the NSF for funding the Varian 500 MHz NMR spectrometer (grant no. CHE- 0420802). The content is solely the responsibility of the authors and does not necessarily reflect the official views of the National Institutes of Health. The authors also thank Dr. Alejandro Ramirez (Mass Spectrometry Core Facility, Baylor University), and Dr. Kevin Klausmeyer (X-ray analysis at Baylor University).

Supplementary data

Supplementary data (Experimental procedures, ¹H NMR, ¹³C NMR, DEPT NMR, HRMS, and HPLC data, along with X-ray crystallographic data) associated with this article can be found, in the online version, at <http://dx.doi.org/10.1016/j.tetlet.2015.01.129>.

CHAPTER SIX

Scale-up Synthesis of Cathepsin L Inhibitor KGP94

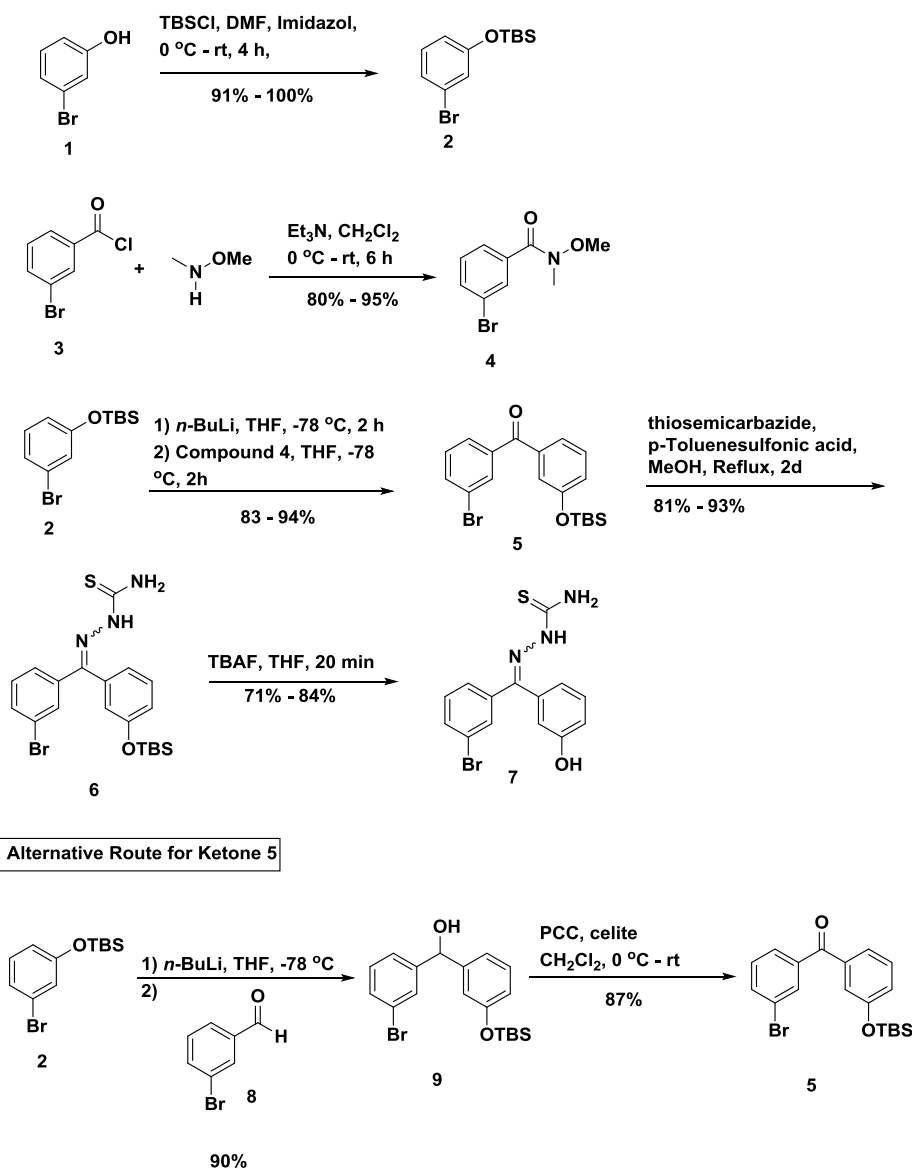
Introduction

The thiosemicarbazone moiety has been recognized for its ability to interact with the cysteine-25 thiolate in the active site of the cysteine protease cruzain.^{194,195} Recent work by the Pinney and Trawick Research Groups has also demonstrated that this moiety is a good warhead for incorporation in small-molecule inhibitors of cathepsin L.^{196–200} Benzophenone thiosemicarbazone derivative KGP94 is a leading cathepsin L inhibitor from a privileged synthetic library, which consists of functionalize benzophenone, thiophene, pyridine, fluorene, thiochromanone, and benzoylbenzophenone thiosemicarbazones.^{140,141,149} KGP94 has been demonstrated to be a competitive inhibitor of Cathepsin L with strong inhibitory activity against cathepsin L ($IC_{50} = 189$ nM).^{140,141,149} In this study, a scale-up synthesis of KGP94 was carried out to obtain 10 grams of **KGP94** to support continuing preclinical studies.

Synthesis

The synthetic route (Scheme 6.1) towards cathepsin L inhibitor KGP94 involved the condensation of the benzophenone intermediate and thiosemicarbazide. The synthesis began with the commercially available 3-bromophenol **1**, which was protected by the *tert*-butyldimethylsilyl group to afford silyl ether **2**. Acyl chloride **3** was treated with *N,O*-dimethylhydroxylamine to form the Weinreb amide **4**. The first two reactions were

carried out in large scales of 100 grams to 200 grams. The benzophenone scaffold **5** was synthesized in 98% yield from reaction between the phenyllithium intermediate, which was obtained from compound **2** and Weinreb amide **4**. Condensation of the resulting *meta* substituted benzophenone analogue **5** with thiosemicarbazide and removal of the protecting group afforded thiosemicarbazone analogue **7** (KGP94).



Scheme 6.1. Synthesis of KGP94

A two-step alternative route towards benzophenone **5** was also evaluated with an overall yield of 78%, where aldehyde **8** was treated with the phenyllithium intermediate, followed by a pyridinium chlorochromate (PCC) oxidation.

Materials and Methods

(3-Bromophenoxy)(tert-butyl)dimethylsilane 2^{197,200}

To a clean dry round bottom flask imidazole (36.8 g, 0.540 mol) was dissolved in *N,N*-dimethylformamide (DMF, 350 mL). The solution was cooled to 0 °C and 3-bromophenol **1** (29.4 ml, 0.278 mol) was added dropwise followed by the addition of *tert*-butyldimethylsilyl chloride (60.5 g, 0.390 mol). The reaction mixture was allowed to warm to room temperature and stirred for 4 h. The reaction was diluted with a 5 % sodium bicarbonate solution (100 mL) and extracted with hexanes (100 ml x 3). The combined organic layer was dried over Na₂SO₄, filtered and concentrated under reduced pressure. Purification of the crude mixture by column chromatography (silica gel, hexane) afforded the silyl ether **2** (79.6 g, 0.277 mmol, 100 % yield) as a colorless liquid.

¹H NMR (500 MHz, CDCl₃) δ 7.10-7.06 (2H, m), 7.01-7.00 (1H, m), 6.78-6.74 (1H, m), 0.98 (9H, s), 0.20 (6H, s).

¹³C NMR (125 MHz, CDCl₃) δ 156.67, 130.55, 124.61, 123.66, 122.61, 118.96, 25.75, 18.33, -4.32.

3-bromo-N-methoxy-N-methylbenzamide 4^{197,200}

N, O-dimethylhydroxylamine hydrochloride (45.0 g, 0.461 mol) was suspended in 450 mL dichloromethane. The solution was cooled to 0 °C and triethylamine (85.7 mL, 0.615 mol) was added dropwise. After the reaction mixture was stirred for 10 min, 3-

bromobenzoyl chloride **3** (67.5 g, 0.308 mol) in dichloromethane (125 mL) was added dropwise. The resulting reaction mixture was allowed to warm to room temperature and stirred for 6 h. Upon completion the reaction was quenched with water (200 mL) and extracted with dichloromethane (100 mL x 4). The combined organic extract was dried over sodium sulfate, filtered and concentrated under reduced pressure. Purification of the crude mixture by column chromatography (silica gel, 90:10 hexane: ethyl acetate then with 80:20 hexane: ethyl acetate followed by 70:30 hexane: ethyl acetate) afforded the Weinreb amide **4** (71.6 g, 0.293 mmol, 95 % yield) as a colorless liquid.

¹H NMR (500 MHz, CDCl₃): 7.83 (1H, t, J = 1.8 Hz), 7.61 (1H, dt, J = 7.7 Hz, 1.3 Hz), 7.59 (1H, ddd, J = 8.0 Hz, 2.1 Hz, 1.1 Hz), 7.28 (1H, m), 3.35 (3H, s), 3.36 (3H, s).

¹³C NMR (125 MHz, CDCl₃): 168.32, 136.06, 133.69, 131.36, 129.74, 126.93, 122.14, 61.33, 33.71.

(3-bromophenyl)(3-((tert-butyldimethylsilyl)oxy)phenyl)methanone **5**^{197,200}

Silyl ether **2** (10.5 g, 36.5 mmol) was dissolved in tetrahydrofuran (60 mL) at -78 °C followed by the dropwise addition of n-Butyllithium (10.3 mL, 1.6 M, 16.4 mmol). The reaction mixture was stirred for 2 h and added dropwise into Weinreb amide **4** (4.67 g, 18.3 mmol) in 40 mL tetrahydrofuran. The reaction was continued to stir at -78 °C for 2 h. Upon completion the solution was quenched with 50 mL 1 M HCl. After stirred for 5 min, the solution was extracted by dichloromethane (50 mL X 4). The combined organic layer was washed by saturated sodium bicarbonate, dried over sodium sulfate, filtered and concentrated under reduced pressure. The crude mixture was subjected to flash column chromatography using a prepacked 350 g silica column [solvent A, EtOAc,

solvent B, hexanes; gradient, 0%A / 100%B (6 CV), 0%A / 100%B → 15%A / 85%B (10 CV), 15%A / 85%B (2 CV); flow rate, 70 mL/min; monitored at 254 and 280 nm] to afford ketone **5** (6.07 g, 15.5 mmol, 94% yield) as a colorless liquid.

¹H NMR (600 MHz, DMSO-d₆) δ 7.89 (1H, ddd, J = 8.0 Hz, 2.1 Hz, 1.0 Hz), 7.83 (1H, t, J = 1.8 Hz), 7.71 (1H, ddd, J = 7.7 Hz, 1.6 Hz, 1.0 Hz), 7.53 (1H, t, J = 7.9 Hz), 7.47 (1H, t, J = 7.9 Hz), 7.34 (1H, ddd, J = 7.6 Hz, 1.6 Hz, 1.0 Hz), 7.20 (1H, ddd, J = 8.1 Hz, 2.6 Hz, 1.0 Hz), 7.14 (1H, dd, J = 2.5 Hz, 1.6 Hz), 0.95 (s, 9H), 0.20 (s, 6H).

¹³C NMR (150 MHz, DMSO-d₆) δ 193.90, 155.11, 139.16, 137.84, 135.32, 131.84, 130.82, 130.19, 128.56, 124.80, 123.09, 121.80, 120.57, 25.55, 18.01, -4.54.

3-(t-Butyldimethylsilyl)oxyphenyl]-(3-bromophenyl)-ketone] thiosemicarbazone **6**^{197,200}

Ketone **5** (7.26 g, 18.6 mmol) and thiosemicarbazide (3.38 g, 37.1 mmol) was added into anhydrous methanol (250 mL) followed by the addition of para-toluenesulfonic acid (0.006 g, 0.04 mmol). The reaction mixture was reflux for 24 h. thiosemicarbazide (1.69 g, 18.6 mmol) and para-toluenesulfonic acid (0.009 g, 0.05 mmol) was added into the solution. The reaction mixture was reflux for another 24 h. Upon completion the reaction was quenched with water (200 mL) followed by extraction with ethyl acetate (100 mL X 3). The combined organic layer was dried over sodium sulfate and concentrated under reduced pressure. The crude mixture was subjected to flash column chromatography using a prepacked 100 g silica column [solvent A, EtOAc, solvent B, hexanes; gradient, 6%A / 94%B (2 CV), 6%A / 94%B → 40%A / 60%B (10 CV), 40%A / 60%B (2 CV); flow rate, 100 mL/min; monitored at 254 and 280 nm] to afford thiosemicarbazone derivative **6** (7.50 g, 16.1 mmol, 87% yield) as a white solid.

¹H-NMR (DMSO-d₆, 600 MHz) δ 8.70 (1H, s), 8.57 (1H, s), 8.45 (1H, s), 8.04 (1H, s), 7.59 (1H, ddd, J = 8.0 Hz, 2.0 Hz, 1.0 Hz), 7.55 (1H, t, J = 7.9 Hz), 7.46 (1H, ddd, J = 8.0 Hz, 1.7 Hz, 1.0 Hz), 7.31 (1H, t, J = 8.0 Hz), 7.10 (1H, ddd, J = 8.3 Hz, 2.5 Hz, 1.0 Hz), 6.94 (1H, ddd, J = 7.5 Hz, 1.5 Hz, 1.0 Hz), 6.81 (1H, dd, J = 2.5 Hz, 1.5 Hz), 0.945 (9H, s), 0.21 (6H, s).

¹³C-NMR (DMSO-d₆, 150 MHz) δ 177.87, 156.21, 146.80, 138.57, 132.36, 132.03, 131.59, 130.43, 129.46, 126.81, 122.18, 121.87, 121.27, 119.73, 25.59, 18.05, -4.51.

[(3-Bromophenyl)-(3-hydroxyphenyl)-ketone] thiosemicarbazone 7^{197,200}

Tetrabutylammonium fluoride trihydrate (TBAF) (10.8 g, 7.77 mmol) was added to the solution of the silyl ether (7.82 g, 16.8 mmol) in dry THF (40 ml). The reaction mixture was stirred at room temperature for 20 min. The reaction mixture was diluted with ethyl acetate (100 mL) and then brine (100 mL). The resulting solution was separated in a separation funnel. The organic layer was dried over sodium sulfate and concentrated under reduced pressure. The crude mixture was subjected to flash column chromatography using a prepacked 100 g silica column [solvent A, EtOAc, solvent B, hexanes, solvent C dichloromethane; gradient, 20%A / 60%B / 20% C(2 CV), 20 %A / 60%B / 20%C→ 50%A / 0%B / 50%C (12CV), 50%A / 0%B / 50%C (2 CV)]; flow rate, 100 mL/min; monitored at 254 and 280 nm] to afford the thiosemicarbazone derivative **7** (4.98 g, 14.2 mmol, 84 % yield) as a solid.

¹H-NMR (DMSO-d₆, 600 MHz) δ 10.00 (1H, s), 8.70 (1H, s), 8.57 (1H, s), 8.40 (1H, s), 8.10 (1H, s), 7.59 (1H, ddd, J = 7.9 Hz, 2.0 Hz, 1.0 Hz), 7.46 (1H, t, J = 7.8 Hz), 7.44 (1H, ddd, J = 7.9 Hz, 1.7 Hz, 1.0 Hz), 7.31 (1H, t, J = 7.9 Hz), 7.00 (1H, ddd, J = 8.3

Hz, 2.5 Hz, 1.0 Hz), 6.73 (1H, ddd, $J = 7.4$ Hz, 1.5 Hz, 1.0 Hz), 6.65 (1H, dd, $J = 2.5$ Hz, 1.5 Hz).

$^{13}\text{C-NMR}$ (DMSO- d_6 , 150 MHz) δ 177.76, 158.53, 147.38, 138.51, 132.38, 131.71, 131.42, 130.46, 129.33, 126.98, 122.21, 118.41, 117.24, 114.53.

HPLC: Method B, 12.0 min.

HRMS (ESI⁺): m/z calculated for $\text{C}_{11}\text{H}_{13}\text{BrN}_3\text{OS}$ $[\text{M}+\text{H}]^+$ 349.9957, found 349.9958.

(3-bromophenyl)(3-((tert-butyldimethylsilyl)oxy)phenyl)methanol 9 (Alternative Route)

Silyl ether **2** (3.50 g, 12.2 mmol) was dissolved in 25 mL tetrahydrofuran at -78 °C followed by the dropwise addition of *n*-Butyllithium (3.4 mL, 1.6 M, 5.5 mmol). The reaction mixture was stirred for 1 h and aldehyde **8** (1.13 g, 6.1 mmol) in tetrahydrofuran (40 mL). The reaction was continued to stir at -78 °C for 1.5 h. Upon completion the solution was quenched with HCl (1 M, 20 mL). After stirred for 5 min, the solution was extracted by dichloromethane (20 mL X 3). The combined organic layer was washed by saturated sodium bicarbonate, dried over sodium sulfate, filtered and concentrated under reduced pressure. The crude mixture was subjected to flash column chromatography using a prepacked 50 g silica column [solvent A, EtOAc, solvent B, hexanes; gradient, 0%A / 100%B (6 CV), 0%A / 100%B \rightarrow 20%A / 80%B (10 CV), 20%A / 80%B (2 CV); flow rate, 100 mL/min; monitored at 254 and 280 nm] to afford secondary alcohol **9** (2.18 g, 5.50 mmol, 90% yield) as a colorless liquid.

$^1\text{H NMR}$ (600 MHz, Chloroform- d) δ 7.54 (s, 1H), 7.38 (d, $J = 7.9$ Hz, 1H), 7.28 (d, $J = 7.7$ Hz, 1H), 7.22 (dq, $J = 7.6, 4.7$ Hz, 2H), 6.92 (d, $J = 7.6$ Hz, 1H), 6.83 (s, 1H),

6.76 (d, $J = 8.1$ Hz, 1H), 5.72 (d, $J = 3.3$ Hz, 1H), 2.27 (d, $J = 3.0$ Hz, 1H), 0.96 (s, 10H), 0.17 (s, 6H).

$^{13}\text{C NMR}$ (151 MHz, CDCl_3) δ 155.93, 145.89, 144.75, 130.58, 130.01, 129.69, 129.51, 125.10, 122.60, 119.57, 119.47, 118.30, 77.26, 77.05, 76.84, 75.40, 25.71, 18.25, -4.38.

(3-Bromophenyl)(3-((tert-butyldimethylsilyl)oxy)phenyl)methanone 5 (Alternative Route)

To a solution of PCC (1.57 g, 7.3 mmol) and celite (1.5 g) in dichloromethane (30 mL), secondary alcohol **8** (1.90 g, 4.8 mmol) was added dropwise at 0 °C. The reaction mixture was stirred at room temperature for 24 h, followed by filtered through a bed of celite and then concentrated under reduced pressure. The residue was then subjected to flash column chromatography using a prepacked 50 g silica column [solvent A, EtOAc, solvent B, hexanes; gradient, 0%A / 100%B (1 CV), 0%A / 100%B \rightarrow 15%A / 85%B (10 CV), 15%A / 85%B (2 CV); flow rate, 100 mL/min; monitored at 254 and 280 nm] to afford benzylphenone **5** (1.64 g, 4.20 mmol, 87% yield) as a colorless liquid.

CHAPTER SEVEN

Conclusion

In summary, a series of small-molecule tubulin binding agents, structurally motivated by 2-aryl-3-aryl indole-based molecular templates, were synthesized and subjected to biochemical and biological evaluation. The most promising new analogue, amino compound **28**, demonstrated inhibition of tubulin assembly comparable to the reference compounds OXi8006 and CA4. The lead indole analogue OXi8006 was also tethered to a cathepsin B cleavable dipeptide linker, designed for selective drug delivery as a drug-linker construct suitable for future antibody incorporation and evaluation as corresponding antibody-drug conjugates (ADCs).

A small library of OXi8006, dihydronaphthalene, and benzosuberene BAPC analogues was prepared to target tumor-associated hypoxia for selective delivery of anticancer agents. Three BAPCs in this library demonstrated moderate hypoxia-selective activation ($HCR > 7$) in the A549 lung cancer cell line. One of them, the monomethyl-nitroimidazole OXi6196 BAPC, demonstrated anti-vascular activity in an orthotopic syngeneic breast tumor mouse model (4T1/BALB/c) as evidenced through BLI.

A carbon-13 isotope labeling strategy was used to explore the mechanistic pathway of the Bischler-Mohlau indole reaction. Analysis of ^{13}C nuclear magnetic resonance (NMR) of the reaction products demonstrated that the indole ring closure, at least in this specific example, required two equivalents of the aniline analogue reactant partner and proceeded through an imine intermediate rather than by direct formation of

the corresponding 3-aryl indole accompanied by a concomitant 1,2-aryl shift rearrangement.

Collectively, these studies have advanced therapeutic approaches towards the targeting of tumor-associated vasculature and hypoxia through the discovery and development of prodrug strategies that enhance selectivity in terms of targeting and delivery of potent anticancer agents that function as small-molecule inhibitors of tubulin polymerization.

APPENDICES

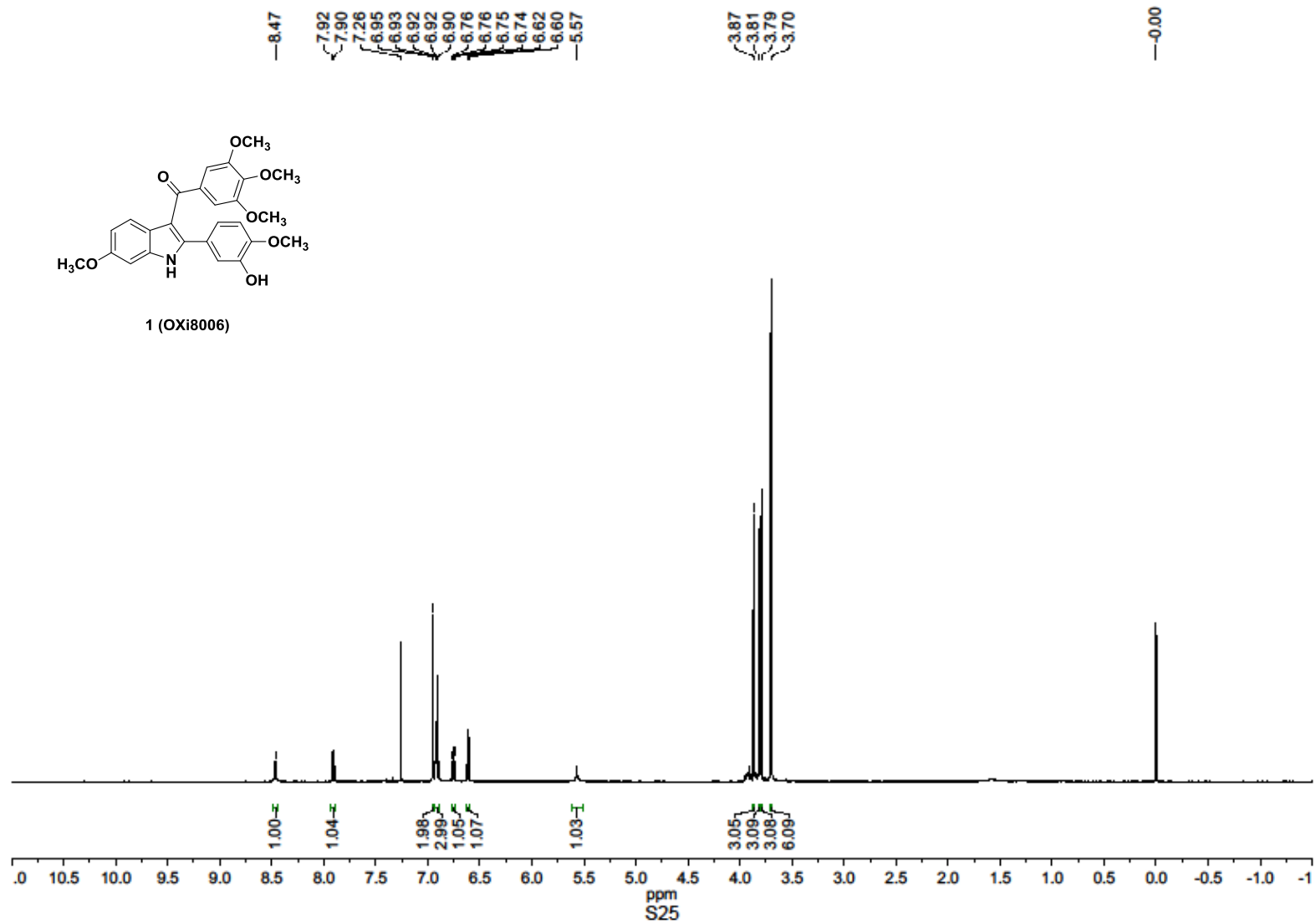
APPENDIX A

Indole-based Vascular Disrupting Agents and Antibody-Drug Conjugates

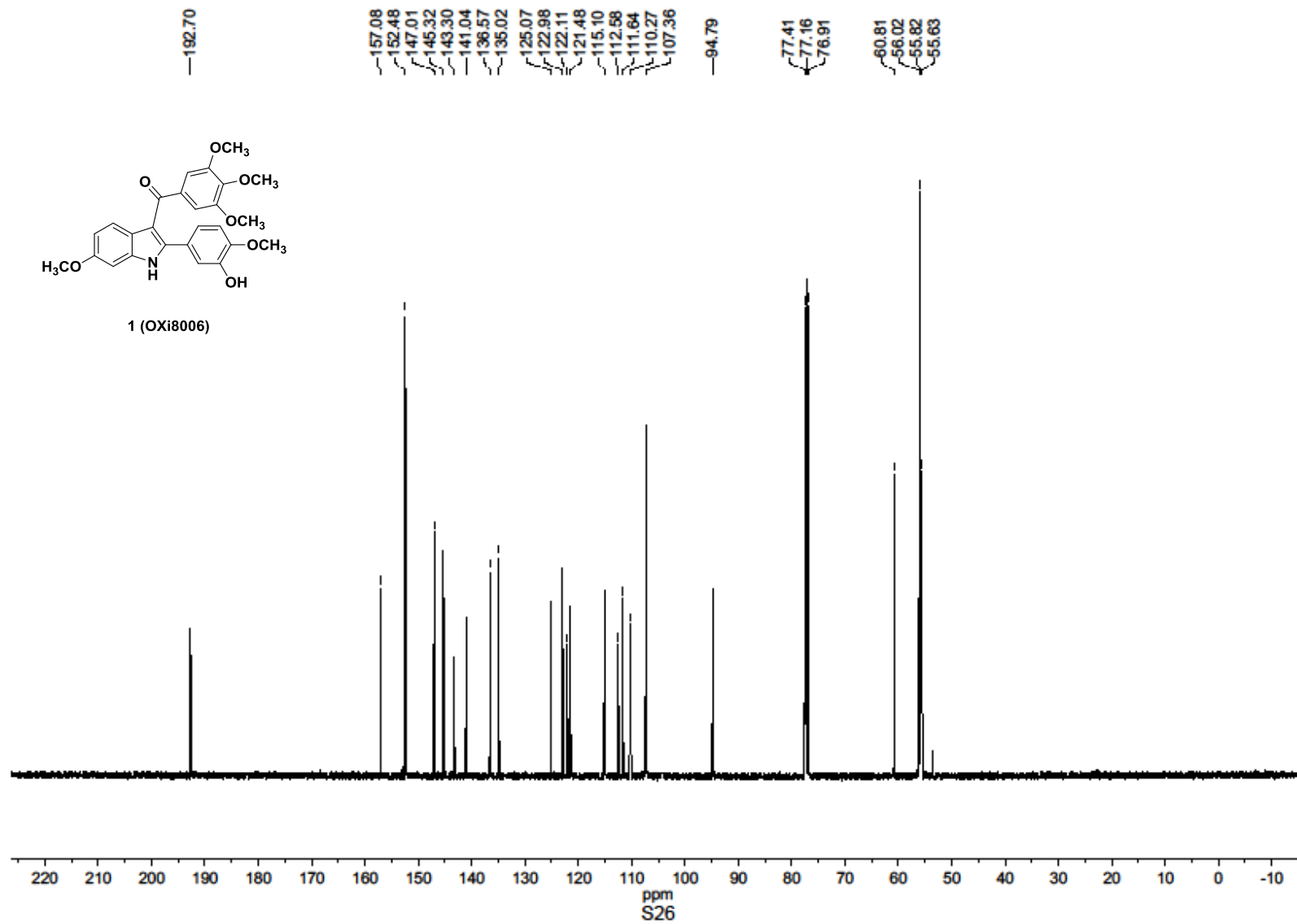
Table of Contents

¹ H, ¹³ C NMR, Mass Spec and HPLC traces of Compound 1	136
¹ H, ¹³ C, ³¹ P NMR, Mass Spec and HPLC traces of Compound 2	143
¹ H, ¹³ C, ³¹ P NMR, Mass Spec and HPLC traces of Compound 5	151
¹ H, ¹³ C NMR, Mass Spec and HPLC traces of Compound 22	160
¹ H NMR, Mass Spec and HPLC traces of Compound 27	167
¹ H, ¹³ C NMR, Mass Spec and HPLC traces of Compound 28	173
¹ H, ¹³ C NMR, Mass Spec and HPLC traces of Compound 35	180
¹ H NMR, Mass Spec and HPLC traces of Compound 54	187

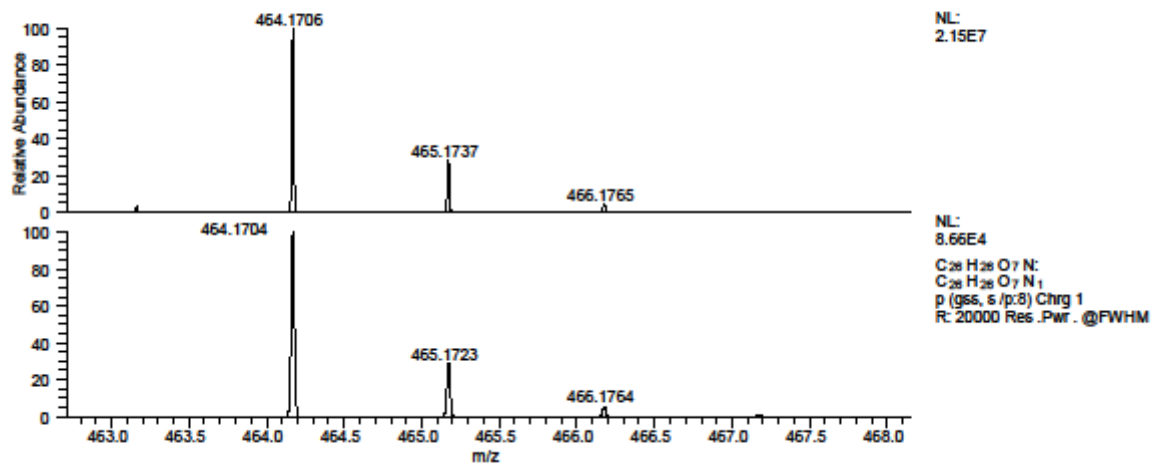
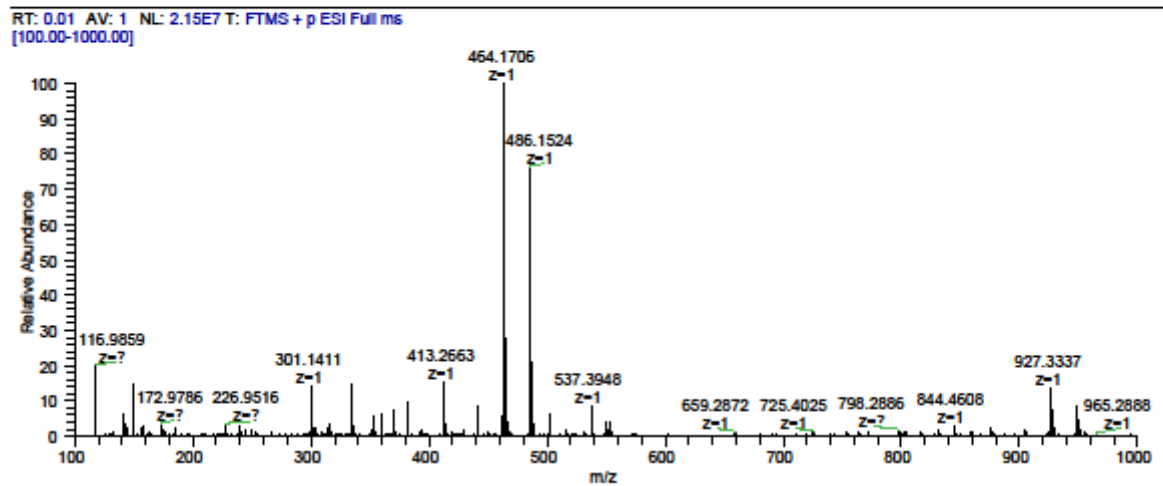
¹H NMR of Compound **1** (OXi8006)



¹³C NMR of Compound 1 (OXi8006)



HRMS of Compound 1 (OXi8006)



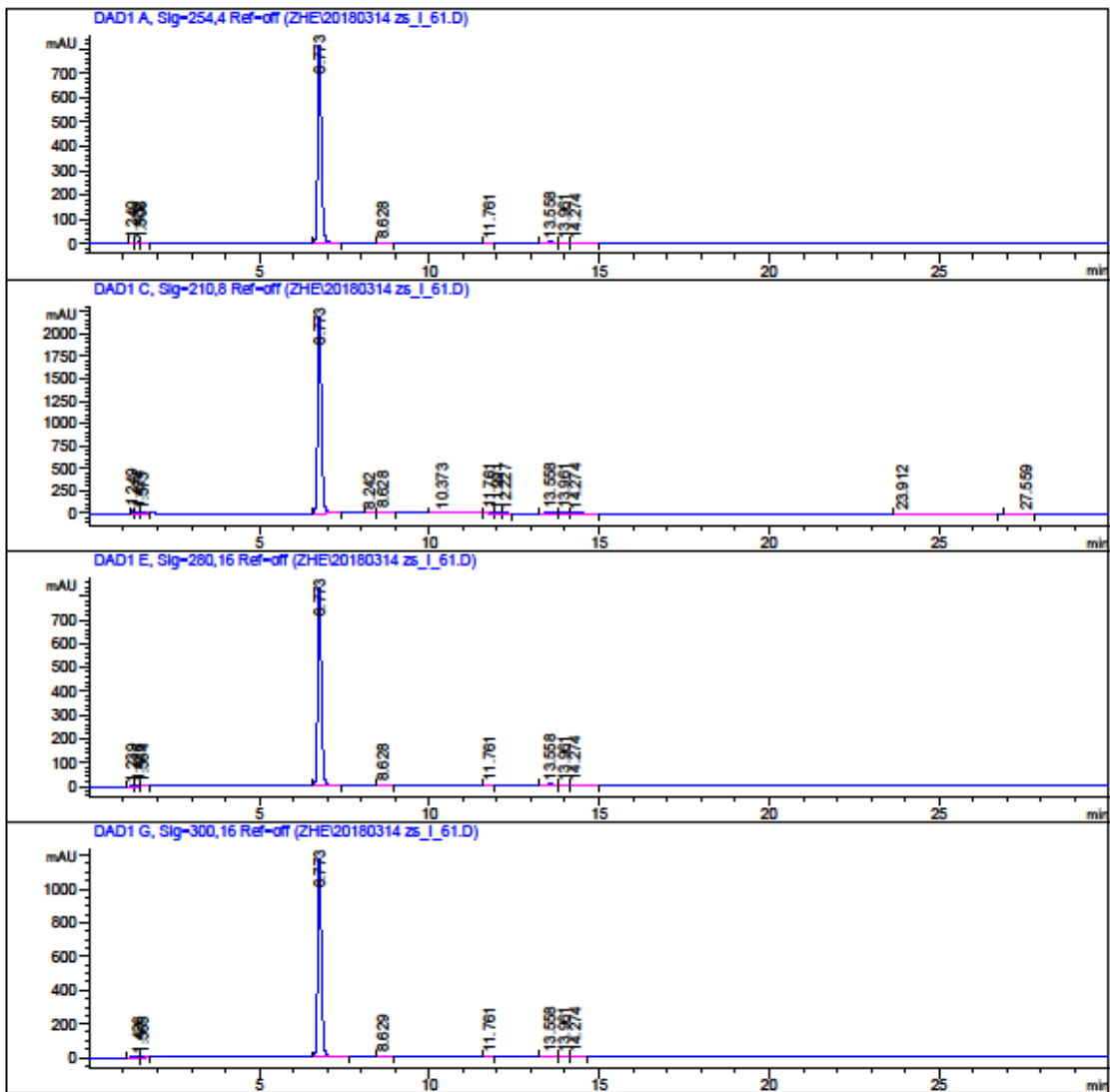
HPLC of Compound 1 (OXi8006)

Data File C:\Chem32\1\Data\ZHE\20180314 zs_I_61.D

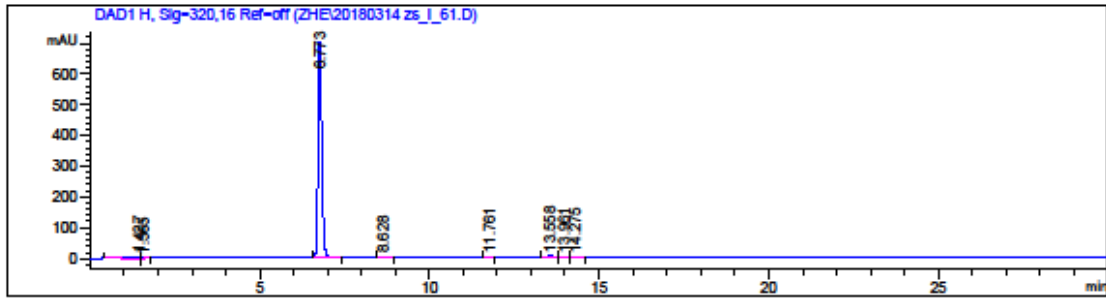
Sample Name: OXi8006

Acq. Operator : SYSTEM
Sample Operator : SYSTEM
Acq. Instrument : 1200 HPLC Location : 1
Injection Date : 3/14/2018 1:55:25 PM Inj Volume : No inj
Acq. Method : C:\CHEM32\1\METHODS\GRAD 2 30-90 ACN.M
Last changed : 4/2/2014 4:04:33 PM by ERICA P
Analysis Method : C:\CHEM32\1\METHODS\RT-ACNWASH 2.M
Last changed : 7/9/2015 2:27:22 PM by Blake
Method Info : General Column Wash Method

Sample Info : OXi8006 zs



Data File C:\Chem32\1\Data\ZHE\20180314 zs_I_61.D
 Sample Name: OXi8006



=====
 Area Percent Report
 =====

Sorted By : Signal
 Multiplier : 1.0000
 Dilution : 1.0000
 Use Multiplier & Dilution Factor with ISTDs

Signal 1: DAD1 A, Sig=254,4 Ref=off

Peak #	RetTime [min]	Type	Width [min]	Area [mAU*s]	Height [mAU]	Area %
1	1.240	BV	0.0644	6.65432	1.48242	0.1016
2	1.432	VV	0.0697	30.61286	6.40725	0.4676
3	1.506	VB	0.0847	29.96033	4.67789	0.4576
4	6.773	BB	0.1186	6340.44873	816.30566	96.8449
5	8.628	BB	0.1419	26.94950	2.76090	0.4116
6	11.761	BB	0.1167	18.05374	2.42974	0.2758
7	13.558	BV	0.1539	54.64087	5.50217	0.8346
8	13.961	VV	0.1399	19.55314	2.11403	0.2987
9	14.274	VB	0.1774	20.13676	1.71016	0.3076

Totals : 6547.01025 843.39022

Signal 2: DAD1 C, Sig=210,8 Ref=off

Peak #	RetTime [min]	Type	Width [min]	Area [mAU*s]	Height [mAU]	Area %
1	1.249	BV	0.0648	214.64099	47.44749	1.1645
2	1.424	VV	0.0979	119.00981	16.16756	0.6457
3	1.573	VB	0.1395	96.76292	9.44871	0.5250
4	6.773	BB	0.1246	1.74198e4	2195.21240	94.5063
5	8.242	BB	0.1198	17.33465	2.25314	0.0940
6	8.628	BB	0.1417	77.74158	7.97959	0.4218
7	10.373	BB	0.3682	33.30708	1.16273	0.1807
8	11.761	BV	0.1260	63.22221	7.68650	0.3430
9	11.991	VV	0.1326	14.46958	1.64545	0.0785
10	12.227	VB	0.1330	11.38415	1.31532	0.0618

Data File C:\Chem32\1\Data\ZHE\20180314 zs_I_61.D
 Sample Name: Oxi8006

Peak #	RetTime [min]	Type	Width [min]	Area [mAU*s]	Height [mAU]	Area %
11	13.558	BV	0.1539	155.81810	15.68387	0.8453
12	13.961	VV	0.1441	58.29197	6.17871	0.3162
13	14.274	VB	0.1928	66.36258	5.06685	0.3600
14	23.912	BB	0.3980	38.03997	1.25364	0.2064
15	27.559	BB	0.2499	46.24069	2.72534	0.2509

Totals : 1.84324e4 2321.22731

Signal 3: DAD1 E, Sig=280,16 Ref=off

Peak #	RetTime [min]	Type	Width [min]	Area [mAU*s]	Height [mAU]	Area %
1	1.239	BV	0.0861	9.15214	1.48139	0.1373
2	1.426	VB	0.0688	22.21363	4.73331	0.3332
3	1.564	BB	0.1108	16.21666	1.99587	0.2432
4	6.773	BB	0.1186	6480.22900	834.09564	97.1957
5	8.628	BB	0.1415	25.54412	2.62518	0.3831
6	11.761	BB	0.1173	16.89900	2.25824	0.2535
7	13.558	BV	0.1531	60.97647	6.18204	0.9146
8	13.961	VV	0.1408	18.05167	1.97236	0.2708
9	14.274	VB	0.1709	17.91190	1.57257	0.2687

Totals : 6667.19460 856.91659

Signal 4: DAD1 G, Sig=300,16 Ref=off

Peak #	RetTime [min]	Type	Width [min]	Area [mAU*s]	Height [mAU]	Area %
1	1.426	BB	0.0970	27.52202	3.86687	0.2940
2	1.565	BB	0.1114	15.39917	1.88240	0.1645
3	6.773	BB	0.1190	9152.51367	1173.47668	97.7791
4	8.629	BB	0.1424	34.15394	3.48433	0.3649
5	11.761	BB	0.1170	22.09877	2.96447	0.2361
6	13.558	BV	0.1528	64.10770	6.51722	0.6849
7	13.961	VV	0.1379	23.02530	2.58649	0.2460
8	14.274	VB	0.1623	21.57463	2.02505	0.2305

Totals : 9360.39519 1196.80351

Signal 5: DAD1 H, Sig=320,16 Ref=off

Peak #	RetTime [min]	Type	Width [min]	Area [mAU*s]	Height [mAU]	Area %
1	1.427	BB	0.2010	53.76475	3.35397	0.9554
2	1.565	BB	0.1166	13.78403	1.59863	0.2449

Data File C:\Chem32\1\Data\ZHE\20180314 zs_I_61.D

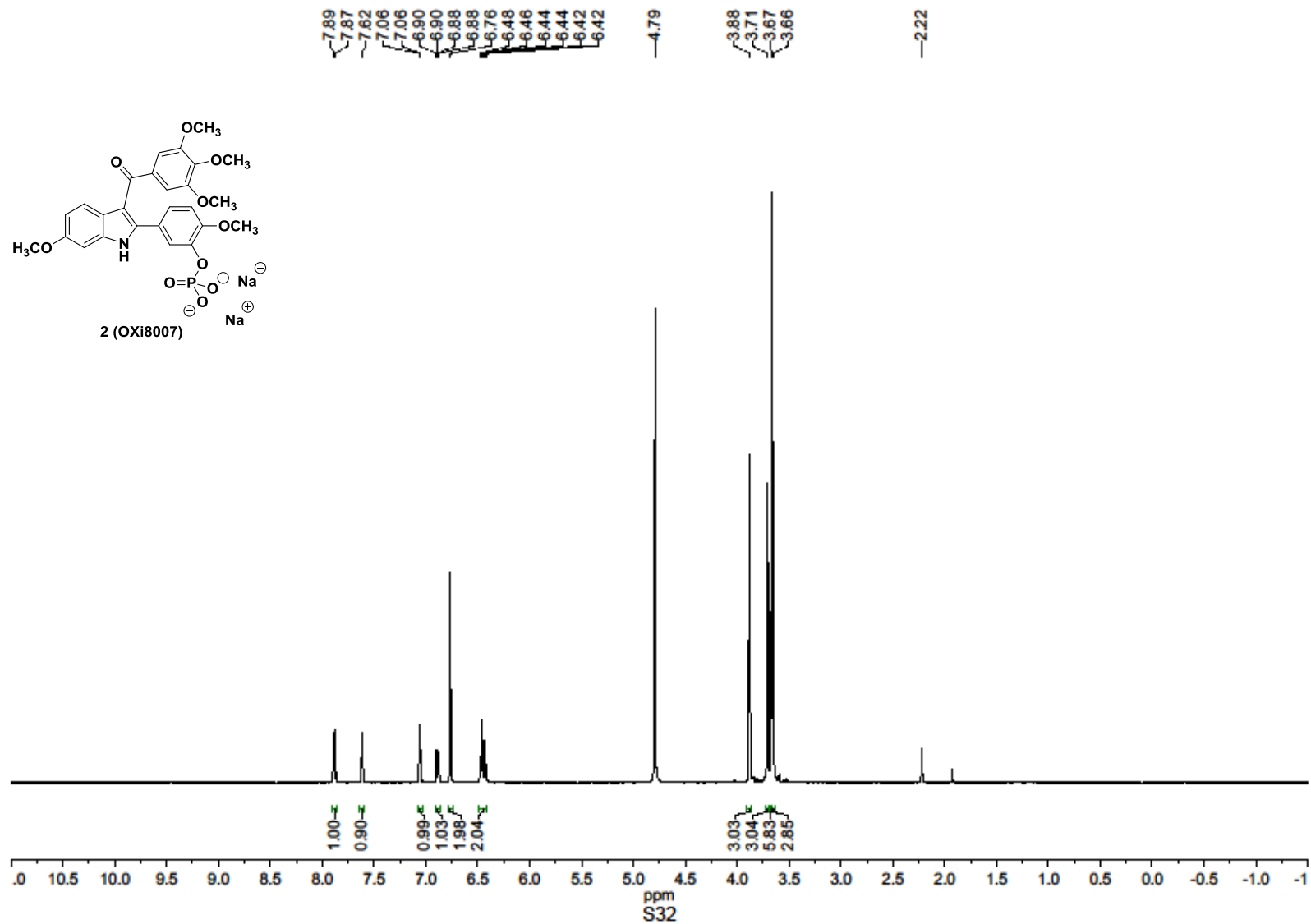
Sample Name: OXi8006

Peak #	RetTime [min]	Type	Width [min]	Area [mAU*s]	Height [mAU]	Area %
3	6.773	BB	0.1188	5456.46582	701.29034	96.9642
4	8.628	BB	0.1424	25.36720	2.58755	0.4508
5	11.761	BB	0.1169	17.22505	2.31377	0.3061
6	13.558	BB	0.1477	33.04178	3.44963	0.5872
7	13.961	BV	0.1317	14.12892	1.68754	0.2511
8	14.275	VB	0.1568	13.52293	1.32745	0.2403

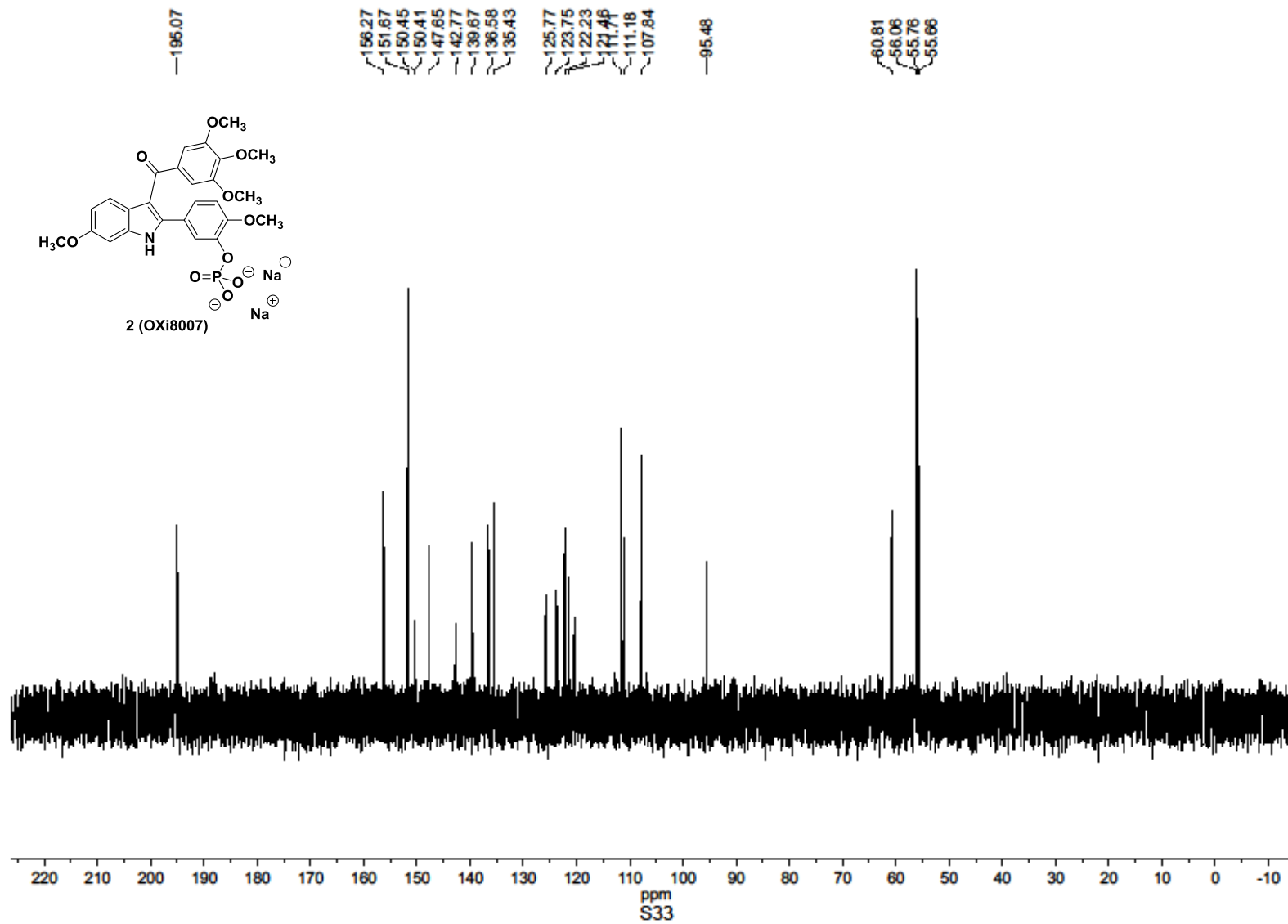
Totals : 5627.30047 717.60888

=====
*** End of Report ***

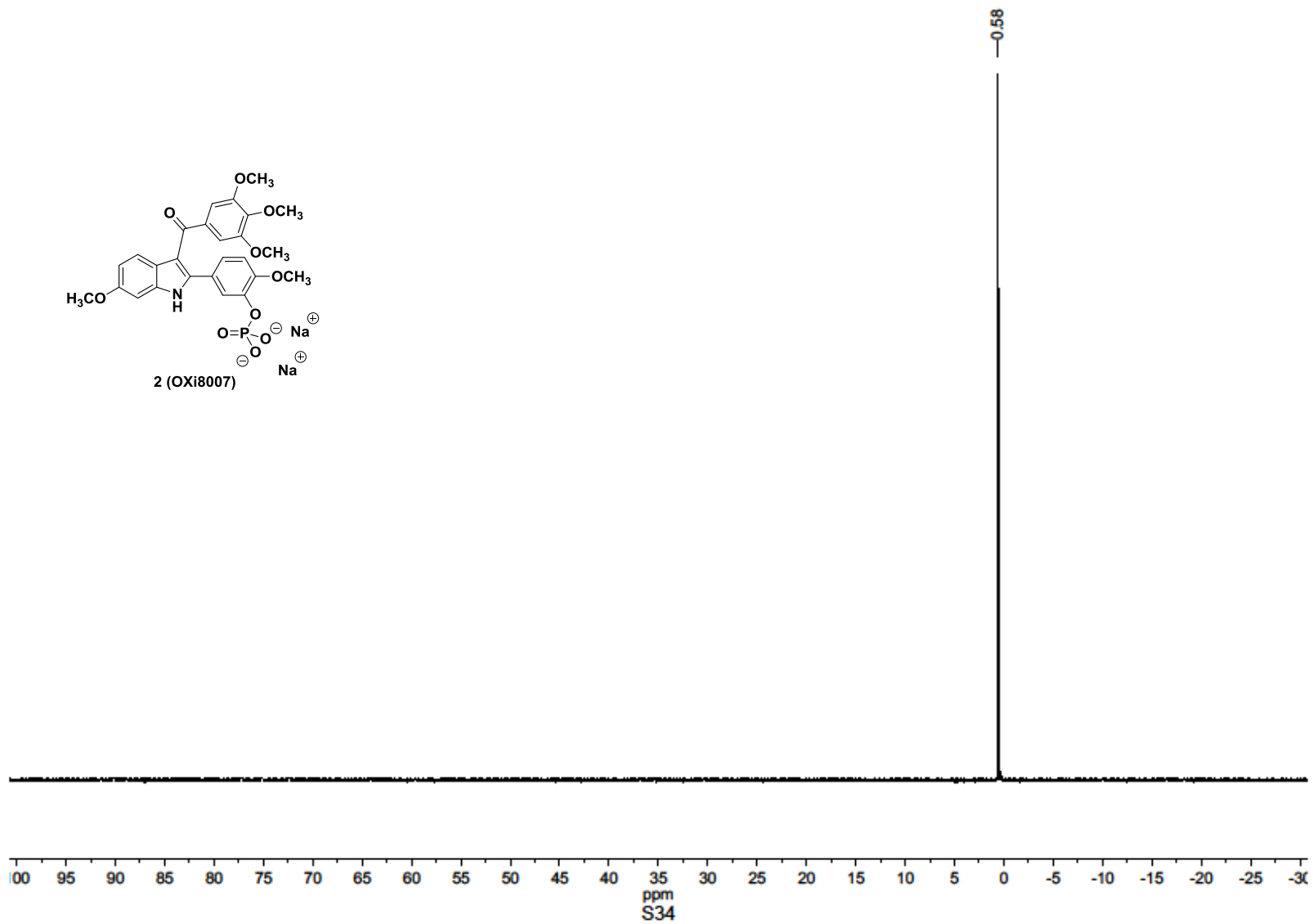
¹H NMR of Compound 2 (OXi8007)



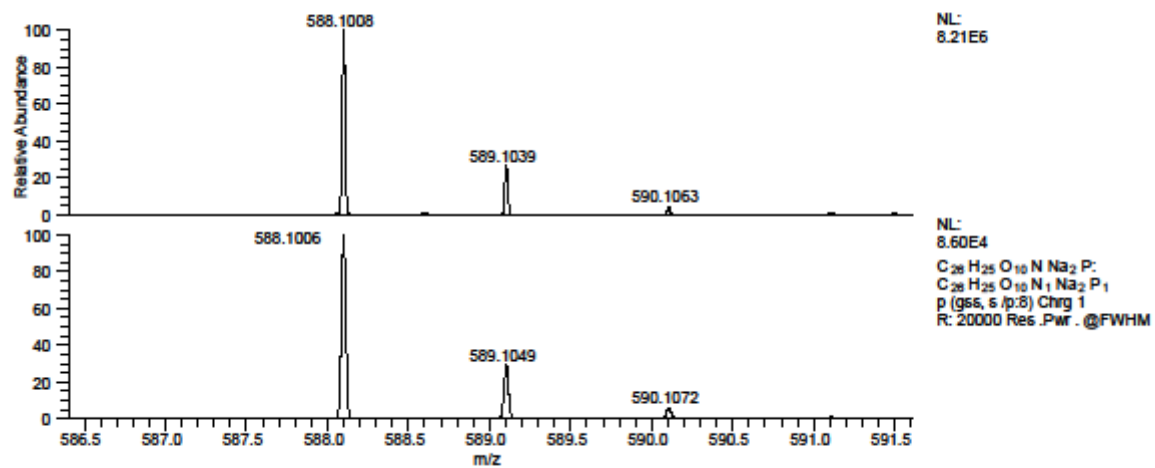
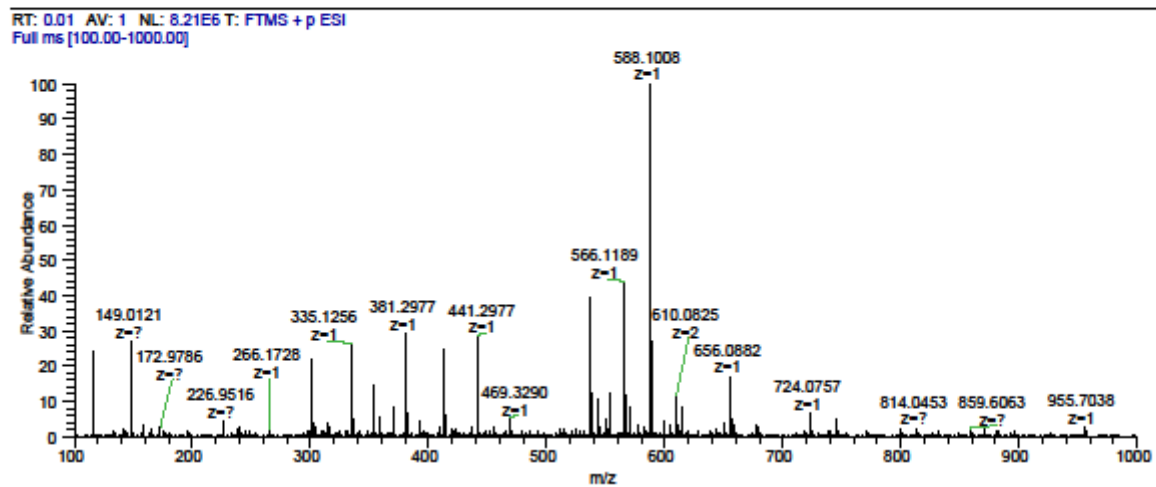
¹³C NMR of Compound 2 (OXi8007)



^{31}P NMR of Compound **2** (OXi8007)



HRMS of Compound 2 (OXi8007)



S39

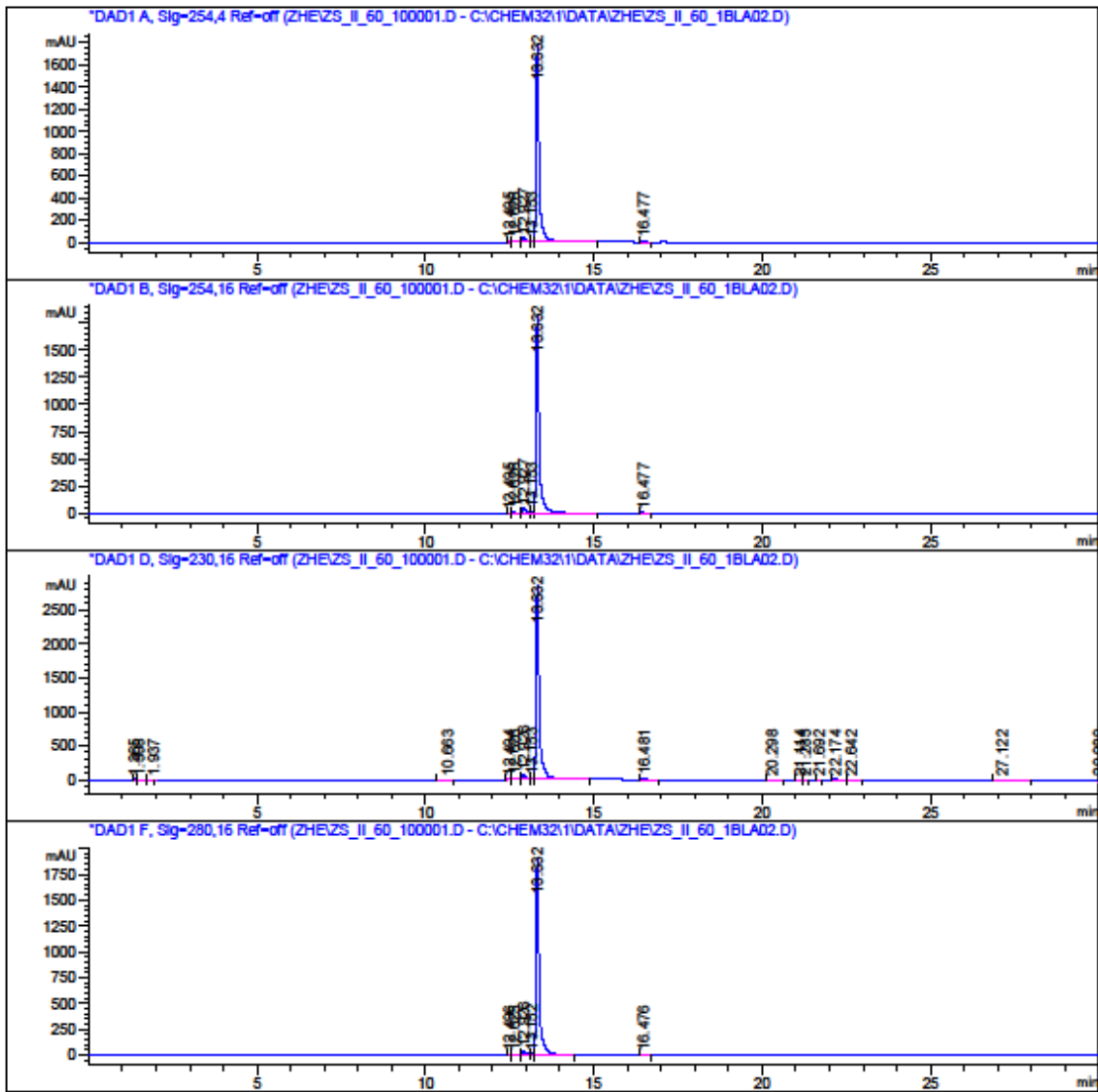
HPLC traces of Compound 2 (OXi8007)

Data File C:\Chem32\1\Data\ZHE\ZS_II_60_100001.D

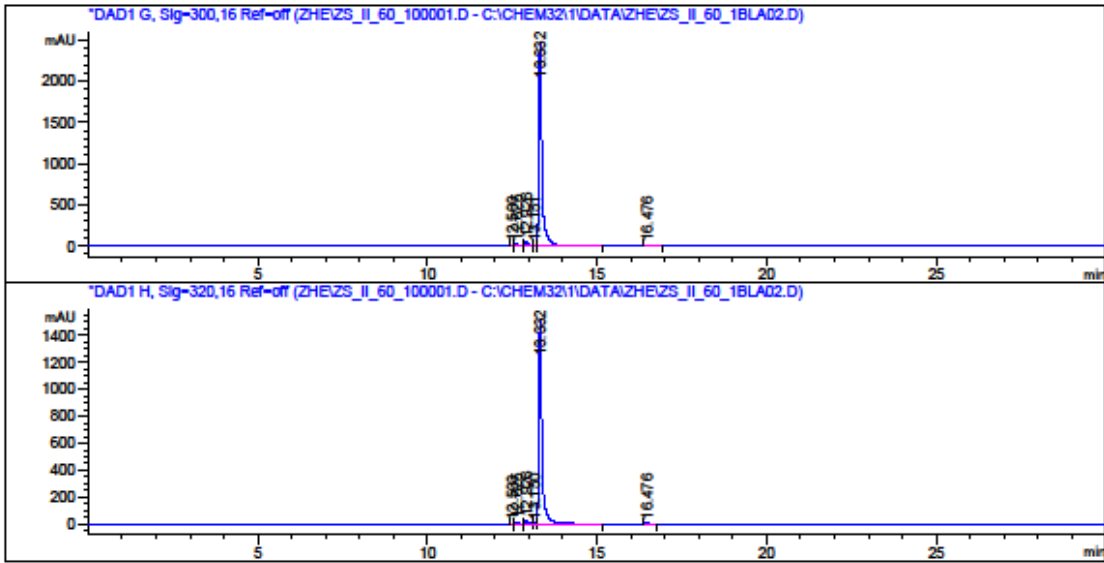
Sample Name: OXi8007

=====
Acq. Operator : Zhe
Acq. Instrument : Instrument 1 Location : -
Injection Date : 7/25/2014 2:52:44 PM
Acq. Method : C:\CHEM32\1\METHODS\MASTERMETHOD02.M
Last changed : 7/25/2014 2:35:32 PM by Laxman
Analysis Method : C:\CHEM32\1\METHODS\RT-ACNWASH 2.M
Last changed : 7/9/2015 2:27:22 PM by Blake
Method Info : General Column Wash Method

Sample Info : zs_II_60_1
OXi8007
Mastermethod 2
TFA 0.1% in H2O



Data File C:\Chem32\1\Data\ZHE\ZS_II_60_100001.D
 Sample Name: Oxi8007



=====
 Area Percent Report
 =====

Sorted By : Signal
 Multiplier : 1.0000
 Dilution : 1.0000
 Use Multiplier & Dilution Factor with ISTDs

Signal 1: DAD1 A, Sig=254,4 Ref-off
 Signal has been modified after loading from rawdata file!

Peak #	RetTime [min]	Type	Width [min]	Area [mAU*s]	Height [mAU]	Area %
1	12.495	BV	0.0795	12.39340	2.42808	0.1077
2	12.626	VB	0.0841	43.99183	7.76432	0.3822
3	12.927	BV	0.1022	252.22702	36.68114	2.1911
4	13.153	VV	0.0726	58.05358	11.95827	0.5043
5	13.332	VB	0.0928	1.11168e4	1781.67322	96.5724
6	16.477	BB	0.0808	27.89583	5.35215	0.2423

Totals : 1.15114e4 1845.85717

Signal 2: DAD1 B, Sig=254,16 Ref-off
 Signal has been modified after loading from rawdata file!

Data File C:\Chem32\1\Data\ZHE\ZS_II_60_100001.D
 Sample Name: Oxi8007

Peak #	RetTime [min]	Type	Width [min]	Area [mAU*s]	Height [mAU]	Area %
1	12.495	BV	0.0797	12.62310	2.46867	0.1074
2	12.626	VB	0.0845	44.41746	7.79347	0.3778
3	12.927	BV	0.1023	257.55658	37.42467	2.1909
4	13.153	VV	0.0727	59.24242	12.17958	0.5039
5	13.332	VB	0.0928	1.13536e4	1818.90979	96.5785
6	16.477	BB	0.0809	28.38755	5.43724	0.2415

Totals : 1.17558e4 1884.21343

Signal 3: DAD1 D, Sig=230,16 Ref=off
 Signal has been modified after loading from rawdata file!

Peak #	RetTime [min]	Type	Width [min]	Area [mAU*s]	Height [mAU]	Area %
1	1.365	BV	0.0615	27.90047	6.85262	0.1424
2	1.508	VB	0.1424	28.85850	2.58198	0.1473
3	1.937	BB	0.0869	15.75779	2.45355	0.0804
4	10.663	BB	0.1200	12.61903	1.47196	0.0644
5	12.494	BV	0.0806	21.31951	4.10706	0.1088
6	12.626	VB	0.0854	79.53583	13.76388	0.4060
7	12.926	BV	0.1026	452.84766	65.55171	2.3114
8	13.153	VV	0.0724	111.88876	23.15592	0.5711
9	13.332	VB	0.0962	1.86046e4	2846.63281	94.9588
10	16.481	BB	0.0891	65.05375	10.98259	0.3320
11	20.298	BB	0.1387	12.08401	1.25080	0.0617
12	21.114	BV	0.1148	12.97643	1.70496	0.0662
13	21.285	VV	0.1093	13.60182	1.85930	0.0694
14	21.692	BV	0.0854	6.14173	1.16725	0.0313
15	22.174	VV	0.1281	34.39015	3.93146	0.1755
16	22.642	VB	0.1263	15.98485	1.82229	0.0816
17	27.122	BB	0.2425	35.00286	2.01674	0.1787
18	29.989	BBA	0.0133	41.72459	52.17110	0.2130

Totals : 1.95923e4 3043.47796

Signal 4: DAD1 F, Sig=280,16 Ref=off
 Signal has been modified after loading from rawdata file!

Peak #	RetTime [min]	Type	Width [min]	Area [mAU*s]	Height [mAU]	Area %
1	12.496	BV	0.0794	12.28356	2.41254	0.1002
2	12.625	VB	0.0859	44.51081	7.64511	0.3630
3	12.926	BV	0.1023	260.27914	37.79521	2.1228
4	13.152	VV	0.0730	52.68259	10.77849	0.4297
5	13.332	VB	0.0923	1.18634e4	1913.20129	96.7549
6	16.476	BB	0.0804	28.13110	5.43327	0.2294

Totals : 1.22613e4 1977.26591

Data File C:\Chem32\1\Data\ZHE\ZS_II_60_100001.D
Sample Name: OXi8007

Signal 5: DAD1 G, Sig=300,16 Ref=off
Signal has been modified after loading from rawdata file!

Peak #	RetTime [min]	Type	Width [min]	Area [mAU*s]	Height [mAU]	Area %
1	12.500	BV	0.0732	12.83738	2.71264	0.0795
2	12.625	VB	0.0822	95.28880	17.31257	0.5903
3	12.926	BV	0.1038	334.77448	47.77440	2.0737
4	13.151	VV	0.0740	59.07925	11.88176	0.3660
5	13.332	VB	0.0936	1.56014e4	2472.82813	96.6413
6	16.476	BB	0.0809	40.23180	7.70837	0.2492

Totals : 1.61436e4 2560.21786

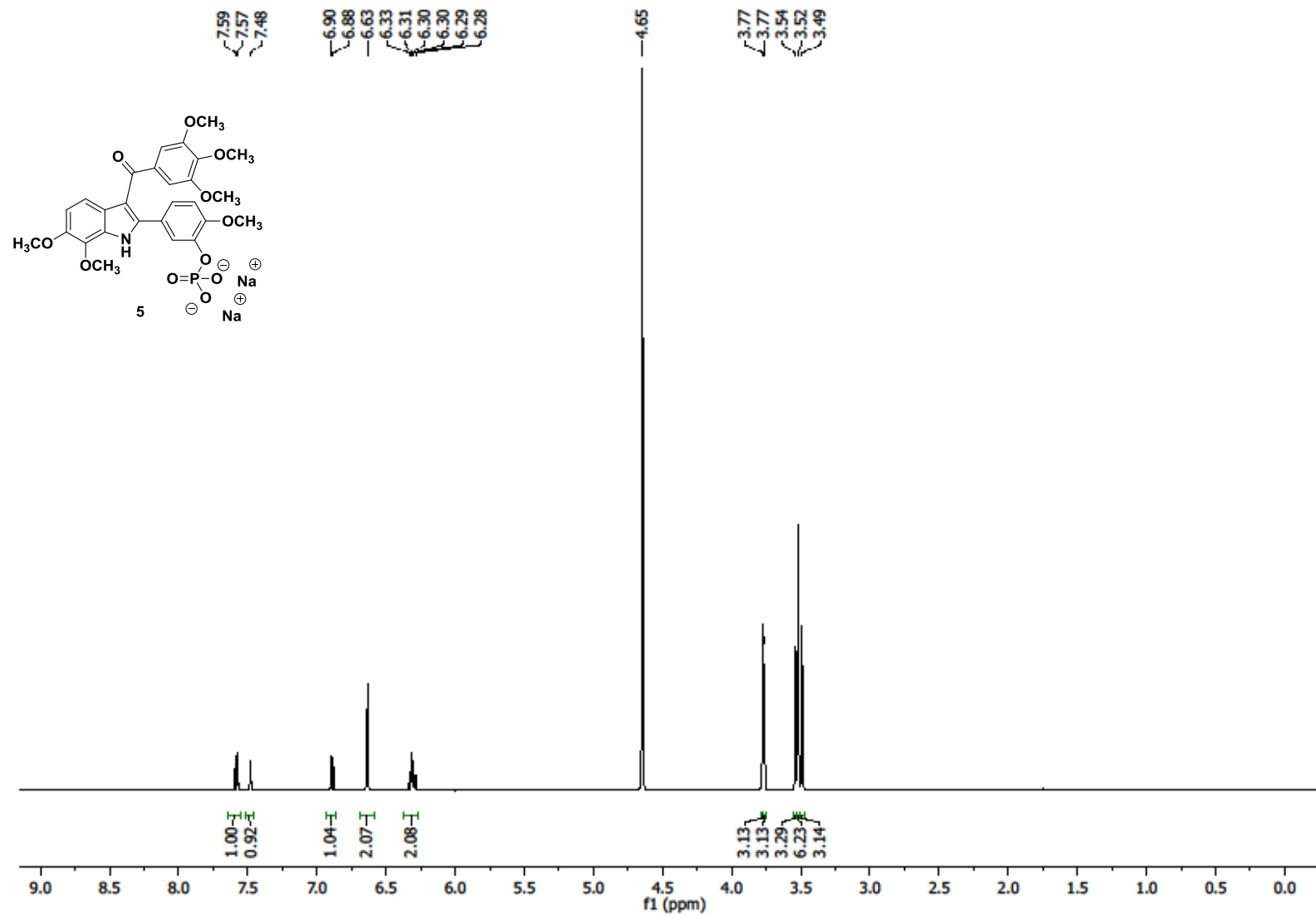
Signal 6: DAD1 H, Sig=320,16 Ref=off
Signal has been modified after loading from rawdata file!

Peak #	RetTime [min]	Type	Width [min]	Area [mAU*s]	Height [mAU]	Area %
1	12.503	BV	0.0718	7.56785	1.64118	0.0772
2	12.625	VB	0.0810	72.44402	13.42175	0.7392
3	12.926	BV	0.1041	196.32983	27.89448	2.0032
4	13.150	VV	0.0737	34.07512	6.88640	0.3477
5	13.332	VB	0.0930	9465.54297	1513.57849	96.5812
6	16.476	BB	0.0805	24.64466	4.74946	0.2515

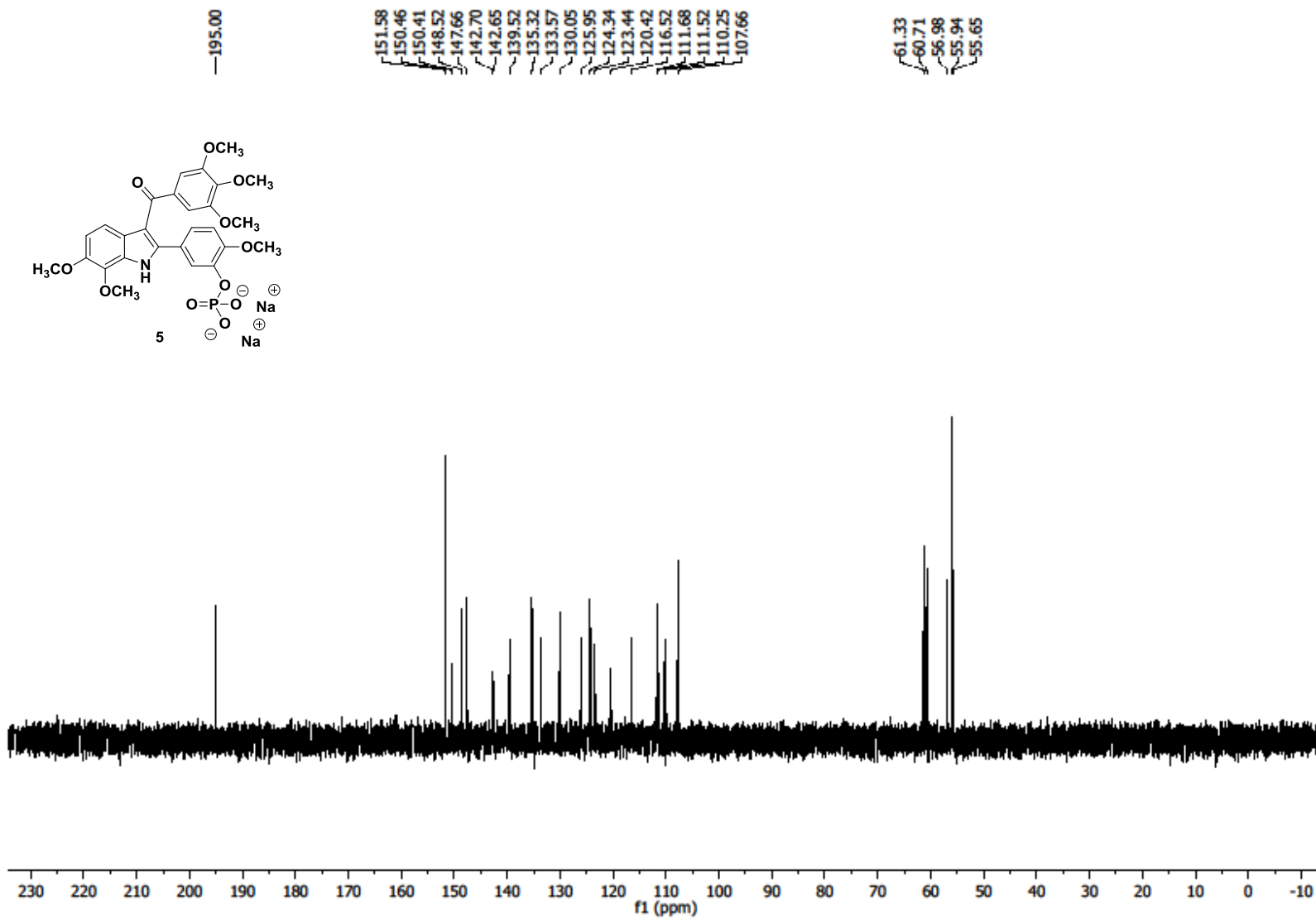
Totals : 9800.60446 1568.17177

=====
*** End of Report ***

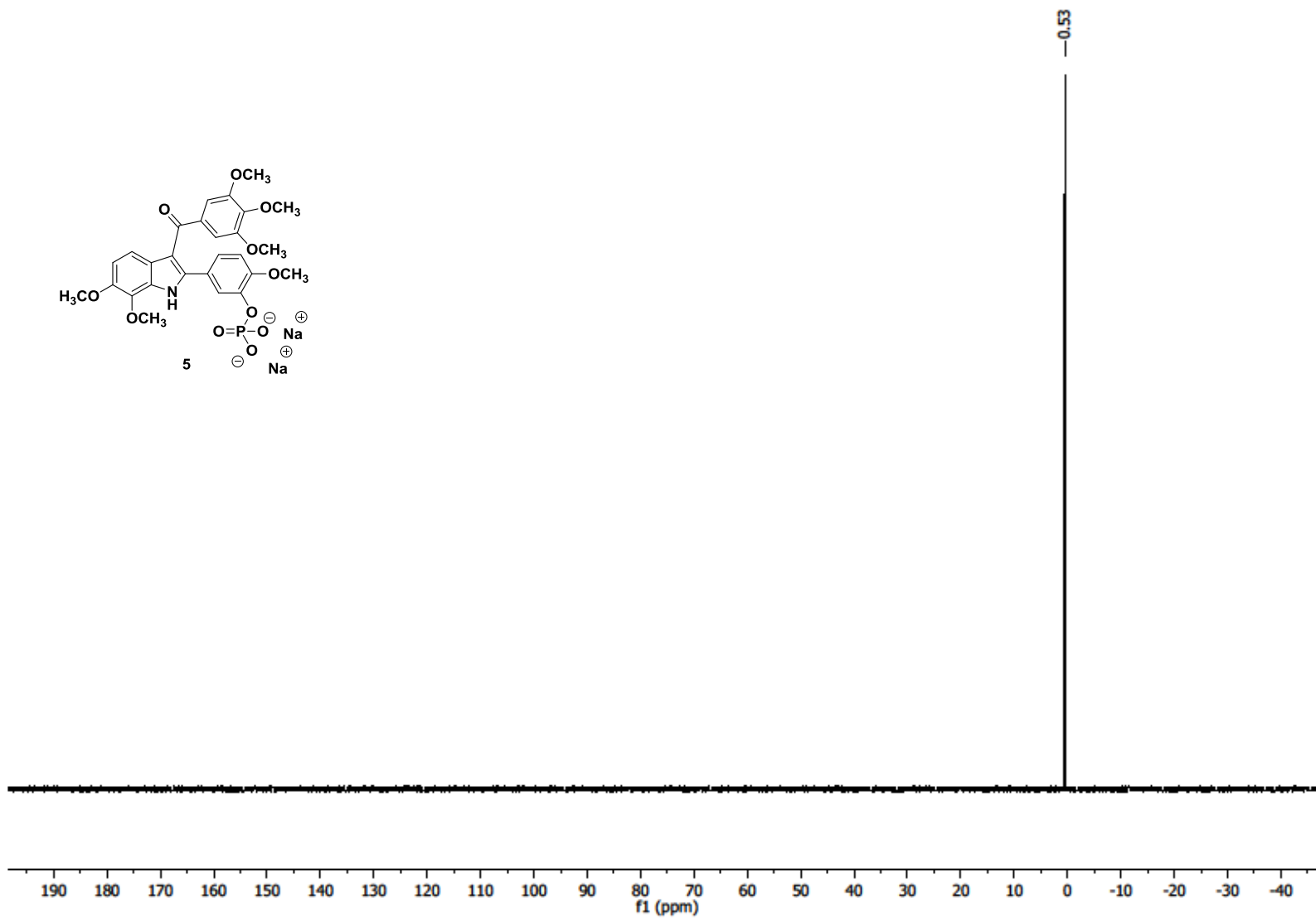
¹H NMR of Compound 5



¹³C NMR of Compound 5



^{31}P NMR of Compound 5

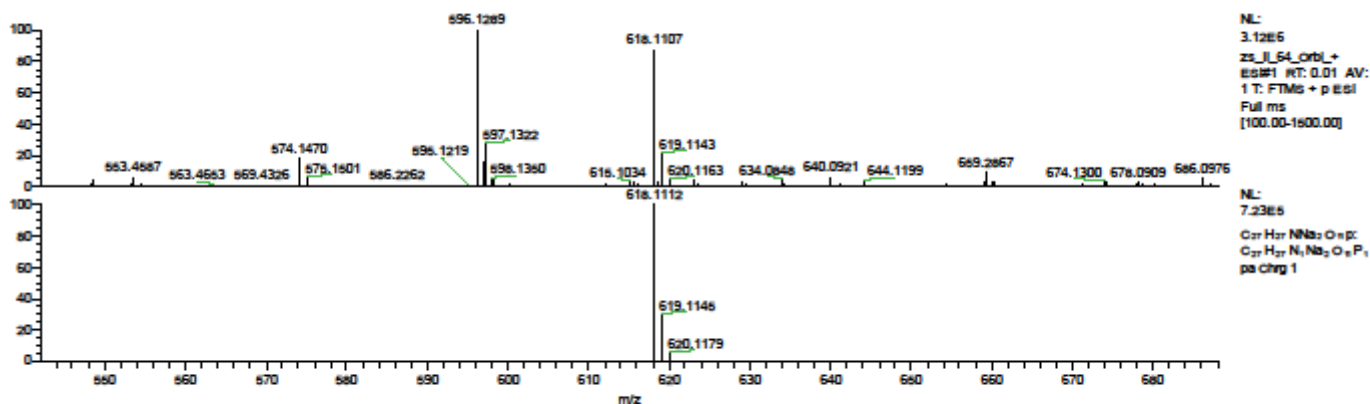
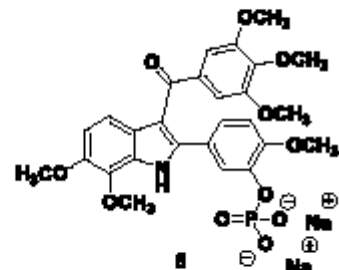
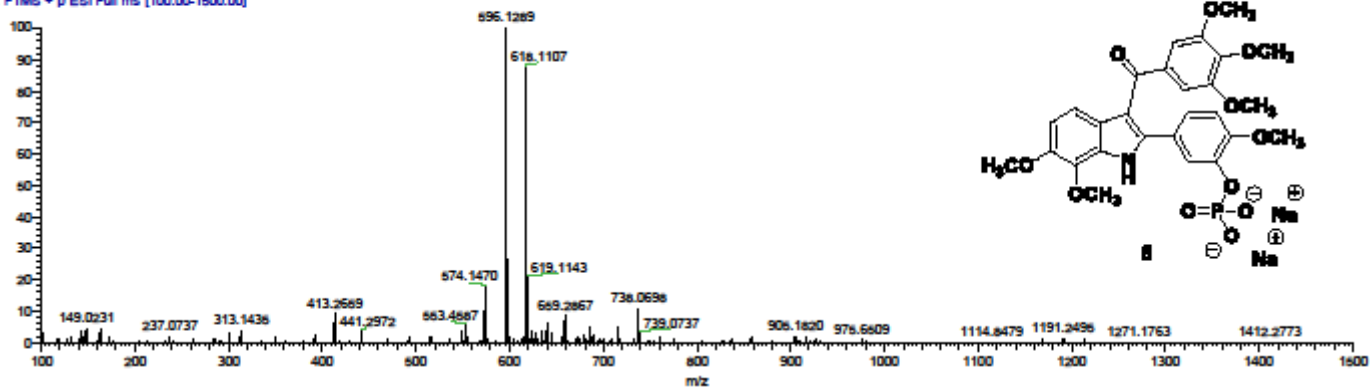


HRMS of Compound 5

C:\Xcalibur...zs_IL54_Orbi_+ESI

8/19/2014 10:18:48 AM

zs_IL54_Orbi_+ESI#1 RT: 0.01 AV: 1 NL: 3
T: FTMs + p ESI Full ms [100.00-1500.00]

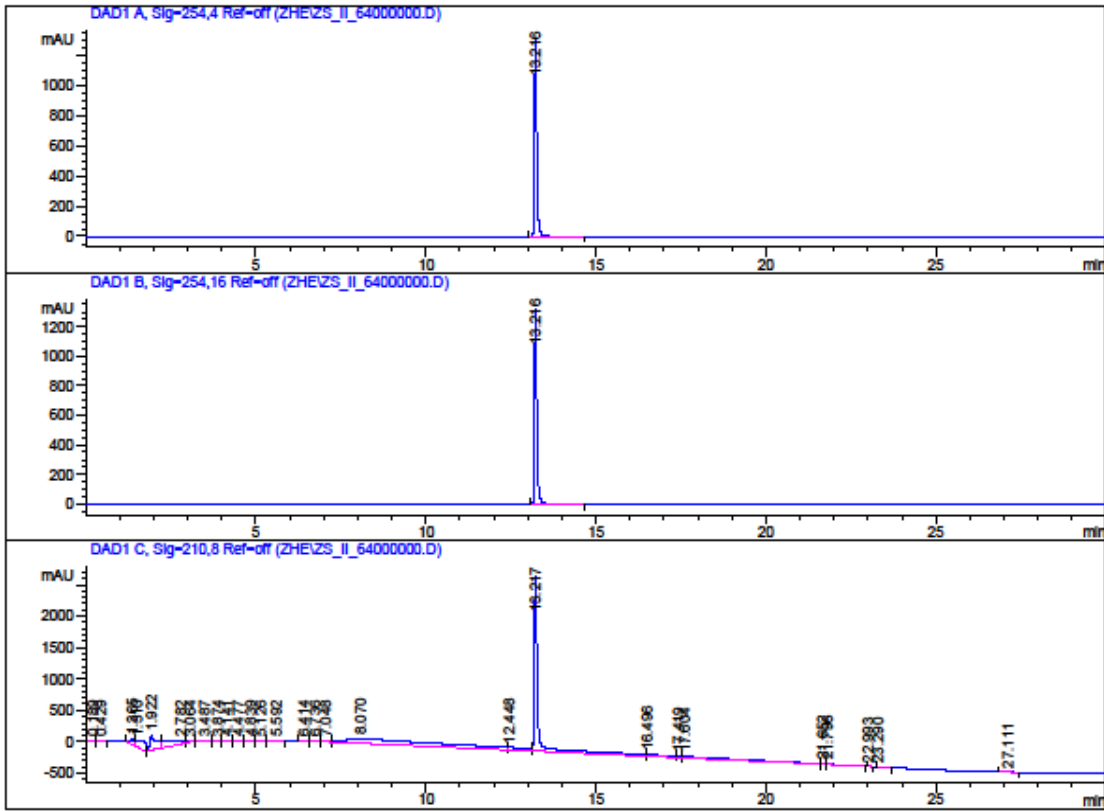


HPLC traces of Compound 5

Data File C:\CHEM32\1\DATA\ZHE\ZS_II_64000000.D

Sample Name: KGP 415

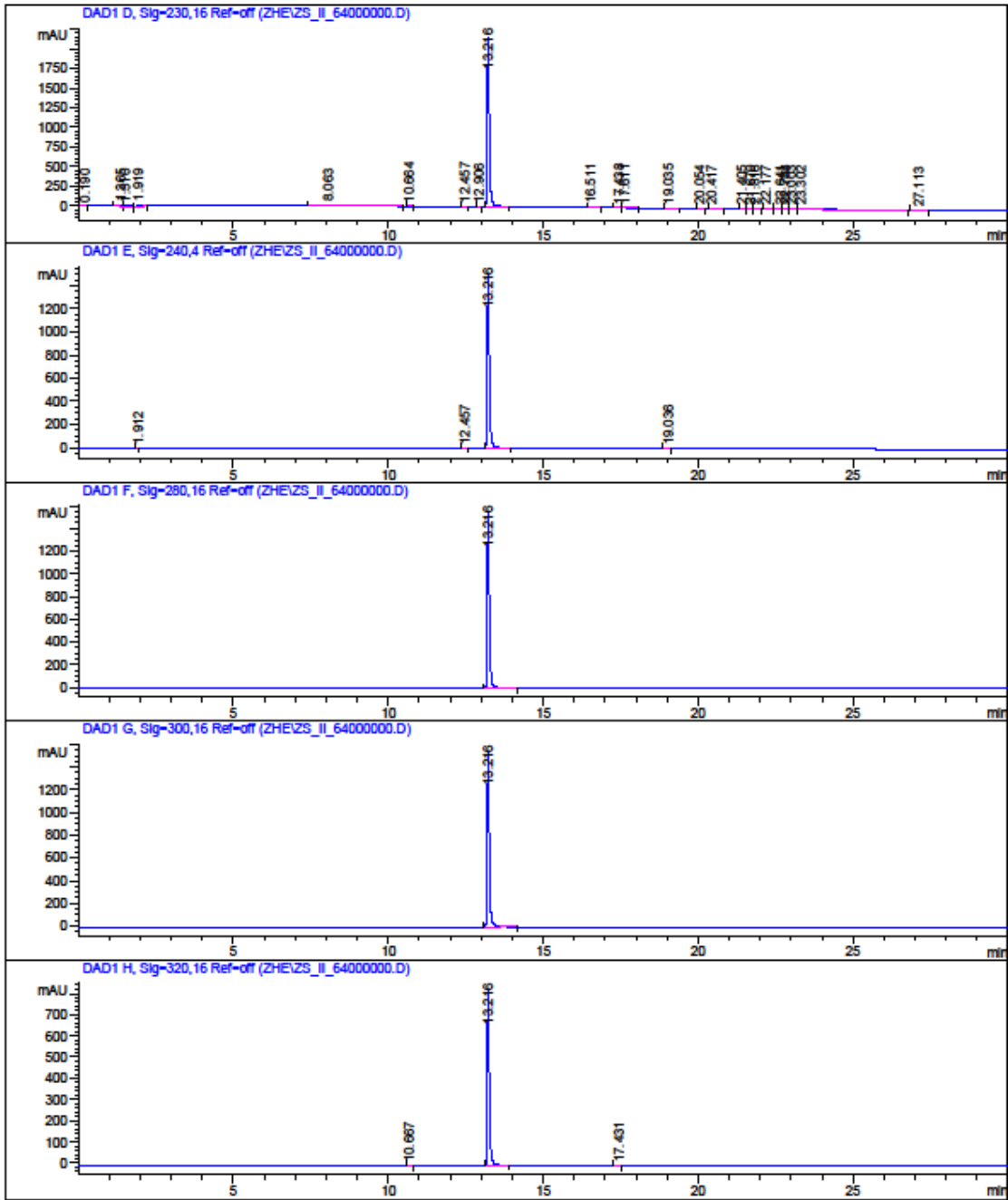
```
=====
Acq. Operator   : Zhe
Acq. Instrument : Instrument 1           Location : -
Injection Date  : 8/6/2014 11:37:50 AM
Acq. Method    : C:\CHEM32\1\METHODS\MASTERMETHOD2.M
Last changed   : 8/6/2014 11:22:45 AM by Zhe
Analysis Method: C:\CHEM32\1\DATA\ZHE\ZS_II_64000000.D\DA.M (MASTERMETHOD2.M)
Last changed   : 8/6/2014 12:18:04 PM by Zhe
Sample Info    : ss_II_64 KGP415
                master method 2
                0.1% TFA
```



Instrument 1 8/6/2014 1:44:16 PM Zhe

Page 1 of 5

Created with novaPDF Printer (www.novapdf.com). Please register to remove this message.



=====
Area Percent Report
=====

Sorted By : Signal
Multiplier : 1.0000
Dilution : 1.0000
Use Multiplier & Dilution Factor with ISTDs

Signal 1: DAD1 A, Sig=254,4 Ref=off

Peak #	RetTime [min]	Type	Width [min]	Area [mAU*s]	Height [mAU]	Area %
1	13.216	BB	0.0768	6531.24219	1295.65454	100.0000

Totals : 6531.24219 1295.65454

Signal 2: DAD1 B, Sig=254,16 Ref=off

Peak #	RetTime [min]	Type	Width [min]	Area [mAU*s]	Height [mAU]	Area %
1	13.216	BB	0.0768	6692.73535	1327.55493	100.0000

Totals : 6692.73535 1327.55493

Signal 3: DAD1 C, Sig=210,8 Ref=off

Peak #	RetTime [min]	Type	Width [min]	Area [mAU*s]	Height [mAU]	Area %
1	0.189	BB	0.0800	75.13561	13.28350	0.1313
2	0.429	BB	0.2254	78.37328	5.59722	0.1369
3	1.365	BV	0.1256	886.32990	92.69025	1.5485
4	1.510	VB	0.2570	2187.33350	105.02055	3.8215
5	1.922	BV	0.1731	3338.16406	244.77377	5.8322
6	2.782	VV	0.7422	3092.31323	50.37460	5.4026
7	3.064	VB	0.2375	261.42422	15.28922	0.4567
8	3.487	BB	0.2369	41.13178	2.87491	0.0719
9	3.874	BB	0.1563	19.03923	2.05058	0.0333
10	4.141	BB	0.1400	16.36439	1.90884	0.0286
11	4.477	BB	0.1563	22.73960	2.36281	0.0397
12	4.839	BV	0.1829	28.16278	2.43588	0.0492
13	5.126	VB	0.1669	18.51681	1.62596	0.0324
14	5.592	BB	0.2041	29.88281	2.23344	0.0522
15	6.414	BB	0.1512	21.94595	2.38779	0.0383
16	6.736	BV	0.2253	80.49945	5.42000	0.1406

Data File C:\CHEM32\1\DATA\ZHE\ZS_II_64000000.D
 Sample Name: KGP 415

Peak #	RetTime [min]	Type	Width [min]	Area [mAU*s]	Height [mAU]	Area %
17	7.048	VV	0.3064	291.14645	14.13098	0.5087
18	8.070	VV	2.6860	1.67952e4	75.59576	29.2433
19	12.448	VV	0.4840	1795.15259	44.94108	3.1363
20	13.217	VV	0.1153	2.22757e4	2785.77563	38.9184
21	16.496	VV	0.5848	1476.85486	30.61629	2.5802
22	17.419	VV	0.1413	275.22180	26.92437	0.4808
23	17.604	VV	1.5956	3705.18506	27.43492	6.4734
24	21.652	VV	0.1192	69.01969	8.11931	0.1206
25	21.796	VB	0.3683	215.26878	7.29487	0.3761
26	22.993	BB	0.0837	9.03658	1.65479	0.0158
27	23.290	BB	0.1958	32.70852	2.14647	0.0571
28	27.111	BB	0.2494	99.10936	6.10576	0.1732

Totals : 5.72370e4 3581.06954

Signal 4: DAD1 D, Sig=230,16 Ref=off

Peak #	RetTime [min]	Type	Width [min]	Area [mAU*s]	Height [mAU]	Area %
1	0.190	BB	0.0876	11.12833	1.97924	0.0849
2	1.365	BV	0.1270	134.78336	13.91810	1.0284
3	1.510	VB	0.2556	320.13950	15.45831	2.4428
4	1.919	BB	0.1180	274.29324	30.78302	2.0929
5	8.063	BB	1.0837	522.85022	6.11413	3.9895
6	10.664	BB	0.0761	7.54185	1.56937	0.0575
7	12.457	BB	0.0704	16.28485	3.62380	0.1243
8	12.906	BB	0.0665	14.98156	3.46301	0.1143
9	13.216	BB	0.0768	1.09238e4	2167.06494	83.3518
10	16.511	BB	0.0942	10.95228	1.72193	0.0836
11	17.438	BV	0.1271	20.98060	2.32815	0.1601
12	17.611	VB	0.1319	23.48243	2.44920	0.1792
13	19.035	BB	0.1390	22.73197	2.30540	0.1735
14	20.054	BB	0.1026	9.84389	1.49945	0.0751
15	20.417	BB	0.0970	13.86986	2.15694	0.1058
16	21.405	VB	0.0975	12.98989	2.06073	0.0991
17	21.670	BV	0.0880	28.89659	4.95541	0.2205
18	21.816	VB	0.1021	36.52095	5.45298	0.2787
19	22.177	BB	0.1015	11.01291	1.65689	0.0840
20	22.641	BV	0.1294	49.07919	5.64419	0.3745
21	22.788	VV	0.1253	42.77975	4.92654	0.3264
22	23.003	VV	0.1756	33.17488	2.52005	0.2531
23	23.302	VB	2.2749	500.31625	2.58396	3.8176
24	27.113	BB	0.2603	63.21421	3.79658	0.4823

Totals : 1.31056e4 2290.03231

Data File C:\CHEM32\1\DATA\ZHE\ZS_II_64000000.D
Sample Name: KGP 415

Signal 5: DAD1 E, Sig=240,4 Ref=off

Peak #	RetTime [min]	Type	Width [min]	Area [mAU*s]	Height [mAU]	Area %
1	1.912	BB	0.0590	22.76381	5.90010	0.3041
2	12.457	BB	0.0708	9.71310	2.14752	0.1298
3	13.216	BB	0.0761	7447.41504	1494.80896	99.4877
4	19.036	BB	0.0921	5.87427	1.00641	0.0785

Totals : 7485.76623 1503.86299

Signal 6: DAD1 F, Sig=280,16 Ref=off

Peak #	RetTime [min]	Type	Width [min]	Area [mAU*s]	Height [mAU]	Area %
1	13.216	BB	0.0764	7692.22559	1536.24902	100.0000

Totals : 7692.22559 1536.24902

Signal 7: DAD1 G, Sig=300,16 Ref=off

Peak #	RetTime [min]	Type	Width [min]	Area [mAU*s]	Height [mAU]	Area %
1	13.216	BB	0.0766	7717.59814	1537.77771	100.0000

Totals : 7717.59814 1537.77771

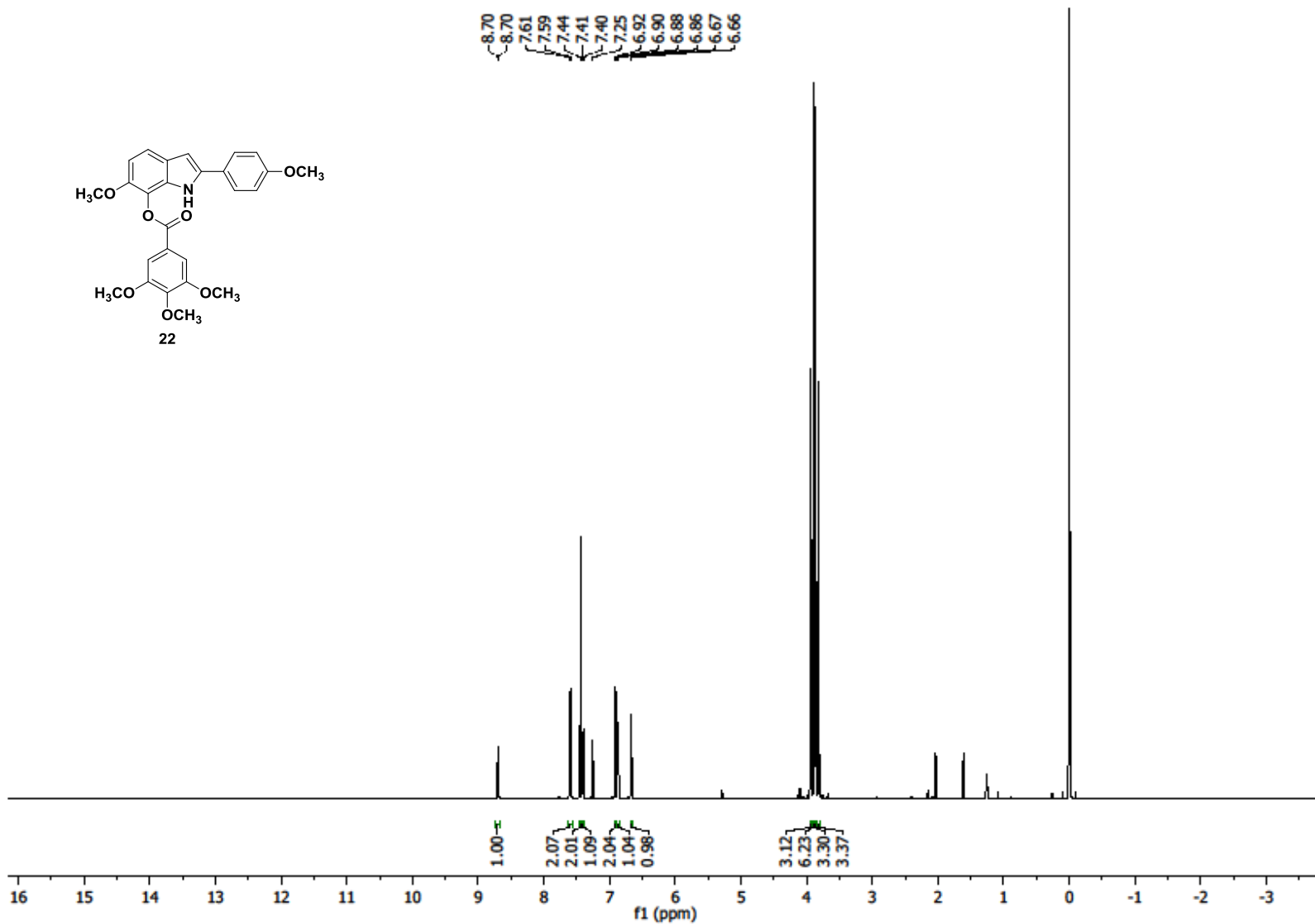
Signal 8: DAD1 H, Sig=320,16 Ref=off

Peak #	RetTime [min]	Type	Width [min]	Area [mAU*s]	Height [mAU]	Area %
1	10.667	BB	0.0774	5.14469	1.04512	0.1250
2	13.216	BB	0.0762	4100.64648	822.51593	99.6377
3	17.431	BV	0.1045	9.76680	1.45211	0.2373

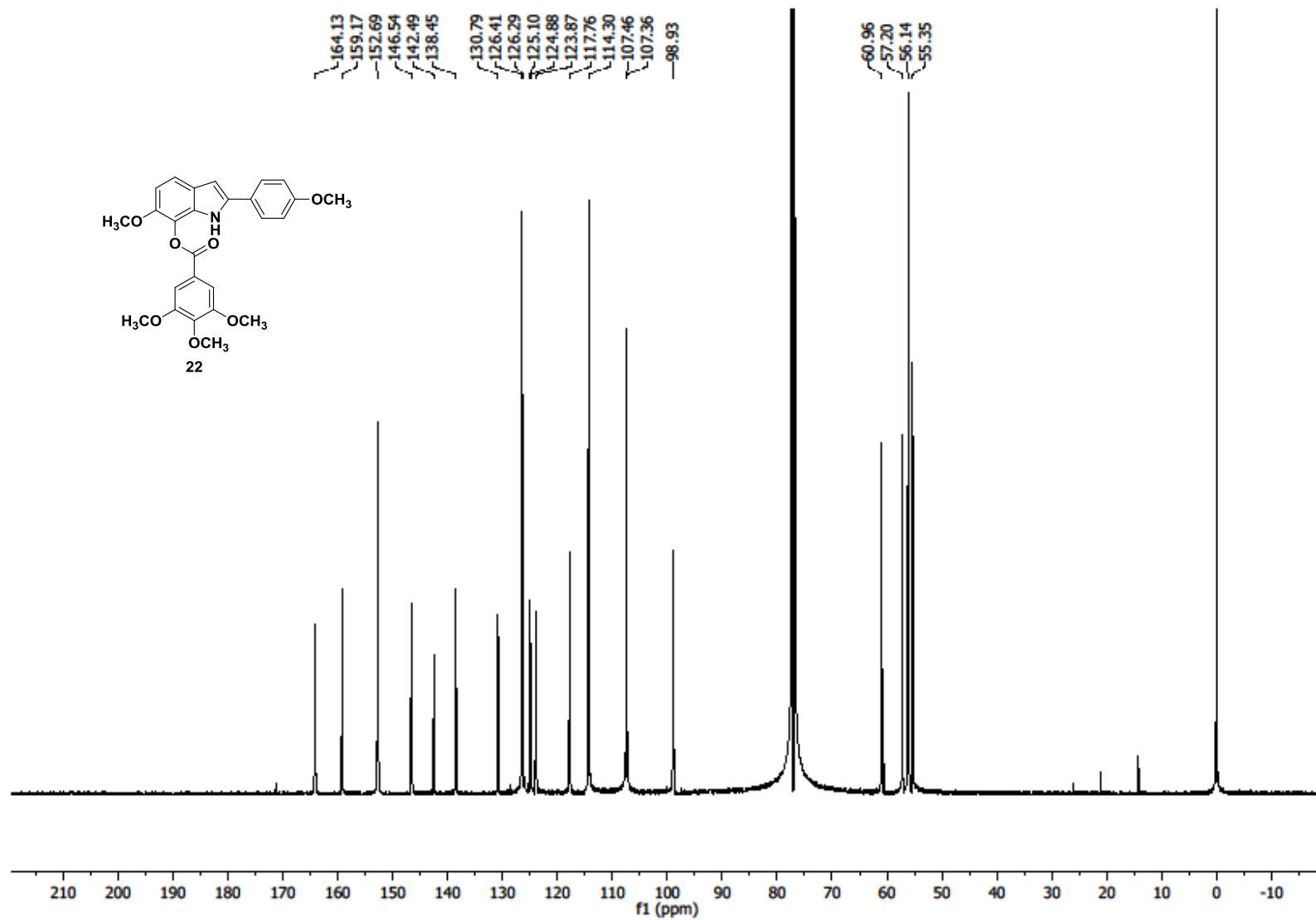
Totals : 4115.55797 825.01316

*** End of Report ***

¹H NMR of Compound 22



¹³C NMR of Compound 22

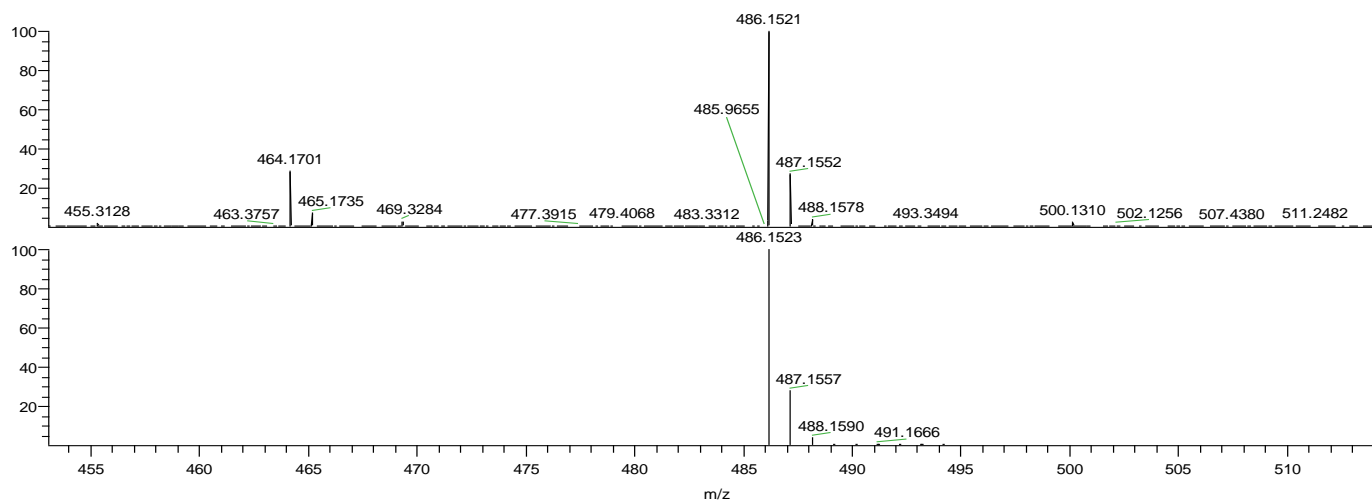
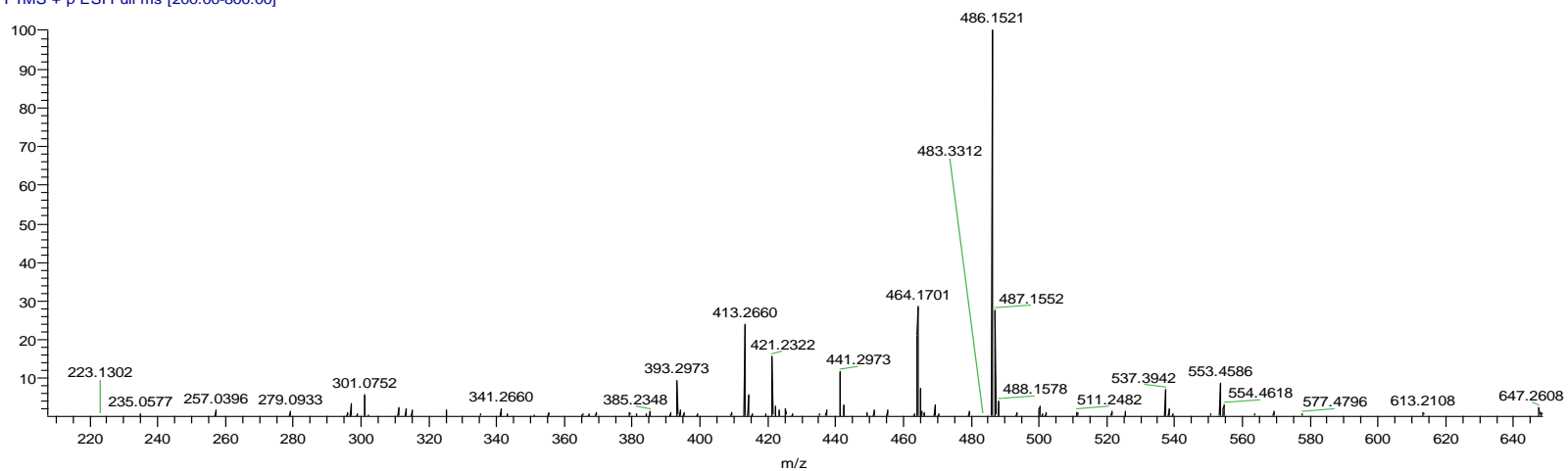


HRMS of Compound 22

9/28/2014 3:03:09 PM

ZS_IL_70_3_8-11_ORBI_+ESI

ZS_IL_70_3_8-11_ORBI_+ESI #2-19 RT: 0.01-0.15
T: FTMS + p ESI Full ms [200.00-800.00]



NL:
1.39E7
ZS_IL_70_3_8-11_ORBI_+
ESI#2-19 RT: 0.01-0.15
AV: 18 T: FTMS + p ESI
Full ms [200.00-800.00]

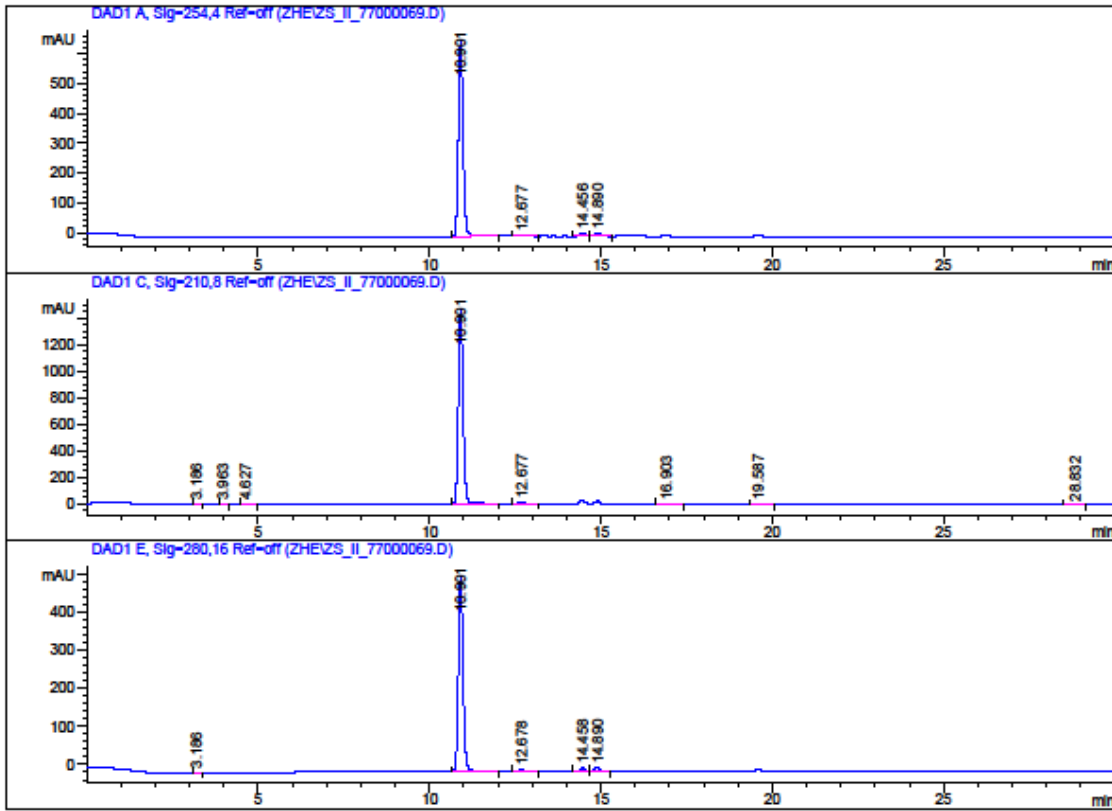
NL:
7.38E5
C₂₆H₂₅NO₇ Na:
C₂₆H₂₅N₁O₇ Na₁
pa Chrg 1

HPLC traces of Compound 22

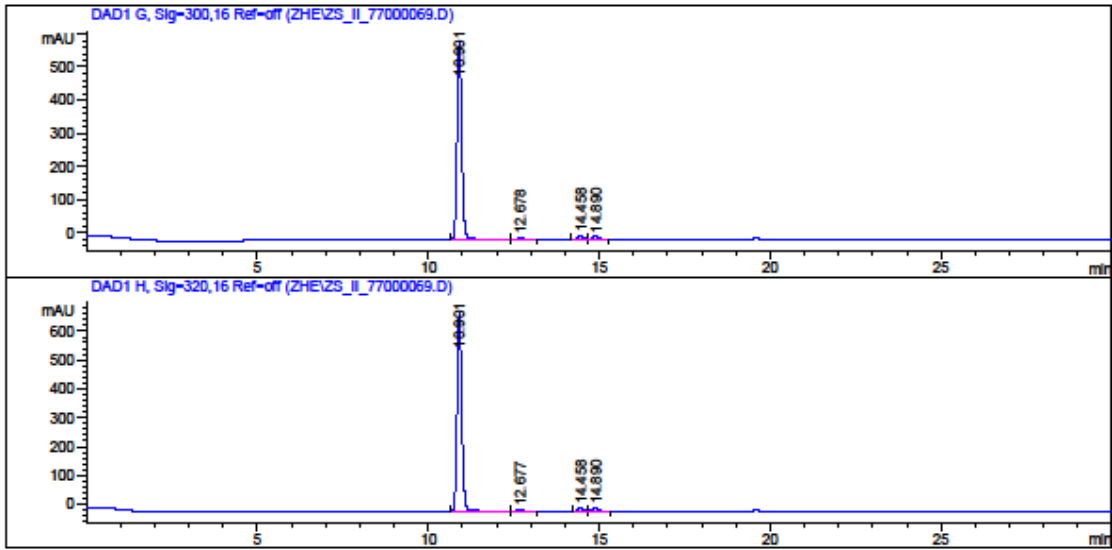
Data File C:\CHEM32\1\DATA\ZHE\ZS_II_77000069.D

Sample Name: ss_II_77

=====
Acq. Operator : she
Acq. Instrument : Instrument 1 Location : -
Injection Date : 7/25/2015 11:48:46 AM
Acq. Method : C:\CHEM32\1\METHODS\GRAD 2 50-90 ACN.M
Last changed : 7/25/2015 11:46:28 AM by Blake
Analysis Method : C:\CHEM32\1\DATA\ZHE\ZS_II_77000069.D\DA.M (GRAD 2 50-90 ACN.M)
Last changed : 7/27/2015 6:01:08 PM by she
Sample Info : ss_II_77
 20150724
 GRAD 2 50-90-ACN



Data File C:\CHEM32\1\DATA\ZHE\ZS_II_77000069.D
 Sample Name: zs_II_77



=====
 Area Percent Report
 =====

Sorted By : Signal
 Multiplier : 1.0000
 Dilution : 1.0000
 Use Multiplier & Dilution Factor with ISTDs

Signal 1: DAD1 A, Sig=254,4 Ref=off

Peak #	RetTime [min]	Type	Width [min]	Area [mAU*s]	Height [mAU]	Area %
1	10.901	BB	0.1470	6239.14063	655.73224	95.2401
2	12.677	BB	0.1551	54.12579	5.30075	0.8262
3	14.456	BV	0.1527	125.43754	12.54448	1.9148
4	14.890	VB	0.1624	132.25436	12.20637	2.0189

Totals : 6550.95821 685.78383

Signal 2: DAD1 C, Sig=210,8 Ref=off

Data File C:\CHEM32\1\DATA\ZHE\ZS_II_77000069.D

Sample Name: zs_II_77

Peak #	RetTime [min]	Type	Width [min]	Area [mAU*s]	Height [mAU]	Area %
1	3.186	BB	0.0756	27.70014	5.61356	0.1916
2	3.963	BB	0.0899	6.58550	1.09917	0.0455
3	4.627	BB	0.1503	13.48362	1.28667	0.0933
4	10.901	BB	0.1481	1.41536e4	1472.83411	97.8943
5	12.677	BB	0.1566	114.37950	11.06427	0.7911
6	16.903	BB	0.2192	39.03370	2.62898	0.2700
7	19.587	BB	0.1736	90.62653	8.03609	0.6268
8	28.832	BB	0.1799	12.63027	1.10072	0.0874

Totals : 1.44580e4 1503.66357

Signal 3: DAD1 E, Sig=280,16 Ref=off

Peak #	RetTime [min]	Type	Width [min]	Area [mAU*s]	Height [mAU]	Area %
1	3.186	BB	0.0751	5.96704	1.21983	0.1166
2	10.901	BB	0.1470	4873.80322	512.45331	95.2626
3	12.678	BB	0.1575	40.68699	3.97113	0.7953
4	14.458	BV	0.1561	96.39175	9.52571	1.8841
5	14.890	VB	0.1630	99.33007	9.12780	1.9415

Totals : 5116.17907 536.29778

Signal 4: DAD1 G, Sig=300,16 Ref=off

Peak #	RetTime [min]	Type	Width [min]	Area [mAU*s]	Height [mAU]	Area %
1	10.901	BB	0.1476	5754.02393	601.48285	95.8778
2	12.678	BB	0.1562	44.09370	4.28085	0.7347
3	14.458	BV	0.1558	105.51485	10.44625	1.7582
4	14.890	VB	0.1623	97.78028	8.89303	1.6293

Totals : 6001.41277 625.10298

Signal 5: DAD1 H, Sig=320,16 Ref=off

Peak #	RetTime [min]	Type	Width [min]	Area [mAU*s]	Height [mAU]	Area %
1	10.901	BB	0.1477	6608.71289	690.19800	96.1304
2	12.677	BB	0.1587	41.99982	4.05920	0.6109
3	14.458	BV	0.1556	107.06859	10.61992	1.5574

Instrument 1 7/27/2015 6:02:35 PM she

Page 3 of 4

Data File C:\CHEM32\1\DATA\ZHE\ZS_II_77000069.D

Sample Name: zs_II_77

Peak #	RetTime [min]	Type	Width [min]	Area [mAU*s]	Height [mAU]	Area %
4	14.890	VB	0.1612	116.95793	10.90296	1.7013
Totals :				6874.73923	715.78007	

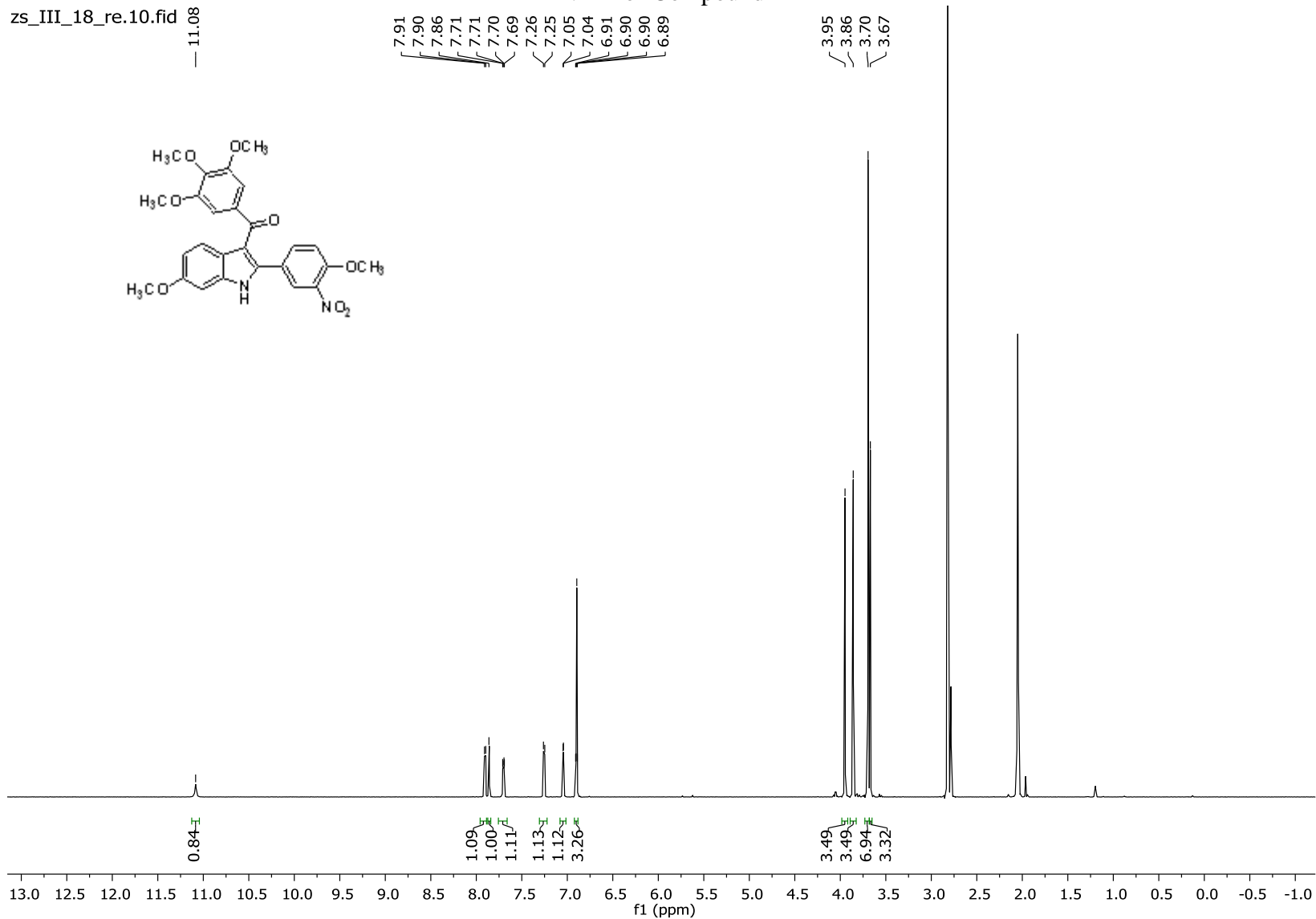
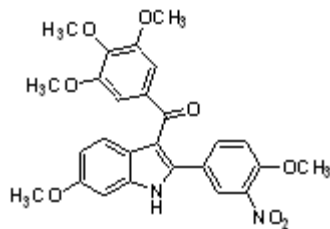
=====
*** End of Report ***

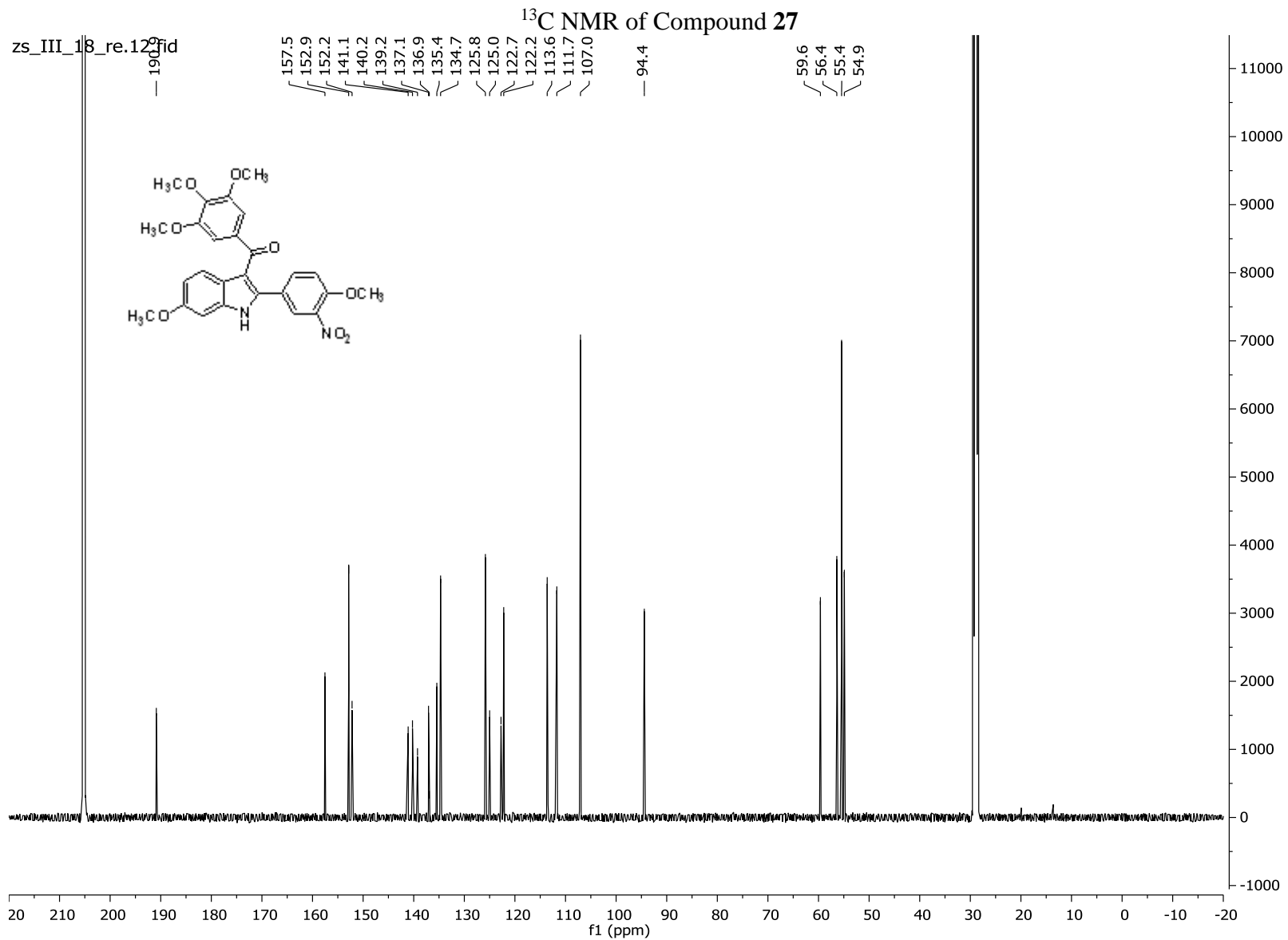
zs_III_18_re.10.fid

— 11.08

¹H NMR of Compound 27

7.91
7.90
7.86
7.71
7.71
7.70
7.69
7.26
7.25
7.05
7.04
6.91
6.90
6.89
3.95
3.86
3.70
3.67



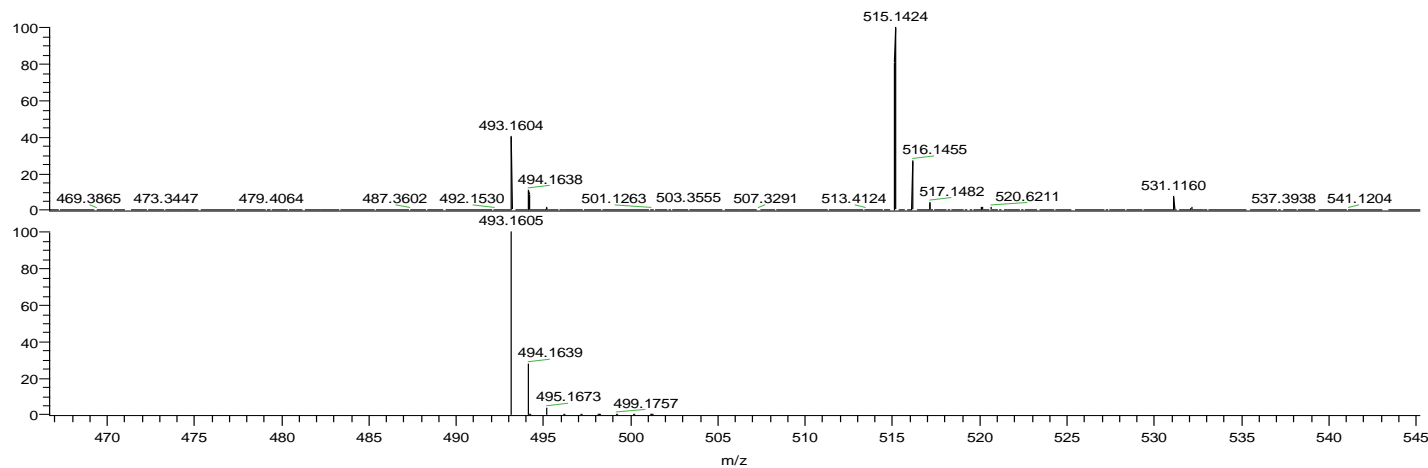
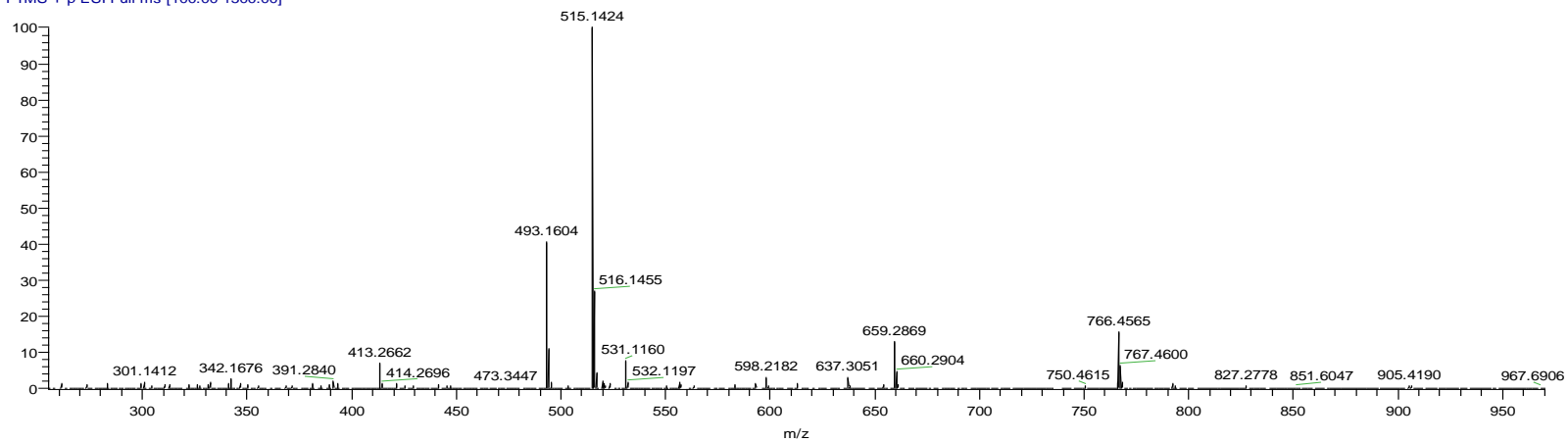


HRMS of Compound 27

C:\Xcalibur\...\zs_III_18_Orbi_+ESI

6/29/2015 12:33:26 PM

zs_III_18_Orbi_+ESI #1 RT: 0.00 AV: 1 NL: 3.
T: FTMS + p ESI Full ms [100.00-1500.00]



NL:
3.37E6
zs_III_18_Orbi_+
ESI#1 RT: 0.00 AV:
1 T: FTMS + p ESI
Full ms
[100.00-1500.00]

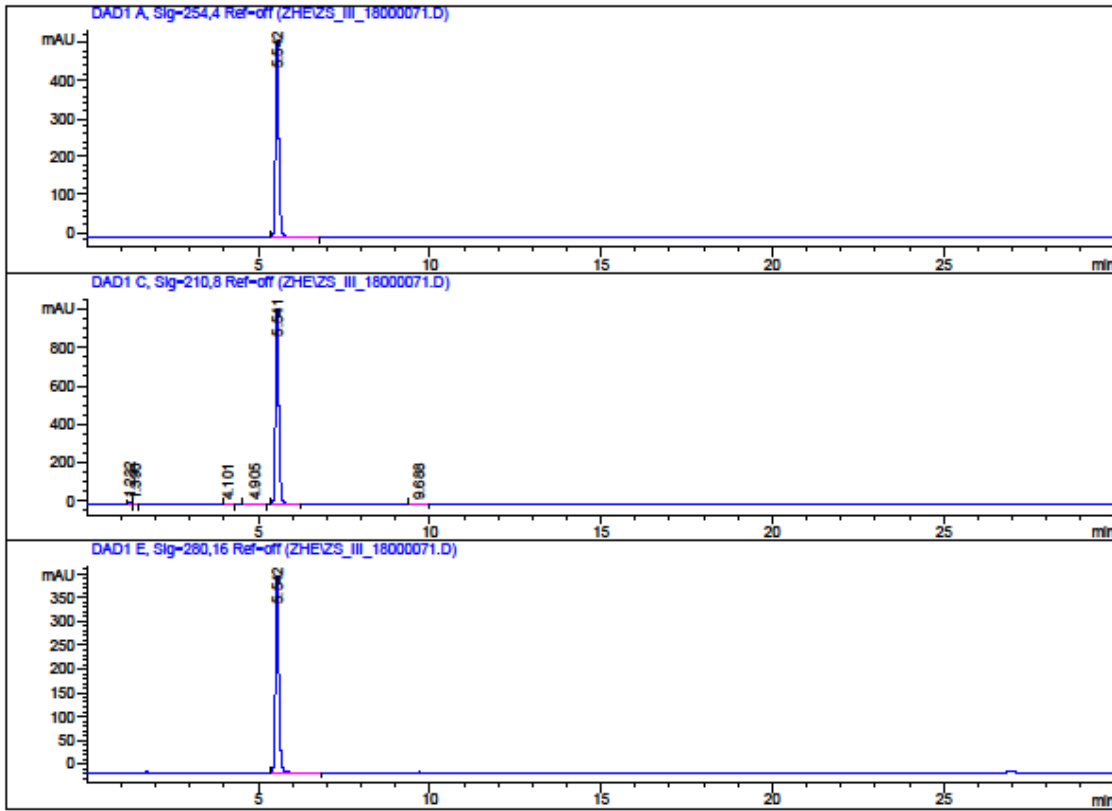
NL:
7.34E5
C₂₆H₂₅N₂O₈:
C₂₆H₂₅N₂O₈
pa Chrg 1

HPLC traces of compound 27

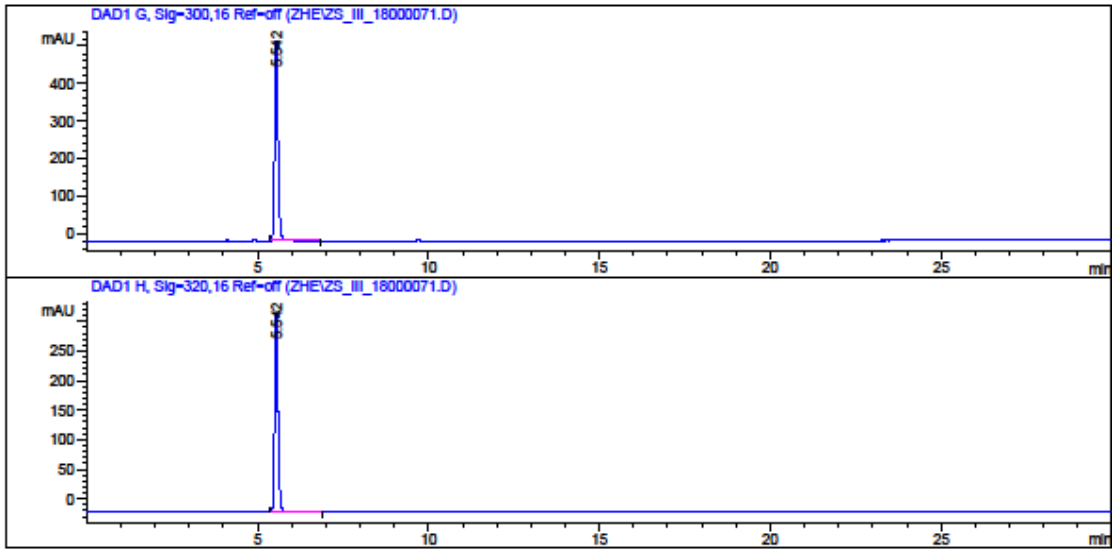
Data File C:\CHEM32\1\DATA\ZHE\ZS_III_18000071.D

Sample Name: ss_III_18

```
=====
Acq. Operator   : she
Acq. Instrument : Instrument 1           Location : -
Injection Date  : 7/25/2015 4:18:01 PM
Acq. Method    : C:\CHEM32\1\METHODS\GRAD 2 50-90 ACN.M
Last changed   : 7/25/2015 4:11:41 PM by she
Analysis Method: C:\CHEM32\1\DATA\ZHE\ZS_III_18000071.D\DA.M (GRAD 2 50-90 ACN.M)
Last changed   : 7/27/2015 6:04:46 PM by she
Sample Info    : ss_III_18
                20150724
                GRAD 2 50-90-ACN
=====
```



Data File C:\CHEM32\1\DATA\ZHE\ZS_III_18000071.D
 Sample Name: zs_III_18



=====
 Area Percent Report
 =====

Sorted By : Signal
 Multiplier : 1.0000
 Dilution : 1.0000
 Use Multiplier & Dilution Factor with ISTDs

Signal 1: DAD1 A, Sig=254,4 Ref=off

Peak #	RetTime [min]	Type	Width [min]	Area [mAU*s]	Height [mAU]	Area %
1	5.542	BB	0.1055	3531.82935	518.12195	100.0000

Totals : 3531.82935 518.12195

Signal 2: DAD1 C, Sig=210,8 Ref=off

Peak #	RetTime [min]	Type	Width [min]	Area [mAU*s]	Height [mAU]	Area %
1	1.232	BV	0.0684	53.55264	12.40019	0.7589
2	1.390	VB	0.0749	7.52131	1.44099	0.1066
3	4.101	BB	0.0884	7.05204	1.23912	0.0999
4	4.905	BB	0.1966	15.27252	1.19934	0.2164

Data File C:\CHEM32\1\DATA\ZHE\ZS_III_18000071.D
Sample Name: zs_III_18

Peak #	RetTime [min]	Type	Width [min]	Area [mAU*s]	Height [mAU]	Area %
5	5.541	BB	0.1055	6955.45752	1020.71185	98.5669
6	9.688	BB	0.1417	17.72804	1.92016	0.2512
Totals :				7056.58407	1038.91165	

Signal 3: DAD1 E, Sig=280,16 Ref=off

Peak #	RetTime [min]	Type	Width [min]	Area [mAU*s]	Height [mAU]	Area %
1	5.542	BB	0.1056	2816.50708	413.00449	100.0000
Totals :				2816.50708	413.00449	

Signal 4: DAD1 G, Sig=300,16 Ref=off

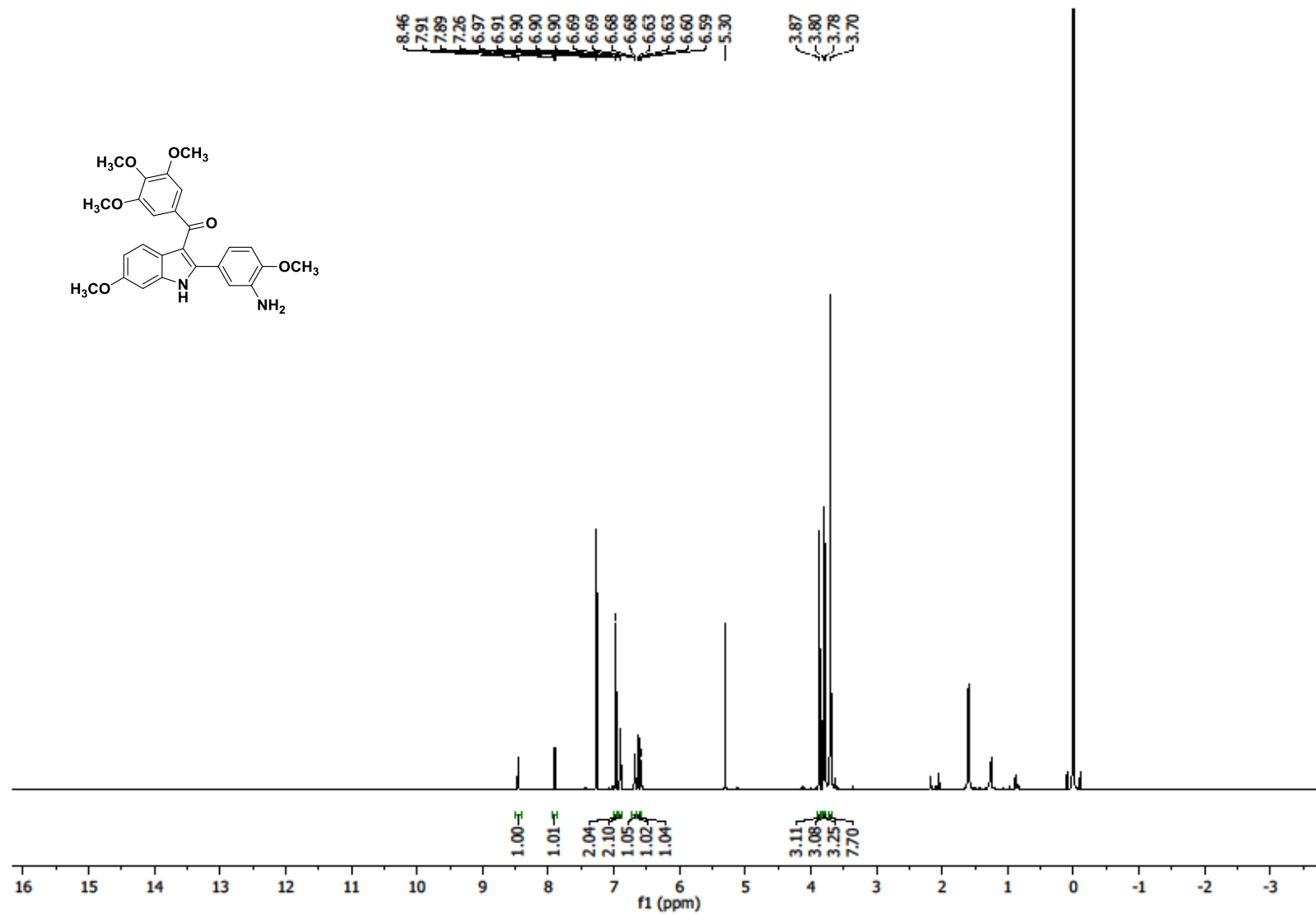
Peak #	RetTime [min]	Type	Width [min]	Area [mAU*s]	Height [mAU]	Area %
1	5.542	BB	0.1056	3639.63867	533.39392	100.0000
Totals :				3639.63867	533.39392	

Signal 5: DAD1 H, Sig=320,16 Ref=off

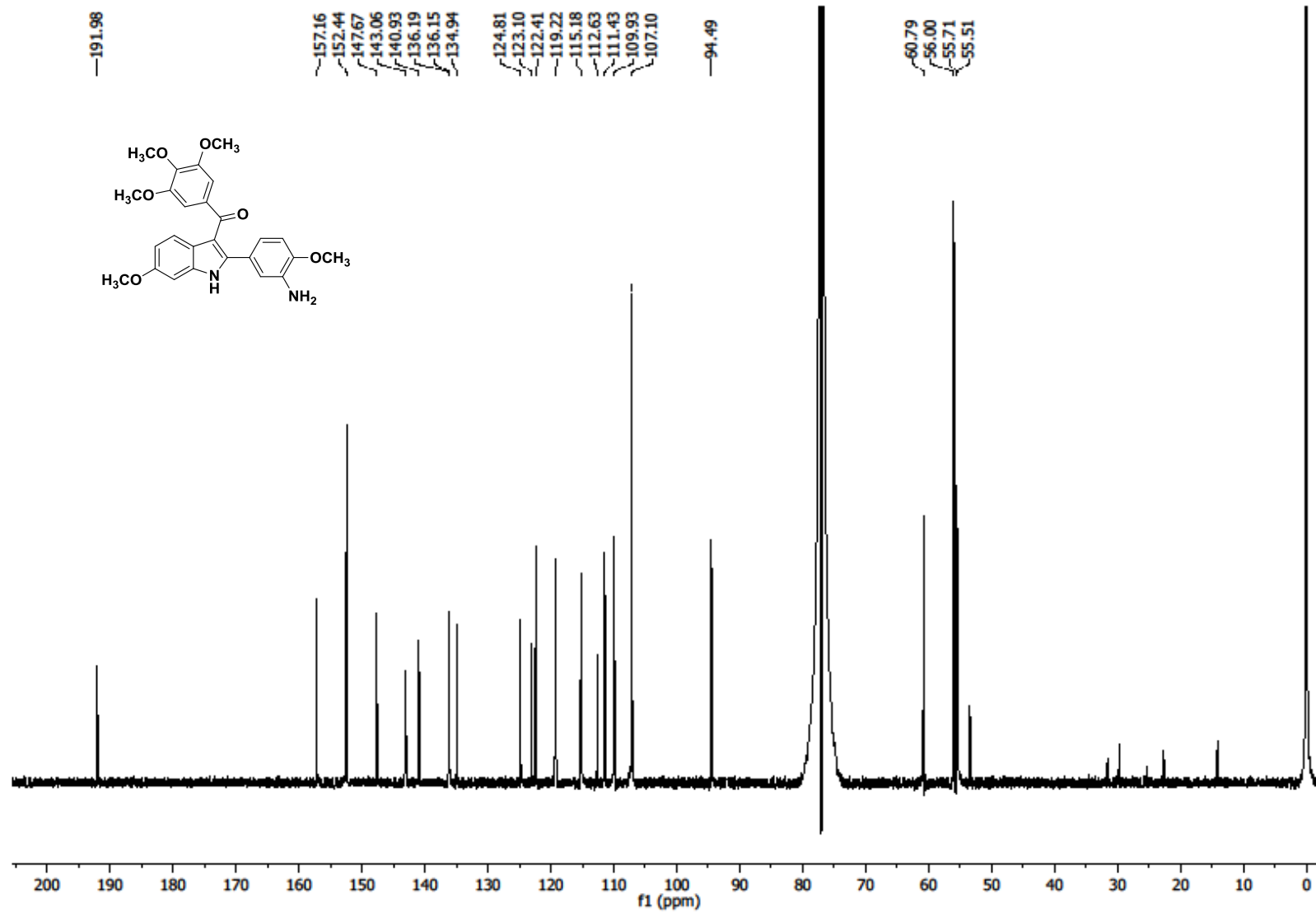
Peak #	RetTime [min]	Type	Width [min]	Area [mAU*s]	Height [mAU]	Area %
1	5.542	BB	0.1056	2303.17480	337.51797	100.0000
Totals :				2303.17480	337.51797	

=====
*** End of Report ***

¹H NMR of Compound 28



¹³C NMR of Compound 28



191.98

157.16
152.44
147.67
143.06
140.93
136.19
136.15
134.94

124.81
123.10
122.41
119.22
115.18
112.63
111.43
109.93
107.10

94.49

60.79
56.00
55.71
55.51

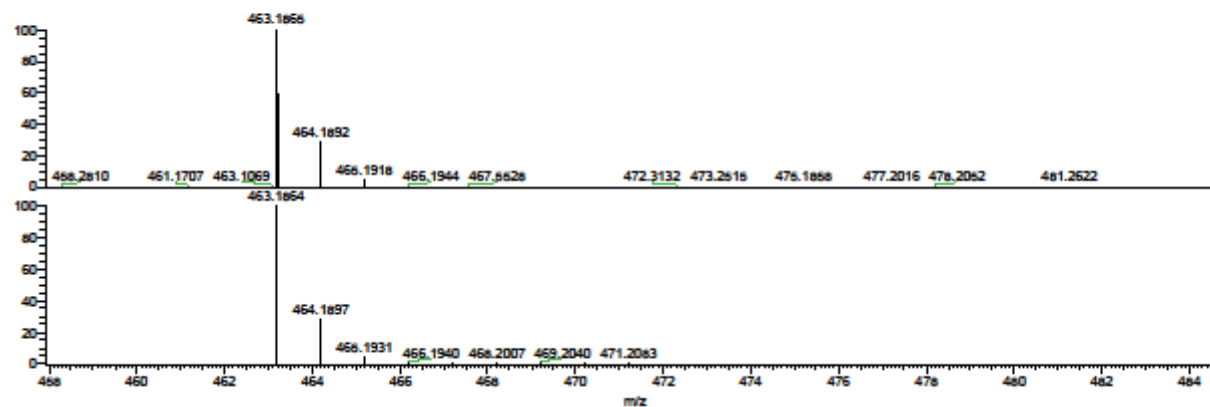
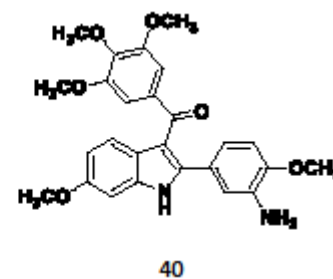
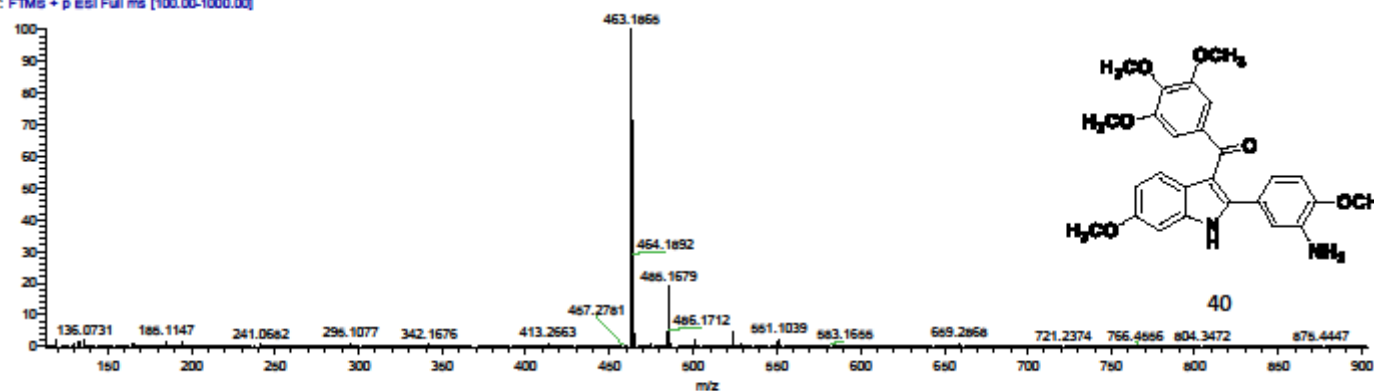
HRMS of Compound 28

C:\Xcalibur\...z5_IL_20_pure_Orbi_+ESI

7/2/2015 11:49:48 AM

z5_IL_20_pure

z5_IL_20_pure_Orbi_+ESI #1 RT: 0.01 AV: 1
T: FTMS + p ESI Full ms [100.00-1000.00]



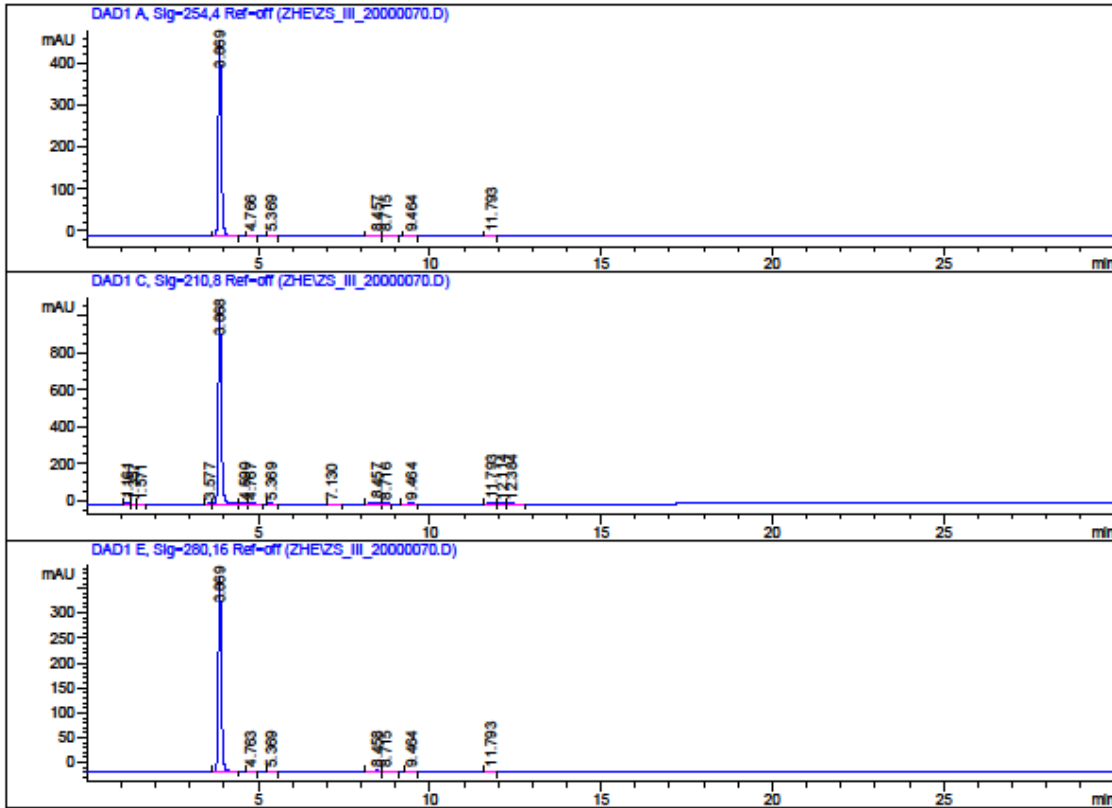
NL:
1.9887
z5_IL_20_pure_Orbi_+
ESI#1 RT: 0.01 AV:
1 T: FTMS + p ESI
Full ms
[100.00-1000.00]

NL:
7.3765
C₂₈H₃₂N₂O₆
C₂₈H₃₂N₂O₆
ps Chrg 1

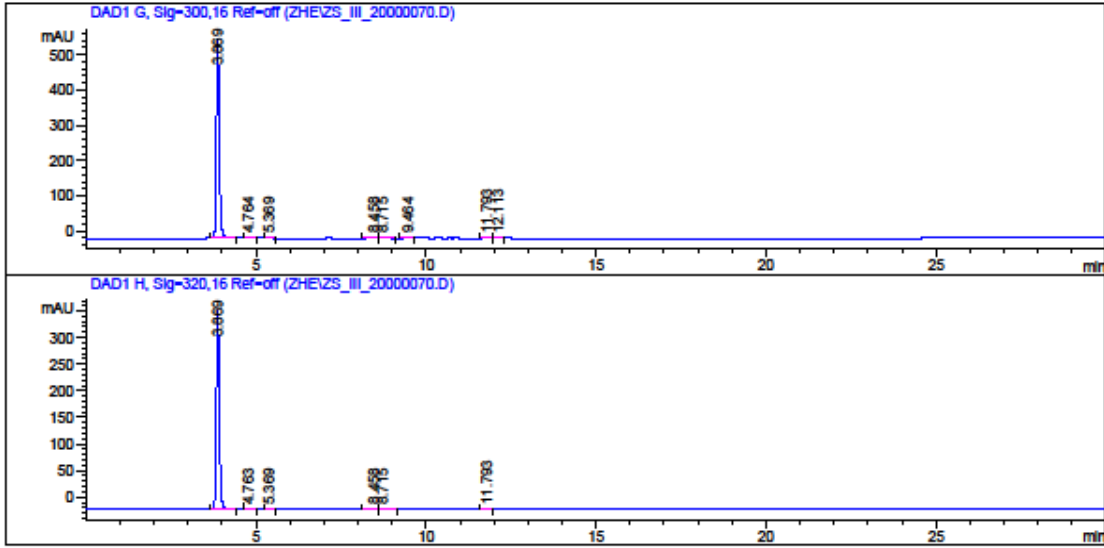
HPLC traces of Compound 28

Data File C:\CHEM32\1\DATA\ZHE\ZS_III_20000070.D
Sample Name: ss_III_20

```
=====
Acq. Operator   : she
Acq. Instrument : Instrument 1           Location : -
Injection Date  : 7/25/2015 12:56:06 PM
Acq. Method     : C:\CHEM32\1\METHODS\GRAD 2 50-90 ACN.M
Last changed    : 7/25/2015 12:29:01 PM by she
Analysis Method : C:\CHEM32\1\DATA\ZHE\ZS_III_20000070.D\DA.M (GRAD 2 50-90 ACN.M)
Last changed    : 7/27/2015 6:04:01 PM by she
                  (modified after loading)
Sample Info     : ss_III_20
                  20150724
                  GRAD 2 50-90-ACN
```



Data File C:\CHEM32\1\DATA\ZHE\ZS_III_20000070.D
 Sample Name: ss_III_20



=====
 Area Percent Report
 =====

Sorted By : Signal
 Multiplier : 1.0000
 Dilution : 1.0000
 Use Multiplier & Dilution Factor with ISTDs

Signal 1: DAD1 A, Sig=254,4 Ref=off

Peak #	RetTime [min]	Type	Width [min]	Area [mAU*s]	Height [mAU]	Area %
1	3.869	VB	0.0916	2789.46094	467.50934	96.7005
2	4.766	BB	0.1171	8.13293	1.06507	0.2819
3	5.369	BB	0.0997	10.08902	1.59808	0.3497
4	8.457	BV	0.1879	33.23231	2.51858	1.1520
5	8.715	VB	0.1742	15.83127	1.31772	0.5488
6	9.464	BB	0.1314	12.56040	1.50401	0.4354
7	11.793	BV	0.1583	15.33231	1.51223	0.5315

Totals : 2884.63916 477.02503

Data File C:\CHEM32\1\DATA\ZHE\ZS_III_20000070.D
 Sample Name: zs_III_20

Signal 2: DAD1 C, Sig=210,8 Ref=off

Peak #	RetTime [min]	Type	Width [min]	Area [mAU*s]	Height [mAU]	Area %
1	1.161	BV	0.0698	37.37536	8.10029	0.5545
2	1.357	VV	0.0859	9.20983	1.49339	0.1366
3	1.571	VB	0.0921	16.50322	2.46679	0.2448
4	3.577	BV	0.0958	16.30973	2.57912	0.2420
5	3.868	VV	0.0922	6366.70215	1058.72461	94.4546
6	4.590	VV	0.1760	35.69058	2.66880	0.5295
7	4.767	VB	0.1682	35.20403	2.92969	0.5223
8	5.369	BB	0.0992	18.45627	2.94114	0.2738
9	7.130	BB	0.1149	10.54125	1.41467	0.1564
10	8.457	BV	0.1781	70.04753	5.66962	1.0392
11	8.716	VB	0.1316	21.09575	2.52120	0.3130
12	9.464	BB	0.1308	21.97367	2.64869	0.3260
13	11.793	BV	0.1599	43.52880	4.23486	0.6458
14	12.114	VV	0.1592	21.63781	2.08365	0.3210
15	12.384	VB	0.1521	16.21356	1.60223	0.2405

Totals : 6740.48954 1102.07877

Signal 3: DAD1 E, Sig=280,16 Ref=off

Peak #	RetTime [min]	Type	Width [min]	Area [mAU*s]	Height [mAU]	Area %
1	3.869	VB	0.0918	2353.67969	393.29330	96.1076
2	4.763	BB	0.1200	9.89361	1.25441	0.4040
3	5.369	BB	0.0988	7.14092	1.14457	0.2916
4	8.458	BV	0.1727	32.78903	2.75740	1.3389
5	8.715	VB	0.1674	16.66070	1.45664	0.6803
6	9.464	BB	0.1299	11.63528	1.41604	0.4751
7	11.793	BV	0.1556	17.20648	1.73628	0.7026

Totals : 2449.00571 403.05865

Signal 4: DAD1 G, Sig=300,16 Ref=off

Peak #	RetTime [min]	Type	Width [min]	Area [mAU*s]	Height [mAU]	Area %
1	3.869	VB	0.0916	3370.28687	564.60181	96.3230
2	4.764	BB	0.1184	12.13207	1.56649	0.3467
3	5.369	BB	0.0989	9.79876	1.56792	0.2800
4	8.458	BV	0.1769	39.76372	3.24728	1.1364
5	8.715	VB	0.1706	20.17021	1.72250	0.5765

Instrument 1 7/27/2015 6:04:16 PM zhe

Page 3 of 4

Data File C:\CHEM32\1\DATA\ZHE\ZS_III_20000070.D
Sample Name: zs_III_20

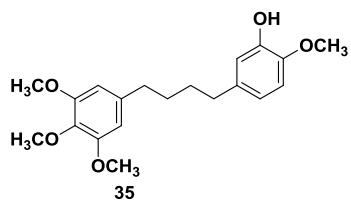
Peak #	RetTime [min]	Type	Width [min]	Area [mAU*s]	Height [mAU]	Area %
6	9.464	BB	0.1294	13.48599	1.64899	0.3854
7	11.793	BV	0.1599	22.07425	2.14790	0.6309
8	12.113	VV	0.1637	11.22981	1.07620	0.3209
Totals :				3498.94167	577.57908	

Signal 5: DAD1 H, Sig=320,16 Ref=off

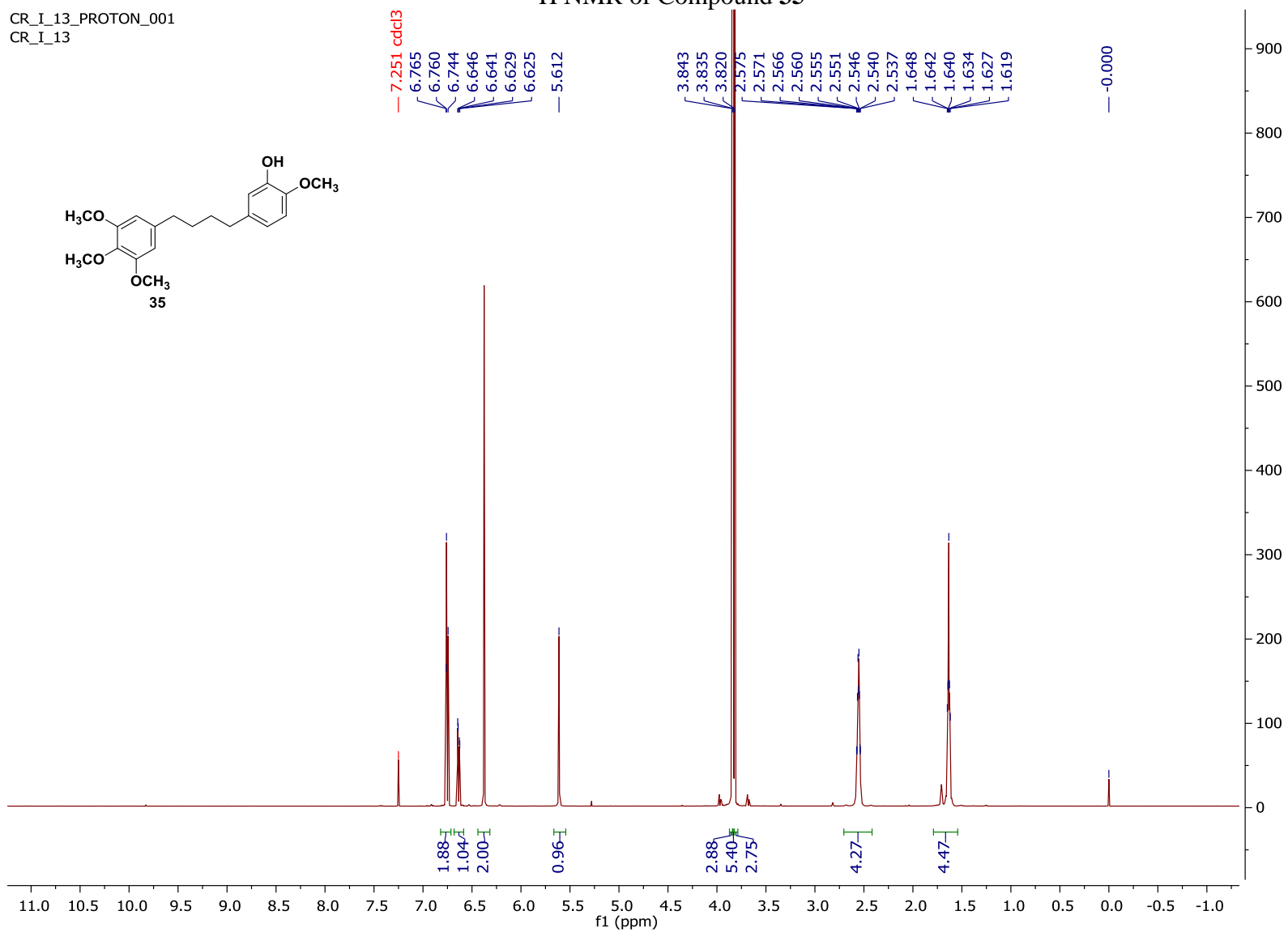
Peak #	RetTime [min]	Type	Width [min]	Area [mAU*s]	Height [mAU]	Area %
1	3.869	BB	0.0917	2238.90576	374.76431	96.7496
2	4.763	BB	0.1198	10.62679	1.35125	0.4592
3	5.369	BB	0.0989	6.98290	1.11814	0.3018
4	8.458	BV	0.1718	26.70467	2.26045	1.1540
5	8.715	VB	0.1709	14.22055	1.21156	0.6145
6	11.793	BV	0.1591	16.68314	1.63365	0.7209
Totals :				2314.12381	382.33936	

=====
*** End of Report ***

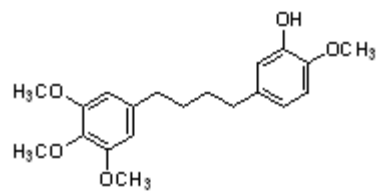
CR_I_13_PROTON_001
CR_I_13



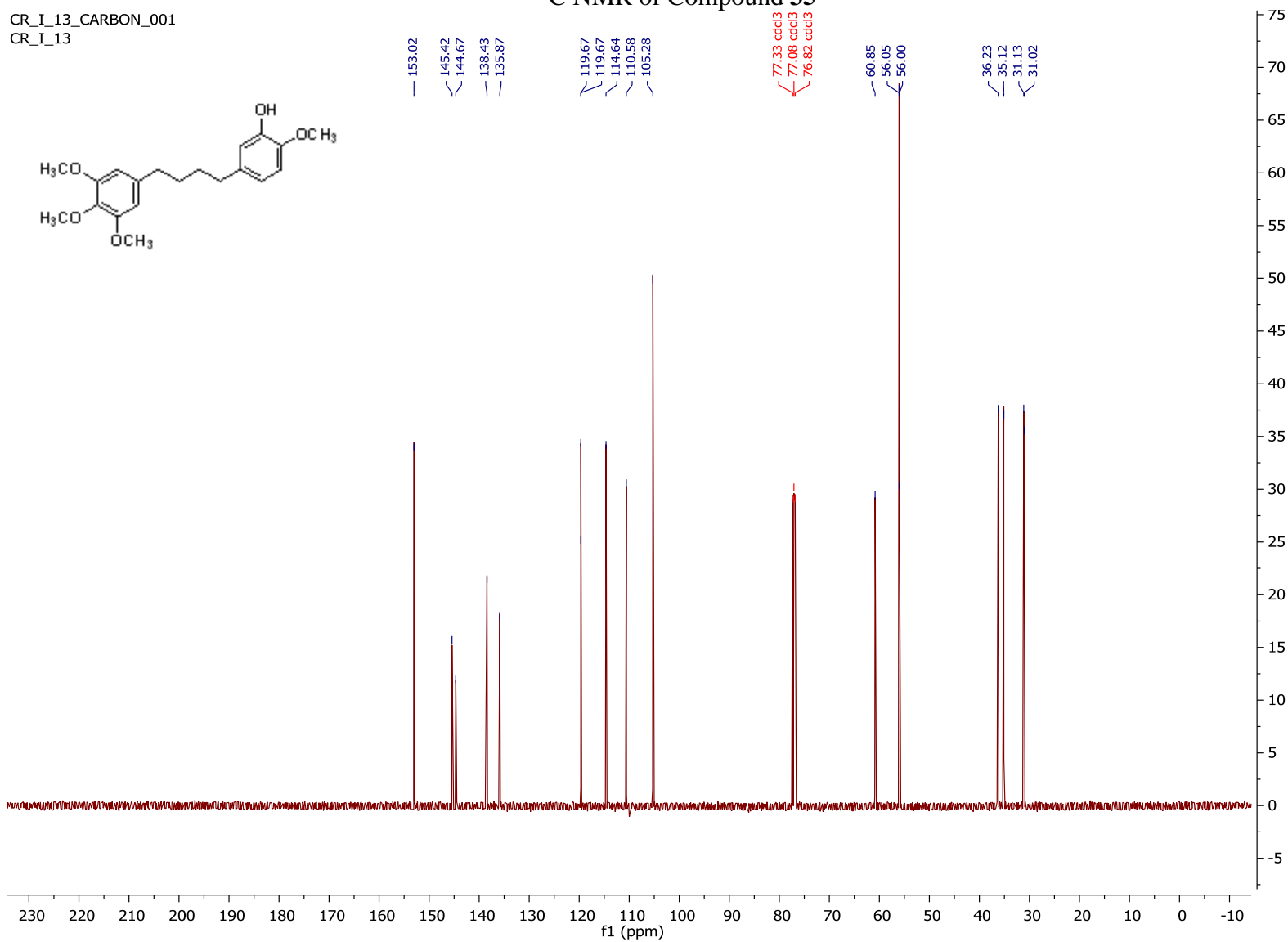
¹H NMR of Compound 35



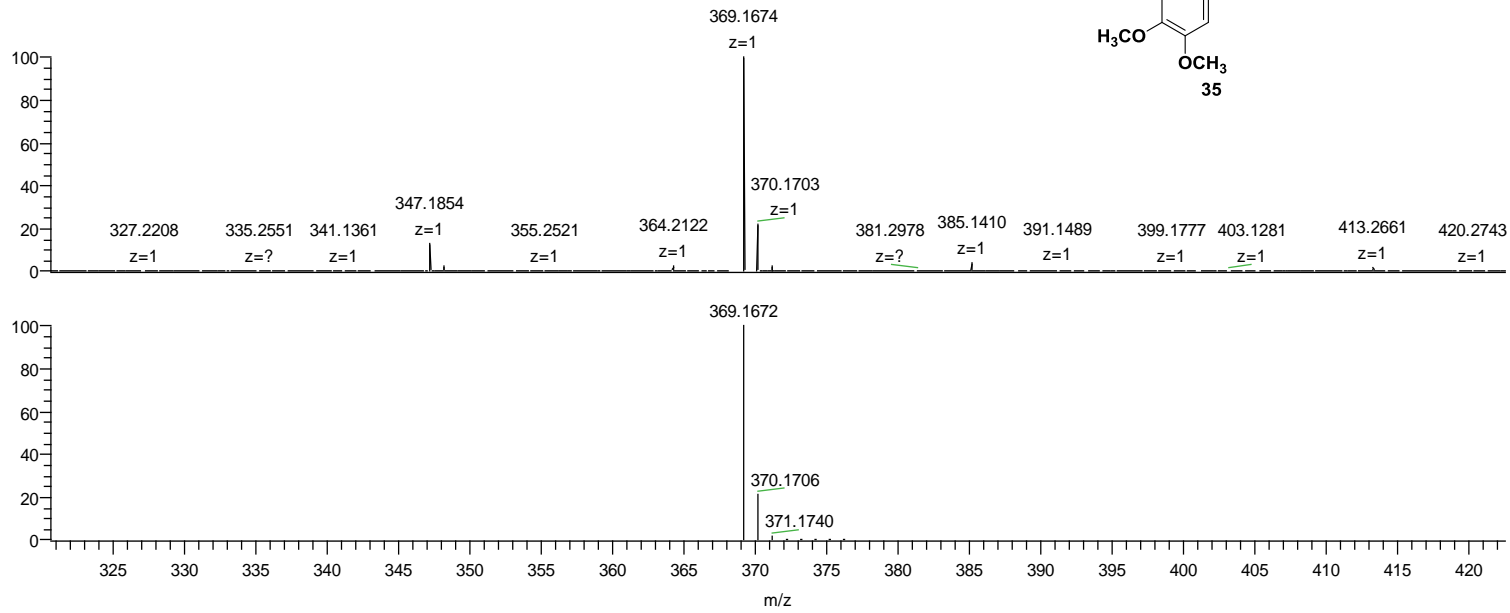
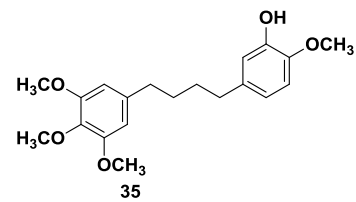
CR_I_13_CARBON_001
CR_I_13



¹³C NMR of Compound 35



HRMS of Compound 35



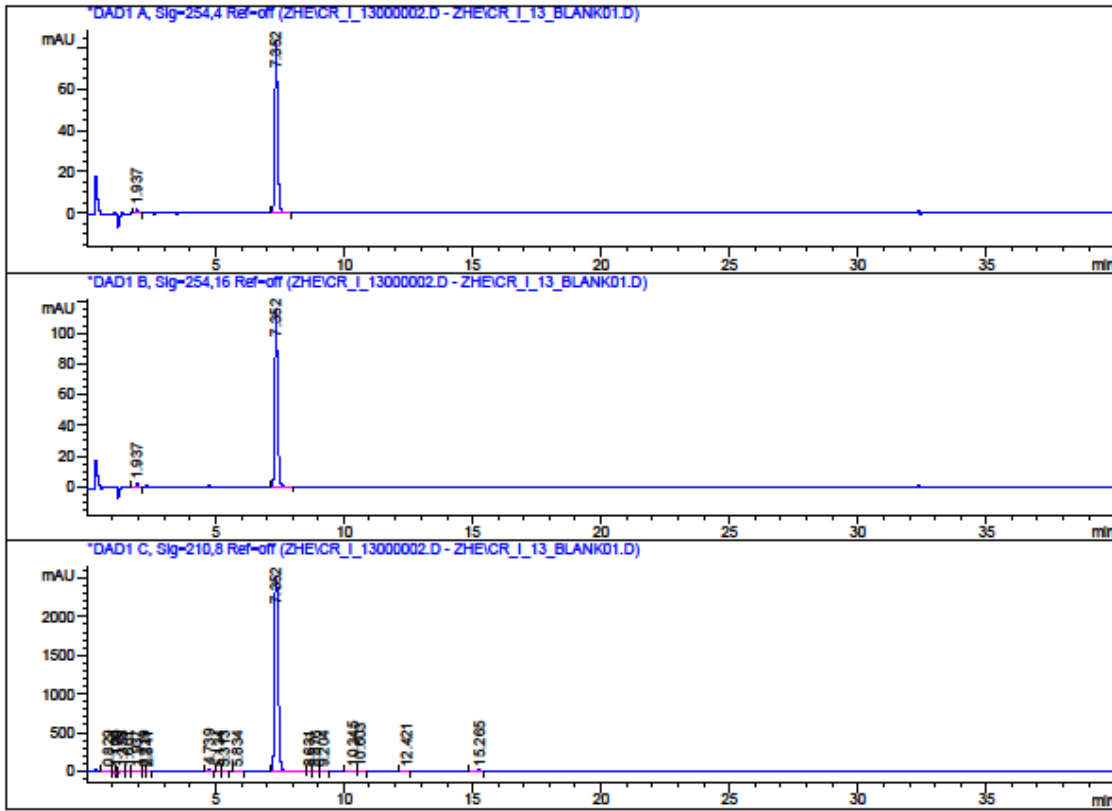
NL:
2.52E8
CR_I_10_Orbi_+
ES#13 RT: 0.10
AV: 1 T: FTMS + p
ESI Full ms
[150.00-700.00]

NL:
7.94E5
C₂₀ H₂₆ NaO₅⁺
C₂₀ H₂₆ Na₁O₅
pa Chrg 1

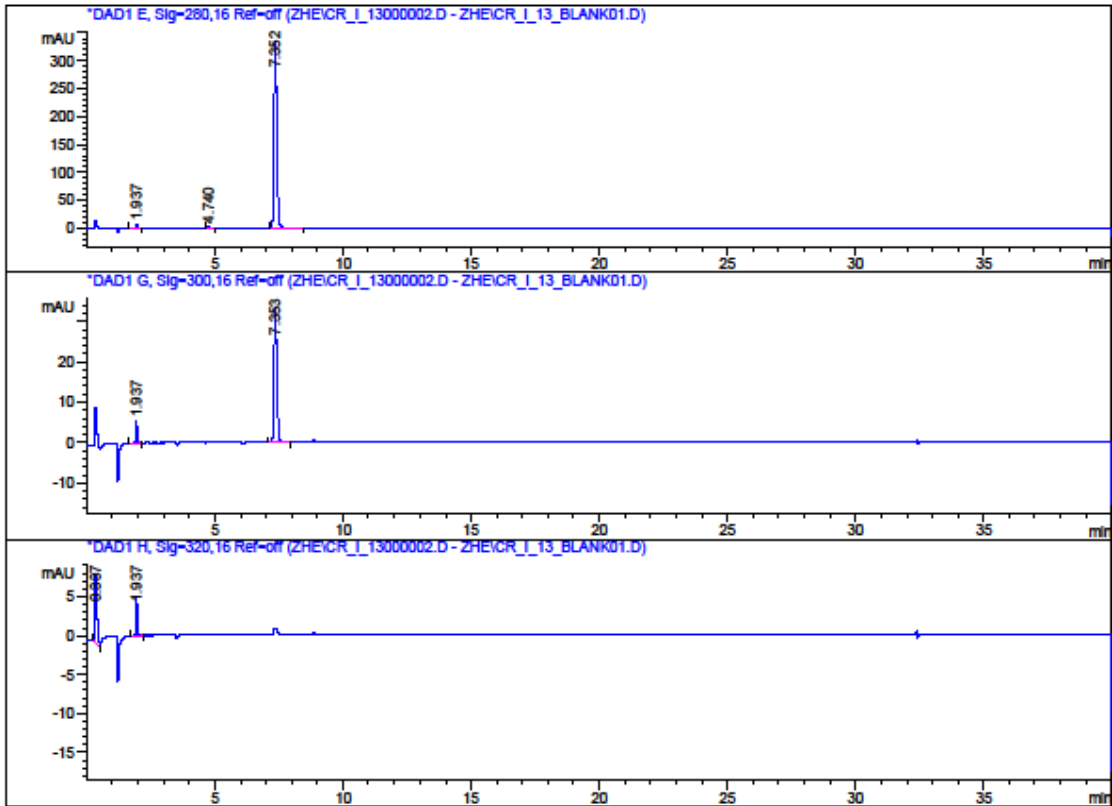
HPLC traces of Compound 35

Data File C:\CHEM32\1\DATA\ZHE\CR_I_13000002.D
Sample Name: CR_I_13

=====
Acq. Operator : Zhe
Acq. Instrument : Instrument 1 Location : -
Injection Date : 6/11/2014 3:28:00 PM
Acq. Method : C:\CHEM32\1\METHODS\GRAD50-100ACN.M
Last changed : 6/11/2014 3:25:44 PM by Zhe
Analysis Method : C:\CHEM32\1\DATA\ZHE\CR_I_13000002.D\DA.M (GRAD50-100ACN.M)
Last changed : 6/11/2014 4:13:11 PM by Zhe
Sample Info : CR_I_13
 GRAD50-100ACN



Data File C:\CHEM32\1\DATA\ZHE\CR_I_13000002.D
 Sample Name: CR_I_13



=====
 Area Percent Report
 =====

Sorted By : Signal
 Multiplier : 1.0000
 Dilution : 1.0000
 Use Multiplier & Dilution Factor with ISTDs

Signal 1: DAD1 A, Sig=254,4 Ref=off
 Signal has been modified after loading from rawdata file!

Peak #	RetTime [min]	Type	Width [min]	Area [mAU*s]	Height [mAU]	Area %
1	1.937	BB	0.0616	9.16731	2.24564	1.4222
2	7.352	BB	0.1168	635.40240	83.46325	98.5778

Totals : 644.56971 85.70889

Data File C:\CHEM32\1\DATA\ZHE\CR_I_13000002.D
Sample Name: CR_I_13

Signal 2: DAD1 B, Sig=254,16 Ref=off
Signal has been modified after loading from rawdata file!

Peak #	RetTime [min]	Type	Width [min]	Area [mAU*s]	Height [mAU]	Area %
1	1.937	BB	0.0625	10.81066	2.60300	1.2194
2	7.352	BB	0.1162	875.72644	115.77881	98.7806
Totals :				886.53710	118.38181	

Signal 3: DAD1 C, Sig=210,8 Ref=off
Signal has been modified after loading from rawdata file!

Peak #	RetTime [min]	Type	Width [min]	Area [mAU*s]	Height [mAU]	Area %
1	0.829	BV	0.2319	171.76660	9.63934	0.6319
2	1.109	VV	0.1329	159.76472	15.17181	0.5877
3	1.170	VB	0.0460	59.41847	19.25142	0.2186
4	1.358	BV	0.1355	141.23851	13.56640	0.5196
5	1.601	VB	0.2489	56.28260	2.94600	0.2070
6	1.937	BB	0.0666	38.77320	8.59495	0.1426
7	2.219	BV	0.0619	14.97322	3.64656	0.0551
8	2.341	VV	0.0831	12.12294	2.17290	0.0446
9	4.739	BB	0.0928	152.07748	25.05950	0.5595
10	5.134	BV	0.0999	33.39083	5.12930	0.1228
11	5.313	VB	0.1062	11.27250	1.56129	0.0415
12	5.834	BB	0.1104	26.18926	3.53767	0.0963
13	7.352	BV	0.1659	2.59359e4	2523.12183	95.4118
14	8.631	VB	0.1229	28.05415	3.37864	0.1032
15	8.876	BV	0.1581	20.05052	1.88447	0.0738
16	9.204	VB	0.1349	25.44459	2.82866	0.0936
17	10.345	BV	0.1663	99.09899	9.01085	0.3646
18	10.603	VB	0.1614	24.59447	2.28897	0.0905
19	12.421	BB	0.1594	14.72597	1.41519	0.0542
20	15.265	BV	0.1594	157.99159	14.94018	0.5812
Totals :				2.71832e4	2669.14591	

Signal 4: DAD1 E, Sig=280,16 Ref=off
Signal has been modified after loading from rawdata file!

Data File C:\CHEM32\1\DATA\ZHE\CR_I_13000002.D
Sample Name: CR_I_13

Peak #	RetTime [min]	Type	Width [min]	Area [mAU*s]	Height [mAU]	Area %
1	1.937	BV	0.0629	30.45411	7.26526	1.1941
2	4.740	BB	0.0933	9.09360	1.48819	0.3566
3	7.352	BB	0.1151	2510.87500	326.41006	98.4494
Totals :				2550.42271	345.16352	

Signal 5: DAD1 G, Sig=300,16 Ref=off
Signal has been modified after loading from rawdata file!

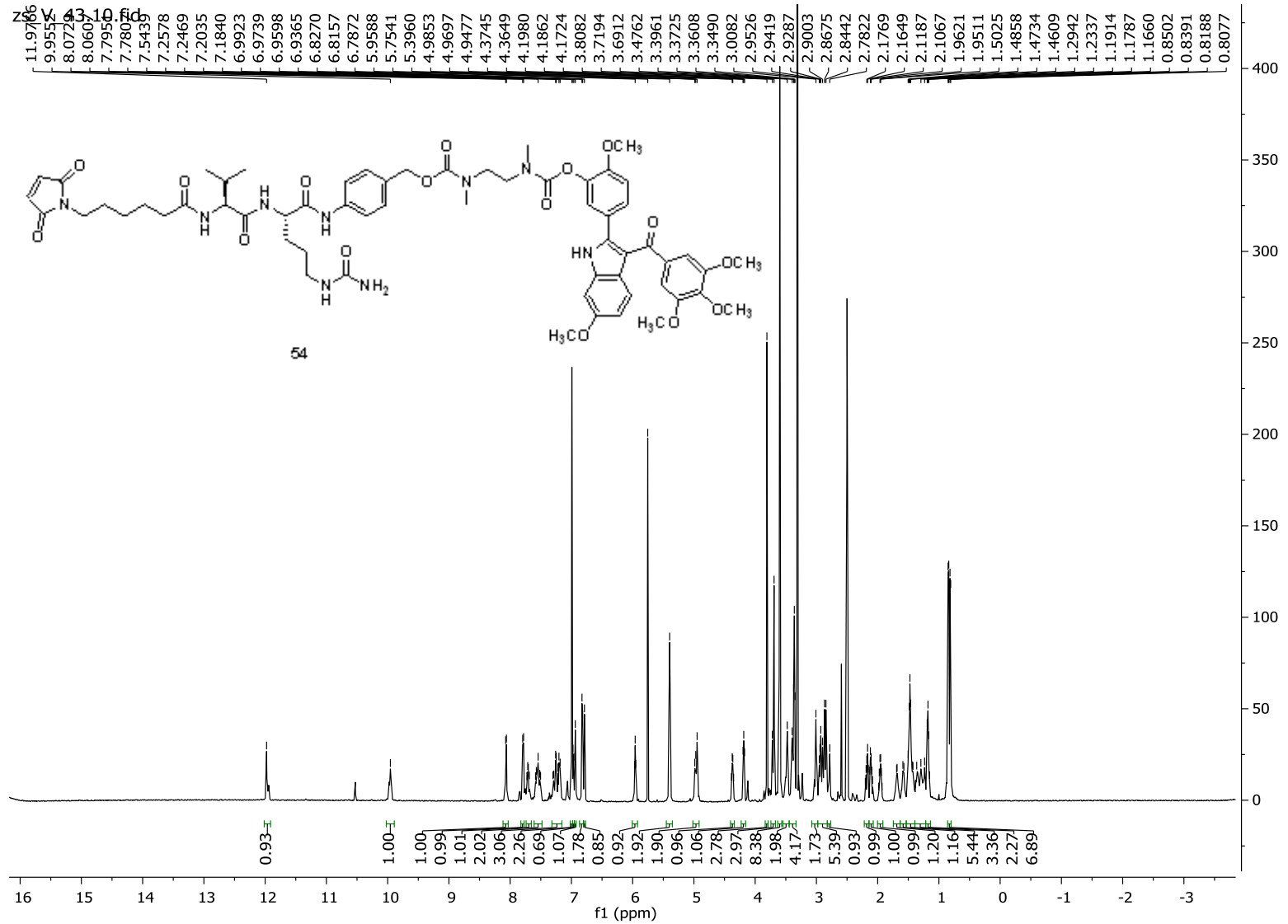
Peak #	RetTime [min]	Type	Width [min]	Area [mAU*s]	Height [mAU]	Area %
1	1.937	BB	0.0627	22.66812	5.43508	8.2045
2	7.353	BB	0.1168	253.61972	33.32097	91.7955
Totals :				276.28784	38.75605	

Signal 6: DAD1 H, Sig=320,16 Ref=off
Signal has been modified after loading from rawdata file!

Peak #	RetTime [min]	Type	Width [min]	Area [mAU*s]	Height [mAU]	Area %
1	0.337	BB	0.0710	43.32848	8.57289	66.6015
2	1.937	BB	0.0631	21.72785	5.16589	33.3985
Totals :				65.05632	13.73878	

=====
*** End of Report ***

¹H NMR of ADC 54

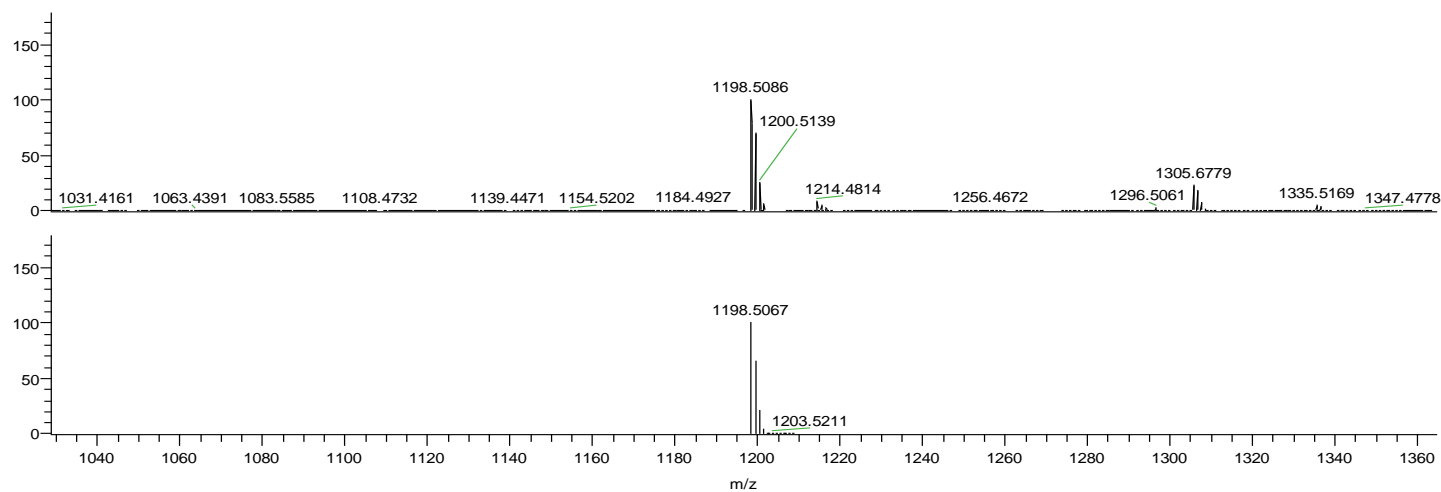
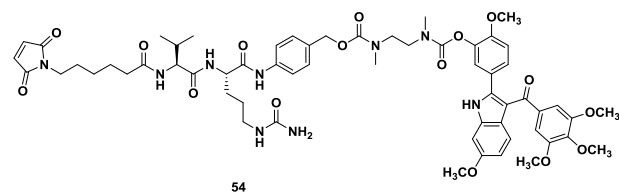
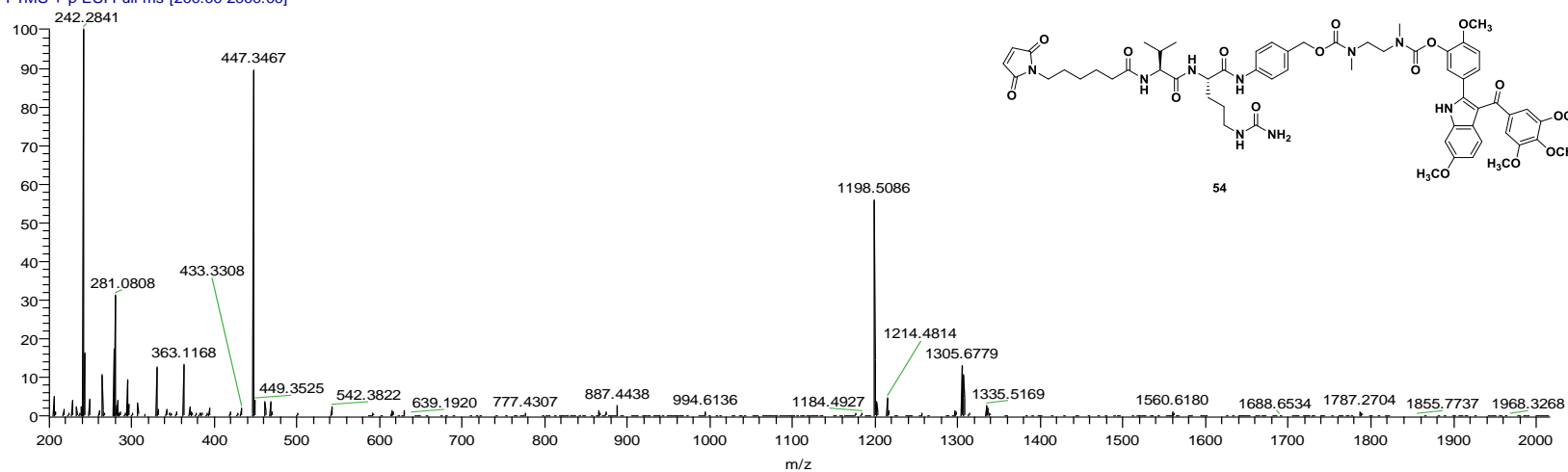


HRMS of ADC 54

2/23/2018 2:41:04 PM

C:\Xcalibur...\Zhe\zs_V_43_1_+ESI

zs_V_43_1_+ESI #2-13 RT: 0.02-0.15 AV: 12
T: FTMS + p ESI Full ms [200.00-2000.00]



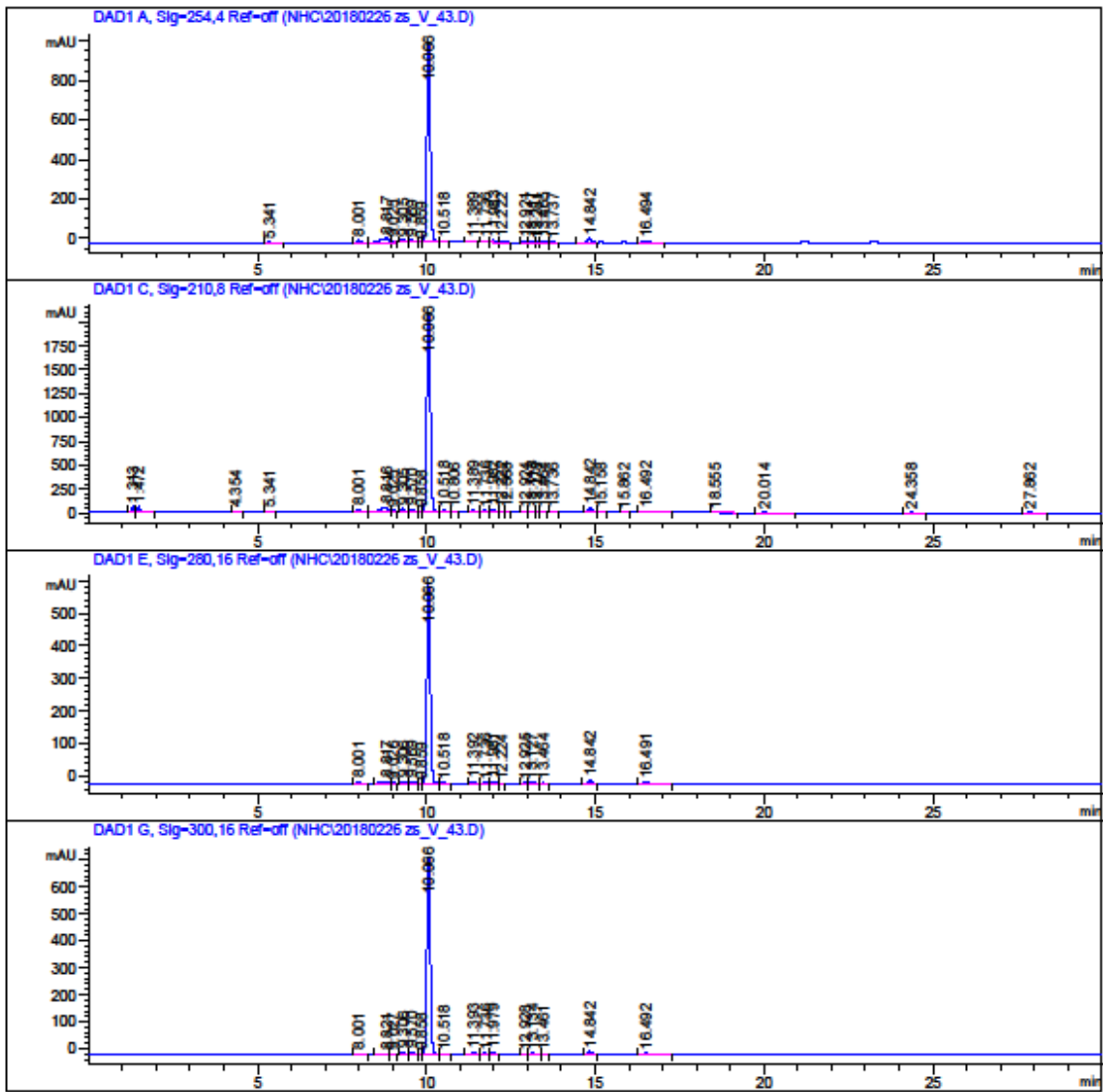
NL:
4.46E6
zs_V_43_1_+
ESI#2-13 RT:
0.02-0.15 AV: 12 T:
FTMS + p ESI Full ms
[200.00-2000.00]

NL:
4.84E5
C₆₀ H₇₃ N₉ O₆ Na:
C₆₀ H₇₃ N₉ O₆ Na₁
pa Chrg 1

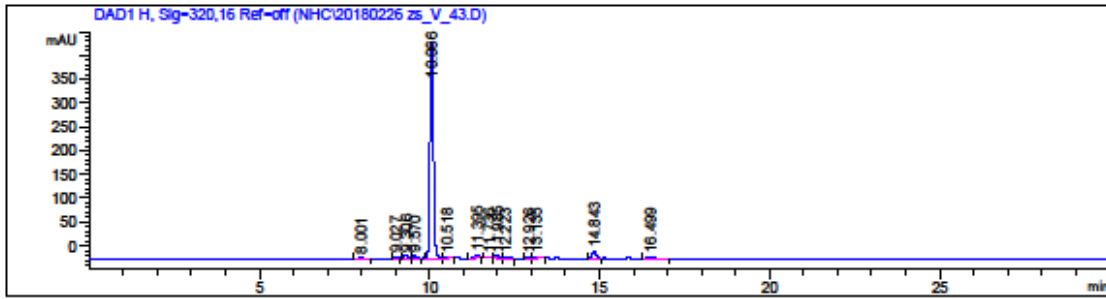
HPLC of ADC 54

Data File C:\Chem32\1\Data\NHC\20180226 zs_V_43.D
Sample Name: zs_V_43

=====
Acq. Operator : SYSTEM
Sample Operator : SYSTEM
Acq. Instrument : 1200 HPLC Location : 1
Injection Date : 2/26/2018 12:52:27 PM Inj Volume : No inj
Acq. Method : C:\CHEM32\1\METHODS\GRAD 2 30-90 ACN.M
Last changed : 4/2/2014 4:04:33 PM by ERICA P
Analysis Method : C:\CHEM32\1\METHODS\RT-ACNWASH 2.M
Last changed : 7/9/2015 2:27:22 PM by Blake
Method Info : General Column Wash Method
Sample Info : GRAD 2 30-90 ACN
20180226



Data File C:\Chem32\1\Data\NHC\20180226 zs_V_43.D
 Sample Name: zs_V_43



=====
 Area Percent Report
 =====

Sorted By : Signal
 Multiplier : 1.0000
 Dilution : 1.0000
 Use Multiplier & Dilution Factor with ISTDs

Signal 1: DAD1 A, Sig=254,4 Ref=off

Peak #	RetTime [min]	Type	Width [min]	Area [mAU*s]	Height [mAU]	Area %
1	5.341	BB	0.1005	20.61787	3.06237	0.2514
2	8.001	BB	0.1076	78.85933	11.27772	0.9615
3	8.817	BV	0.1960	316.25577	21.96337	3.8558
4	9.025	VB	0.1045	37.20697	5.38908	0.4536
5	9.305	BV	0.1054	89.28493	13.11554	1.0886
6	9.569	VB	0.1366	97.38895	11.51781	1.1874
7	9.859	BV	0.0768	9.40652	1.93253	0.1147
8	10.066	VV	0.1069	6945.38428	1001.18597	84.6790
9	10.518	VB	0.1159	31.42906	4.07833	0.3832
10	11.389	BB	0.1174	48.70319	6.50207	0.5938
11	11.736	BV	0.1094	43.85822	6.28944	0.5347
12	11.983	VV	0.1554	99.43372	10.23036	1.2123
13	12.222	VB	0.1386	32.36553	3.35362	0.3946
14	12.921	BV	0.1231	29.21477	3.65984	0.3562
15	13.117	VV	0.1424	49.45594	5.22518	0.6030
16	13.281	VV	0.1002	15.34558	2.23157	0.1871
17	13.465	VB	0.1235	24.71082	3.08321	0.3013
18	13.737	BB	0.1200	8.49728	1.10190	0.1036
19	14.842	BV	0.1265	162.29958	19.62482	1.9788
20	16.494	BB	0.1591	62.29515	5.99940	0.7595

Totals : 8202.01346 1140.82415

Data File C:\Chem32\1\Data\NHC\20180226 zs_V_43.D
 Sample Name: zs_V_43

Signal 2: DAD1 C, Sig=210,8 Ref=off

Peak #	RetTime [min]	Type	Width [min]	Area [mAU*s]	Height [mAU]	Area %
1	1.313	BB	0.0536	189.25438	53.03495	1.0147
2	1.472	BB	0.0840	308.56772	51.39600	1.6543
3	4.354	BB	0.0910	10.46381	1.76847	0.0561
4	5.341	BB	0.0989	34.01527	5.15739	0.1824
5	8.001	BB	0.1079	133.08250	18.96366	0.7135
6	8.816	BV	0.1955	685.32043	47.74666	3.6742
7	9.025	VB	0.1041	77.69532	11.31646	0.4165
8	9.305	BV	0.1053	224.52692	33.02016	1.2038
9	9.570	VB	0.1367	223.89299	26.47769	1.2004
10	9.858	BV	0.0763	21.47610	4.44939	0.1151
11	10.066	VV	0.1158	1.51013e4	2054.57568	80.9631
12	10.518	VB	0.1156	73.63119	9.58761	0.3948
13	10.806	BB	0.1033	12.31768	1.90832	0.0660
14	11.389	BB	0.1173	121.18683	16.18966	0.6497
15	11.736	BV	0.1090	91.12369	13.12916	0.4885
16	11.982	VV	0.1540	224.60695	23.40005	1.2042
17	12.222	VV	0.1157	57.98127	7.54260	0.3109
18	12.368	VB	0.0913	16.81611	2.83150	0.0902
19	12.924	BV	0.1196	57.42982	7.47491	0.3079
20	13.118	VV	0.1358	102.84863	11.55762	0.5514
21	13.278	VB	0.0812	15.14659	2.88787	0.0812
22	13.464	BB	0.1036	28.70004	4.42684	0.1539
23	13.736	BV	0.1285	26.07346	3.08737	0.1398
24	14.842	VV	0.1245	341.28415	42.13326	1.8297
25	15.158	VB	0.1243	16.68338	2.02045	0.0894
26	15.862	BB	0.1216	12.76190	1.66183	0.0684
27	16.492	BB	0.1615	158.64658	14.98323	0.8506
28	18.555	BB	0.1504	17.39082	1.77327	0.0932
29	20.014	BB	0.3925	47.37663	1.82691	0.2540
30	24.358	BB	0.1754	72.02349	6.30000	0.3861
31	27.862	BB	0.1918	148.46678	11.88001	0.7960

Totals : 1.86521e4 2494.50977

Signal 3: DAD1 E, Sig=280,16 Ref=off

Peak #	RetTime [min]	Type	Width [min]	Area [mAU*s]	Height [mAU]	Area %
1	8.001	BB	0.1078	39.17150	5.58345	0.8039
2	8.817	BV	0.1936	118.29580	8.23420	2.4278
3	9.026	VB	0.1046	22.40325	3.24134	0.4598
4	9.306	BV	0.1053	52.66414	7.74342	1.0808
5	9.569	VB	0.1367	58.68945	6.93916	1.2045
6	9.859	BV	0.0770	5.66839	1.16019	0.1163
7	10.066	VV	0.1068	4197.80713	605.89099	86.1523
8	10.518	VB	0.1162	18.91942	2.44728	0.3883
9	11.392	BB	0.1159	39.57376	5.37462	0.8122
10	11.736	BV	0.1084	25.35138	3.67864	0.5203

Data File C:\Chem32\1\Data\NHC\20180226 zs_V_43.D

Sample Name: zs_V_43

Peak #	RetTime [min]	Type	Width [min]	Area [mAU*s]	Height [mAU]	Area %
11	11.981	VV	0.1458	57.16606	6.18751	1.1732
12	12.224	VV	0.1118	10.57574	1.40450	0.2170
13	12.925	BV	0.1245	19.89448	2.45484	0.4083
14	13.127	VV	0.1695	51.00711	4.26530	1.0468
15	13.464	VB	0.1221	14.76531	1.83073	0.3030
16	14.842	BV	0.1228	89.43332	11.24829	1.8355
17	16.491	BB	0.1522	51.15547	5.13695	1.0499
Totals :				4872.54171	682.82142	

Signal 4: DAD1 G, Sig=300,16 Ref=off

Peak #	RetTime [min]	Type	Width [min]	Area [mAU*s]	Height [mAU]	Area %
1	8.001	BB	0.1091	25.90895	3.63885	0.4539
2	8.821	BV	0.1940	33.48712	2.29755	0.5866
3	9.027	VB	0.1045	25.30528	3.76261	0.4433
4	9.306	BV	0.1055	63.62440	9.34263	1.1145
5	9.570	VB	0.1370	71.02799	8.36698	1.2442
6	9.858	BV	0.0773	7.11675	1.44893	0.1247
7	10.066	VV	0.1070	5093.81348	734.12860	89.2310
8	10.518	VV	0.1282	28.16729	3.21402	0.4934
9	11.393	BB	0.1175	52.96440	7.06109	0.9278
10	11.736	BV	0.1066	29.09484	4.31806	0.5097
11	11.979	VV	0.1438	58.20720	6.54246	1.0196
12	12.928	BV	0.1266	17.45311	2.10719	0.3057
13	13.134	VV	0.1636	48.76984	4.25783	0.8543
14	13.461	VB	0.1206	10.50892	1.32371	0.1841
15	14.842	BV	0.1249	87.04623	10.93710	1.5248
16	16.492	BB	0.1558	56.07471	5.55411	0.9823
Totals :				5708.57051	808.30170	

Signal 5: DAD1 H, Sig=320,16 Ref=off

Peak #	RetTime [min]	Type	Width [min]	Area [mAU*s]	Height [mAU]	Area %
1	8.001	BB	0.1106	10.96641	1.51263	0.3070
2	9.027	BB	0.0993	13.64479	2.17262	0.3820
3	9.306	BV	0.1057	39.12141	5.72812	1.0951
4	9.570	VB	0.1371	43.19882	5.08494	1.2093
5	10.066	VV	0.1068	3141.87158	453.44620	87.9514
6	10.518	VB	0.1177	14.08270	1.79156	0.3942
7	11.395	BB	0.1118	45.72948	6.36763	1.2801
8	11.736	BV	0.1061	17.10805	2.55626	0.4789
9	11.985	VV	0.1438	45.47075	5.01472	1.2729
10	12.223	VB	0.1344	15.25533	1.67224	0.4270
11	12.926	BV	0.1206	8.91657	1.14790	0.2496

Data File C:\Chem32\1\Data\NHC\20180226 zs_V_43.D

Sample Name: zs_V_43

Peak #	RetTime [min]	Type	Width [min]	Area [mAU*s]	Height [mAU]	Area %
12	13.135	VB	0.1326	27.07506	3.07971	0.7579
13	14.843	BB	0.1234	110.71606	14.13317	3.0993
14	16.499	BB	0.1709	39.12258	3.59599	1.0952

Totals : 3572.27960 507.30368

=====
*** End of Report ***

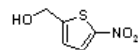
APPENDIX B

Synthesis of Bioreductively Activatable Prodrug Conjugates based-on OXi8006 and 3-Bromopyruvic Acid

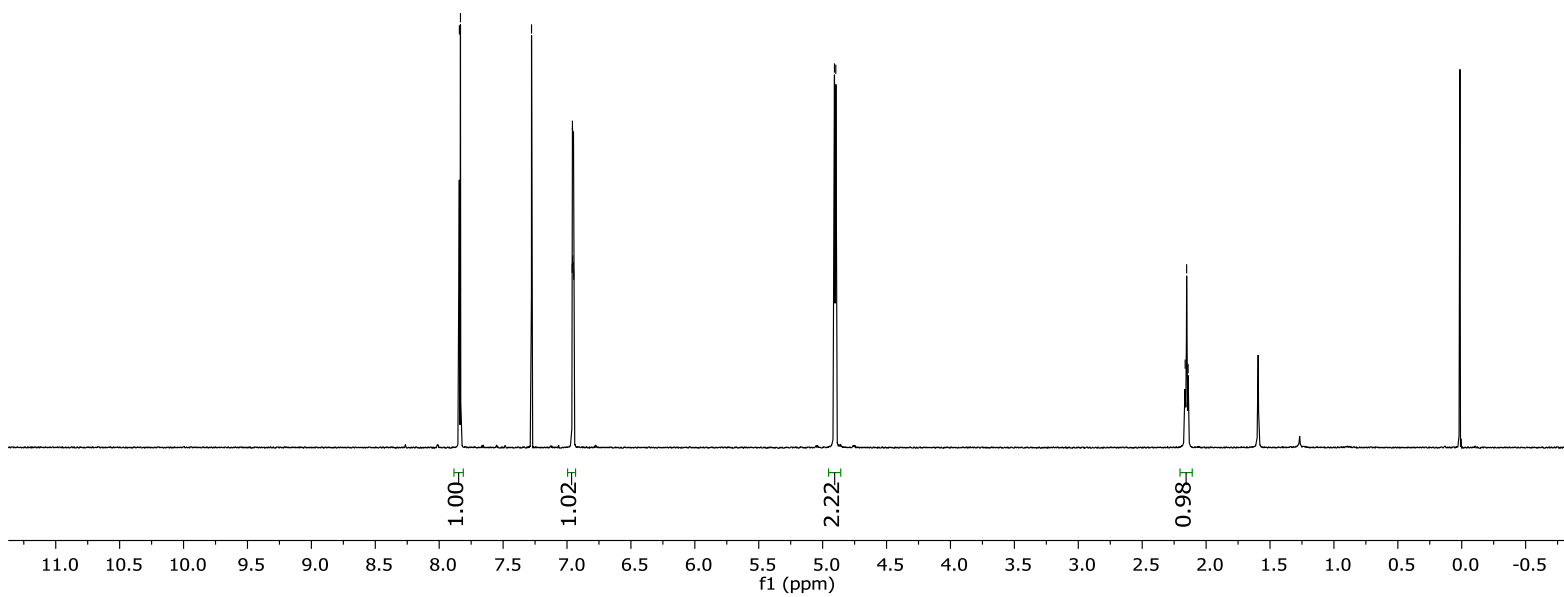
Table of Contents

¹ H and ¹³ C NMR of Compound 2	195
¹ H and ¹³ C NMR of Compound 3	197
¹ H and ¹³ C NMR of Compound 4	199
¹ H and ¹³ C NMR of Compound 5	201
¹ H and ¹³ C NMR of Compound 7	203
¹ H and ¹³ C NMR of Compound 8	205
¹ H and ¹³ C NMR of Compound 9	207
¹ H and ¹³ C NMR of Compound 10	209
¹ H and ¹³ C NMR of Compound 14	211
¹ H and ¹³ C NMR of Compound 15	213
¹ H and ¹³ C NMR of Compound 16	215
¹ H and ¹³ C NMR of Compound 17	217
¹ H and ¹³ C NMR of Compound 18	219
¹ H and ¹³ C NMR of Compound 22	221
¹ H and ¹³ C NMR of Compound 24	223
¹ H, ¹³ C NMR, HRMS and HPLC traces of Compound 26	225
¹ H, ¹³ C NMR, HRMS and HPLC traces of Compound 28	232

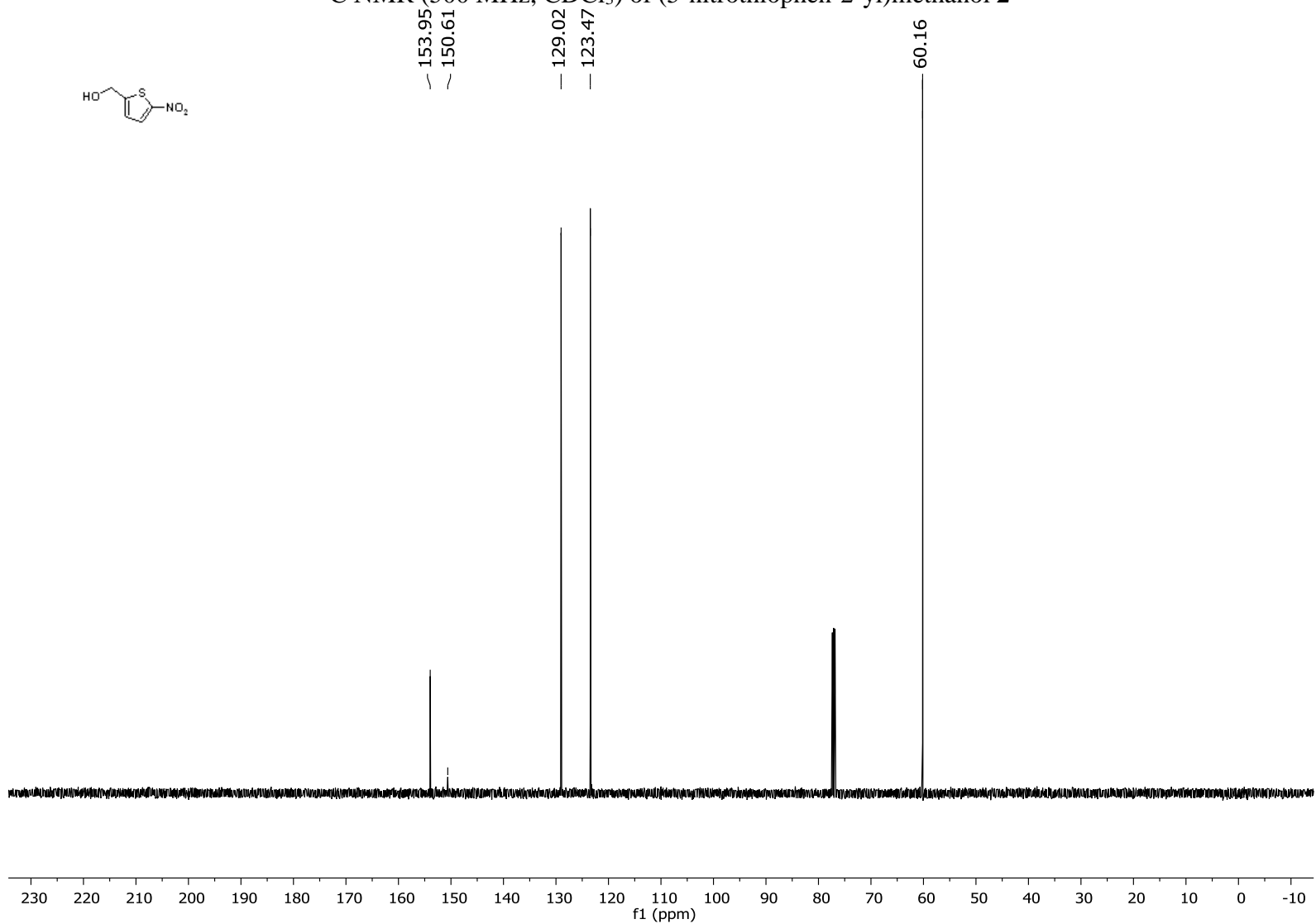
¹H NMR (500 MHz, CDCl₃) of (5-nitrothiophen-2-yl)methanol **2**



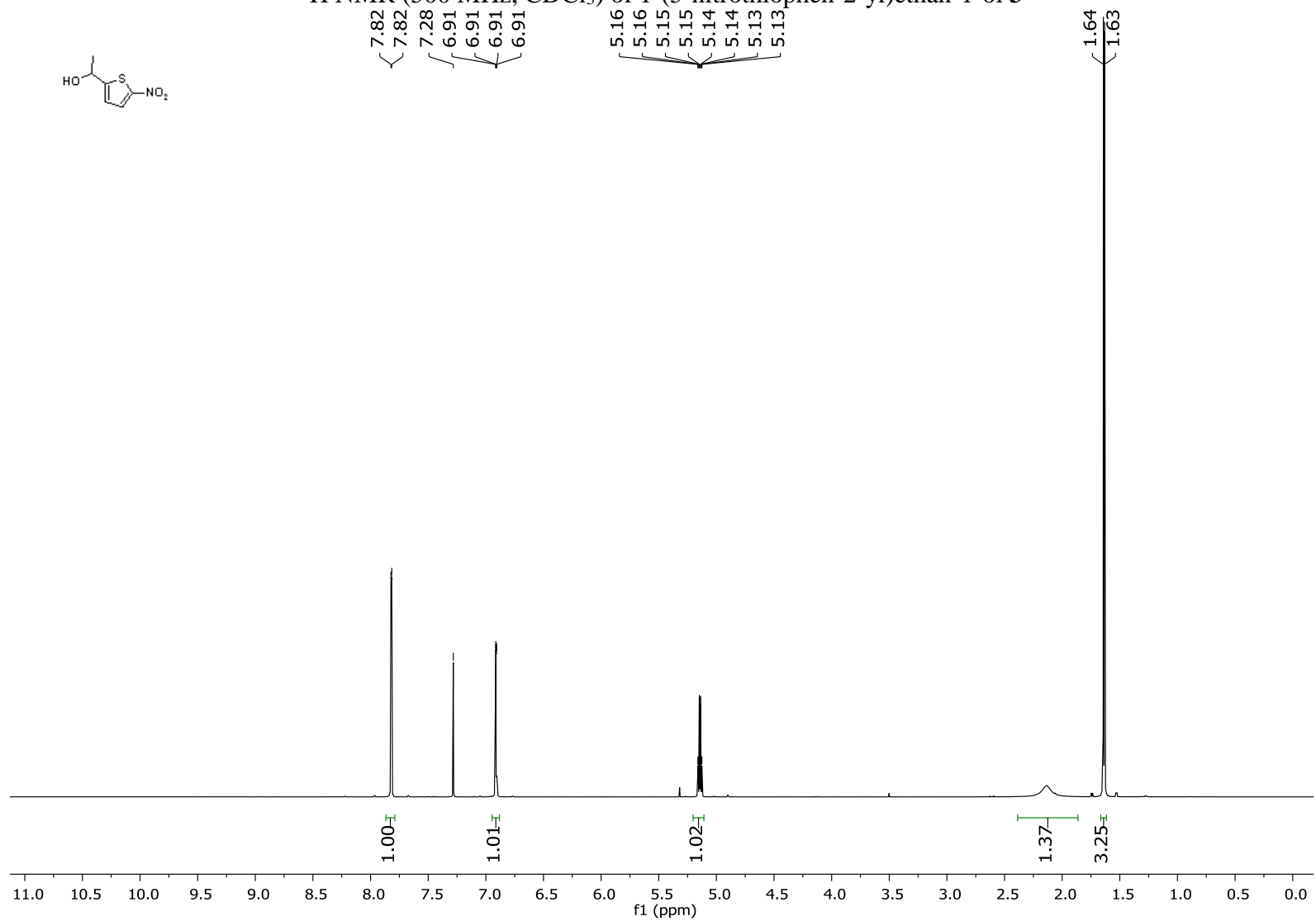
7.84
7.83
7.28
6.96
6.96
6.96
6.95
6.95
6.95
4.91
4.90
2.16
2.15
2.14



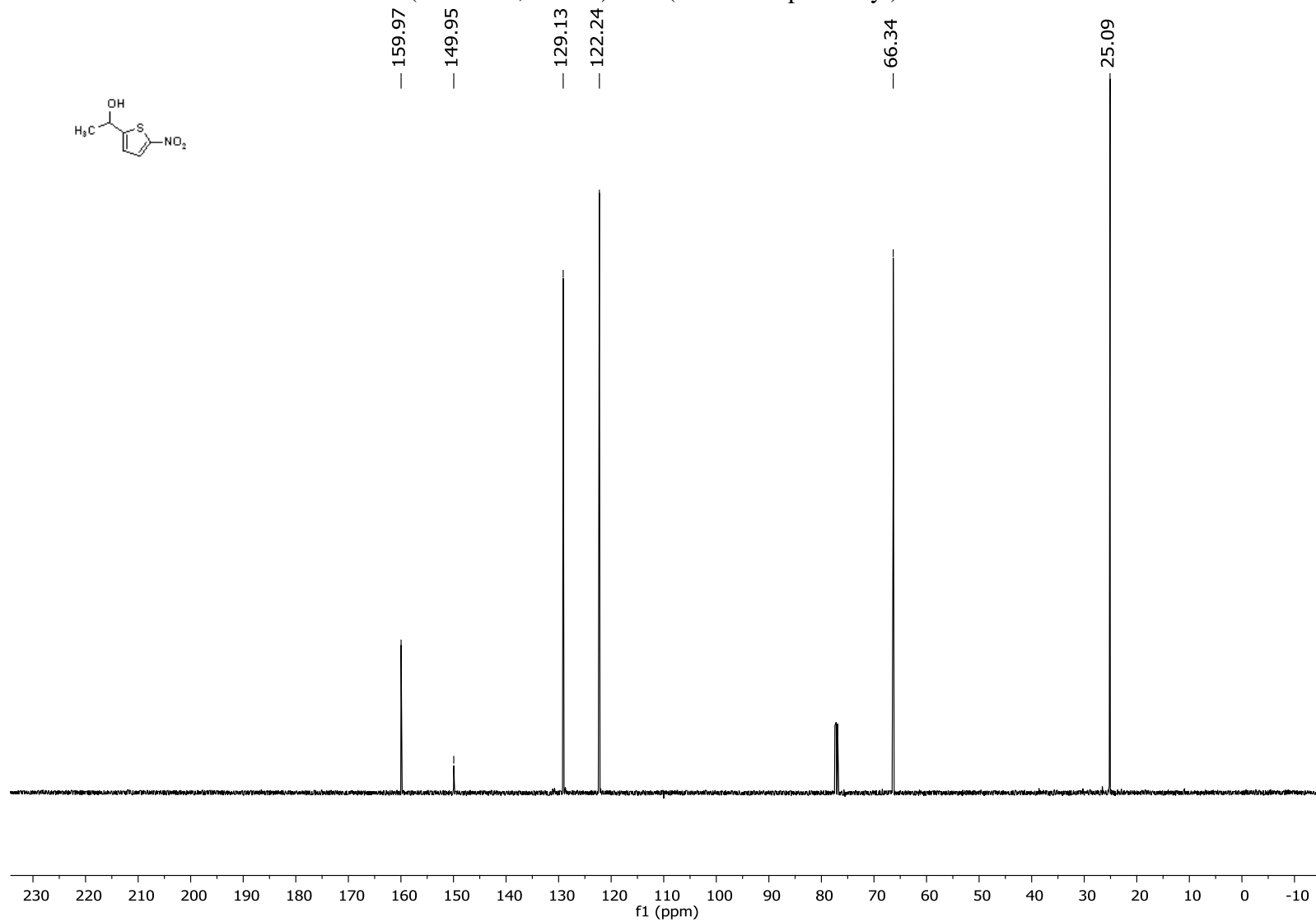
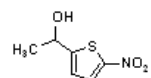
¹³C NMR (500 MHz, CDCl₃) of (5-nitrothiophen-2-yl)methanol **2**



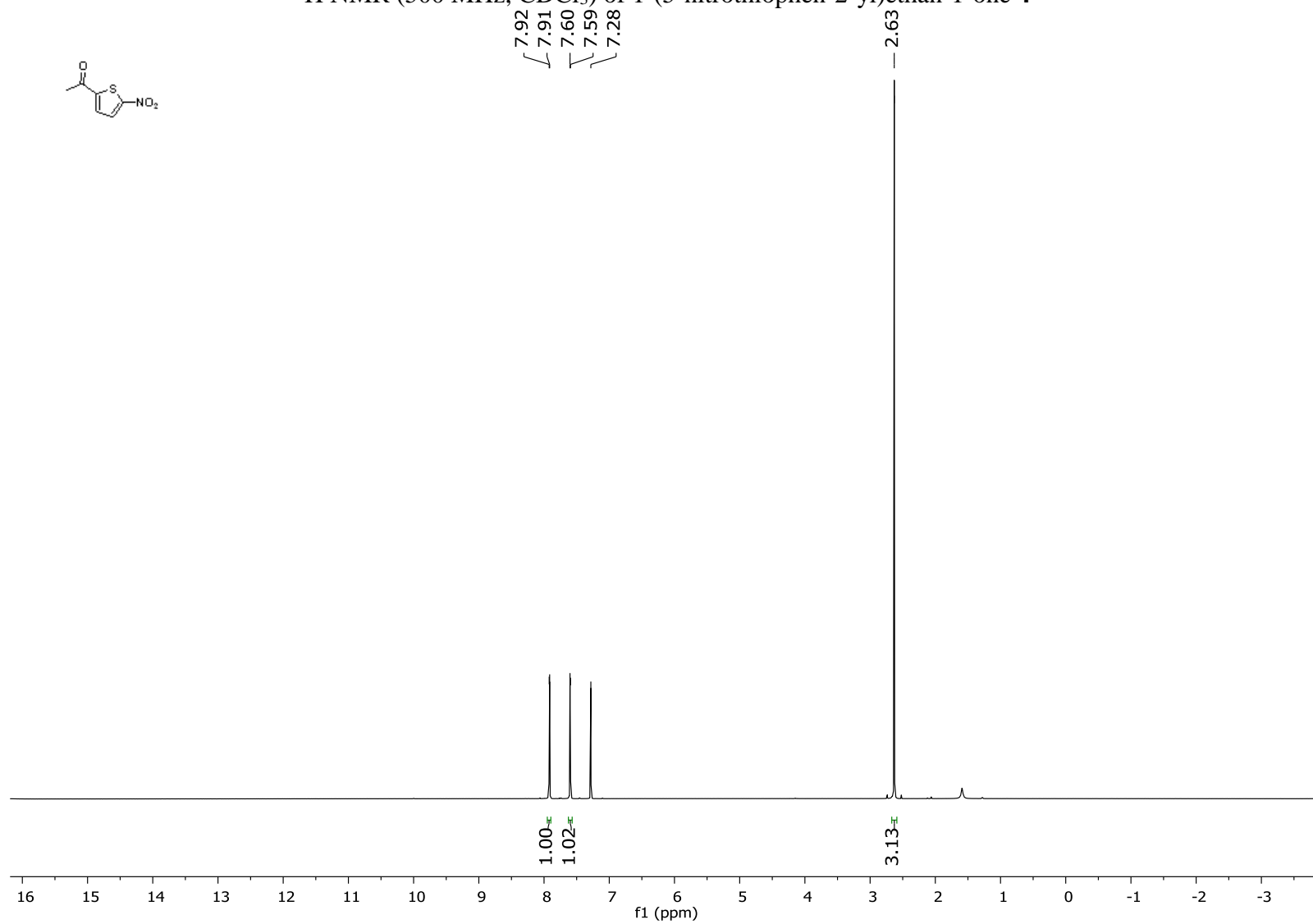
¹H NMR (500 MHz, CDCl₃) of 1-(5-nitrothiophen-2-yl)ethan-1-ol **3**

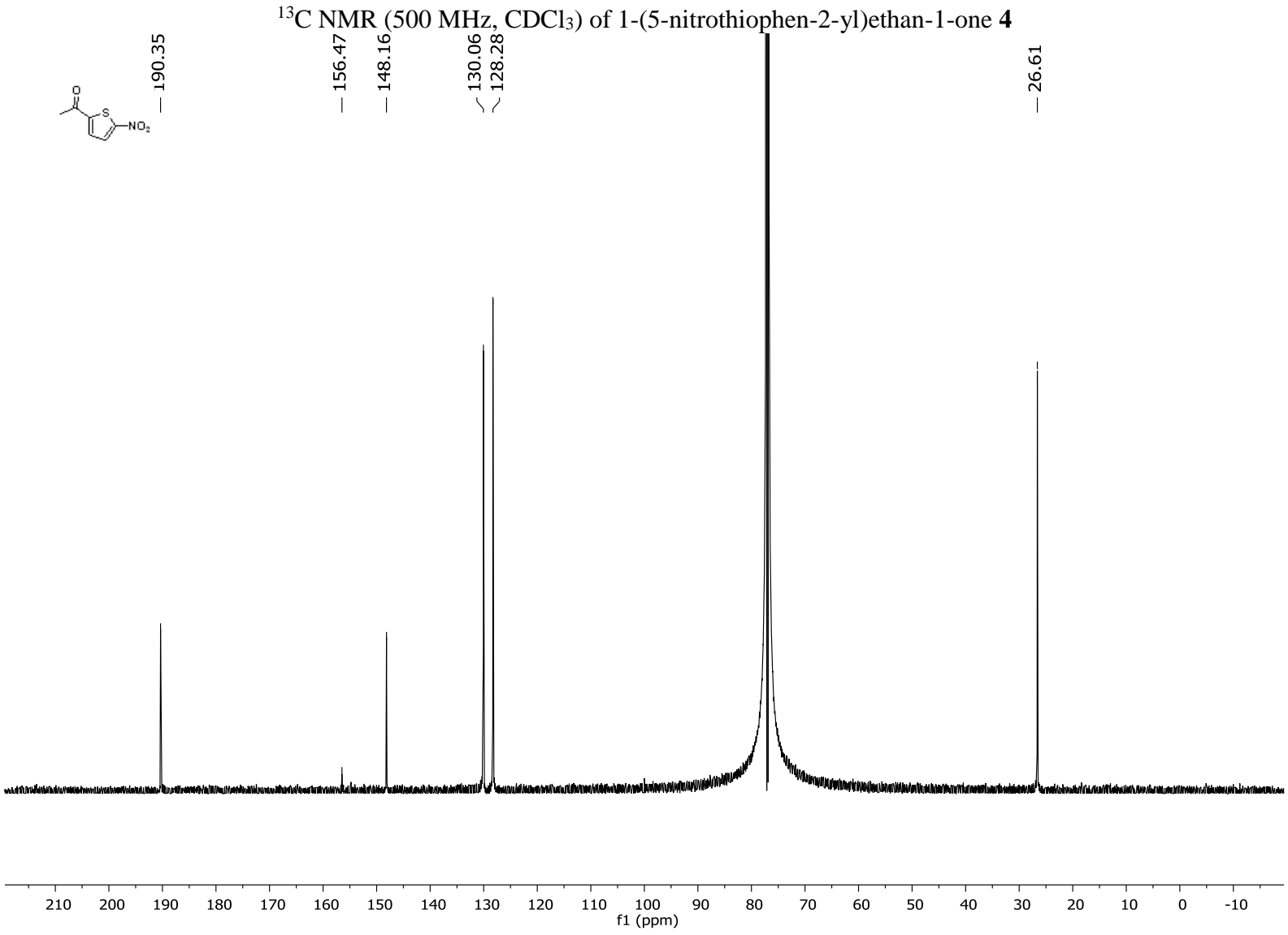


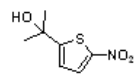
^{13}C NMR (500 MHz, CDCl_3) of 1-(5-nitrothiophen-2-yl)ethan-1-ol **3**



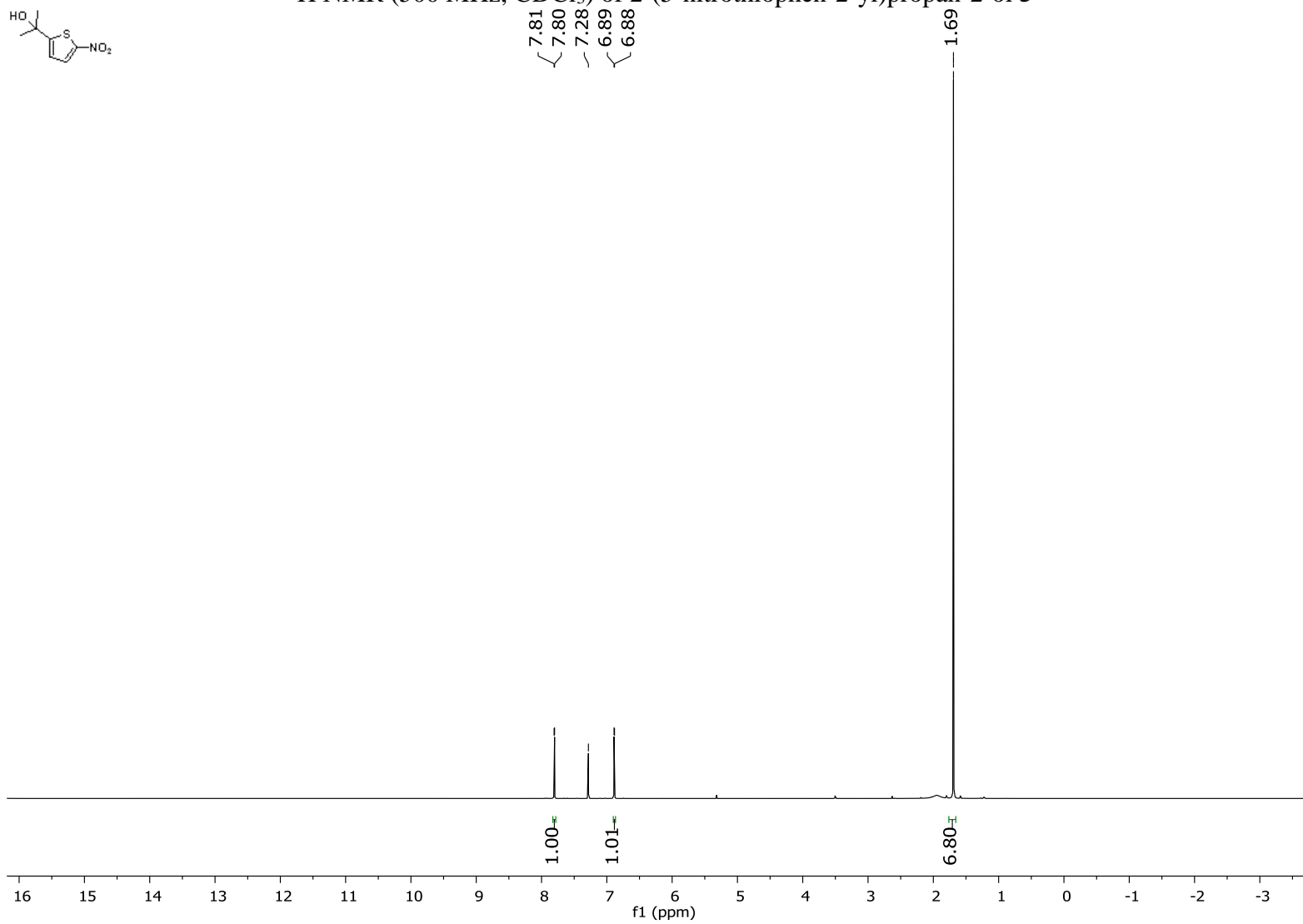
^1H NMR (500 MHz, CDCl_3) of 1-(5-nitrothiophen-2-yl)ethan-1-one **4**

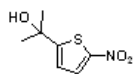




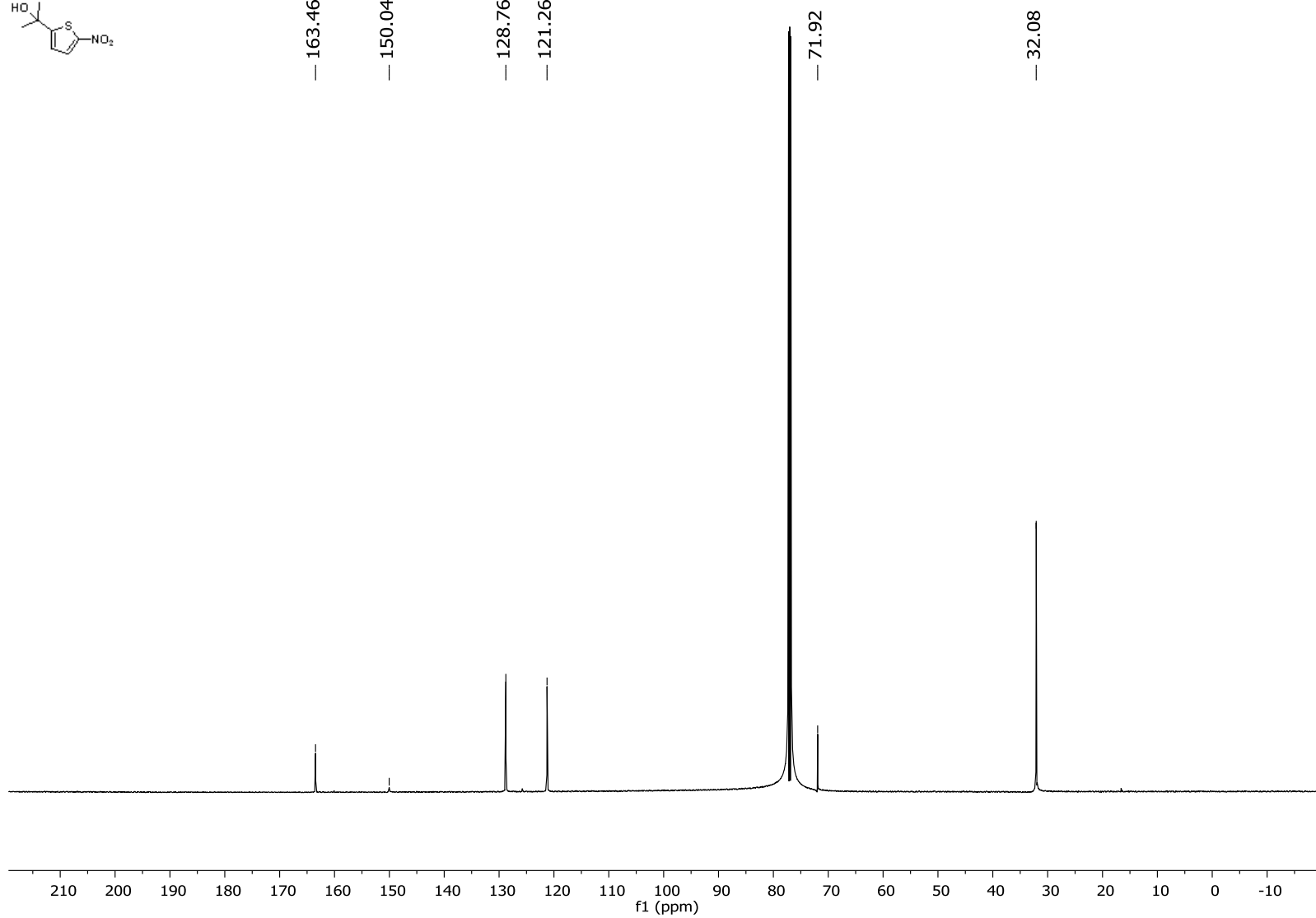


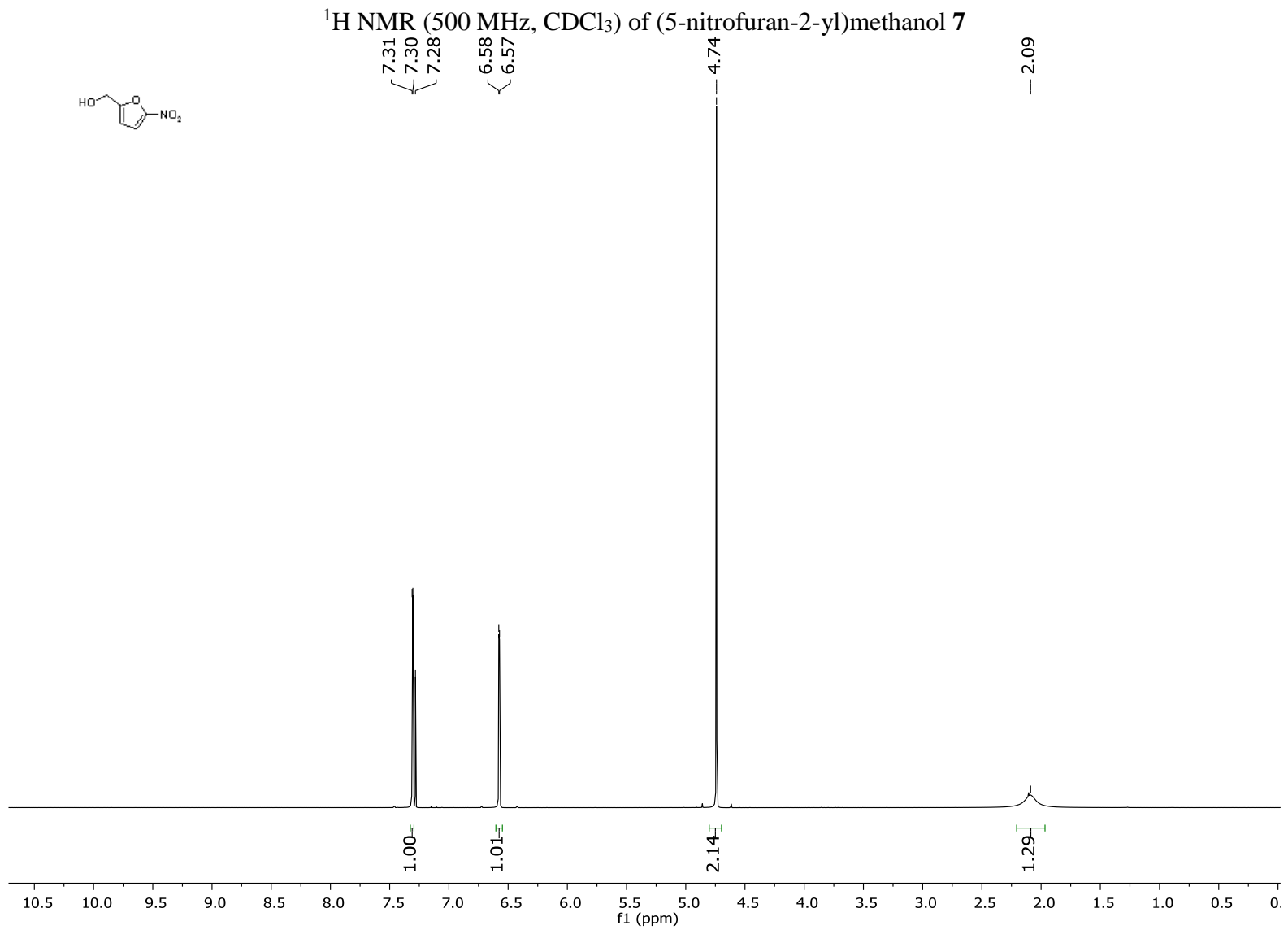
^1H NMR (500 MHz, CDCl_3) of 2-(5-nitrothiophen-2-yl)propan-2-ol **5**

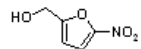




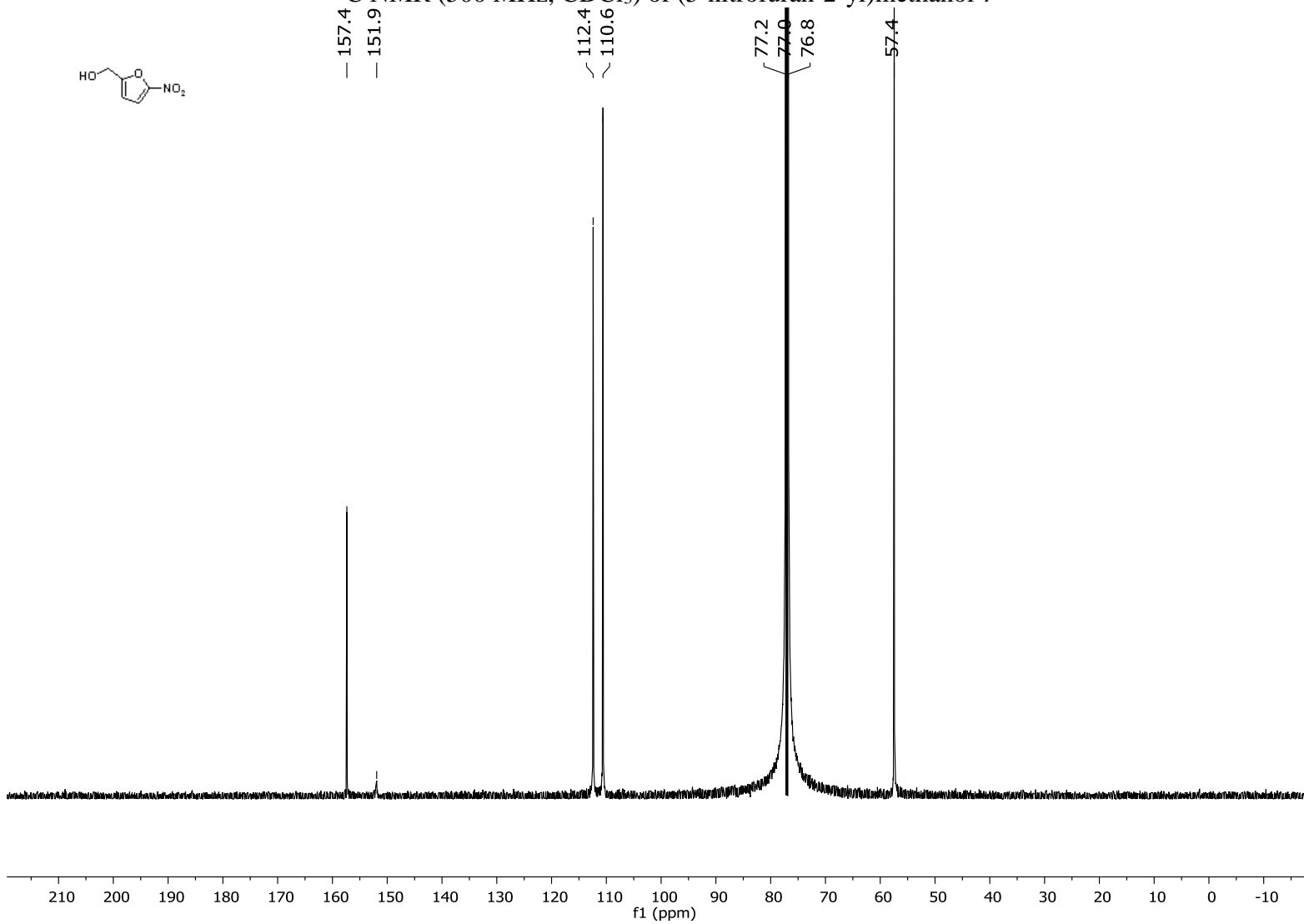
¹³C NMR (500 MHz, CDCl₃) of 2-(5-nitrothiophen-2-yl)propan-2-ol **5**

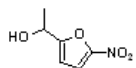




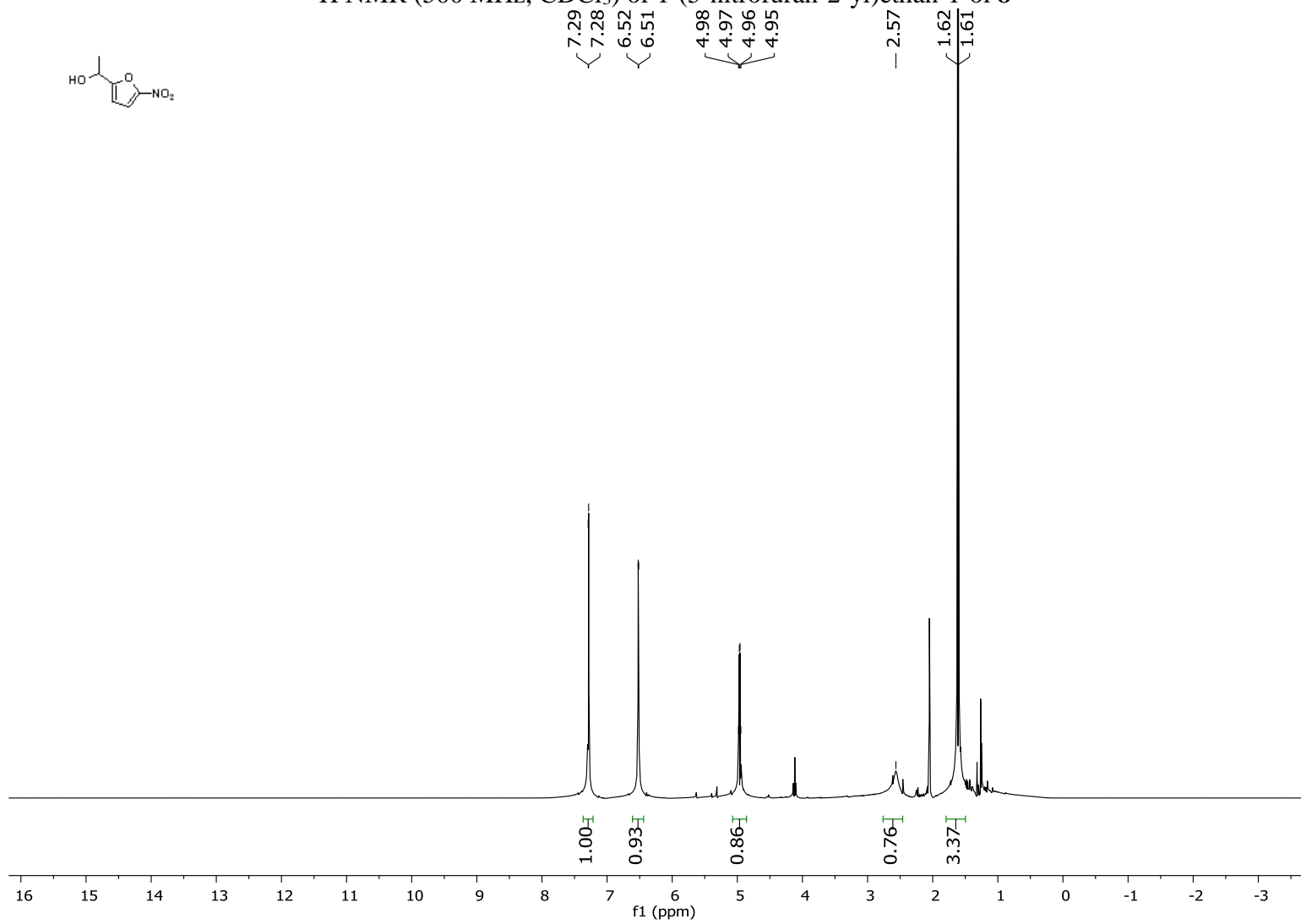


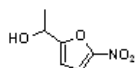
¹³C NMR (500 MHz, CDCl₃) of (5-nitrofur-2-yl)methanol **7**





^1H NMR (500 MHz, CDCl_3) of 1-(5-nitrofur-2-yl)ethan-1-ol **8**





^{13}C NMR (500 MHz, CDCl_3) of 1-(5-nitrofur-2-yl)ethan-1-ol **8**

— 161.27

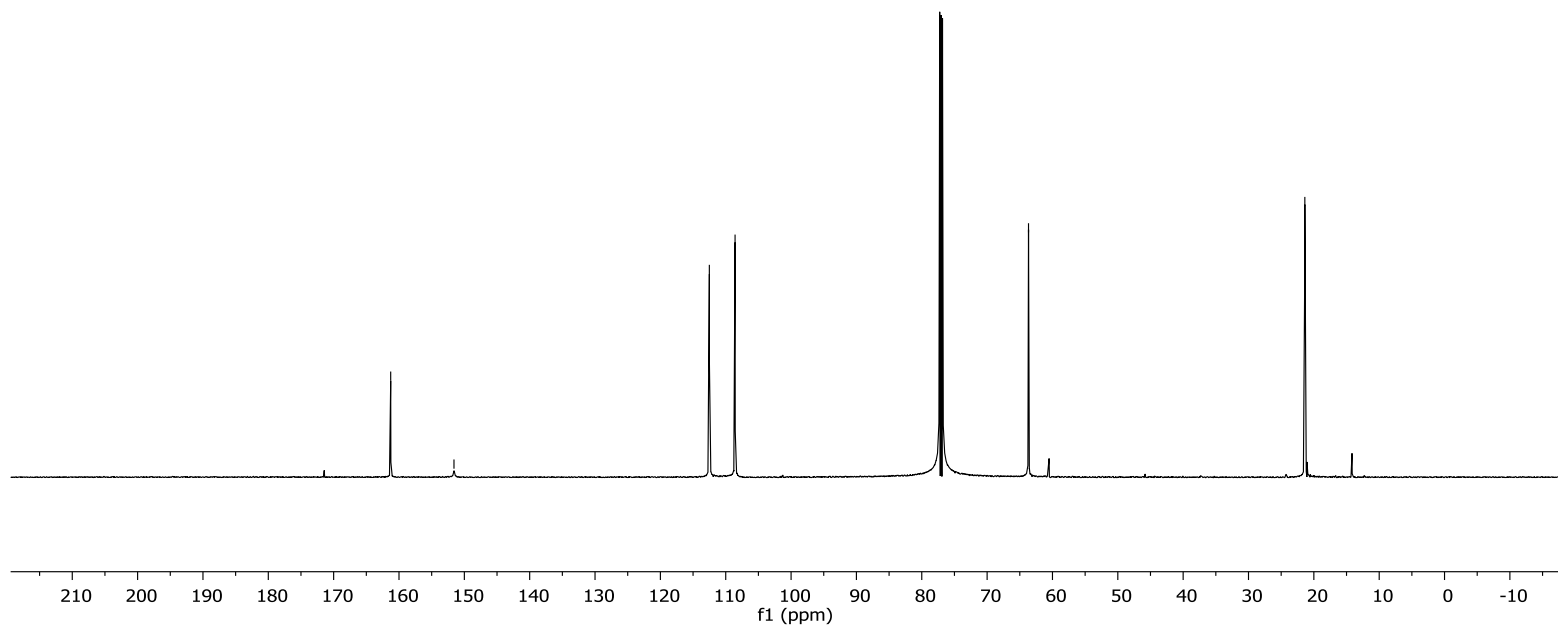
— 151.59

— 112.51

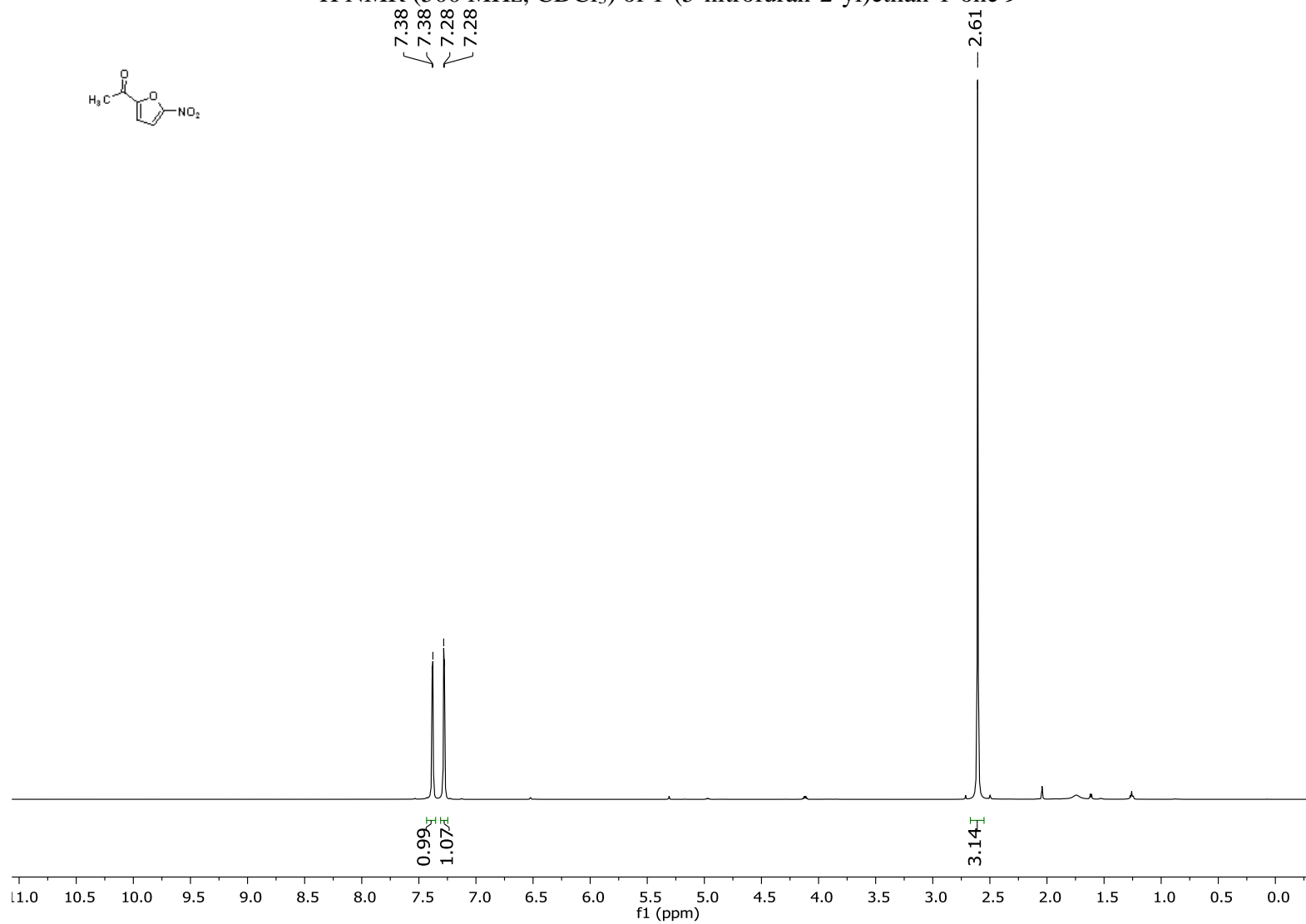
— 108.57

— 63.66

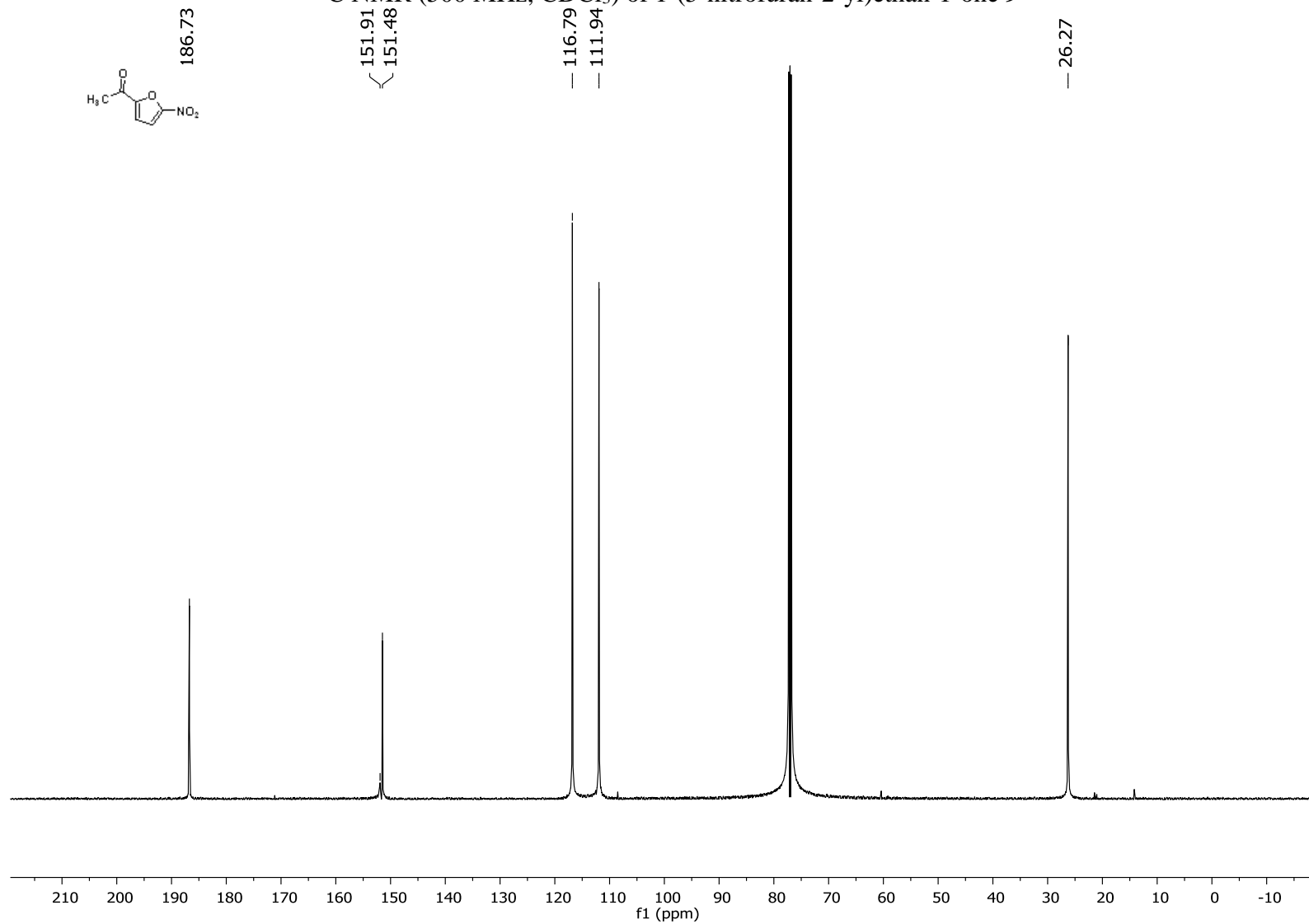
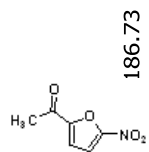
— 21.38



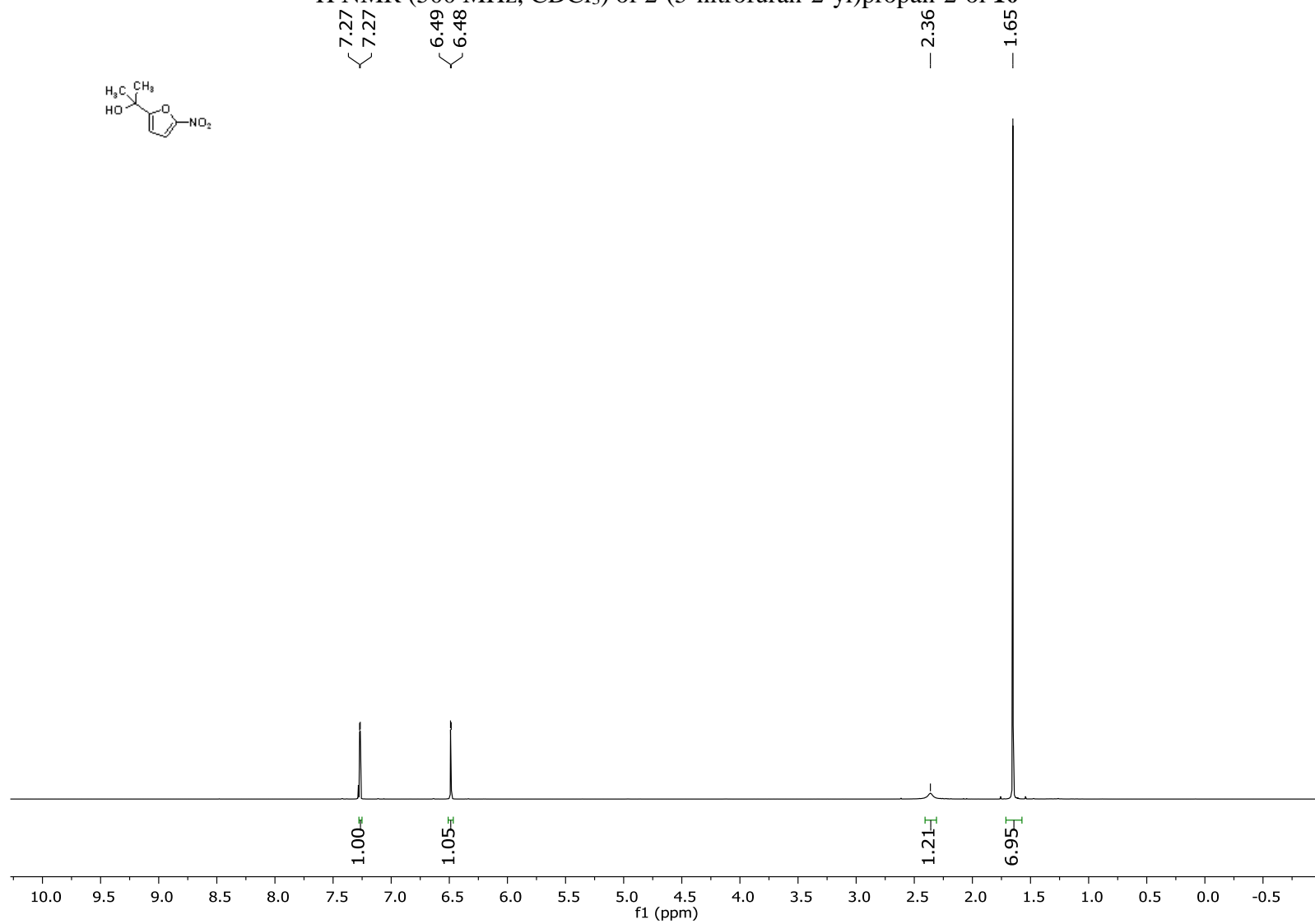
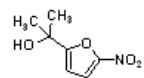
¹H NMR (500 MHz, CDCl₃) of 1-(5-nitrofur-2-yl)ethan-1-one **9**



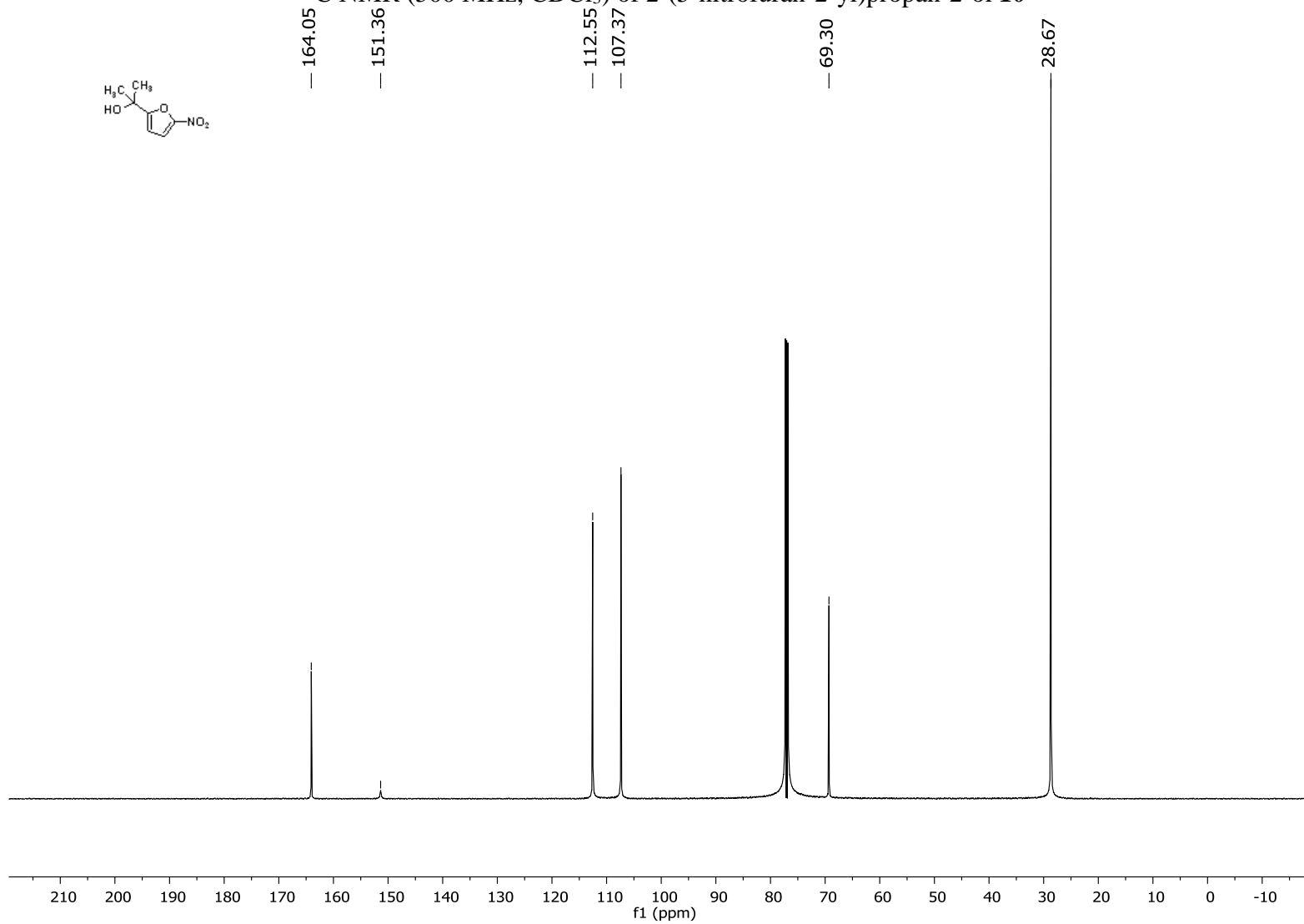
¹³C NMR (500 MHz, CDCl₃) of 1-(5-nitrofur-2-yl)ethan-1-one **9**



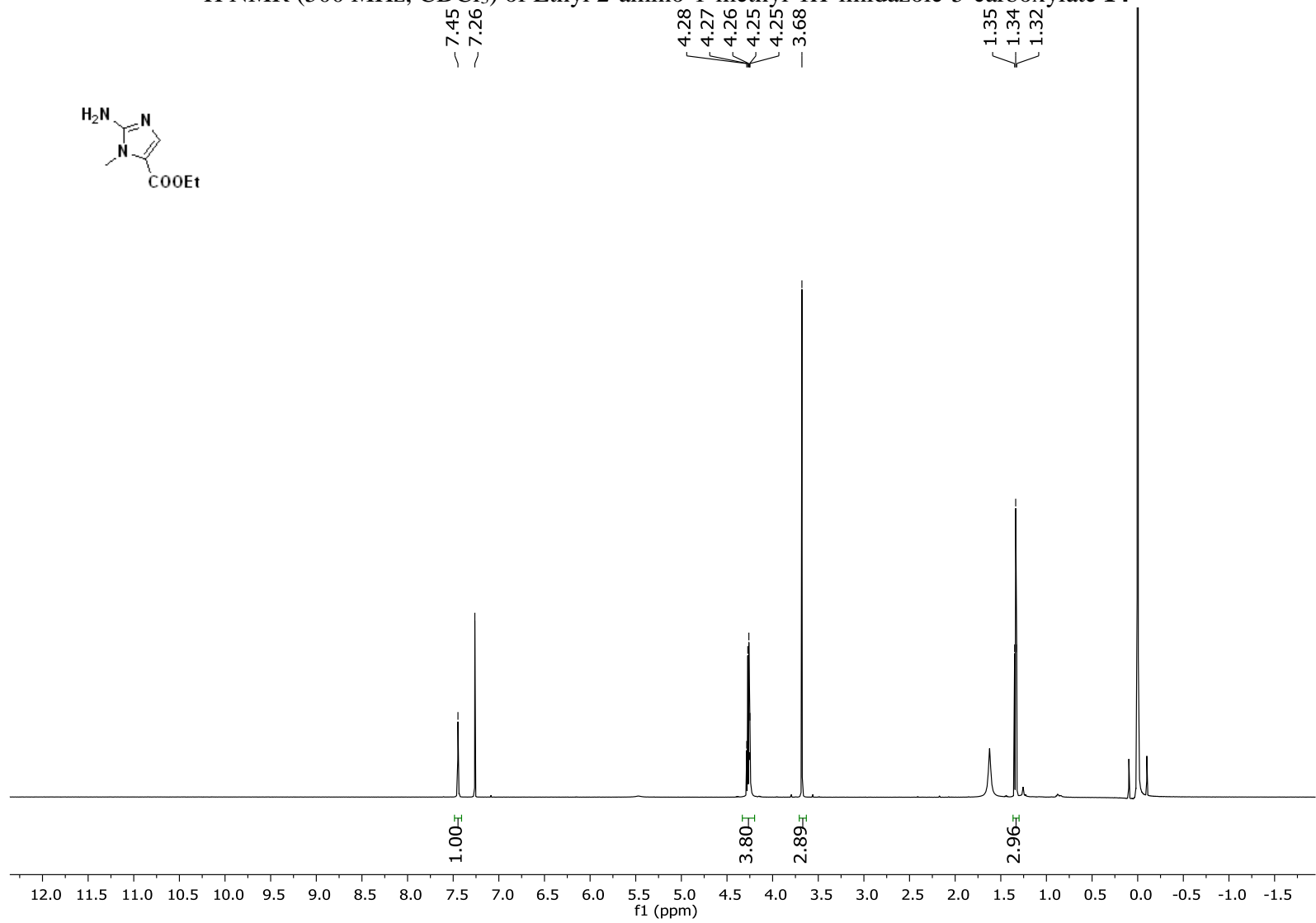
¹H NMR (500 MHz, CDCl₃) of 2-(5-nitrofur-2-yl)propan-2-ol **10**



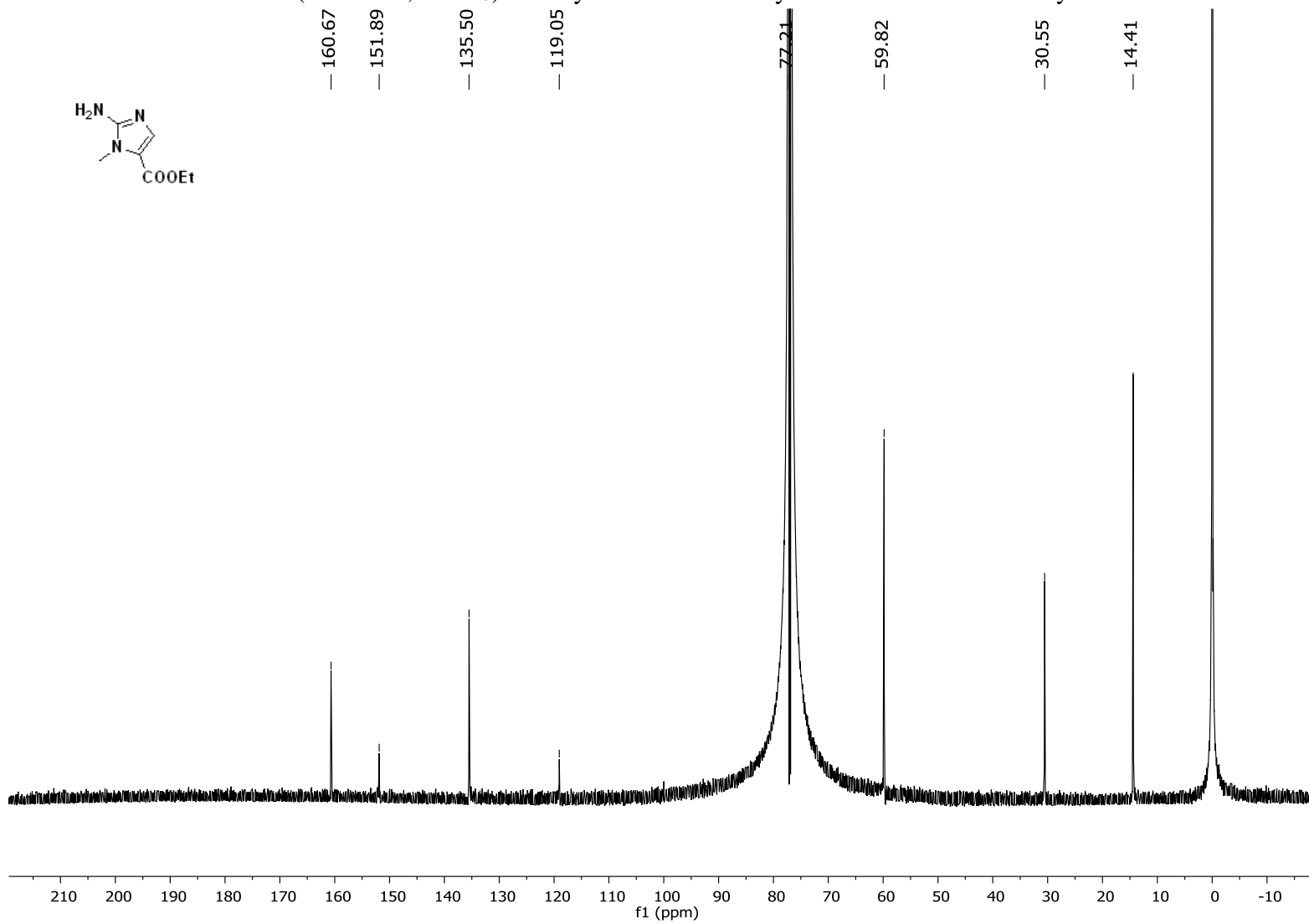
¹³C NMR (500 MHz, CDCl₃) of 2-(5-nitrofur-2-yl)propan-2-ol **10**



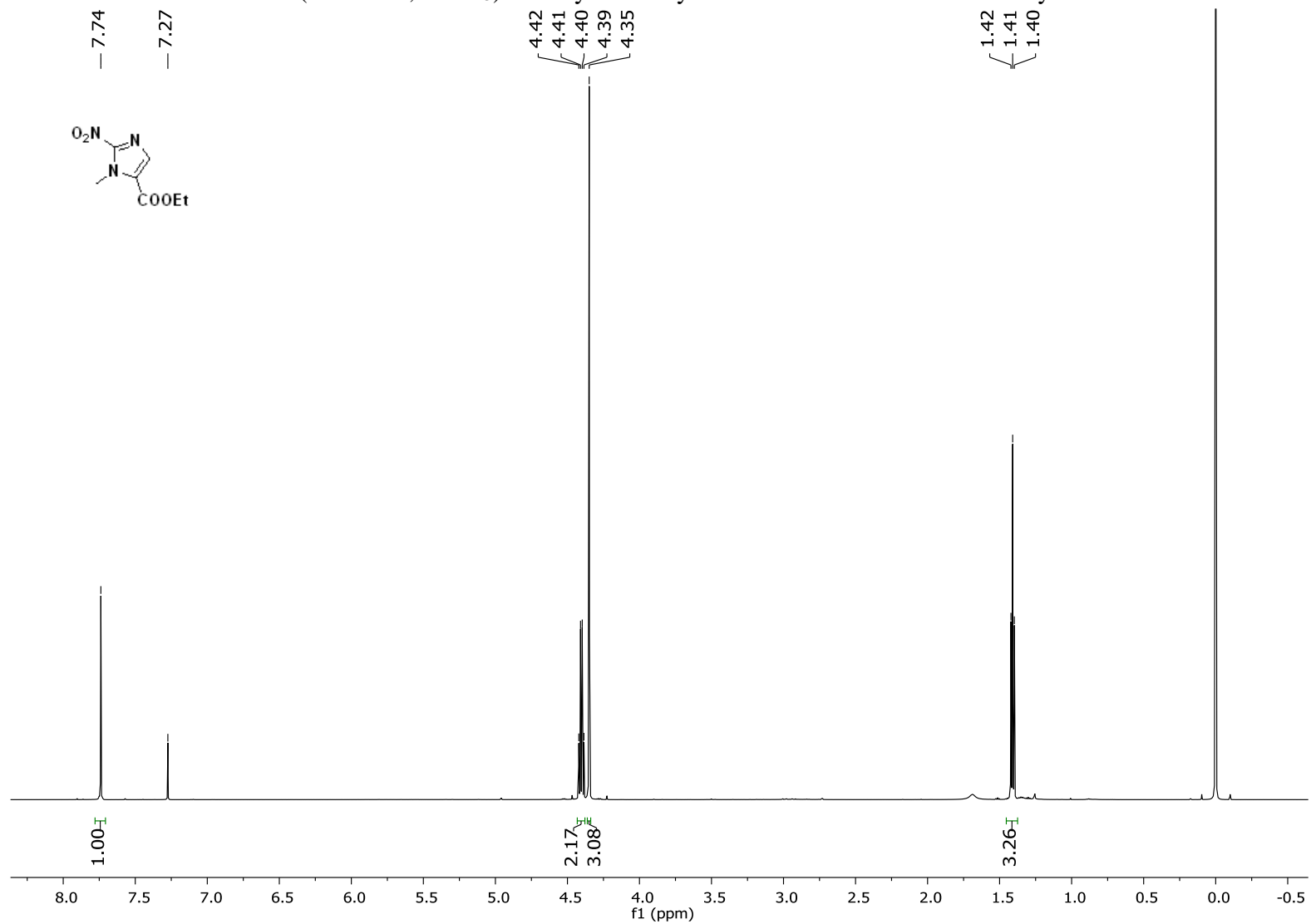
¹H NMR (500 MHz, CDCl₃) of Ethyl 2-amino-1-methyl-1*H*-imidazole-5-carboxylate **14**



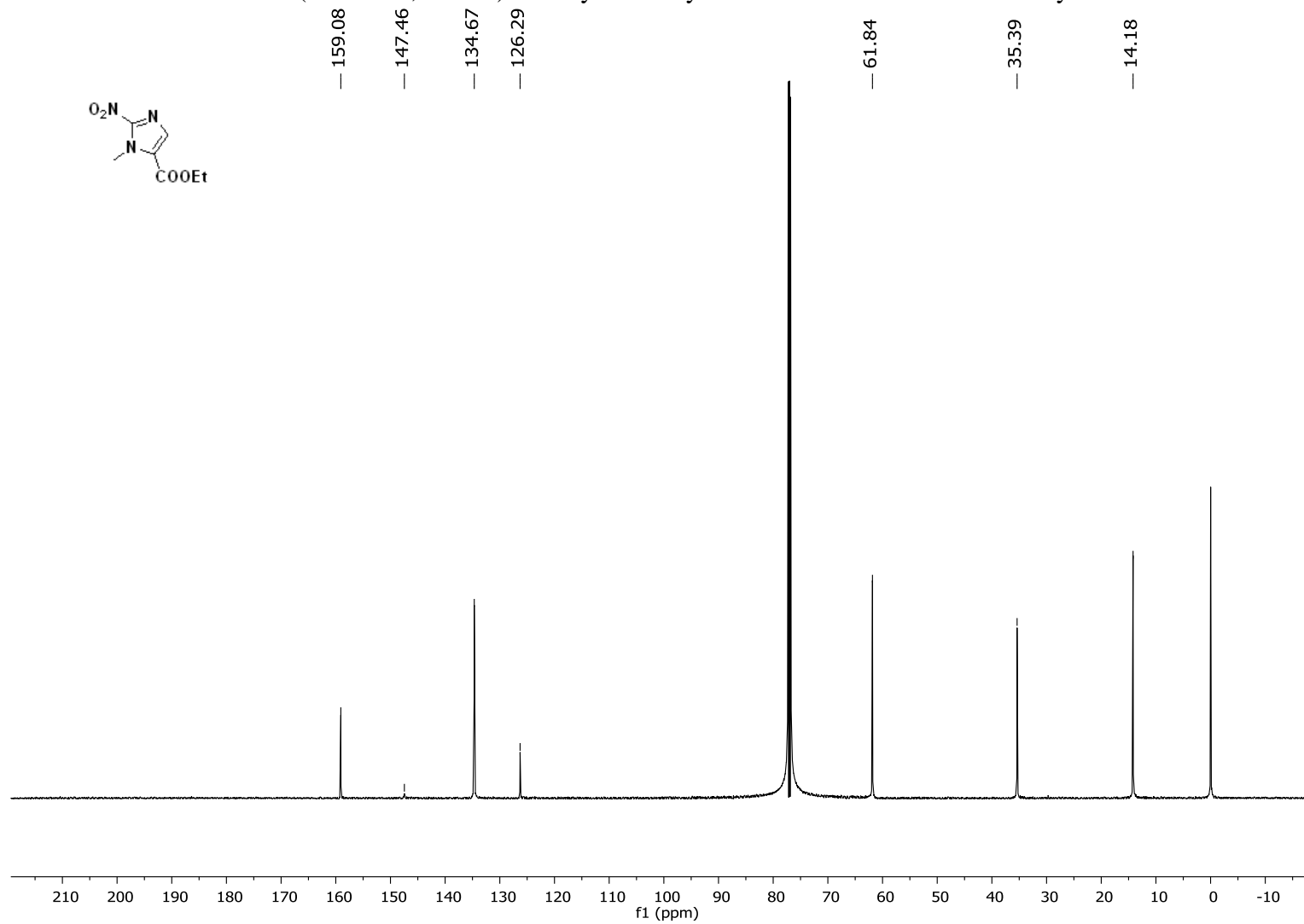
¹³C NMR (500 MHz, CDCl₃) of Ethyl 2-amino-1-methyl-1*H*-imidazole-5-carboxylate **14**



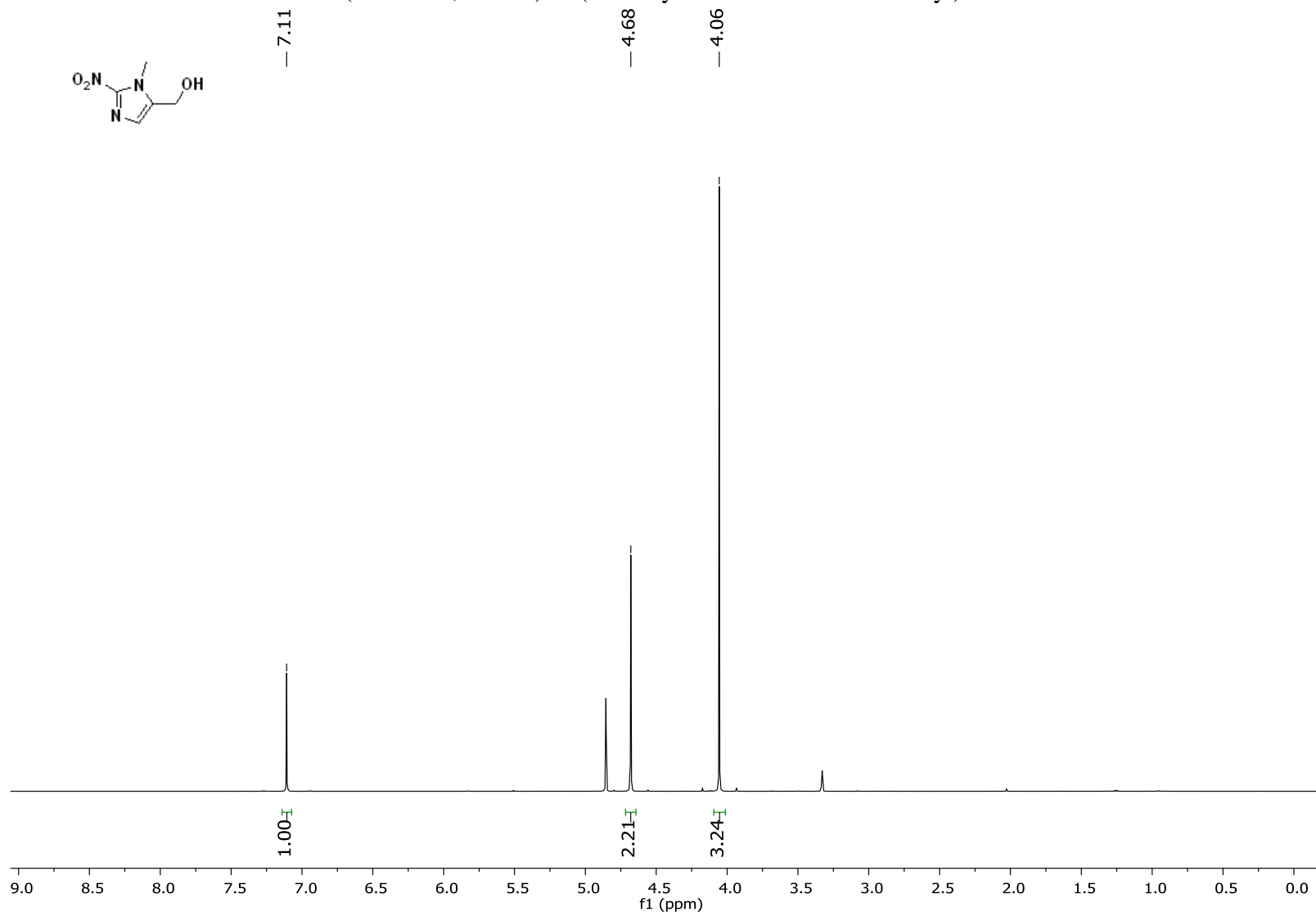
¹H NMR (500 MHz, CDCl₃) of Ethyl 1-methyl-2-nitro-1*H*-imidazole-5-carboxylate **15**



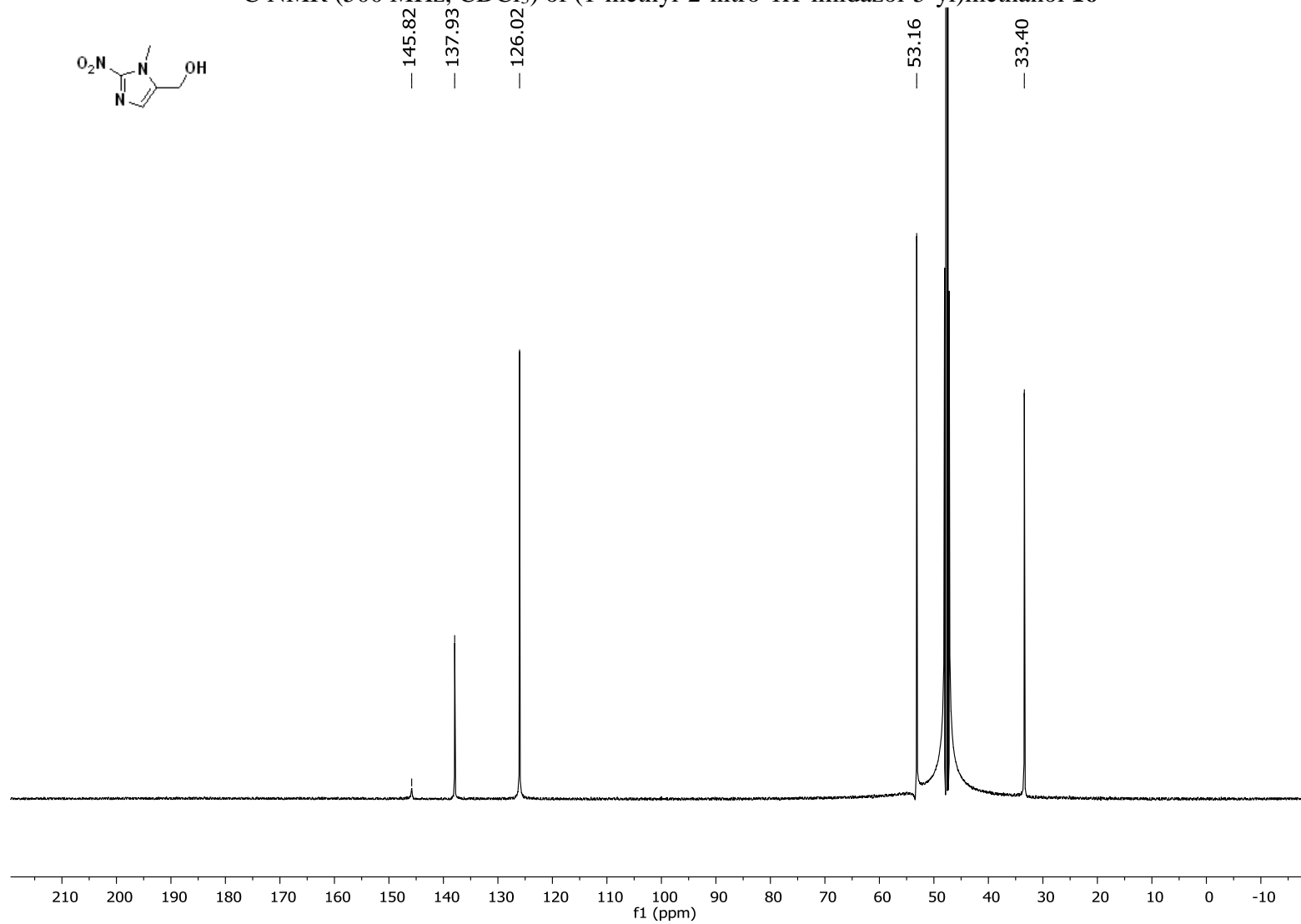
¹³C NMR (500 MHz, CDCl₃) of Ethyl 1-methyl-2-nitro-1*H*-imidazole-5-carboxylate **15**



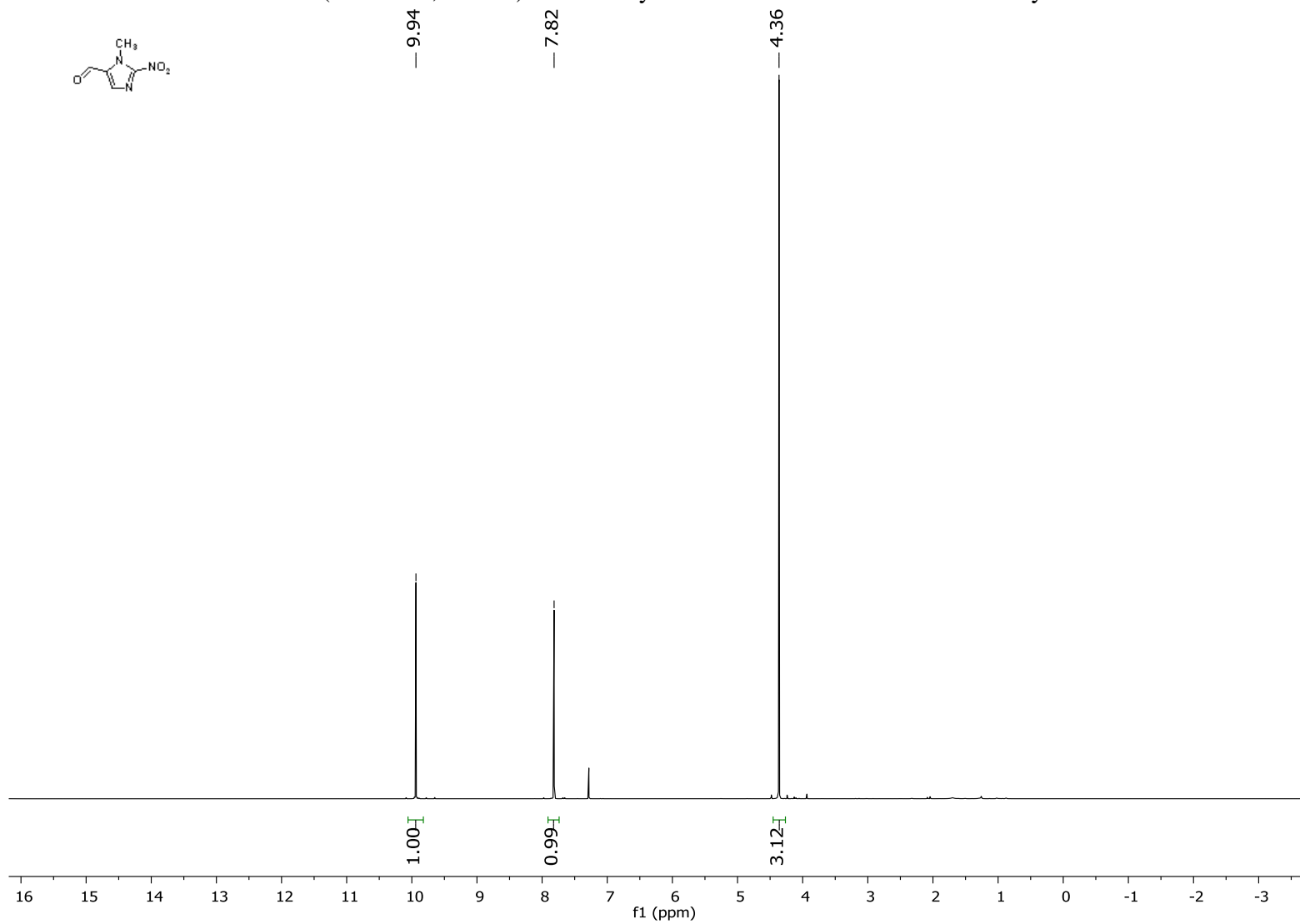
¹H NMR (500 MHz, CDCl₃) of (1-methyl-2-nitro-1*H*-imidazol-5-yl)methanol **16**

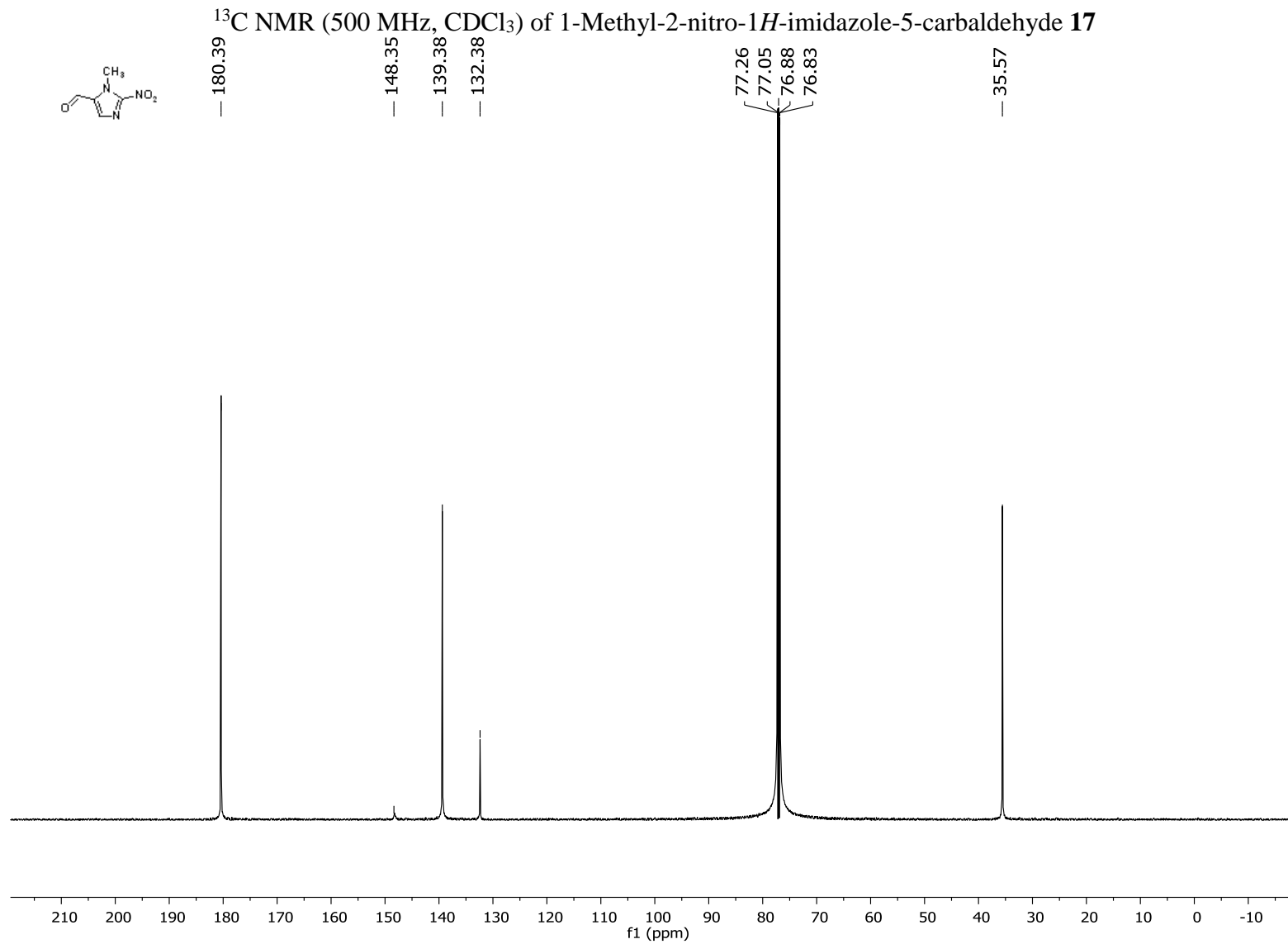


¹³C NMR (500 MHz, CDCl₃) of (1-methyl-2-nitro-1*H*-imidazol-5-yl)methanol **16**

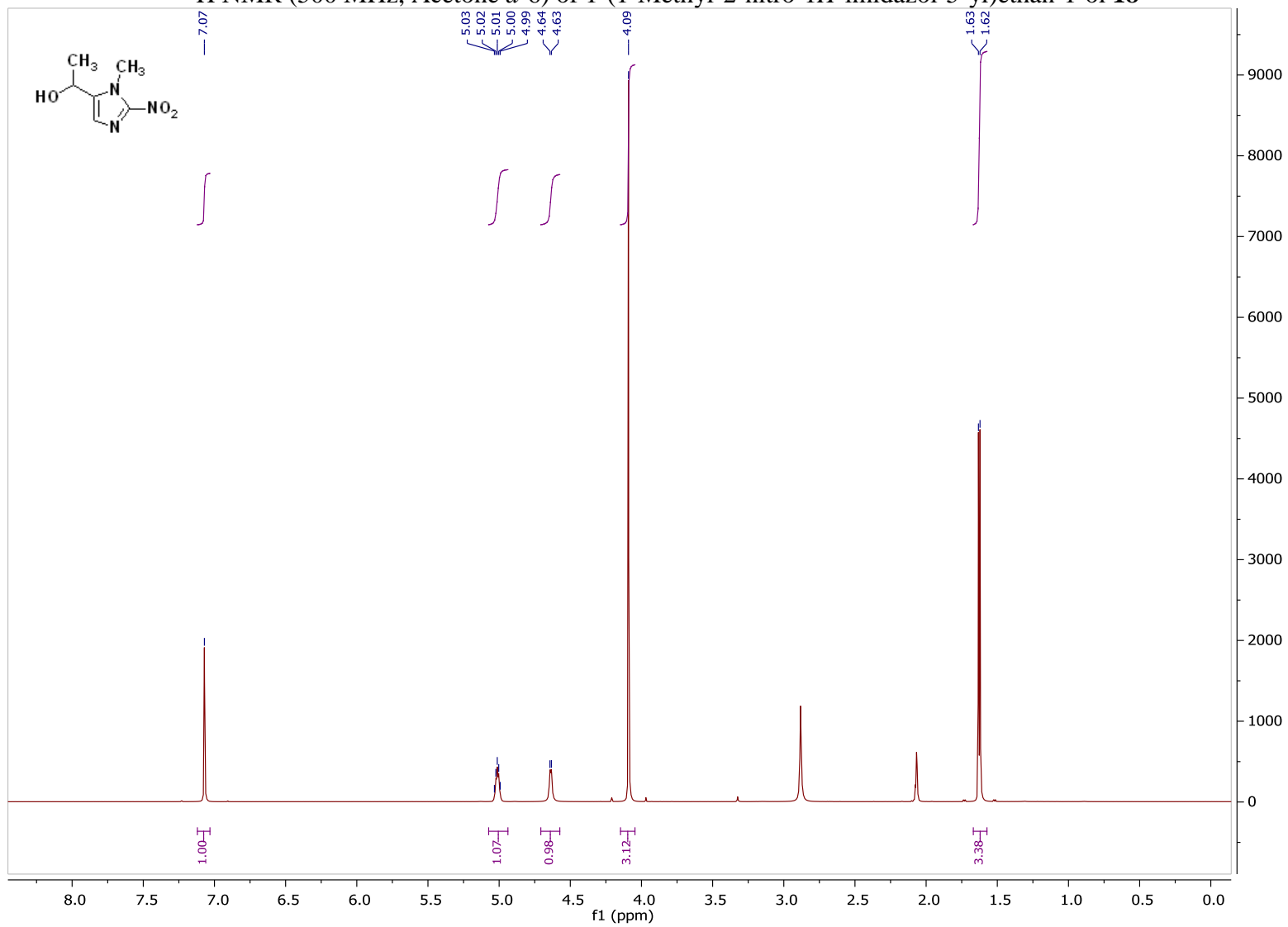


¹H NMR (500 MHz, CDCl₃) of 1-Methyl-2-nitro-1*H*-imidazole-5-carbaldehyde **17**

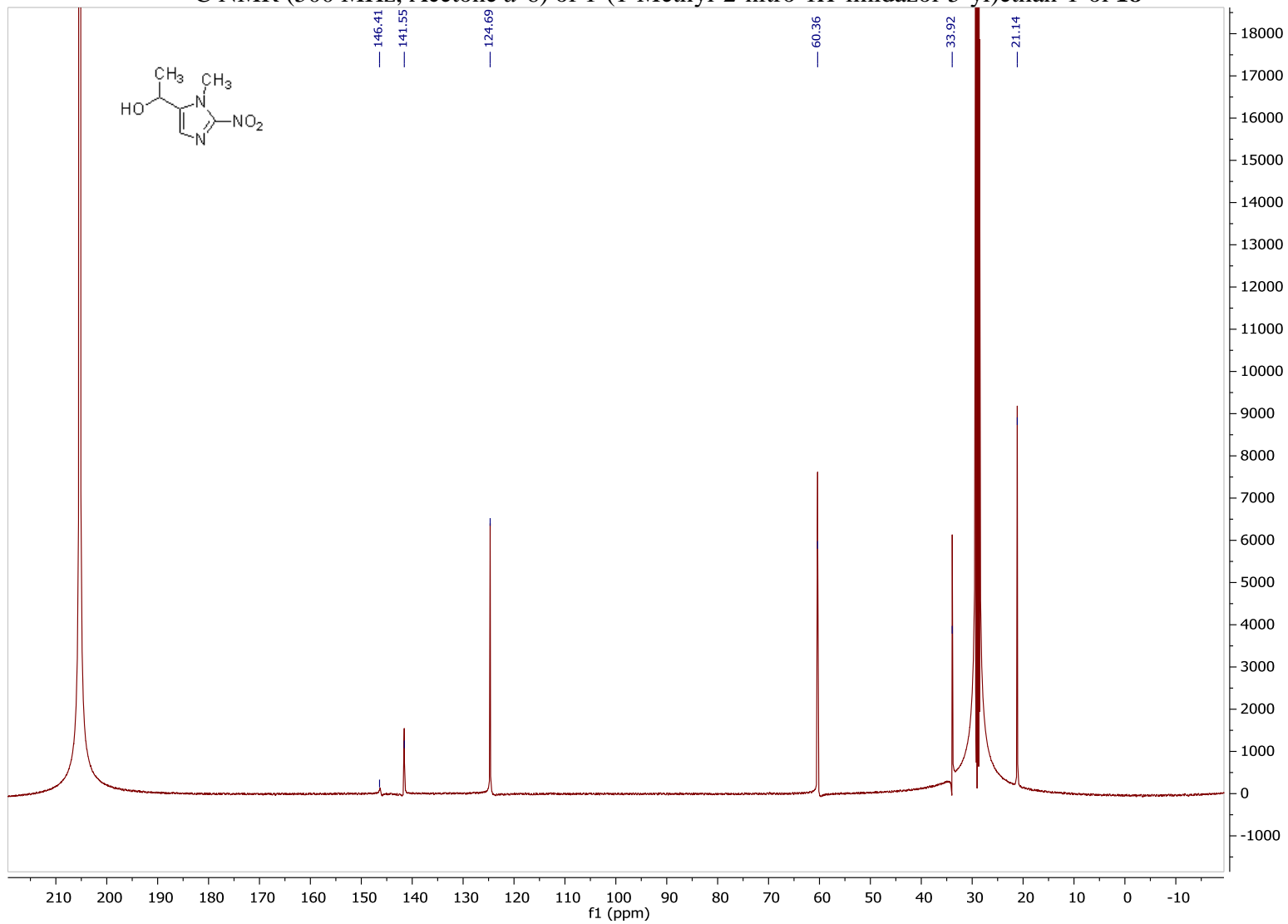


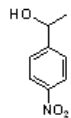


¹H NMR (500 MHz, Acetone *d*-6) of 1-(1-Methyl-2-nitro-1*H*-imidazol-5-yl)ethan-1-ol **18**

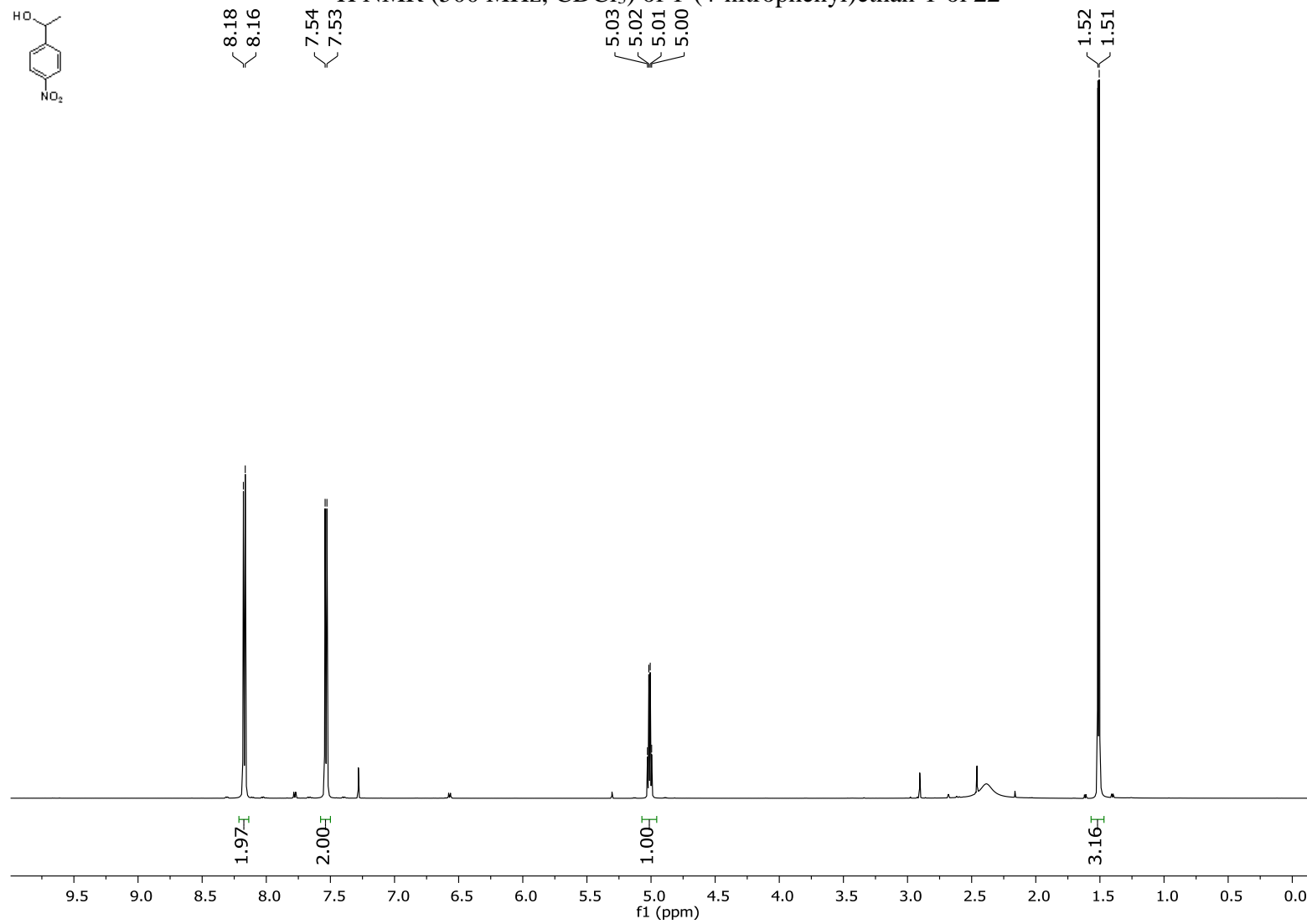


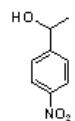
¹³C NMR (500 MHz, Acetone *d*-6) of 1-(1-Methyl-2-nitro-1*H*-imidazol-5-yl)ethan-1-ol **18**





¹H NMR (500 MHz, CDCl₃) of 1-(4-nitrophenyl)ethan-1-ol **22**





^{13}C NMR (500 MHz, CDCl_3) of 1-(4-nitrophenyl)ethan-1-ol **22**

— 153.22

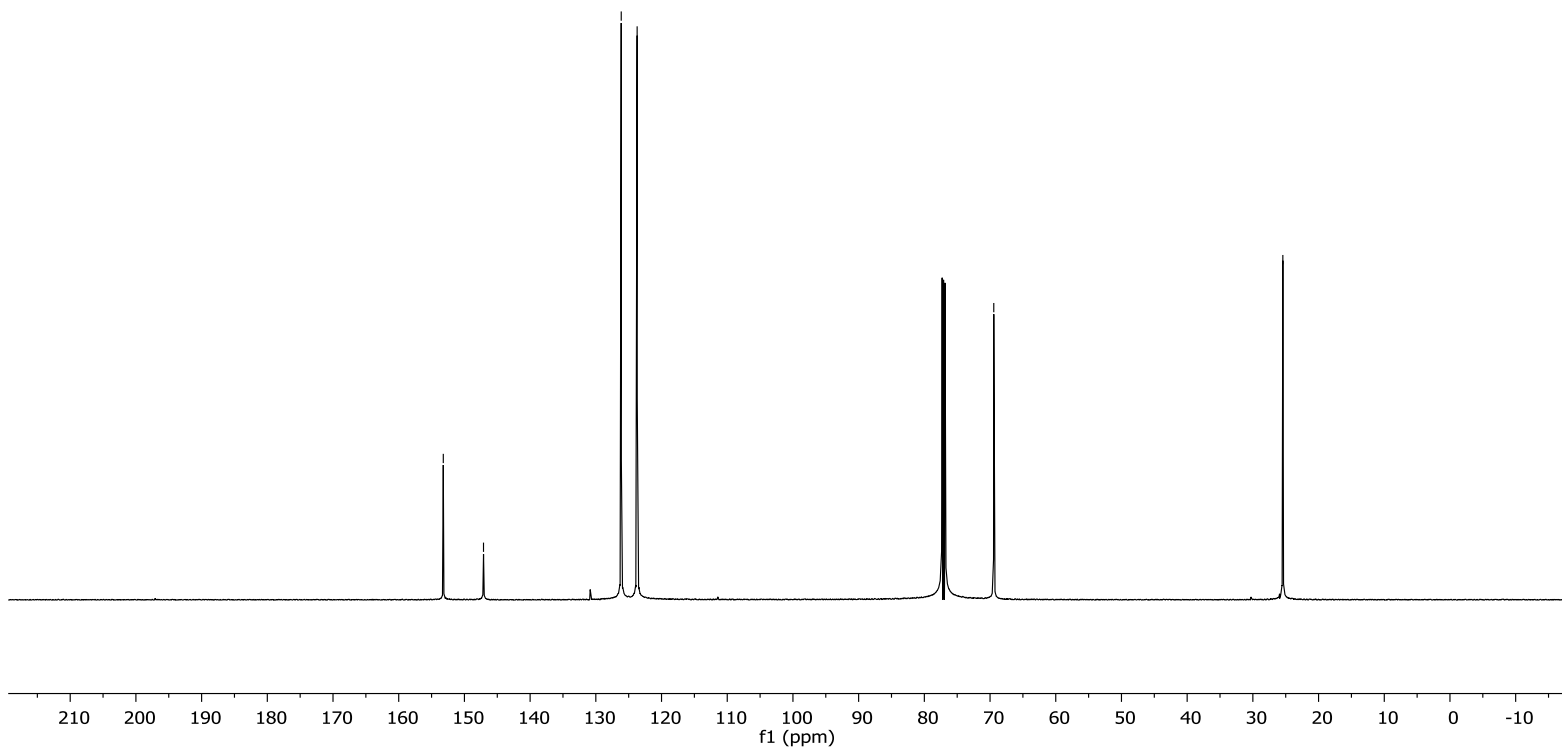
— 147.09

~ 126.13

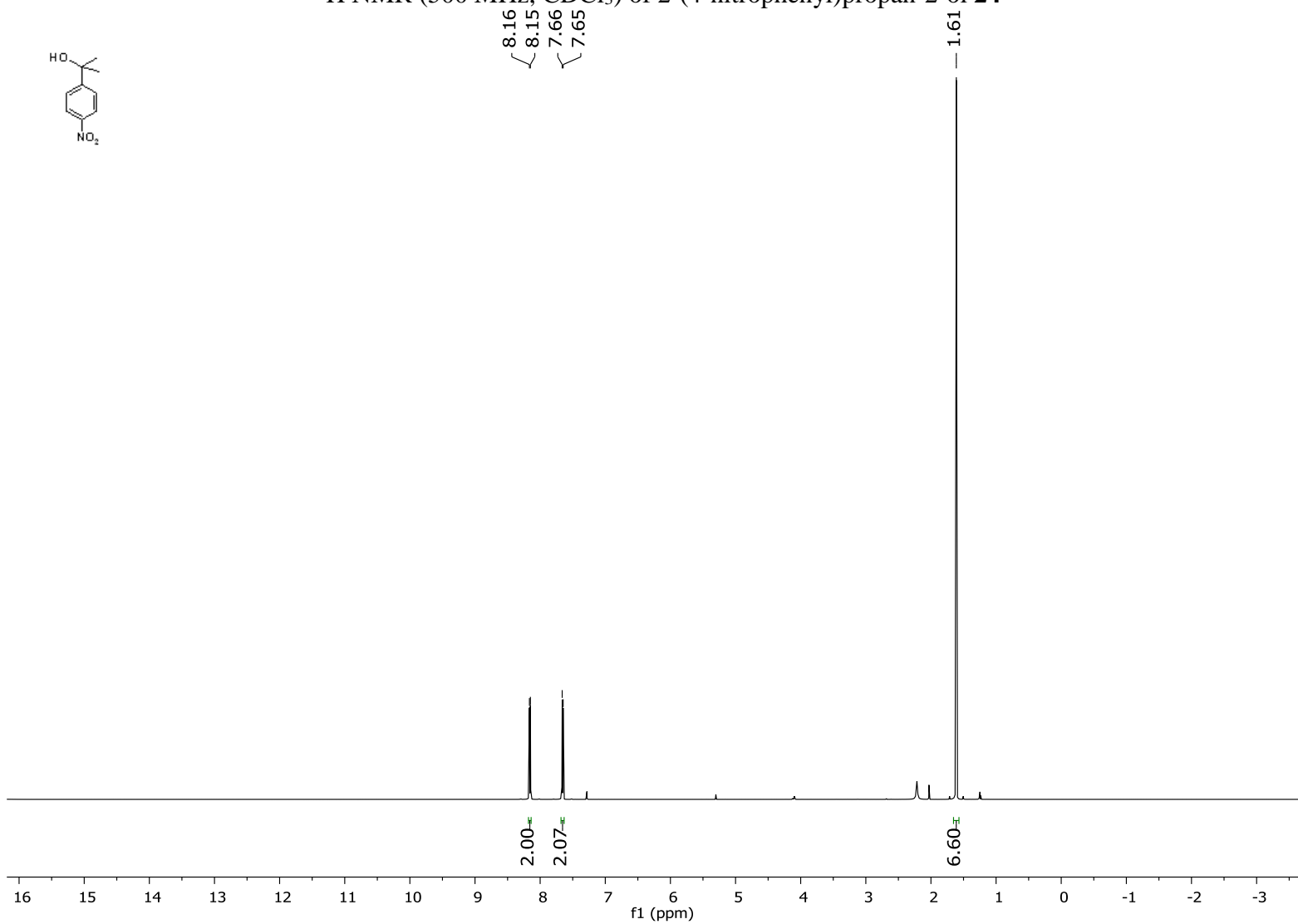
~ 123.71

— 69.43

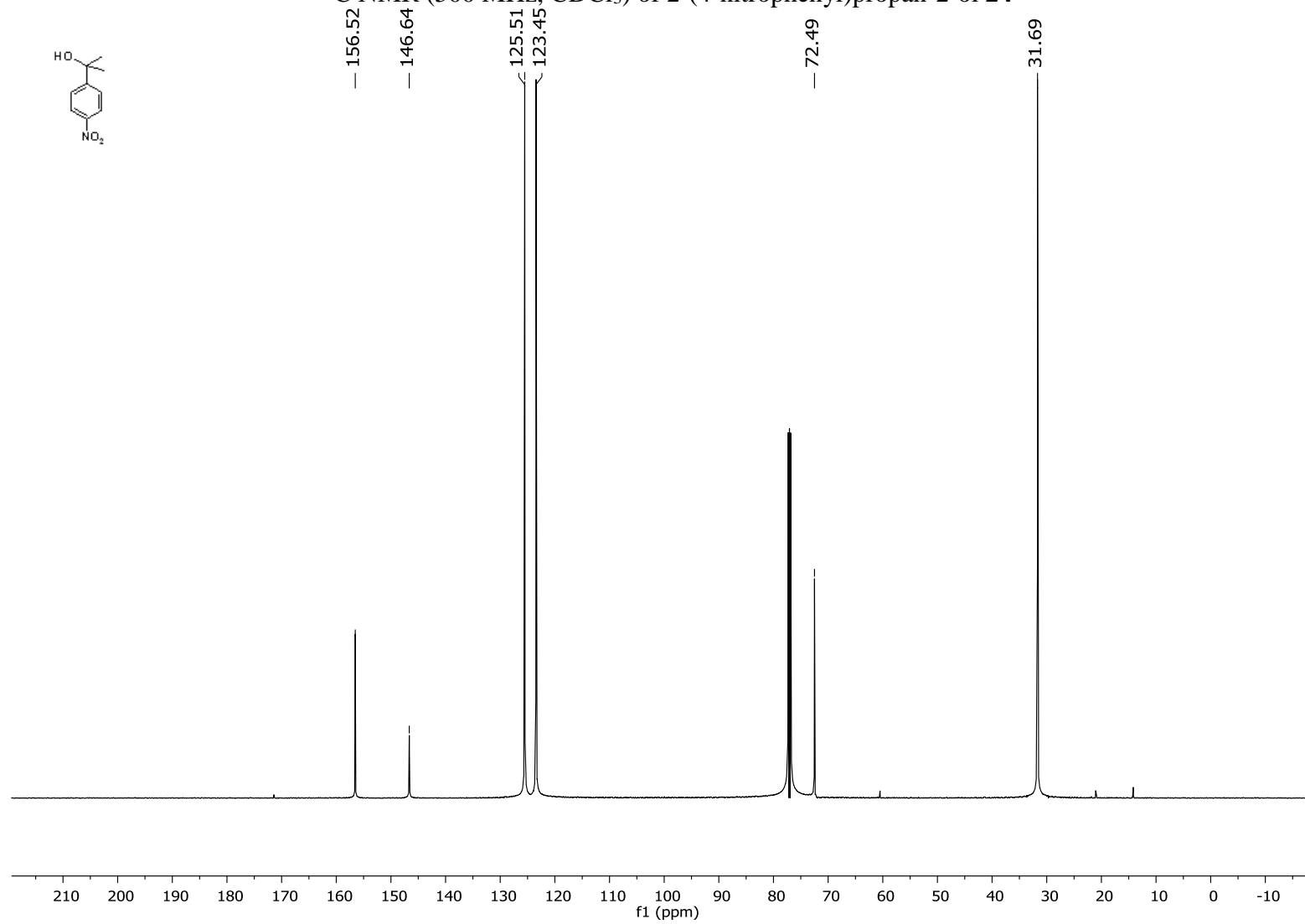
— 25.44



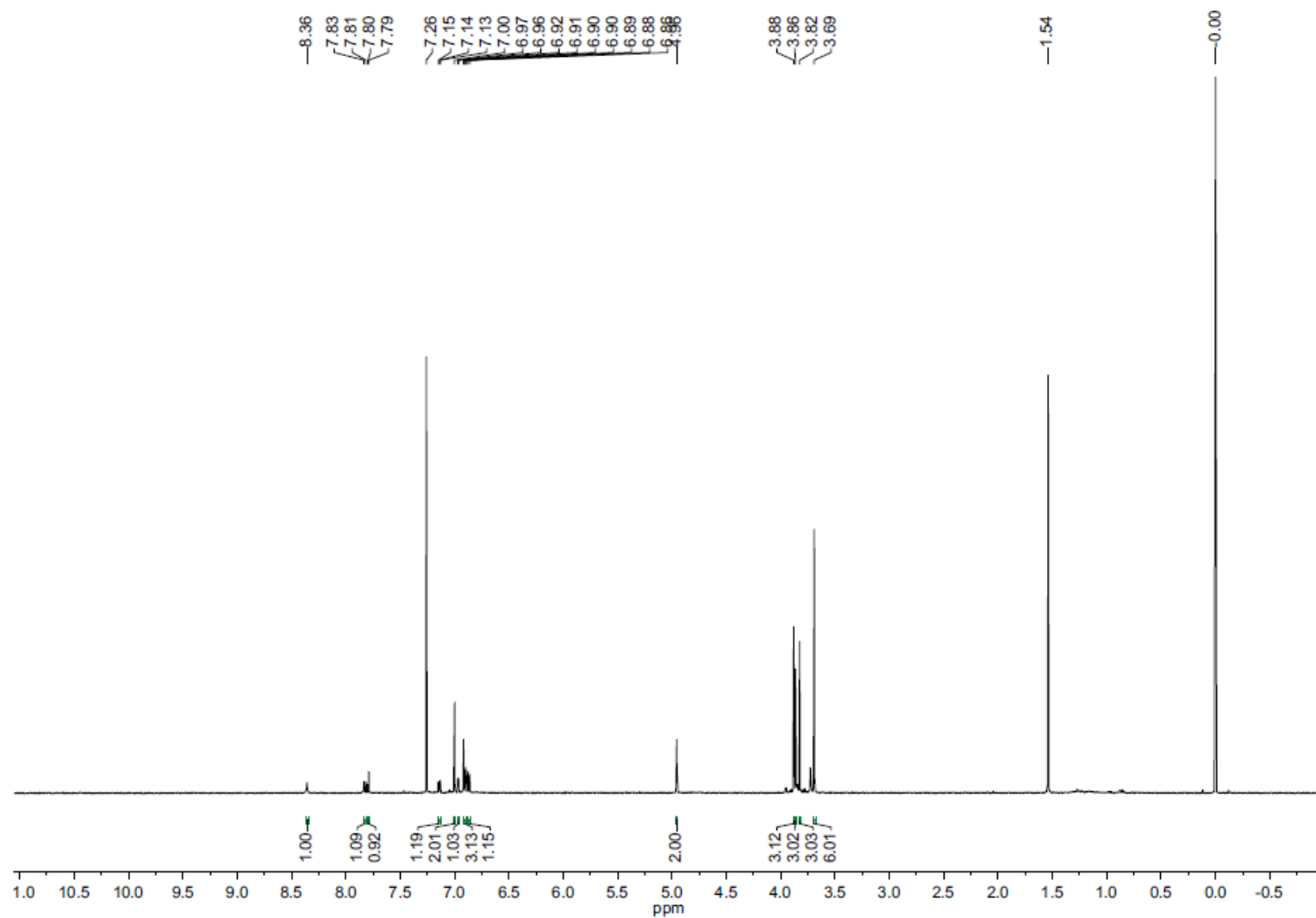
^1H NMR (500 MHz, CDCl_3) of 2-(4-nitrophenyl)propan-2-ol **24**



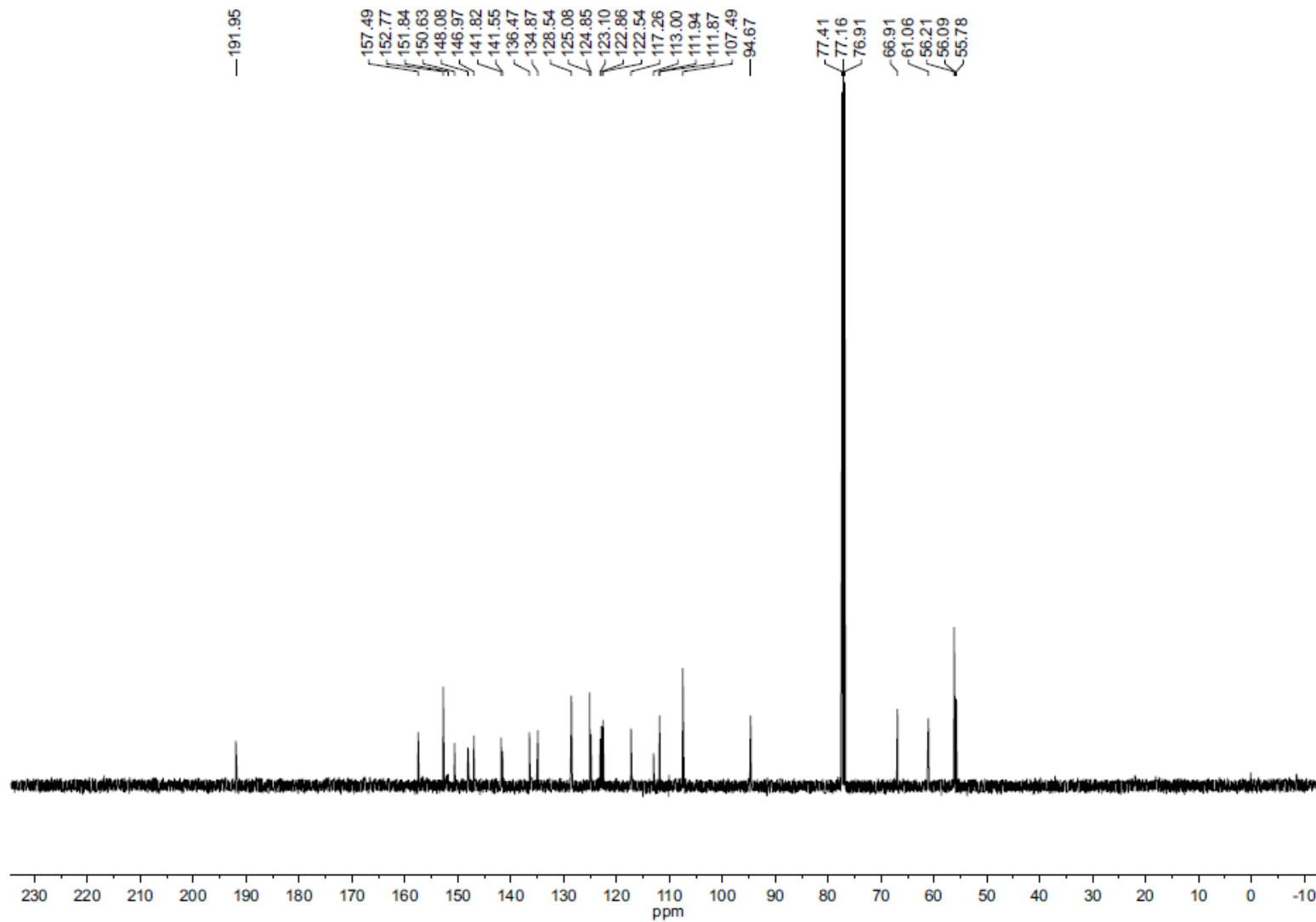
¹³C NMR (500 MHz, CDCl₃) of 2-(4-nitrophenyl)propan-2-ol **24**



¹H NMR of OXi8006-normethylthiophene BAPC 26

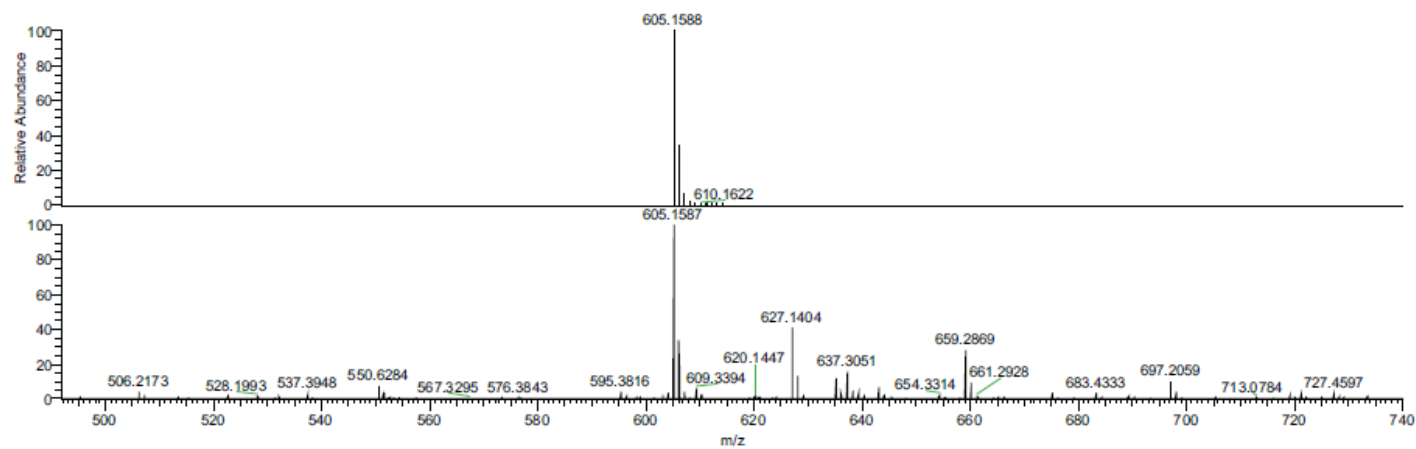
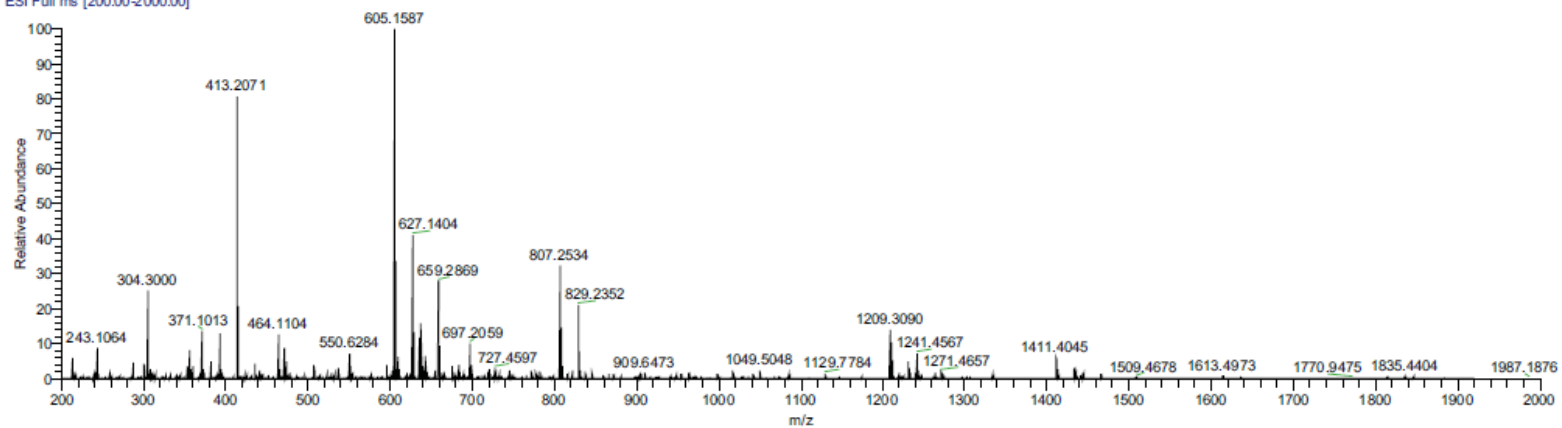


¹³C NMR of OXi8006-normethylthiophene BAPC 26



HRMS of OXi8006-normethylthiophene BAPC 26

RT: 0.06 AV: 1 NL: 2.22E7 T: FTMS + p
ESI Full ms [200.00-2000.00]



NL:
6.58E5
C₂₁H₂₅O₉N₂S:
C₂₁H₂₅O₉N₂S:
pa Chrg 1

NL:
2.22E7
MTM-III-95_+ESI#8
RT: 0.06 AV: 1 T:
FTMS + p ESI Full
ms
[200.00-2000.00]

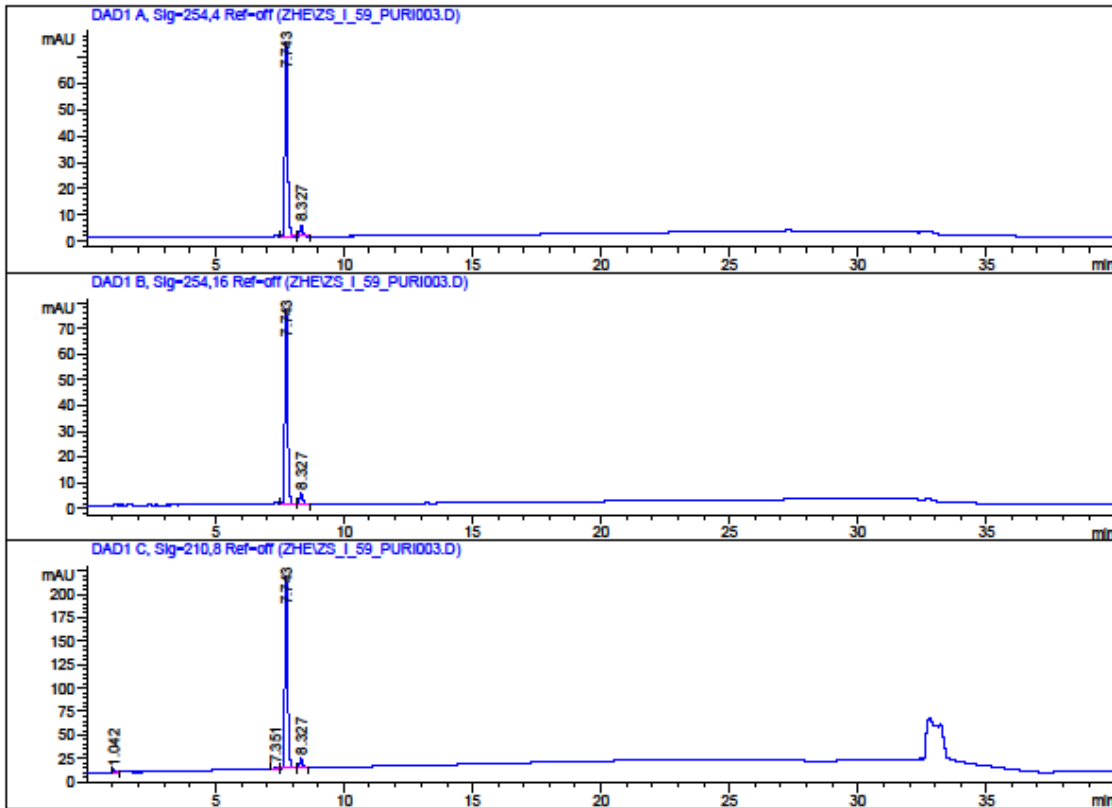
HPLC traces of OXi8006-normethylthiophene BAPC 26

Data File C:\CHEM32\1\DATA\ZHE\ZS_I_59_PURI003.D

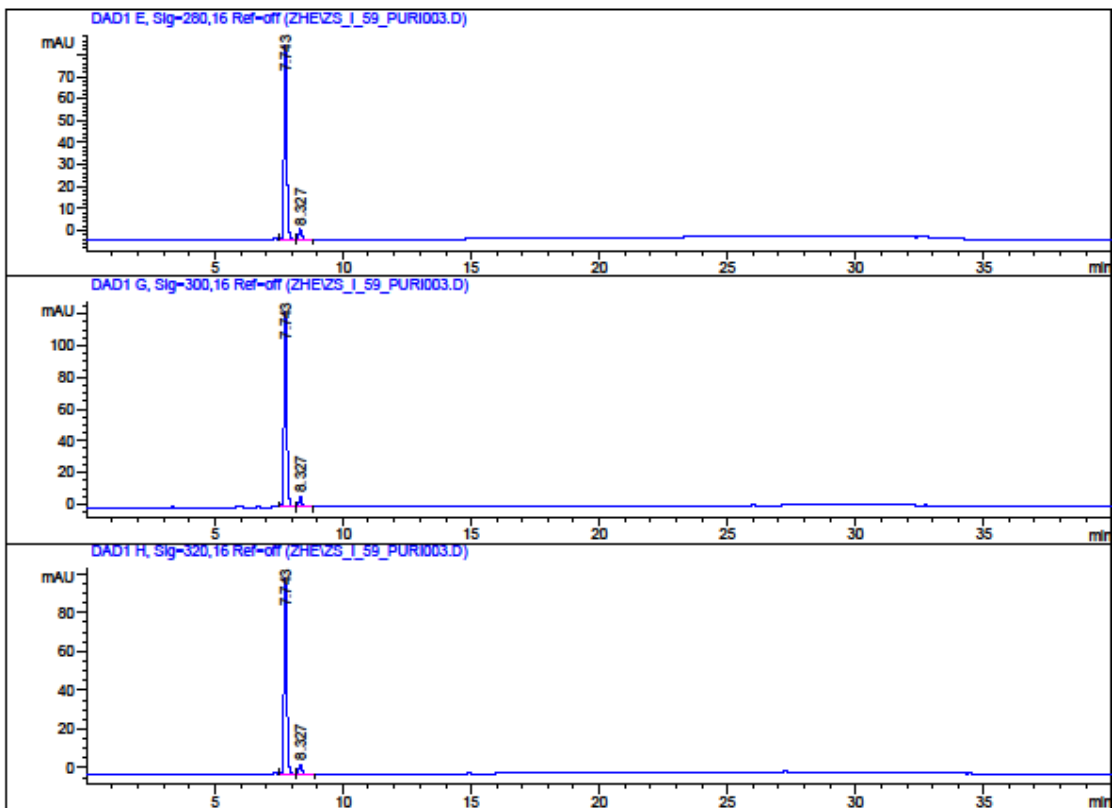
Sample Name: wash

```
=====
Acq. Operator   : Zhe
Acq. Instrument : Instrument 1           Location : -
Injection Date  : 12/20/2013 1:02:38 PM
Acq. Method     : C:\CHEM32\1\METHODS\GRAD50-100ACN.M
Last changed    : 12/20/2013 12:51:50 PM by Zhe
Analysis Method : C:\CHEM32\1\DATA\ZHE\ZS_I_59_PURI003.D\DA.M (GRAD50-100ACN.M)
Last changed    : 12/30/2013 2:51:07 PM by Christine
                  (modified after loading)
Sample Info     : wash
```

```
Method:
0-25 Min 50/50 to 100/0 ACN/Water
25-30 min 100% ACN
30-35 min 100/0 to 50/50 ACN/Water
35-40 min 50/50 ACN/Water
```



Data File C:\CHEM32\1\DATA\ZHE\ZS_I_59_PURI003.D
 Sample Name: wash



=====
 Area Percent Report
 =====

Sorted By : Signal
 Multiplier : 1.0000
 Dilution : 1.0000
 Use Multiplier & Dilution Factor with ISTDs

Signal 1: DAD1 A, Sig=254,4 Ref=off

Peak #	RetTime [min]	Type	Width [min]	Area [mAU*s]	Height [mAU]	Area %
1	7.743	BB	0.1160	557.93005	73.99174	94.6666
2	8.327	BB	0.1176	31.43339	4.09376	5.3334

Totals : 589.36345 78.08550

Data File C:\CHEM32\1\DATA\ZHE\ZS_I_59_PURI003.D
Sample Name: wash

Signal 2: DAD1 B, Sig=254,16 Ref=off

Peak #	RetTime [min]	Type	Width [min]	Area [mAU*s]	Height [mAU]	Area %
1	7.743	BB	0.1160	572.83990	75.96780	94.7063
2	8.327	BB	0.1175	32.01962	4.17416	5.2937
Totals :				604.85952	80.14196	

Signal 3: DAD1 C, Sig=210,8 Ref=off

Peak #	RetTime [min]	Type	Width [min]	Area [mAU*s]	Height [mAU]	Area %
1	1.042	BB	0.0745	15.65550	2.92207	0.9504
2	7.351	BB	0.1119	13.95538	1.89595	0.8472
3	7.743	BV	0.1160	1540.47729	204.17958	93.5228
4	8.327	VB	0.1181	77.07970	9.98401	4.6795
Totals :				1647.16788	218.98161	

Signal 4: DAD1 E, Sig=280,16 Ref=off

Peak #	RetTime [min]	Type	Width [min]	Area [mAU*s]	Height [mAU]	Area %
1	7.743	BV	0.1161	670.97308	88.83448	94.5841
2	8.327	VB	0.1195	38.41978	4.89697	5.4159
Totals :				709.39286	93.73145	

Signal 5: DAD1 G, Sig=300,16 Ref=off

Peak #	RetTime [min]	Type	Width [min]	Area [mAU*s]	Height [mAU]	Area %
1	7.743	VV	0.1162	931.85590	123.30495	94.4860
2	8.327	VB	0.1197	54.38060	6.92157	5.5140
Totals :				986.23649	130.22652	

Data File C:\CHEM32\1\DATA\ZHE\ZS_I_59_PURI003.D
Sample Name: wash

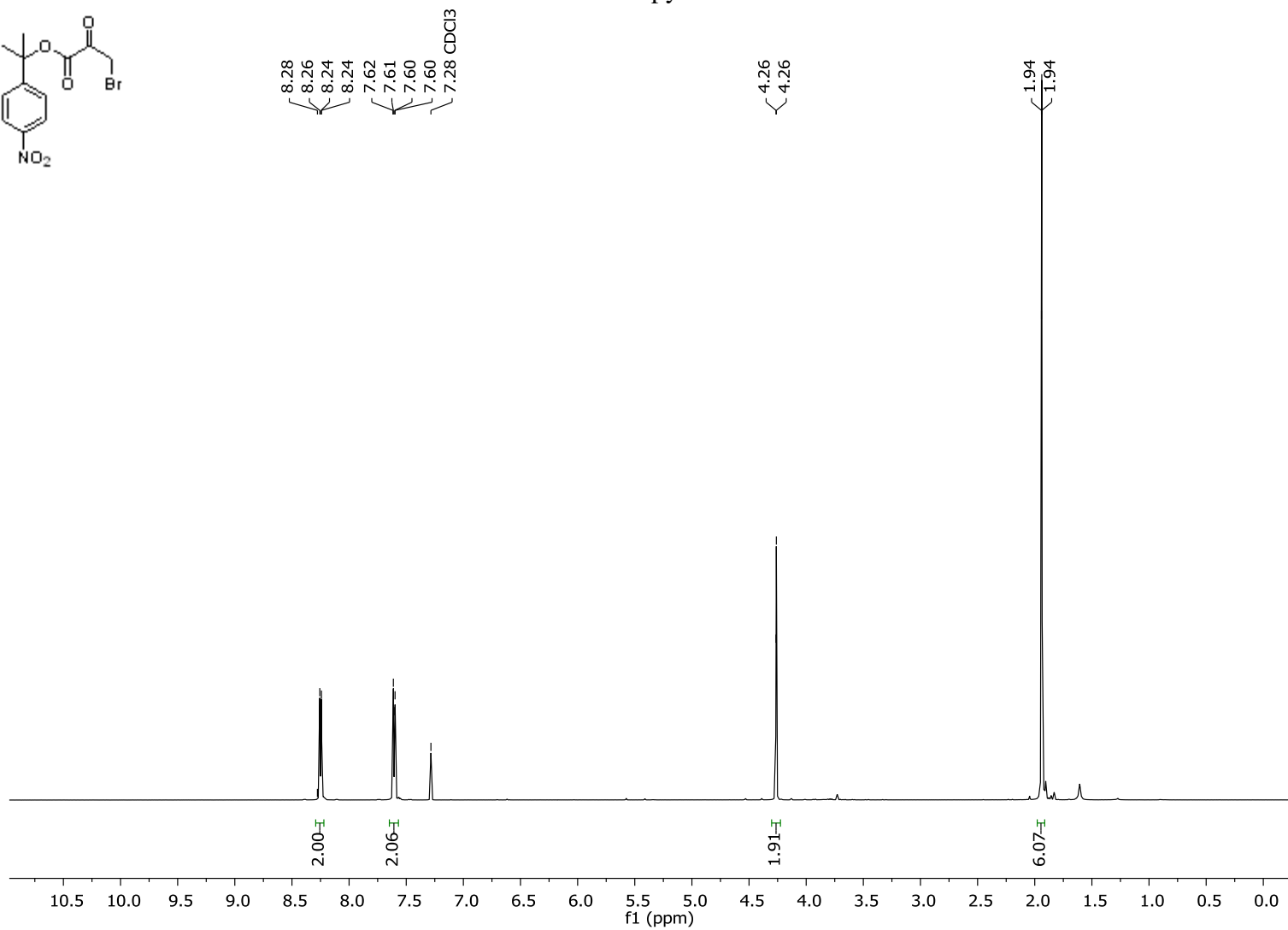
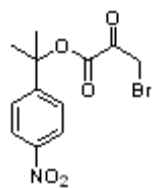
Signal 6: DAD1 H, Sig=320,16 Ref=off

Peak #	RetTime [min]	Type	Width [min]	Area [mAU*s]	Height [mAU]	Area %
1	7.743	VV	0.1162	761.59857	100.75832	94.9257
2	8.327	VB	0.1200	40.71147	5.16180	5.0743

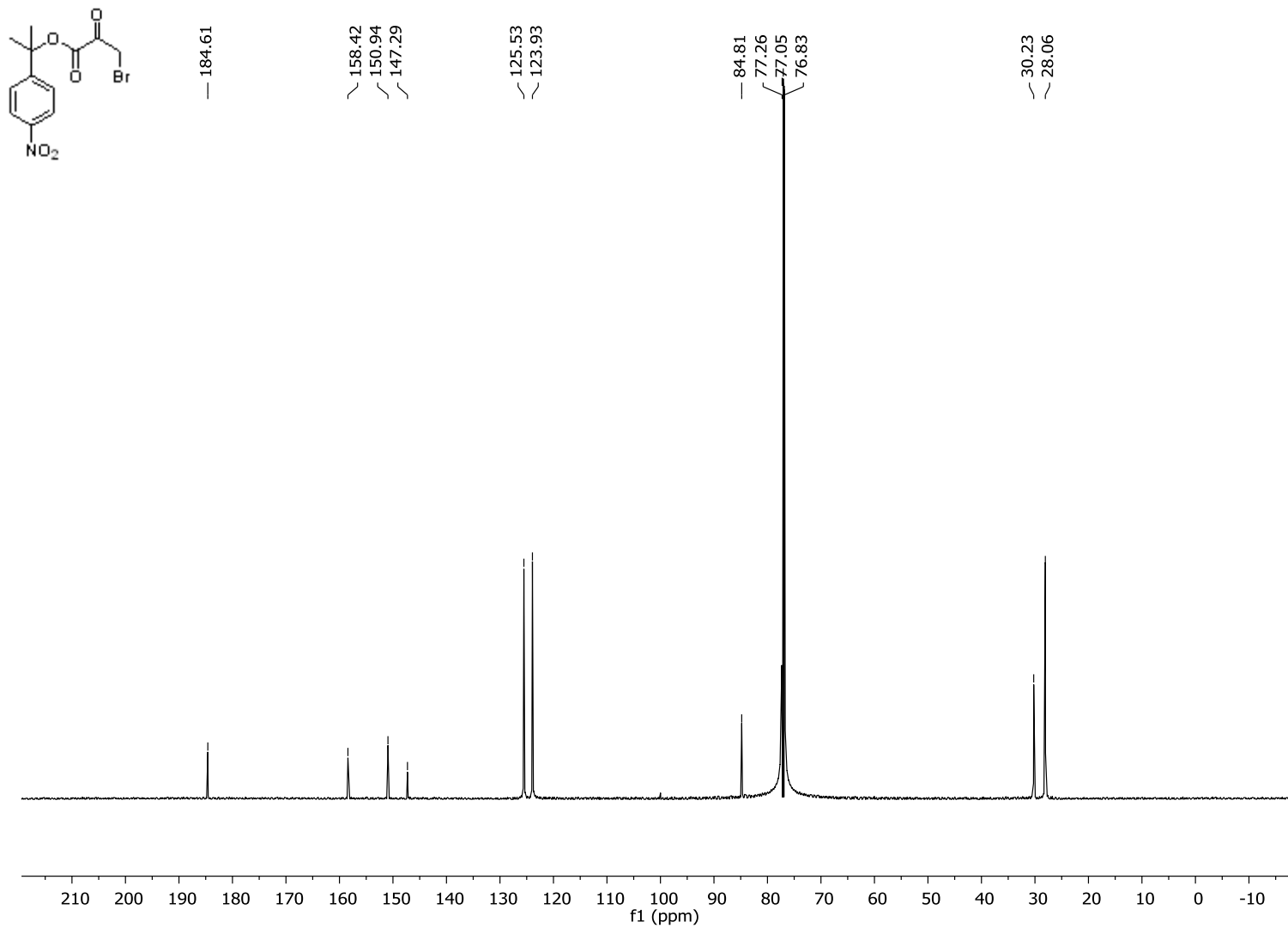
Totals : 802.31004 105.92013

=====
*** End of Report ***

¹H NMR of Bromopyruvate BAPC 28



¹³C NMR of Bromopyruvate BAPC **28**

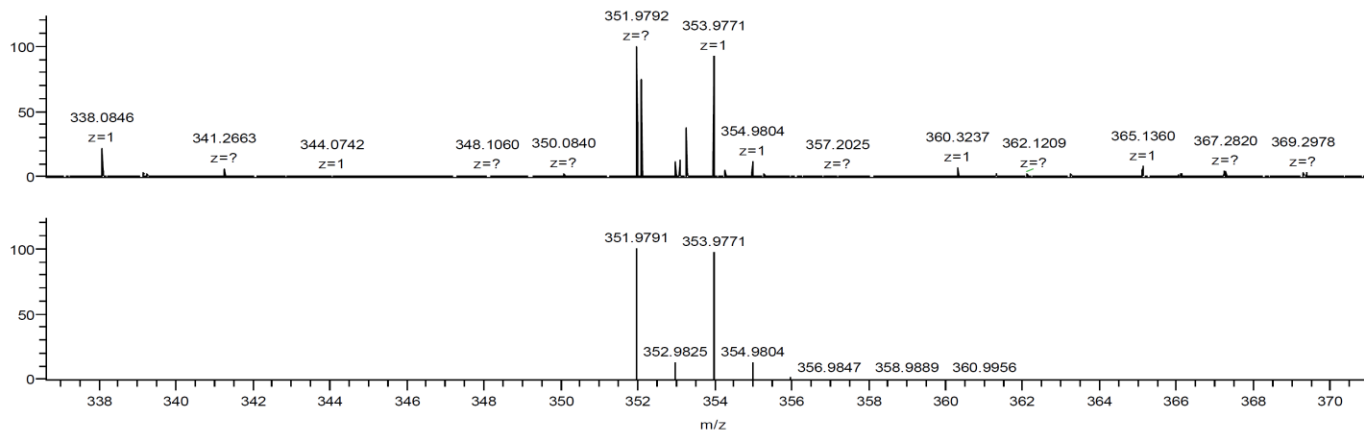
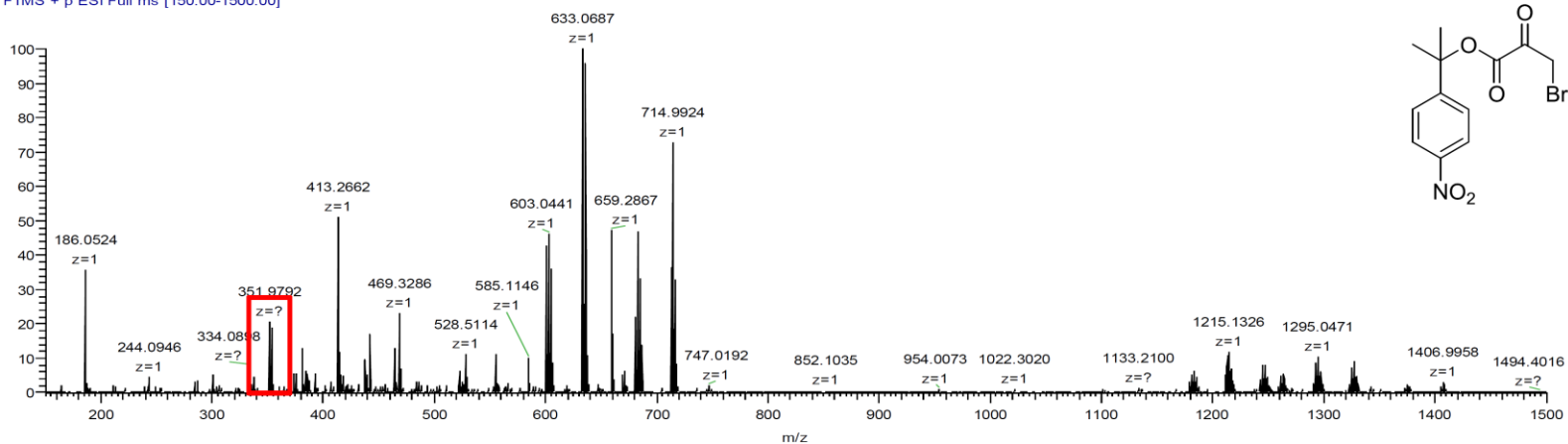


HRMS of Bromopyruvate BAPC 28

zs_ll_86_pure_MeOH_Orbi_+ESI

1/29/2015 5:38:40 PM

zs_ll_86_pure_MeOH_Orbi_+ESI #20 RT: 0.16 /
T: FTMS + p ESI Full ms [150.00-1500.00]



NL:
1.02E6
zs_ll_86_pure_MeOH_Or
bi_+ESI#20 RT: 0.16
AV: 1 T: FTMS + p ESI
Full ms
[150.00-1500.00]

NL:
4.38E5
C₆H₆BrNNaO₅
C₆H₆Br₁N₁Na₁O₅
pa Chrg 1

APPENDIX C

Targeting Tumor Hypoxia with Bioreductively Activatable Prodrug Conjugates Derived from Dihydronaphthalene, and Benzosuberene-Based Vascular Disrupting Agents

This appendix will be published as: “Targeting Tumor Hypoxia with Bioreductively Activatable Prodrug Conjugates Derived from Dihydronaphthalene, and Benzosuberene-Based Vascular Disrupting Agents” Zhe Shi, Rajsekhar Guddneppanavar, Blake A. Winn, Clinton S. George, Tracy E. Strecker, Jeni Gerberich, Alex Winters, Elisa Lin, Casey J. Maguire, Jacob Ford, Ernest Hamel, David J. Chaplin, Ralph P. Mason, Mary Lynn Trawick, Kevin G. Pinney.

The author Zhe Shi contributed to this manuscript through synthesizing four of the eight BAPCs reported in this manuscript and full characterization of all eight final compounds including NMR, HPLC and HRMS. In addition, Zhe Shi contributed a significant amount to the preparation of the manuscript and the supporting material.

Supplementary Data

Targeting Tumor Hypoxia with Bioreductively Activatable Prodrug Conjugates Based on
Small-Molecule Inhibitors of Tubulin Polymerization

Zhe Shi¹, Rajsekhar Guddneppanavar¹, Blake A. Winn¹, Clinton S. George¹, Tracy E. Strecker¹, Jeni Gerberich², Alex Winters², Elisa Lin², Casey J. Maguire¹, Jacob Ford¹, Ernest Hamel³, David J. Chaplin⁴, Ralph P. Mason², Mary Lynn Trawick¹, Kevin G. Pinney^{1*}

¹Department of Chemistry and Biochemistry, Baylor University, Waco, TX;

²Department of Radiology, University of Texas Southwestern Medical Center, Dallas, TX;

³Screening Technologies Branch, Developmental Therapeutics Program, Division of Cancer Treatment and Diagnosis, National Cancer Institute, Frederick National Laboratory for Cancer Research, National Institutes of Health, Frederick, MD;

⁴Mateon Therapeutics, Inc., South San Francisco, CA.

*Corresponding author.

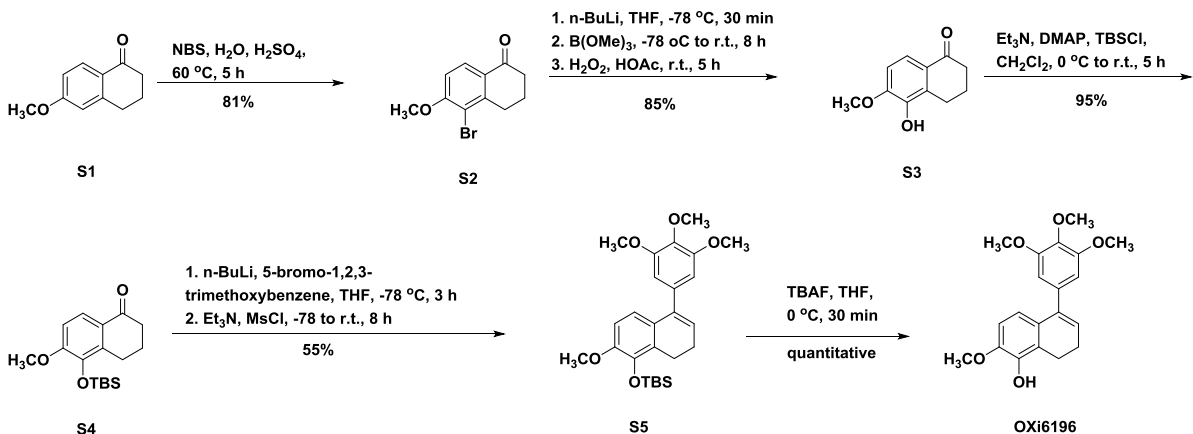
Tel.: 254-710-4117

Email address: Kevin.Pinney@baylor.edu

Appendix C Table of Contents

Synthesis of OXi6196	238
Synthesis of KGP18.....	243
NMR Spectra, HPLC Traces, and HRMS Data for Compound 10	250
NMR Spectra, HPLC Traces, and HRMS Data for Compound 11	256
NMR Spectra, HPLC Traces, and HRMS Data for Compound 12	263
NMR Spectra, HPLC Traces, and HRMS Data for Compound 13	269
NMR Spectra, HPLC Traces, and HRMS Data for Compound 14	275
NMR Spectra, HPLC Traces, and HRMS Data for Compound 15	281
NMR Spectra, HPLC Traces, and HRMS Data for Compound 16	287
NMR Spectra, HPLC Traces, and HRMS Data for Compound 17	293

Synthesis of OXi6196



Scheme C.1. Synthesis of OXi6196

The synthesis to OXi6196 was begun with 6-methoxy-1-tetralone which is commercially available. Regioselective bromination of the tetralone followed by lithium halogen exchange provided a means to direct the hydroxylation to the correct position with a 69% yield in 2 steps.^{49,187,188} The phenolic tetralone **S3** was subsequently converted to its corresponding silyl ether **S4** upon treatment with TBSCl. Installation of the trimethoxy aryl ring and elimination of the resulting tertiary alcohol to generate the OXi6196 core structure was accomplished in a one-pot reaction. The appropriate aryllithium intermediate (prepared *in situ* from the corresponding aryl bromide) was allowed to react with the tetralone, the resulting tertiary alcohol (*in situ*) was treated with triethyl amine and mesly chloride to furnish the OXi6196-silyl ether derivative **S5**.¹⁸⁹ Desilylation with TBAF afforded **OXi6196** in a 5-step synthesis with a 36% yield overall.

5-Bromo-6-methoxy-3,4-dihydronaphthalen-1(2H)-one S2

6-methoxy-1-tetralone **S1** (1.06 g, 6.02 mmol) was stirred in 60 mL of H₂O. *N*-bromosuccinimide (1.07g, 6.01 mmol) was added and the reaction mixture was heated to 60 °C. H₂SO₄ (0.67 mL) was then added to the reaction mixture and the reaction was heated for 5 hours. The reaction was extracted with EtOAc and the organic layers were dried over Na₂SO₄ and filtered. The solvent was then removed in vacuo and the resulting solid was dissolve in methanol and recrystallized. The crystals were filtered and washed with cold methanol affording 5-bromo-6-methoxy-3,4-dihydronaphthalen-1(2H)-one **S2** (1.22 g, 4.78 mmol, 81% yield) as a white solid.

¹H NMR (CDCl₃, 600 MHz): δ 8.09 (1H, d, *J* = 8.7 Hz), 6.91 (1H, d, *J* = 8.7 Hz), 4.00 (3H, s), 3.06 (2H, t, *J* = 6.2 Hz), 2.66 (2H, m), 2.15 (2H, p, *J* = 6.3 Hz).

¹³C NMR (CDCl₃, 151 MHz): δ 196.8, 159.8, 145.5, 128.4, 127.6, 113.0, 109.6, 56.5, 38.0, 30.5, 22.5.

HRMS, *m/z*: observed 255.0016 [M + H]⁺, (calcd for C₁₁H₁₂BrO₂⁺ 255.0015).

5-Hydroxy-6-methoxy-3,4-dihydronaphthalen-1(2H)-one (S3)

To a well-stirred solution of 5-bromo-6-methoxy-3,4-dihydronaphthalen-1(2H)-one **S2** (0.50 g, 1.96 mmol) in Et₂O at -78 °C, *n*-BuLi (4.90 mL, 7.84 mmol) was added dropwise. After the addition was complete, the reaction mixture was stirred at -78 °C for 1 hour then allowed to warm to room temperature. B(OMe)₃ (0.45 mL, 3.92 mmol) was added dropwise and the reaction mixture was stirred for 1 hour at room temperature. Glacial acetic acid (0.22 mL) was added dropwise, followed by the addition of 35 wt.% H₂O₂ (0.48 mL) added dropwise. The reaction mixture was then stirred at room temperature for 12 hours. Saturated NH₄Cl (20 mL) was added to the solution and the

mixture was extracted with Et₂O (3 x 50 mL). The combined organic phases were washed with brine and dried over Na₂SO₄, filtered, and concentrated in vacuo. Purification by flash column chromatography afforded the phenol **S3** (0.32 g, 1.66 mmol, 85% yield) as a tan solid.

¹H NMR (CDCl₃, 600 MHz): δ 7.70 (1H, d, *J* = 8.6 Hz), 6.86 (1H, d, *J* = 8.6 Hz), 5.76 (1H, s), 3.98 (3H, s), 2.95 (2H, t, *J* = 6.2 Hz), 2.65 (2H, m), 2.13 (2H, p, *J* = 6.4 Hz).

¹³C NMR (CDCl₃, 151 MHz): δ 197.9, 149.9, 141.9, 130.4, 126.8, 120.0, 108.3, 56.1, 38.8, 22.9, 22.7.

HRMS, *m/z*: observed 215.0679 [M + Na]⁺, (calcd for C₁₁H₁₂NaO₃⁺ 215.0679).

5-((tert-Butyldimethylsilyl)oxy)-6-methoxy-3,4-dihydronaphthalen-1(2H)-one (S4)

5-hydroxy-6-methoxy-3,4-dihydronaphthalen-1(2H)-one **S3** (1.05 g, 5.46 mmol) was stirred in 10 mL of CH₂Cl₂ at 0 °C. Triethylamine (0.84 mL, 6.03 mmol) and DMAP (0.27 g, 2.18 mmol) were then added. The reaction was stirred for an additional 10 minutes before adding TBSCl (0.90g, 5.97 mmol). The reaction was quenched with 100 mL of H₂O after 1 hour. The reaction was extracted with CH₂Cl₂ (3x 100 mL) and the organic layer was dried over sodium sulfate. The organic layer was then filtered and the solvent was removed in vacuo. The crude mixture was purified by flash chromatography afforded the silyl ether **S4** (1.58 g, 5.16 mmol, 95% yield) as an orange oil.

¹H NMR (CDCl₃, 600 MHz): δ 7.54 (1H, d, *J* = 8.6 Hz), 6.64 (1H, d, *J* = 8.7 Hz), 3.67 (3H, s), 2.72 (2H, t, *J* = 6.1 Hz), 2.42 (2H, m), 1.89 (2H, p, *J* = 6.4 Hz), 0.83 (9H, s), 0.00 (6H, s).

¹³C NMR (CDCl₃, 151 MHz): δ 198.0, 154.0, 141.3, 136.1, 126.8, 121.5, 109.2, 54.9, 38.7, 26.1, 24.4, 22.9, 18.9, -3.8.

HRMS, *m/z*: observed 307.1727 [M + H]⁺, (calcd for C₁₇H₂₇O₃Si⁺ 307.1724).

tert-Butyl((2-methoxy-5-(3,4,5-trimethoxyphenyl)-7,8-dihydronaphthalen-1-yl)oxy)dimethylsilane (**S5**)

To a solution of 3,4,5- trimethoxybromobenzene (1.62g, 6.55 mmol) in anhydrous THF (20 mL), *n*-BuLi (2.62 mL, 6.55 mmol) was added dropwise at -78 °C. The reaction mixture was stirred for 30 minutes at -78 °C. A solution of 5-((*tert*-butyldimethylsilyl)oxy)-6-methoxy-3,4-dihydronaphthalen-1(2H)-one **S4** (1.00g, 3.27 mmol) in THF (10 mL) was added dropwise and the reaction mixture was then allowed warm to 0 °C over 3 hours. The reaction was then cooled to -78 °C and triethylamine (3.68 mL, 26.16 mmol) and MsCl (1.01 mL, 13.08 mmol) were added dropwise to the solution. The reaction was allowed to warm to room temperature over a period of 8 hours. The reaction was quenched with H₂O (100 mL) and the reaction mixture was then extracted with EtOAc (2 x 100 mL). The combined organic phases were washed with brine and dried over sodium sulfate, filtered and the solvent was evaporated under reduced pressure. The resulting crude product was then subjected to flash column chromatography to afford *tert*-butyl((2-methoxy-5-(3,4,5-trimethoxyphenyl)-7,8-dihydronaphthalen-1-yl)oxy)dimethylsilane **S5** (0.82g, 1.80 mmol, 55% yield).

¹H NMR (CDCl₃, 600 MHz): δ 6.44 (1H, d, *J* = 8.4 Hz), 6.40 (1H, d, *J* = 8.5 Hz), 6.37 (2H, s), 5.75 (1H, t, *J* = 4.6 Hz), 3.69 (3H, s), 3.65 (6H, s), 3.58 (3H, s), 2.69-2.64 (2H, m), 2.13 (2H, td, *J* = 7.9, 4.7 Hz), 0.83 (9H, s), 0.00 (6H, s).

¹³C NMR (CDCl₃, 151 MHz): δ 152.9, 149.7, 141.4, 139.8, 137.0, 137.0, 128.7, 128.1, 124.9, 118.9, 108.1, 106.0, 60.9, 56.1, 26.1, 23.1 21.7, 18.9, -3.9.

2-Methoxy-5-(3,4,5-trimethoxyphenyl)-7,8-dihydronaphthalen-1-ol (OXi6196)

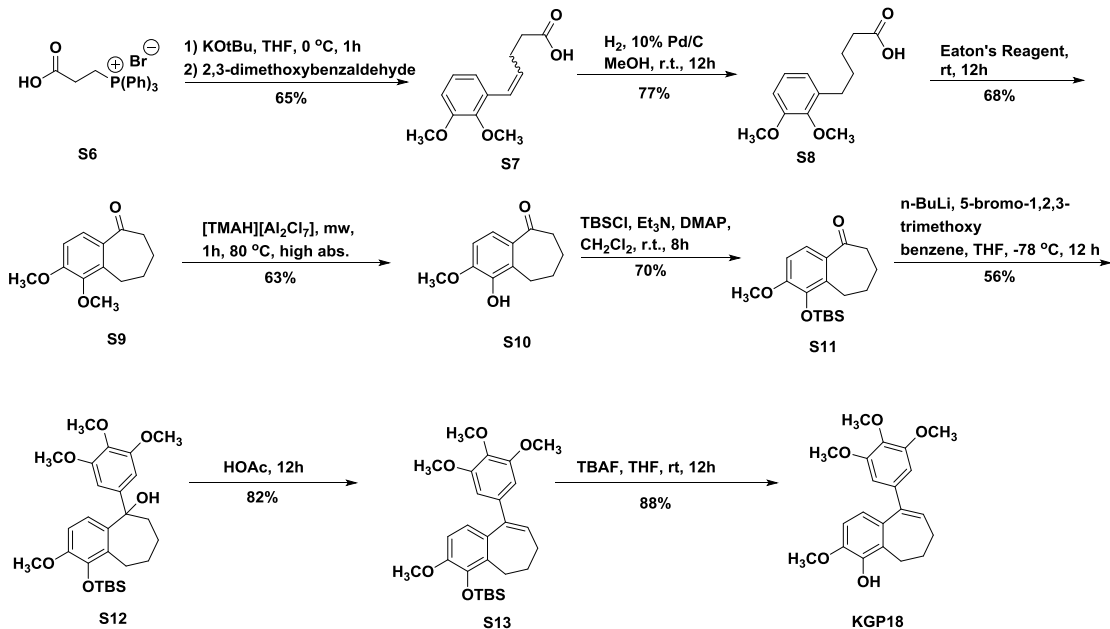
tert-Butyl((2-methoxy-5-(3,4,5-trimethoxyphenyl)-7,8-dihydronaphthalen-1-yl)oxy)dimethylsilane **S5** (0.82g, 1.80 mmol) was dissolved in THF and cooled to 0 °C. TBAF (0.71g, 2.70mmol) was added to the solution. The reaction was stirred 30 minutes and then quenched with 50 mL of H₂O. The aqueous layer was then extracted with EtOAc (3x 100 mL) and the organic layer was dried over Na₂SO₄. The Organic layer was then filtered and the solvent was removed in vacuo. Purification by flash chromatography afforded 2-methoxy-5-(3,4,5-trimethoxyphenyl)-7,8-dihydronaphthalen-1-ol **OXi6196** (0.62 g, 1.80 mmol, quantitative yield) as a white solid.

¹H NMR (CDCl₃, 600 MHz): δ 6.65 (1H, d, *J* = 8.4 Hz), 6.61 (1H, d, *J* = 8.4 Hz), 6.58 (2H, s), 5.99 (1H, t, *J* = 4.7 Hz), 5.74 (1H, s), 3.86 (6H, s), 2.93 (2H, t, *J* = 8.4 Hz), 2.40 (2H, td, *J* = 8.0, 4.7 Hz).

¹³C NMR (CDCl₃, 151 MHz): δ 152.9, 145.8, 142.0, 139.5, 136.9, 129.0, 125.4, 122.3, 117.4, 107.2, 105.8, 61.0, 56.1, 56.0, 22.8, 20.2.

HRMS, *m/z*: observed 343.1541 [M + H]⁺, (calcd for C₂₀H₂₃O₅⁺ 343.1540).

Synthesis of KGP18



Scheme C.2. Synthesis of KGP18

The KGP18 synthesis developed by the Pinney Research Group utilizes two key reactions to generate the benzosuberene CA4 analogue- a cyclization employing Eaton's reagent to form the seven membered ring and a lithium-halogen exchange to install the trimethoxy aryl ring system.⁵¹ The Wittig olefination reaction was used to generate alkene **S7** from phosphonium salt **S6** and 2,3 dimethoxybenzaldehyde (Scheme C2). Reduction of alkene **S7** yielded carboxylic acid **S8**, which was then cyclized, upon treatment with Eaton's reagent, to produce benzosuberene **S9**. Benzosuberene **S9** was demethylated by ionic liquid to generate phenol **S10**, which was then silylated to form the protected benzosuberene **S11**. Installation of the trimethoxy aryl ring and elimination of the resulting tertiary alcohol to generate **S13**, which was then deprotected to yield **KGP18**.

5-(2,3-Dimethoxyphenyl)pent-4-enoic acid S7

(2-Carboxyethyl)triphenylphosphonium bromide **S6** (16.7 g, 39.0 mmol) was dissolved in THF (400 mL). Potassium *tert*-butoxide (11.7 g, 104 mmol) was added to the reaction and it was stirred for 1 h at room temperature. 2,3-Dimethoxybenzaldehyde (5.39 g, 32.0 mmol) was added to the reaction mixture and it was stirred for 8 h. The reaction was then quenched with HCl (2 M, 50 mL) and evaporated under reduced pressure. EtOAc (80 mL) was added to the residue and the layers were partitioned. The aqueous layer was extracted with EtOAc (3 x 40 mL). The combined organic layers were washed with brine (50 mL), dried over Na₂SO₄, and evaporated under reduced pressure. The crude product was purified by flash chromatography using a pre-packed 100 g silica column [solvent A: EtOAc; solvent B: hexanes; gradient 10%A / 90%B (1 CV), 10%A / 90%B → 50%A / 50%B (13 CV), 50%A / 50%B (2 CV); flow rate: 100 mL/min; monitored at 254 and 280 nm] to afford compound **S7** (6.00 g, 25.4 mmol, 65%) as a light yellow solid. NMR characterization was conducted after the next step.

5-(2,3-Dimethoxyphenyl)pentanoic acid S8

5-(2,3-Dimethoxyphenyl)pent-4-enoic acid **S7** (5.39 g, 21.5 mmol) was added to an empty flask flushed under N₂, followed by 10 % palladium on carbon (0.430 g, 0.404 mmol). Methanol (100 mL) was added slowly to the reagents, and then the flask was purged under N₂. The flask was placed under vacuum, and then H₂ was added and the reaction was stirred for 12 h at room temperature. The reaction was then filtered through Celite in a frit funnel, rinsed with EtOAc (3 x 50 mL), and the combined organic phases were evaporated under reduced pressure. The crude product was purified by flash chromatography using a pre-packed 100 g silica column [solvent A: EtOAc; solvent B:

hexanes; gradient 7% A / 93% B (1 CV), 7% A / 93% B → 40% A / 60% B (13 CV), 40% A / 60% B (2 CV); flow rate: 100 mL/min; monitored at 254 and 280 nm] to afford compound **S8** (6.00 g, 25.4 mmol, 77%) as a clear oil.

¹H NMR (500 MHz, CDCl₃) δ 6.97 (1H, t, *J* = 7.9 Hz), 6.76 (2H, m), 3.85 (3H, s), 3.81 (3H, s), 2.64 (2H, t, *J* = 7.3 Hz), 2.38 (2H, t, *J* = 7.1 Hz), 1.74 – 1.60 (4H, m).

¹³C NMR (125 MHz, CDCl₃) δ 179.5, 152.7, 147.0, 135.9, 123.8, 121.8, 110.1, 60.6, 55.6, 33.8, 30.1, 29.4, 24.5.

1,2-Dimethoxy-6,7,8,9-tetrahydro-5H-benzo[7]annulen-5-one S9

5-(2,3-Dimethoxyphenyl)pentanoic acid **S8** (3.55 g, 14.9 mmol) was dissolved in Eaton's reagent (29 mL, 7.7 wt.%) and stirred for 12 h at room temperature. The reaction was poured over ice and neutralized with saturated sodium bicarbonate. The layers were partitioned, then the aqueous layer was extracted with EtOAc (3 x 50 mL). The combined organic layers were washed with brine (40 mL), dried over Na₂SO₄, and evaporated under reduced pressure. The crude product was purified by flash chromatography using a pre-packed 100 g silica column [solvent A: EtOAc; solvent B: hexanes; gradient 7% A / 93% B (1 CV), 7% A / 93% B → 40% A / 60% B (13 CV), 40% A / 60% B (2 CV); flow rate: 100 mL/min; monitored at 254 and 280 nm] to afford compound **S9** (2.22 g, 10.1 mmol, 68%) as a yellow solid.

¹H NMR (500 MHz, CDCl₃) δ 7.53 (1H, d, *J* = 8.6 Hz), 6.84 (1H, d, *J* = 8.6 Hz), 3.90 (3H, s), 3.79 (3H, s), 3.00 (2H, t, *J* = 6.1 Hz), 2.69 (2H, t, *J* = 6.1 Hz), 1.89 – 1.81 (2H, m), 1.81 – 1.72 (2H, m).

¹³C NMR (125 MHz, CDCl₃) δ 204.9, 156.1, 145.9, 135.7, 132.8, 125.5, 109.7, 61.1, 55.8, 40.6, 24.9, 23.2, 20.9.

1-Hydroxy-2-methoxy-6,7,8,9-tetrahydro-5H-benzo[7]annulen-5-one S10

[TMAH][Al₂Cl₇] (18.3 mL, 9.08 mmol) was added to 1,2-dimethoxy-6,7,8,9-tetrahydro-5H-benzo[7]annulen-5-one **S9** (1.01 g, 4.54 mmol) in a 20 mL microwave vial. The reaction mixture was then exposed to microwave irradiation for 1 h on high absorbance at 80 °C. The reaction was then poured into water (50 mL) and EtOAc (40 mL) was added. The layers were partitioned and the aqueous layer was extracted (3 x 40 mL). The combined organic layers were washed with brine (50 mL), dried over Na₂SO₄, and evaporated under reduced pressure. The crude product was purified by flash chromatography using a pre-packed 50 g silica column [solvent A: EtOAc; solvent B: hexanes; gradient 7% A / 93% B (1 CV), 7% A / 93% B → 60% A / 40% B (13 CV), 60% A / 40% B (2 CV); flow rate: 50 mL/min; monitored at 254 and 280 nm] to afford compound **S10** (0.590 g, 2.86 mmol, 63%) as a yellow solid.

¹H NMR (500 MHz, CDCl₃) δ 7.34 (1H, d, *J* = 8.5 Hz), 6.79 (1H, d, *J* = 8.5 Hz), 5.77 (1H, s), 3.94 (3H, s), 3.01 (2H, dd, *J* = 7.2, 5.0 Hz), 2.76 – 2.66 (2H, m), 1.83 (4H, m).

¹³C NMR (125 MHz, CDCl₃) δ 205.1, 149.2, 142.4, 133.3, 127.7, 120.8, 107.9, 56.1, 40.8, 24.5, 23.0, 21.3.

1-((tert-Butyldimethylsilyl)oxy)-2-methoxy-6,7,8,9-tetrahydro-5H-benzo[7]annulen-5-one S11

1-Hydroxy-2-methoxy-6,7,8,9-tetrahydro-5H-benzo[7]annulen-5-one **S10** (2.00 g, 9.70 mmol) was dissolved in CH₂Cl₂ (80 mL). Triethylamine (1.64 mL, 11.6 mmol), *tert*-butyldimethylsilyl chloride (1.61 g, 10.7 mmol) and DMAP (0.0650 g, 0.532 mmol) were added to the reaction mixture and it was stirred for 8 h. The reaction was quenched with

water (40 mL) and the layers were partitioned. The aqueous layer was extracted with CH₂Cl₂ (3 x 40 mL). The combined organic layers were washed with brine (50 mL), dried over Na₂SO₄, and evaporated under reduced pressure. The crude product was purified by flash chromatography using a pre-packed 50 g silica column [solvent A: EtOAc; solvent B: hexanes; gradient 2% A / 98% B (1 CV), 2% A / 98% B → 20% A / 80% B (13 CV), 20% A / 80% B (2 CV); flow rate: 50 mL/min; monitored at 254 and 280 nm] to afford compound **S11** (2.18 g, 6.79 mmol, 70%) as light tan crystals.

¹H NMR (500 MHz, CDCl₃) δ 7.37 (1H, d, *J* = 8.5 Hz), 6.76 (1H, d, *J* = 8.6 Hz), 3.82 (3H, s), 3.00 (2H, dd, *J* = 7.0, 5.1 Hz), 2.69 (2H, dd, *J* = 7.3, 4.4 Hz), 1.84 – 1.73 (4H, m), 1.01 (9H, s), 0.18 (6H, s).

¹³C NMR (125 MHz, CDCl₃) δ 205.3, 153.2, 141.7, 133.1, 133.1, 122.3, 108.7, 54.8, 40.7, 26.1, 25.6, 24.7, 23.9, 21.2, -3.9.

1-((tert-Butyldimethylsilyl)oxy)-2-methoxy-5-(3,4,5-trimethoxyphenyl)-6,7,8,9-tetrahydro-5H-benzo[7]annulen-5-ol S12

3,4,5-Trimethoxybromobenzene (4.13 g, 16.7 mmol) was dissolved in THF (80 mL) at -78 °C. n-Butyllithium (1.6M, 7.06 mL, 16.8 mmol) was added dropwise to the reaction mixture and it was stirred for 1 h. 1-((*tert*-Butyldimethylsilyl)oxy)-2-methoxy-6,7,8,9-tetrahydro-5H-benzo[7]annulen-5-one **S11** (3.99 g, 12.4 mmol) was added to the reaction mixture and it was stirred for 8 h while warming from -78 °C to room temperature. The reaction was quenched with water (50 mL) and the layers were partitioned. The aqueous layer was extracted with EtOAc (3 x 60 mL). The combined organic layers were washed with brine (60 mL), dried over Na₂SO₄, and evaporated under reduced pressure. The crude product was purified by flash chromatography using a

pre-packed 100 g silica column [solvent A: EtOAc; solvent B: hexanes; gradient 7% A / 93% B (1 CV), 7% A / 93% B → 60% A / 40% B (13 CV), 60% A / 40% B (2 CV); flow rate: 100 mL/min; monitored at 254 and 280 nm] to afford compound **S12** (4.57 g, 9.35 mmol, 56%) as a clear oil. NMR characterization was performed after the next step.

tert-butyl((3-methoxy-9-(3,4,5-trimethoxyphenyl)-6,7-dihydro-5H-benzo[7]annulen-4-yl)oxy)dimethylsilane **S13**

1-((*tert*-Butyldimethylsilyl)oxy)-2-methoxy-5-(3,4,5-trimethoxyphenyl)-6,7,8,9-tetrahydro-5H-benzo[7]annulen-5-ol **S12** (4.57 g, 9.35 mmol) was dissolved in glacial acetic acid (50 mL) and the reaction mixture was stirred for 12 h at room temperature. The reaction was quenched with water (50 mL), the mixture was evaporated under reduced pressure, and the residue was dissolved in EtOAc (60 mL) and water (40 mL). The layers were partitioned, and then the aqueous layer was extracted with EtOAc (3 x 50 mL). The combined organic layers were washed with brine (50 mL), dried over Na₂SO₄, and evaporated under reduced pressure. The crude product was purified by flash chromatography using a pre-packed 100 g silica column [solvent A: EtOAc; solvent B: hexanes; gradient 7% A / 93% B (1 CV), 7% A / 93% B → 60% A / 40% B (13 CV), 60% A / 40% B (2 CV); flow rate: 100 mL/min; monitored at 254 and 280 nm] to afford compound **S13** (3.61 g, 7.67 mmol, 82%) as a clear oil.

¹H NMR (500 MHz, CDCl₃) δ 6.69 (1H d, *J* = 8.5 Hz), 6.61 (1H, d, *J* = 8.4 Hz), 6.48 (2H, s), 6.32 (1H, t, *J* = 7.3 Hz), 3.85 (3H, s), 3.80 (3H, s), 3.79 (6H, s), 2.76 (2H, t, *J* = 6.9 Hz), 2.10 (2H, p, *J* = 7.1 Hz), 1.95 (2H, q, *J* = 7.2 Hz), 1.04 (9H, s), 0.23 (6H, s).

¹³C NMR (125 MHz, CDCl₃) δ 152.8, 148.6, 143.0, 141.5, 138.6, 137.2, 133.8, 133.3, 126.9, 122.4, 108.3, 105.2, 60.9, 56.1, 54.6, 33.9, 26.2, 25.6, 24.2, 19.0, 3.8.

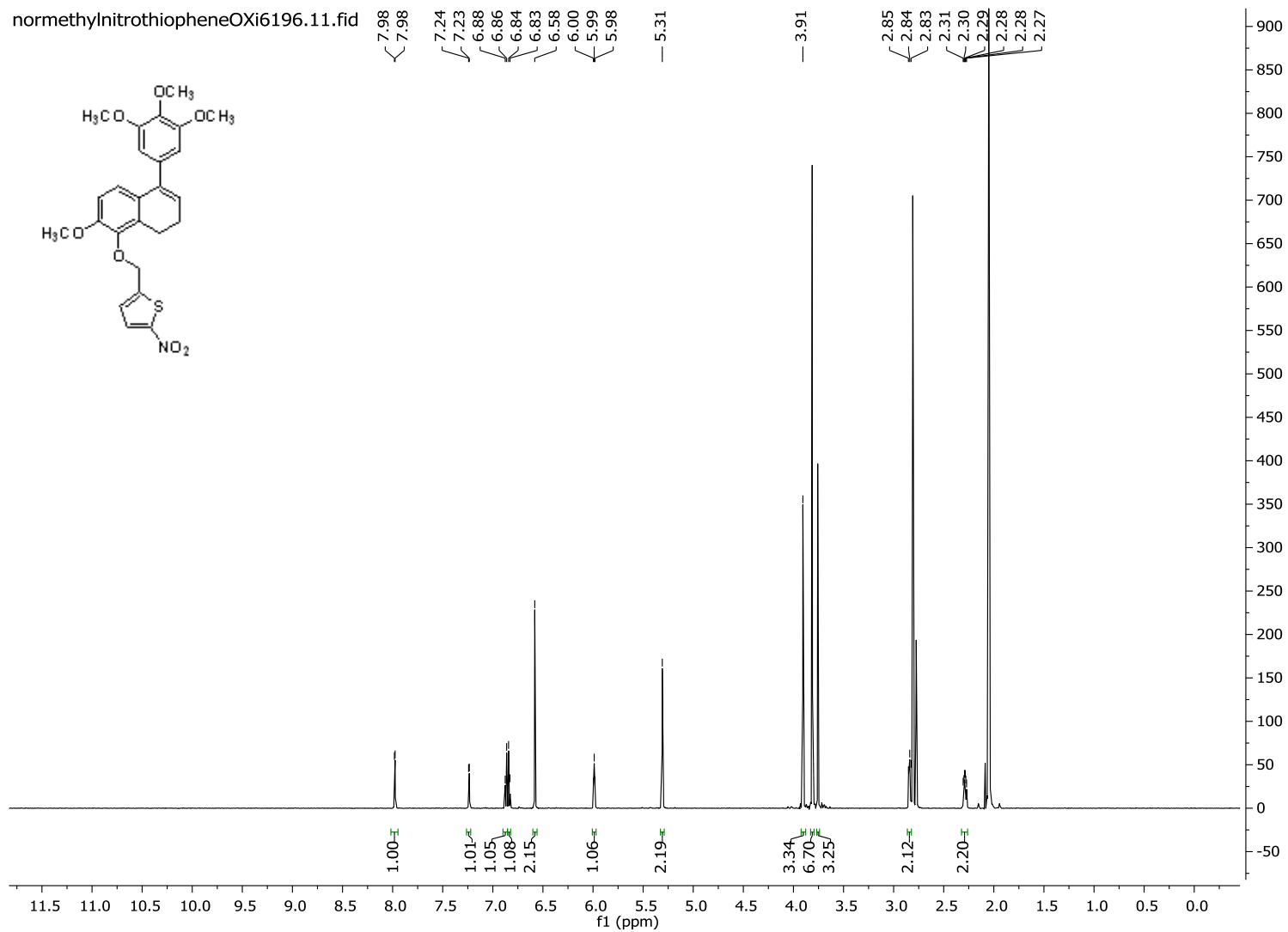
3-methoxy-9-(3,4,5-trimethoxyphenyl)-6,7-dihydro-5H-benzo[7]annulen-4-ol **OXi6196**

tert-Butyl((3-methoxy-9-(3,4,5-trimethoxyphenyl)-6,7-dihydro-5H-benzo[7]annulen-4-yl)oxy)dimethylsilane **S13** (3.61 g, 7.67 mmol) was dissolved in THF (80 mL). TBAF (1M, 9.00 mL, 9.00 mmol) was added dropwise to the reaction mixture and it was stirred for 12 h at room temperature. The reaction was quenched with water (50 mL), the mixture was evaporated under reduced pressure, and the residue was dissolved in EtOAc (60 mL) and water (40 mL). The layers were partitioned, and then the aqueous layer was extracted with EtOAc (3 x 50 mL). The combined organic layers were washed with brine (50 mL), dried over Na₂SO₄, and evaporated under reduced pressure. The crude product was purified by flash chromatography using a pre-packed 100 g silica column [solvent A: EtOAc; solvent B: hexanes; gradient 10% A / 90% B (1 CV), 10% A / 90% B → 80% A / 20% B (13 CV), 80% A / 20% B (2 CV); flow rate: 100 mL/min; monitored at 254 and 280 nm] to afford **OXi6196** (2.40 g, 6.73 mmol, 88%) as a white solid.

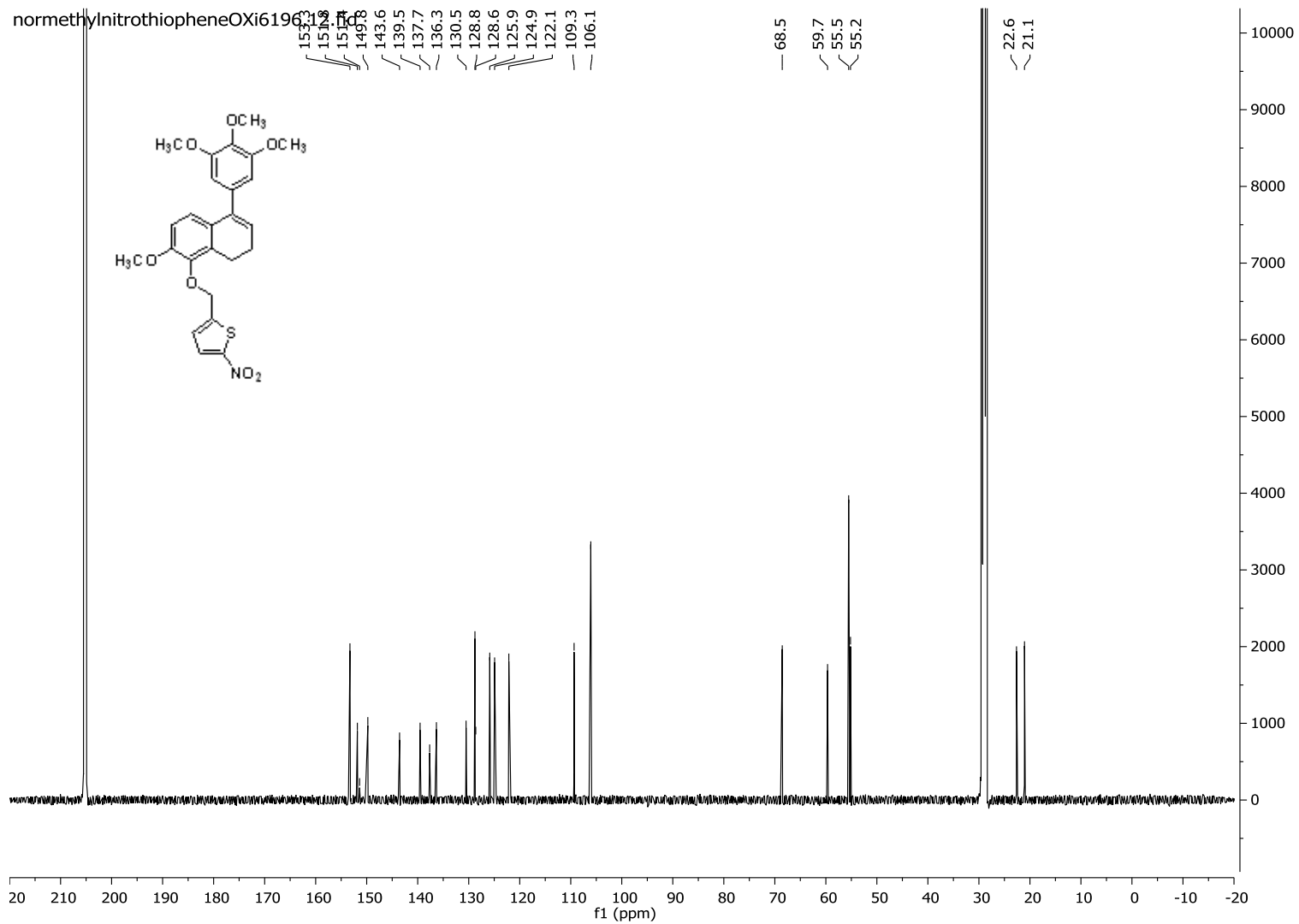
¹H NMR (500 MHz, CDCl₃) δ 6.71 (1H, d, *J* = 8.4 Hz), 6.57 (1H, d, *J* = 8.4 Hz), 6.50 (2H, s), 6.33 (1H, t, *J* = 7.4 Hz), 3.91 (3H, s), 3.86 (3H, s), 3.80 (6H, s), 2.76 (2H, t, *J* = 7.0 Hz), 2.14 (2H, p, *J* = 7.1 Hz), 1.96 (2H, q, *J* = 7.2 Hz).

¹³C NMR (125 MHz, CDCl₃) δ 152.8, 145.0, 142.8, 142.3, 138.5, 137.2, 134.2, 127.7, 127.2, 120.8, 107.6, 105.2, 60.9, 56.1, 55.9, 33.6, 25.7, 23.5.

¹H NMR of 2-(((2-methoxy-5-(3,4,5-trimethoxyphenyl)-7,8-dihydronaphthalen-1-yl)oxy)methyl)-5-nitrothiophene



¹³C NMR of 2-(((2-methoxy-5-(3,4,5-trimethoxyphenyl)-7,8-dihydronaphthalen-1-yl)oxy)methyl)-5-nitrothiophene **10**

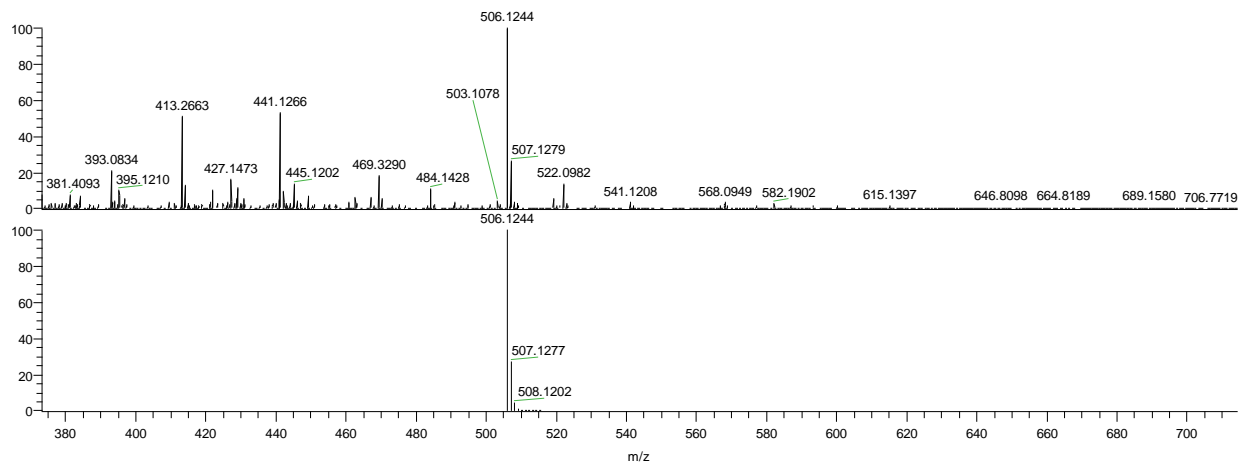
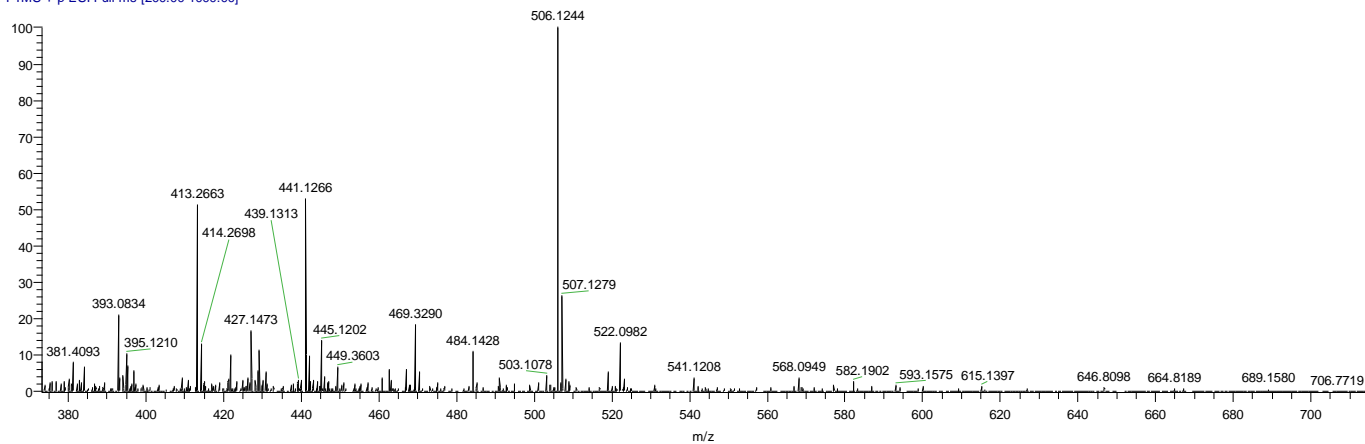


HRMS of 2-(((2-methoxy-5-(3,4,5-trimethoxyphenyl)-7,8-dihydronaphthalen-1-yl)oxy)methyl)-5-nitrothiophene 10

C:\Xcalibur...\Zhe\20180409\KGP24_+es'

4/9/2018 2:35:46 PM

KGP24_+esi #2-15 RT: 0.01-0.15 AV: 14 NL:
T: FTMS + p ESI Full ms [200.00-1000.00]



NL:
2.11E5
KGP24_+esi#2-15
RT: 0.01-0.15 AV:
14 T: FTMS + p ESI
Full ms
[200.00-1000.00]

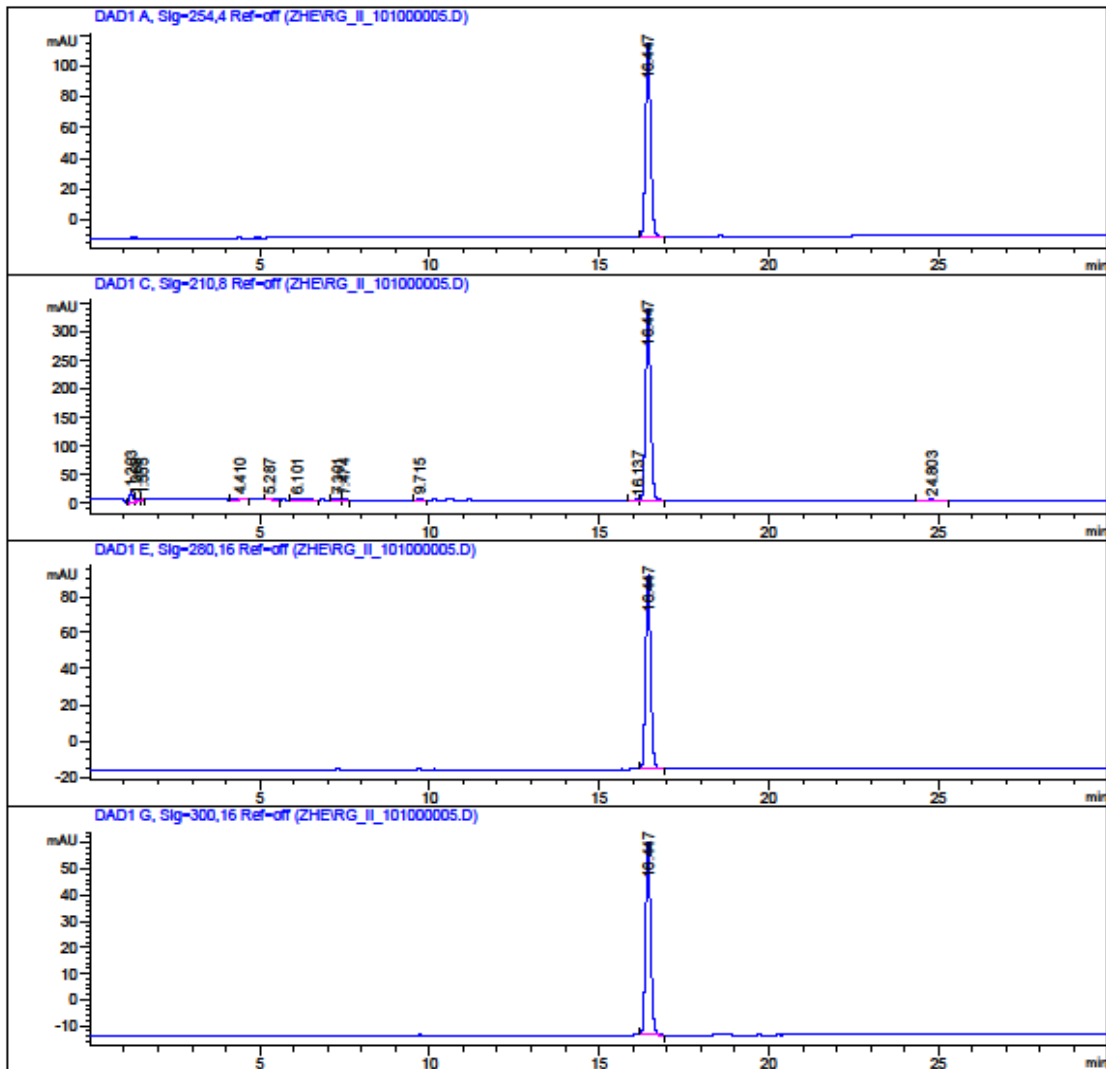
NL:
7.09E5
C₂₅H₂₅NNaO₇S:
C₂₅H₂₅N₁Na₁O₇S₁
pa Chrg 1

HPLC traces of Compound 10

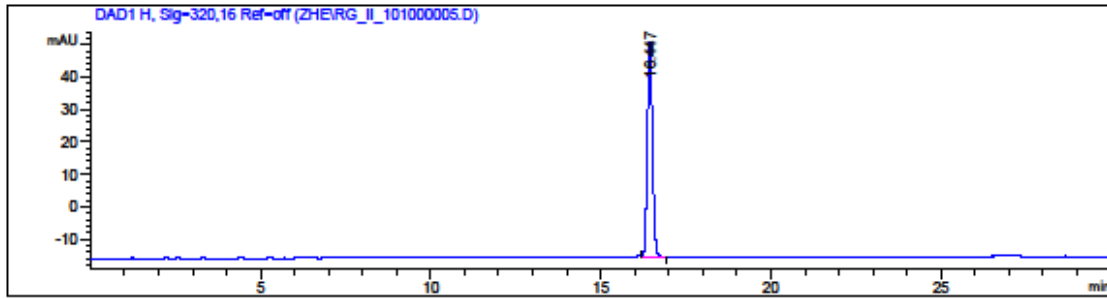
Data File C:\Chem32\1\Data\ZHE\RG_II_101000005.D
Sample Name: RG_II_101 KGP24

Acq. Operator : zhe
Acq. Instrument : Instrument 1 Location : -
Injection Date : 4/15/2016 1:16:44 PM
Acq. Method : C:\CHEM32\1\METHODS\GRAD 2 50-90 ACN.M
Last changed : 4/15/2016 12:57:29 PM by zhe
Analysis Method : C:\CHEM32\1\METHODS\RT-ACNWASH 2.M
Last changed : 7/9/2015 2:27:22 PM by Blake
Method Info : General Column Wash Method

Sample Info : RG_II_101
 KGP 24
 GRAD 2 50-90 ACN
 20160415



Data File C:\Chem32\1\Data\ZHE\RG_II_101000005.D
 Sample Name: RG_II_101 KGP24



=====
 Area Percent Report
 =====

Sorted By : Signal
 Multiplier : 1.0000
 Dilution : 1.0000
 Use Multiplier & Dilution Factor with ISTDs

Signal 1: DAD1 A, Sig=254,4 Ref=off

Peak #	RetTime [min]	Type	Width [min]	Area [mAU*s]	Height [mAU]	Area %
1	16.447	BB	0.1609	1294.19678	124.91805	100.0000

Totals : 1294.19678 124.91805

Signal 2: DAD1 C, Sig=210,8 Ref=off

Peak #	RetTime [min]	Type	Width [min]	Area [mAU*s]	Height [mAU]	Area %
1	1.203	BV	0.0741	113.21812	21.96493	2.9580
2	1.368	VV	0.1305	58.40009	5.84936	1.5258
3	1.555	VB	0.0716	9.78534	1.91627	0.2557
4	4.410	BB	0.1234	13.53947	1.58860	0.3537
5	5.287	BB	0.1190	22.72482	2.91246	0.5937
6	6.101	BB	0.1895	29.48074	2.10344	0.7702
7	7.301	BV	0.1327	23.20275	2.58537	0.6062
8	7.474	VB	0.1196	13.06872	1.66504	0.3414
9	9.715	BB	0.1323	23.90842	2.83733	0.6246
10	16.137	BV	0.1356	15.07104	1.69788	0.3938
11	16.447	VB	0.1614	3475.58081	334.06122	90.8051
12	24.803	BB	0.2261	29.53568	1.97870	0.7717

Totals : 3827.51601 381.16058

Data File C:\Chem32\1\Data\ZHE\RG_II_101000005.D
Sample Name: RG_II_101 KGP24

Signal 3: DAD1 E, Sig=280,16 Ref=off

Peak #	RetTime [min]	Type	Width [min]	Area [mAU*s]	Height [mAU]	Area %
1	16.447	BB	0.1610	1108.23608	106.89331	100.0000

Totals : 1108.23608 106.89331

Signal 4: DAD1 G, Sig=300,16 Ref=off

Peak #	RetTime [min]	Type	Width [min]	Area [mAU*s]	Height [mAU]	Area %
1	16.447	BB	0.1608	765.70856	73.96243	100.0000

Totals : 765.70856 73.96243

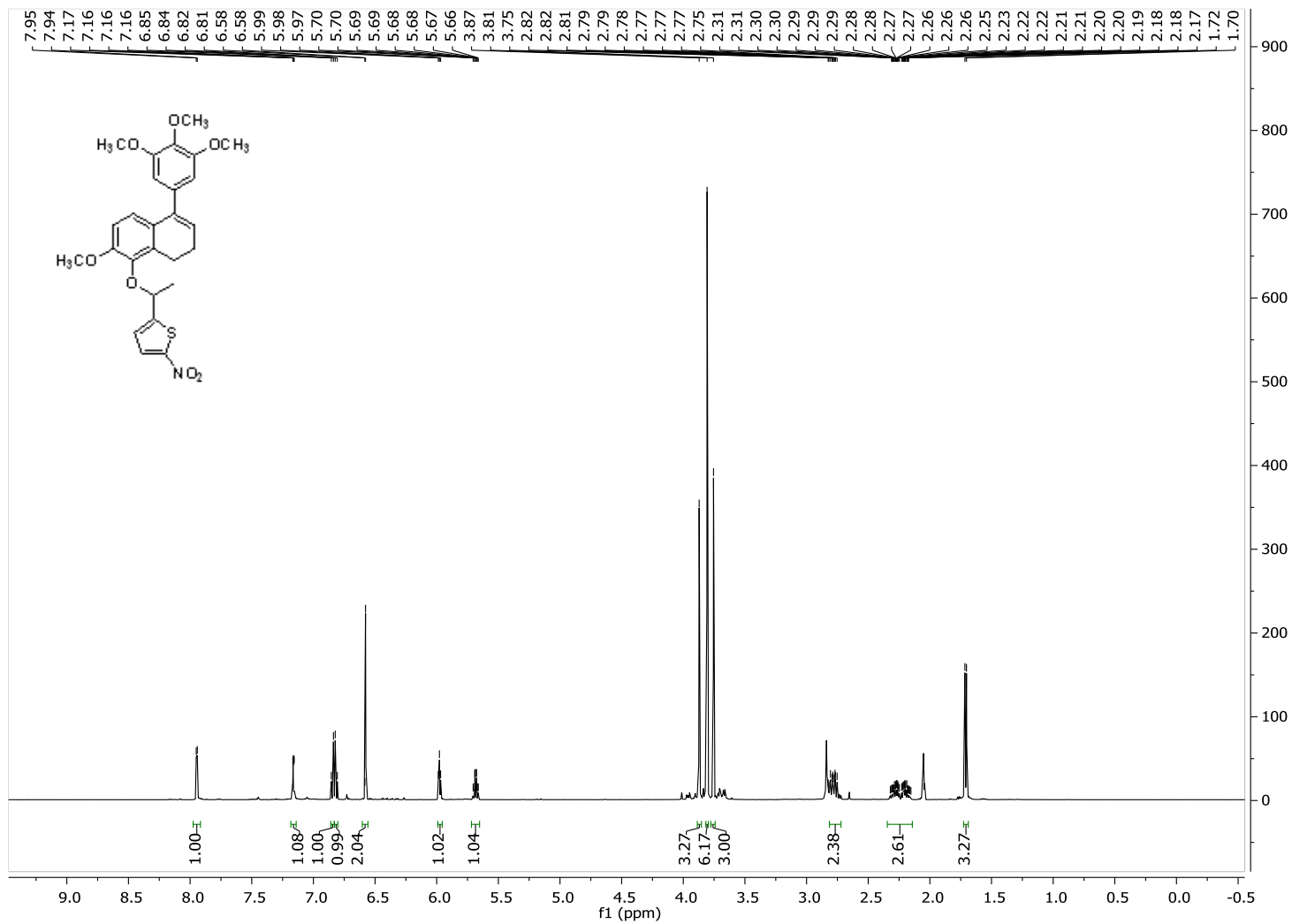
Signal 5: DAD1 H, Sig=320,16 Ref=off

Peak #	RetTime [min]	Type	Width [min]	Area [mAU*s]	Height [mAU]	Area %
1	16.447	BB	0.1606	684.04120	66.14884	100.0000

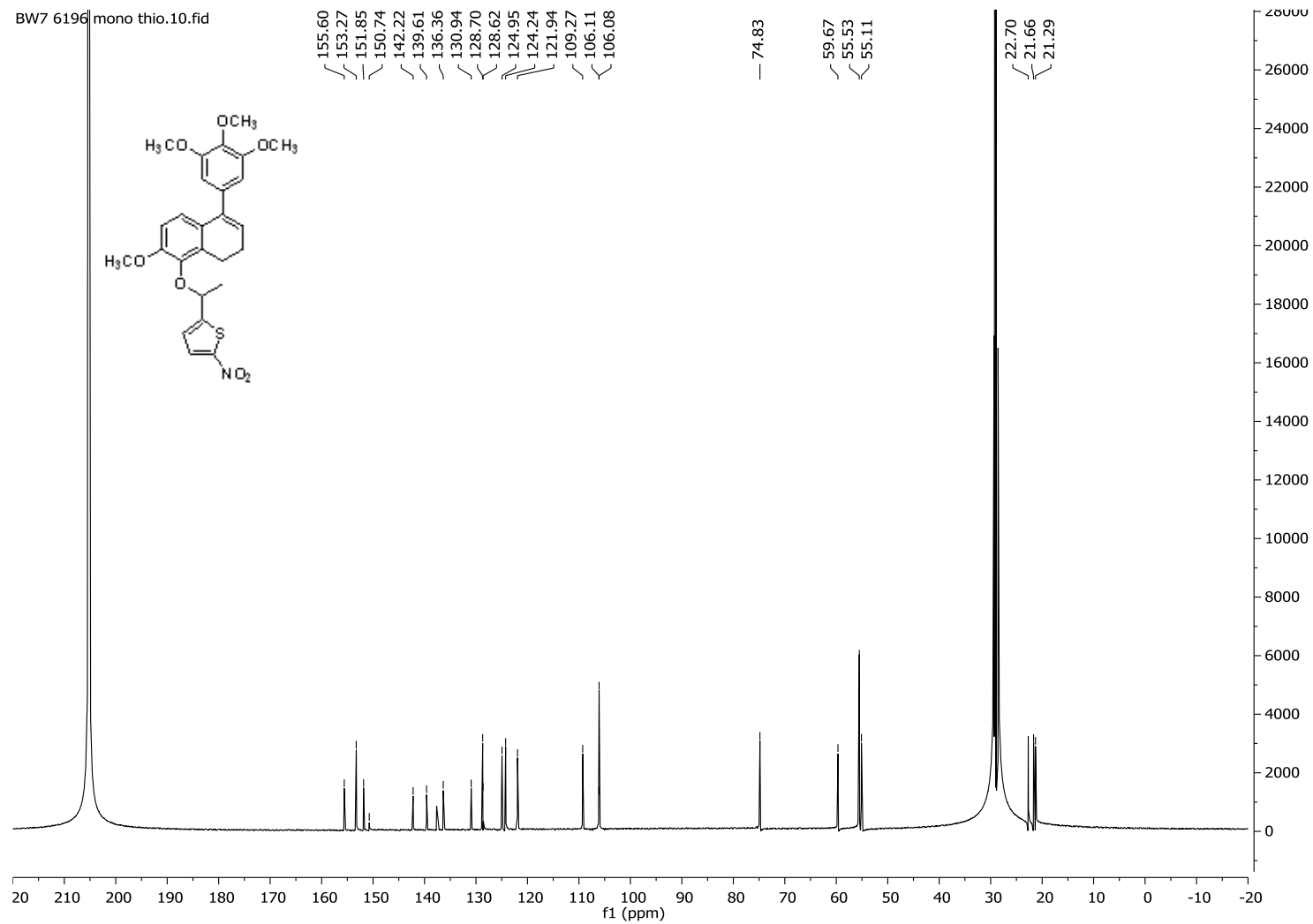
Totals : 684.04120 66.14884

=====
*** End of Report ***

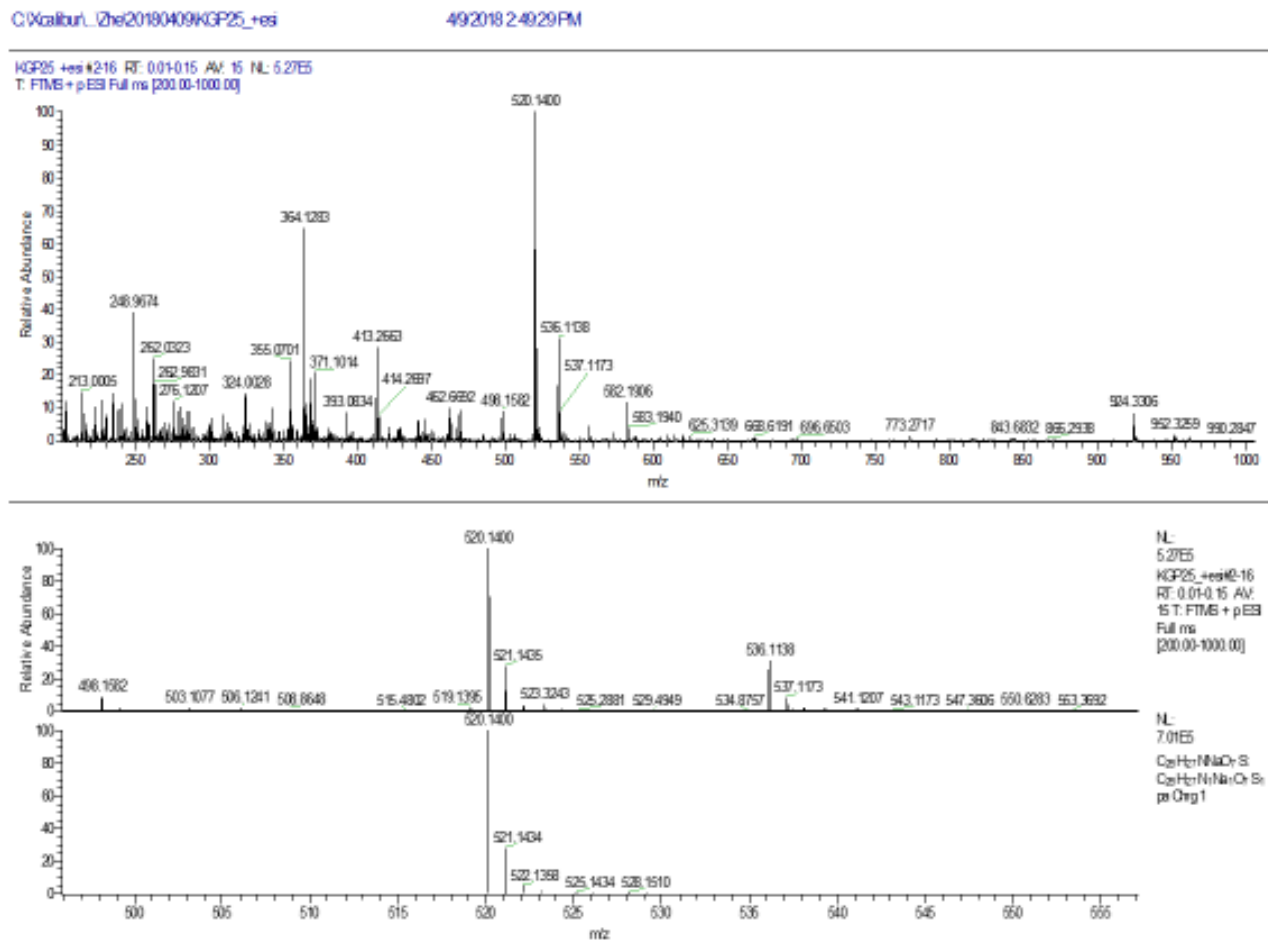
¹H NMR of 2-(1-((2-methoxy-5-(3,4,5-trimethoxyphenyl)-7,8-dihydronaphthalen-1-yl)oxy)ethyl)-5-nitrothiophene **11**



¹³C NMR of 2-(1-((2-methoxy-5-(3,4,5-trimethoxyphenyl)-7,8-dihydronaphthalen-1-yl)oxy)ethyl)-5-nitrothiophene **11**



HRMS of 2-(1-((2-methoxy-5-(3,4,5-trimethoxyphenyl)-7,8-dihydronaphthalen-1-yl)oxy)ethyl)-5-nitrothiophene **11**

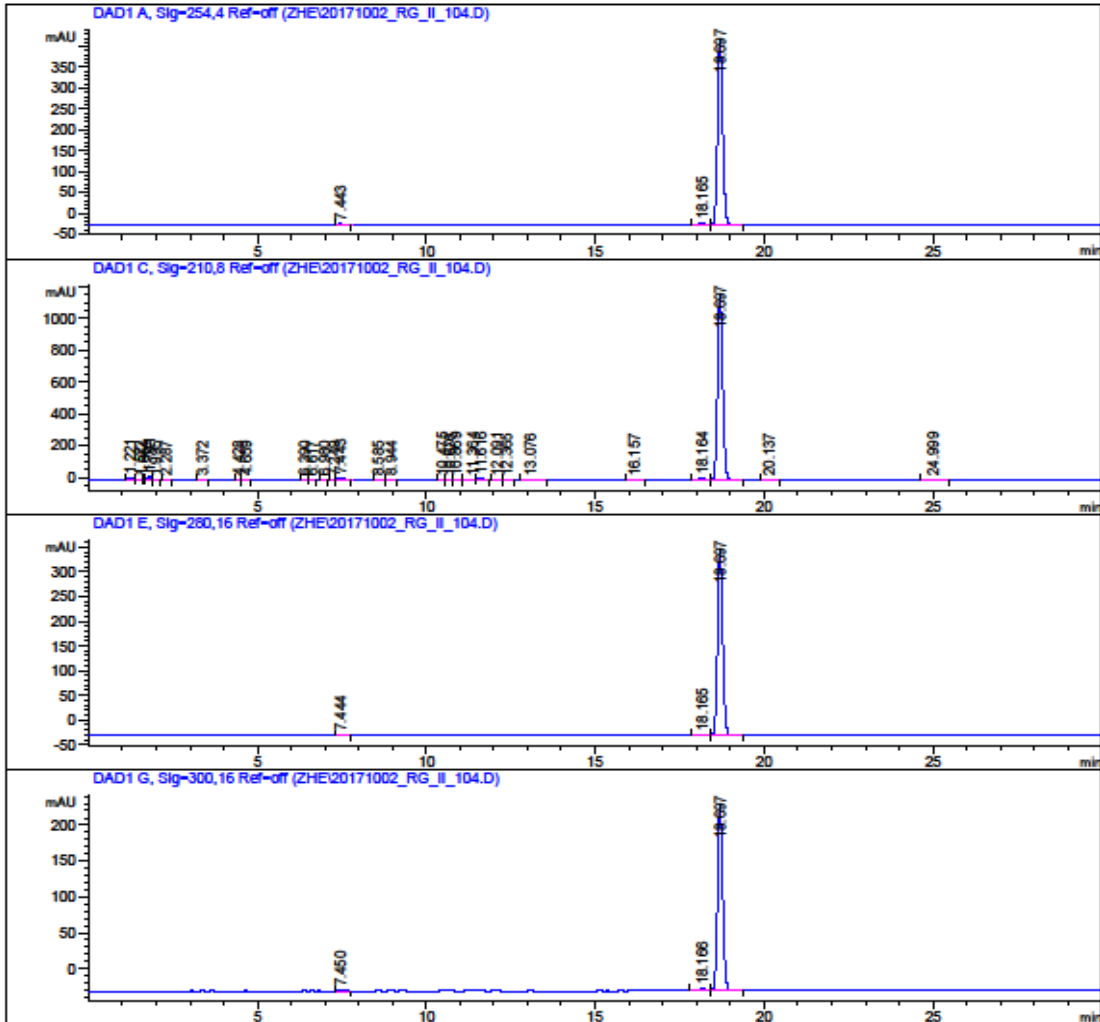


HPLC traces of Compound 11

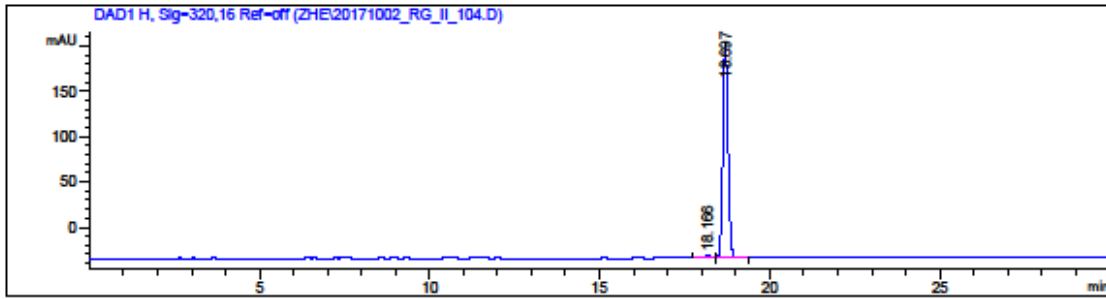
Data File C:\Chem32\1\Data\ZHE\20171002_RG_II_104.D
Sample Name: 20171002_RG_II_104

Acq. Operator : SYSTEM
Sample Operator : SYSTEM
Acq. Instrument : 1200 HPLC Location : 1
Injection Date : 10/2/2017 11:15:08 AM Inj Volume : No inj
Acq. Method : C:\CHEM32\1\METHODS\GRAD 2 50-90 ACN.M
Last changed : 4/30/2014 1:53:57 AM by ERICAP
Analysis Method : C:\CHEM32\1\METHODS\RT-ACNWASH 2.M
Last changed : 7/9/2015 2:27:22 PM by Blake
Method Info : General Column Wash Method

Sample Info : RG_II_104
GRAD 2 50-90 ACN
20171002



Data File C:\Chem32\1\Data\ZHE\20171002_RG_II_104.D
 Sample Name: 20171002_RG_II_104



=====
 Area Percent Report
 =====

Sorted By : Signal
 Multiplier : 1.0000
 Dilution : 1.0000
 Use Multiplier & Dilution Factor with ISTDs

Signal 1: DAD1 A, Sig=254,4 Ref=off

Peak #	RetTime [min]	Type	Width [min]	Area [mAU*s]	Height [mAU]	Area %
1	7.443	BB	0.1498	33.21056	3.23443	0.6895
2	18.165	BV	0.1638	34.54362	3.25448	0.7171
3	18.697	VB	0.1658	4749.10059	447.63040	98.5934

Totals : 4816.85477 454.11932

Signal 2: DAD1 C, Sig=210,8 Ref=off

Peak #	RetTime [min]	Type	Width [min]	Area [mAU*s]	Height [mAU]	Area %
1	1.221	BV	0.1078	102.97834	14.32981	0.7501
2	1.522	VV	0.1471	52.56194	5.06268	0.3829
3	1.654	VV	0.0692	17.88513	3.78305	0.1303
4	1.791	VB	0.0803	106.73665	20.66155	0.7775
5	1.995	BB	0.1042	13.83065	1.82896	0.1007
6	2.287	BB	0.0833	11.35046	2.02862	0.0827
7	3.372	BB	0.0898	6.12888	1.02480	0.0446
8	4.428	BV	0.0977	6.84383	1.08398	0.0499
9	4.659	VB	0.1137	9.03924	1.20314	0.0658
10	6.390	BV	0.1179	22.63209	2.93812	0.1649
11	6.617	VB	0.1262	13.48842	1.63535	0.0983
12	6.980	BB	0.1062	6.93827	1.06240	0.0505
13	7.249	BV	0.0981	7.18235	1.13102	0.0523
14	7.443	VB	0.1638	117.73193	10.26825	0.8576
15	8.585	VV	0.1411	17.93737	1.91895	0.1307
16	8.944	VV	0.1368	35.99319	4.08469	0.2622

Data File C:\Chem32\1\Data\ZHE\20171002_RG_II_104.D
 Sample Name: 20171002_RG_II_104

Peak #	RetTime [min]	Type	Width [min]	Area [mAU*s]	Height [mAU]	Area %
17	10.475	BV	0.1333	26.63588	3.12849	0.1940
18	10.676	VV	0.1238	19.73938	2.35495	0.1438
19	10.869	VB	0.1429	38.85814	4.16476	0.2830
20	11.364	BV	0.1620	54.65991	4.83132	0.3982
21	11.616	VB	0.1971	109.36239	8.67617	0.7966
22	12.091	BV	0.1624	31.34126	3.03582	0.2283
23	12.365	VB	0.1515	19.30640	1.98416	0.1406
24	13.076	BB	0.1633	23.35310	2.20997	0.1701
25	16.157	BB	0.1942	15.54489	1.24081	0.1132
26	18.164	BV	0.1657	134.63341	12.70155	0.9807
27	18.697	VB	0.1667	1.25503e4	1173.78503	91.4183
28	20.137	BB	0.1820	55.92270	4.79765	0.4073
29	24.999	BB	0.2034	99.51420	7.56836	0.7249

Totals : 1.37284e4 1304.52442

Signal 3: DAD1 E, Sig=280,16 Ref=off

Peak #	RetTime [min]	Type	Width [min]	Area [mAU*s]	Height [mAU]	Area %
1	7.444	BB	0.1465	22.54143	2.22013	0.5561
2	18.165	BV	0.1643	25.91957	2.43294	0.6395
3	18.697	VB	0.1657	4004.91895	377.58429	98.8044

Totals : 4053.37994 382.23735

Signal 4: DAD1 G, Sig=300,16 Ref=off

Peak #	RetTime [min]	Type	Width [min]	Area [mAU*s]	Height [mAU]	Area %
1	7.450	BB	0.1761	14.73961	1.14534	0.5258
2	18.166	BV	0.1619	34.88275	3.28485	1.2442
3	18.697	VB	0.1658	2753.91309	259.55505	98.2300

Totals : 2803.53544 263.98524

Signal 5: DAD1 H, Sig=320,16 Ref=off

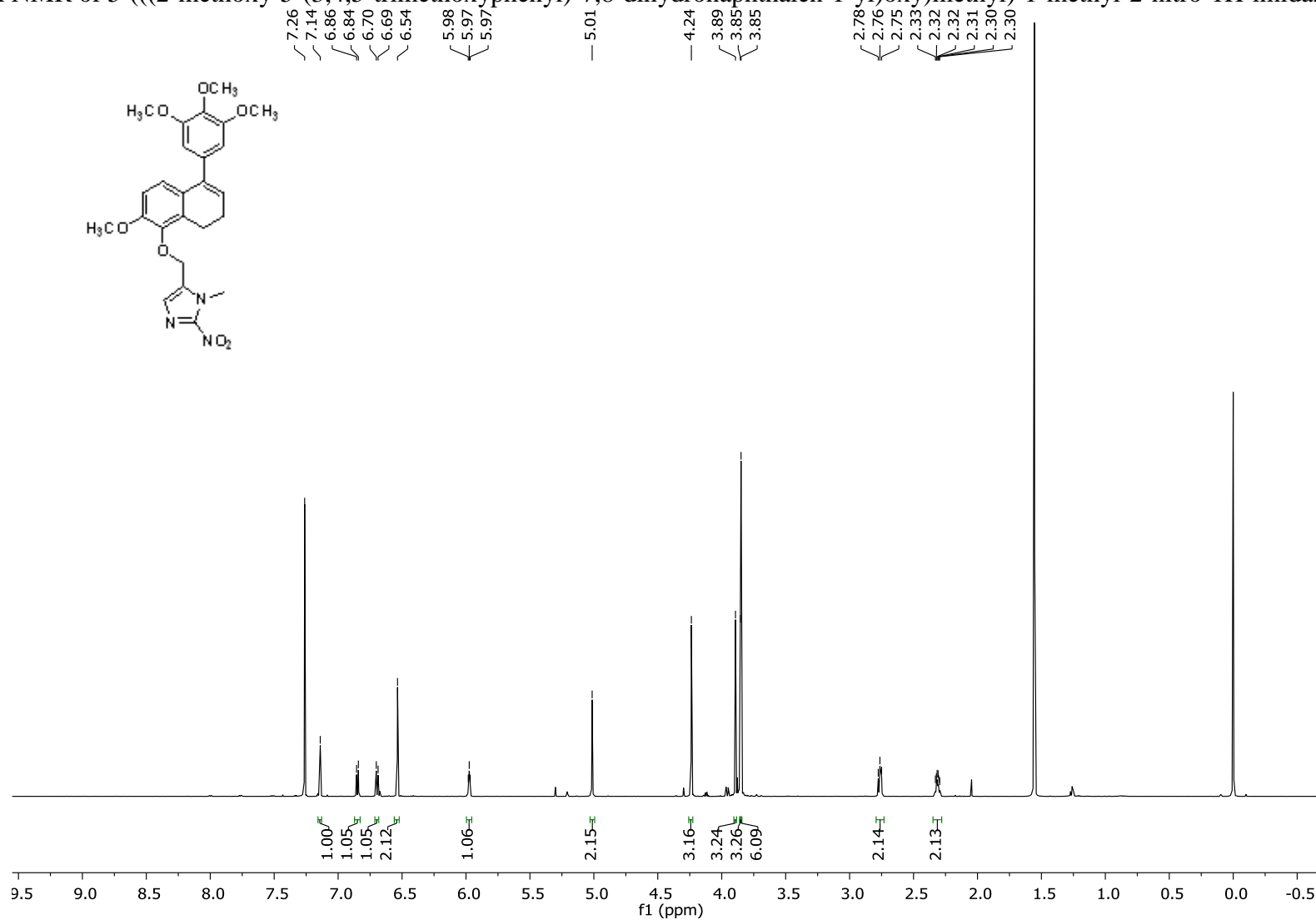
Peak #	RetTime [min]	Type	Width [min]	Area [mAU*s]	Height [mAU]	Area %
1	18.166	BV	0.1647	34.98343	3.27187	1.3653
2	18.697	VB	0.1658	2527.30688	238.23128	98.6347

Totals : 2562.29032 241.50315

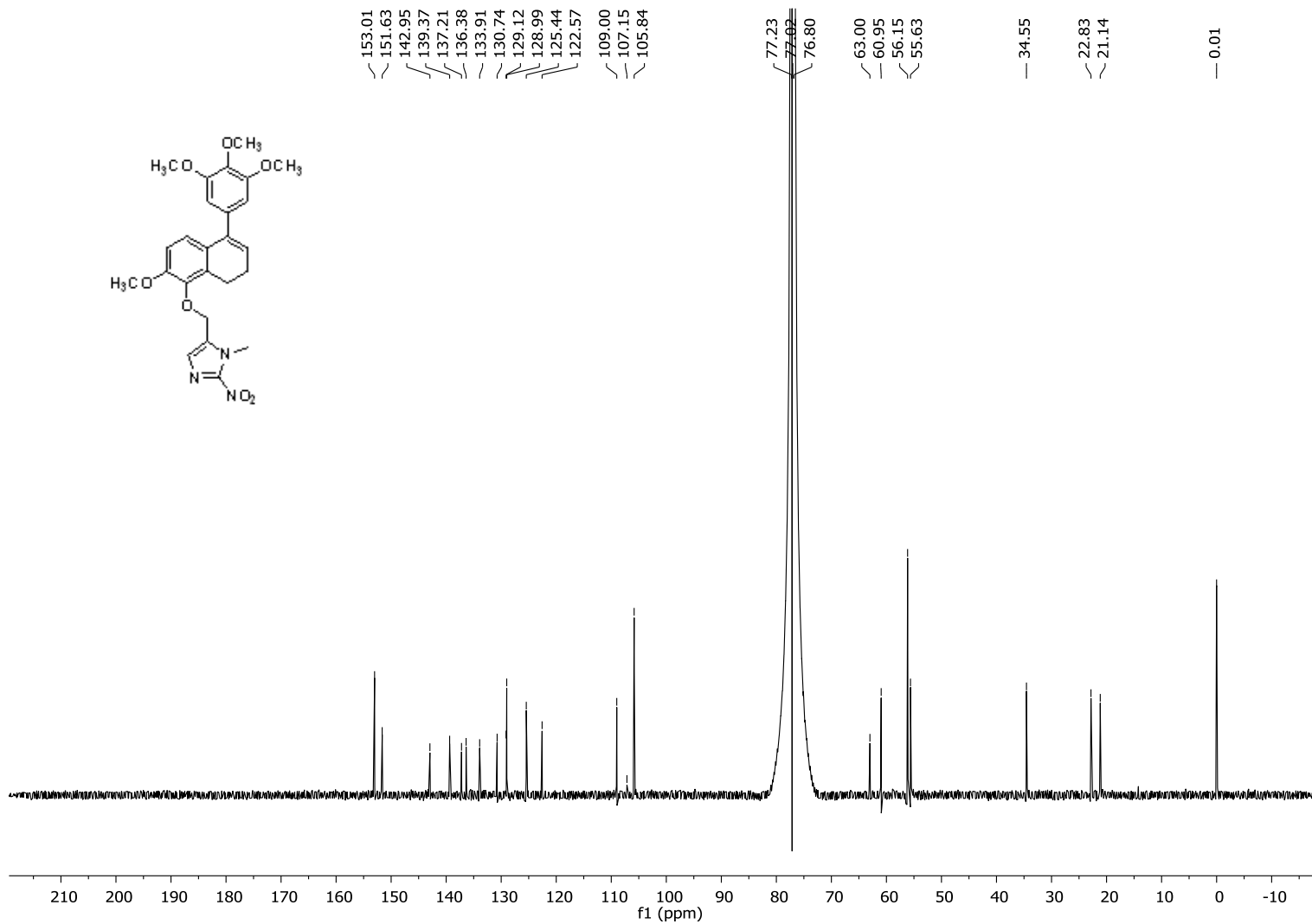
Data File C:\Chem32\1\Data\ZHE\20171002_RG_II_104.D
Sample Name: 20171002_RG_II_104

=====
*** End of Report ***

¹H NMR of 5-(((2-methoxy-5-(3,4,5-trimethoxyphenyl)-7,8-dihydronaphthalen-1-yl)oxy)methyl)-1-methyl-2-nitro-1H-imidazole



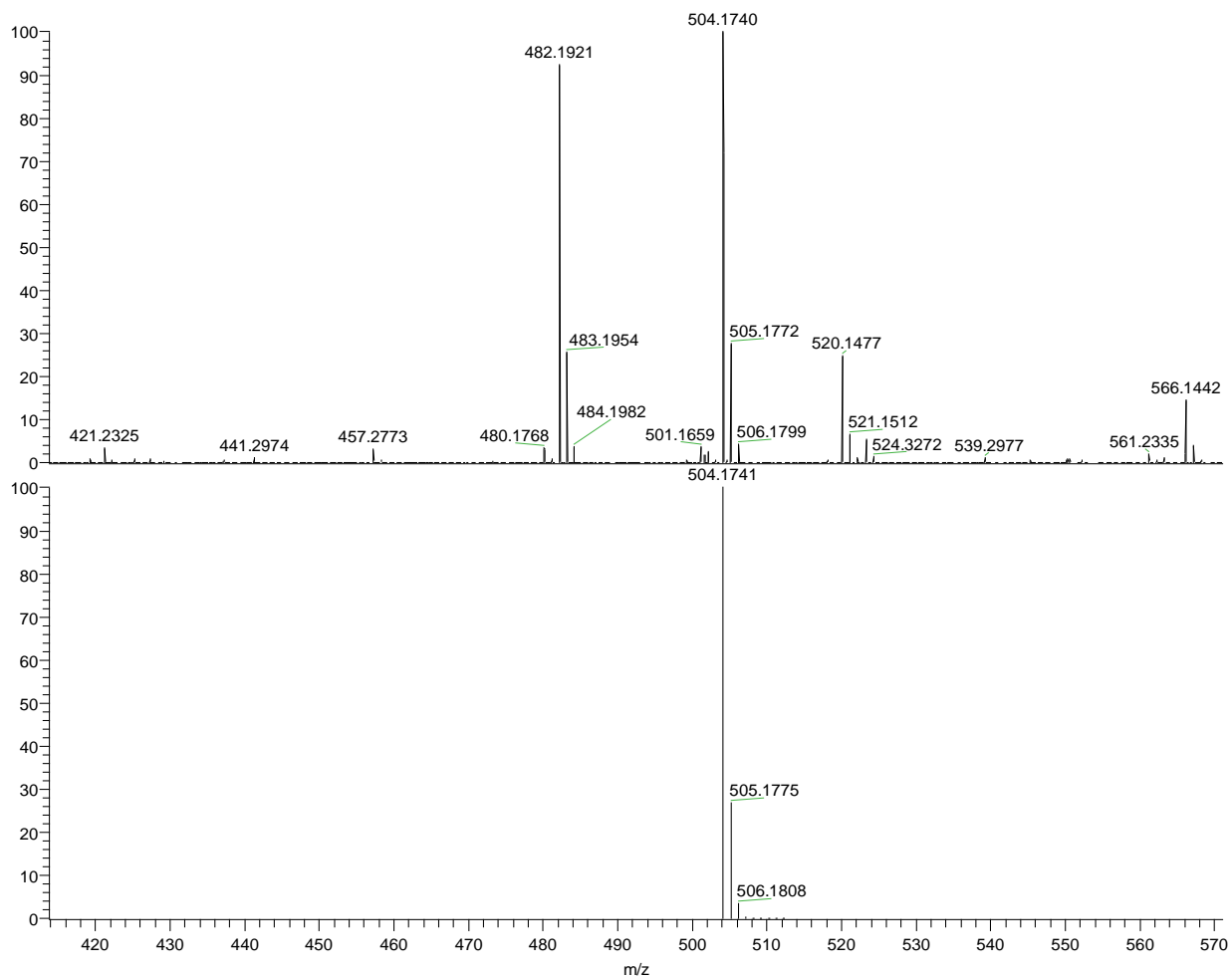
¹³C NMR of 5-(((2-methoxy-5-(3,4,5-trimethoxyphenyl)-7,8-dihydronaphthalen-1-yl)oxy)methyl)-1-methyl-2-nitro-1H-imidazole **12**



HRMS of 5-(((2-methoxy-5-(3,4,5-trimethoxyphenyl)-7,8-dihydronaphthalen-1-yl)oxy)methyl)-1-methyl-2-nitro-1H-imidazole **12**

C:\Xcalibur\...20160121\vs_III_107_+ESI

1/21/2016 2:28:44 PM



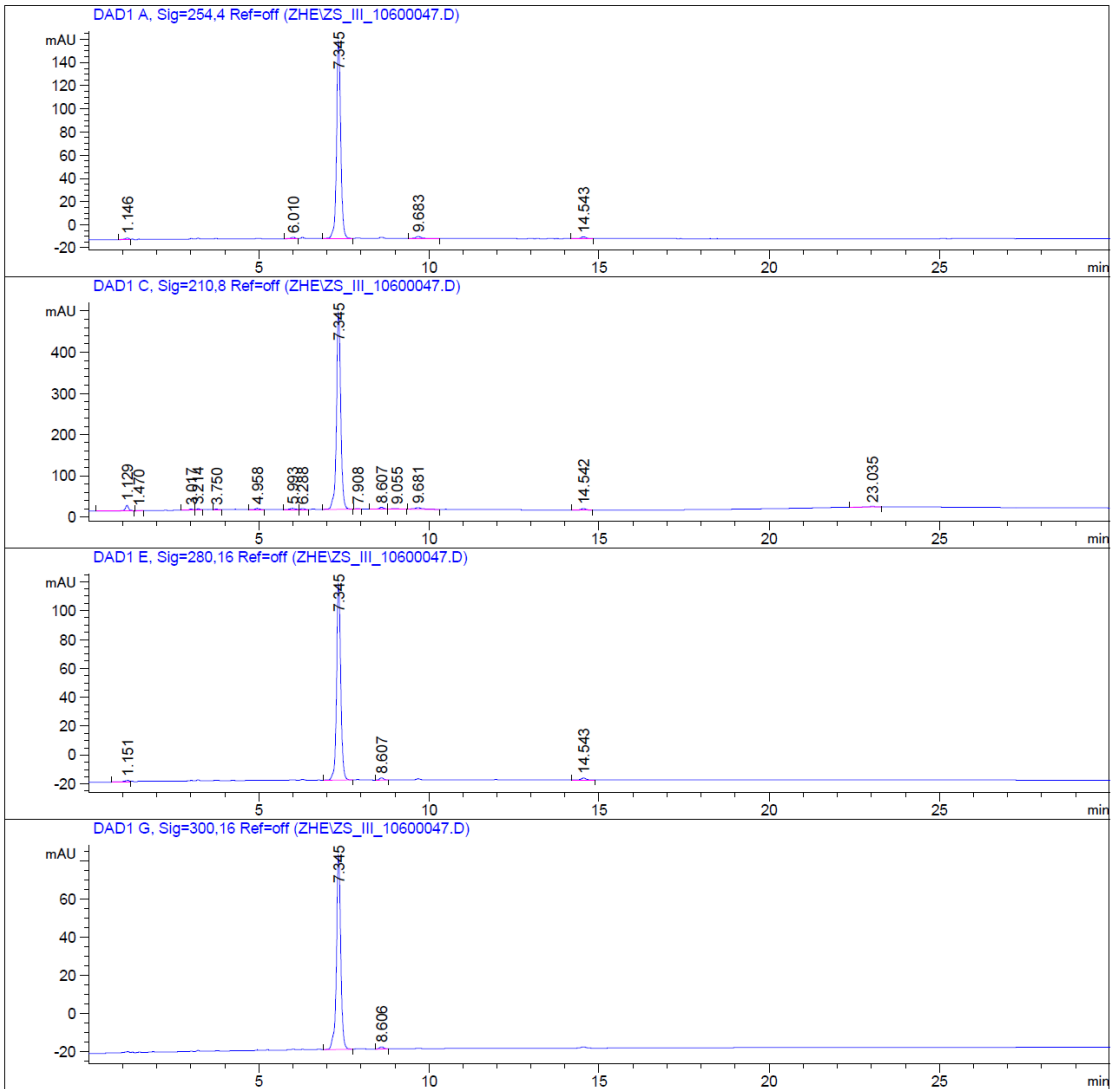
NL:
1.07E7
zs_III_107_+ESI#2-12
RT: 0.01-0.09 AV:
11 T: FTMS + p ESI
Full ms
[200.00-1000.00]

NL:
7.41E5
C₂₅ H₂₇ N₃ NaO₇:
C₂₅ H₂₇ N₃ Na₁ O₇
pa Chrg 1

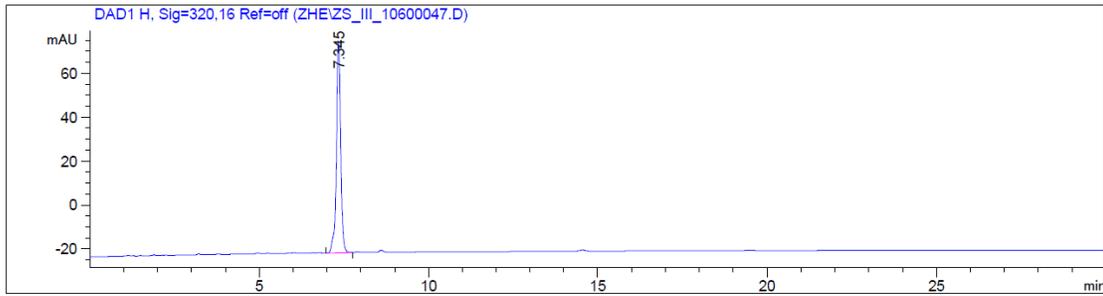
HPLC traces of compound 12

Data File C:\Chem32\1\Data\ZHE\ZS_III_10600047.D
Sample Name: zs_III_106

```
=====
Acq. Operator   : zhe
Acq. Instrument : Instrument 1           Location : -
Injection Date  : 6/13/2016 4:53:29 PM
Acq. Method     : C:\CHEM32\1\METHODS\GRAD 2 50-90 ACN.M
Last changed    : 4/30/2014 1:53:57 AM by ERICAP
Analysis Method : C:\Chem32\1\Methods\DEF_LC.M
Last changed    : 6/22/2014 3:13:01 PM by SYSTEM
Sample Info     : zs_III_106
                  GRAD 2 50-90 ACN
                  checking for OXi6196
                  20160613
```



Data File C:\Chem32\1\Data\ZHE\ZS_III_10600047.D
 Sample Name: zs_III_106



=====
 Area Percent Report
 =====

Sorted By : Signal
 Multiplier : 1.0000
 Dilution : 1.0000
 Use Multiplier & Dilution Factor with ISTDs

Signal 1: DAD1 A, Sig=254,4 Ref=off

Peak #	RetTime [min]	Type	Width [min]	Area [mAU*s]	Height [mAU]	Area %
1	1.146	BV	0.1225	14.50789	1.65133	0.9533
2	6.010	BV	0.1416	10.73883	1.12269	0.7056
3	7.345	BB	0.1304	1463.31226	170.11348	96.1542
4	9.683	BB	0.1668	18.27984	1.55920	1.2012
5	14.543	BB	0.1627	15.00034	1.40349	0.9857

Totals : 1521.83916 175.85019

Signal 2: DAD1 C, Sig=210,8 Ref=off

Peak #	RetTime [min]	Type	Width [min]	Area [mAU*s]	Height [mAU]	Area %
1	1.129	BB	0.1194	114.46228	13.99465	2.4845
2	1.470	BB	0.1120	9.27811	1.08261	0.2014
3	3.017	BV	0.1166	19.83439	2.44635	0.4305
4	3.214	VV	0.1009	19.90868	2.87203	0.4321
5	3.750	VB	0.1196	9.08917	1.15818	0.1973
6	4.958	BB	0.1201	24.10078	2.98917	0.5231
7	5.993	BV	0.1532	29.46825	2.88322	0.6396
8	6.288	VB	0.1122	17.46011	2.41898	0.3790
9	7.345	BB	0.1320	4174.38184	477.42743	90.6098
10	7.908	BB	0.1058	8.32523	1.24921	0.1807
11	8.607	BV	0.1375	42.01498	4.64822	0.9120
12	9.055	VB	0.1989	19.14094	1.32226	0.4155
13	9.681	BB	0.2065	65.06004	4.25249	1.4122
14	14.542	BB	0.1595	36.76067	3.53028	0.7979

Data File C:\Chem32\1\Data\ZHE\ZS_III_10600047.D
Sample Name: zs_III_106

Peak #	RetTime [min]	Type	Width [min]	Area [mAU*s]	Height [mAU]	Area %
15	23.035	BB	0.2213	17.70357	1.19172	0.3843
Totals :				4606.98903	523.46678	

Signal 3: DAD1 E, Sig=280,16 Ref=off

Peak #	RetTime [min]	Type	Width [min]	Area [mAU*s]	Height [mAU]	Area %
1	1.151	BV	0.1316	11.28998	1.12047	0.9390
2	7.345	BB	0.1298	1163.81067	136.00249	96.7981
3	8.607	BB	0.1309	13.15300	1.55119	1.0940
4	14.543	BB	0.1610	14.05339	1.33285	1.1689
Totals :				1202.30703	140.00700	

Signal 4: DAD1 G, Sig=300,16 Ref=off

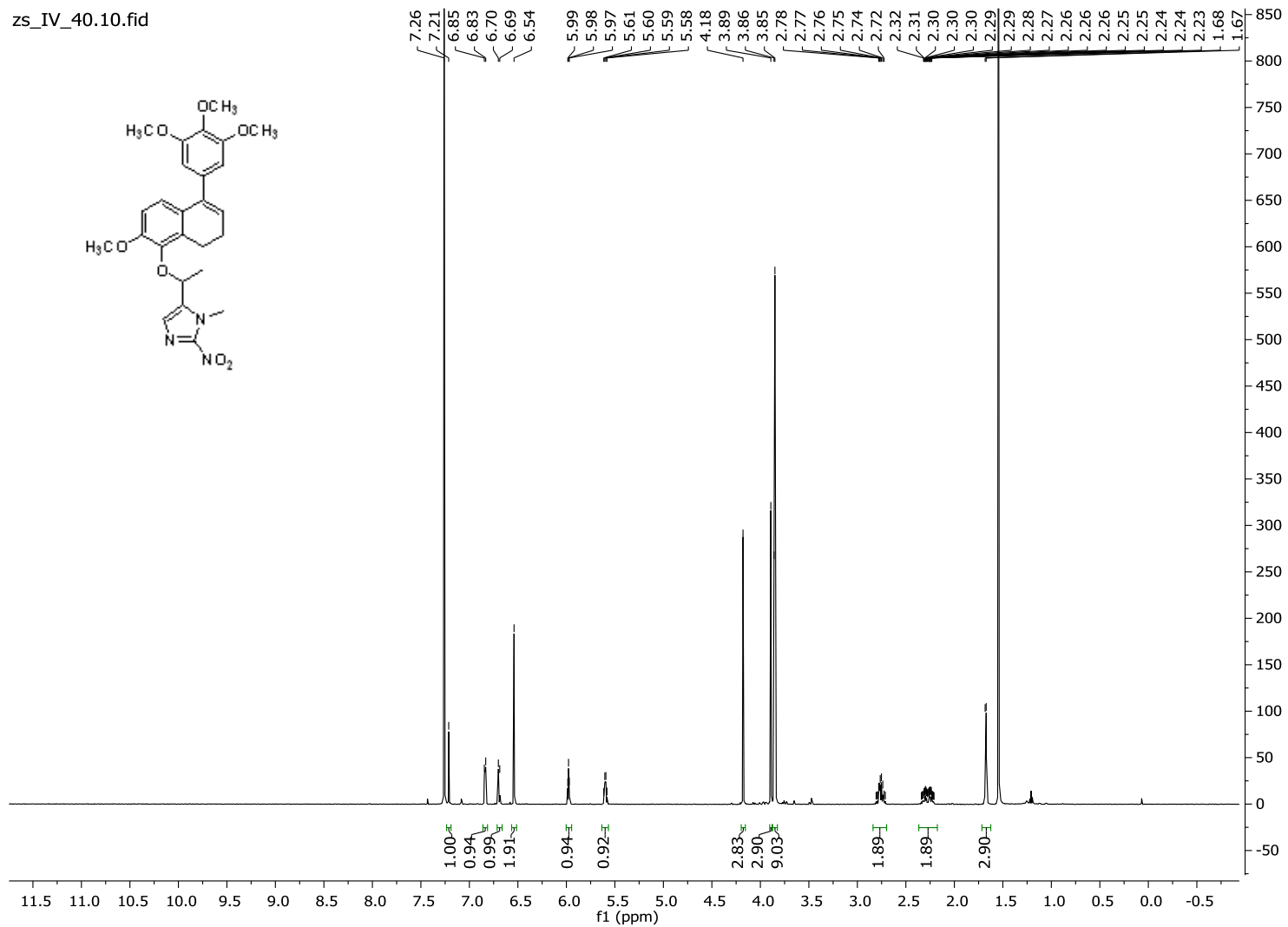
Peak #	RetTime [min]	Type	Width [min]	Area [mAU*s]	Height [mAU]	Area %
1	7.345	BB	0.1330	899.99927	101.95317	98.8688
2	8.606	BB	0.1332	10.29763	1.21165	1.1312
Totals :				910.29690	103.16482	

Signal 5: DAD1 H, Sig=320,16 Ref=off

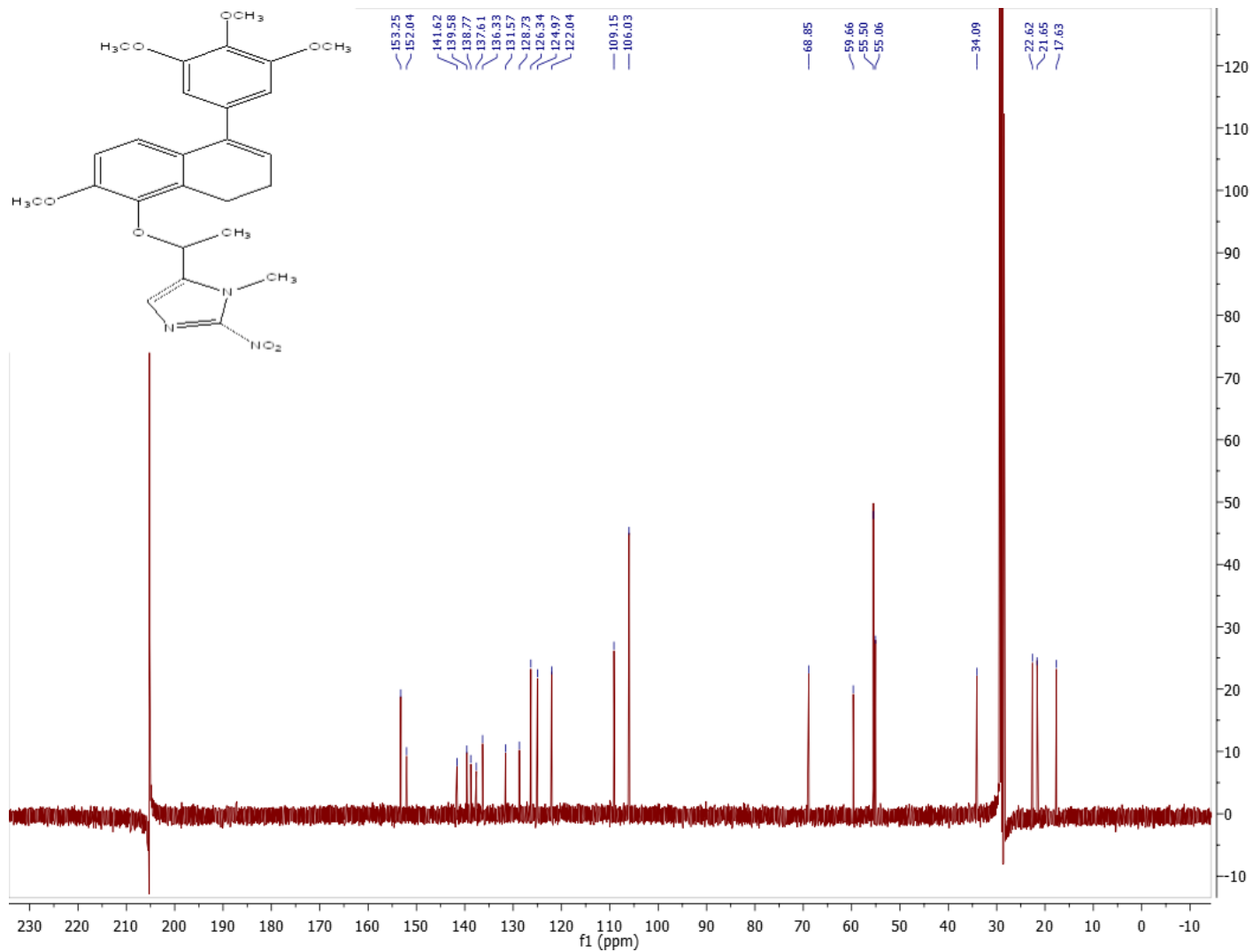
Peak #	RetTime [min]	Type	Width [min]	Area [mAU*s]	Height [mAU]	Area %
1	7.345	BB	0.1334	852.90222	96.21187	100.0000
Totals :				852.90222	96.21187	

=====
*** End of Report ***

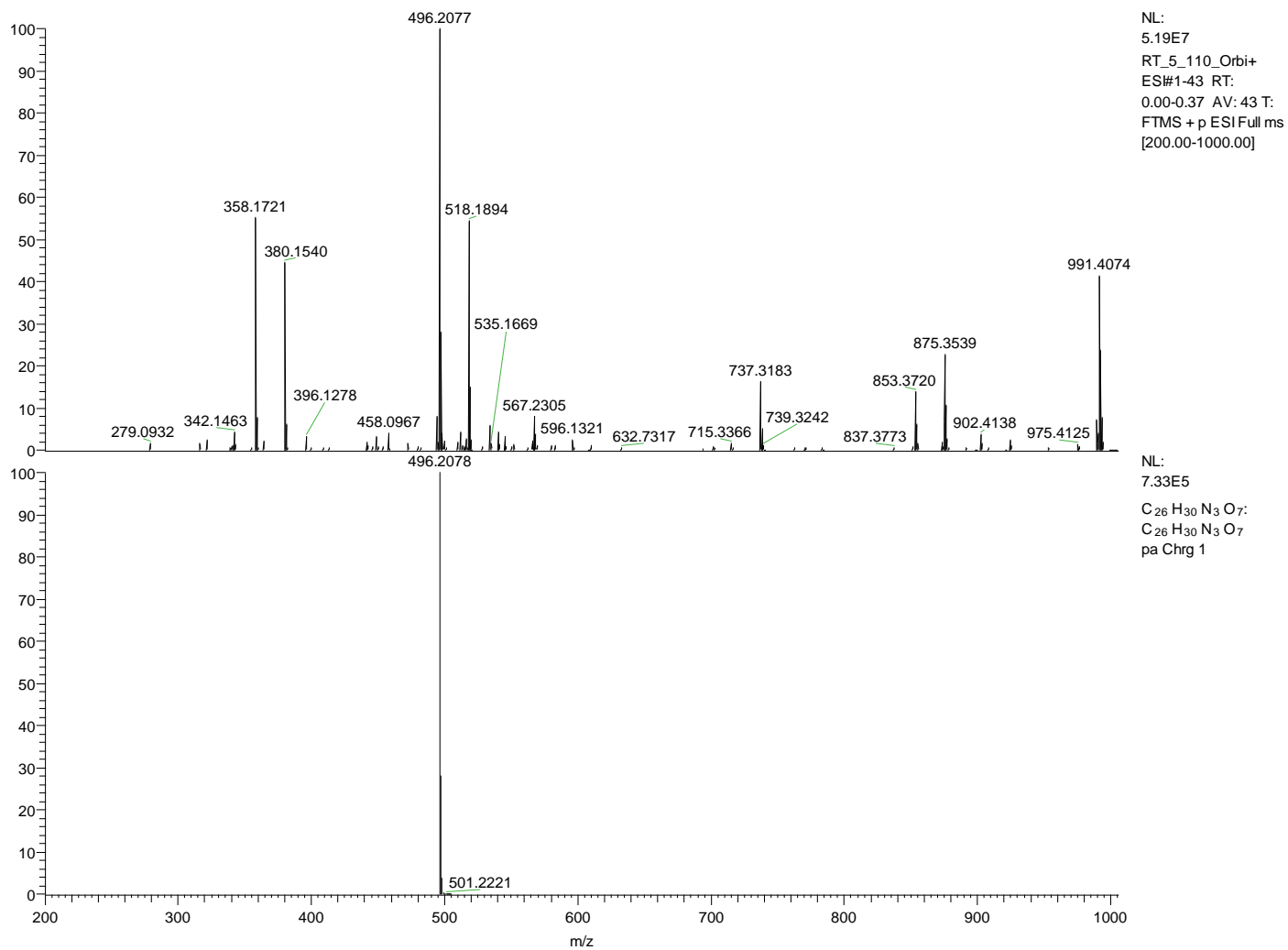
¹H NMR of 5-(1-((2-methoxy-5-(3,4,5-trimethoxyphenyl)-7,8-dihydronaphthalen-1-yl)oxy)ethyl)-1-methyl-2-nitro-1H-imidazole **13**



¹³C NMR of 5-(1-((2-methoxy-5-(3,4,5-trimethoxyphenyl)-7,8-dihydronaphthalen-1-yl)oxy)ethyl)-1-methyl-2-nitro-1H-imidazole **13**



HRMS of 5-(1-((2-methoxy-5-(3,4,5-trimethoxyphenyl)-7,8-dihydronaphthalen-1-yl)oxy)ethyl)-1-methyl-2-nitro-1H-imidazole **13**

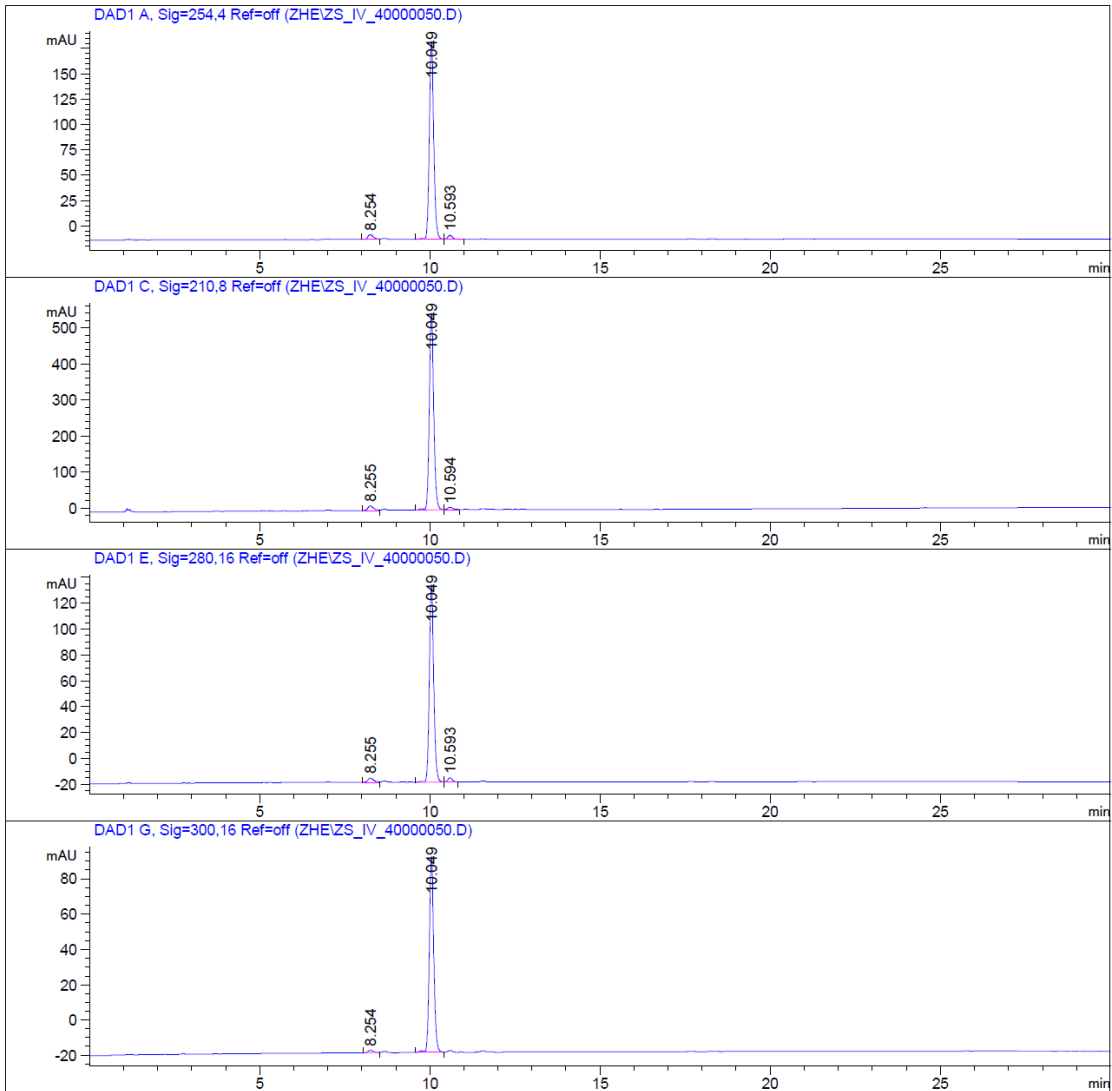


HPLC traces of Compound 13

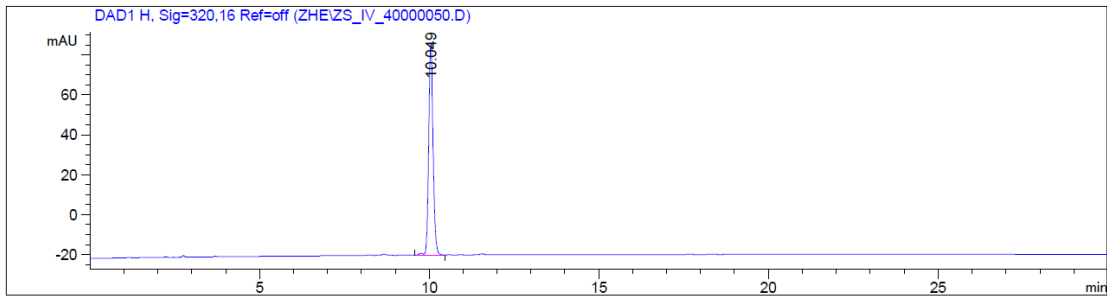
Data File C:\Chem32\1\Data\ZHE\ZS_IV_40000050.D
Sample Name: zs_IV_40

```
=====
Acq. Operator   : zhe
Acq. Instrument : Instrument 1           Location : -
Injection Date  : 6/14/2016 1:13:14 PM
Acq. Method     : C:\CHEM32\1\METHODS\GRAD 2 50-90 ACN.M
Last changed    : 4/30/2014 1:53:57 AM by ERICAP
Analysis Method : C:\Chem32\1\Methods\DEF_LC.M
Last changed    : 6/22/2014 3:13:01 PM by SYSTEM
Sample Info     : zs_IV_40
                  GRAD 2 50-90 ACN
                  checking for OXi6196
                  20160613
```

Additional Info : Peak(s) manually integrated



Data File C:\Chem32\1\Data\ZHE\ZS_IV_40000050.D
 Sample Name: zs_IV_40



=====
 Area Percent Report
 =====

Sorted By : Signal
 Multiplier : 1.0000
 Dilution : 1.0000
 Use Multiplier & Dilution Factor with ISTDs

Signal 1: DAD1 A, Sig=254,4 Ref=off

Peak #	RetTime [min]	Type	Width [min]	Area [mAU*s]	Height [mAU]	Area %
1	8.254	BV	0.1762	56.55766	4.84522	3.0398
2	10.049	VV R	0.1395	1766.42224	195.27231	94.9382
3	10.593	VB	0.1461	37.62222	3.91615	2.0220

Totals : 1860.60212 204.03367

Signal 2: DAD1 C, Sig=210,8 Ref=off

Peak #	RetTime [min]	Type	Width [min]	Area [mAU*s]	Height [mAU]	Area %
1	8.255	BV	0.1761	145.61433	12.47793	2.8203
2	10.049	VV R	0.1392	4952.49658	545.70105	95.9208
3	10.594	VB	0.1448	64.99823	6.84419	1.2589

Totals : 5163.10915 565.02318

Signal 3: DAD1 E, Sig=280,16 Ref=off

Peak #	RetTime [min]	Type	Width [min]	Area [mAU*s]	Height [mAU]	Area %
1	8.255	BV	0.1770	38.75599	3.30042	2.6811
2	10.049	VV R	0.1393	1377.34216	152.55774	95.2831
3	10.593	VB	0.1411	29.42853	3.20475	2.0358

Data File C:\Chem32\1\Data\ZHE\ZS_IV_40000050.D
Sample Name: zs_IV_40

Peak #	RetTime [min]	Type	Width [min]	Area [mAU*s]	Height [mAU]	Area %
Totals :				1445.52668	159.06291	

Signal 4: DAD1 G, Sig=300,16 Ref=off

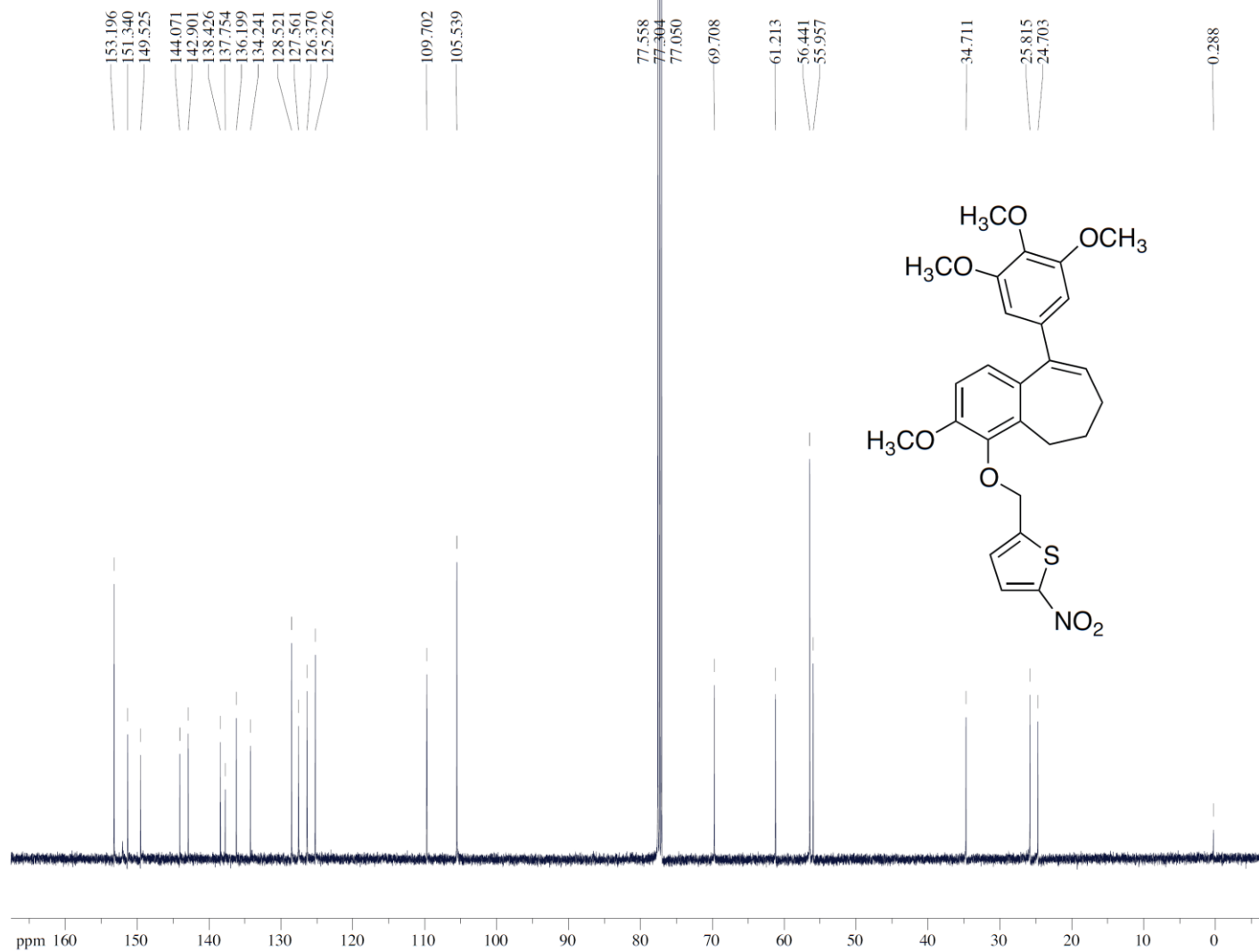
Peak #	RetTime [min]	Type	Width [min]	Area [mAU*s]	Height [mAU]	Area %
1	8.254	BB	0.1619	13.44318	1.26573	1.3209
2	10.049	VB R	0.1397	1004.31458	110.81192	98.6791
Totals :				1017.75776	112.07765	

Signal 5: DAD1 H, Sig=320,16 Ref=off

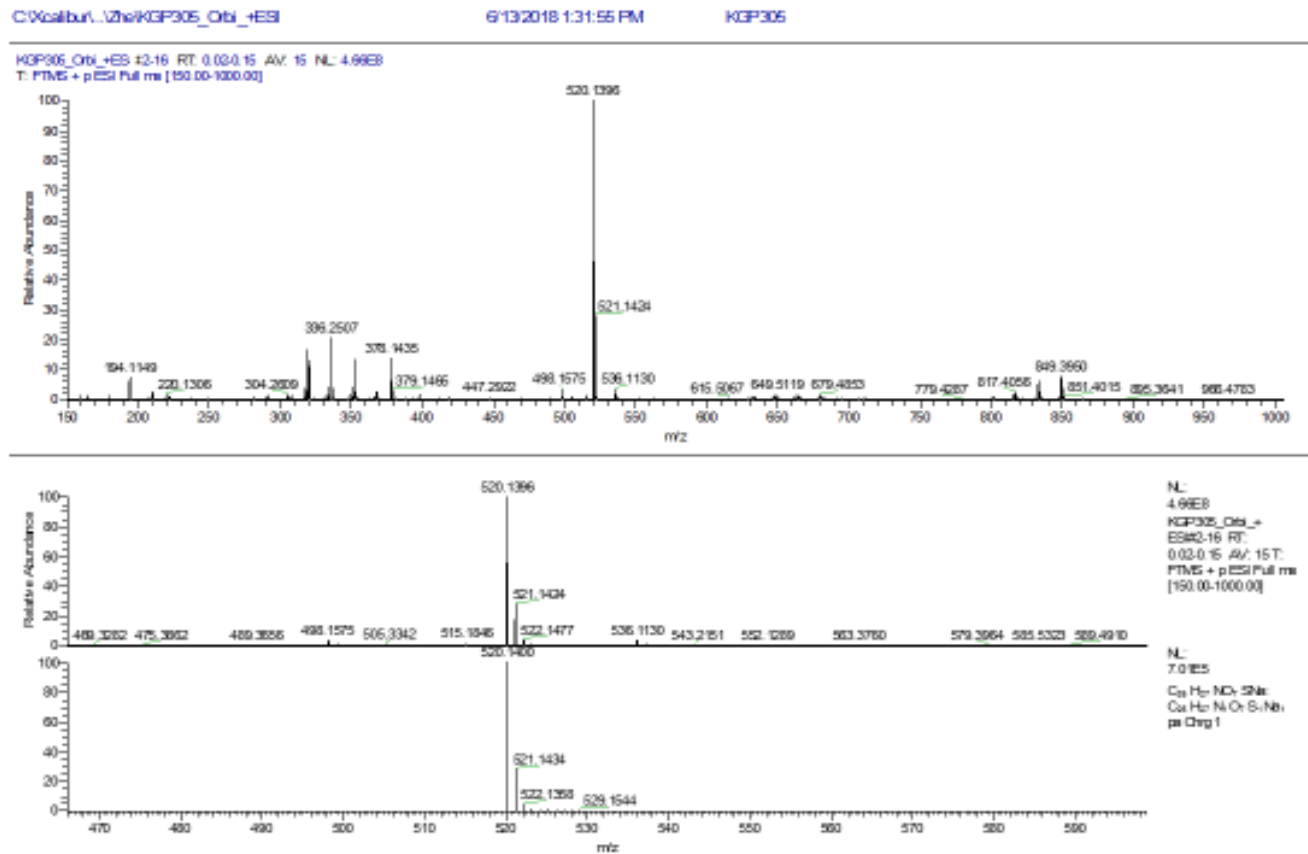
Peak #	RetTime [min]	Type	Width [min]	Area [mAU*s]	Height [mAU]	Area %
1	10.049	VB R	0.1390	967.01086	106.53122	100.0000
Totals :				967.01086	106.53122	

=====
*** End of Report ***

¹³C NMR of 2-(1-((3-methoxy-9-(3,4,5-trimethoxyphenyl)-6,7-dihydro-5H-benzo[7]annulen-4-yl)oxy)methyl)-5-nitrothiophene **14**



HRMS of 2-(1-((3-methoxy-9-(3,4,5-trimethoxyphenyl)-6,7-dihydro-5H-benzo[7]annulen-4-yl)oxy)methyl)-5-nitrothiophene 14

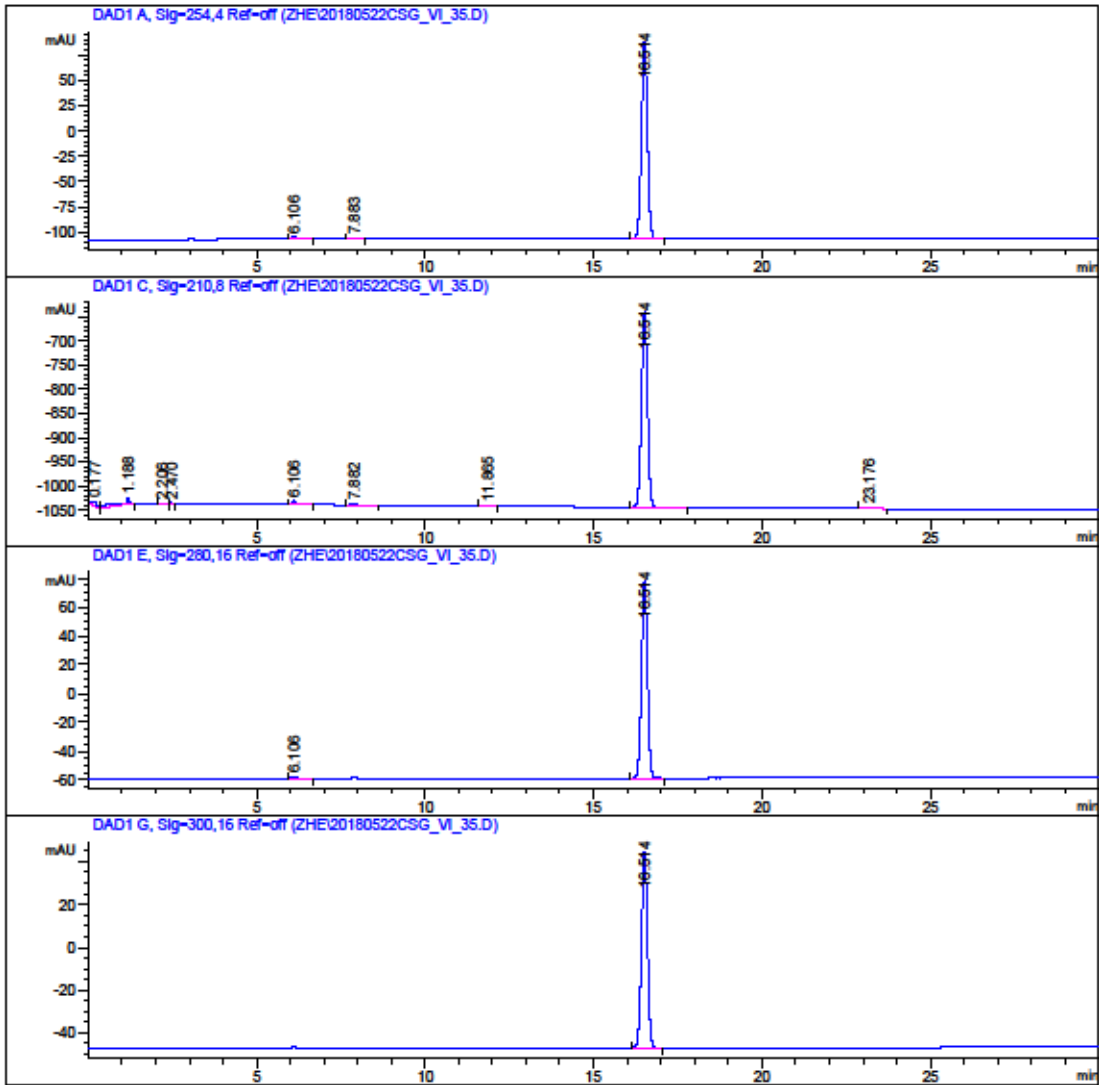


HPLC traces of Compound 14

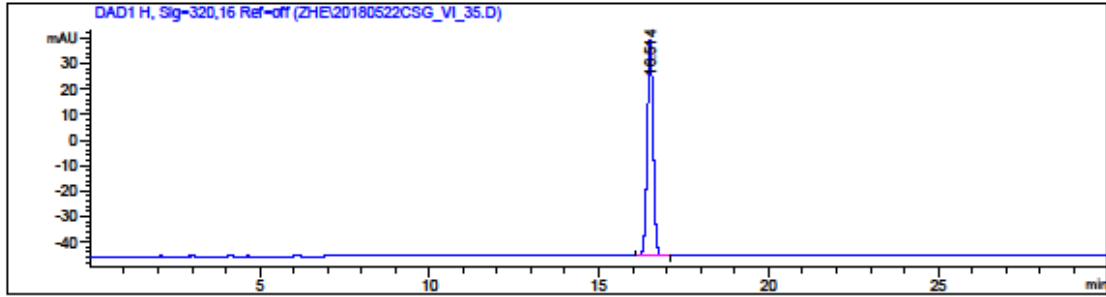
Data File C:\Chem32\1\Data\ZHE\20180522CSG_VI_35.D

Sample Name: KGP305

Acq. Operator : SYSTEM
Sample Operator : SYSTEM
Acq. Instrument : 1200 HPLC Location : 1
Injection Date : 5/22/2018 11:49:34 AM Inj Volume : No inj
Acq. Method : C:\CHEM32\1\METHODS\GRAD 2 50-90 ACN.M
Last changed : 4/30/2014 1:53:57 AM by ERICAP
Analysis Method : C:\CHEM32\1\METHODS\RT-ACNWASH 2.M
Last changed : 7/9/2015 2:27:22 PM by Blake
Method Info : General Column Wash Method
Sample Info : 20180522CSG_VI_35
GRAD 2 50-90 ACN



Data File C:\Chem32\1\Data\ZHE\20180522CSG_VI_35.D
 Sample Name: KGP305



=====
 Area Percent Report
 =====

Sorted By : Signal
 Multiplier : 1.0000
 Dilution : 1.0000
 Use Multiplier & Dilution Factor with ISTDs

Signal 1: DAD1 A, Sig=254,4 Ref-off

Peak #	RetTime [min]	Type	Width [min]	Area [mAU*s]	Height [mAU]	Area %
1	6.106	BB	0.1287	18.78357	2.22060	0.7819
2	7.883	BB	0.1451	9.71985	1.03958	0.4046
3	16.514	BB	0.1886	2373.84180	194.15721	98.8135

Totals : 2402.34521 197.41739

Signal 2: DAD1 C, Sig=210,8 Ref-off

Peak #	RetTime [min]	Type	Width [min]	Area [mAU*s]	Height [mAU]	Area %
1	0.177	BB	0.1450	89.12038	8.59009	1.6410
2	1.188	BB	0.2122	246.89737	14.53000	4.5461
3	2.206	BB	0.1762	19.99943	1.71323	0.3682
4	2.470	BB	0.0824	15.19208	2.84144	0.2797
5	6.106	BB	0.1275	58.44517	6.99209	1.0761
6	7.882	BB	0.1486	26.80206	2.72940	0.4935
7	11.865	BB	0.1666	11.98730	1.08741	0.2207
8	16.514	BB	0.1890	4944.76465	403.40457	91.0472
9	23.176	BB	0.2176	17.78183	1.23800	0.3274

Totals : 5430.99028 443.12622

Data File C:\Chem32\1\Data\ZHE\20180522CSG_VI_35.D
Sample Name: KGP305

Signal 3: DAD1 E, Sig=280,16 Ref=off

Peak #	RetTime [min]	Type	Width [min]	Area [mAU*s]	Height [mAU]	Area %
1	6.106	BB	0.1281	13.03988	1.55095	0.7756
2	16.514	BB	0.1887	1668.26929	136.43387	99.2244

Totals : 1681.30916 137.98482

Signal 4: DAD1 G, Sig=300,16 Ref=off

Peak #	RetTime [min]	Type	Width [min]	Area [mAU*s]	Height [mAU]	Area %
1	16.514	BB	0.1887	1124.02905	91.90234	100.0000

Totals : 1124.02905 91.90234

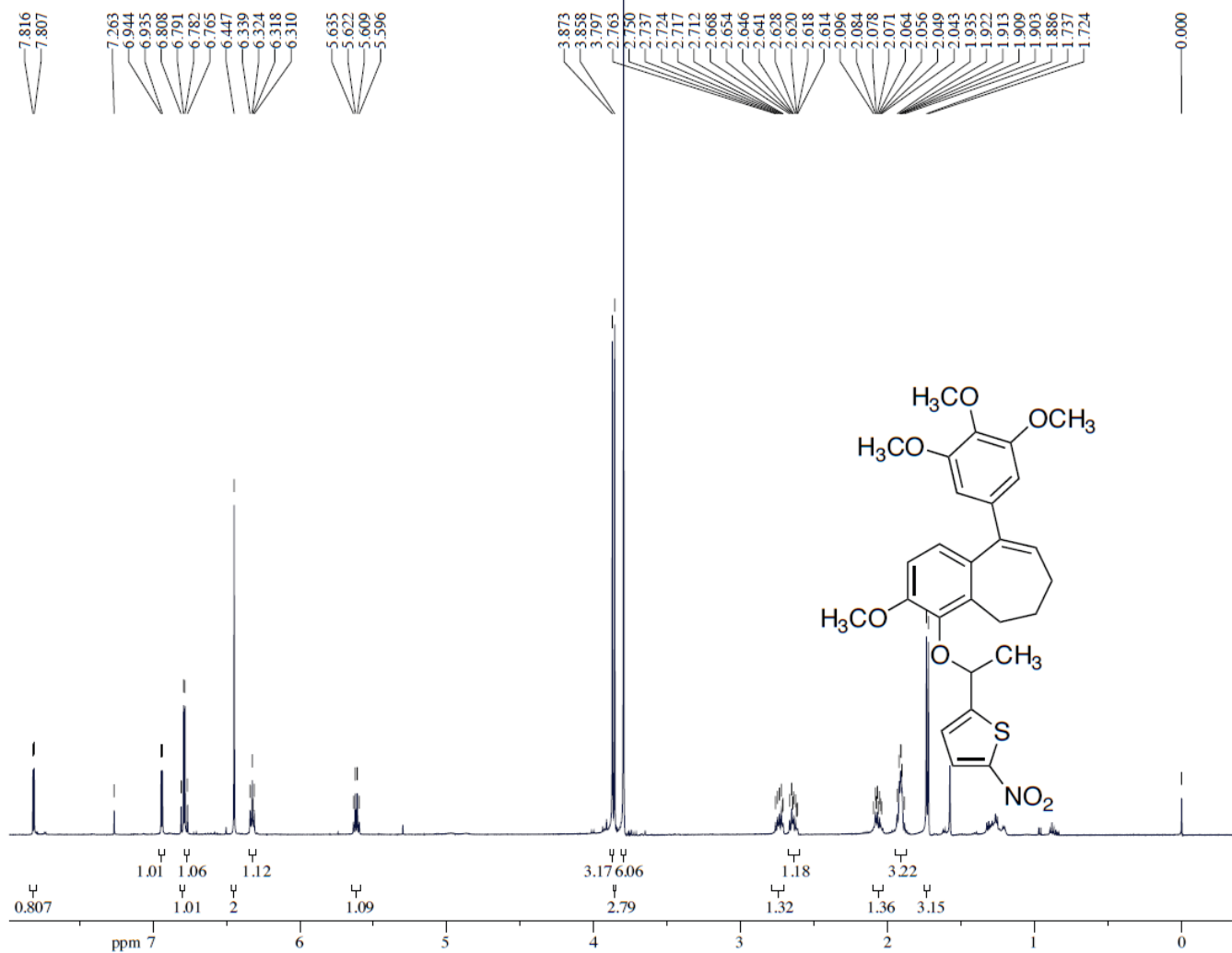
Signal 5: DAD1 H, Sig=320,16 Ref=off

Peak #	RetTime [min]	Type	Width [min]	Area [mAU*s]	Height [mAU]	Area %
1	16.514	BB	0.1887	1035.16174	84.64111	100.0000

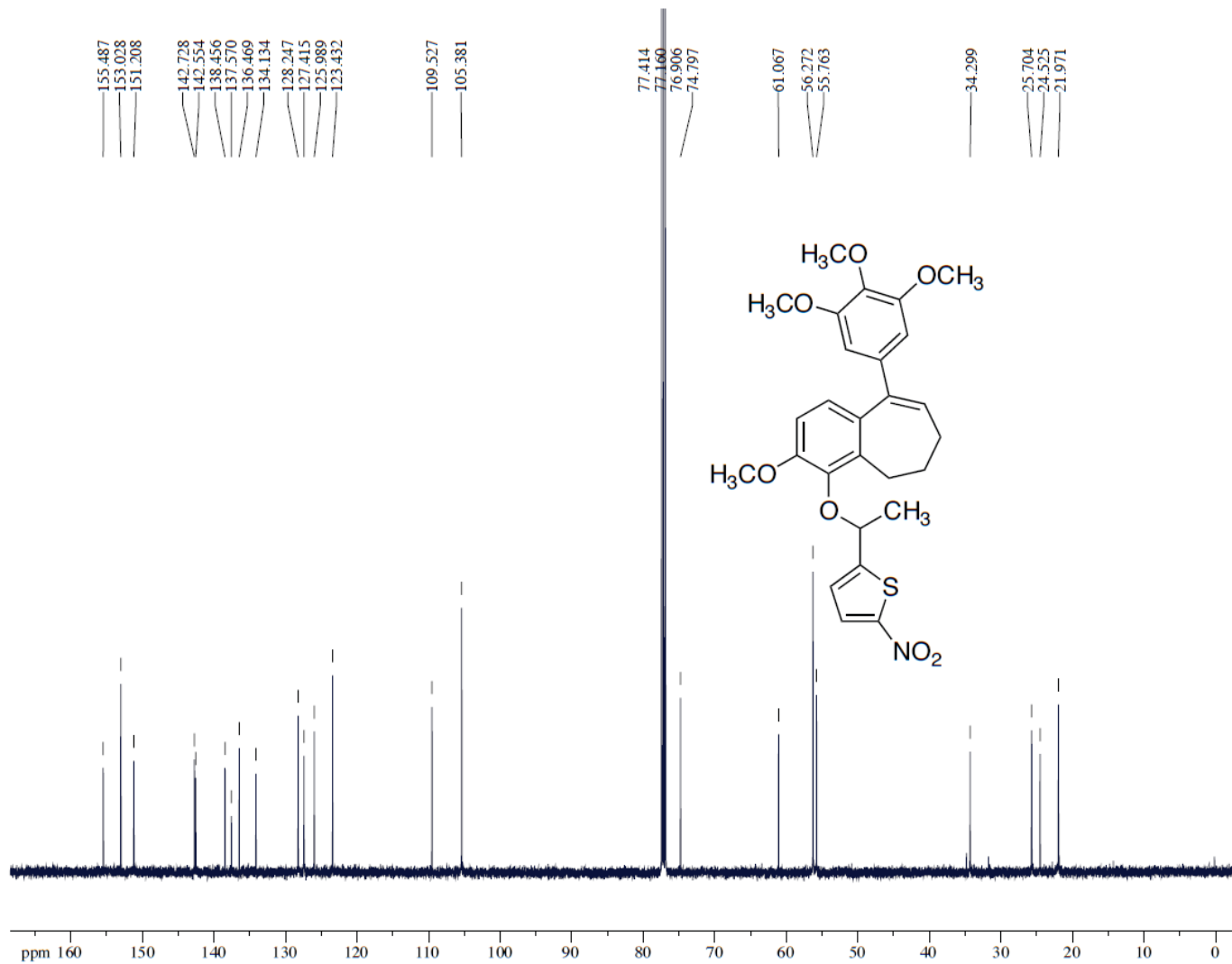
Totals : 1035.16174 84.64111

=====
*** End of Report ***

¹H NMR of 2-(1-((3-methoxy-9-(3,4,5-trimethoxyphenyl)-6,7-dihydro-5H-benzo[7]annulen-4-yl)oxy)ethyl)-5-nitrothiophene **15**



¹³C NMR of 2-(1-((3-methoxy-9-(3,4,5-trimethoxyphenyl)-6,7-dihydro-5H-benzo[7]annulen-4-yl)oxy)ethyl)-5-nitrothiophene **15**



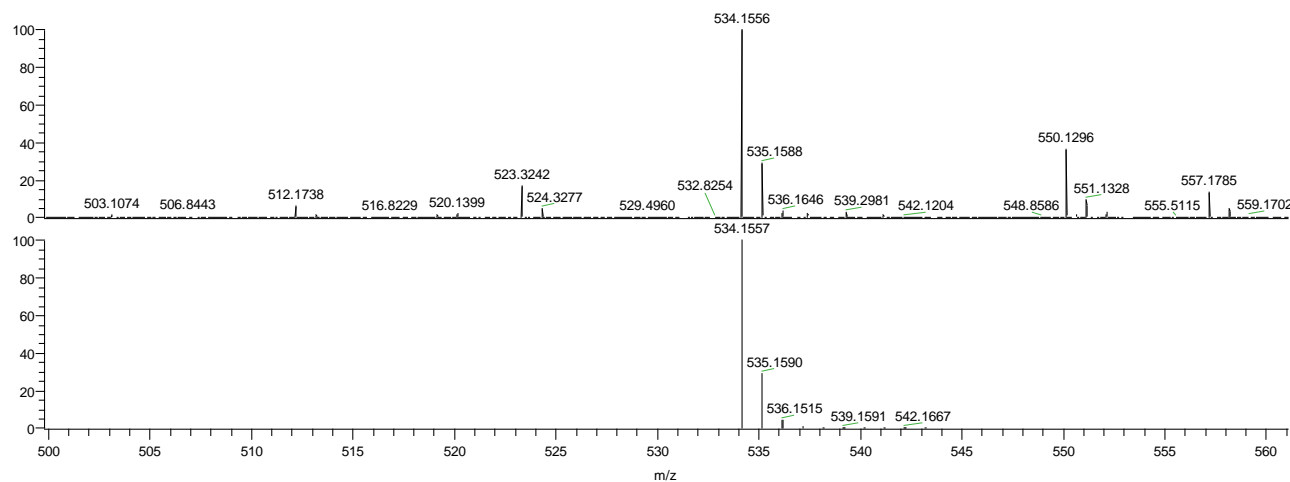
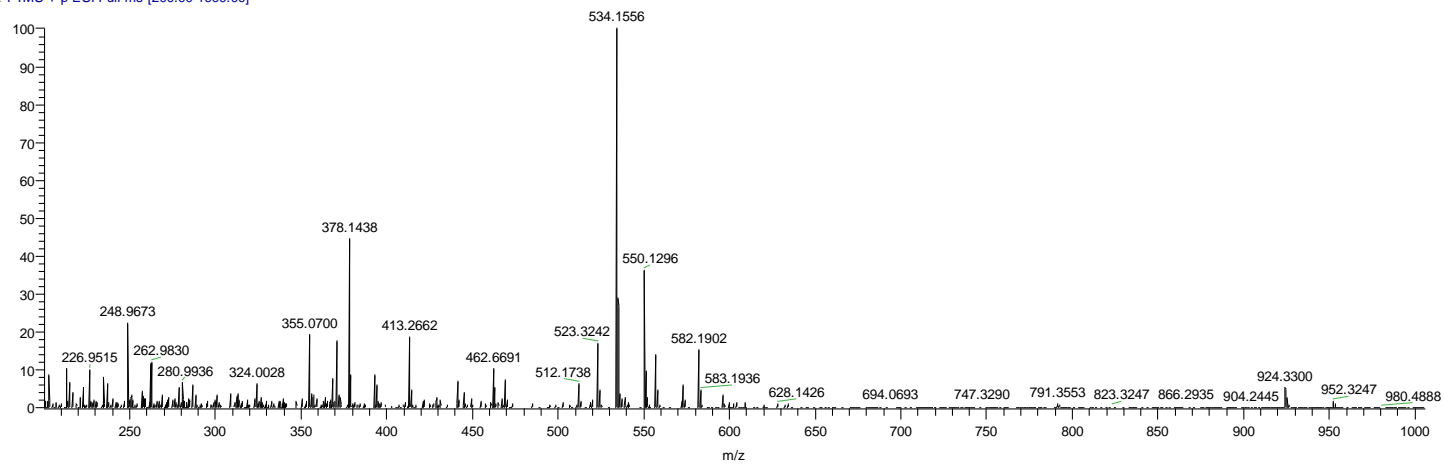
HRMS of 2-(1-((3-methoxy-9-(3,4,5-trimethoxyphenyl)-6,7-dihydro-5H-benzo[7]annulen-4-yl)oxy)ethyl)-5-nitrothiophene 15

C:\Xcalibur\...Zhe\20180409\KGP304_+e⁻

4/9/2018 3:06:18 PM

KGP304_+esi #2-16 RT: 0.01-0.15 AV: 15 NL

T: FTMS + p ESI Full ms [200.00-1000.00]



NL:
7.38E5
KGP304_+esi#2-16
RT: 0.01-0.15 AV: 15
T: FTMS + p ESI Full
ms [200.00-1000.00]

NL:
6.93E5
C₂₇H₂₉NNaO₇S:
C₂₇H₂₉N₁Na₁O₇S₁
pa Chrg 1

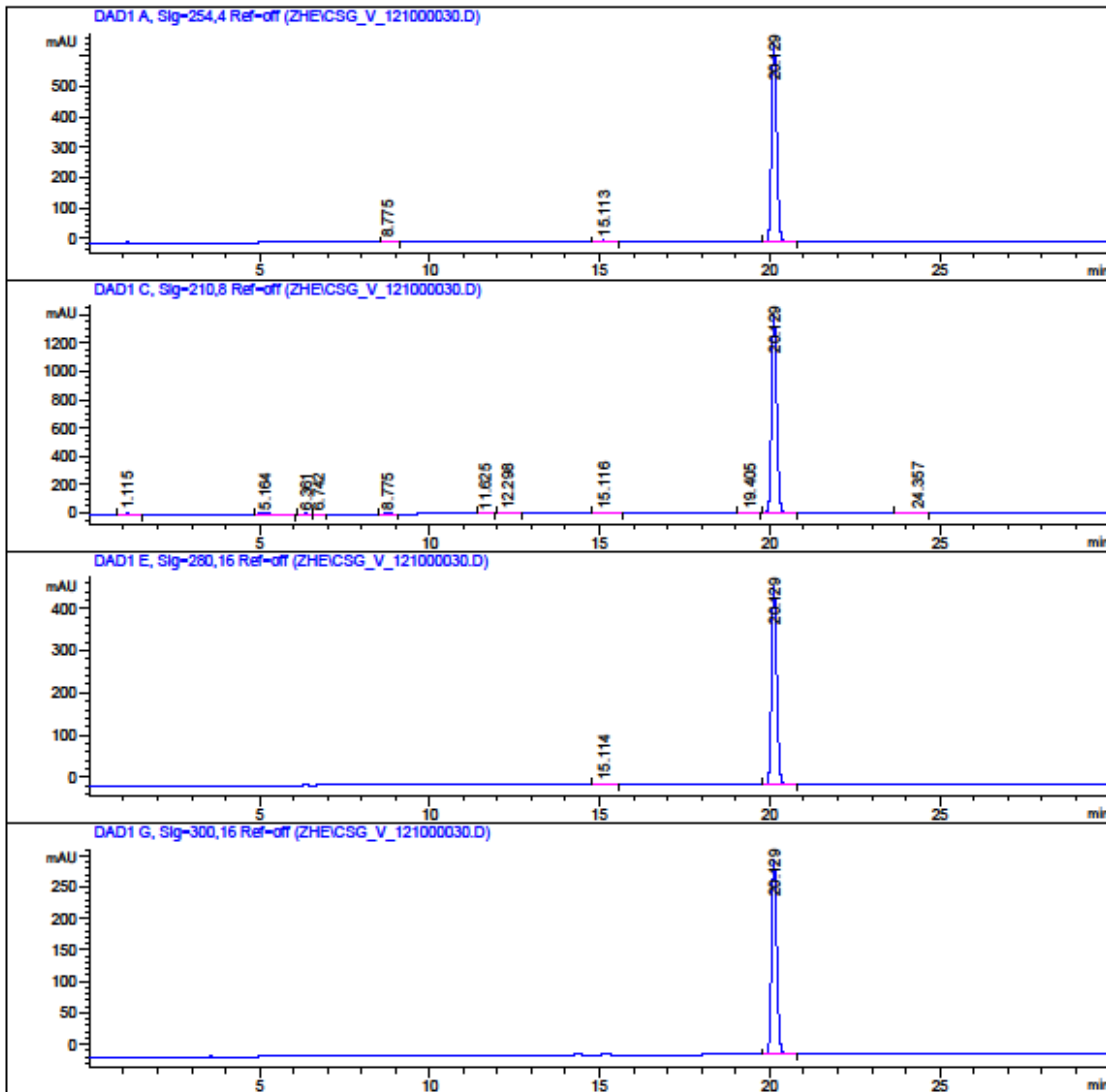
HPLC traces of compound 15

Data File C:\Chem32\1\Data\ZHE\CSG_V_121000030.D

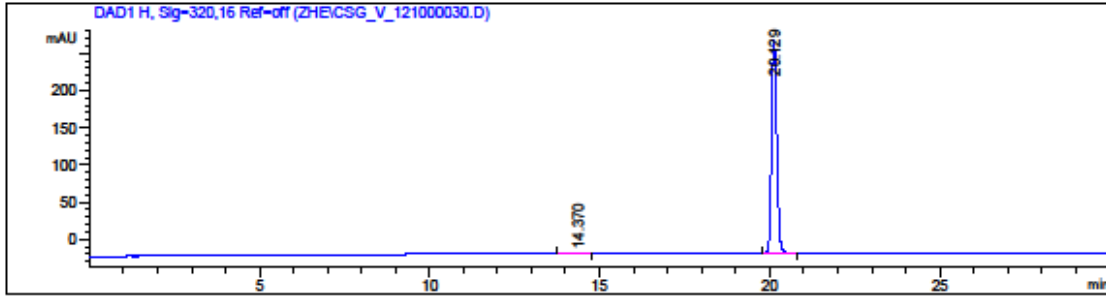
Sample Name: csg_v_121

=====
Acq. Operator : zhe
Acq. Instrument : Instrument 1 Location : -
Injection Date : 5/26/2016 12:27:54 PM
Acq. Method : C:\CHEM32\1\METHODS\GRAD 2 50-90 ACN.M
Last changed : 5/26/2016 12:21:16 PM by zhe
Analysis Method : C:\CHEM32\1\METHODS\RT-ACNWASH 2.M
Last changed : 7/9/2015 2:27:22 PM by Blake
Method Info : General Column Wash Method

Sample Info : csg_v_121
 monomethylnitrothiophene-KGP18
 GRAD 2 50-90 ACN
 20160526



Data File C:\Chem32\1\Data\ZHE\CSG_V_121000030.D
 Sample Name: csg_v_121



=====
 Area Percent Report
 =====

Sorted By : Signal
 Multiplier : 1.0000
 Dilution : 1.0000
 Use Multiplier & Dilution Factor with ISTDs

Signal 1: DAD1 A, Sig=254,4 Ref-off

Peak #	RetTime [min]	Type	Width [min]	Area [mAU*s]	Height [mAU]	Area %
1	8.775	BB	0.1512	13.57231	1.37441	0.1970
2	15.113	BB	0.1725	57.65867	5.00151	0.8369
3	20.129	BB	0.1620	6818.50244	652.01569	98.9661
Totals :				6889.73343	658.39160	

Signal 2: DAD1 C, Sig=210,8 Ref-off

Peak #	RetTime [min]	Type	Width [min]	Area [mAU*s]	Height [mAU]	Area %
1	1.115	BB	0.0835	69.99749	11.74304	0.4592
2	5.164	BB	0.3443	158.17261	5.79756	1.0375
3	6.361	BB	0.1363	33.63096	3.76306	0.2206
4	6.742	BB	0.1317	14.17675	1.65870	0.0930
5	8.775	BB	0.1487	34.68475	3.59144	0.2275
6	11.625	BB	0.1868	24.73398	1.93875	0.1622
7	12.298	BB	0.1690	23.68892	2.17614	0.1554
8	15.116	BB	0.2334	168.22318	9.84212	1.1035
9	19.405	BB	0.1927	30.23411	2.34099	0.1983
10	20.129	BB	0.1628	1.46480e4	1391.95850	96.0845
11	24.357	BB	0.2060	39.37650	2.87048	0.2583
Totals :				1.52449e4	1437.68077	

Data File C:\Chem32\1\Data\ZHE\CSG_V_12100030.D
Sample Name: csg_v_121

Signal 3: DAD1 E, Sig=280,16 Ref=off

Peak #	RetTime [min]	Type	Width [min]	Area [mAU*s]	Height [mAU]	Area %
1	15.114	BB	0.1810	32.63206	2.62612	0.6635
2	20.129	BB	0.1620	4885.21436	467.15475	99.3365
Totals :				4917.84642	469.78087	

Signal 4: DAD1 G, Sig=300,16 Ref=off

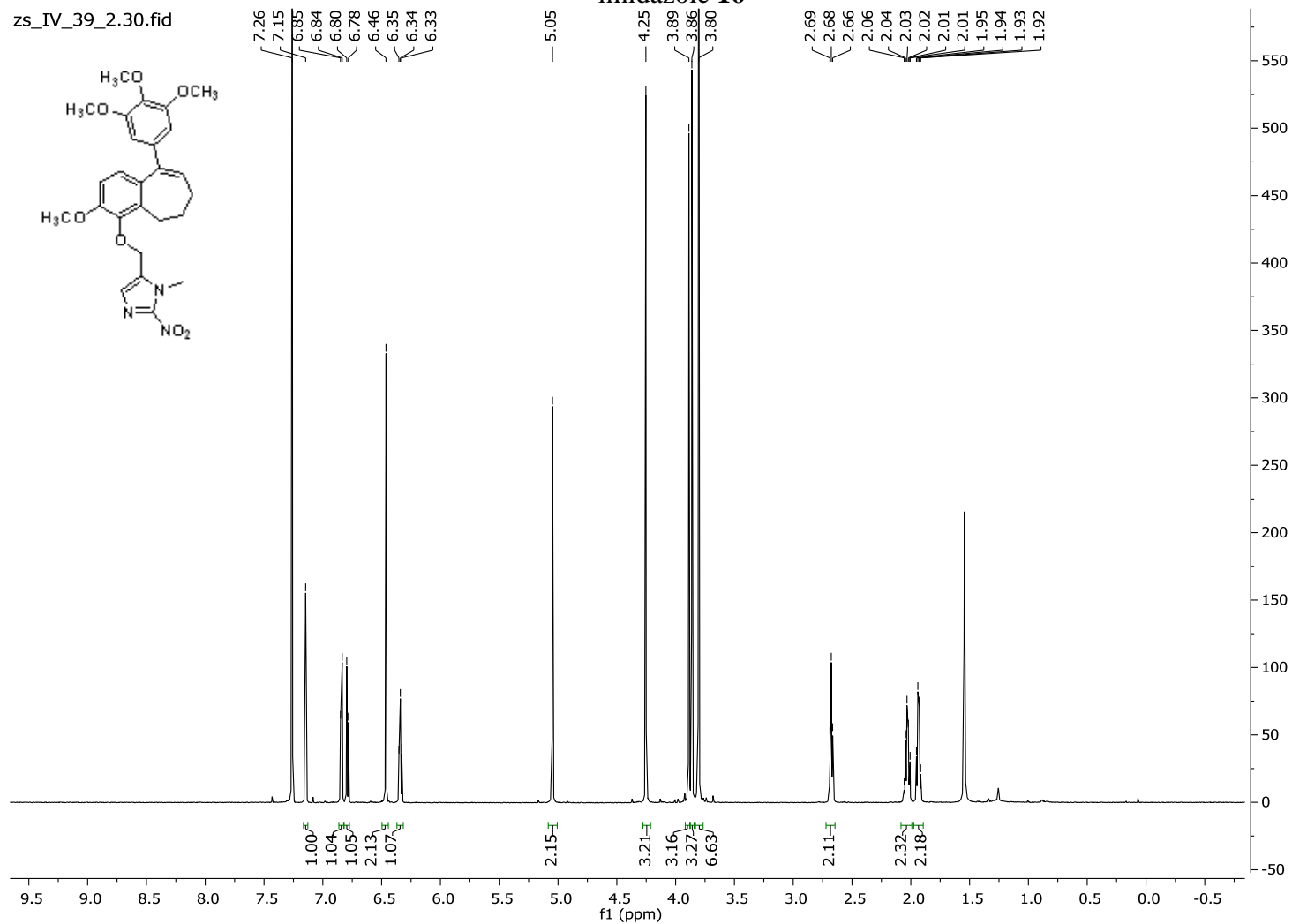
Peak #	RetTime [min]	Type	Width [min]	Area [mAU*s]	Height [mAU]	Area %
1	20.129	BB	0.1621	3257.06250	311.31851	100.0000
Totals :				3257.06250	311.31851	

Signal 5: DAD1 H, Sig=320,16 Ref=off

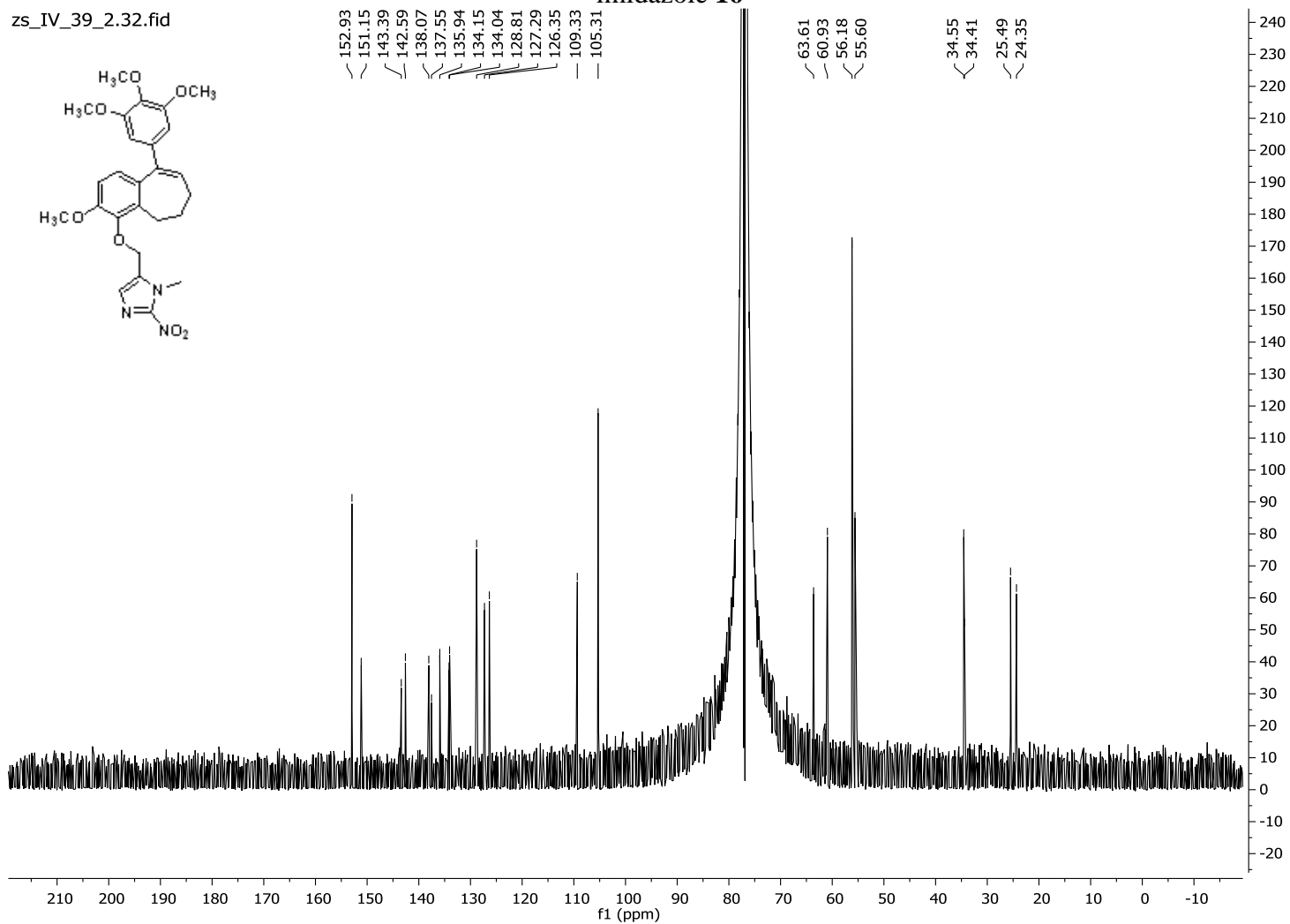
Peak #	RetTime [min]	Type	Width [min]	Area [mAU*s]	Height [mAU]	Area %
1	14.370	BB	0.2870	28.37486	1.49796	0.9392
2	20.129	BB	0.1620	2992.67383	286.07428	99.0608
Totals :				3021.04869	287.57224	

=====
*** End of Report ***

¹H NMR of 5-(((3-methoxy-9-(3,4,5-trimethoxyphenyl)-6,7-dihydro-5H-benzo[7]annulen-4-yl)oxy)methyl)-1-methyl-2-nitro-1H-imidazole **16**



¹H NMR of 5-(((3-methoxy-9-(3,4,5-trimethoxyphenyl)-6,7-dihydro-5H-benzo[7]annulen-4-yl)oxy)methyl)-1-methyl-2-nitro-1H-imidazole **16**

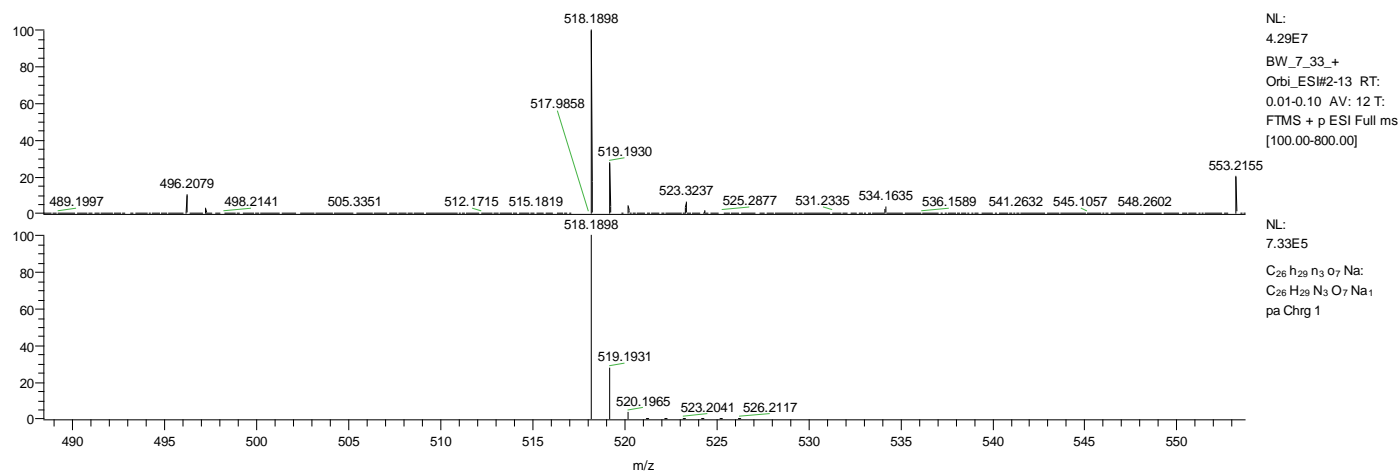
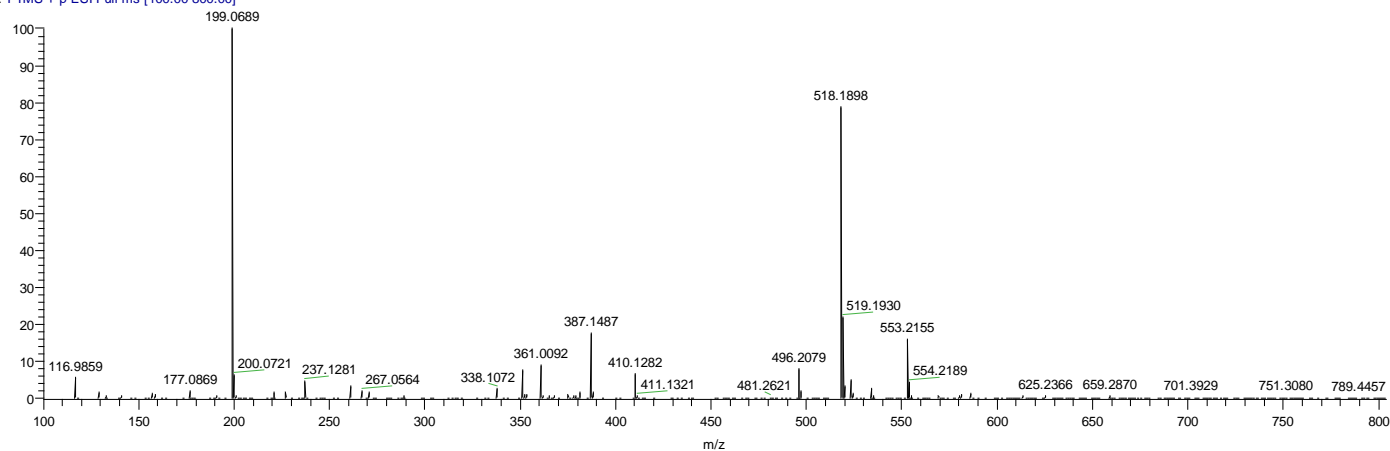


HRMS of 5-(((3-methoxy-9-(3,4,5-trimethoxyphenyl)-6,7-dihydro-5H-benzo[7]annulen-4-yl)oxy)methyl)-1-methyl-2-nitro-1H-imidazole **16**

C:\Xcalibur\...BW_7_33_+Orbi_ESI

4/27/2016 1:46:17 PM

BW_7_33_+Orbi_ESI #2-13 RT: 0.01-0.10 AV:
T: FTMS + p ESI Full ms [100.00-800.00]



NL:
4.29E7
BW_7_33_+
Orbi_ESI#2-13 RT:
0.01-0.10 AV: 12 T:
FTMS + p ESI Full ms
[100.00-800.00]

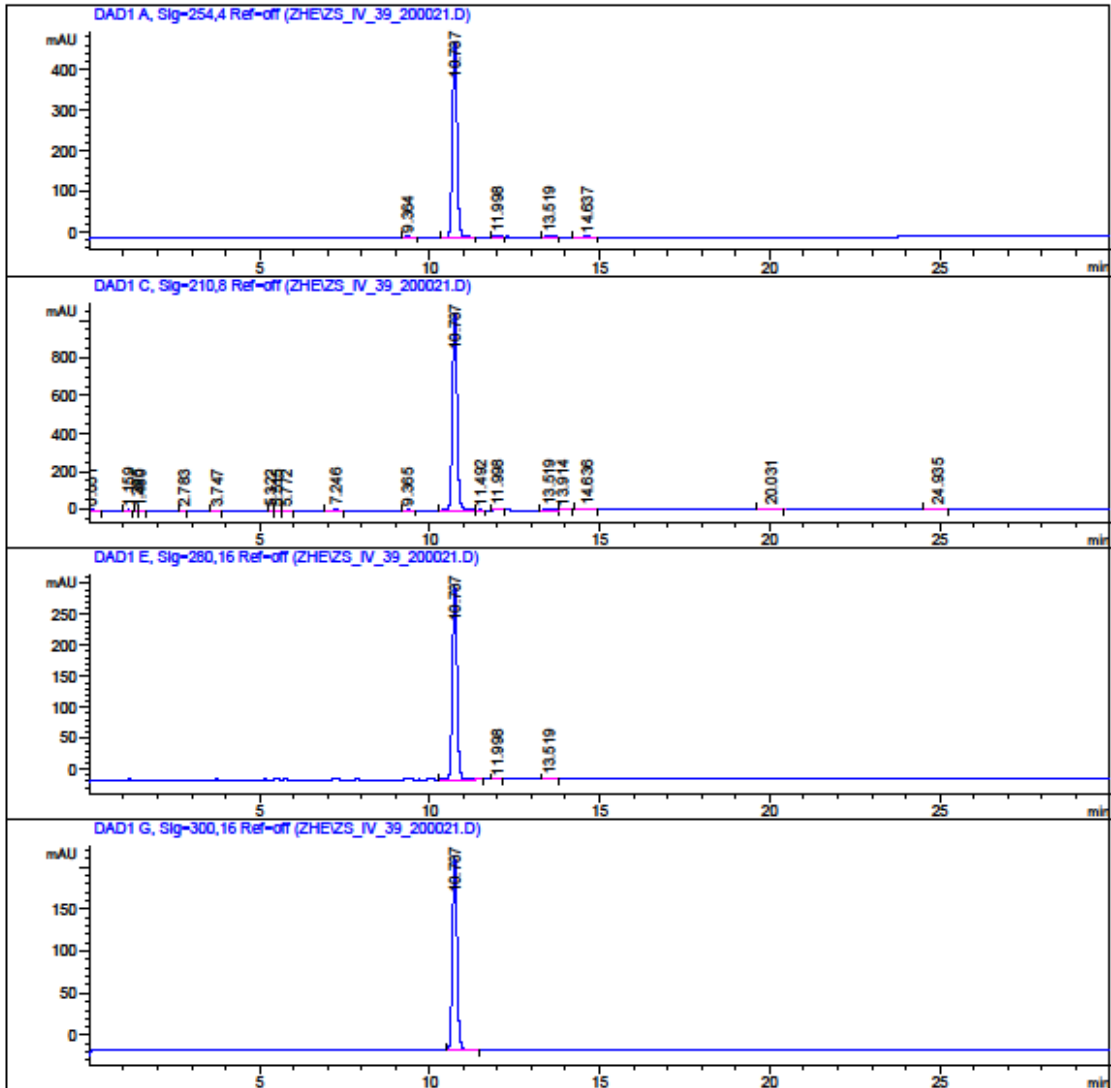
NL:
7.33E5
C₂₆H₂₉N₃O₇Na
C₂₆H₂₉N₃O₇Na
pa Chrg 1

HPLC traces of compound 16

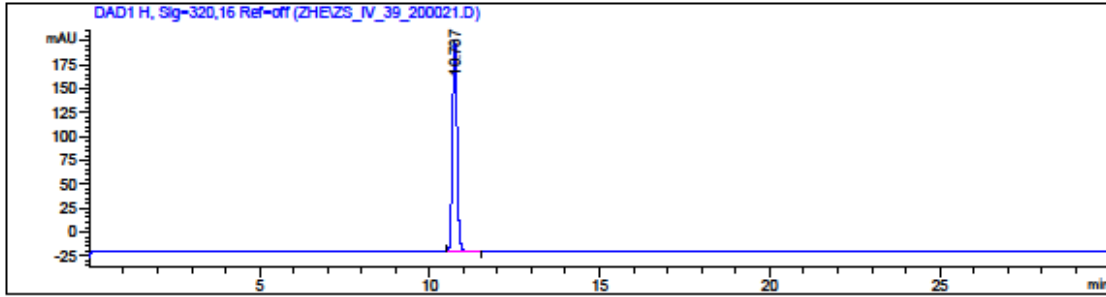
Data File C:\Chem32\1\Data\ZHE\ZS_IV_39_200021.D
Sample Name: zs_IV_39_2

Acq. Operator : Zhe
Acq. Instrument : Instrument 1 Location : -
Injection Date : 5/25/2016 12:24:32 PM
Acq. Method : C:\CHEM32\1\METHODS\GRAD 2 50-90 ACN.M
Last changed : 5/25/2016 12:22:35 PM by Zhe
Analysis Method : C:\CHEM32\1\METHODS\RT-ACNWASH 2.M
Last changed : 7/9/2015 2:27:22 PM by Blake
Method Info : General Column Wash Method

Sample Info : zs_IV_39_2
KGP 293
normethylnitroimidazole-KGP18
GRAD 2 50-90 ACN
20160525



Data File C:\Chem32\1\Data\ZHE\ZS_IV_39_200021.D
 Sample Name: zs_IV_39_2



=====
 Area Percent Report
 =====

Sorted By : Signal
 Multiplier : 1.0000
 Dilution : 1.0000
 Use Multiplier & Dilution Factor with ISTDs

Signal 1: DAD1 A, Sig=254,4 Ref=off

Peak #	RetTime [min]	Type	Width [min]	Area [mAU*s]	Height [mAU]	Area %
1	9.364	BB	0.1481	10.64091	1.10784	0.2329
2	10.737	BB	0.1424	4483.29834	482.45068	98.1124
3	11.998	BV	0.1491	26.46362	2.77853	0.5791
4	13.519	BB	0.1803	33.96112	2.82498	0.7432
5	14.637	BB	0.1659	15.18865	1.40725	0.3324

Totals : 4569.55263 490.56929

Signal 2: DAD1 C, Sig=210,8 Ref=off

Peak #	RetTime [min]	Type	Width [min]	Area [mAU*s]	Height [mAU]	Area %
1	0.051	BB	0.1066	41.25443	5.68900	0.4007
2	1.159	BB	0.0634	40.82954	9.26910	0.3965
3	1.395	BV	0.0595	6.40275	1.64135	0.0622
4	1.480	VB	0.0833	6.22000	1.01708	0.0604
5	2.783	BB	0.0793	6.71858	1.32192	0.0653
6	3.747	BV	0.0903	14.63146	2.42814	0.1421
7	5.322	VV	0.1097	11.44702	1.55894	0.1112
8	5.515	VV	0.1137	16.63885	2.21422	0.1616
9	5.772	VB	0.1258	8.65554	1.03230	0.0841
10	7.246	BB	0.1326	58.78048	6.68392	0.5709
11	9.365	BB	0.1478	27.24378	2.89511	0.2646
12	10.737	BV	0.1433	9793.47168	1045.34851	95.1141
13	11.492	VB	0.1425	10.14302	1.09025	0.0985
14	11.998	BB	0.1428	53.51123	5.95866	0.5197

Data File C:\Chem32\1\Data\ZHE\ZS_IV_39_200021.D
Sample Name: zs_IV_39_2

Peak #	RetTime [min]	Type	Width [min]	Area [mAU*s]	Height [mAU]	Area %
15	13.519	BV	0.1894	93.14103	7.27567	0.9046
16	13.914	VB	0.1581	10.75116	1.02733	0.1044
17	14.636	BB	0.1677	36.43460	3.38132	0.3539
18	20.031	BB	0.1938	20.10485	1.56616	0.1953
19	24.935	BB	0.2022	40.17056	3.03976	0.3901
Totals :				1.02966e4	1104.43875	

Signal 3: DAD1 E, Sig=280,16 Ref=off

Peak #	RetTime [min]	Type	Width [min]	Area [mAU*s]	Height [mAU]	Area %
1	10.737	BB	0.1426	2938.32471	315.77563	99.0735
2	11.998	BV	0.1466	11.02297	1.18411	0.3717
3	13.519	BB	0.1787	16.45601	1.38402	0.5549
Totals :				2965.80369	318.34377	

Signal 4: DAD1 G, Sig=300,16 Ref=off

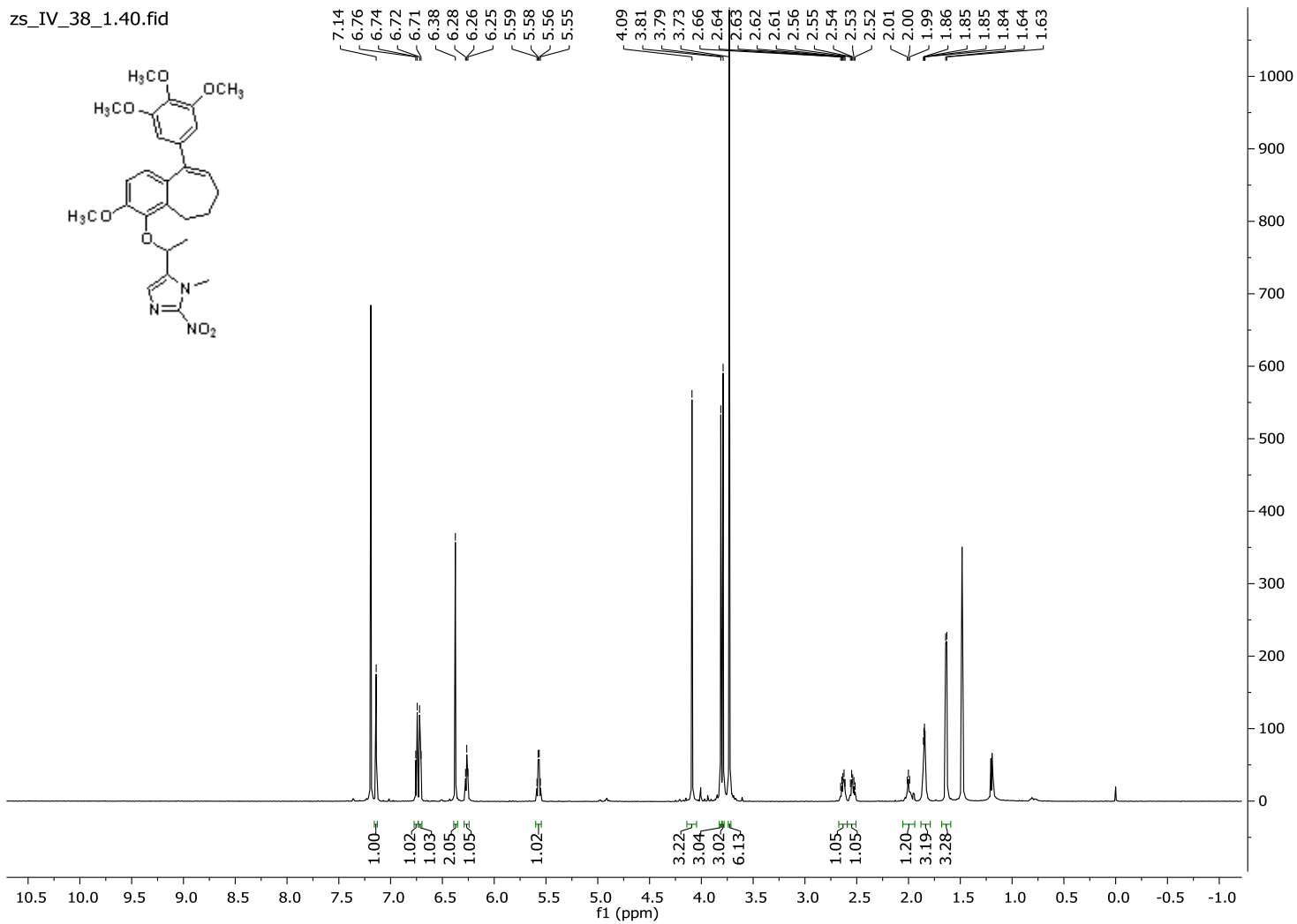
Peak #	RetTime [min]	Type	Width [min]	Area [mAU*s]	Height [mAU]	Area %
1	10.737	BB	0.1420	2133.37476	230.35779	100.0000
Totals :				2133.37476	230.35779	

Signal 5: DAD1 H, Sig=320,16 Ref=off

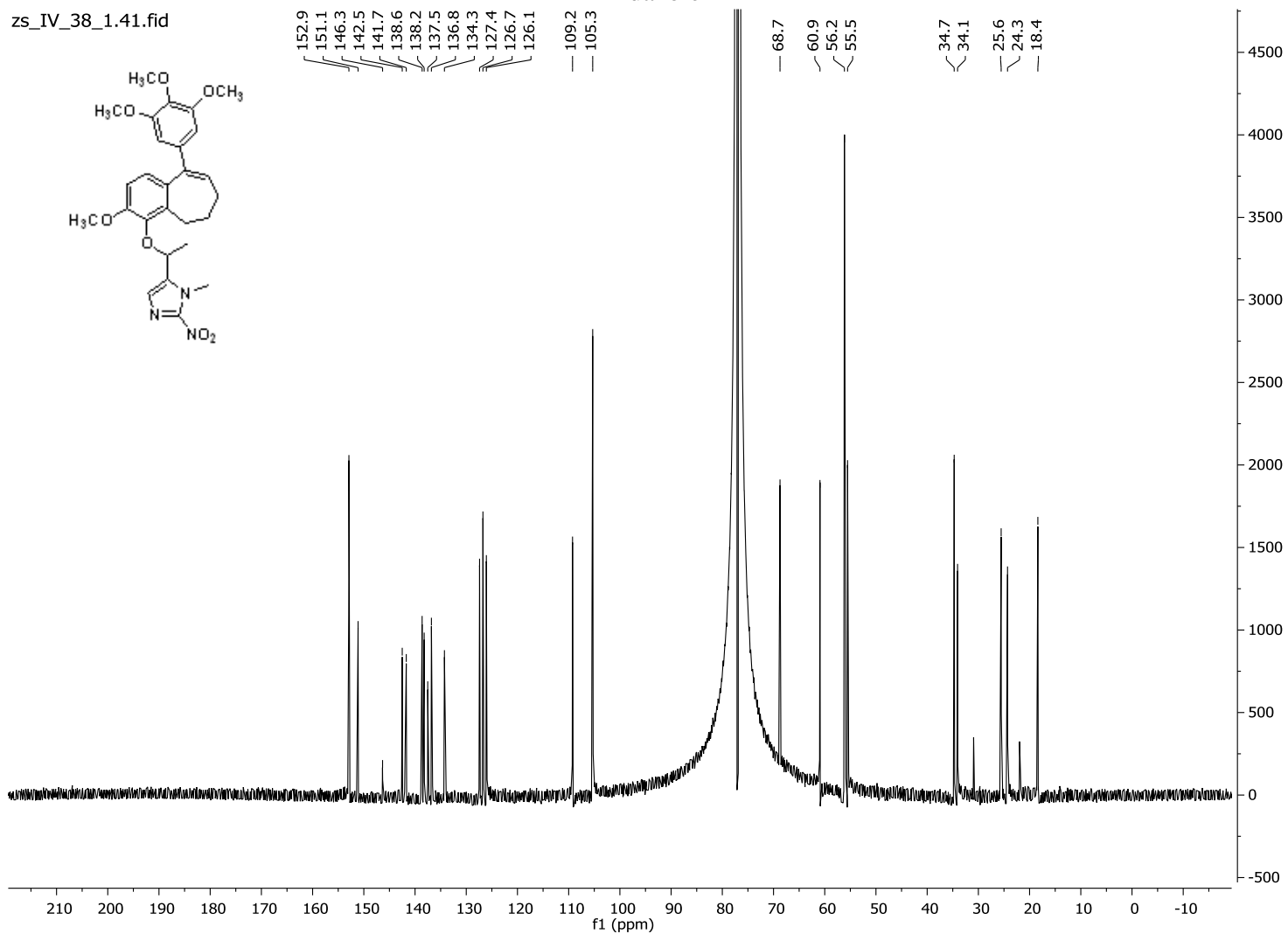
Peak #	RetTime [min]	Type	Width [min]	Area [mAU*s]	Height [mAU]	Area %
1	10.737	BB	0.1420	2049.19653	221.43524	100.0000
Totals :				2049.19653	221.43524	

=====
*** End of Report ***

¹H NMR of 5-(1-((3-methoxy-9-(3,4,5-trimethoxyphenyl)-6,7-dihydro-5H-benzo[7]annulen-4-yl)oxy)ethyl)-1-methyl-2-nitro-1H-imidazole **17**



¹³C NMR of 5-(1-((3-methoxy-9-(3,4,5-trimethoxyphenyl)-6,7-dihydro-5H-benzo[7]annulen-4-yl)oxy)ethyl)-1-methyl-2-nitro-1H-imidazole **17**

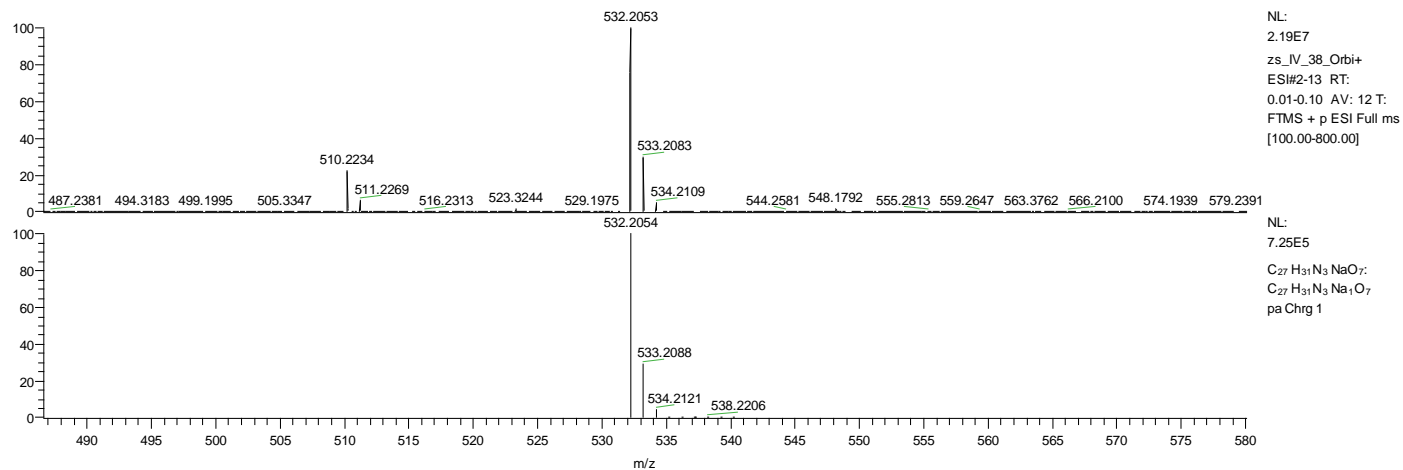
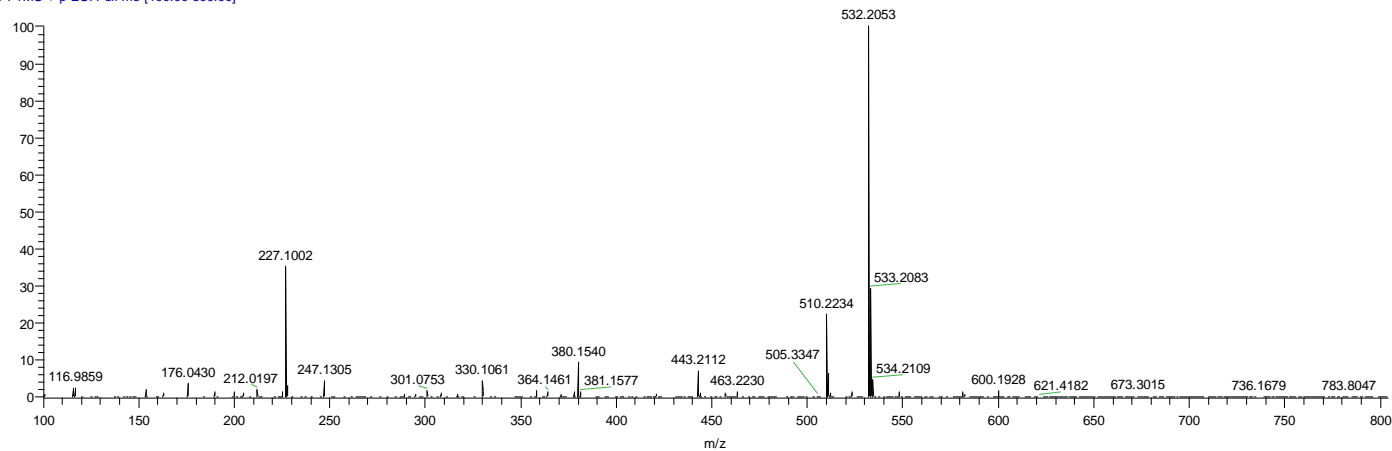


HRMS of 5-(1-((3-methoxy-9-(3,4,5-trimethoxyphenyl)-6,7-dihydro-5H-benzo[7]annulen-4-yl)oxy)ethyl)-1-methyl-2-nitro-1H-imidazole 17

C:\Xcalibur\...zs_IV_38_Orbi+ESI

5/2/2016 3:34:08 PM

zs_IV_38_Orbi+ESI #2-13 RT: 0.01-0.10 AV: 1:
T: FTMS + p ESI Full ms [100.00-800.00]



NL:
2.19E7
zs_IV_38_Orbi+
ESI#2-13 RT:
0.01-0.10 AV: 12 T:
FTMS + p ESI Full ms
[100.00-800.00]

NL:
7.25E5
C₂₇H₃₁N₃NaO₇:
C₂₇H₃₁N₃Na₁O₇:
pa Chrg 1

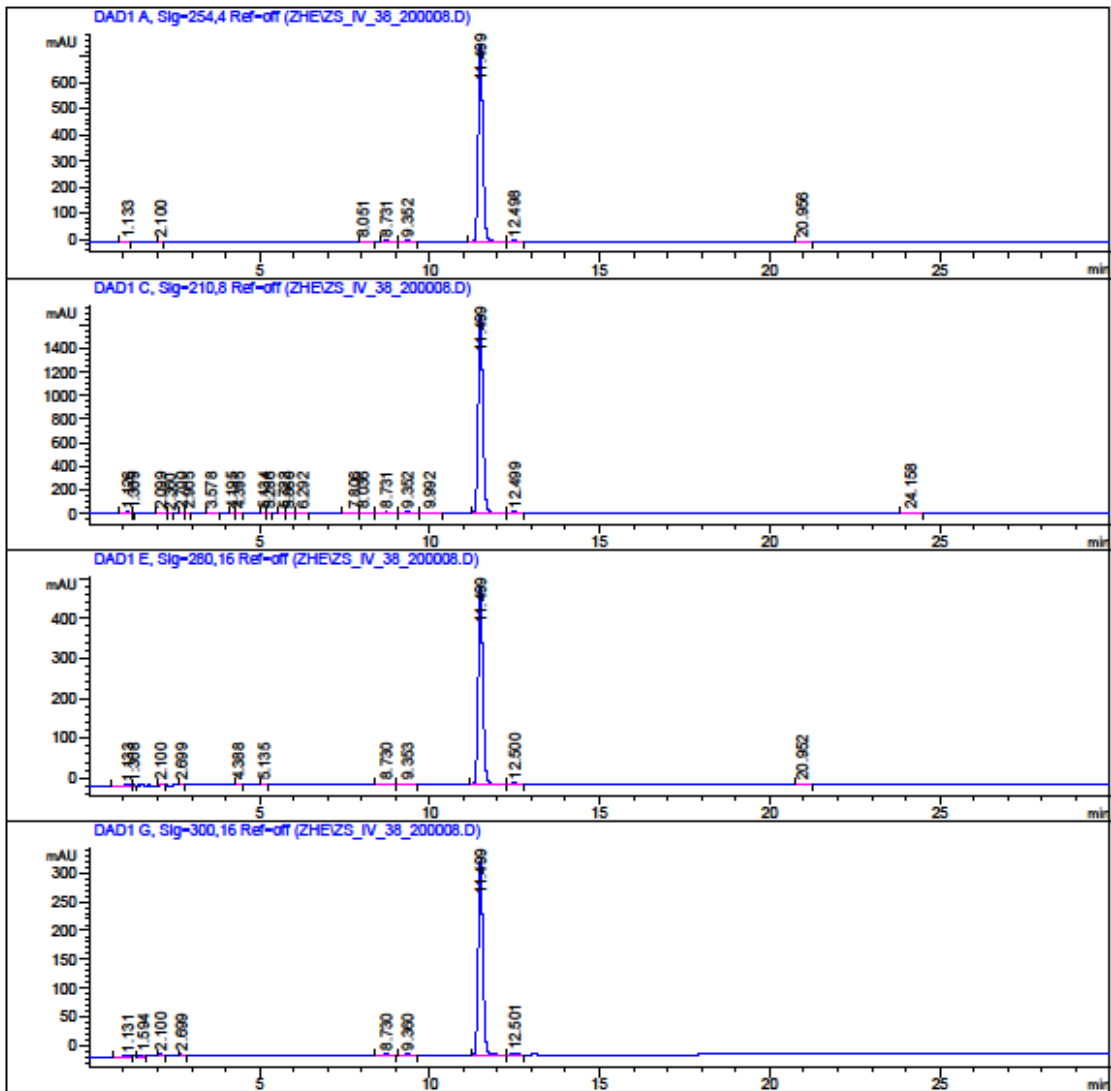
HPLC traces of Compound 17

Data File C:\Chem32\1\Data\ZHE\ZS_IV_38_200008.D

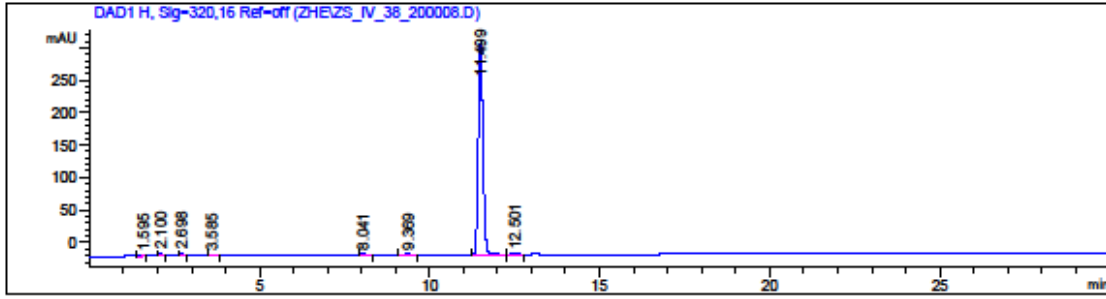
Sample Name: zs_IV_38_2

=====
Acq. Operator : zhe
Acq. Instrument : Instrument 1 Location : -
Injection Date : 5/5/2016 12:03:07 PM
Acq. Method : C:\CHEM32\1\METHODS\GRAD 2 50-90 ACN.M
Last changed : 5/5/2016 11:51:25 AM by zhe
Analysis Method : C:\CHEM32\1\METHODS\RT-ACNWASH 2.M
Last changed : 7/9/2015 2:27:22 PM by Blake
Method Info : General Column Wash Method

Sample Info : zs_IV_38_2
KGP18-monomethyl nitroimidazole
GRAD2 ACN 50-90



Sample Name: zs_IV_38_2



=====
 Area Percent Report
 =====

Sorted By : Signal
 Multiplier : 1.0000
 Dilution : 1.0000
 Use Multiplier & Dilution Factor with ISTDs

Signal 1: DAD1 A, Sig=254,4 Ref=off

Peak #	RetTime [min]	Type	Width [min]	Area [mAU*s]	Height [mAU]	Area %
1	1.133	BB	0.0924	9.27913	1.45485	0.1266
2	2.100	BV	0.0580	6.46301	1.71326	0.0882
3	8.051	BB	0.1354	10.94999	1.23606	0.1494
4	8.731	BB	0.1383	34.64928	3.87737	0.4726
5	9.352	BB	0.1515	49.93470	5.04215	0.6811
6	11.499	BV	0.1456	7146.90625	760.60394	97.4804
7	12.498	VB	0.1558	48.08035	4.76298	0.6558
8	20.956	BB	0.2606	25.37336	1.60372	0.3461

Totals : 7331.63608 780.29433

Signal 2: DAD1 C, Sig=210,8 Ref=off

Peak #	RetTime [min]	Type	Width [min]	Area [mAU*s]	Height [mAU]	Area %
1	1.126	BV	0.0833	80.91444	14.90394	0.4844
2	1.309	VV	0.0567	7.45635	1.94705	0.0446
3	2.099	BV	0.0776	15.72043	2.88344	0.0941
4	2.360	VB	0.0651	6.67961	1.58807	0.0400
5	2.700	BV	0.0696	17.16201	3.73572	0.1027
6	2.905	VV	0.0758	6.62650	1.33727	0.0397
7	3.578	BB	0.1048	17.86118	2.51697	0.1069
8	4.195	VV	0.0911	17.36708	2.84933	0.1040
9	4.395	VV	0.1013	13.71676	2.07060	0.0821
10	5.134	BV	0.0937	18.59568	3.02740	0.1113
11	5.286	VB	0.0980	10.67476	1.68193	0.0639

Data File C:\Chem32\1\Data\ZHE\ZS_IV_38_200008.D

Sample Name: zs_IV_38_2

Peak #	RetTime [min]	Type	Width [min]	Area [mAU*s]	Height [mAU]	Area %
12	5.722	BV	0.1337	21.27279	2.18244	0.1273
13	5.860	VB	0.1106	18.20321	2.45211	0.1090
14	6.292	BB	0.1253	12.25700	1.46969	0.0734
15	7.806	BV	0.1349	45.46303	4.96064	0.2721
16	8.036	VB	0.1438	62.68601	6.53897	0.3752
17	8.731	BB	0.1415	95.28065	10.33580	0.5704
18	9.352	BV	0.1579	140.55745	13.67223	0.8414
19	9.992	VB	0.2555	27.73345	1.50149	0.1660
20	11.499	BV	0.1467	1.59298e4	1679.48901	95.3560
21	12.499	VB	0.1524	120.07780	12.03566	0.7188
22	24.158	BB	0.1896	19.50130	1.56271	0.1167

Totals : 1.67056e4 1774.74247

Signal 3: DAD1 E, Sig=280,16 Ref=off

Peak #	RetTime [min]	Type	Width [min]	Area [mAU*s]	Height [mAU]	Area %
1	1.133	BV	0.1311	14.51148	1.55142	0.3009
2	1.308	VB	0.0633	5.32972	1.26033	0.1105
3	2.100	BB	0.0581	8.32161	2.20213	0.1725
4	2.699	BB	0.0667	5.14825	1.18580	0.1067
5	4.388	BB	0.0913	6.79379	1.17842	0.1409
6	5.135	BB	0.0890	6.98379	1.25374	0.1448
7	8.730	BB	0.1429	25.02022	2.68090	0.5187
8	9.353	BB	0.1535	30.43494	3.07317	0.6310
9	11.499	BV	0.1456	4667.32764	496.72919	96.7685
10	12.500	VB	0.1518	36.16943	3.64322	0.7499
11	20.952	BB	0.2675	17.14849	1.06702	0.3555

Totals : 4823.18937 515.82534

Signal 4: DAD1 G, Sig=300,16 Ref=off

Peak #	RetTime [min]	Type	Width [min]	Area [mAU*s]	Height [mAU]	Area %
1	1.131	BV	0.1201	8.26240	1.00280	0.2497
2	1.594	BV	0.0739	8.13209	1.53150	0.2458
3	2.100	BV	0.0614	16.32239	4.01500	0.4933
4	2.699	BB	0.0678	12.69180	2.85899	0.3836
5	8.730	BB	0.1445	12.70976	1.31765	0.3841
6	9.360	BB	0.1499	15.29956	1.56725	0.4624
7	11.499	BB	0.1455	3213.00366	342.38644	97.1032
8	12.501	BB	0.1462	22.43407	2.37462	0.6780

Totals : 3308.85573 357.05426

Data File C:\Chem32\1\Data\ZHE\ZS_IV_38_200008.D
Sample Name: zs_IV_38_2

Signal 5: DAD1 H, Sig=320,16 Ref=off

Peak #	RetTime [min]	Type	Width [min]	Area [mAU*s]	Height [mAU]	Area %
1	1.595	BV	0.0682	12.10355	2.60457	0.3780
2	2.100	BV	0.0645	18.00180	4.15635	0.5622
3	2.698	BB	0.0675	19.07925	4.31986	0.5959
4	3.585	BB	0.0842	7.96521	1.40347	0.2488
5	8.041	VB	0.1351	10.68806	1.20914	0.3338
6	9.369	BB	0.1388	13.32180	1.45494	0.4161
7	11.499	BB	0.1454	3099.98657	330.51221	96.8177
8	12.501	BB	0.1465	20.73283	2.18976	0.6475

Totals : 3201.87906 347.85029

=====
*** End of Report ***

APPENDIX D

Mechanistic Considerations in the Synthesis of 2-Aryl-Indole Analogues under Bischler-Mohlau Conditions

This appendix published as: MacDonough, M. T.; Shi, Z.; Pinney, K. G. Mechanistic considerations in the synthesis of 2-aryl-indole analogues under Bischler–Mohlau conditions. *Tetrahedron Letters*, **2015**, *56*, 3624-3629.

The author Zhe Shi contributed to this manuscript through re-synthesis of the ^{13}C isotope labelled indole analogue and full characterization of this final compound including NMR, HPLC, HRMS and crystallization. In addition, Zhe Shi contributed a significant amount to the preparation of the supporting material and editing of the manuscript.

Supplementary Data

Mechanistic Considerations in the Synthesis of 2-Aryl-Indole Analogues under
Bischler-Mohrlau Conditions

Matthew T. MacDonough^a, Zhe Shi^a, and Kevin G. Pinney^{a,*}

^aDepartment of Chemistry and Biochemistry, Baylor University, One Bear Place #97348,
Waco, Texas 76798-7348, United States of America (USA)

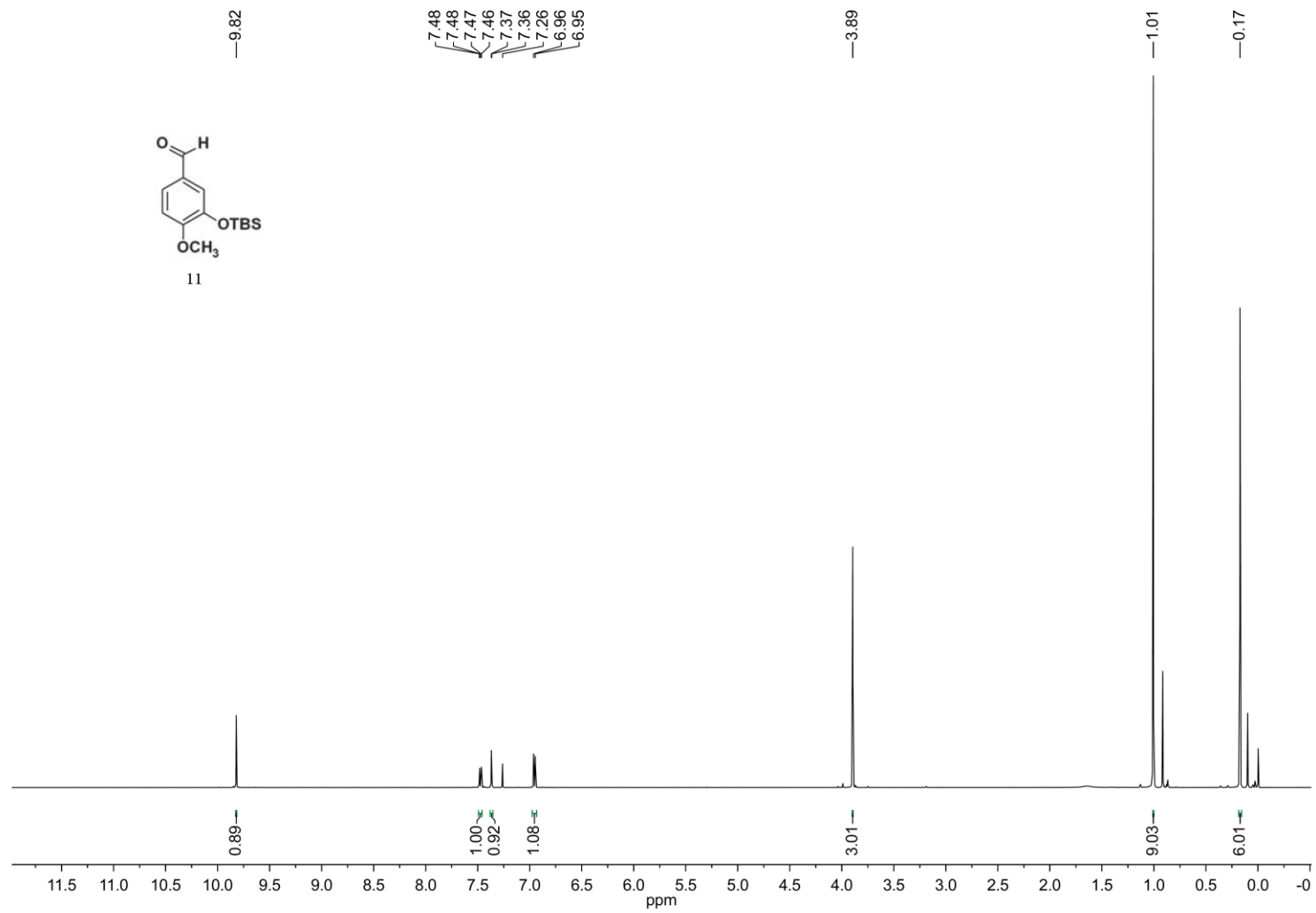
*Corresponding author. Tel.: 254-710-4117

Email address: Kevin_Pinney@baylor.edu

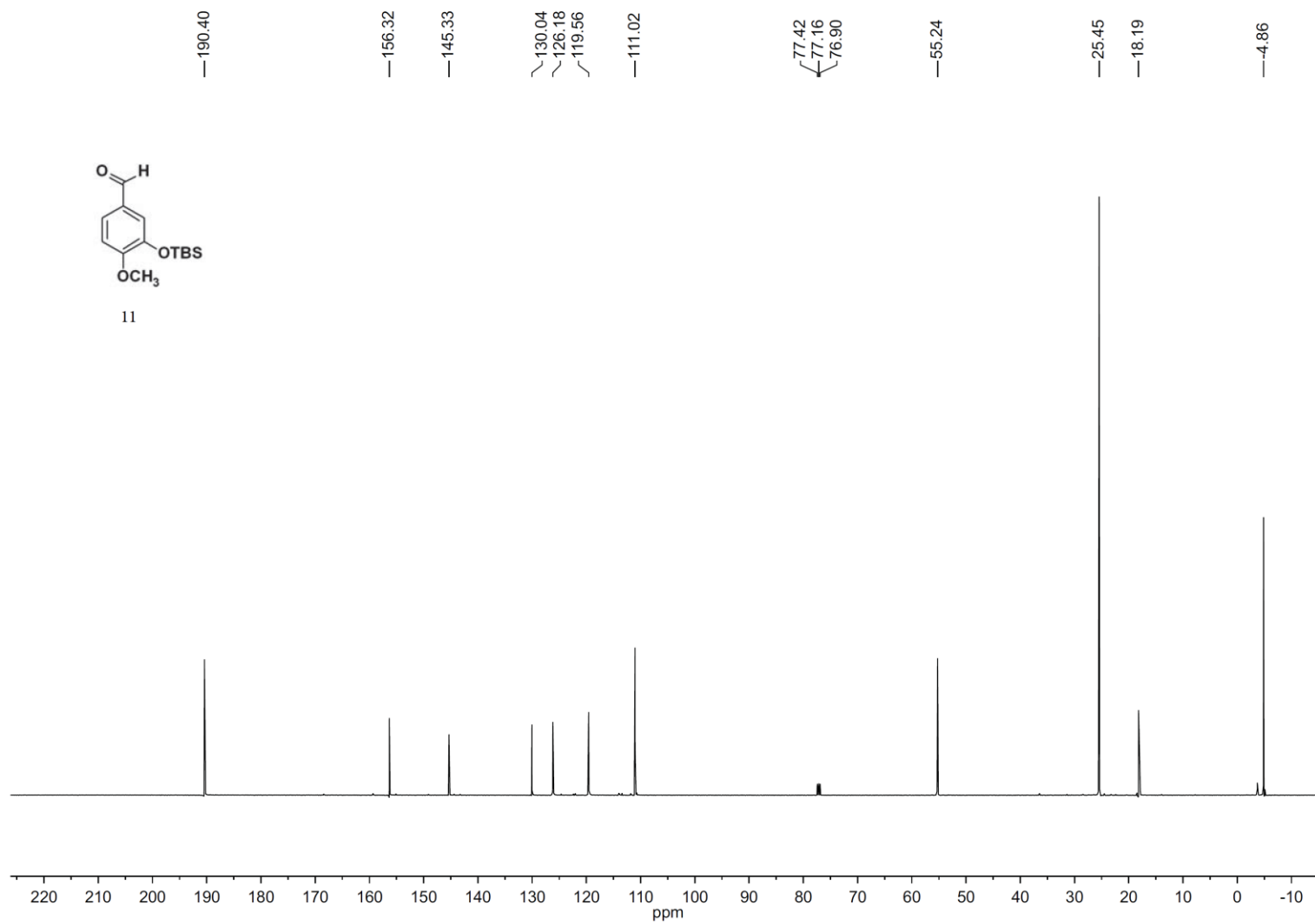
Appendix D Table of Contents

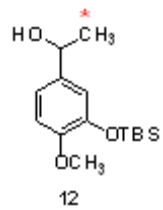
NMR Spectra, HPLC Traces, and HRMS Data for Compounds	303
DEPT NMR for ¹³ C Labeled Indole 16	323
Predicted (ChemBioDraw, Version 13.0.2.3020) ¹³ C NMR Values for Possible Indole Regioisomers.....	329
X-ray Crystallographic Data for ¹³ C Labeled Indole 16	330

¹H NMR (500 MHz, CDCl₃) of Compound **11**

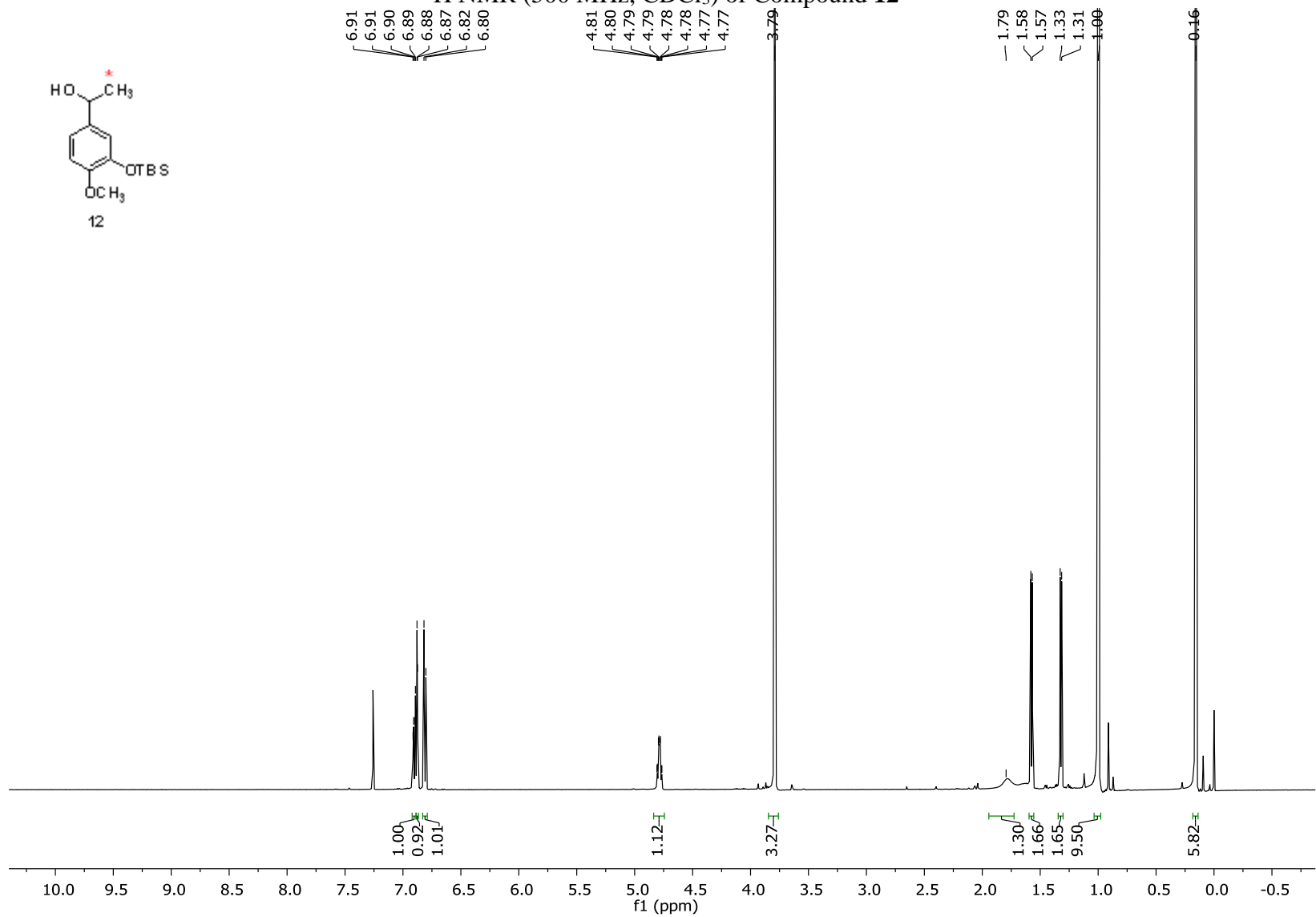


¹³C NMR (125 MHz, CDCl₃) of Compound **11**

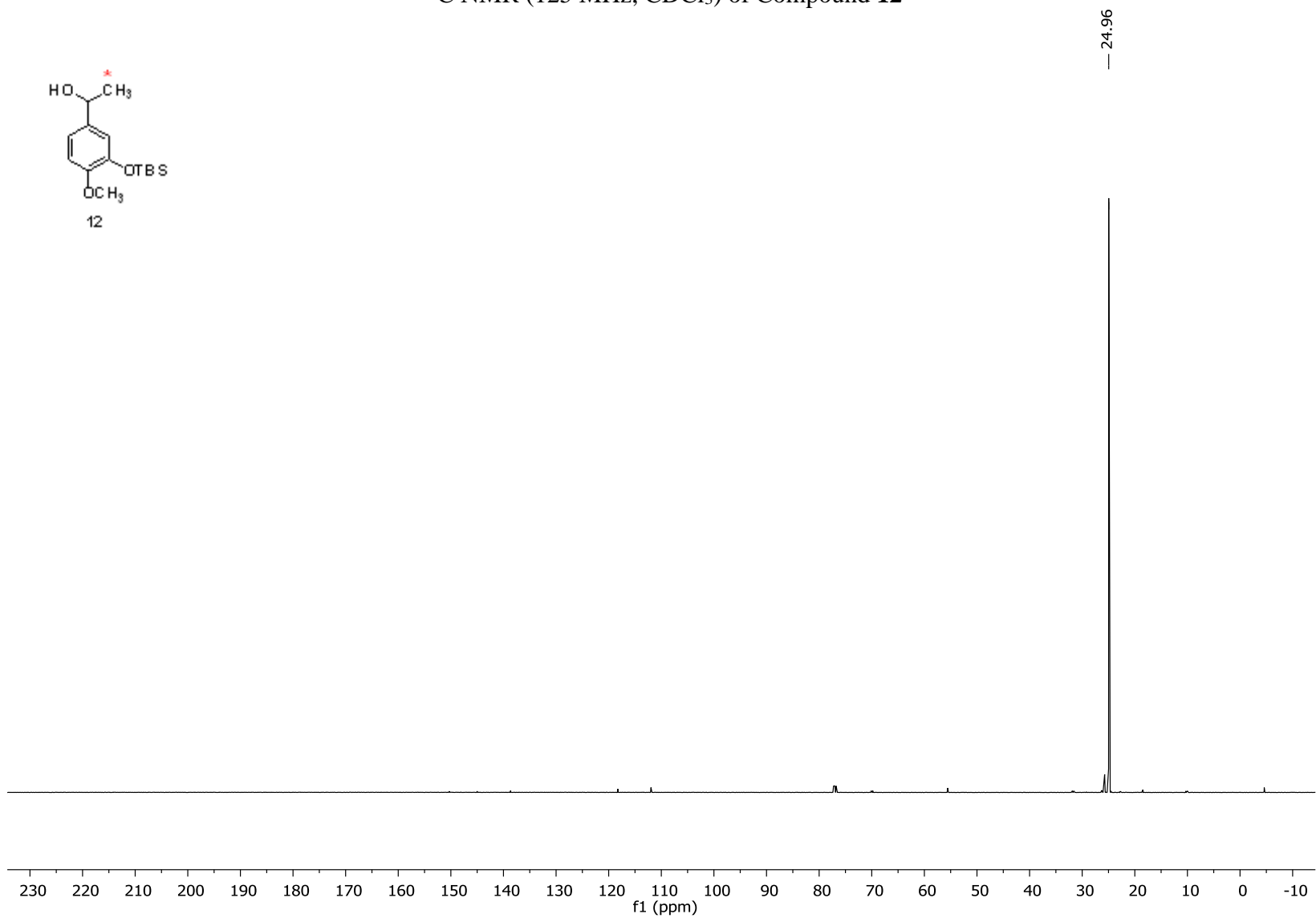
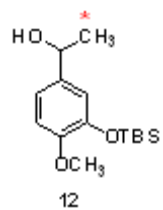




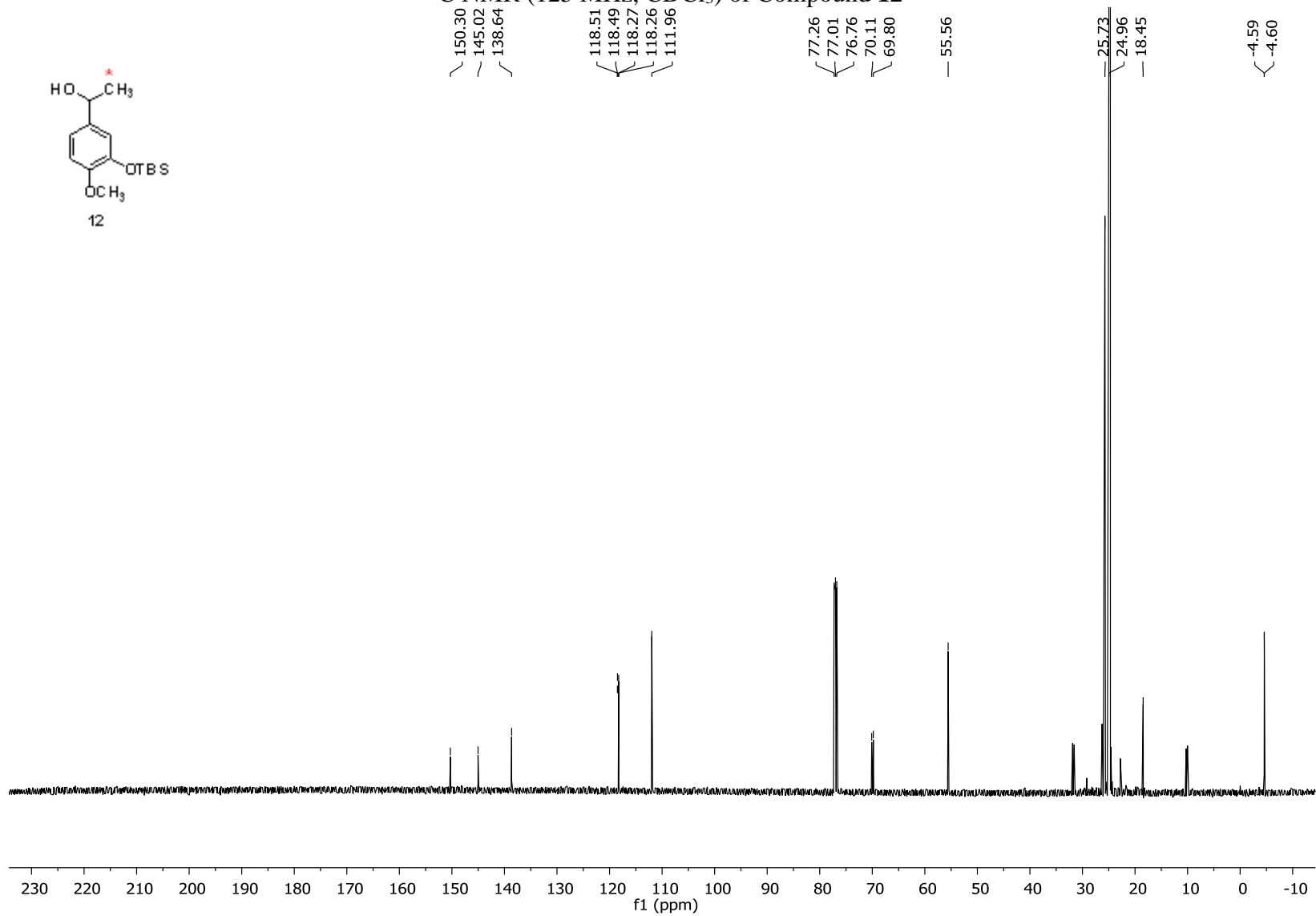
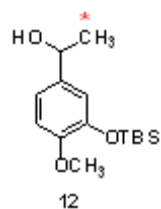
^1H NMR (500 MHz, CDCl_3) of Compound **12**



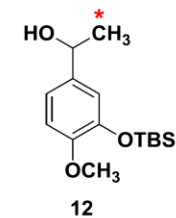
^{13}C NMR (125 MHz, CDCl_3) of Compound **12**



¹³C NMR (125 MHz, CDCl₃) of Compound **12**



HRMS of Compound 12

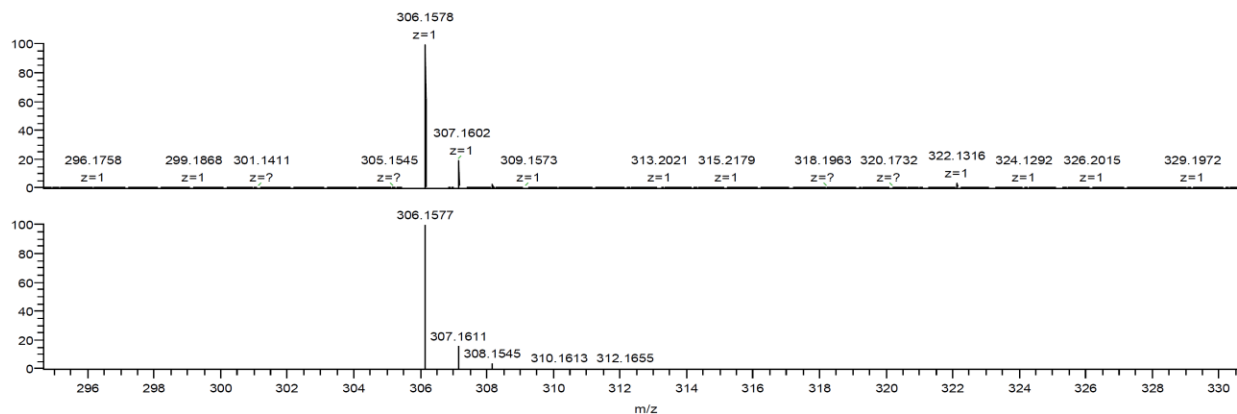
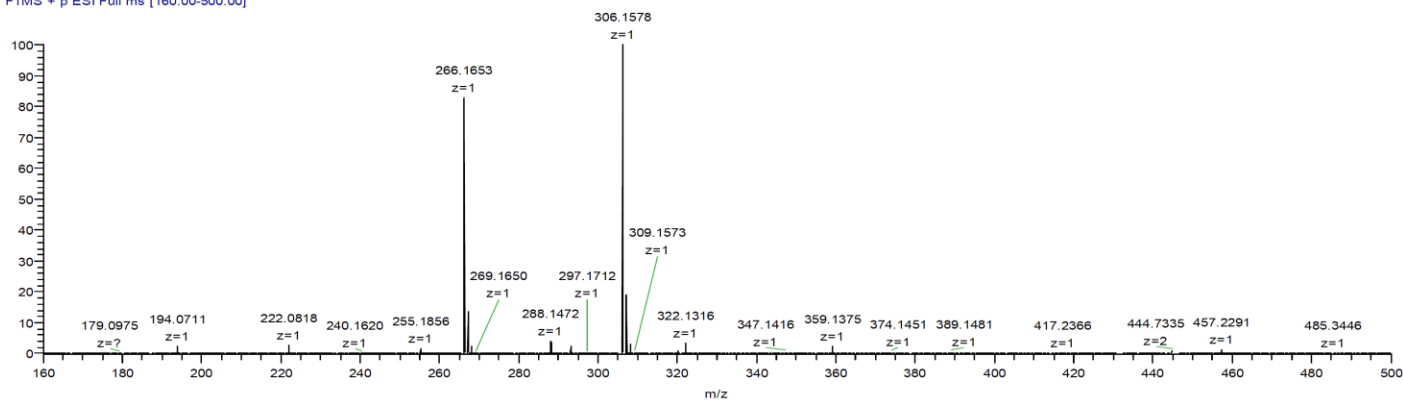


C:\Xcalibur\...MTM-IV-35_Orbi_+ESI
in MEOH

8/14/2013 2:53:57 PM

MTM-IV-35

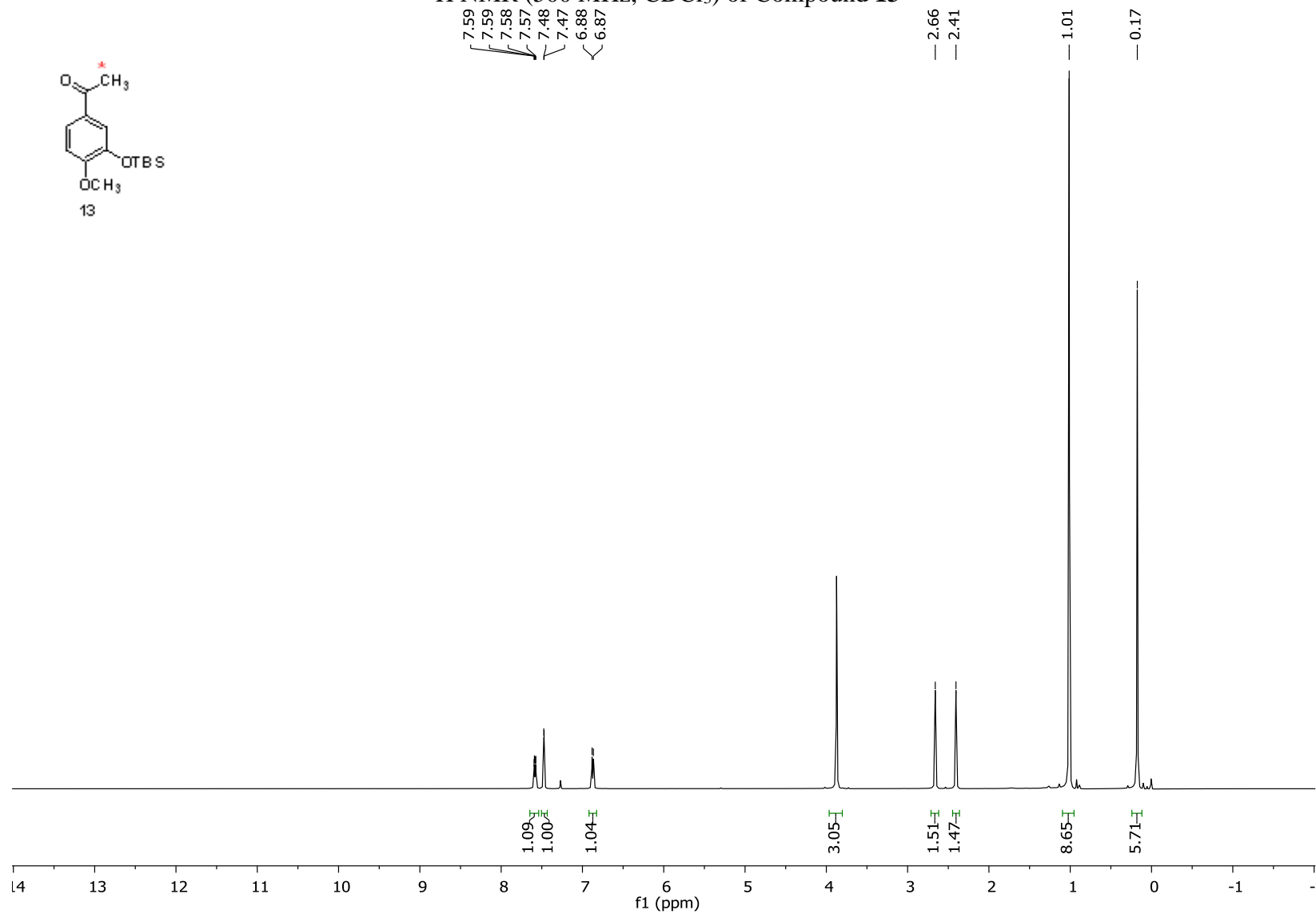
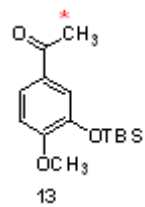
MTM-IV-35_Orbi_+ESI #50 RT: 0.39 AV: 1 NL:
T: FTMS + p ESI Full ms [160.00-500.00]



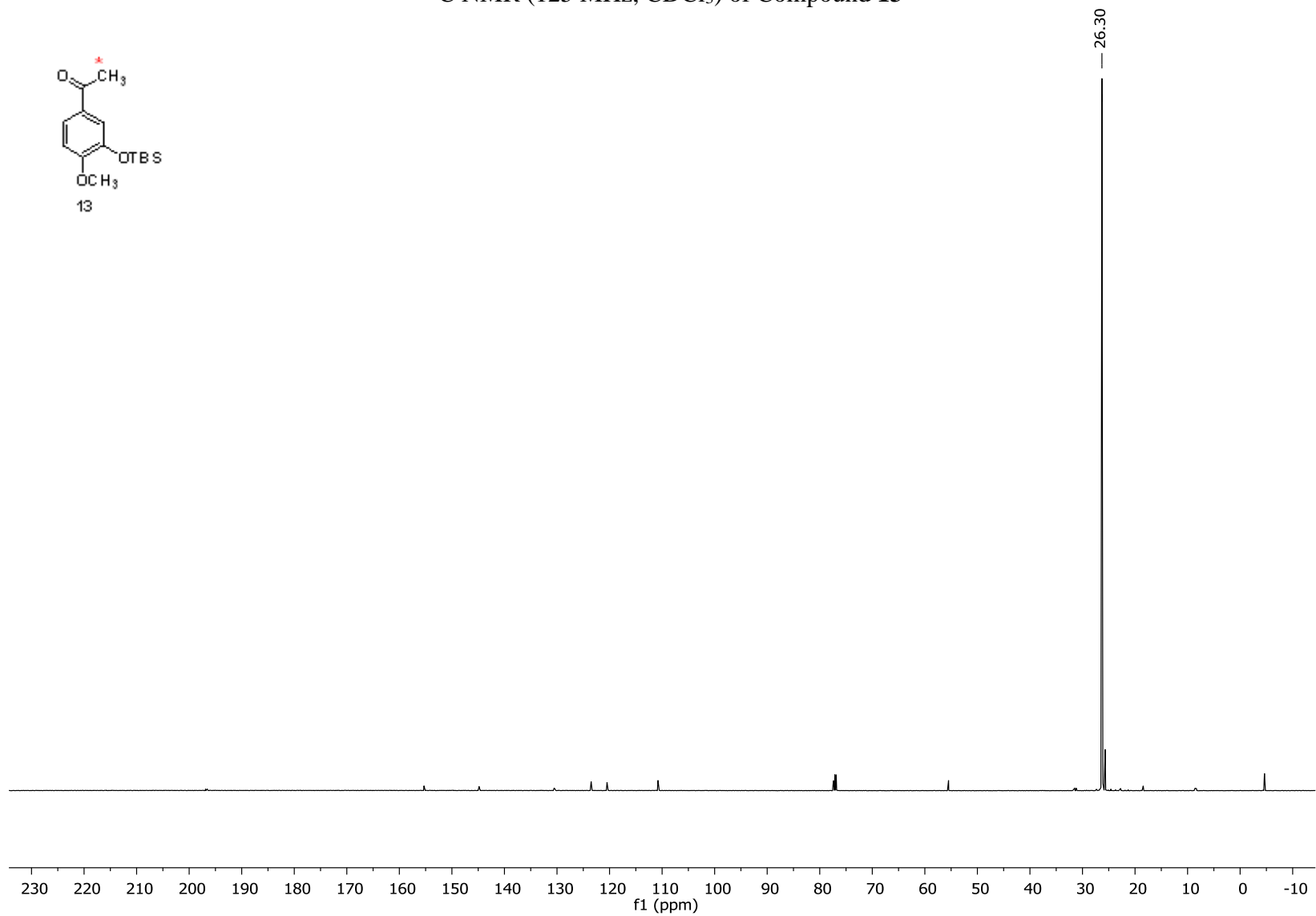
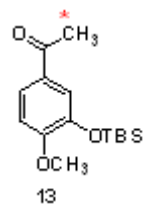
NL:
1.41E9
MTM-IV-35_Orbi_+
ESI#50 RT: 0.39
AV: 1 T: FTMS + p
ESI Full ms
[160.00-500.00]

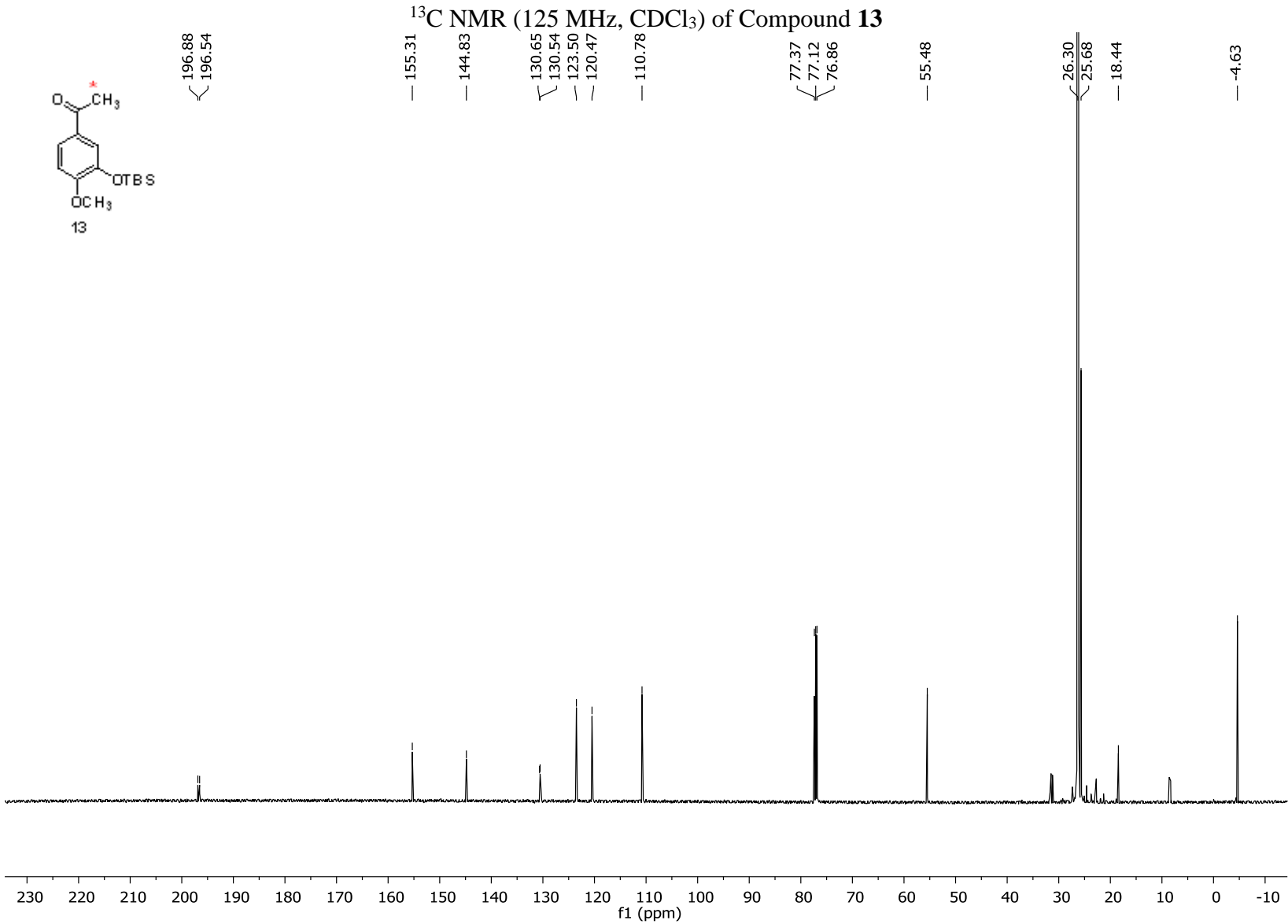
NL:
7.85E5
C₁₄ H₁₈ O₃ Si
C₁₄ H₁₇ O₃ Si
pa Chrg 1

¹H NMR (500 MHz, CDCl₃) of Compound **13**

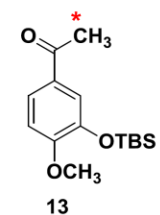


^{13}C NMR (125 MHz, CDCl_3) of Compound **13**





HRMS of Compound 13

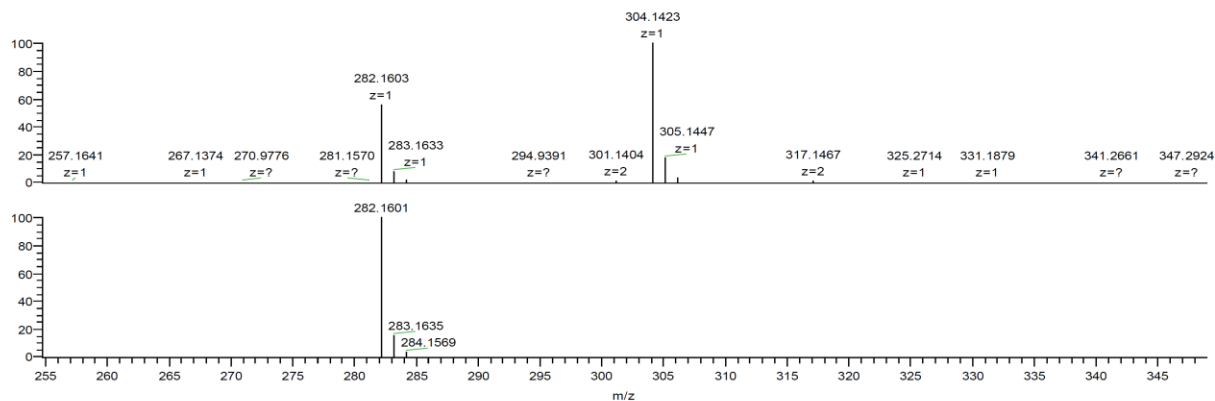
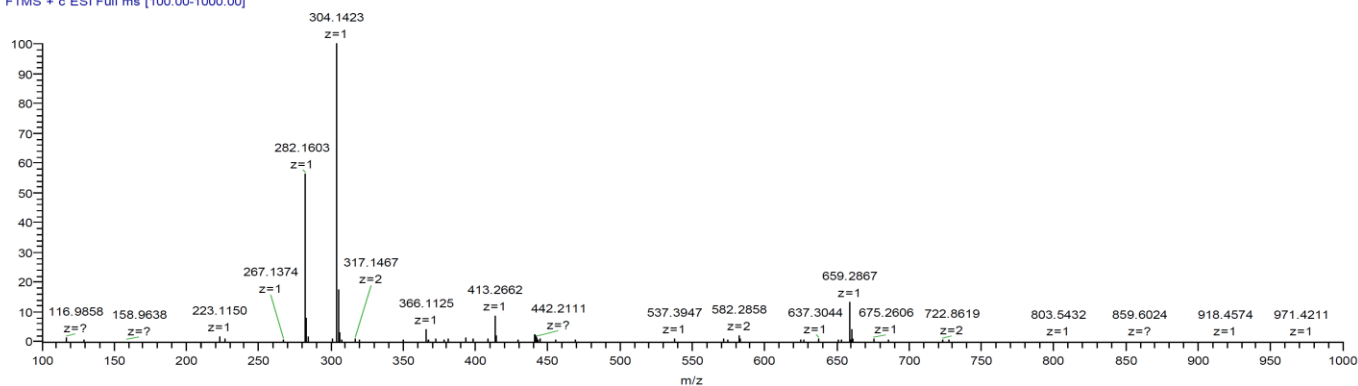


C:\Xcalibur\...MTM_IV_37_Orbi_+ESI

12/31/2014 1:13:46 AM

MTM_IV_37

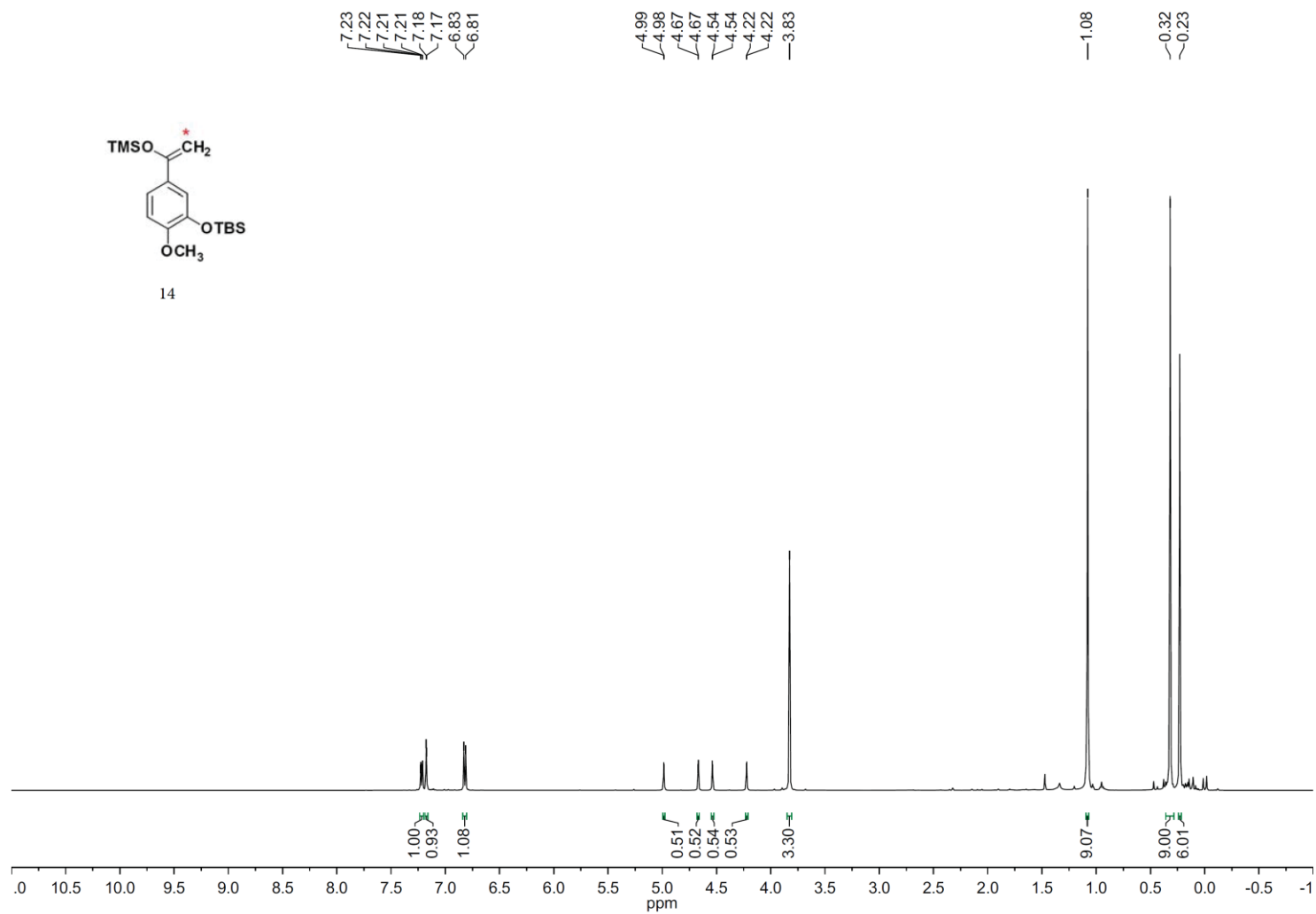
MTM_IV_37_Orbi_+ESI #20 RT: 0.24 AV: 1 NL
T: FTMS + c ESI Full ms [100.00-1000.00]



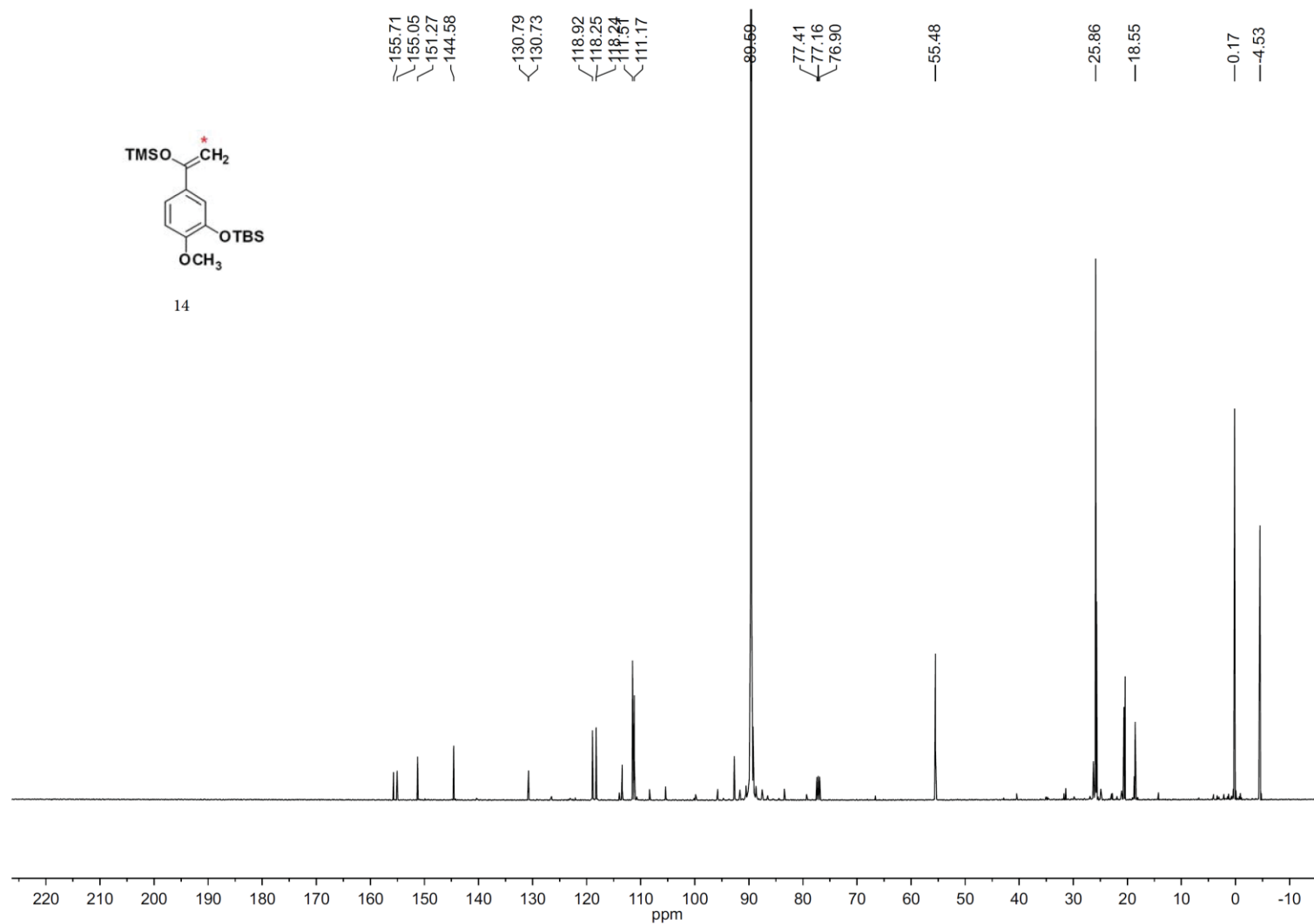
NL:
4.06E6
MTM_IV_37_Orbi_+
ESI#20 RT: 0.24
AV: 1 T: FTMS + c
ESI Full ms
[100.00-1000.00]

NL:
7.85E5
C₁₄H₁₉CH₂₅O₃Si:
C₁₄H₁₉C₁H₂₅O₃Si₁
pa Chrg 1

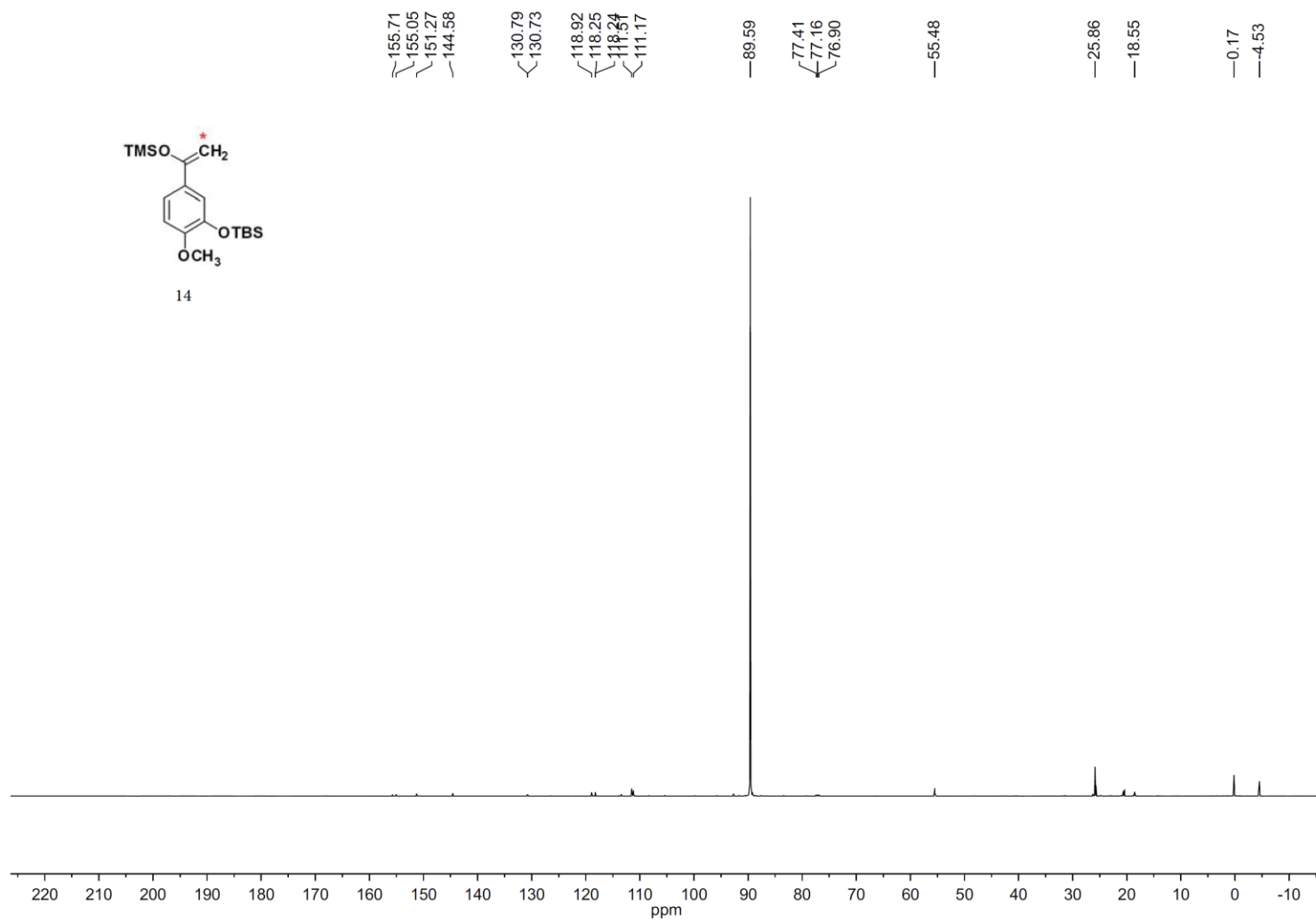
^1H NMR (500 MHz, CDCl_3) of Compound **14**



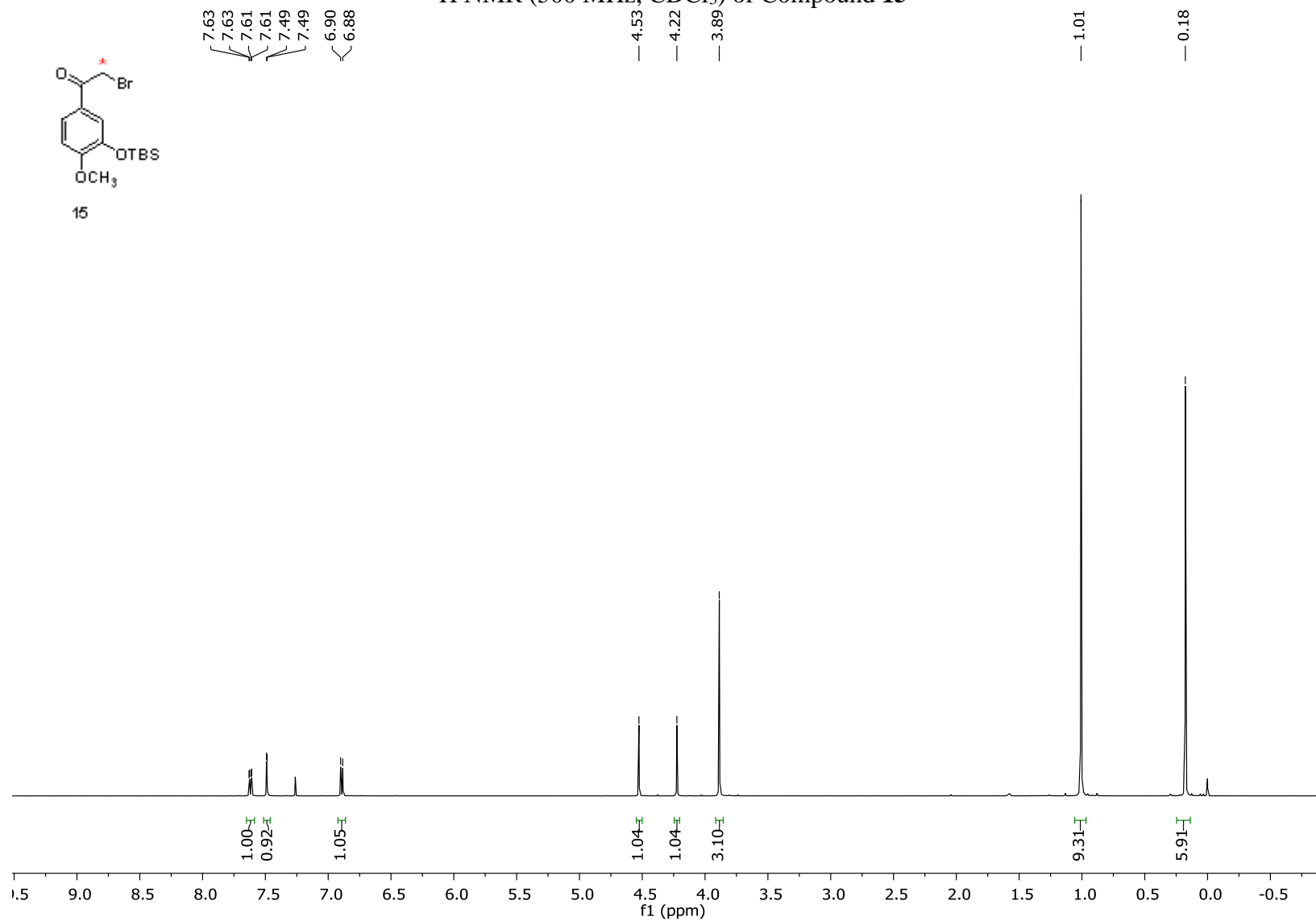
¹³C NMR (125 MHz, CDCl₃) of Compound **14**



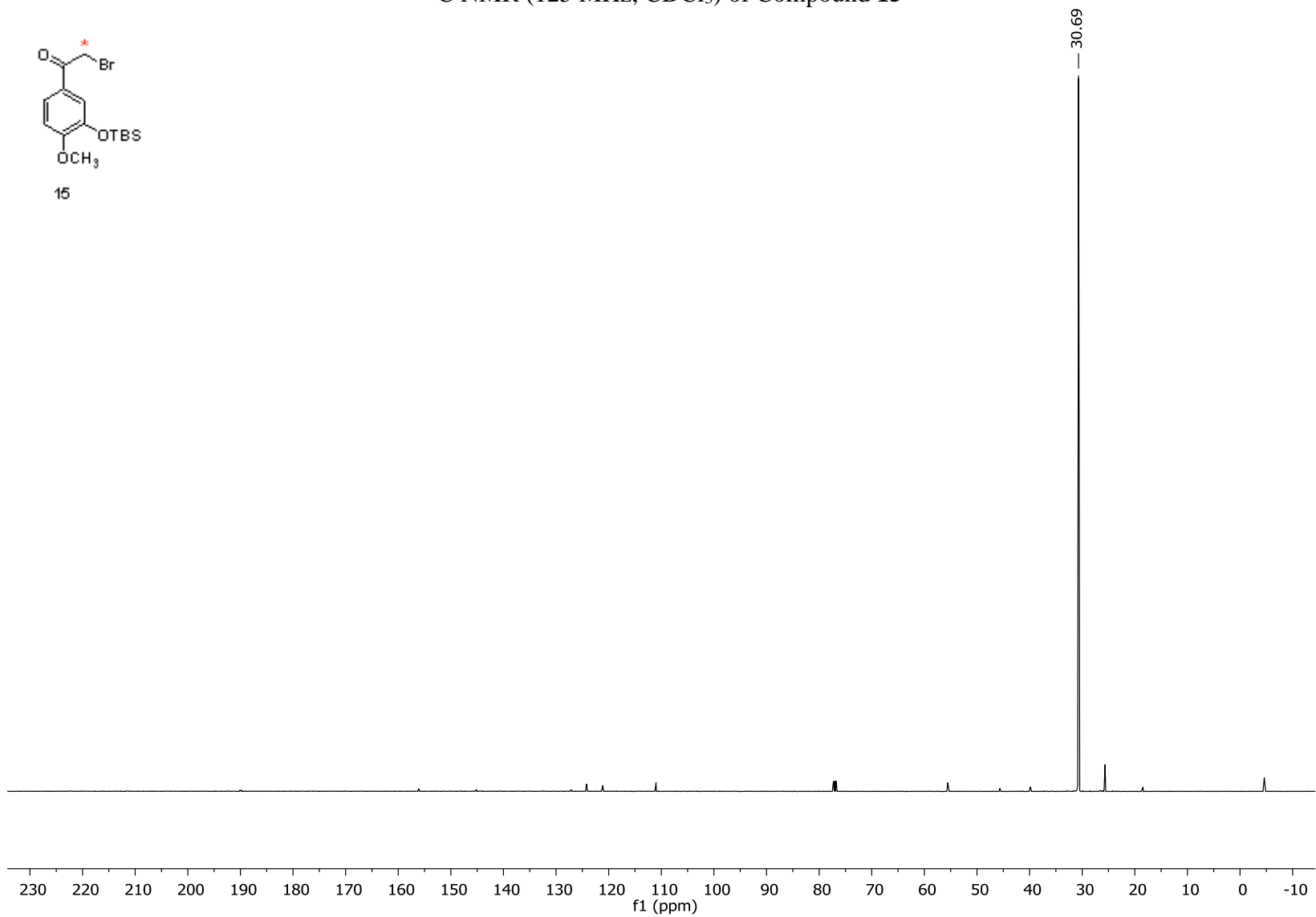
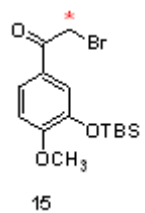
^{13}C NMR (500 MHz, CDCl_3) of Compound **14**

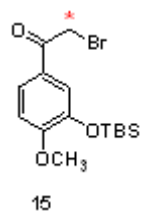


^1H NMR (500 MHz, CDCl_3) of Compound **15**

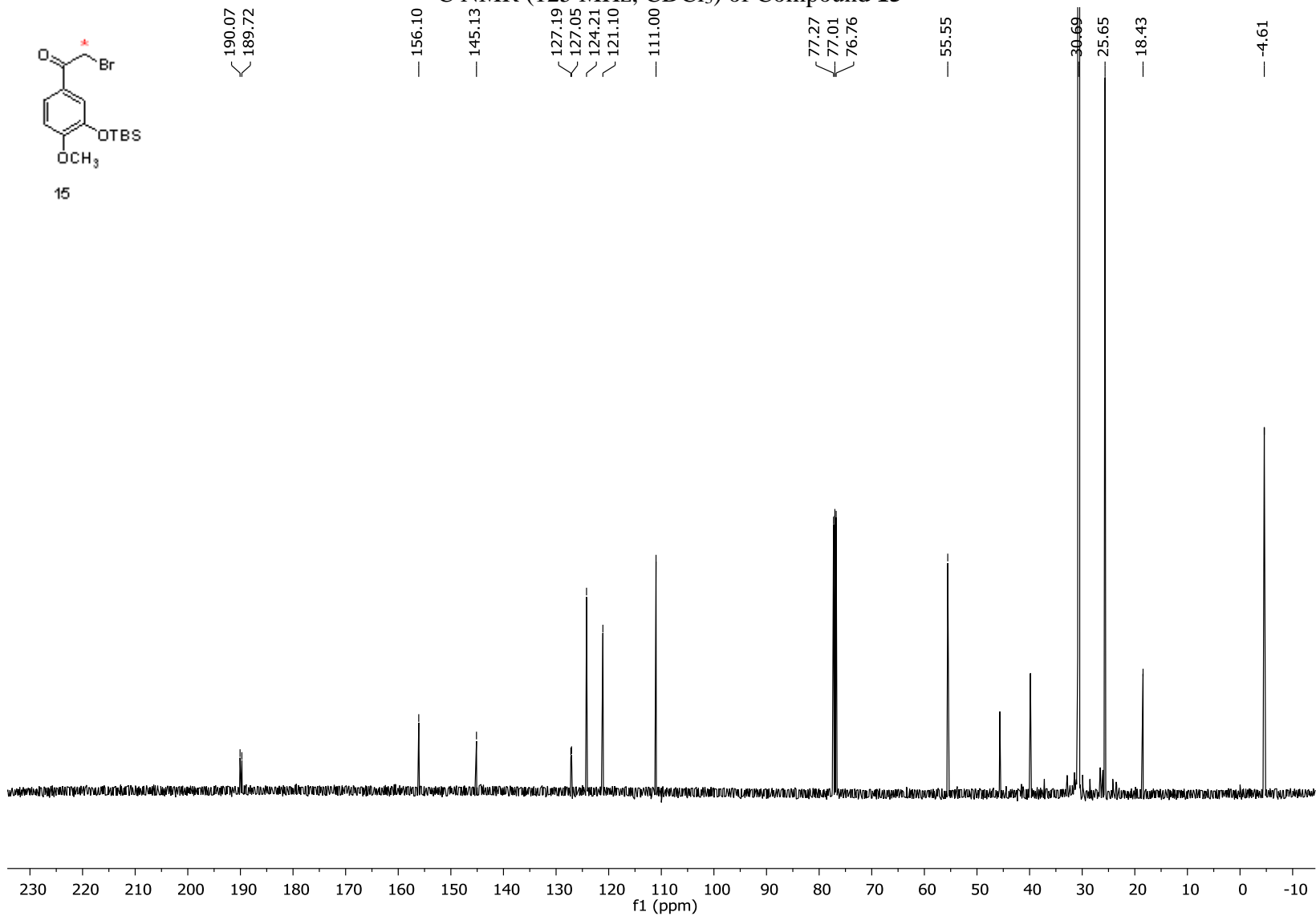


^{13}C NMR (125 MHz, CDCl_3) of Compound **15**

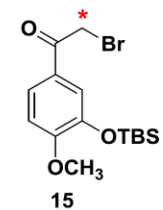




¹³C NMR (125 MHz, CDCl₃) of Compound 15



HRMS of Compound 15

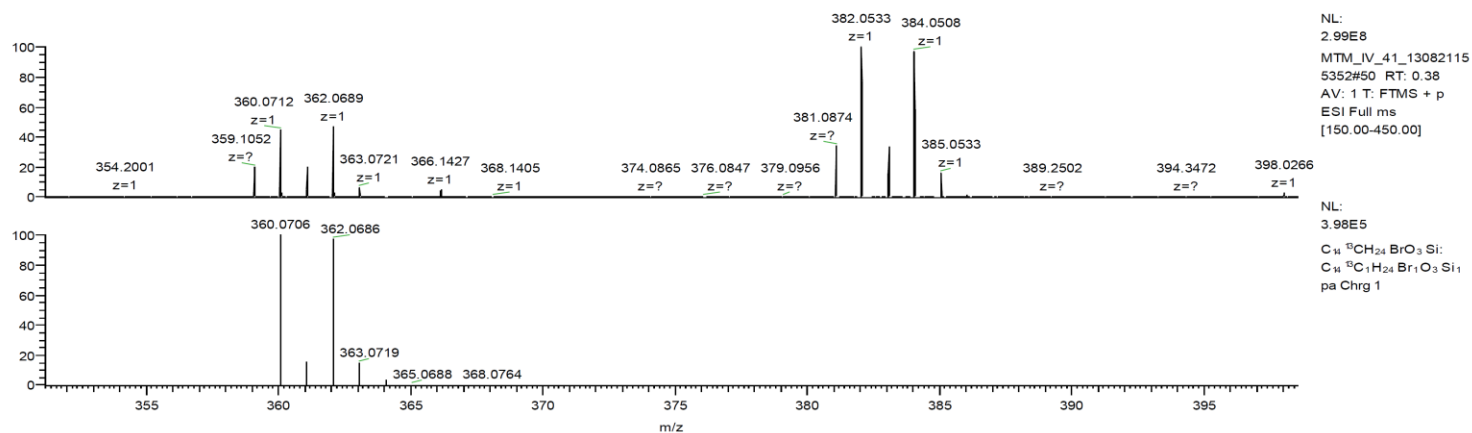
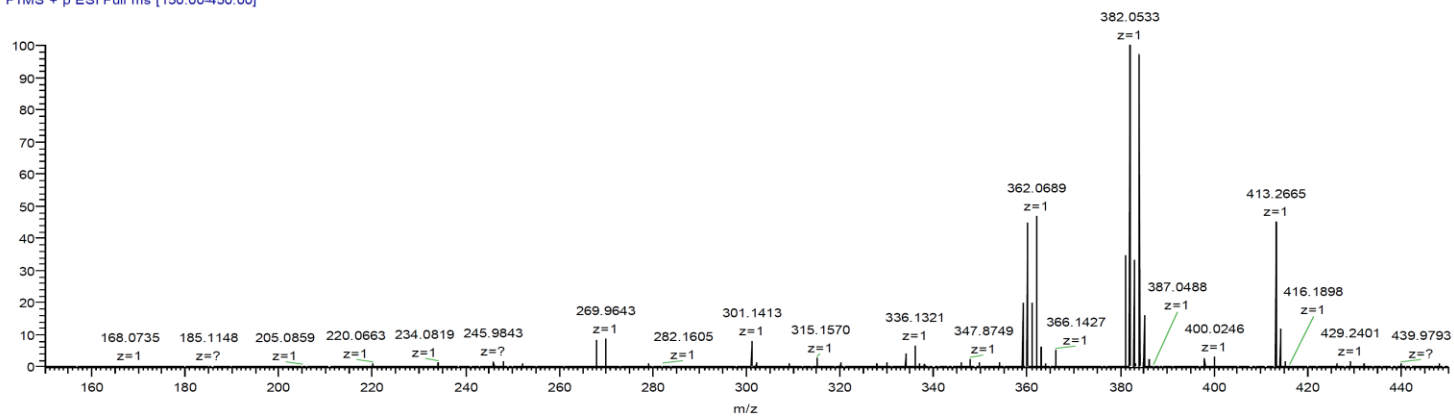


C:\Xcalibur\...MTM_IV_41_130821155352

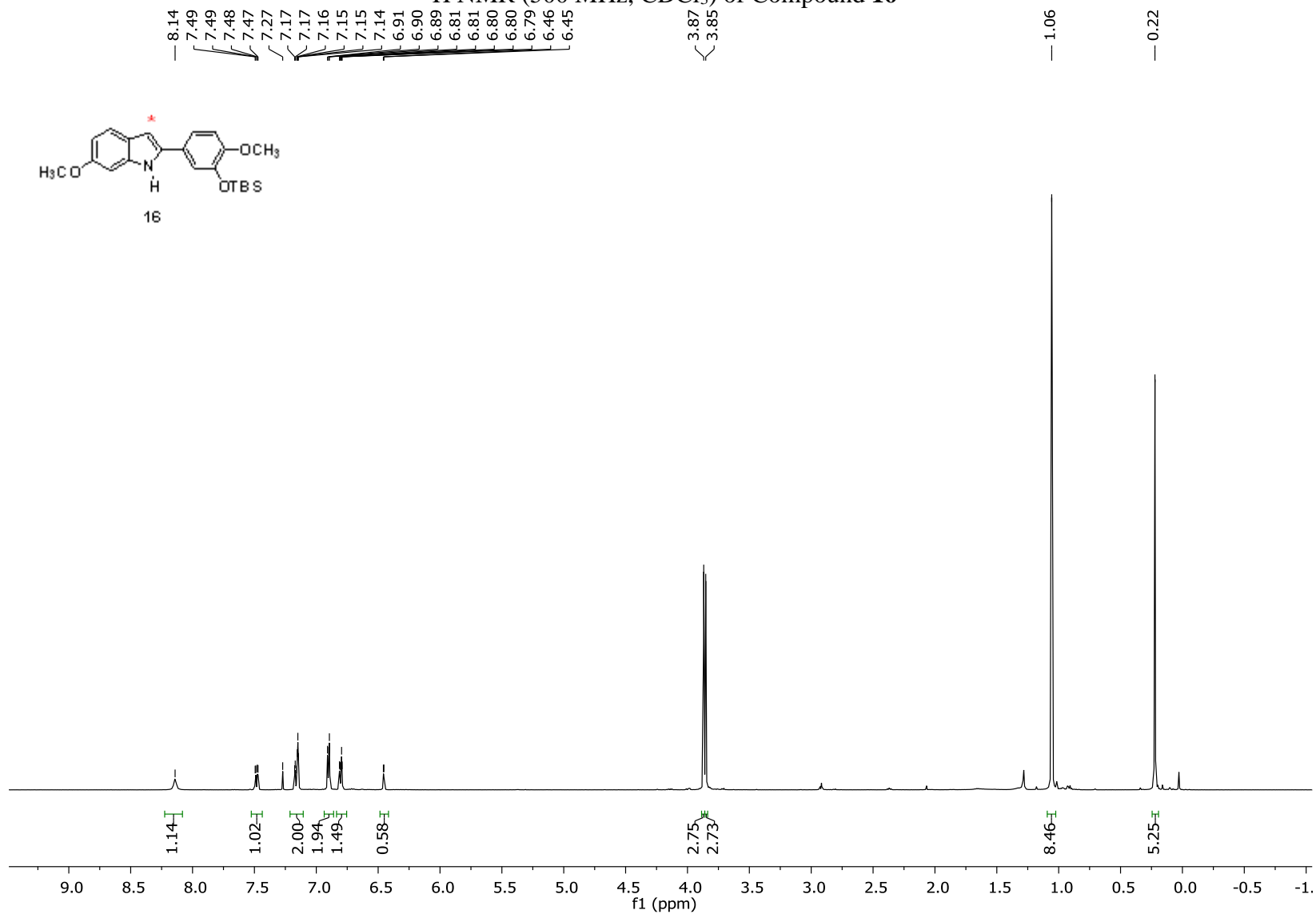
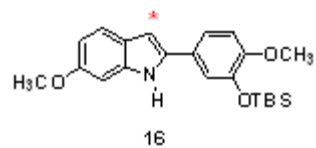
8/21/2013 3:53:52 PM

MTM_IV_41

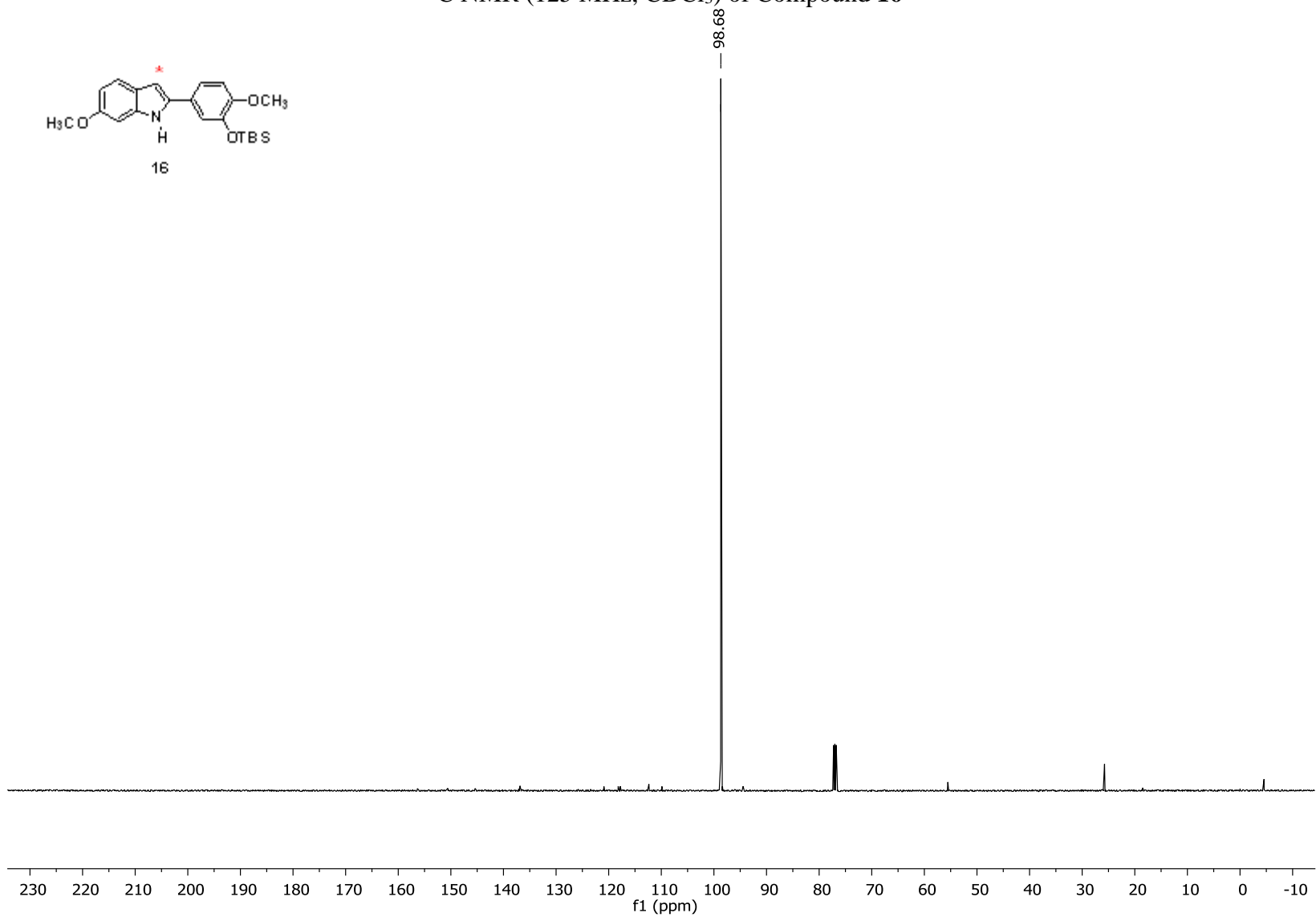
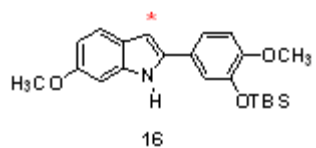
MTM_IV_41_130821155352 #50 RT: 0.38 AV: 1
T: FTMS + p ESI Full ms [150.00-450.00]



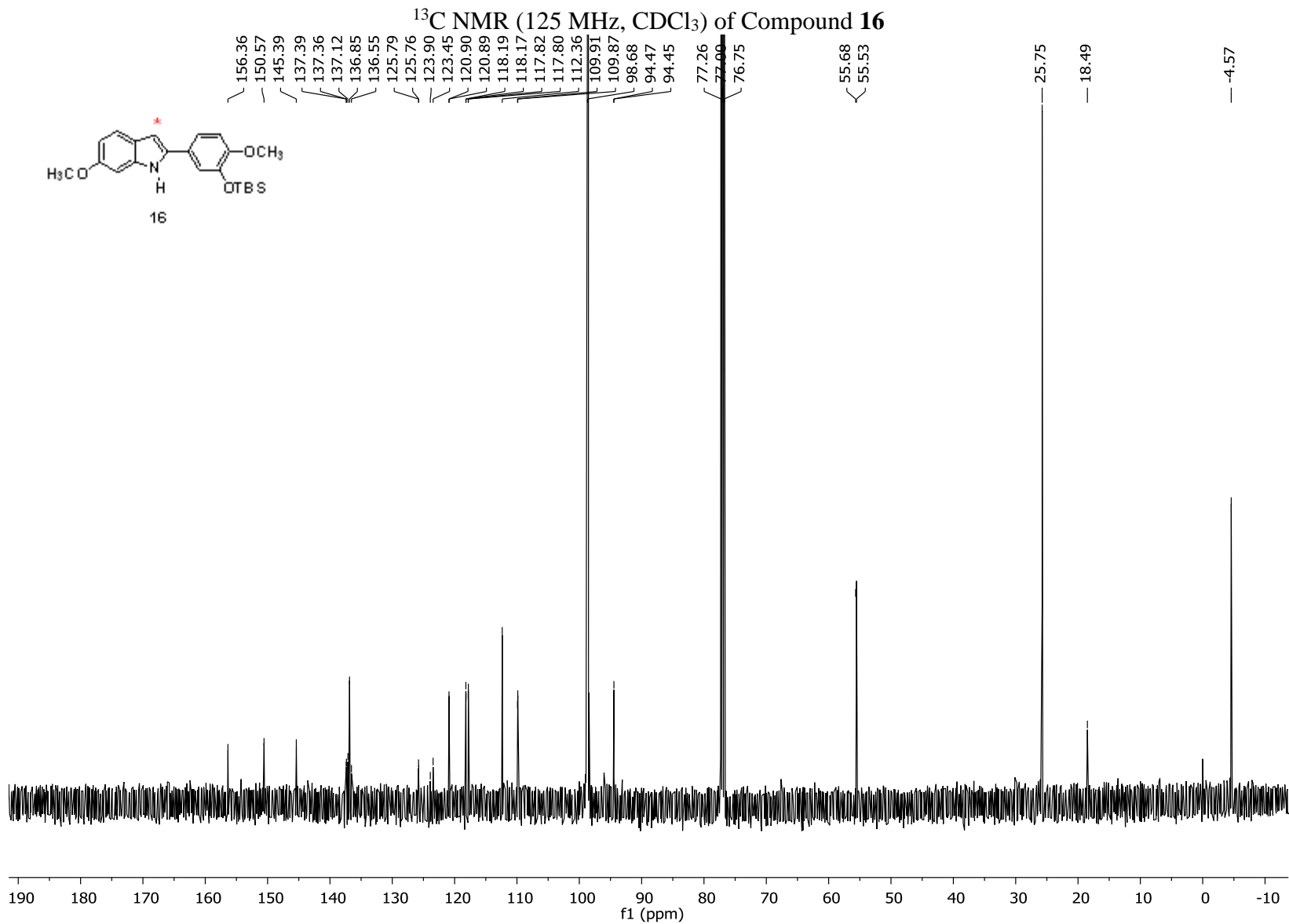
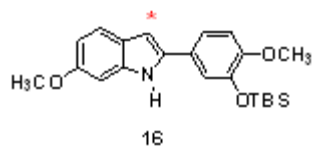
¹H NMR (500 MHz, CDCl₃) of Compound **16**



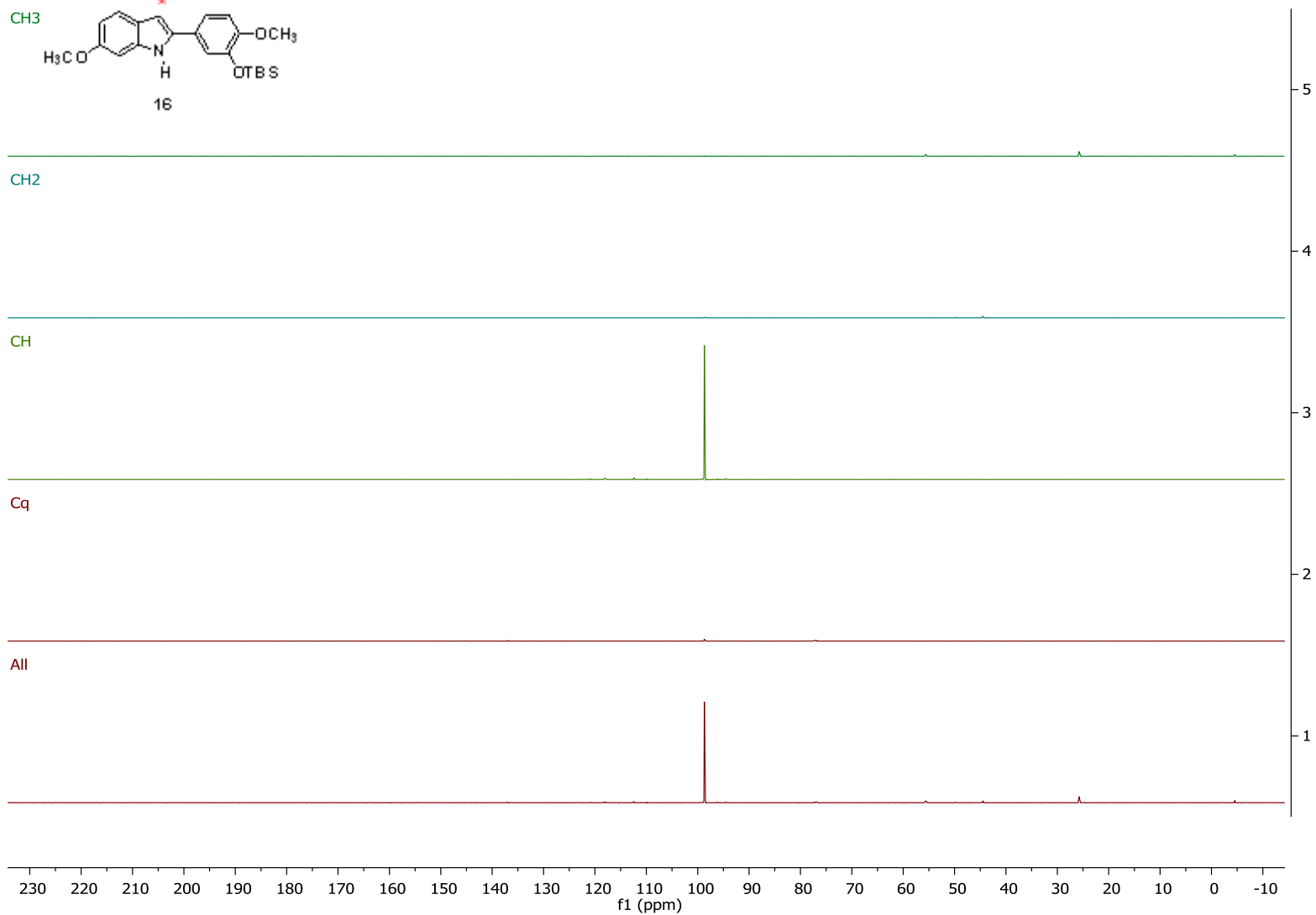
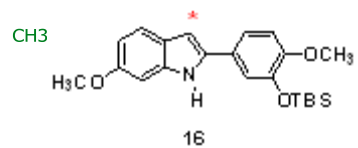
^{13}C NMR (125 MHz, CDCl_3) of Compound **16**



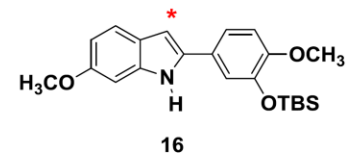
¹³C NMR (125 MHz, CDCl₃) of Compound 16



DEPT of Compound 16



HRMS of Compound 16

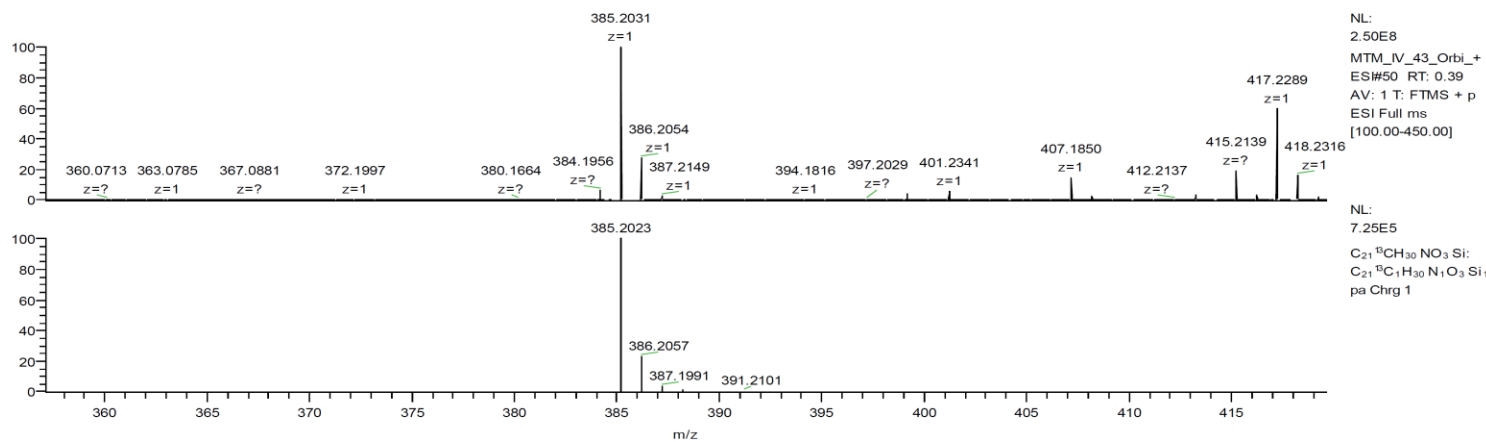
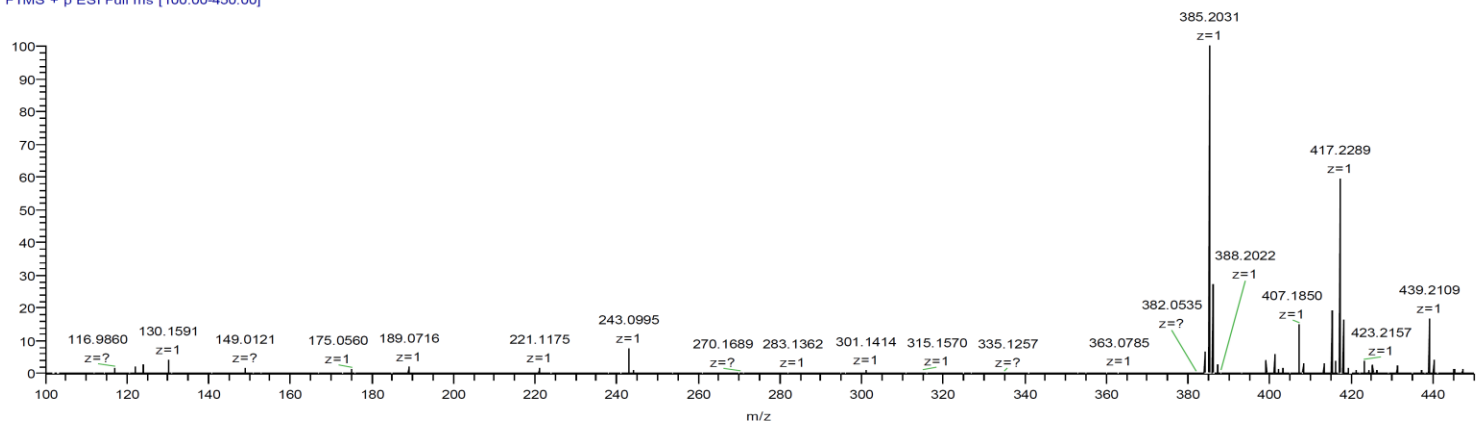


C:\Xcalibur\...MTM_IV_43_Orbi_+ESI

8/21/2013 3:17:34 PM

MTM_IV_43

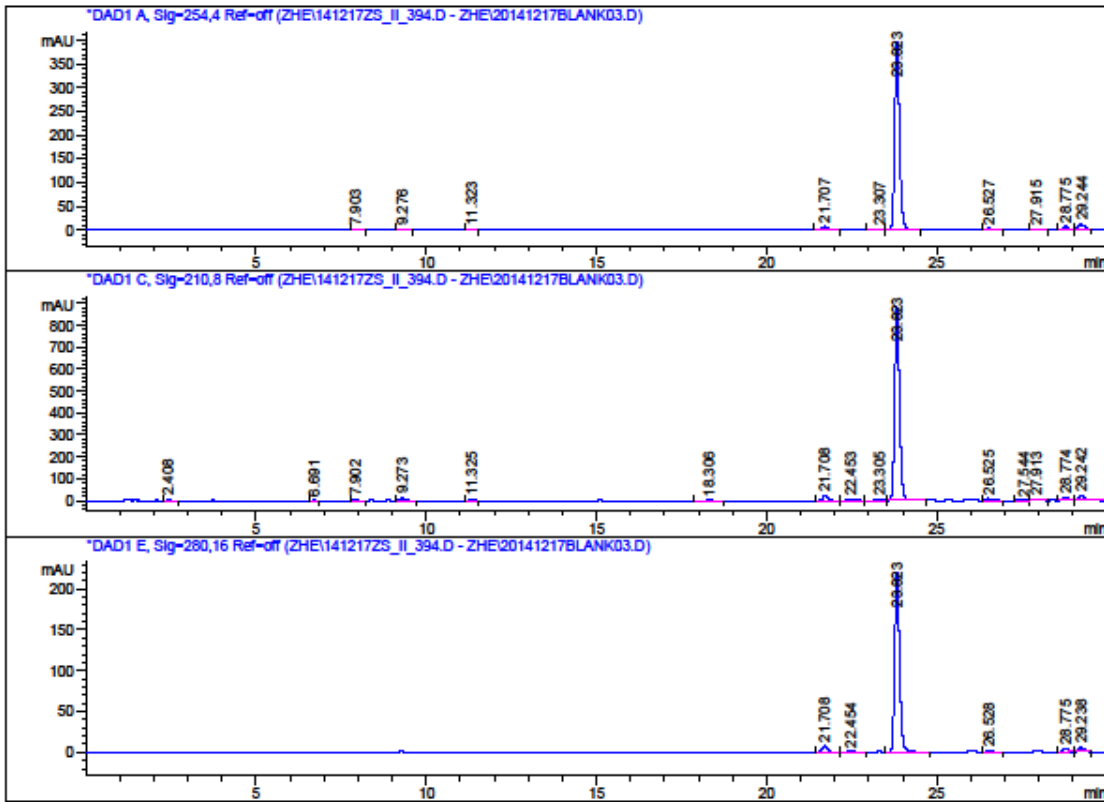
MTM_IV_43_Orbi_+ESI #50 RT: 0.39 AV: 1 NL
T: FTMS + p ESI Full ms [100.00-450.00]



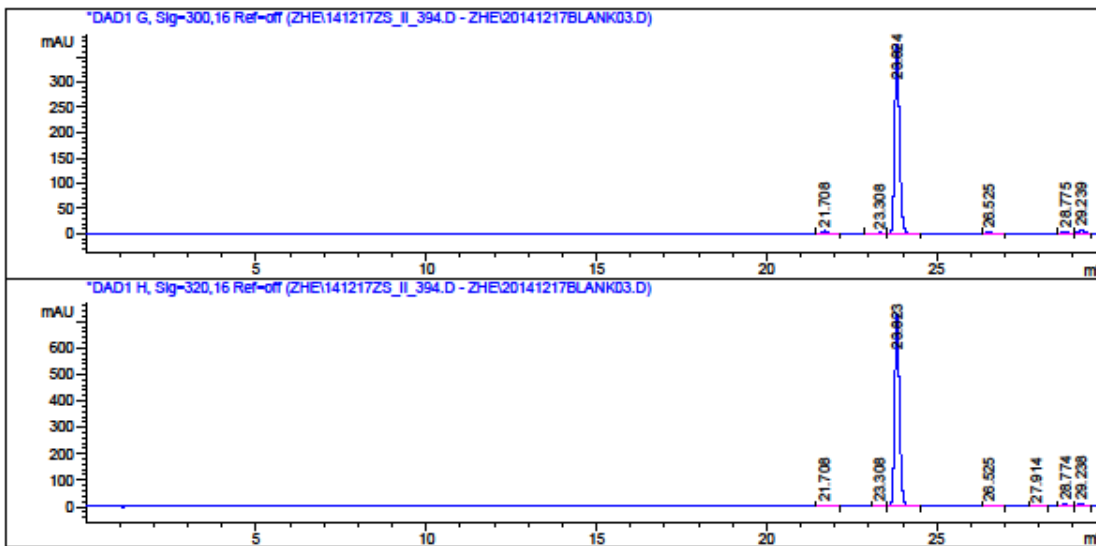
HPLC of Compound 16

Data File C:\CHEM32\1\DATA\ZHE\141217ZS_II_394.D
Sample Name: C13indole

```
=====
Acq. Operator   : HAICHAN NIU
Acq. Instrument : Instrument 1           Location : -
Injection Date  : 12/17/2014 1:24:43 PM
Acq. Method     : C:\CHEM32\1\METHODS\GRAD 2 50-90 ACN.M
Last changed    : 12/17/2014 1:22:13 PM by HAICHAN NIU
Analysis Method : C:\CHEM32\1\DATA\ZHE\141217ZS_II_394.D\DA.M (GRAD 2 50-90 ACN.M)
Last changed    : 12/30/2014 4:47:19 PM by ERICAP
Sample Info     : GRAD 2 50 -90 ACN
                  C13indole
                  20141217
=====
```



Sample Name: Cl3indole



=====
 Area Percent Report
 =====

Sorted By : Signal
 Multiplier : 1.0000
 Dilution : 1.0000
 Use Multiplier & Dilution Factor with ISTDs

Signal 1: DAD1 A, Sig=254,4 Ref=off
 Signal has been modified after loading from rawdata file!

Peak #	RetTime [min]	Type	Width [min]	Area [mAU*s]	Height [mAU]	Area %
1	7.903	BB	0.1237	8.97274	1.09440	0.2070
2	9.276	BB	0.1403	16.84550	1.81463	0.3886
3	11.323	BB	0.1362	12.08191	1.35247	0.2787
4	21.707	BB	0.1573	72.22176	6.94540	1.6662
5	23.307	BB	0.1472	14.23725	1.49431	0.3285
6	23.823	BB	0.1541	3944.59912	396.45770	91.0046
7	26.527	BB	0.1736	37.00466	3.09254	0.8537
8	27.915	BB	0.1954	23.40132	1.75668	0.5399
9	28.775	BB	0.1618	70.08858	6.71465	1.6170
10	29.244	BB	0.1943	135.05341	10.91752	3.1158

Totals : 4334.50624 431.64030

Sample Name: Cl3indole

Signal 2: DAD1 C, Sig=210,8 Ref=off

Signal has been modified after loading from rawdata file!

Peak #	RetTime [min]	Type	Width [min]	Area [mAU*s]	Height [mAU]	Area %
1	2.408	BB	0.0683	22.30968	4.97948	0.2266
2	6.691	VB	0.1052	8.28824	1.19031	0.0842
3	7.902	BB	0.1218	25.92144	3.22458	0.2633
4	9.273	BB	0.1402	112.41674	12.11774	1.1418
5	11.325	BB	0.1379	28.51899	3.20380	0.2897
6	18.306	BB	0.1813	17.94281	1.44024	0.1823
7	21.708	BB	0.1557	202.23770	19.70864	2.0542
8	22.453	BB	0.1920	45.83818	3.47165	0.4656
9	23.305	BB	0.1578	29.30734	2.80739	0.2977
10	23.823	BB	0.1541	8799.65332	884.17999	89.3806
11	26.525	BB	0.1619	95.05730	8.80946	0.9655
12	27.544	BV	0.2140	17.40180	1.16646	0.1768
13	27.913	VB	0.1982	39.21973	2.89218	0.3984
14	28.774	BV	0.1639	143.44379	13.50203	1.4570
15	29.242	VB	0.2077	257.59482	19.05302	2.6165

Totals : 9845.15189 981.74698

Signal 3: DAD1 E, Sig=280,16 Ref=off

Signal has been modified after loading from rawdata file!

Peak #	RetTime [min]	Type	Width [min]	Area [mAU*s]	Height [mAU]	Area %
1	21.708	BB	0.1556	81.35815	7.93701	3.3271
2	22.454	BB	0.1947	14.99190	1.10235	0.6131
3	23.823	BB	0.1549	2214.12866	221.04308	90.5459
4	26.528	BB	0.1712	19.06033	1.62073	0.7795
5	28.775	BB	0.1619	48.55169	4.64699	1.9855
6	29.238	BB	0.1939	67.21884	5.44941	2.7489

Totals : 2445.30957 241.79956

Signal 4: DAD1 G, Sig=300,16 Ref=off

Signal has been modified after loading from rawdata file!

Peak #	RetTime [min]	Type	Width [min]	Area [mAU*s]	Height [mAU]	Area %
1	21.708	BB	0.1539	59.15012	5.85095	1.4892
2	23.308	BB	0.1493	18.53098	1.90773	0.4666
3	23.824	BB	0.1539	3725.80444	375.04620	93.8063

Data File C:\CHEM32\1\DATA\ZHE\14121728_II_394.D

Sample Name: Cl3indole

Peak #	RetTime [min]	Type	Width [min]	Area [mAU*s]	Height [mAU]	Area %
4	26.525	BB	0.1657	34.37233	3.04487	0.8654
5	28.775	BB	0.1619	55.19741	5.28453	1.3897
6	29.239	BB	0.1927	78.75215	6.43651	1.9828

Totals : 3971.80744 397.57080

Signal 5: DAD1 H, Sig=320,16 Ref=off

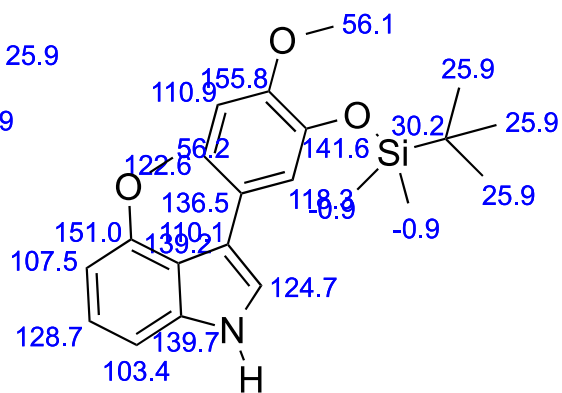
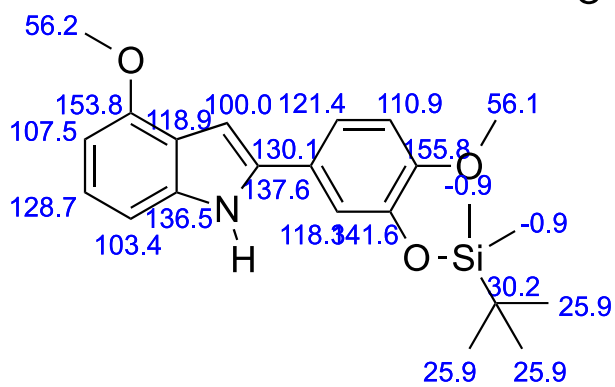
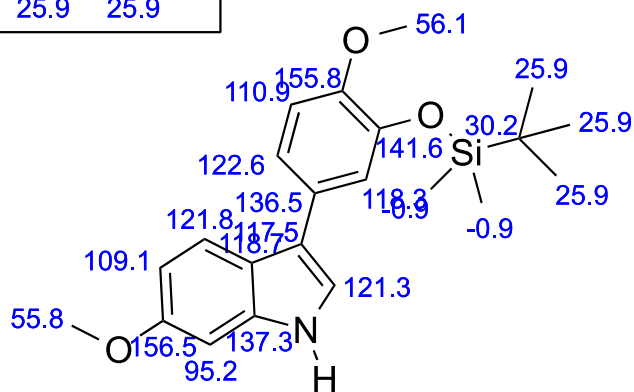
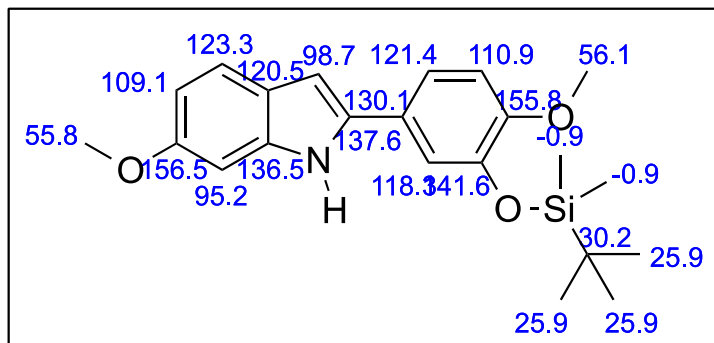
Signal has been modified after loading from rawdata file!

Peak #	RetTime [min]	Type	Width [min]	Area [mAU*s]	Height [mAU]	Area %
1	21.708	BB	0.1544	23.81687	2.34698	0.3156
2	23.308	BB	0.1461	19.31839	2.04754	0.2560
3	23.823	BB	0.1537	7247.35693	730.59741	96.0400
4	26.525	BB	0.1665	35.64434	3.13880	0.4723
5	27.914	BB	0.1906	13.79213	1.09783	0.1828
6	28.774	BB	0.1616	87.57129	8.40103	1.1605
7	29.238	BB	0.1930	118.68315	9.68232	1.5728

Totals : 7546.18311 757.31191

=====
*** End of Report ***

¹³C-NMR Predicted (ChemBioDraw, Version 13.0.2.3020) Chemical Shifts for Possible Indole Regioisomers



X-ray Crystallographic Data for ¹³C Labeled Indole 16

X-ray crystallographic data were collected at 110 K on a Bruker X8 Apex using Mo KR radiation ($\lambda = 0.71073 \text{ \AA}$). The structure was solved by direct methods after correction of the data using SADABS. All data were processed using the Bruker AXS SHELXTL software, version 6.10.

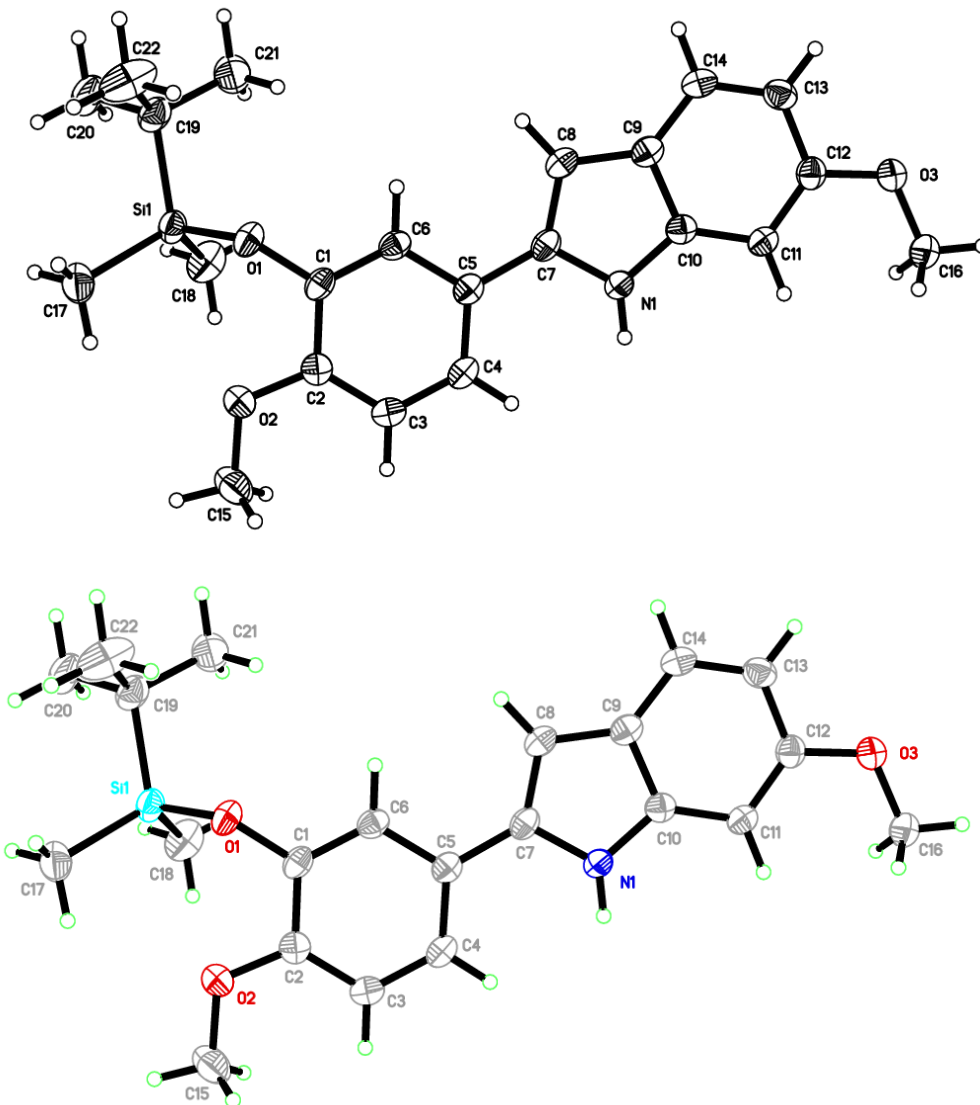


Table D.1. Crystal data and structure refinement for Indole **16**.

Identification code	kp66	
Empirical formula	C ₂₂ H ₂₉ N O ₃ Si	
Formula weight	383.55	
Temperature	150(2) K	
Wavelength	0.71073 Å	
Crystal system	Monoclinic	
Space group	P2(1)/c	
Unit cell dimensions	a = 12.5182(6) Å	α = 90°.
	b = 23.1476(10) Å	β = 100.7843(17)°.
	c = 7.5208(3) Å	γ = 90°.
Volume	2140.79(16) Å ³	
Z	4	
Density (calculated)	1.190 Mg/m ³	
Absorption coefficient	0.130 mm ⁻¹	
F(000)	824	
Crystal size	0.38 x 0.16 x 0.12 mm ³	
Theta range for data collection	2.42 to 26.85°.	
Index ranges	-15 ≤ h ≤ 15, -29 ≤ k ≤ 25, -9 ≤ l ≤ 9	
Reflections collected	25973	
Independent reflections	4565 [R(int) = 0.0410]	
Completeness to theta = 26.85°	99.4 %	
Absorption correction	Semi-empirical from equivalents	
Max. and min. transmission	0.9843 and 0.9526	
Refinement method	Full-matrix least-squares on F ²	
Data / restraints / parameters	4565 / 0 / 251	
Goodness-of-fit on F ²	1.569	
Final R indices [I > 2σ(I)]	R1 = 0.0419, wR2 = 0.1071	
R indices (all data)	R1 = 0.0590, wR2 = 0.1115	
Largest diff. peak and hole	0.307 and -0.225 e.Å ⁻³	

Table D.2. Atomic coordinates ($\times 10^4$) and equivalent isotropic displacement parameters ($\text{\AA}^2 \times 10^3$) for indole **16**. $U(\text{eq})$ is defined as one third of the trace of the orthogonalized U^{ij} tensor.

	x	y	z	U(eq)
Si(1)	-2359(1)	615(1)	10812(1)	28(1)
O(1)	-1718(1)	1161(1)	9999(1)	29(1)
O(2)	-1373(1)	1655(1)	13280(1)	33(1)
O(3)	5990(1)	2021(1)	6358(1)	33(1)
N(1)	2891(1)	1943(1)	9526(2)	25(1)
C(1)	-729(1)	1406(1)	10656(2)	25(1)
C(2)	-534(1)	1682(1)	12347(2)	25(1)
C(3)	451(1)	1958(1)	12936(2)	27(1)
C(4)	1238(1)	1962(1)	11862(2)	27(1)
C(5)	1069(1)	1687(1)	10190(2)	23(1)
C(6)	65(1)	1405(1)	9622(2)	25(1)
C(7)	1881(1)	1681(1)	9018(2)	24(1)
C(8)	1838(1)	1437(1)	7346(2)	26(1)
C(9)	2848(1)	1544(1)	6794(2)	25(1)
C(10)	3495(1)	1863(1)	8189(2)	24(1)
C(11)	4555(1)	2038(1)	8135(2)	25(1)
C(12)	4965(1)	1880(1)	6621(2)	26(1)
C(13)	4339(1)	1563(1)	5201(2)	29(1)
C(14)	3297(1)	1398(1)	5277(2)	29(1)
C(15)	-1193(1)	1901(1)	15046(2)	45(1)
C(16)	6666(1)	2332(1)	7773(2)	38(1)
C(17)	-3537(1)	901(1)	11724(2)	45(1)
C(18)	-1395(1)	230(1)	12588(2)	45(1)
C(19)	-2826(1)	149(1)	8766(2)	34(1)
C(20)	-3455(1)	-377(1)	9276(2)	43(1)
C(21)	-1833(2)	-63(1)	8029(3)	57(1)
C(22)	-3569(2)	496(1)	7300(3)	59(1)

Table D.3. Bond lengths [\AA] and angles [$^\circ$] for indole **16**.

Si(1)-O(1)	1.6721(10)
Si(1)-C(18)	1.8536(16)
Si(1)-C(17)	1.8602(16)
Si(1)-C(19)	1.8804(16)
O(1)-C(1)	1.3674(16)
O(2)-C(2)	1.3690(17)
O(2)-C(15)	1.4236(18)
O(3)-C(12)	1.3744(17)
O(3)-C(16)	1.4253(17)
N(1)-C(10)	1.3785(17)
N(1)-C(7)	1.3892(17)
C(1)-C(6)	1.3717(19)
C(1)-C(2)	1.403(2)
C(2)-C(3)	1.386(2)
C(3)-C(4)	1.385(2)
C(4)-C(5)	1.3909(19)
C(5)-C(6)	1.4090(19)
C(5)-C(7)	1.4651(19)
C(7)-C(8)	1.3703(19)
C(8)-C(9)	1.4244(19)
C(9)-C(14)	1.404(2)
C(9)-C(10)	1.4078(19)
C(10)-C(11)	1.3953(19)
C(11)-C(12)	1.382(2)
C(12)-C(13)	1.4077(19)
C(13)-C(14)	1.371(2)
C(19)-C(22)	1.531(2)
C(19)-C(21)	1.533(2)
C(19)-C(20)	1.538(2)
O(1)-Si(1)-C(18)	109.52(6)
O(1)-Si(1)-C(17)	109.55(7)
C(18)-Si(1)-C(17)	111.09(8)

O(1)-Si(1)-C(19)	103.37(6)
C(18)-Si(1)-C(19)	111.97(8)
C(17)-Si(1)-C(19)	111.05(7)
C(1)-O(1)-Si(1)	130.24(9)
C(2)-O(2)-C(15)	117.18(12)
C(12)-O(3)-C(16)	116.89(11)
C(10)-N(1)-C(7)	109.62(12)
O(1)-C(1)-C(6)	119.82(12)
O(1)-C(1)-C(2)	120.58(13)
C(6)-C(1)-C(2)	119.54(13)
O(2)-C(2)-C(3)	125.42(13)
O(2)-C(2)-C(1)	115.06(12)
C(3)-C(2)-C(1)	119.52(14)
C(4)-C(3)-C(2)	120.28(14)
C(3)-C(4)-C(5)	121.31(13)
C(4)-C(5)-C(6)	117.51(13)
C(4)-C(5)-C(7)	122.88(13)
C(6)-C(5)-C(7)	119.61(12)
C(1)-C(6)-C(5)	121.83(13)
C(8)-C(7)-N(1)	108.04(12)
C(8)-C(7)-C(5)	130.01(13)
N(1)-C(7)-C(5)	121.95(12)
C(7)-C(8)-C(9)	108.10(12)
C(14)-C(9)-C(10)	118.06(13)
C(14)-C(9)-C(8)	134.94(13)
C(10)-C(9)-C(8)	106.99(12)
N(1)-C(10)-C(11)	129.53(13)
N(1)-C(10)-C(9)	107.25(12)
C(11)-C(10)-C(9)	123.21(13)
C(12)-C(11)-C(10)	116.66(13)
O(3)-C(12)-C(11)	123.82(13)
O(3)-C(12)-C(13)	114.63(12)
C(11)-C(12)-C(13)	121.54(13)
C(14)-C(13)-C(12)	120.84(13)
C(13)-C(14)-C(9)	119.67(13)

C(22)-C(19)-C(21)	109.39(15)
C(22)-C(19)-C(20)	108.96(13)
C(21)-C(19)-C(20)	108.91(13)
C(22)-C(19)-Si(1)	110.02(11)
C(21)-C(19)-Si(1)	109.30(11)
C(20)-C(19)-Si(1)	110.23(11)

Symmetry transformations used to generate equivalent atoms:

Table D.4. Anisotropic displacement parameters ($\text{\AA}^2 \times 10^3$) for indole **16**. The anisotropic displacement factor exponent takes the form: $-2\pi^2 [h^2 a^{*2} U^{11} + \dots + 2 h k a^* b^* U^{12}]$

	U ¹¹	U ²²	U ³³	U ²³	U ¹³	U ¹²
Si(1)	24(1)	25(1)	35(1)	0(1)	7(1)	-4(1)
O(1)	25(1)	29(1)	32(1)	1(1)	2(1)	-7(1)
O(2)	31(1)	35(1)	35(1)	-7(1)	12(1)	-2(1)
O(3)	28(1)	38(1)	33(1)	-6(1)	10(1)	-6(1)
N(1)	26(1)	25(1)	24(1)	-2(1)	4(1)	-4(1)
C(1)	24(1)	18(1)	30(1)	3(1)	1(1)	-3(1)
C(2)	27(1)	22(1)	28(1)	2(1)	6(1)	1(1)
C(3)	30(1)	26(1)	25(1)	-2(1)	2(1)	0(1)
C(4)	24(1)	24(1)	30(1)	0(1)	-1(1)	-4(1)
C(5)	25(1)	19(1)	25(1)	4(1)	2(1)	-1(1)
C(6)	29(1)	20(1)	24(1)	1(1)	2(1)	-3(1)
C(7)	23(1)	19(1)	28(1)	3(1)	1(1)	-2(1)
C(8)	25(1)	21(1)	29(1)	-1(1)	-1(1)	-2(1)
C(9)	28(1)	19(1)	26(1)	1(1)	1(1)	0(1)
C(10)	29(1)	18(1)	24(1)	2(1)	4(1)	0(1)
C(11)	26(1)	22(1)	27(1)	-2(1)	2(1)	-2(1)
C(12)	28(1)	23(1)	29(1)	3(1)	6(1)	0(1)
C(13)	34(1)	26(1)	28(1)	-3(1)	9(1)	2(1)
C(14)	32(1)	25(1)	28(1)	-5(1)	1(1)	0(1)
C(15)	38(1)	67(1)	32(1)	-5(1)	10(1)	9(1)
C(16)	30(1)	45(1)	42(1)	-10(1)	12(1)	-10(1)
C(17)	36(1)	46(1)	58(1)	-10(1)	19(1)	-9(1)
C(18)	47(1)	36(1)	48(1)	10(1)	0(1)	-4(1)
C(19)	32(1)	26(1)	42(1)	-3(1)	6(1)	-7(1)
C(20)	35(1)	32(1)	60(1)	-4(1)	6(1)	-8(1)
C(21)	54(1)	50(1)	75(1)	-29(1)	29(1)	-18(1)
C(22)	77(2)	43(1)	48(1)	0(1)	-14(1)	-12(1)

NOTE:

Crystallographic data for ¹³C labeled indole regioisomer **16** presented in this paper have been deposited with the Cambridge Crystallographic Data Centre (CCDC deposition number 1041417). Copies of the data can be obtained, free of charge, on application to CCDC, 12 Union Road, Cambridge CB2 1EZ, UK, (fax: +44-(0)1223-336033 or e-mail: deposit@ccdc.cam.ac.uk).

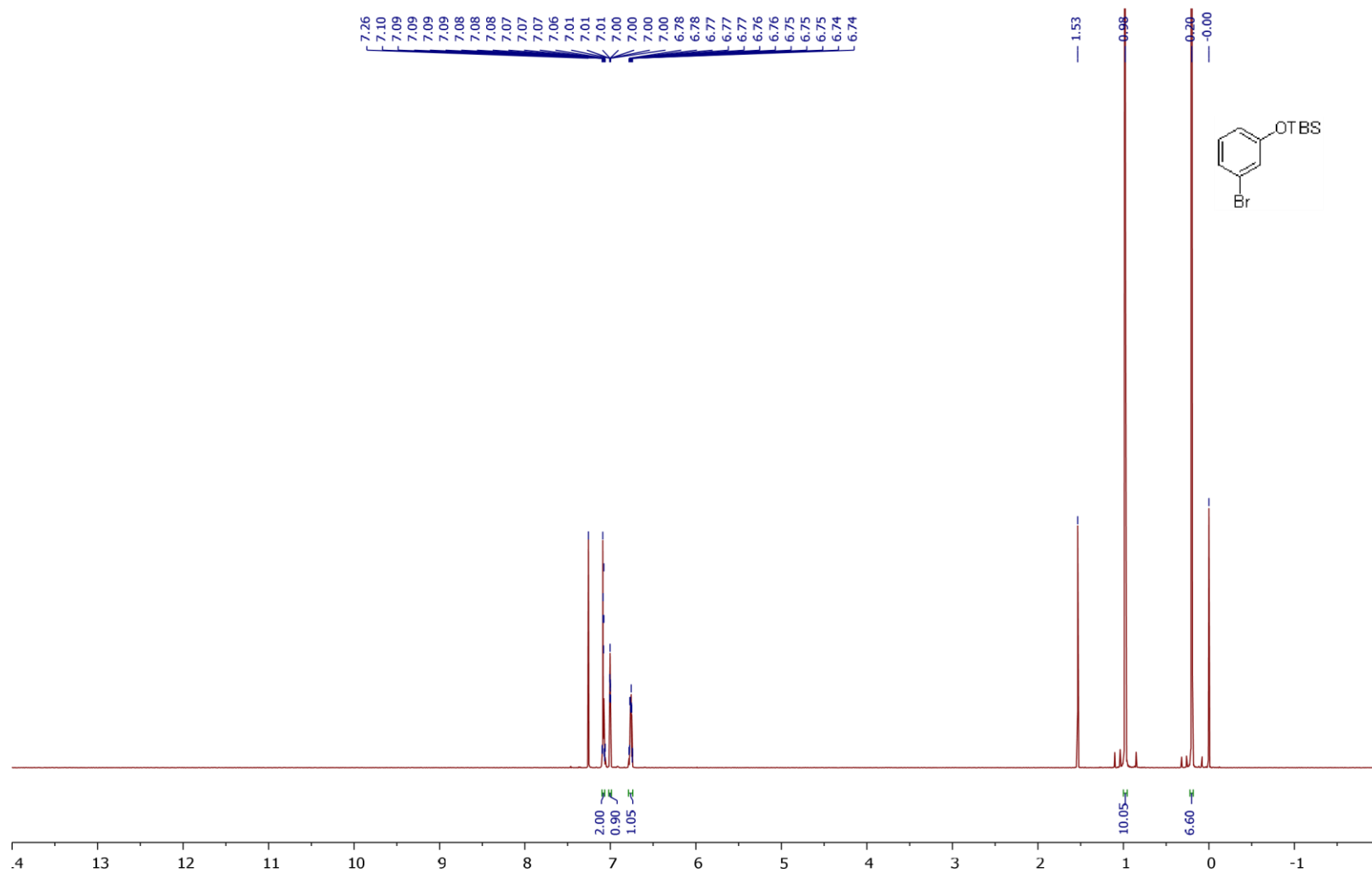
APPENDIX E

Scale-up Synthesis of Cathepsin L Inhibitor KGP94

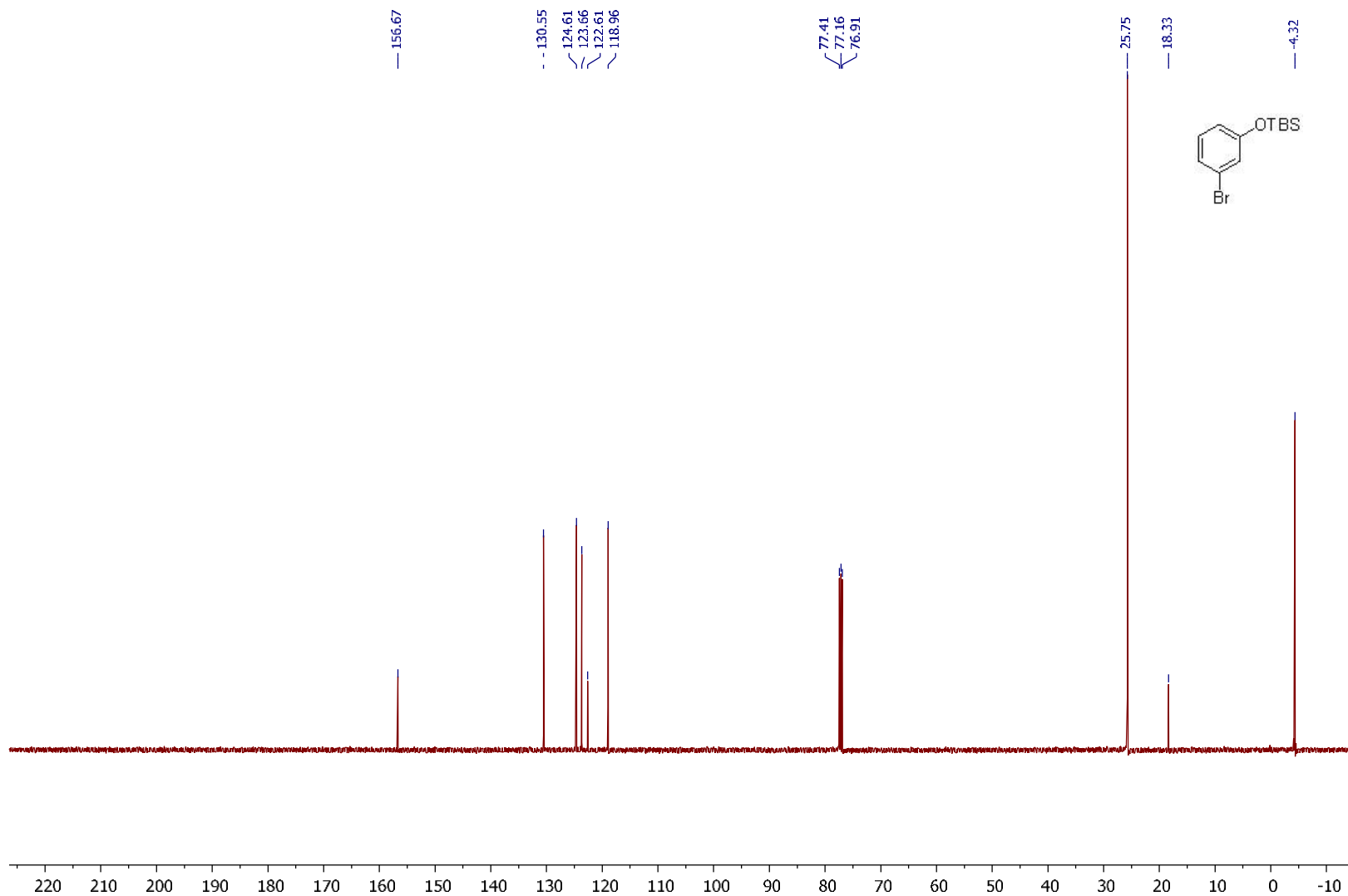
Table of Contents

¹ H and ¹³ C NMR of Compound 2.....	338
¹ H and ¹³ C NMR of Compound 4.....	340
¹ H and ¹³ C NMR of Compound 5.....	342
¹ H and ¹³ C NMR of Compound 6.....	344
¹ H, ¹³ C NMR, Mass Spec and HPLC traces of Compound 7	346
¹ H and ¹³ C NMR of Compound 9.....	349

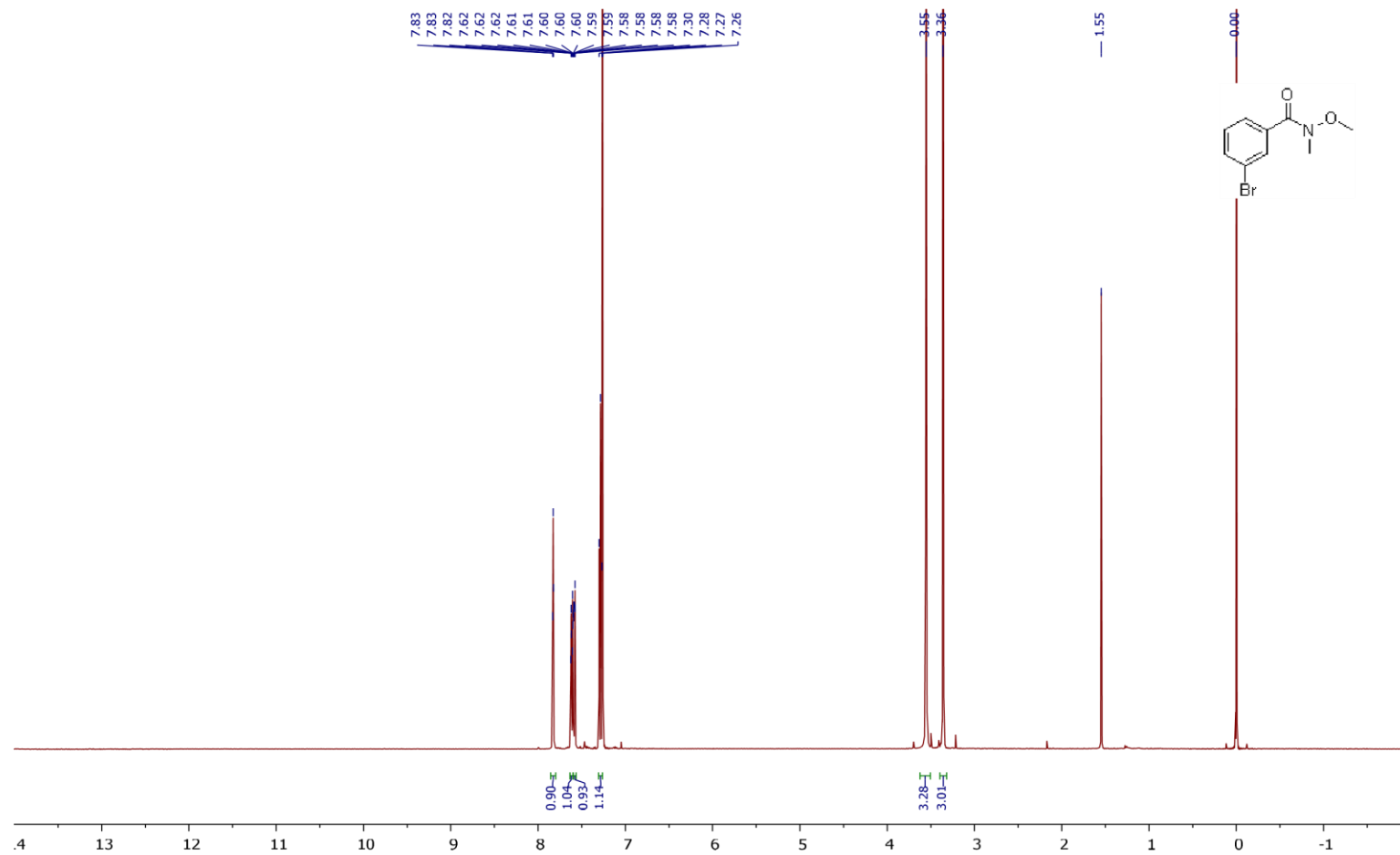
¹H NMR (500 MHz, CDCl₃) of Compound 2



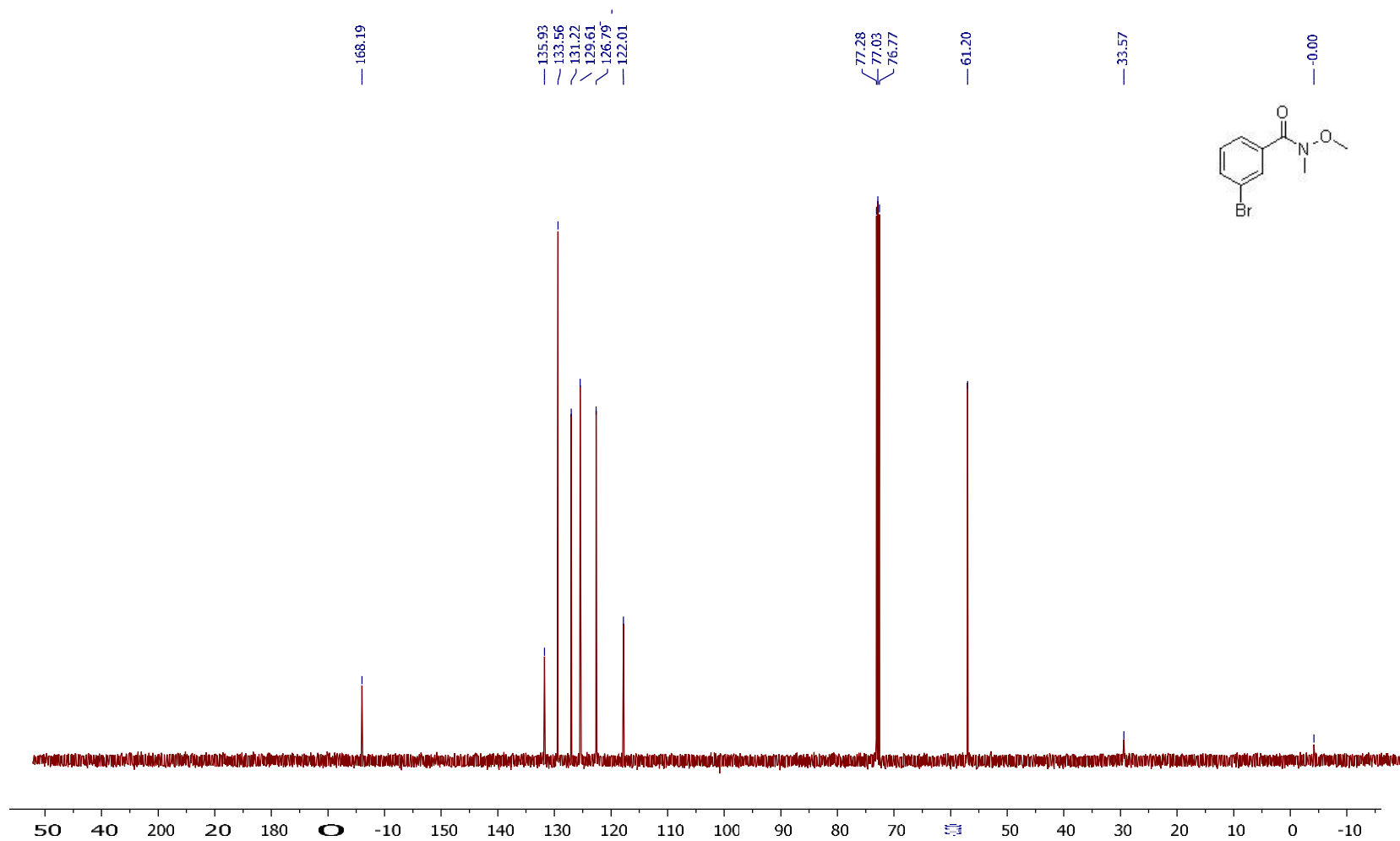
^{13}C NMR (125 MHz, CDCl_3) of Compound **2**



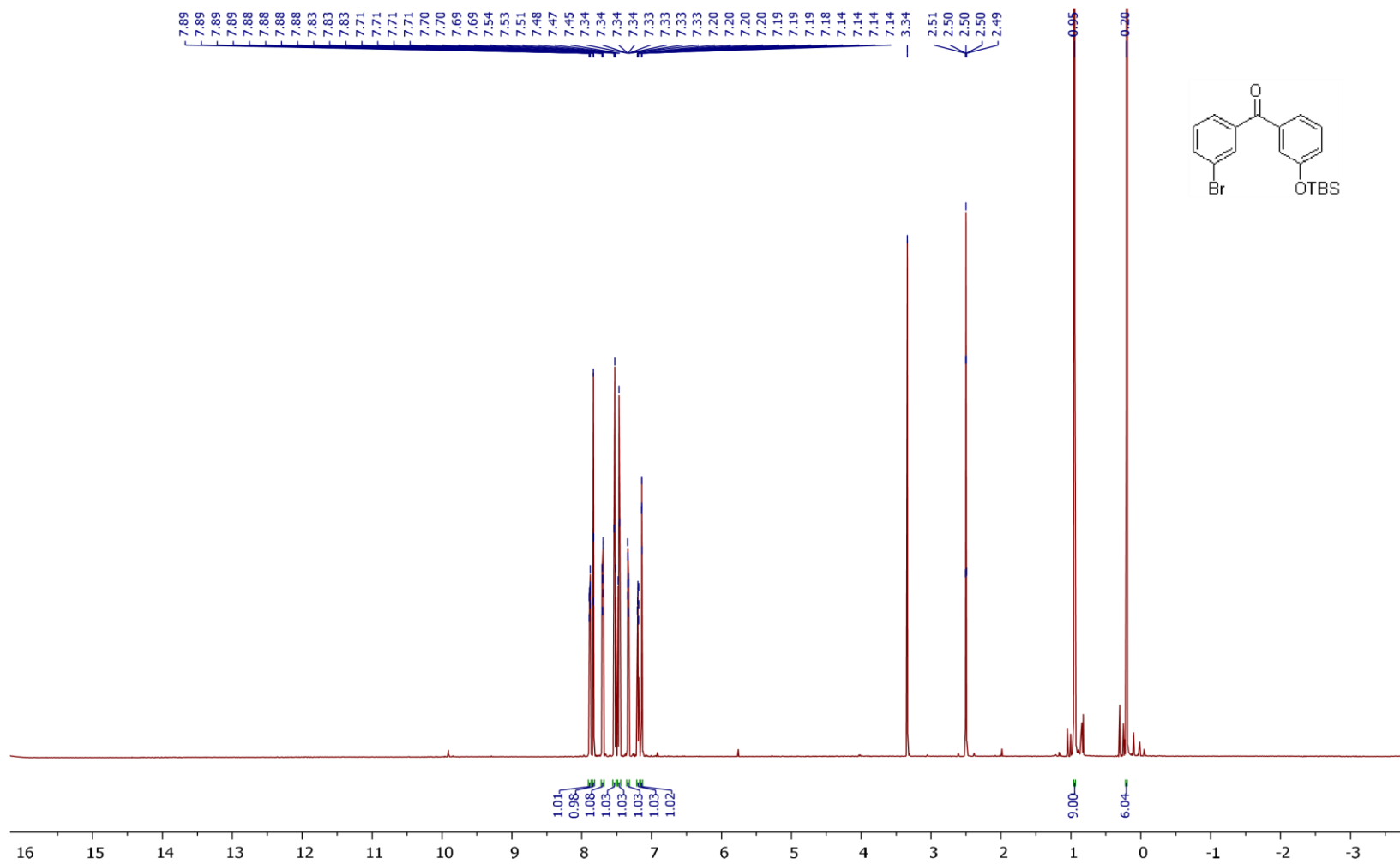
¹H NMR (500 MHz, CDCl₃) of Compound 4



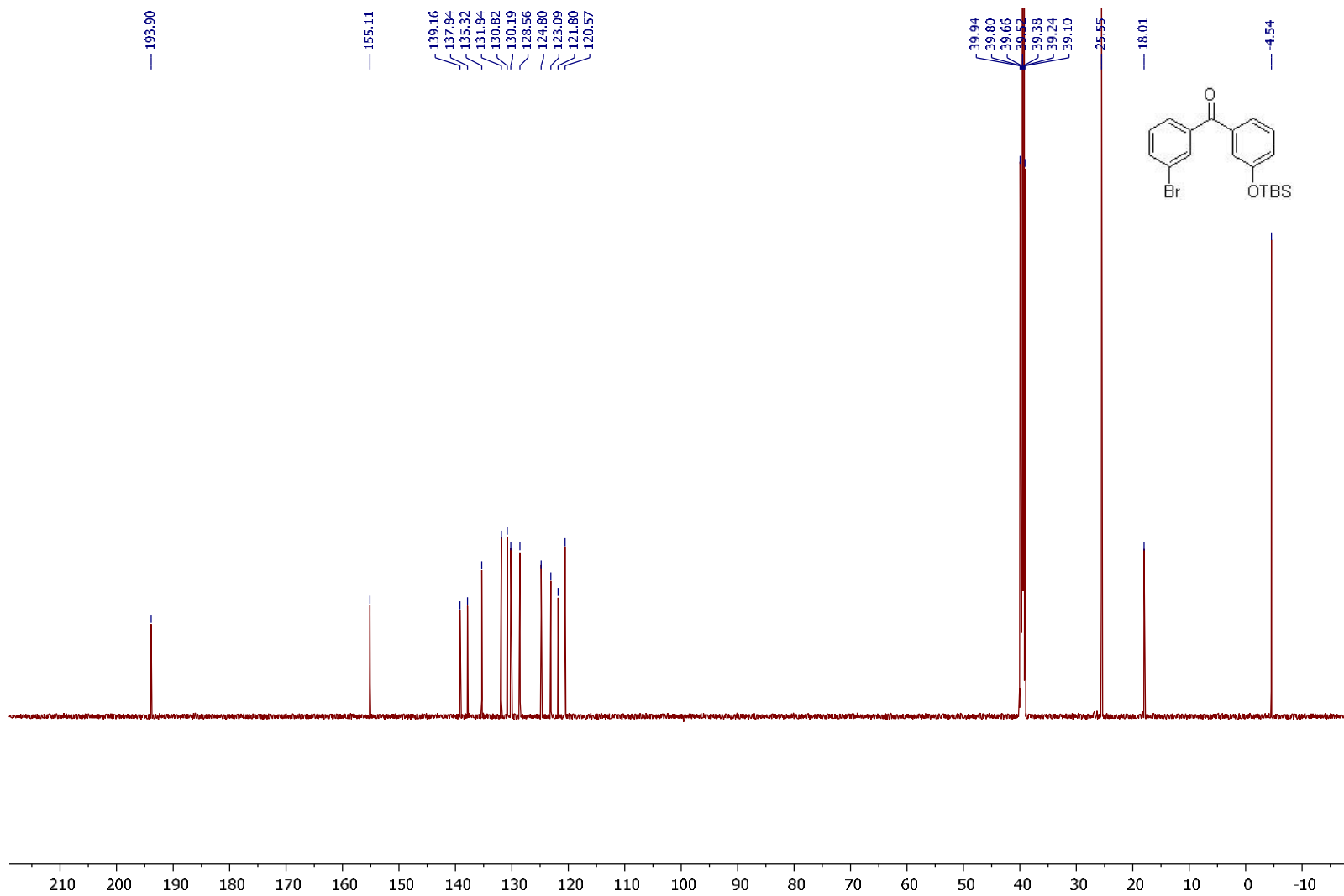
^{13}C NMR (125 MHz, CDCl_3) of Compound 4



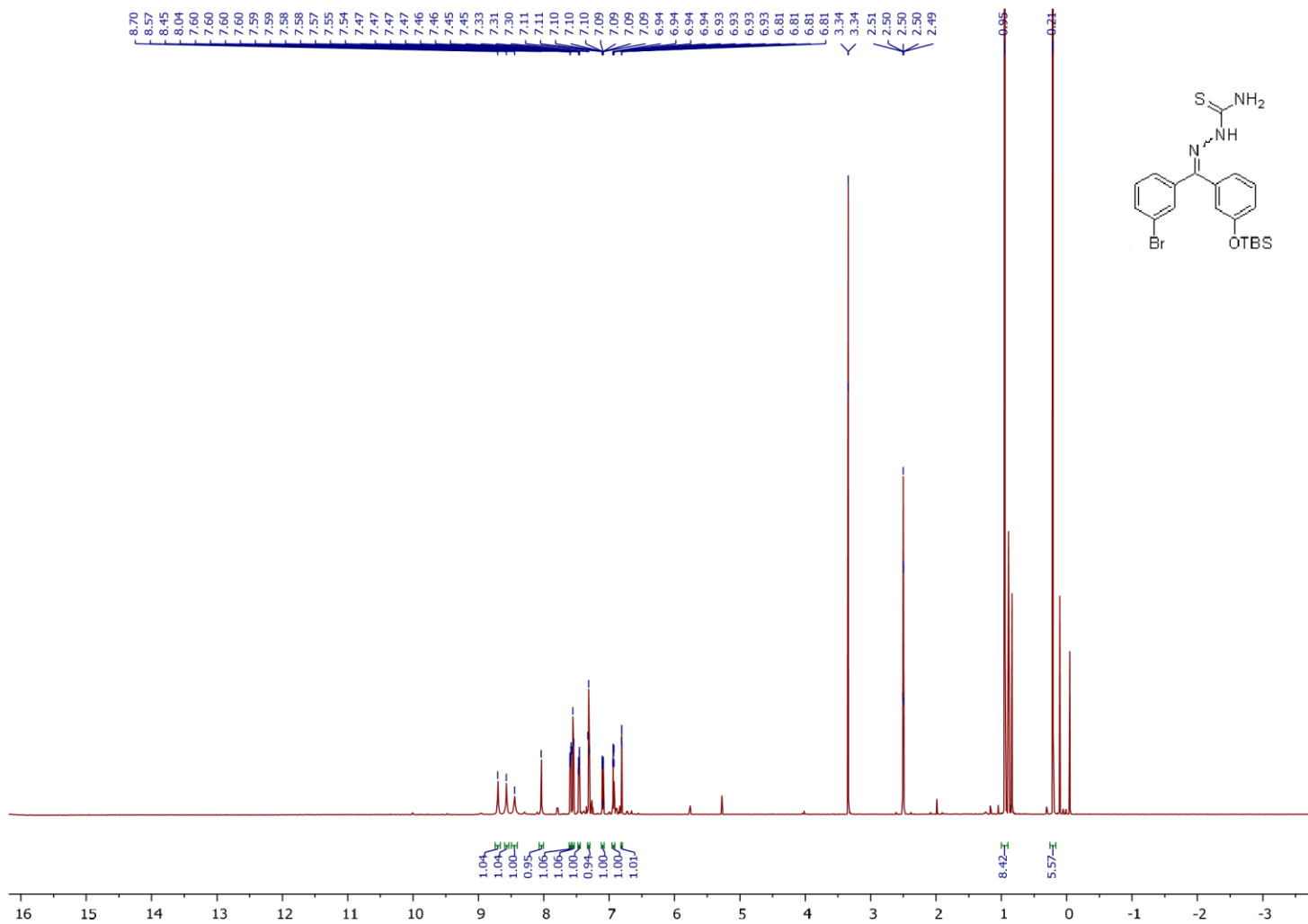
¹H NMR (600 MHz, CDCl₃) of Compound **5**



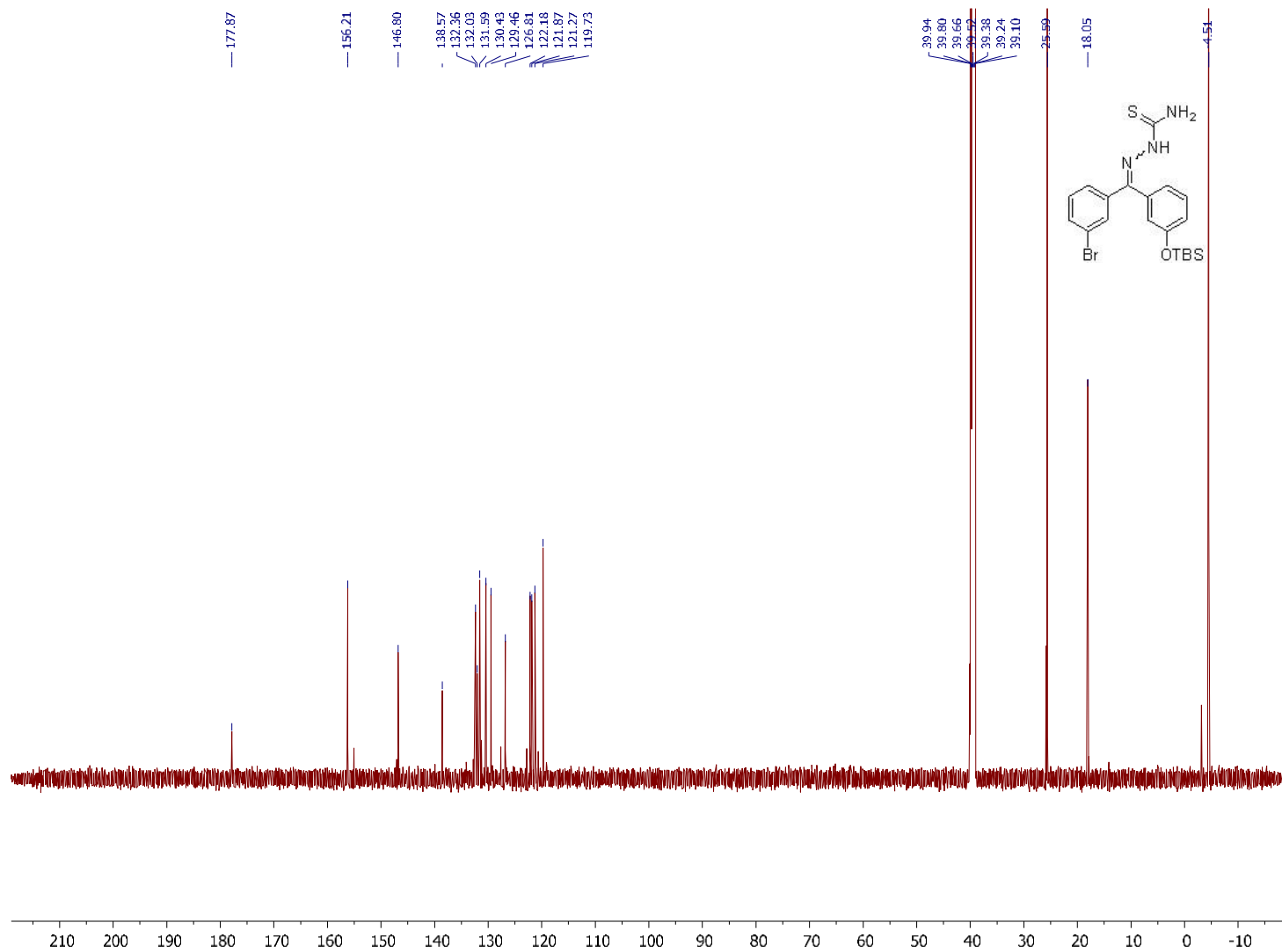
¹³C NMR (150 MHz, CDCl₃) of Compound 5



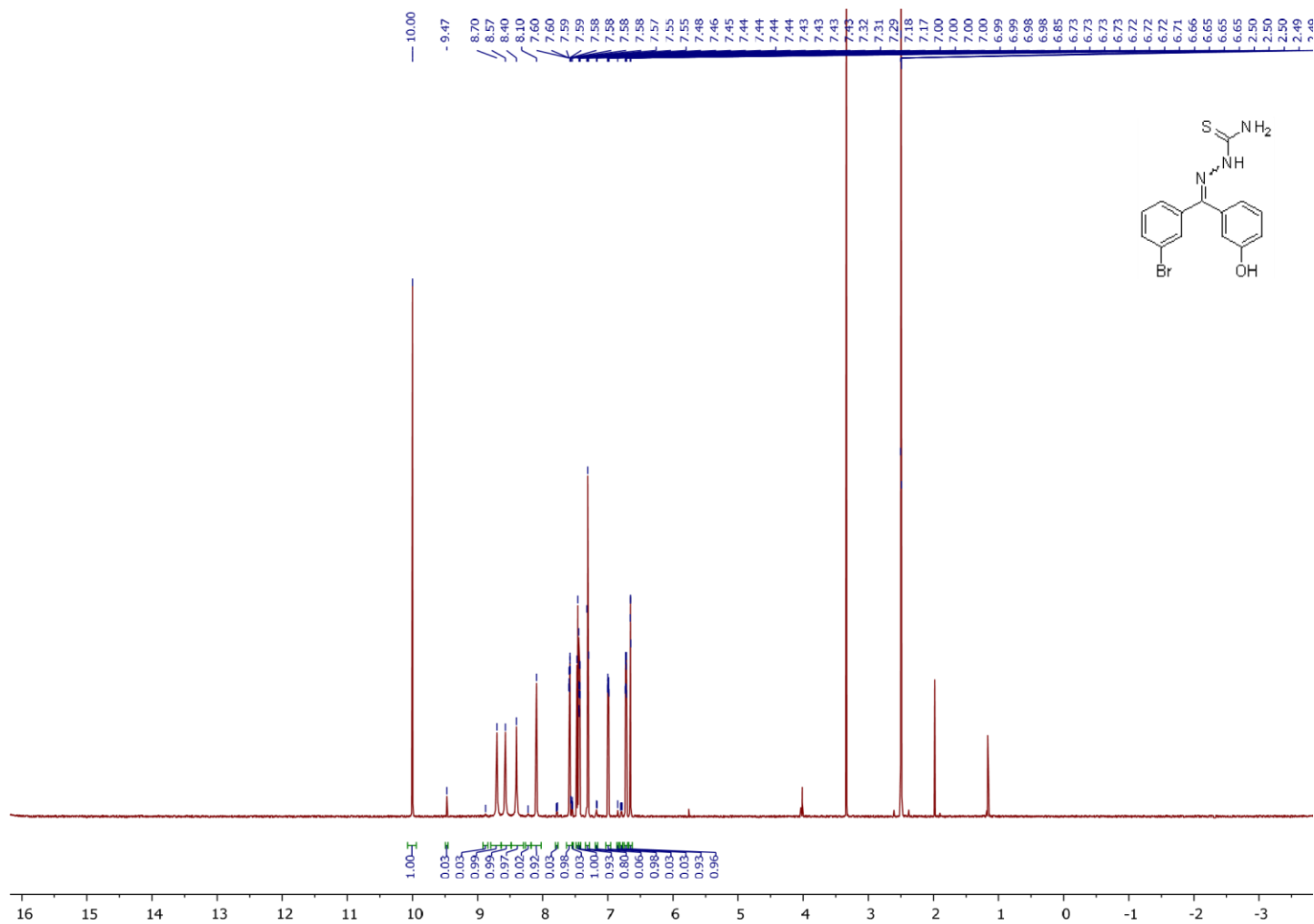
¹H NMR (DMSO-d₆, 600 MHz) of Compound 6



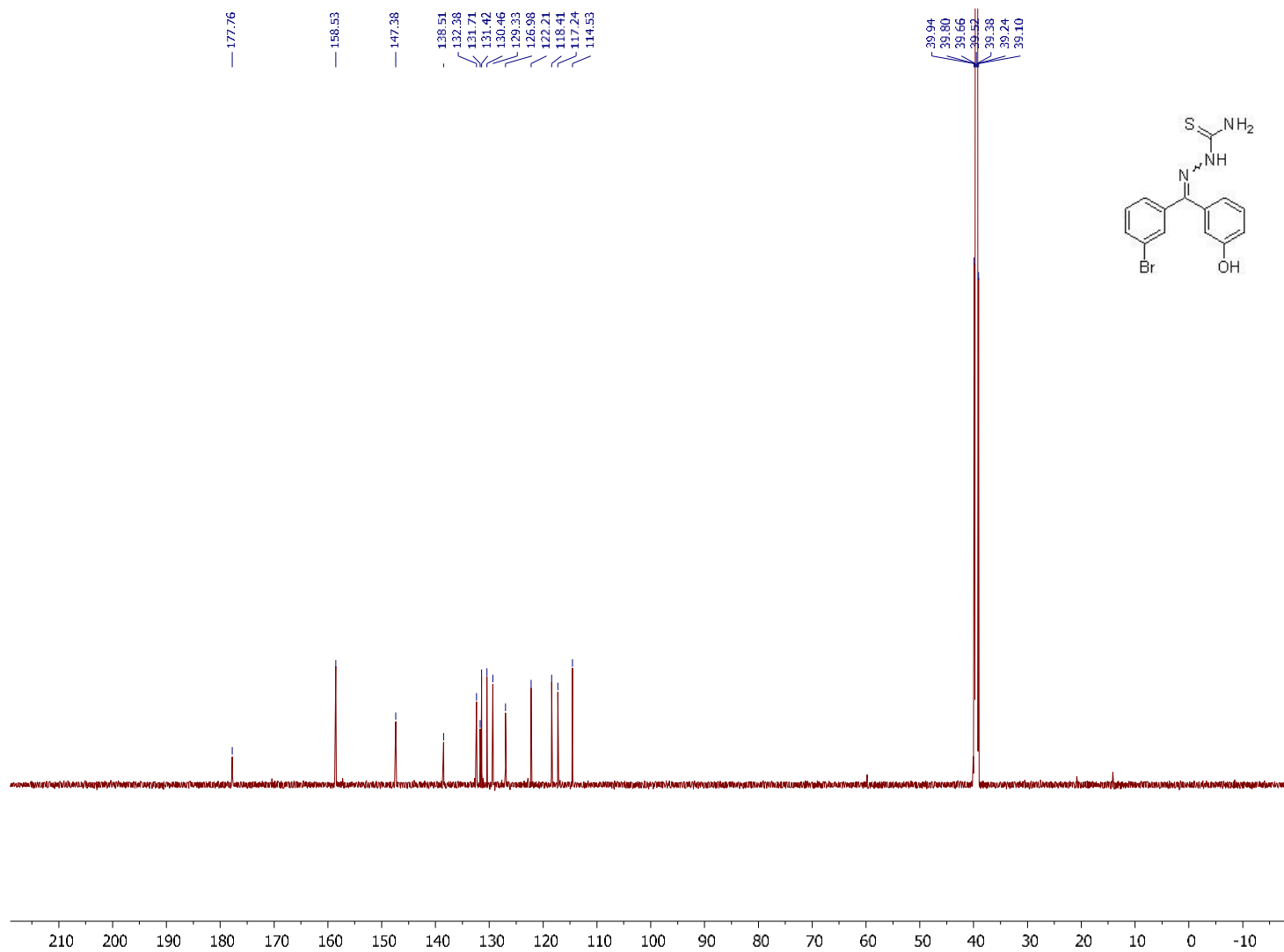
^{13}C NMR (DMSO-d₆, 600 MHz) of Compound **6**



¹H NMR (DMSO-d₆, 600 MHz) of Compound 7

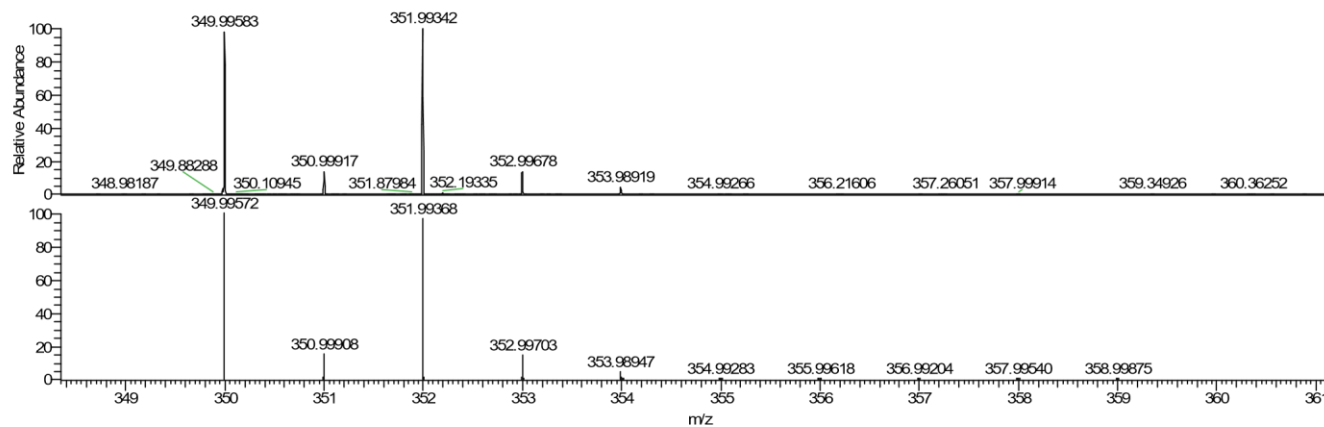
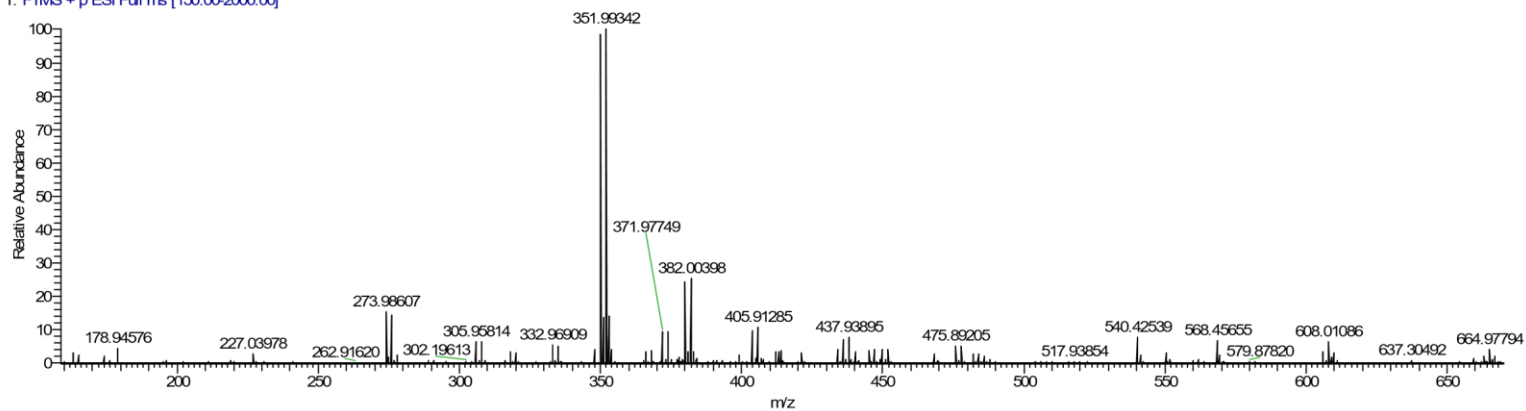


¹³C-NMR (DMSO-d₆, 150 MHz) of Compound 7



Mass Spec of Compound 7

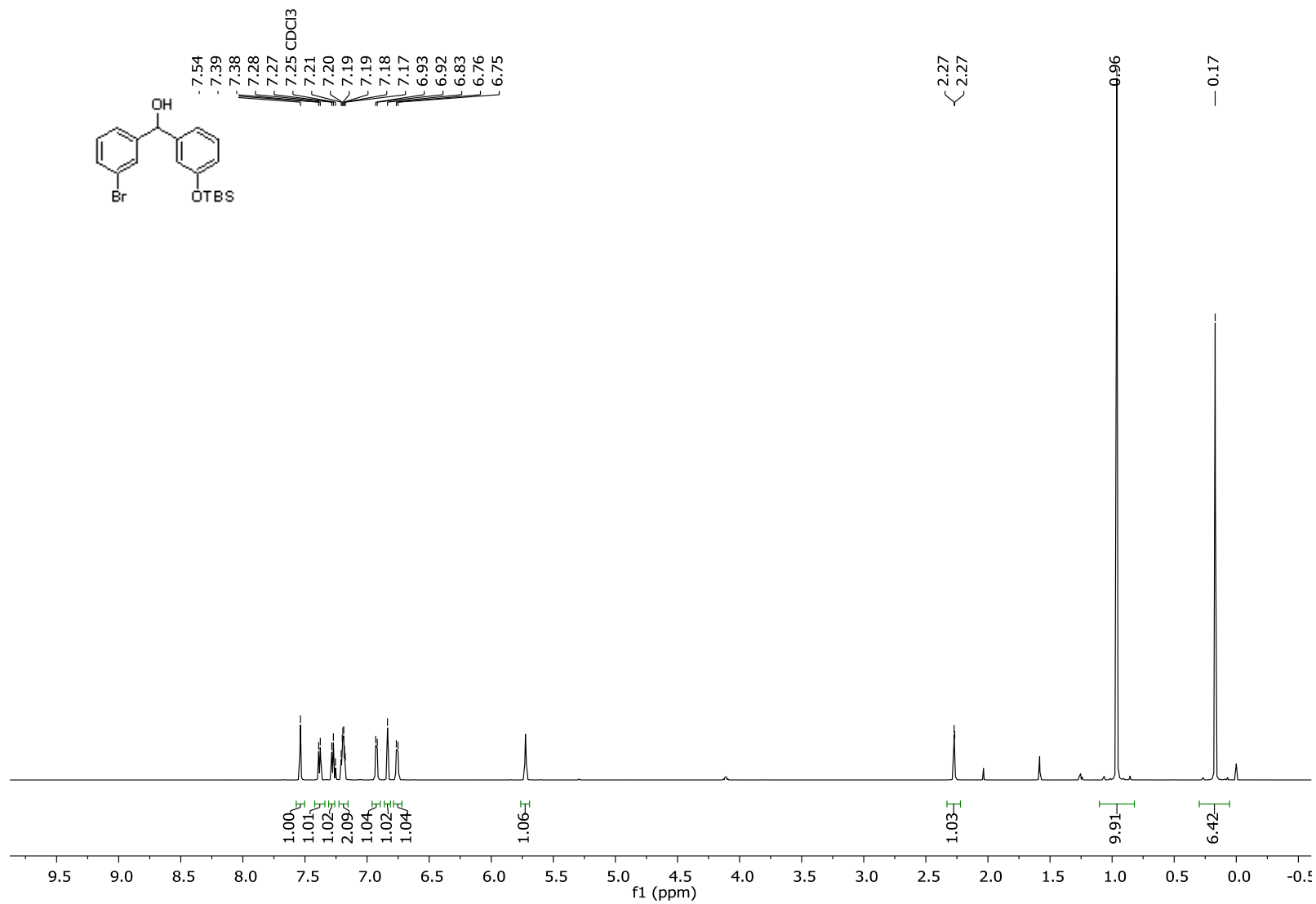
ENP-II-94C2a_Orbi_+ESI #2-13 RT: 0.01-0.10 AV: 12 NL: 2.08E7
T: FTMS + p ESI Full ms [150.00-2000.00]



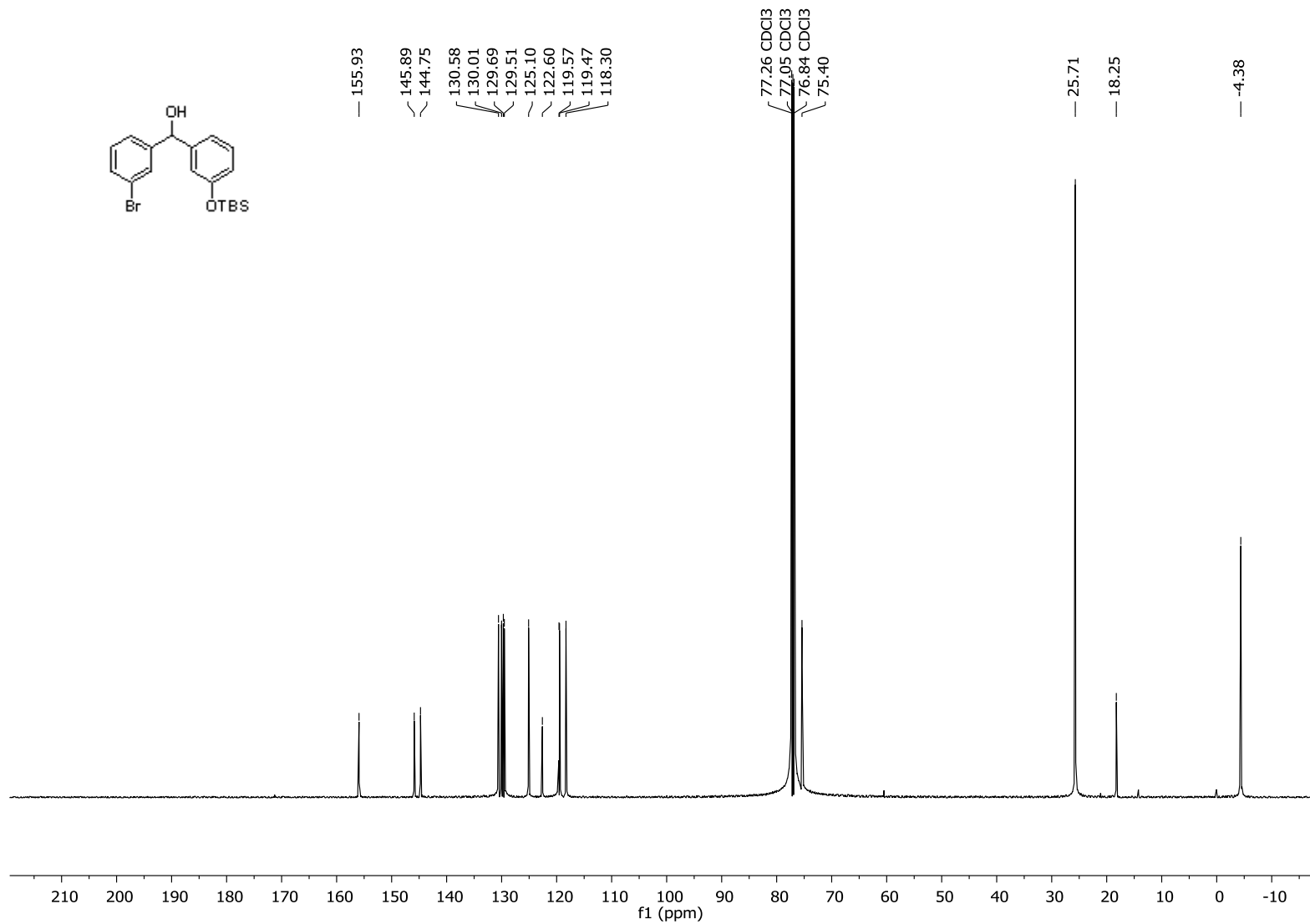
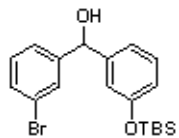
NL:
2.08E7
ENP-II-94C2a_Orbi_+
ESI#2-13 RT: 0.01-0.10
AV: 12 T: FTMS + p ESI
Full ms [150.00-2000.00]

NL:
4.08E5
C11H2BrN3OS+H
C11H3Br1N3O1S1
pa Chrg 1

^1H NMR (DMSO- d_6 , 600 MHz) of Compound **9**



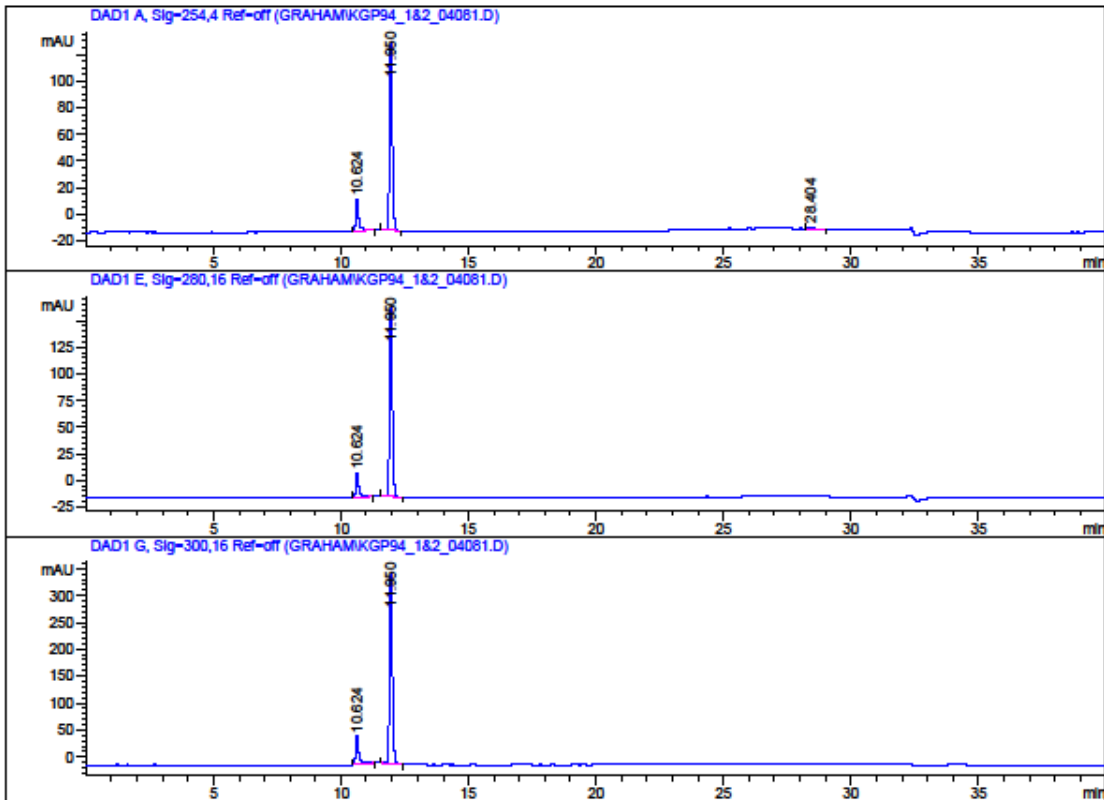
¹³C NMR (DMSO-d₆, 150 MHz) of Compound **9**



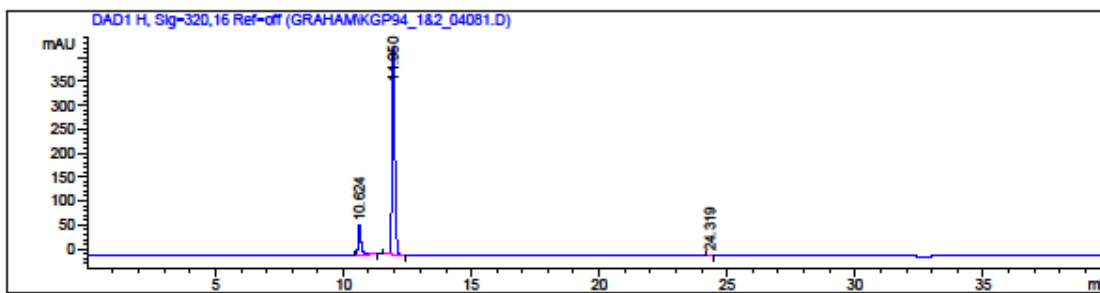
HPLC of Compound 7 (KGP94)

Data File C:\CHEM32\1\DATA\GRAHAM\KGP94_1&2_04081.D
Sample Name: kgp94

```
=====
Acq. Operator   : Graham
Acq. Instrument : Instrument 1           Location : -
Injection Date  : 4/8/2015 1:43:43 PM
Acq. Method    : C:\CHEM32\1\METHODS\KGP94.M
Last changed   : 4/8/2015 1:28:57 PM by Graham
Analysis Method: C:\CHEM32\1\DATA\GRAHAM\KGP94_1&2_04081.D\DA.M (KGP94.M)
Last changed   : 4/15/2015 4:25:50 PM by Zhe
Sample Info    : 4/8/15
                KGP94 batch 1&2 raf_I_23
                method: KGP94
=====
```



Data File C:\CHEM32\1\DATA\GRAHAM\KGP94_1&2_04081.D
Sample Name: kgp94



=====
Area Percent Report
=====

Sorted By : Signal
Multiplier : 1.0000
Dilution : 1.0000
Use Multiplier & Dilution Factor with ISTDs

Signal 1: DAD1 A, Sig=254,4 Ref=off

Peak #	RetTime [min]	Type	Width [min]	Area [mAU*s]	Height [mAU]	Area %
1	10.624	BB	0.1279	207.91383	23.80215	16.1681
2	11.950	BB	0.1138	1065.84668	141.70499	82.8840
3	28.404	BB	0.1180	12.18920	1.48084	0.9479

Totals : 1285.94971 166.98797

Signal 2: DAD1 E, Sig=280,16 Ref=off

Peak #	RetTime [min]	Type	Width [min]	Area [mAU*s]	Height [mAU]	Area %
1	10.624	BB	0.1275	201.38797	23.15149	13.0152
2	11.950	BB	0.1138	1345.93921	178.76274	86.9848

Totals : 1547.32718 201.91423

Data File C:\CHEM32\1\DATA\GRAHAM\KGP94_1&2_04081.D
Sample Name: kgp94

Signal 3: DAD1 G, Sig=300,16 Ref=off

Peak #	RetTime [min]	Type	Width [min]	Area [mAU*s]	Height [mAU]	Area %
1	10.624	BB	0.1278	452.82950	51.87541	14.4533
2	11.950	BB	0.1139	2680.21460	355.78809	85.5467
Totals :				3133.04410	407.66349	

Signal 4: DAD1 H, Sig=320,16 Ref=off

Peak #	RetTime [min]	Type	Width [min]	Area [mAU*s]	Height [mAU]	Area %
1	10.624	BB	0.1280	552.90387	63.26136	14.4322
2	11.950	BB	0.1139	3271.04858	434.03421	85.3826
3	24.319	BB	0.1068	7.09734	1.05102	0.1853
Totals :				3831.04979	498.34660	

=====
*** End of Report ***

APPENDIX F

Permissions

6/12/2018

RightsLink Printable License

JOHN WILEY AND SONS LICENSE TERMS AND CONDITIONS

Jun 12, 2018

This Agreement between Zhe Shi ("You") and John Wiley and Sons ("John Wiley and Sons") consists of your license details and the terms and conditions provided by John Wiley and Sons and Copyright Clearance Center.

License Number	4366030921755
License date	Jun 11, 2018
Licensed Content Publisher	John Wiley and Sons
Licensed Content Publication	CA: Cancer Journal for Clinicians
Licensed Content Title	Cancer statistics, 2018
Licensed Content Author	Rebecca L. Siegel, Kimberly D. Miller, Ahmedin Jemal
Licensed Content Date	Jan 4, 2018
Licensed Content Volume	68
Licensed Content Issue	1
Licensed Content Pages	24
Type of use	Dissertation/Thesis
Requestor type	University/Academic
Format	Print and electronic
Portion	Figure/table
Number of figures/tables	1
Original Wiley figure/table number(s)	Figure 1
Will you be translating?	No
Title of your thesis / dissertation	Small-molecule Inhibitors of Tubulin Polymerization as Vascular Disrupting Agents and Prodrugs Targeting Tumor-Associated Hypoxia
Expected completion date	Aug 2018
Expected size (number of pages)	400
Requestor Location	Zhe Shi 3309 Robinson Dr. Apt 510 WACO, TX 76706 United States Attn: Zhe Shi
Publisher Tax ID	EU826007151
Total	0.00 USD
Terms and Conditions	

TERMS AND CONDITIONS

This copyrighted material is owned by or exclusively licensed to John Wiley & Sons, Inc. or one of its group companies (each a "Wiley Company") or handled on behalf of a society with which a Wiley Company has exclusive publishing rights in relation to a particular work

<https://s100.copyright.com/CustomAdmin/PLF.jsp?ref=7a4cd26c-2397-43aa-b908-0392a8e58384>

1/5

(collectively "WILEY"). By clicking "accept" in connection with completing this licensing transaction, you agree that the following terms and conditions apply to this transaction (along with the billing and payment terms and conditions established by the Copyright Clearance Center Inc., ("CCC's Billing and Payment terms and conditions"), at the time that you opened your RightsLink account (these are available at any time at <http://myaccount.copyright.com>).

Terms and Conditions

- The materials you have requested permission to reproduce or reuse (the "Wiley Materials") are protected by copyright.
- You are hereby granted a personal, non-exclusive, non-sub licensable (on a stand-alone basis), non-transferable, worldwide, limited license to reproduce the Wiley Materials for the purpose specified in the licensing process. This license, and any CONTENT (PDF or image file) purchased as part of your order, is for a one-time use only and limited to any maximum distribution number specified in the license. The first instance of republication or reuse granted by this license must be completed within two years of the date of the grant of this license (although copies prepared before the end date may be distributed thereafter). The Wiley Materials shall not be used in any other manner or for any other purpose, beyond what is granted in the license. Permission is granted subject to an appropriate acknowledgement given to the author, title of the material/book/journal and the publisher. You shall also duplicate the copyright notice that appears in the Wiley publication in your use of the Wiley Material. Permission is also granted on the understanding that nowhere in the text is a previously published source acknowledged for all or part of this Wiley Material. Any third party content is expressly excluded from this permission.
- With respect to the Wiley Materials, all rights are reserved. Except as expressly granted by the terms of the license, no part of the Wiley Materials may be copied, modified, adapted (except for minor reformatting required by the new Publication), translated, reproduced, transferred or distributed, in any form or by any means, and no derivative works may be made based on the Wiley Materials without the prior permission of the respective copyright owner. For STM Signatory Publishers clearing permission under the terms of the [STM Permissions Guidelines](#) only, the terms of the license are extended to include subsequent editions and for editions in other languages, provided such editions are for the work as a whole in situ and does not involve the separate exploitation of the permitted figures or extracts, You may not alter, remove or suppress in any manner any copyright, trademark or other notices displayed by the Wiley Materials. You may not license, rent, sell, loan, lease, pledge, offer as security, transfer or assign the Wiley Materials on a stand-alone basis, or any of the rights granted to you hereunder to any other person.
- The Wiley Materials and all of the intellectual property rights therein shall at all times remain the exclusive property of John Wiley & Sons Inc, the Wiley Companies, or their respective licensors, and your interest therein is only that of having possession of and the right to reproduce the Wiley Materials pursuant to Section 2 herein during the continuance of this Agreement. You agree that you own no right, title or interest in or to the Wiley Materials or any of the intellectual property rights therein. You shall have no rights hereunder other than the license as provided for above in Section 2. No right, license or interest to any trademark, trade name, service mark or other branding ("Marks") of WILEY or its licensors is granted hereunder, and you agree that you shall not assert any such right, license or interest with respect thereto

- NEITHER WILEY NOR ITS LICENSORS MAKES ANY WARRANTY OR REPRESENTATION OF ANY KIND TO YOU OR ANY THIRD PARTY, EXPRESS, IMPLIED OR STATUTORY, WITH RESPECT TO THE MATERIALS OR THE ACCURACY OF ANY INFORMATION CONTAINED IN THE MATERIALS, INCLUDING, WITHOUT LIMITATION, ANY IMPLIED WARRANTY OF MERCHANTABILITY, ACCURACY, SATISFACTORY QUALITY, FITNESS FOR A PARTICULAR PURPOSE, USABILITY, INTEGRATION OR NON-INFRINGEMENT AND ALL SUCH WARRANTIES ARE HEREBY EXCLUDED BY WILEY AND ITS LICENSORS AND WAIVED BY YOU.
- WILEY shall have the right to terminate this Agreement immediately upon breach of this Agreement by you.
- You shall indemnify, defend and hold harmless WILEY, its Licensors and their respective directors, officers, agents and employees, from and against any actual or threatened claims, demands, causes of action or proceedings arising from any breach of this Agreement by you.
- IN NO EVENT SHALL WILEY OR ITS LICENSORS BE LIABLE TO YOU OR ANY OTHER PARTY OR ANY OTHER PERSON OR ENTITY FOR ANY SPECIAL, CONSEQUENTIAL, INCIDENTAL, INDIRECT, EXEMPLARY OR PUNITIVE DAMAGES, HOWEVER CAUSED, ARISING OUT OF OR IN CONNECTION WITH THE DOWNLOADING, PROVISIONING, VIEWING OR USE OF THE MATERIALS REGARDLESS OF THE FORM OF ACTION, WHETHER FOR BREACH OF CONTRACT, BREACH OF WARRANTY, TORT, NEGLIGENCE, INFRINGEMENT OR OTHERWISE (INCLUDING, WITHOUT LIMITATION, DAMAGES BASED ON LOSS OF PROFITS, DATA, FILES, USE, BUSINESS OPPORTUNITY OR CLAIMS OF THIRD PARTIES), AND WHETHER OR NOT THE PARTY HAS BEEN ADVISED OF THE POSSIBILITY OF SUCH DAMAGES. THIS LIMITATION SHALL APPLY NOTWITHSTANDING ANY FAILURE OF ESSENTIAL PURPOSE OF ANY LIMITED REMEDY PROVIDED HEREIN.
- Should any provision of this Agreement be held by a court of competent jurisdiction to be illegal, invalid, or unenforceable, that provision shall be deemed amended to achieve as nearly as possible the same economic effect as the original provision, and the legality, validity and enforceability of the remaining provisions of this Agreement shall not be affected or impaired thereby.
- The failure of either party to enforce any term or condition of this Agreement shall not constitute a waiver of either party's right to enforce each and every term and condition of this Agreement. No breach under this agreement shall be deemed waived or excused by either party unless such waiver or consent is in writing signed by the party granting such waiver or consent. The waiver by or consent of a party to a breach of any provision of this Agreement shall not operate or be construed as a waiver of or consent to any other or subsequent breach by such other party.
- This Agreement may not be assigned (including by operation of law or otherwise) by you without WILEY's prior written consent.
- Any fee required for this permission shall be non-refundable after thirty (30) days from receipt by the CCC.

- These terms and conditions together with CCC's Billing and Payment terms and conditions (which are incorporated herein) form the entire agreement between you and WILEY concerning this licensing transaction and (in the absence of fraud) supersedes all prior agreements and representations of the parties, oral or written. This Agreement may not be amended except in writing signed by both parties. This Agreement shall be binding upon and inure to the benefit of the parties' successors, legal representatives, and authorized assigns.
- In the event of any conflict between your obligations established by these terms and conditions and those established by CCC's Billing and Payment terms and conditions, these terms and conditions shall prevail.
- WILEY expressly reserves all rights not specifically granted in the combination of (i) the license details provided by you and accepted in the course of this licensing transaction, (ii) these terms and conditions and (iii) CCC's Billing and Payment terms and conditions.
- This Agreement will be void if the Type of Use, Format, Circulation, or Requestor Type was misrepresented during the licensing process.
- This Agreement shall be governed by and construed in accordance with the laws of the State of New York, USA, without regards to such state's conflict of law rules. Any legal action, suit or proceeding arising out of or relating to these Terms and Conditions or the breach thereof shall be instituted in a court of competent jurisdiction in New York County in the State of New York in the United States of America and each party hereby consents and submits to the personal jurisdiction of such court, waives any objection to venue in such court and consents to service of process by registered or certified mail, return receipt requested, at the last known address of such party.

WILEY OPEN ACCESS TERMS AND CONDITIONS

Wiley Publishes Open Access Articles in fully Open Access Journals and in Subscription journals offering Online Open. Although most of the fully Open Access journals publish open access articles under the terms of the Creative Commons Attribution (CC BY) License only, the subscription journals and a few of the Open Access Journals offer a choice of Creative Commons Licenses. The license type is clearly identified on the article.

The Creative Commons Attribution License

The [Creative Commons Attribution License \(CC-BY\)](#) allows users to copy, distribute and transmit an article, adapt the article and make commercial use of the article. The CC-BY license permits commercial and non-

Creative Commons Attribution Non-Commercial License

The [Creative Commons Attribution Non-Commercial \(CC-BY-NC\) License](#) permits use, distribution and reproduction in any medium, provided the original work is properly cited and is not used for commercial purposes. (see below)

Creative Commons Attribution-Non-Commercial-NoDerivs License

The [Creative Commons Attribution Non-Commercial-NoDerivs License \(CC-BY-NC-ND\)](#) permits use, distribution and reproduction in any medium, provided the original work is properly cited, is not used for commercial purposes and no modifications or adaptations are made. (see below)

Use by commercial "for-profit" organizations

Use of Wiley Open Access articles for commercial, promotional, or marketing purposes requires further explicit permission from Wiley and will be subject to a fee.

Further details can be found on Wiley Online Library
<http://olabout.wiley.com/WileyCDA/Section/id-410895.html>

Other Terms and Conditions:

v1.10 Last updated September 2015

Questions? customer care@copyright.com or +1-855-239-3415 (toll free in the US) or
+1-978-646-2777.

**ELSEVIER LICENSE
TERMS AND CONDITIONS**

Jun 11, 2018

This Agreement between Zhe Shi ("You") and Elsevier ("Elsevier") consists of your license details and the terms and conditions provided by Elsevier and Copyright Clearance Center.

License Number	4366100592662
License date	Jun 11, 2018
Licensed Content Publisher	Elsevier
Licensed Content Publication	Cancer Treatment Reviews
Licensed Content Title	The unique characteristics of tumor vasculature and preclinical evidence for its selective disruption by Tumor-Vascular Disrupting Agents
Licensed Content Author	Dietmar W. Siemann
Licensed Content Date	Feb 1, 2011
Licensed Content Volume	37
Licensed Content Issue	1
Licensed Content Pages	12
Start Page	63
End Page	74
Type of Use	reuse in a thesis/dissertation
Portion	figures/tables/illustrations
Number of figures/tables/illustrations	1
Format	both print and electronic
Are you the author of this Elsevier article?	No
Will you be translating?	No
Original figure numbers	Figure 1
Title of your thesis/dissertation	Small-molecule Inhibitors of Tubulin Polymerization as Vascular Disrupting Agents and Prodrugs Targeting Tumor-Associated Hypoxia
Expected completion date	Aug 2018
Estimated size (number of pages)	400
Requestor Location	Zhe Shi 3309 Robinson Dr. Apt 510 WACO, TX 76706 United States Attn: Zhe Shi
Publisher Tax ID	98-0397604
Total	0.00 USD
Terms and Conditions	

<https://s100.copyright.com/AppDispatchServlet>

1/6

**SPRINGER NATURE LICENSE
TERMS AND CONDITIONS**

Jun 11, 2018

This Agreement between Zhe Shi ("You") and Springer Nature ("Springer Nature") consists of your license details and the terms and conditions provided by Springer Nature and Copyright Clearance Center.

License Number	4366110654076
License date	Jun 11, 2018
Licensed Content Publisher	Springer Nature
Licensed Content Publication	Nature Reviews Cancer
Licensed Content Title	Disrupting tumour blood vessels
Licensed Content Author	Gillian M. Tozer, Chryso Kanthou, Bruce C. Baguley
Licensed Content Date	Jun 1, 2005
Licensed Content Volume	5
Licensed Content Issue	6
Type of Use	Thesis/Dissertation
Requestor type	academic/university or research institute
Format	print and electronic
Portion	figures/tables/illustrations
Number of figures/tables/illustrations	1
High-res required	no
Will you be translating?	no
Circulation/distribution	<501
Author of this Springer Nature content	no
Title	Small-molecule Inhibitors of Tubulin Polymerization as Vascular Disrupting Agents and Prodrugs Targeting Tumor-Associated Hypoxia
Instructor name	n/a
Institution name	n/a
Expected presentation date	Aug 2018
Portions	Figure 3 Proposed mechanisms for rapid tumour vascular shutdown after treatment with CA-4-P or DMXAA.
Requestor Location	Zhe Shi 3309 Robinson Dr. Apt 510 WACO, TX 76706 United States Attn: Zhe Shi
Billing Type	Invoice
Billing Address	Zhe Shi 3309 Robinson Dr. Apt 510 WACO, TX 76706 United States Attn: Zhe Shi
Total	0.00 USD
Terms and Conditions	

<https://s100.copyright.com/AppDispatchServlet>

1/3

**ELSEVIER LICENSE
TERMS AND CONDITIONS**

Jun 11, 2018

This Agreement between Zhe Shi ("You") and Elsevier ("Elsevier") consists of your license details and the terms and conditions provided by Elsevier and Copyright Clearance Center.

License Number	4366120235056
License date	Jun 11, 2018
Licensed Content Publisher	Elsevier
Licensed Content Publication	Cancer Letters
Licensed Content Title	The vascular disrupting activity of OXi8006 in endothelial cells and its phosphate prodrug OXi8007 in breast tumor xenografts
Licensed Content Author	Tracy E. Strecker, Samuel O. Odutola, Ramona Lopez, Morgan S. Cooper, Justin K. Tidmore, Amanda K. Charlton-Sevcik, Li Li, Matthew T. MacDonough, Mallinath B. Hadimani, Anjan Ghatak, Li Liu, David J. Chaplin, Ralph P. Mason, Kevin G. Pinney, Mary Lynn Trawick
Licensed Content Date	Dec 1, 2015
Licensed Content Volume	369
Licensed Content Issue	1
Licensed Content Pages	13
Start Page	229
End Page	241
Type of Use	reuse in a thesis/dissertation
Intended publisher of new work	other
Portion	figures/tables/illustrations
Number of figures/tables/illustrations	1
Format	both print and electronic
Are you the author of this Elsevier article?	No
Will you be translating?	No
Original figure numbers	Figure 10
Title of your thesis/dissertation	Small-molecule Inhibitors of Tubulin Polymerization as Vascular Disrupting Agents and Prodrugs Targeting Tumor-Associated Hypoxia
Expected completion date	Aug 2018
Estimated size (number of pages)	400
Requestor Location	Zhe Shi 3309 Robinson Dr. Apt 510 WACO, TX 76706 United States Attn: Zhe Shi

REFERENCE

- (1) Street, W. Cancer Facts & Figures 2018. **2018**, 76.
- (2) Siegel, R. L.; Miller, K. D.; Jemal, A. Cancer Statistics, 2018. *CA. Cancer J. Clin.* **2018**, *68* (1), 7–30.
- (3) Cancer of Any Site - Cancer Stat Facts
<https://seer.cancer.gov/statfacts/html/all.html> (accessed May 15, 2018).
- (4) Sudhakar, A. History of Cancer, Ancient and Modern Treatment Methods. *J. Cancer Sci. Ther.* **2009**, *1* (2), 1–4.
- (5) Types of Cancer Treatment <https://www.cancer.gov/about-cancer/treatment/types> (accessed May 15, 2018).
- (6) Syn, N. L.; Teng, M. W. L.; Mok, T. S. K.; Soo, R. A. De-Novo and Acquired Resistance to Immune Checkpoint Targeting. *Lancet Oncol.* **2017**, *18* (12), e731–e741.
- (7) Siemann, D. W. The Unique Characteristics of Tumor Vasculature and Preclinical Evidence for Its Selective Disruption by Tumor-Vascular Disrupting Agents. *Cancer Treat. Rev.* **2011**, *37* (1), 63–74.
- (8) Horsman, M. R.; Vaupel, P. Pathophysiological Basis for the Formation of the Tumor Microenvironment. *Front. Oncol.* **2016**, *6*.
- (9) Folkman, J. Tumor Angiogenesis: Therapeutic Implications. *N. Engl. J. Med.* **1971**, *285* (21), 1182–1186.
- (10) Folkman, J.; Merler, E.; Abernathy, C.; Williams, G. Isolation of a Tumor Factor Responsible for Angiogenesis. *J. Exp. Med.* **1971**, *133* (2), 275–288.
- (11) Less, J. R.; Skalak, T. C.; Sevick, E. M.; Jain, R. K. Microvascular Architecture in a Mammary Carcinoma: Branching Patterns and Vessel Dimensions. *Cancer Res.* **1991**, *51* (1), 265–273.
- (12) Dudley, A. C. Tumor Endothelial Cells. *Cold Spring Harb. Perspect. Med.* **2012**, *2* (3).

- (13) Dvorak, H. F.; Nagy, J. A.; Dvorak, J. T.; Dvorak, A. M. Identification and Characterization of the Blood Vessels of Solid Tumors That Are Leaky to Circulating Macromolecules. *Am. J. Pathol.* **1988**, *133* (1), 95–109.
- (14) Folkman, J.; Long, D. M.; Becker, F. F. Growth and Metastasis of Tumor in Organ Culture. *Cancer* **1963**, *16*, 453–467.
- (15) Gimbrone, M. A.; Aster, R. H.; Cotran, R. S.; Corkery, J.; Jandl, J. H.; Folkman, J. Preservation of Vascular Integrity in Organs Perfused in Vitro with a Platelet-Rich Medium. *Nature* **1969**, *222* (5188), 33–36.
- (16) Denekamp, J. Endothelial Cell Proliferation as a Novel Approach to Targeting Tumour Therapy. *Br. J. Cancer* **1982**, *45* (1), 136–139.
- (17) Siemann, D. W.; Chaplin, D. J.; Horsman, M. R. Realizing the Potential of Vascular Targeted Therapy: The Rationale for Combining Vascular Disrupting Agents and Anti-Angiogenic Agents to Treat Cancer. *Cancer Invest.* **2017**, *35* (8), 519–534.
- (18) Birbrair, A.; Zhang, T.; Wang, Z.-M.; Messi, M. L.; Olson, J. D.; Mintz, A.; Delbono, O. Type-2 Pericytes Participate in Normal and Tumoral Angiogenesis. *Am. J. Physiol.-Cell Physiol.* **2014**, *307* (1), C25–C38.
- (19) Gotink, K. J.; Verheul, H. M. W. Anti-Angiogenic Tyrosine Kinase Inhibitors: What Is Their Mechanism of Action? *Angiogenesis* **2010**, *13* (1), 1–14.
- (20) Goto, F.; Goto, K.; Weindel, K.; Folkman, J. Synergistic Effects of Vascular Endothelial Growth Factor and Basic Fibroblast Growth Factor on the Proliferation and Cord Formation of Bovine Capillary Endothelial Cells within Collagen Gels. *Lab. Investig. J. Tech. Methods Pathol.* **1993**, *69* (5), 508–517.
- (21) Ornitz, D. M.; Itoh, N. Fibroblast Growth Factors. *Genome Biol.* **2001**, *2*, reviews3005.
- (22) Vasudev, N. S.; Reynolds, A. R. Anti-Angiogenic Therapy for Cancer: Current Progress, Unresolved Questions and Future Directions. *Angiogenesis* **2014**, *17* (3), 471–494.
- (23) Shih, T.; Lindley, C. Bevacizumab: An Angiogenesis Inhibitor for the Treatment of Solid Malignancies. *Clin. Ther.* **2006**, *28* (11), 1779–1802.
- (24) Los, M.; Roodhart, J. M. L.; Voest, E. E. Target Practice: Lessons from Phase III Trials with Bevacizumab and Vatalanib in the Treatment of Advanced Colorectal Cancer. *The Oncologist* **2007**, *12* (4), 443–450.

- (25) Gridelli, C.; Rossi, A.; Maione, P.; Rossi, E.; Castaldo, V.; Sacco, P. C.; Colantuoni, G. Vascular Disrupting Agents: A Novel Mechanism of Action in the Battle Against Non-Small Cell Lung Cancer. *The Oncologist* **2009**, *14* (6), 612–620.
- (26) Hinnen, P.; Eskens, F. a. L. M. Vascular Disrupting Agents in Clinical Development. *Br. J. Cancer* **2007**, *96* (8), 1159–1165.
- (27) Pettit, G. R.; Singh, S. B.; Hamel, E.; Lin, C. M.; Alberts, D. S.; Garcia-Kendal, D. Isolation and Structure of the Strong Cell Growth and Tubulin Inhibitor Combretastatin A-4. *Experientia* **1989**, *45* (2), 209–211.
- (28) Tozer, G. M.; Prise, V. E.; Wilson, J.; Cemazar, M.; Shan, S.; Dewhirst, M. W.; Barber, P. R.; Vojnovic, B.; Chaplin, D. J. Mechanisms Associated with Tumor Vascular Shut-down Induced by Combretastatin A-4 Phosphate: Intravital Microscopy and Measurement of Vascular Permeability. *Cancer Res.* **2001**, *61* (17), 6413–6422.
- (29) Lominadze, D.; Mchedlishvili, G. Red Blood Cell Behavior at Low Flow Rate in Microvessels. *Microvasc. Res.* **1999**, *58* (2), 187–189.
- (30) Tozer, G. M.; Kanthou, C.; Baguley, B. C. Disrupting Tumour Blood Vessels. *Nat. Rev. Cancer* **2005**, *5* (6), 423–435.
- (31) Graham, W.; Roberts, J. B. Intravenous Colchicine in the Management of Gouty Arthritis. *Ann. Rheum. Dis.* **1953**, *12* (1), 16–19.
- (32) Dasgeb, B.; Kornreich, D.; McGuinn, K.; Okon, L.; Brownell, I.; Sackett, D. L. Colchicine: An Ancient Drug with Novel Applications. *Br. J. Dermatol.* *178* (2), 350–356.
- (33) Levy, M.; Spino, M.; Read, S. E. Colchicine: A State-of-the-Art Review. *Pharmacotherapy* **1991**, *11* (3), 196–211.
- (34) Slobodnick, A.; Shah, B.; Pillinger, M. H.; Krasnokutsky, S. COLCHICINE: OLD AND NEW. *Am. J. Med.* **2015**, *128* (5), 461–470.
- (35) Pilat, M. J.; LoRusso, P. M. Vascular Disrupting Agents. *J. Cell. Biochem.* *99* (4), 1021–1039.
- (36) Pettit, G. R.; Singh, S. B.; Niven, M. L.; Hamel, E.; Schmidt, J. M. Isolation, Structure, and Synthesis of Combretastatins A-1 and B-1, Potent New Inhibitors of Microtubule Assembly, Derived from Combretum Caffrum. *J. Nat. Prod.* **1987**, *50* (1), 119–131.

- (37) Pettit, G. R.; Singh, S. B.; Boyd, M. R.; Hamel, E.; Pettit, R. K.; Schmidt, J. M.; Hogan, F. Antineoplastic Agents. 291. Isolation and Synthesis of Combretastatins A-4, A-5, and A-6. *J. Med. Chem.* **1995**, *38* (10), 1666–1672.
- (38) Dark, G. G.; Hill, S. A.; Prise, V. E.; Tozer, G. M.; Pettit, G. R.; Chaplin, D. J. Combretastatin A-4, an Agent That Displays Potent and Selective Toxicity toward Tumor Vasculature. *Cancer Res.* **1997**, *57* (10), 1829–1834.
- (39) Patterson, D. M.; Zweifel, M.; Middleton, M. R.; Price, P. M.; Folkes, L. K.; Stratford, M. R. L.; Ross, P.; Halford, S.; Peters, J.; Balkissoon, J.; et al. Phase I Clinical and Pharmacokinetic Evaluation of the Vascular-Disrupting Agent OXi4503 in Patients with Advanced Solid Tumors. *Clin. Cancer Res.* **2012**, *18* (5), 1415–1425.
- (40) Grisham, R.; Ky, B.; Tewari, K. S.; Chaplin, D. J.; Walker, J. Clinical Trial Experience with CA4P Anticancer Therapy: Focus on Efficacy, Cardiovascular Adverse Events, and Hypertension Management. *Gynecol. Oncol. Res. Pract.* **2018**, *5*.
- (41) Chaplin, D. J.; Hill, S. A. The Development of Combretastatin A4 Phosphate as a Vascular Targeting Agent. *Int. J. Radiat. Oncol.* **2002**, *54* (5), 1491–1496.
- (42) Meyer, T.; Gaya, A. M.; Dancey, G.; Stratford, M. R. L.; Othman, S.; Sharma, S. K.; Wellsted, D.; Taylor, N. J.; Stirling, J. J.; Poupard, L.; et al. A Phase I Trial of Radioimmunotherapy with ¹³¹I-A5B7 Anti-CEA Antibody in Combination with Combretastatin-A4-Phosphate in Advanced Gastrointestinal Carcinomas. *Clin. Cancer Res. Off. J. Am. Assoc. Cancer Res.* **2009**, *15* (13), 4484–4492.
- (43) Rustin, G. J.; Shreeves, G.; Nathan, P. D.; Gaya, A.; Ganesan, T. S.; Wang, D.; Boxall, J.; Poupard, L.; Chaplin, D. J.; Stratford, M. R. L.; et al. A Phase Ib Trial of CA4P (Combretastatin A-4 Phosphate), Carboplatin, and Paclitaxel in Patients with Advanced Cancer. *Br. J. Cancer* **2010**, *102* (9), 1355–1360.
- (44) Nathan, P.; Zweifel, M.; Padhani, A. R.; Koh, D.-M.; Ng, M.; Collins, D. J.; Harris, A.; Carden, C.; Smythe, J.; Fisher, N.; et al. Phase I Trial of Combretastatin A4 Phosphate (CA4P) in Combination with Bevacizumab in Patients with Advanced Cancer. *Clin. Cancer Res.* **2012**, *18* (12), 3428–3439.
- (45) Ng, Q.-S.; Mandeville, H.; Goh, V.; Alonzi, R.; Milner, J.; Carnell, D.; Meer, K.; Padhani, A. R.; Saunders, M. I.; Hoskin, P. J. Phase Ib Trial of Radiotherapy in Combination with Combretastatin-A4-Phosphate in Patients with Non-Small-Cell Lung Cancer, Prostate Adenocarcinoma, and Squamous Cell Carcinoma of the Head and Neck. *Ann. Oncol. Off. J. Eur. Soc. Med. Oncol.* **2012**, *23* (1), 231–237.

- (46) Kretzschmann, V. K.; Fürst, R. Plant-Derived Vascular Disrupting Agents: Compounds, Actions, and Clinical Trials. *Phytochem. Rev.* **2014**, *13* (1), 191–206.
- (47) Mooney, C. J.; Nagaiah, G.; Fu, P.; Wasman, J. K.; Cooney, M. M.; Savvides, P. S.; Bokar, J. A.; Dowlati, A.; Wang, D.; Agarwala, S. S.; et al. A Phase II Trial of Fosbretabulin in Advanced Anaplastic Thyroid Carcinoma and Correlation of Baseline Serum-Soluble Intracellular Adhesion Molecule-1 with Outcome. *Thyroid Off. J. Am. Thyroid Assoc.* **2009**, *19* (3), 233–240.
- (48) Therapeutics, M. Mateon Announces New Preclinical Data Demonstrating Enhanced Tumor Immune Responses when CA4P is Given in Combination with Checkpoint Inhibitors <http://globenewswire.com/news-release/2018/01/08/1284927/0/en/Mateon-Announces-New-Preclinical-Data-Demonstrating-Enhanced-Tumor-Immune-Responses-when-CA4P-is-Given-in-Combination-with-Checkpoint-Inhibitors.html> (accessed Jun 5, 2018).
- (49) Pinney, K.; Mocharla, V.; Chen, Z.; Garner, C.; Ghatak, A.; Hadimani, M.; Kessler, J.; Dorsey, J.; Edvardsen, K.; Chaplin, D.; et al. Tubulin Binding Agents and Corresponding Prodrug Constructs. US20040043969A1, March 4, 2004.
- (50) Sriram, M.; Hall, J. J.; Grohmann, N. C.; Strecker, T. E.; Wootton, T.; Franken, A.; Trawick, M. L.; Pinney, K. G. Design, Synthesis and Biological Evaluation of Dihydronaphthalene and Benzosuberene Analogs of the Combretastatins as Inhibitors of Tubulin Polymerization in Cancer Chemotherapy. *Bioorg. Med. Chem.* **2008**, *16* (17), 8161–8171.
- (51) Tanpure, R. P.; George, C. S.; Strecker, T. E.; Devkota, L.; Tidmore, J. K.; Lin, C.-M.; Herdman, C. A.; MacDonough, M. T.; Sriram, M.; Chaplin, D. J.; et al. Synthesis of Structurally Diverse Benzosuberene Analogues and Their Biological Evaluation as Anti-Cancer Agents. *Bioorg. Med. Chem.* **2013**, *21* (24), 8019–8032.
- (52) Herdman, C. A.; Devkota, L.; Lin, C.-M.; Niu, H.; Strecker, T. E.; Lopez, R.; Liu, L.; George, C. S.; Tanpure, R. P.; Hamel, E.; et al. Structural Interrogation of Benzosuberene-Based Inhibitors of Tubulin Polymerization. *Bioorg. Med. Chem.* **2015**, *23* (24), 7497–7520.
- (53) Herdman, C. A.; Strecker, T. E.; Tanpure, R. P.; Chen, Z.; Winters, A.; Gerberich, J.; Liu, L.; Hamel, E.; Mason, R. P.; Chaplin, D. J.; et al. Synthesis and Biological Evaluation of Benzocyclooctene-Based and Indene-Based Anticancer Agents That Function as Inhibitors of Tubulin Polymerization. *MedChemComm* **2016**, *7* (12), 2418–2427.

- (54) Hadimani, M. B.; MacDonough, M. T.; Ghatak, A.; Strecker, T. E.; Lopez, R.; Sriram, M.; Nguyen, B. L.; Hall, J. J.; Kessler, R. J.; Shirali, A. R.; et al. Synthesis of a 2-Aryl-3-Aroyl Indole Salt (OXi8007) Resembling Combretastatin A-4 with Application as a Vascular Disrupting Agent. *J. Nat. Prod.* **2013**, *76* (9), 1668–1678.
- (55) MacDonough, M. T.; Strecker, T. E.; Hamel, E.; Hall, J. J.; Chaplin, D. J.; Trawick, M. L.; Pinney, K. G. Synthesis and Biological Evaluation of Indole-Based, Anti-Cancer Agents Inspired by the Vascular Disrupting Agent 2-(3'-Hydroxy-4'-Methoxyphenyl)-3-(3'',4'',5''-Trimethoxybenzoyl)-6-Methoxyindole (OXi8006). *Bioorg. Med. Chem.* **2013**, *21* (21), 6831–6843.
- (56) Mullica, D. F.; Pinney, K. G.; Mocharla, V. P.; Dingeman, K. M.; Bounds, A. D.; Sappenfield, E. L. Characterization and Structural Analyses of Trimethoxy and Triethoxybenzo[b]Thiophene. *J. Chem. Crystallogr.* **1998**, *28* (4), 289–295.
- (57) Pinney, K. G.; Bounds, A. D.; Dingeman, K. M.; Mocharla, V. P.; Pettit, G. R.; Bai, R.; Hamel, E. A New Anti-Tubulin Agent Containing the Benzo[b]Thiophene Ring System. *Bioorg. Med. Chem. Lett.* **1999**, *9* (8), 1081–1086.
- (58) Tron, G. C.; Pirali, T.; Sorba, G.; Pagliai, F.; Busacca, S.; Genazzani, A. A. Medicinal Chemistry of Combretastatin A4: Present and Future Directions. *J. Med. Chem.* **2006**, *49* (11), 3033–3044.
- (59) Pinney, K. G.; Bounds, A. D.; Dingeman, K. M.; Mocharla, V. P.; Pettit, G. R.; Bai, R.; Hamel, E. A New Anti-Tubulin Agent Containing the Benzo[b]Thiophene Ring System. *Bioorg. Med. Chem. Lett.* **1999**, *9* (8), 1081–1086.
- (60) Pettit, G. R.; Grealish, M. P.; Herald, D. L.; Boyd, M. R.; Hamel, E.; Pettit, R. K. Antineoplastic Agents. 443. Synthesis of the Cancer Cell Growth Inhibitor Hydroxyphenstatin and Its Sodium Diphosphate Prodrug. *J. Med. Chem.* **2000**, *43* (14), 2731–2737.
- (61) Tanpure, R. P.; Nguyen, B. L.; Strecker, T. E.; Aguirre, S.; Sharma, S.; Chaplin, D. J.; Siim, B. G.; Hamel, E.; Lippert, J. W.; Pettit, G. R.; et al. Regioselective Synthesis of Water-Soluble Monophosphate Derivatives of Combretastatin A-1. *J. Nat. Prod.* **2011**, *74* (7), 1568–1574.
- (62) Flynn, B. L.; Hamel, E.; Jung, M. K. One-Pot Synthesis of Benzo[b]Furan and Indole Inhibitors of Tubulin Polymerization. *J. Med. Chem.* **2002**, *45* (12), 2670–2673.

- (63) Strecker, T. E.; Odutola, S. O.; Lopez, R.; Cooper, M. S.; Tidmore, J. K.; Charlton-Sevcik, A. K.; Li, L.; MacDonough, M. T.; Hadimani, M. B.; Ghatak, A.; et al. The Vascular Disrupting Activity of OXi8006 in Endothelial Cells and Its Phosphate Prodrug OXi8007 in Breast Tumor Xenografts. *Cancer Lett.* **2015**, *369* (1), 229–241.
- (64) Vaupel, P.; Mayer, A. Hypoxia in Cancer: Significance and Impact on Clinical Outcome. *Cancer Metastasis Rev.* **2007**, *26* (2), 225–239.
- (65) Dewhirst, M. W.; Cao, Y.; Moeller, B. Cycling Hypoxia and Free Radicals Regulate Angiogenesis and Radiotherapy Response. *Nat. Rev. Cancer* **2008**, *8* (6), 425–437.
- (66) Brown, J. M.; Wilson, W. R. Exploiting Tumour Hypoxia in Cancer Treatment. *Nat. Rev. Cancer* **2004**, *4* (6), 437.
- (67) Hoppe-Seyler, K.; Mändl, J.; Adrian, S.; Kuhn, B. J.; Hoppe-Seyler, F. Virus/Host Cell Crosstalk in Hypoxic HPV-Positive Cancer Cells. *Viruses* **2017**, *9* (7), 174.
- (68) Graeber, T. G.; Osmanian, C.; Jacks, T.; Housman, D. E.; Koch, C. J.; Lowe, S. W.; Giaccia, A. J. Hypoxia-Mediated Selection of Cells with Diminished Apoptotic Potential in Solid Tumours. *Nature* **1996**, *379* (6560), 88–91.
- (69) Bristow, R. G.; Hill, R. P. Hypoxia and Metabolism. Hypoxia, DNA Repair and Genetic Instability. *Nat. Rev. Cancer* **2008**, *8* (3), 180–192.
- (70) Liao, D.; Johnson, R. S. Hypoxia: A Key Regulator of Angiogenesis in Cancer. *Cancer Metastasis Rev.* **2007**, *26* (2), 281–290.
- (71) Semenza, G. L. Regulation of Cancer Cell Metabolism by Hypoxia-Inducible Factor 1. *Semin. Cancer Biol.* **2009**, *19* (1), 12–16.
- (72) Chang, Q.; Jurisica, I.; Do, T.; Hedley, D. W. Hypoxia Predicts Aggressive Growth and Spontaneous Metastasis Formation from Orthotopically Grown Primary Xenografts of Human Pancreatic Cancer. *Cancer Res.* **2011**, *71* (8), 3110–3120.
- (73) Viry, E.; Paggetti, J.; Baginska, J.; Mgrditchian, T.; Berchem, G.; Moussay, E.; Janji, B. Autophagy: An Adaptive Metabolic Response to Stress Shaping the Antitumor Immunity. *Biochem. Pharmacol.* **2014**, *92* (1), 31–42.
- (74) Yotnda, P.; Wu, D.; Swanson, A. M. Hypoxic Tumors and Their Effect on Immune Cells and Cancer Therapy. *Methods Mol. Biol. Clifton NJ* **2010**, *651*, 1–29.

- (75) Talks, K. L.; Turley, H.; Gatter, K. C.; Maxwell, P. H.; Pugh, C. W.; Ratcliffe, P. J.; Harris, A. L. The Expression and Distribution of the Hypoxia-Inducible Factors HIF-1alpha and HIF-2alpha in Normal Human Tissues, Cancers, and Tumor-Associated Macrophages. *Am. J. Pathol.* **2000**, *157* (2), 411–421.
- (76) Meng, F.; Evans, J. W.; Bhupathi, D.; Banica, M.; Lan, L.; Lorente, G.; Duan, J.-X.; Cai, X.; Mowday, A. M.; Guise, C. P.; et al. Molecular and Cellular Pharmacology of the Hypoxia-Activated Prodrug TH-302. *Mol. Cancer Ther.* **2012**, *11* (3), 740–751.
- (77) Patterson, A. V.; Silva, S.; Guise, C.; Bull, M.; Abbattista, M.; Hsu, A.; Sun, J. D.; Hart, C. P.; Pearce, T. E.; Smaill, J. B. TH-4000, a Hypoxia-Activated EGFR/Her2 Inhibitor to Treat EGFR-TKI Resistant T790M-Negative NSCLC. *J. Clin. Oncol.* **2015**, *33* (15_suppl), e13548–e13548.
- (78) Reddy, S. B.; Williamson, S. K. Tirapazamine: A Novel Agent Targeting Hypoxic Tumor Cells. *Expert Opin. Investig. Drugs* **2009**, *18* (1), 77–87.
- (79) Konopleva, M.; Thall, P. F.; Yi, C. A.; Borthakur, G.; Coveler, A.; Bueso-Ramos, C.; Benito, J.; Konoplev, S.; Gu, Y.; Ravandi, F.; et al. Phase I/II Study of the Hypoxia-Activated Prodrug PR104 in Refractory/Relapsed Acute Myeloid Leukemia and Acute Lymphoblastic Leukemia. *Haematologica* **2015**, *100* (7), 927–934.
- (80) Caramés Masana, F.; de Reijke, T. M. The Efficacy of Apaziquone in the Treatment of Bladder Cancer. *Expert Opin. Pharmacother.* **2017**, *18* (16), 1781–1788.
- (81) Thomson, P.; Naylor, M. A.; Everett, S. A.; Stratford, M. R. L.; Lewis, G.; Hill, S.; Patel, K. B.; Wardman, P.; Davis, P. D. Synthesis and Biological Properties of Bioreductively Targeted Nitrothienyl Prodrugs of Combretastatin A-4. *Mol. Cancer Ther.* **2006**, *5* (11), 2886–2894.
- (82) Davis, P.; Naylor, M.; Thomson, P.; Everett, S.; Stratford, M.; Wardman, P. Bioreductively-Activated Prodrugs. WO2004085421 (A2), October 7, 2004.
- (83) Wilson, W. R.; Hay, M. P. Targeting Hypoxia in Cancer Therapy. *Nat. Rev. Cancer* **2011**, *11* (6), 393–410.
- (84) Denny, W. A. The Role of Hypoxia-Activated Prodrugs in Cancer Therapy. *Lancet Oncol.* **2000**, *1* (1), 25–29.
- (85) Thomlinson, R. H.; Gray, L. H. The Histological Structure of Some Human Lung Cancers and the Possible Implications for Radiotherapy. *Br. J. Cancer* **1955**, *9* (4), 539–549.

- (86) Phillips, R. M. Targeting the Hypoxic Fraction of Tumours Using Hypoxia-Activated Prodrugs. *Cancer Chemother. Pharmacol.* **2016**, *77* (3), 441–457.
- (87) Guise, C. P.; Mowday, A. M.; Ashoorzadeh, A.; Yuan, R.; Lin, W.-H.; Wu, D.-H.; Smaill, J. B.; Patterson, A. V.; Ding, K. Bioreductive Prodrugs as Cancer Therapeutics: Targeting Tumor Hypoxia. *Chin. J. Cancer* **2014**, *33* (2), 80–86.
- (88) Zeman, E. M.; Brown, J. M.; Lemmon, M. J.; Hirst, V. K.; Lee, W. W. SR-4233: A New Bioreductive Agent with High Selective Toxicity for Hypoxic Mammalian Cells. *Int. J. Radiat. Oncol.* **1986**, *12* (7, Part 1), 1239–1242.
- (89) Ahn, G.-O.; Brown, M. Targeting Tumors with Hypoxia-Activated Cytotoxins. *Front. Biosci. J. Virtual Libr.* **2007**, *12*, 3483–3501.
- (90) Shinde, S. S.; Hay, M. P.; Patterson, A. V.; Denny, W. A.; Anderson, R. F. Spin Trapping of Radicals Other Than the •OH Radical upon Reduction of the Anticancer Agent Tirapazamine by Cytochrome P450 Reductase. *J. Am. Chem. Soc.* **2009**, *131* (40), 14220–14221.
- (91) DiSilvestro, P. A.; Ali, S.; Craighead, P. S.; Lucci, J. A.; Lee, Y.-C.; Cohn, D. E.; Spirtos, N. M.; Tewari, K. S.; Muller, C.; Gajewski, W. H.; et al. Phase III Randomized Trial of Weekly Cisplatin and Irradiation versus Cisplatin and Tirapazamine and Irradiation in Stages IB2, IIA, IIB, IIIB, and IVA Cervical Carcinoma Limited to the Pelvis: A Gynecologic Oncology Group Study. *J. Clin. Oncol. Off. J. Am. Soc. Clin. Oncol.* **2014**, *32* (5), 458–464.
- (92) Rischin, D.; Peters, L. J.; O’Sullivan, B.; Giralt, J.; Fisher, R.; Yuen, K.; Trotti, A.; Bernier, J.; Bourhis, J.; Ringash, J.; et al. Tirapazamine, Cisplatin, and Radiation Versus Cisplatin and Radiation for Advanced Squamous Cell Carcinoma of the Head and Neck (TROG 02.02, HeadSTART): A Phase III Trial of the Trans-Tasman Radiation Oncology Group. *J. Clin. Oncol.* **2010**, *28* (18), 2989–2995.
- (93) Williamson, S. K.; Crowley, J. J.; Lara, P. N.; McCoy, J.; Lau, D. H. M.; Tucker, R. W.; Mills, G. M.; Gandara, D. R.; Southwest Oncology Group Trial S0003. Phase III Trial of Paclitaxel plus Carboplatin with or without Tirapazamine in Advanced Non-Small-Cell Lung Cancer: Southwest Oncology Group Trial S0003. *J. Clin. Oncol. Off. J. Am. Soc. Clin. Oncol.* **2005**, *23* (36), 9097–9104.
- (94) Duan, J.-X.; Jiao, H.; Kaizerman, J.; Stanton, T.; Evans, J. W.; Lan, L.; Lorente, G.; Banica, M.; Jung, D.; Wang, J.; et al. Potent and Highly Selective Hypoxia-Activated Achiral Phosphoramidate Mustards as Anticancer Drugs. *J. Med. Chem.* **2008**, *51* (8), 2412–2420.

- (95) Clinical Trial Testing TH-302 in Combination With Gemcitabine in Previously Untreated Subjects With Metastatic or Locally Advanced Unresectable Pancreatic Adenocarcinoma - Full Text View - ClinicalTrials.gov
<https://clinicaltrials.gov/ct2/show/NCT01746979> (accessed May 30, 2018).
- (96) Lee, A. T. J.; Pollack, S. M.; Huang, P.; Jones, R. L. Phase III Soft Tissue Sarcoma Trials: Success or Failure? *Curr. Treat. Options Oncol.* **2017**, *18* (3).
- (97) Inc, T. P. Threshold Pharmaceuticals Announces First Patient Dosed in Immunotherapy Clinical Trial of Evofosfamide and Ipilimumab
<http://globenewswire.com/news-release/2017/06/13/1018187/0/en/Threshold-Pharmaceuticals-Announces-First-Patient-Dosed-in-Immunotherapy-Clinical-Trial-of-Evofosfamide-and-Ipilimumab.html> (accessed May 30, 2018).
- (98) Brenner, A.; Zuniga, R.; Sun, J. D.; Floyd, J.; Hart, C. P.; Kroll, S.; Fichtel, L.; Cavazos, D.; Caflisch, L.; Gruslova, A.; et al. Hypoxia-Activated Evofosfamide for Treatment of Recurrent Bevacizumab-Refractory Glioblastoma: A Phase I Surgical Study. *Neuro-Oncol.*
- (99) Winn, B. A.; Shi, Z.; Carlson, G. J.; Wang, Y.; Nguyen, B. L.; Kelly, E. M.; Ross, R. D.; Hamel, E.; Chaplin, D. J.; Trawick, M. L.; et al. Bioreductively Activatable Prodrug Conjugates of Phenstatin Designed to Target Tumor Hypoxia. *Bioorg. Med. Chem. Lett.* **2017**, *27* (3), 636–641.
- (100) Matteucci, M.; Duan, J.-X.; Jiao, H.; Kaizerman, J.; Ammons, S. Phosphoramidate Alkylator Prodrugs. WO2007002931 A3, April 23, 2009.
- (101) O'Connor, L. J.; Cazares-Körner, C.; Saha, J.; Evans, C. N. G.; Stratford, M. R. L.; Hammond, E. M.; Conway, S. J. Efficient Synthesis of 2-Nitroimidazole Derivatives and the Bioreductive Clinical Candidate Evofosfamide (TH-302). *Org. Chem.* **2015**, *2* (9), 1026–1029.
- (102) O'Connor, L. J.; Cazares-Körner, C.; Saha, J.; Evans, C. N. G.; Stratford, M. R. L.; Hammond, E. M.; Conway, S. J. Design, Synthesis and Evaluation of Molecularly Targeted Hypoxia-Activated Prodrugs. *Nat. Protoc.* **2016**, *11* (4), 781–794.
- (103) Pinney, K. G.; Trawick, M. L.; Mason, R. P.; Liu, L.; Chaplin, D. J.; Winn, B. A.; Devkota, L.; Strecker, T. E.; Gerberich, J.; Winters, A.; Wang, Y.; MacDonough, M. T. Targeting Tumor Hypoxia with Prodrug Conjugates of Potent Small-Molecule Inhibitors of Tubulin Polymerization, Abstract No. 3203, American Association for Cancer Research (AACR) Annual Meeting, Washington, DC, April 1-5, 2017. Poster presented on Tuesday April 4, 2017.
- (104) Tan, S. Y.; Grimes, S. Paul Ehrlich (1854-1915): Man with the Magic Bullet. *Singapore Med. J.* **2010**, *51* (11), 842–843.

- (105) Strebhardt, K.; Ullrich, A. Paul Ehrlich's Magic Bullet Concept: 100 Years of Progress. *Nat. Rev. Cancer* **2008**, *8* (6), 473–480.
- (106) Senter, P. D.; Sievers, E. L. The Discovery and Development of Brentuximab Vedotin for Use in Relapsed Hodgkin Lymphoma and Systemic Anaplastic Large Cell Lymphoma. *Nat. Biotechnol.* **2012**, *30* (7), 631–637.
- (107) Beck, A.; Goetsch, L.; Dumontet, C.; Corvaia, N. Strategies and Challenges for the next Generation of Antibody-Drug Conjugates. *Nat. Rev. Drug Discov.* **2017**, *16* (5), 315–337.
- (108) Barok, M.; Joensuu, H.; Isola, J. Trastuzumab Emtansine: Mechanisms of Action and Drug Resistance. *Breast Cancer Res.* **2014**, *16*, 209.
- (109) Verma, S.; Miles, D.; Gianni, L.; Krop, I. E.; Welslau, M.; Baselga, J.; Pegram, M.; Oh, D.-Y.; Diéras, V.; Guardino, E.; et al. Trastuzumab Emtansine for HER2-Positive Advanced Breast Cancer <https://www.nejm.org/doi/10.1056/NEJMoa1209124> (accessed May 31, 2018).
- (110) Köhler, G.; Milstein, C. Continuous Cultures of Fused Cells Secreting Antibody of Predefined Specificity. *Nature* **1975**, *256* (5517), 495–497.
- (111) Appelbaum, F. R.; Bernstein, I. D. Gemtuzumab Ozogamicin for Acute Myeloid Leukemia. *Blood* **2017**, blood-2017-09-797712.
- (112) Ansell, S. M. Brentuximab Vedotin. *Blood* **2014**, *124* (22), 3197–3200.
- (113) Connors, J. M.; Jurczak, W.; Straus, D. J.; Ansell, S. M.; Kim, W. S.; Gallamini, A.; Younes, A.; Alekseev, S.; Illés, Á.; Picardi, M.; et al. Brentuximab Vedotin with Chemotherapy for Stage III or IV Hodgkin's Lymphoma. *N. Engl. J. Med.* **2017**.
- (114) Dubowchik, G. M.; Firestone, R. A. Cathepsin B-Sensitive Dipeptide Prodrugs. 1. A Model Study of Structural Requirements for Efficient Release of Doxorubicin. *Bioorg. Med. Chem. Lett.* **1998**, *8* (23), 3341–3346.
- (115) Pinney, K. G.; Lin, C.-M.; Mondal, D.; Ford, J. Drug-Linker Conjugate Pharmaceutical Compositions. WO2017066668A1, April 20, 2017.
- (116) de Groot, F. M. H.; van Berkom, L. W. A.; Scheeren, H. W. Synthesis and Biological Evaluation of 2'-Carbamate-Linked and 2'-Carbonate-Linked Prodrugs of Paclitaxel: Selective Activation by the Tumor-Associated Protease Plasmin. *J. Med. Chem.* **2000**, *43* (16), 3093–3102.

- (117) Roughley, S. D.; Jordan, A. M. The Medicinal Chemist's Toolbox: An Analysis of Reactions Used in the Pursuit of Drug Candidates. *J. Med. Chem.* **2011**, *54* (10), 3451–3479.
- (118) Fischer Indole Synthesis. In *Indole Ring Synthesis*; Wiley-Blackwell, 2016; pp 41–115.
- (119) Bischler, A. Ueber Die Entstehung Einiger Substituierter Indole. *Berichte Dtsch. Chem. Ges.* *25* (2), 2860–2879.
- (120) Li, J. J. Bischler–Möhlau Indole Synthesis. In *Name Reactions*; Springer, Berlin, Heidelberg, 2009; pp 46–47.
- (121) Taber, D. F.; Tirunahari, P. K. Indole Synthesis: A Review and Proposed Classification. *Tetrahedron* **2011**, *67* (38), 7195–7210.
- (122) Fischer, E.; Jourdan, F. Ueber Die Hydrazine Der Brenztraubensäure. *Berichte Dtsch. Chem. Ges.* *16* (2), 2241–2245.
- (123) Bischler, A. Ueber Die Entstehung Einiger Substituierter Indole. *Berichte Dtsch. Chem. Ges.* *25* (2), 2860–2879.
- (124) Bischler, A.; Fireman, P. Zur Kenntniss Einiger α - β - Diphenylindole. *Berichte Dtsch. Chem. Ges.* *26* (2), 1336–1349.
- (125) Vara, Y.; Aldaba, E.; Arrieta, A.; Pizarro, J. L.; Arriortua, M. I.; Cossío, F. P. Regiochemistry of the Microwave-Assisted Reaction between Aromatic Amines and Alpha-Bromoketones to Yield Substituted 1H-Indoles. *Org. Biomol. Chem.* **2008**, *6* (10), 1763–1772.
- (126) MacDonough, M. T.; Shi, Z.; Pinney, K. G. Mechanistic Considerations in the Synthesis of 2-Aryl-Indole Analogues under Bischler–Möhlau Conditions. *Tetrahedron Lett.* **2015**, *56* (23), 3624–3629.
- (127) Guan, X. Cancer Metastases: Challenges and Opportunities. *Acta Pharm. Sin. B* **2015**, *5* (5), 402–418.
- (128) Meyer, T.; Hart, I. . Mechanisms of Tumour Metastasis. *Eur. J. Cancer* **1998**, *34* (2), 214–221.
- (129) Seyfried, T. N.; Huysentruyt, L. C. On the Origin of Cancer Metastasis. *Crit. Rev. Oncog.* **2013**, *18* (1–2), 43–73.
- (130) Rawlings, N. D.; Morton, F. R.; Barrett, A. J. MEROPS: The Peptidase Database. *Nucleic Acids Res.* **2006**, *34* (Database issue), D270–272.

- (131) Mohamed, M. M.; Sloane, B. F. Cysteine Cathepsins: Multifunctional Enzymes in Cancer. *Nat. Rev. Cancer* **2006**, *6* (10), 764–775.
- (132) Lin, L.; Aggarwal, S.; Glover, T. W.; Orringer, M. B.; Hanash, S.; Beer, D. G. A Minimal Critical Region of the 8p22-23 Amplicon in Esophageal Adenocarcinomas Defined Using Sequence Tagged Site-Amplification Mapping and Quantitative Polymerase Chain Reaction Includes the GATA-4 Gene. *Cancer Res.* **2000**, *60* (5), 1341–1347.
- (133) Baici, A.; Müntener, K.; Willmann, A.; Zwicky, R. Regulation of Human Cathepsin B by Alternative mRNA Splicing: Homeostasis, Fatal Errors and Cell Death. *Biol. Chem.* **2006**, *387* (8), 1017–1021.
- (134) Rao, J. S. Molecular Mechanisms of Glioma Invasiveness: The Role of Proteases. *Nat. Rev. Cancer* **2003**, *3* (7), 489–501.
- (135) Jean, D.; Rousselet, N.; Frade, R. Expression of Cathepsin L in Human Tumor Cells Is under the Control of Distinct Regulatory Mechanisms. *Oncogene* **2006**, *25* (10), 1474–1484.
- (136) Brömme, D.; Wilson, S. Role of Cysteine Cathepsins in Extracellular Proteolysis. In *Extracellular Matrix Degradation; Biology of Extracellular Matrix*; Springer, Berlin, Heidelberg, 2011; pp 23–51.
- (137) Lankelma, J. M.; Voorend, D. M.; Barwari, T.; Koetsveld, J.; Van der Spek, A. H.; De Porto, A. P. N. A.; Van Rooijen, G.; Van Noorden, C. J. F. Cathepsin L, Target in Cancer Treatment? *Life Sci.* **2010**, *86* (7), 225–233.
- (138) Barbarin, A.; Frade, R. Procathepsin L Secretion, Which Triggers Tumour Progression, Is Regulated by Rab4a in Human Melanoma Cells. *Biochem. J.* **2011**, *437* (1), 97–107.
- (139) Ullah, M. F.; Aatif, M. The Footprints of Cancer Development: Cancer Biomarkers. *Cancer Treat. Rev.* **2009**, *35* (3), 193–200.
- (140) Palermo, C.; Joyce, J. A. Cysteine Cathepsin Proteases as Pharmacological Targets in Cancer. *Trends Pharmacol. Sci.* **2008**, *29* (1), 22–28.
- (141) Lankelma, J. M.; Voorend, D. M.; Barwari, T.; Koetsveld, J.; Van der Spek, A. H.; De Porto, A. P. N. A.; Van Rooijen, G.; Van Noorden, C. J. F. Cathepsin L, Target in Cancer Treatment? *Life Sci.* **2010**, *86* (7), 225–233.
- (142) Sudhan, D. R.; Siemann, D. W. Cathepsin L Inhibition by the Small Molecule KGP94 Suppresses Tumor Microenvironment Enhanced Metastasis Associated Cell Functions of Prostate and Breast Cancer Cells. *Clin. Exp. Metastasis* **2013**, *30* (7), 891–902.

- (143) Sudhan, D. R.; Pampo, C.; Rice, L.; Siemann, D. W. Cathepsin L Inactivation Leads to Multimodal Inhibition of Prostate Cancer Cell Dissemination in a Preclinical Bone Metastasis Model. *Int. J. Cancer* **2016**, *138* (11), 2665–2677.
- (144) Du, X.; Guo, C.; Hansell, E.; Doyle, P. S.; Caffrey, C. R.; Holler, T. P.; McKerrow, J. H.; Cohen, F. E. Synthesis and Structure–Activity Relationship Study of Potent Trypanocidal Thio Semicarbazone Inhibitors of the Trypanosomal Cysteine Protease Cruzain. *J. Med. Chem.* **2002**, *45* (13), 2695–2707.
- (145) Greenbaum, D. C.; Mackey, Z.; Hansell, E.; Doyle, P.; Gut, J.; Caffrey, C. R.; Lehrman, J.; Rosenthal, P. J.; McKerrow, J. H.; Chibale, K. Synthesis and Structure–Activity Relationships of Parasiticidal Thiosemicarbazone Cysteine Protease Inhibitors against *Plasmodium Falciparum*, *Trypanosoma Brucei*, and *Trypanosoma Cruzi*. *J. Med. Chem.* **2004**, *47* (12), 3212–3219.
- (146) Siles, R.; Chen, S.-E.; Zhou, M.; Pinney, K. G.; Trawick, M. L. Design, Synthesis, and Biochemical Evaluation of Novel Cruzain Inhibitors with Potential Application in the Treatment of Chagas’ Disease. *Bioorg. Med. Chem. Lett.* **2006**, *16* (16), 4405–4409.
- (147) Kumar, G. D. K.; Chavarria, G. E.; Charlton-Sevcik, A. K.; Yoo, G. K.; Song, J.; Strecker, T. E.; Siim, B. G.; Chaplin, D. J.; Trawick, M. L.; Pinney, K. G. Functionalized Benzophenone, Thiophene, Pyridine, and Fluorene Thiosemicarbazone Derivatives as Inhibitors of Cathepsin L. *Bioorg. Med. Chem. Lett.* **2010**, *20* (22), 6610–6615.
- (148) Mallari, J. P.; Shelat, A. A.; Kosinski, A.; Caffrey, C. R.; Connelly, M.; Zhu, F.; McKerrow, J. H.; Guy, R. K. Structure-Guided Development of Selective TbcatB Inhibitors. *J. Med. Chem.* **2009**, *52* (20), 6489–6493.
- (149) Chavarria, G. E.; Horsman, M. R.; Arispe, W. M.; Kumar, G. D. K.; Chen, S.-E.; Strecker, T. E.; Parker, E. N.; Chaplin, D. J.; Pinney, K. G.; Trawick, M. L. Initial Evaluation of the Antitumour Activity of KGP94, a Functionalized Benzophenone Thiosemicarbazone Inhibitor of Cathepsin L. *Eur. J. Med. Chem.* **2012**, *58*, 568–572.
- (150) Parker, E. N.; Song, J.; Kishore Kumar, G. D.; Odutola, S. O.; Chavarria, G. E.; Charlton-Sevcik, A. K.; Strecker, T. E.; Barnes, A. L.; Sudhan, D. R.; Wittenborn, T. R.; et al. Synthesis and Biochemical Evaluation of Benzoylbenzophenone Thiosemicarbazone Analogues as Potent and Selective Inhibitors of Cathepsin L. *Bioorg. Med. Chem.* **2015**, *23* (21), 6974–6992.

- (151) Parker, E. N.; Odutola, S. O.; Wang, Y.; Strecker, T. E.; Mukherjee, R.; Shi, Z.; Chaplin, D. J.; Trawick, M. L.; Pinney, K. G. Synthesis and Biological Evaluation of a Water-Soluble Phosphate Prodrug Salt and Structural Analogues of KGP94, a Lead Inhibitor of Cathepsin L. *Bioorg. Med. Chem. Lett.* **2017**, *27* (5), 1304–1310.
- (152) Hadimani, M. B.; Kessler, R. J.; Kautz, J. A.; Ghatak, A.; Shirali, A. R.; O'Dell, H.; Garner, C. M.; Pinney, K. G. 2-(3-Tert-Butyldimethylsiloxy-4-Methoxyphenyl)-6-Methoxy-3-(3,4,5-Trimethoxybenzoyl)Indole. *Acta Crystallogr. C* **2002**, *58* (Pt 6), o330-332.
- (153) Macdonough, M. T.; Strecker, T. E.; Hamel, E.; Hall, J. J.; Chaplin, D. J.; Trawick, M. L.; Pinney, K. G. Synthesis and Biological Evaluation of Indole-Based, Anti-Cancer Agents Inspired by the Vascular Disrupting Agent 2-(3'-Hydroxy-4'-Methoxyphenyl)-3-(3'',4'',5''-Trimethoxybenzoyl)-6-Methoxyindole (OXi8006). *Bioorg. Med. Chem.* **2013**, *21* (21), 6831–6843.
- (154) Hadimani, M. B.; MacDonough, M. T.; Ghatak, A.; Strecker, T. E.; Lopez, R.; Sriram, M.; Nguyen, B. L.; Hall, J. J.; Kessler, R. J.; Shirali, A. R.; et al. Synthesis of a 2-Aryl-3-Aroyl Indole Salt (OXi8007) Resembling Combretastatin A-4 with Application as a Vascular Disrupting Agent. *J. Nat. Prod.* **2013**, *76* (9), 1668–1678.
- (155) Getahun, Z.; Jurd, L.; Chu, P. S.; Lin, C. M.; Hamel, E. Synthesis of Alkoxy-Substituted Diaryl Compounds and Correlation of Ring Separation with Inhibition of Tubulin Polymerization: Differential Enhancement of Inhibitory Effects under Suboptimal Polymerization Reaction Conditions. *J. Med. Chem.* **1992**, *35* (6), 1058–1067.
- (156) Bidwell, G. L.; Fokt, I.; Priebe, W.; Raucher, D. Development of Elastin-like Polypeptide for Thermally Targeted Delivery of Doxorubicin. *Biochem. Pharmacol.* **2007**, *73* (5), 620–631.
- (157) George R. Pettit; Matthew P. Grealish; Delbert L. Herald; Michael R. Boyd; Ernest Hamel, and; Pettit, R. K. Antineoplastic Agents. 443. Synthesis of the Cancer Cell Growth Inhibitor Hydroxyphenstatin and Its Sodium Diphosphate Prodrug <https://pubs.acs.org/doi/abs/10.1021/jm000045a> (accessed Jun 23, 2018).
- (158) Tanpure, R. P.; Harkrider, A. R.; Strecker, T. E.; Hamel, E.; Trawick, M. L.; Pinney, K. G. Application of the McMurry Coupling Reaction in the Synthesis of Tri- and Tetra-Arylethylene Analogues as Potential Cancer Chemotherapeutic Agents. *Bioorg. Med. Chem.* **2009**, *17* (19), 6993–7001.
- (159) Pinney, K.; Wang, F.; Hadimani, M. Indole-Containing and Combretastatin-Related Anti-Mitotic and Anti-Tubulin Polymerization Agents. US6849656 B1, February 1, 2005.

- (160) Hadimani, M. B.; MacDonough, M. T.; Ghatak, A.; Strecker, T. E.; Lopez, R.; Sriram, M.; Nguyen, B. L.; Hall, J. J.; Kessler, R. J.; Shirali, A. R.; et al. Synthesis of a 2-Aryl-3-Aroyl Indole Salt (OXi8007) Resembling Combretastatin A-4 with Application as a Vascular Disrupting Agent. *J. Nat. Prod.* **2013**, *76* (9), 1668–1678.
- (161) Reetz, M. T.; Kyung, S. H.; Hüllmann, M. CH₃Li/TiCl₄: A Non-Basic and Highly Selective Grignard Analogue. *Tetrahedron* **1986**, *42* (11), 2931–2935.
- (162) J. O'Connor, L.; Cazares-Körner, C.; Saha, J.; G. Evans, C. N.; L. Stratford, M. R.; M. Hammond, E.; J. Conway, S. Efficient Synthesis of 2-Nitroimidazole Derivatives and the Bioreductive Clinical Candidate Evofosfamide (TH-302). *Org. Chem. Front.* **2015**, *2* (9), 1026–1029.
- (163) Cavalleri, B.; Volpe, G.; Arioli, V.; Lancini, G. Synthesis and Biological Activity of Two Metabolites of 1-Methyl-5-(1-Methylethyl)-2-Nitro-1H-Imidazole, an Antiprotozoal Agent. *J. Med. Chem.* **1977**, *20* (11), 1522–1525.
- (164) Pedersen, P. L. 3-Bromopyruvate (3BP) a Fast Acting, Promising, Powerful, Specific, and Effective “Small Molecule” Anti-Cancer Agent Taken from Labside to Bedside: Introduction to a Special Issue. *J. Bioenerg. Biomembr.* **2012**, *44* (1), 1–6.
- (165) Xing, X.; Ho, P.; Bourquin, G.; Yeh, L.-A.; Cuny, G. D. Synthesis, Stereochemistry Confirmation and Biological Activity Evaluation of a Constituent from *Isodon Excisus*. *Tetrahedron* **2003**, *59* (50), 9961–9969.
- (166) Chaplin, D. J.; Olive, P. L.; Durand, R. E. Intermittent Blood Flow in a Murine Tumor: Radiobiological Effects. *Cancer Res.* **1987**, *47* (2), 597–601.
- (167) Baran, N.; Konopleva, M. Molecular Pathways: Hypoxia-Activated Prodrugs in Cancer Therapy. *Clin. Cancer Res.* **2017**, *23* (10), 2382–2390.
- (168) Brown, J. M. Tumor Hypoxia in Cancer Therapy. In *Methods in Enzymology; Oxygen Biology and Hypoxia*; Academic Press, 2007; Vol. 435, pp 295–321.
- (169) Hasani, A.; Leighl, N. Classification and Toxicities of Vascular Disrupting Agents. *Clin. Lung Cancer* **2011**, *12* (1), 18–25.
- (170) Pettit, G. R.; Toki, B.; Herald, D. L.; Verdier-Pinard, P.; Boyd, M. R.; Hamel, E.; Pettit, R. K. Antineoplastic Agents. 379. Synthesis of Phenstatin Phosphate. *J. Med. Chem.* **1998**, *41* (10), 1688–1695.
- (171) Swamy, K. C. K.; Kumar, N. N. B.; Balaraman, E.; Kumar, K. V. P. P. Mitsunobu and Related Reactions: Advances and Applications. *Chem. Rev.* **2009**, *109* (6), 2551–2651.

- (172) Pulaski, B. A.; Ostrand-Rosenberg, S. Reduction of Established Spontaneous Mammary Carcinoma Metastases Following Immunotherapy with Major Histocompatibility Complex Class II and B7.1 Cell-Based Tumor Vaccines. *Cancer Res.* **1998**, *58* (7), 1486–1493.
- (173) Tao, K.; Fang, M.; Alroy, J.; Sahagian, G. G. Imagable 4T1 Model for the Study of Late Stage Breast Cancer. *BMC Cancer* **2008**, *8*, 228.
- (174) Zhang, Y.; Hong, H.; Nayak, T. R.; Valdovinos, H. F.; Myklejord, D. V.; Theuer, C. P.; Barnhart, T. E.; Cai, W. Imaging Tumor Angiogenesis in Breast Cancer Experimental Lung Metastasis with Positron Emission Tomography, near-Infrared Fluorescence, and Bioluminescence. *Angiogenesis* **2013**, *16* (3), 663–674.
- (175) Baklaushev, V. P.; Grinenko, N. F.; Yusubaliev, G. M.; Abakumov, M. A.; Gubskii, I. L.; Cherepanov, S. A.; Kashparov, I. A.; Burenkov, M. S.; Rabinovich, E. Z.; Ivanova, N. V.; et al. Modeling and Integral X-Ray, Optical, and MRI Visualization of Multiorgan Metastases of Orthotopic 4T1 Breast Carcinoma in BALB/c Mice. *Bull. Exp. Biol. Med.* **2015**, *158* (4), 581–588.
- (176) Wankhede, M.; Dedeugd, C.; Siemann, D. W.; Sorg, B. S. In Vivo Functional Differences in Microvascular Response of 4T1 and Caki-1 Tumors after Treatment with OXi4503. *Oncol. Rep.* **2010**, *23* (3), 685–692.
- (177) Zhiron, A. M.; Aksenov, A. V. Azodicarboxylates: Synthesis and Functionalization of Organic Compounds. *Russ. Chem. Rev.* **2014**, *83* (6), 502–522.
- (178) Chen, Z.; Mocharla, V. P.; Farmer, J. M.; Pettit, G. R.; Hamel, E.; Pinney, K. G. Preparation of New Anti-Tubulin Ligands through a Dual-Mode, Addition–Elimination Reaction to a Bromo-Substituted α,β -Unsaturated Sulfoxide. *J. Org. Chem.* **2000**, *65* (25), 8811–8815.
- (179) Hadimani, M. B.; Kessler, R. J.; Kautz, J. A.; Ghatak, A.; Shirali, A. R.; O’Dell, H.; Garner, C. M.; Pinney, K. G. 2-(3-Tert-Butyldimethylsiloxy-4-Methoxyphenyl)-6-Methoxy-3-(3,4,5-Trimethoxybenzoyl)Indole. *Acta Crystallogr. C* **2002**, *58* (Pt 6), o330-332.
- (180) Mason, R. P.; Zhao, D.; Liu, L.; Trawick, M. L.; Pinney, K. G. A Perspective on Vascular Disrupting Agents That Interact with Tubulin: Preclinical Tumor Imaging and Biological Assessment. *Integr. Biol. Quant. Biosci. Nano Macro* **2011**, *3* (4), 375–387.
- (181) Roughley, S. D.; Jordan, A. M. The Medicinal Chemist’s Toolbox: An Analysis of Reactions Used in the Pursuit of Drug Candidates. *J. Med. Chem.* **2011**, *54* (10), 3451–3479.

- (182) Fischer, E.; Jourdan, F. Ueber Die Hydrazine Der Brenztraubensäure. *Berichte Dtsch. Chem. Ges.* **16** (2), 2241–2245.
- (183) Bischler, A.; Fireman, P. Zur Kenntniss Einiger α - β - Diphenylindole. *Berichte Dtsch. Chem. Ges.* **26** (2), 1336–1349.
- (184) Bigot, P.; Saint-Ruf, G.; Buu-Hoï, N. P. Carcinogenic Nitrogen Compounds. Part LXXXII. Polycyclic Indoles by Means of the Möhlau–Bischler Synthesis. *J. Chem. Soc. [Perkin 1]* **1972**, 0 (0), 2573–2576.
- (185) Bancroft, K. C. C.; Ward, T. J.; Brown, K. Application of the Bischler Reaction to the Preparations of Some Pyrrolopyridines and the Novel Dipyrrolopyridine System. *J. Chem. Soc. [Perkin 1]* **1974**, 0 (0), 1852–1858.
- (186) Bunescu, A.; Piemontesi, C.; Wang, Q.; Zhu, J. Heteroannulation of Arynes with N-Aryl- α -Aminoketones for the Synthesis of Unsymmetrical N-Aryl-2,3-Disubstituted Indoles: An Aryne Twist of Bischler–Möhlau Indole Synthesis. *Chem. Commun.* **2013**, 49 (87), 10284–10286.
- (187) Laube, M.; Tondera, C.; Sharma, S. K.; Bechmann, N.; Pietzsch, F.-J.; Pigorsch, A.; Köckerling, M.; Wuest, F.; Pietzsch, J.; Kniess, T. 2,3-Diaryl-Substituted Indole Based COX-2 Inhibitors as Leads for Imaging Tracer Development. *RSC Adv.* **2014**, 4 (73), 38726–38742.
- (188) Henry, J. R.; Dodd, J. H. Synthesis of RWJ 68354: A Potent Inhibitor of the MAP Kinase P38. *Tetrahedron Lett.* **1998**, 39 (48), 8763–8764.
- (189) Vara, Y.; Aldaba, E.; Arrieta, A.; Pizarro, J. L.; Arriortua, M. I.; Cossío, F. P. Regiochemistry of the Microwave-Assisted Reaction between Aromatic Amines and α -Bromoketones to Yield Substituted 1H-Indoles. *Org. Biomol. Chem.* **2008**, 6 (10), 1763–1772.
- (190) Nelson, K. L.; Seefeld, R. L. The Mechanistic Fate of Carbonyl Oxygen in the Rearrangement of 2-Anilino-1-Phenyl-1-Propanone. *J. Am. Chem. Soc.* **1958**, 80 (22), 5957–5959.
- (191) MacDonough, M. T. The Design, Synthesis, and Biological Evaluation of Indole-Based Anticancer Agents. Thesis, 2013.
- (192) Jones, C. D.; Jevnikar, M. G.; Pike, A. J.; Peters, M. K.; Black, L. J.; Thompson, A. R.; Falcone, J. F.; Clemens, J. A. Antiestrogens. 2. Structure-Activity Studies in a Series of 3-Aroyl-2-Arylbenzo[b]Thiophene Derivatives Leading to [6-Hydroxy-2-(4-Hydroxyphenyl)Benzo[b]Thien-3-Yl]-[4-[2-(1-Piperidinyl)Ethoxy]Phenyl]Methanone Hydrochloride (LY 156758), a Remarkably Effective Estrogen Antagonist with Only Minimal Intrinsic Estrogenicity. *J. Med. Chem.* **1984**, 27 (8), 1057–1066.

- (193) Kaufmann, D.; Pojarová, M.; Vogel, S.; Liebl, R.; Gastpar, R.; Gross, D.; Nishino, T.; Pfaller, T.; von Angerer, E. Antimitotic Activities of 2-Phenylindole-3-Carbaldehydes in Human Breast Cancer Cells. *Bioorg. Med. Chem.* **2007**, *15* (15), 5122–5136.
- (194) Du, X.; Guo, C.; Hansell, E.; Doyle, P. S.; Caffrey, C. R.; Holler, T. P.; McKerrow, J. H.; Cohen, F. E. Synthesis and Structure–Activity Relationship Study of Potent Trypanocidal Thio Semicarbazone Inhibitors of the Trypanosomal Cysteine Protease Cruzain. *J. Med. Chem.* **2002**, *45* (13), 2695–2707.
- (195) Greenbaum, D. C.; Mackey, Z.; Hansell, E.; Doyle, P.; Gut, J.; Caffrey, C. R.; Lehrman, J.; Rosenthal, P. J.; McKerrow, J. H.; Chibale, K. Synthesis and Structure–Activity Relationships of Parasitocidal Thiosemicarbazone Cysteine Protease Inhibitors against Plasmodium Falciparum, Trypanosoma Brucei, and Trypanosoma Cruzi. *J. Med. Chem.* **2004**, *47* (12), 3212–3219.
- (196) Kishore Kumar, G. D.; Chavarria, G. E.; Charlton-Sevcik, A. K.; Arispe, W. M.; MacDonough, M. T.; Strecker, T. E.; Chen, S.-E.; Siim, B. G.; Chaplin, D. J.; Trawick, M. L.; et al. Design, Synthesis, and Biological Evaluation of Potent Thiosemicarbazone Based Cathepsin L Inhibitors. *Bioorg. Med. Chem. Lett.* **2010**, *20* (4), 1415–1419.
- (197) Chavarria, G. E.; Horsman, M. R.; Arispe, W. M.; Kumar, G. D. K.; Chen, S.-E.; Strecker, T. E.; Parker, E. N.; Chaplin, D. J.; Pinney, K. G.; Trawick, M. L. Initial Evaluation of the Antitumour Activity of KGP94, a Functionalized Benzophenone Thiosemicarbazone Inhibitor of Cathepsin L. *Eur. J. Med. Chem.* **2012**, *58*, 568–572.
- (198) Song, J.; Jones, L. M.; Chavarria, G. E.; Charlton-Sevcik, A. K.; Jantz, A.; Johansen, A.; Bayeh, L.; Soeung, V.; Snyder, L. K.; Lade, S. D.; et al. Small-Molecule Inhibitors of Cathepsin L Incorporating Functionalized Ring-Fused Molecular Frameworks. *Bioorg. Med. Chem. Lett.* **2013**, *23* (9), 2801–2807.
- (199) Parker, E. N.; Song, J.; Kishore Kumar, G. D.; Odutola, S. O.; Chavarria, G. E.; Charlton-Sevcik, A. K.; Strecker, T. E.; Barnes, A. L.; Sudhan, D. R.; Wittenborn, T. R.; et al. Synthesis and Biochemical Evaluation of Benzoylbenzophenone Thiosemicarbazone Analogues as Potent and Selective Inhibitors of Cathepsin L. *Bioorg. Med. Chem.* **2015**, *23* (21), 6974–6992.
- (200) Parker, E. N.; Odutola, S. O.; Wang, Y.; Strecker, T. E.; Mukherjee, R.; Shi, Z.; Chaplin, D. J.; Trawick, M. L.; Pinney, K. G. Synthesis and Biological Evaluation of a Water-Soluble Phosphate Prodrug Salt and Structural Analogues of KGP94, a Lead Inhibitor of Cathepsin L. *Bioorg. Med. Chem. Lett.* **2017**, *27* (5), 1304–1310.